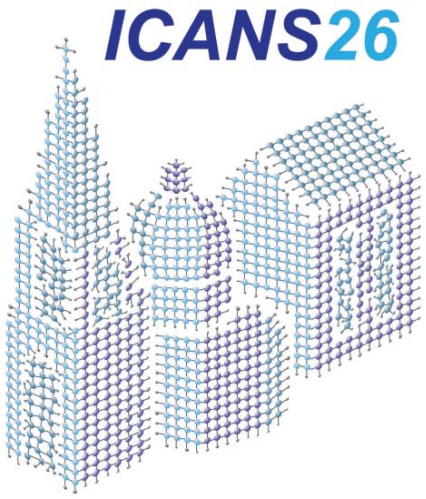

ICANS26

26th International Conference on Amorphous and Nanocrystalline Semiconductors

Abstracts and Program

13-18 September, 2015, Aachen, Germany

	September, 14. (Monday)			September, 15. (Tuesday)			September, 16. (Wednesday)			September, 17. (Thursday)			September, 18. (Friday)		
	Brüssel	Berlin 1	Berlin 2	Brüssel	Berlin 1	Berlin 2	Brüssel	Berlin 1	Berlin 2	Brüssel	Berlin 1	Berlin 2	Brüssel	Berlin 1	Berlin 2
08:40-09:00															
09:00-09:20				Uwe Kortshagen: Gas phase synthesis of semi-conductor nanoparticles and their electronic and plasmonic properties			Vanessa Wood: Charge Transport and Recombination in Colloidal Nanocrystal Solids			Koen Vandewal: Molecular factors influencing charge carrier recombination at donor-acceptor interfaces for organic photovoltaics			Takuya Matsui: Progress and challenges in a-Si:H based solar cells		
09:20-09:40	Opening Remarks 09:30-10:00														
09:40-10:00				**Coffee/Tea**			**Coffee/Tea**			**Coffee/Tea**			**Coffee/Tea**		
10:00-10:20	John Robertson: What has Bonding Done for Us?			Si particles	Organic homo/hetero junction	Alloys	Polysilicon/ growth	Modelling & simulation	Chalco-genides	SHJ III	Organics II	Phase change materials	TFS solar cells II	Oxides & chalcogenides	Devices III
10:20-10:40															
10:40-11:00	**Coffee/Tea**														
11:00-11:20	IGZO & TFTS	Nano-structures	Characteri-zation												
11:20-11:40															
11:40-12:00													Closing, announcement		
12:00-12:20															
12:20-14:00	**Lunch break**			**Lunch break**			ICANS 26 Conference Excursion to Monschau 13:00 - 22:00			**Lunch & IAC Meeting**					
14:00-14:20	Sang Il Seok: Recent Progress of Nanocrystalline Semiconductor-Based Inorganic/Organic Hybrid Solar Cells			SHJ I	TFS solar cells I	Transport				Perovskite	Solar materials & cells	Growth & properties of nanostructures			
14:20-14:40															
14:40-15:00	Devices I	Chalco-genides & transport	2D Materials												
15:00-15:20															
15:20-15:40															
15:40-16:00				**Coffee/Tea**											
16:00-16:20	**Coffee/Tea**									**Coffee/Tea**					
16:20-16:40	Organics & Perovskites	Sensors	Stability	SHJ II	Organics I	Electro-chemistry				Voids & Hydrogen	Devices II	Methods and materials			
16:40-17:00															
17:00-17:20															
17:20-17:40															
17:40-18:00															
18:00-18:20	Poster			Poster											
18:20-18:40															
18:40-19:00															
19:00-19:20										ICANS 26 Conference Banquet 19:00 - 23:00 (Coronation Hall in Aachen's Town Hall)					
19:20-19:40															
19:40-20:00															

Dear conference participants,

Welcome to ICANS26 in Aachen, Germany!

It is our pleasure to welcome you to the 26th International Conference on Amorphous and Nanocrystalline Semiconductors in Aachen, Germany. This is the third conference of the series to be held in Germany; after two meetings in Garmisch-Partenkirchen in 1973 and 1991 in the south, this time in Aachen we welcome you to the far west close to the meeting point of Germany, The Netherlands, and Belgium.

Having celebrated the 25th conference two years ago in Toronto this year we can celebrate 50 years since the beginning of this conference series. The Conference series started in Prague in 1965 named International Conference on Amorphous and Liquid Semiconductors (ICALS) and since then saw a slight change of name (ICAxS; x=L,_,M,N) to express the changing scientific focus of the conference. Until 1995, the conference was typically held in Europe, however in the more recent years the hosts of the conference have been equally distributed between Europe, America and Asia demonstrating the growing interest in the fascinating science of amorphous and nanocrystalline materials all over the world.

Initially, and for many years the scientific focus of the conference was on the fundamental physics of amorphous semiconductors, in particular those principally formed from chalcogenides and group IV elements. This was followed by an almost two-decade long period predominated by amorphous and microcrystalline silicon, particularly for solar cell and transistor applications. Currently, the scope of the conference covers the preparation, characterization and theory of a wide range of amorphous, organic and nanocrystalline semiconductors including the effects of disorder in semiconductors and dielectrics, both in the bulk and at interfaces. Sessions on devices and applications in technological areas such as electronics, photovoltaics and data storage among many others, form another significant part of the meeting. Finally, there will be several sessions on recent material and device developments in photovoltaic technologies where nanocrystalline or disordered materials play an essential role, such as silicon heterojunction solar cells, perovskites and organic solar cells.

We are confident, that the conference will provide an excellent forum for information and discussions on the latest developments in the field of amorphous, organic and nanocrystalline semiconductors and their various applications as well as the role of disorder on the optoelectronic properties of materials in general. We hope that the program and the charming environment will help to stimulate the exchange of ideas, identification of problems common across the different areas, and cross-border solutions, as well as new collaborations and friendships.

The scientific program will open in the traditional way on Monday morning with the Mott lecture, this year given by John Robertson entitled *What has bonding done for us?* with the Monday keynote lecture in the early afternoon. All other days will begin with the keynote lecture. The remaining program is organized into 3 parallel sessions each day with a total 18 invited talks and 129 contributed oral presentations. Two poster sessions with a total of 146 posters will take place on Monday and Tuesday evenings.

The tutorial program on Sunday will feature distinguished lecturers on the topics of hybrid organic/inorganic solar cells, high-efficiency silicon heterojunction solar cells, effects of disorder in semiconductors, and theory and simulation for structurally disordered semiconductors.

Finally, the Organizers would like to express their sincere thanks to the numerous friends and colleagues for helping to make this conference a success. We are very grateful to the local organizing

Committee headed by Friedhelm Finger and consisting of Maurice Nuys, Jan Adamczak, Urs Aeberhard, Josef Klomfaß, Astrid Nogga, Olexander Astakhov, Stefan Muthmann and many more for the taking care of all the details needed to make the conference enjoyable. We are indebted to the members of the International Advisory Committee, the program committee headed by Ruud Schropp, and the reviewers of the abstracts for their efforts and their suggestions regarding the program. Last but not least we are deeply thankful to all institutions, universities and companies for their generous financial support.
We hope you enjoy all this Conference has to offer and look forward to sharing this time with you in Aachen.

On behalf of the organizers

Reinhard Carius

Chair, ICANS26

INTERNATIONAL ADVISORY COMMITTEE

Sergei Baranovski, University of Marburg, Germany
Kunji Chen, Nanjing University, China
Reuben Collins, Colorado School of Mines, USA
Hiroaki Fujiwara, Gifu University, Japan
Hideo Hosono, Tokyo Institute of Technology, Japan
Jin Jang, Kyung Hee University, Korea
Safa Kasap, University of Saskatchewan, Canada
Jan Kočka, Academy of Sciences of Czech Republic
Sandor Kugler, Budapest University, Hungary
Rodrigo Martins, UNINOVA, Portugal
John Robertson, University of Cambridge, UK
Pere Roca i Cabarrocas, Ecole Polytechnique, France
Ruud Schropp, Eindhoven University of Technology, the Netherlands
Robert Street, Palo Alto Research Center, USA
Martin Stutzmann, University of Munich, Germany
John Wager, Oregon State University, USA
Sigurd Wagner (Chair), Princeton University, USA
Baojie Yan, Wintek Electro-Optics Corporation, Ann Arbor, Michigan, USA

ORGANISING COMMITTEE

R. Carius (Chair), Forschungszentrum Jülich, Germany
F. Finger (Co-Chair), Forschungszentrum Jülich, Germany
R. Schropp (Program Chair), Eindhoven University of Technology, the Netherlands
M. Wuttig, RWTH Aachen University, Germany
M. Stutzmann, Technical University of Munich, Germany
K. Lips, Helmholtz Center Berlin, Germany
M. Schubert, University of Stuttgart, Germany
D. Neher, University of Potsdam, Germany
U. Rau, Forschungszentrum Jülich, Germany
T. Kirchartz, Forschungszentrum Jülich, Germany
M. Nuys, Forschungszentrum Jülich, Germany
U. Aeberhard, Forschungszentrum Jülich, Germany

CONFERENCE DESK

The desk will be opened during the following hours

Sunday 13th September
8:30h – 9:15h (for Tutorials participants only)
17:00h – 20:00h

Monday 14th and Tuesday 15th September
8:15h – 18:00h

Tuesday 15th September
8:30h – 18:00h

Wednesday 16th September
8:30h – 12:15h

Thursday 17th September
8:30h – 18:00h

Friday 18th September
8:30h – 12:30h

SOCIAL PROGRAM

ON-SITE REGISTRATION FOR THE EXCURSION AND THE CONFERENCE DINNER IS POSSIBLE AS LONG AS SPACE IS AVAILABLE

Reception on Sunday 13th September, 2015 / 18:00h – 21:30h

Reception takes place at the Eurogress Conference Center. All conference participants will be welcomed by the conference organizers with a variety of drinks & snacks framed by easy listening live music. The conference opening by Organizing Committee Chair will start at 18:00h.

Pre registration to pick up your conference materials will be available too, starting Sunday afternoon.

Excursion to Monschau and Botrange on Wednesday 16th September, 2015 / 13:30h – 22:00h

ICANS Excursion visits the sights of the Hohes Venn – Eifel Nature Park region with the historical town of Monschau. Monschau is located half an hour from Aachen in the hills of the North Eifel, within the Hohes Venn – Eifel Nature Park in the narrow valley of the Rur river. The historic town center of Monschau has many preserved half-timbered houses and small streets which have remained nearly unchanged for 300 years. The 13th century castle closely above the town center completes the remarkable picturesque sight.

You have the choice between three different tours:

1. Guided Tour in the historical Town Monschau with local specialities
2. Guided Hiking Tour in the National Park High Venn
3. Guided Walking Tour along the river Rur

45 € - Price include transportation, 1 tour fee, catering (lunch bags and evening reception)

Excursion will start (13:30h) and end (22:00h) in front of Eurogress Aachen. Participants will be picked up by Bus and brought to the starting points of their guided tour. Lunch bags will be prepared at the start.

After tours end all participants will meet for a reception in Monschau old markethall (17:30h) with traditional hearty potatoe and pea soup and drinks such as regionally brewed beer. Departure to Aachen will be at 21:00h.

The old market hall is situated directly in the heart of Monschau old town, Address: Rurstraße 9, 52156 Monschau.

Information about the tours

1. Guided Tour in the historical Town Monschau with local specialities - A Bite of Monschau (1.5h)

You will be guided through the historical town of Monschau and experience the regional specialties such as Printen (regional gingerbread), Monschau Mustard and many more free of charge.

2. Guided Hiking Tour in the National Park High Venn (2h)

You will visit the biggest hill moor in the European Union with an extension of 600 skm across the Belgian-German border. A specially trained guide will explain about the ecological impact for the surrounding countries.

The unique landscape can be described best: Gnarled downy birches, roundish shrubs of the eared willow, spruces, and sweeping sorbs give the bog bizarre silhouettes.

3. Hiking tour for experienced hiker through the unique landscape of High Venn.

All-weather clothing and hiking boots are recommended.

Guided Walking Tour along the river Rur (2h)

Walk along the gurgling waters through the narrow Rur valley passing by historical half-timbered houses.

All-weather clothing and walking shoes are recommended.

Conference Dinner on Thursday 17th September, 2015 / 19:00h – 23:00h

Conference Dinner will be hosted at Aachen Coronation hall. The Coronation hall with its famous Rethel frescoes dating from the 19th century and copies of the Imperial Crown Jewels as well as the gothic and baroque furniture of the building is a very special location. In the past several coronations of emperors set place in the Coronation Hall.

These days there is an annually assembly for the award of Karls's prize.

All guests will be welcomed with a sparkling wine reception and will experience short stories of Aachens history.

Dinner will present a fine 3 course menu/buffet and corresponding drinks. During dinner there will be another short presentation of regional tradition. After dinner the coronation hall is still open for the conference get together with DJ at set.

LUNCHES

Lunch is not included in the Conference fee. Close to the Eurogress Aachen there are several bars and restaurants within walking distance to reach (cf. map below).

ICANS26 – 2015 Restaurants in Aachen

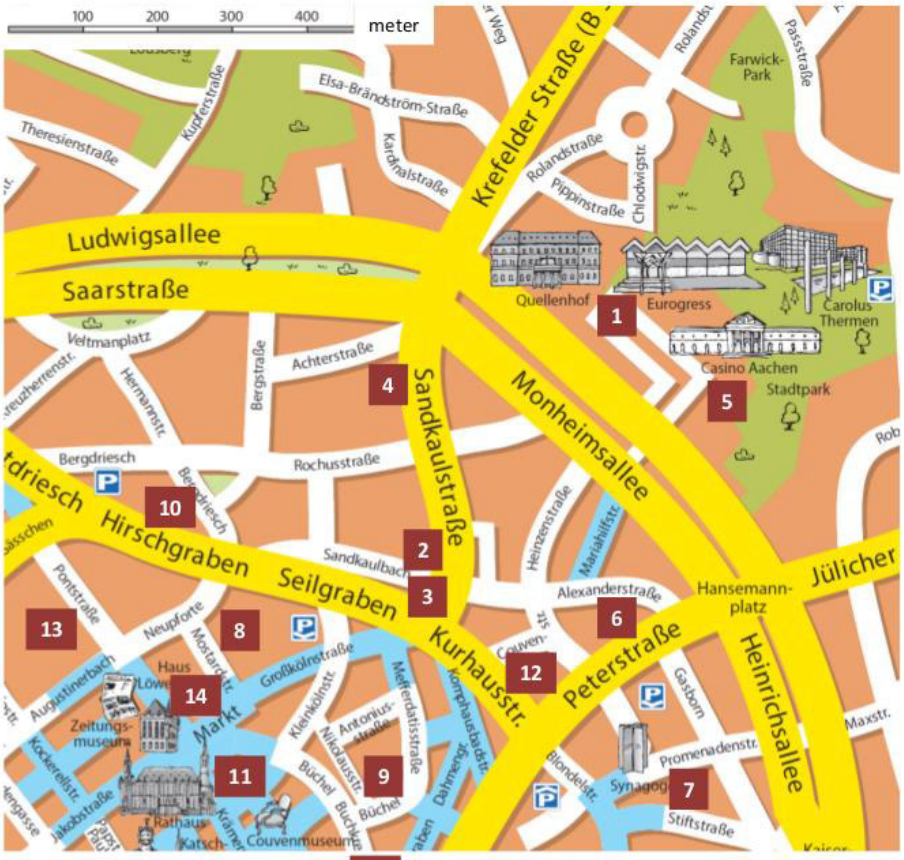

several Bars & Restaurants:

12 Kurhausstraße

13 Pontstraße

14 *Tijuana*
Markt 47

1 *La Brasserie*
Monheimsallee 52

2 *Kolumbianisches Restaurant „Karibik“*
Sandkaulstraße 5

3 *Kanpai Running Sushi & Lounge*
Alexanderstraße 17

4 *Café & Bar Zuhause*
Sandkaulstraße 109

5 *Café Kurhaus*
Monheimsallee 40

6 *Restaurant One & Only*
Peterstraße 81-83

7 *Justus K*
Promenadenstraße 36

8 *Mostard Restaurant*
Mostardstraße 20

9 *Nudeloper*
Büchel 41

10 *Am Knipp*
Bergdriesch 3

11 *Ratskeller*
Markt 40

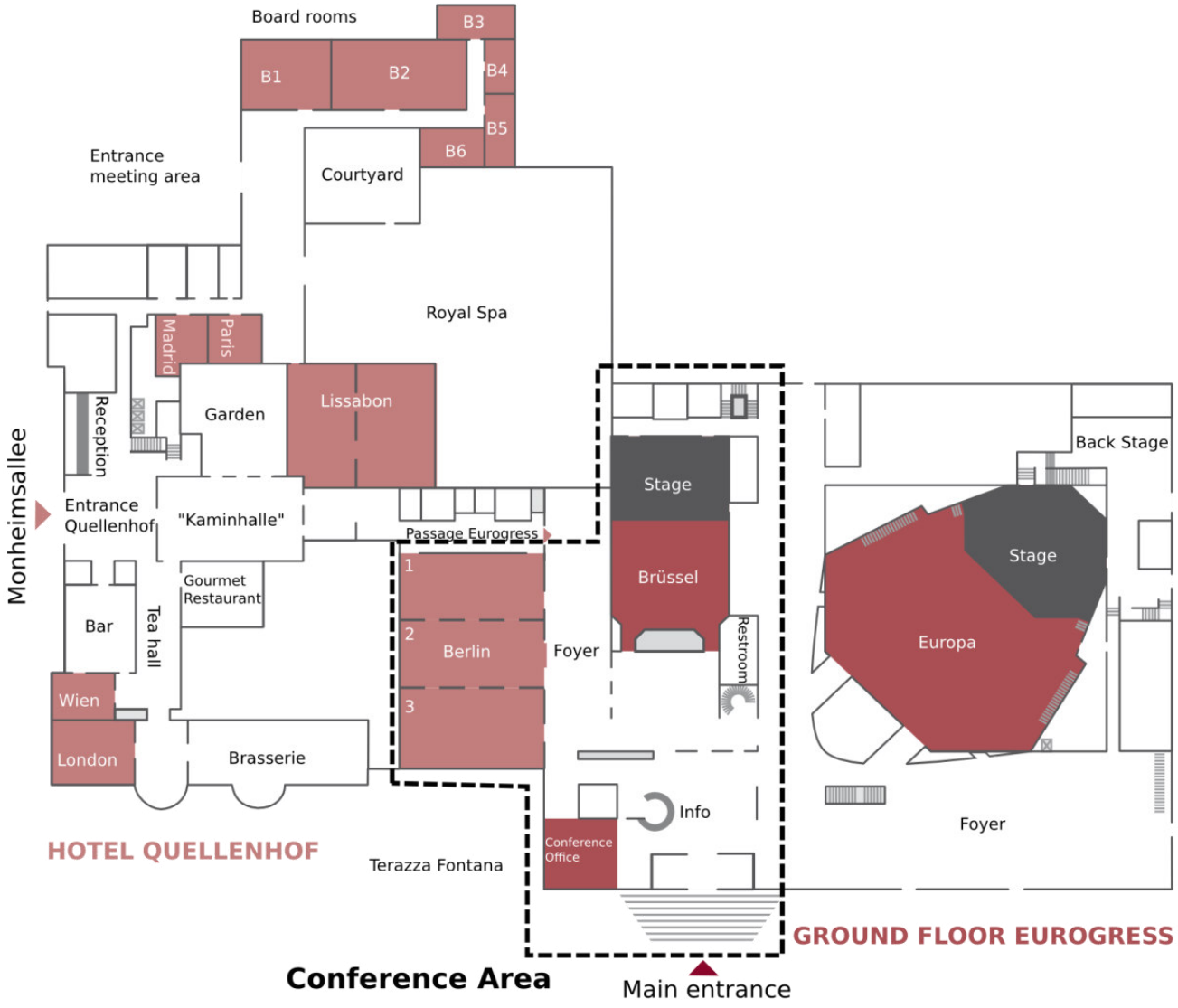
Board rooms
B3
B1
B2
B4
B5
B6
Entrance
meeting area
Courtyard
Royal Spa
Madrid
Paris
Garden
Lissabon
Reception
Monheimsallee
Entrance
Quellenhof
"Kaminhalle"
Passage Eurogress
Gourmet
Restaurant
Bar
Tea hall
Wien
London
Brasserie
HOTEL QUELLENHOF
Terazza Fontana
1
2
Berlin
3
Foyer
Stage
Brüssel
Restroom
Info
Conference
Office
Conference Area
Main entrance
Back Stage
Stage
Europa
Foyer
GROUND FLOOR EUROGRESS

MOTT LECTURE

John Robertson – Cambridge
What has Bonding Done for Us? (ID 278)

KEYNOTE LECTURES

Uwe Kortshagen – University of Minnesota
Gas phase synthesis of semiconductor nanoparticles and their electronic and plasmonic properties.

Takuya Matsui – Advanced Industria Science and Technology (AIST)
Progress and challenges in a-Si:H based solar cells (ID 274)

Sang Il Seok – Korea Research Institute of Chemical Technology (KRICT)
Recent Progress of Nanocrystalline Semiconductor-Based Inorganic/Organic Hybrid Solar Cells (ID 287)

Koen Vandewal – University of Dresden
Molecular factors influencing charge carrier recombination at donor-acceptor interfaces for organic photovoltaics (ID 281)

Vanessa Wood – ETH Zürich
Charge Transport and Recombination in Colloidal Nanocrystal Solids

INVITED LECTURES

Shane Ardo – University California Irvine
Light-Driven Vectorial Ion Transport: Using Interdigitated Back-Contact Semiconductors and Organic Photovoltaics for the Photoelectrochemical Generation of Drinking Water from Seawater (ID 228)

Daniel Amkreutz *– Helmholtz-Zentrum Berlin*
Advances in liquid phase crystallized silicon on glass: growth, electronic properties and solar cell concepts (ID 276)

Wolfhard Beyer - Helmholtz-Zentrum Berlin and Forschungszentrum Jülich GmbH
Hydrogen incorporation, stability and release effects in thin film silicon (ID 283)

Wallace Choy – University of Hong Kong
Novel Approaches to Improve Optical Absorption and Carrier Extraction of Organic Photovoltaic Cells (ID 284)

João Pedro Conde – University of Lisbon
Thin-film silicon MEMS and NEMS (ID 275)

Richard Curry – University of Surrey
Non-equilibrium doping of amorphous chalcogenide materials and devices

David Drabold – Ohio University
Disordered Materials by design (ID 14)

Jarvist Frost – University of Bath
The dynamic solid-state physics of hybrid halide perovskites

Neil Greenham – Cambridge
Singlet Fission – Using Organic Semiconductors and Nanocrystals to Break Efficiency Limits in Photovoltaics (ID 286)

Robert A. de Groot – Radboud University Nijmegen
The amorphous / crystalline interface: a computational point of view. (ID 247)

Yongtaek Hong – Seol National University
Inkjet-printed nano materials for stretchable electronic system

Jenny Nelson – Imperial College London
Relating material properties to charge recombination in organic heterojunction solar cells (ID 288)

Thomas Niehaus – University of Regensburg
Inverse quantum confinement in luminescent Silicon quantum dots (ID 277)

Shunri Oda – Tokyo Institute of Technology
Silicon nanocrystals for future electronics and photonics (ID 282)

Jean-Yves Raty – University of Liege
Stability and Aging of Phase Change Materials : An Ab Initio (ID 279)

Jan-Willem Schüttauf – EPFL STI IMT PV-LAB
Triple- and quadruple-junction thin-film silicon solar cells (ID 176)

Masaki Shima – Panasonic Corporation
Technological Progress in HIT(R) - on the long way towards the limit – (ID 285)

Nenad Vukmirovic – University of Belgrade
Simulation Insights into Electronic Properties of Disordered Organic Semiconductors (ID 65)

Xiaodan Zhang – University Nankai
High efficiency single-, double- and triple- junction silicon based thin film solar cells (ID 280)

TUTORIALS PROGRAM

The tutorial lectures will take place on 13th September 2015. The tutorials cover the following topics: (1) hybrid organic/inorganic perovskite solar cells, (2) silicon heterojunction solar cells, (3) effects of disorder in semiconductors, and (4) theory and simulation for structurally disordered materials.

9:00 – 10:30: Tutorial I

David Cahen with Gary Hodes - Weizmann Institute of Science, Rehovot, Israel
Hybrid Organic/Inorganic Perovskite Solar Cells

10:30 – 11:00: Break

11:00 – 12:30: Tutorial II

Stefaan De Wolf - PV-Lab, IMT, EPFL, Neuchâtel, Switzerland
High-Efficiency Silicon Heterojunction Solar cells - Processing, Properties and Perspectives

12:30 – 13:30: Lunch Break

13:30 – 15:00: Tutorial III

Martin Stutzmann und Matthias Wuttig – TU München und RWTH Aachen, Germany
Effects of disorder in semiconductors

15:00 – 15:30: Break

15:30 – 17:00: Tutorial IV

David Drabold – Ohio University, United States of America
Theory and simulation for structurally disordered materials

Tutorials Abstracts

Tutorial I: Hybrid Organic/Inorganic Perovskite Solar Cells

David Cahen with Gary Hodes - Weizmann Institute of Science, Rehovot, Israel

With solution-processed, organic-inorganic hybrid lead halide perovskite-based solar cell developments being meteoric over the last few years, the questions of

- how these materials form,
- how hard or easy it is to decompose the compounds, and
- how can and do solar cells that are made with them work,

are topics of significant fundamental interest. They are quite relevant also for our understanding of what are “good” PV materials and, more generally, what are “good” optoelectronic materials. In this tutorial we will consider the above-phrased questions and issues and review

- the question of how the materials form and decompose, and
- our present understanding of how both iodide and bromide cells are likely to operate, including microscopy studies,

By combining insights in these and other aspects we may then be able to provide an idea of realistic future prospects for these materials and for devices made with them.

Tutorial II: High-Efficiency Silicon Heterojunction Solar cells - Processing, Properties and Perspectives

Stefaan De Wolf - PV-Lab, IMT, EPFL, Neuchâtel, Switzerland

Silicon heterojunction technology (HJT) uses silicon thin-film deposition techniques to fabricate photovoltaic devices from mono-crystalline silicon wafers (c-Si). This enables energy-conversion efficiencies above 21%, also at industrial-production level. In this tutorial we review the present status of this technology, with a focus on the actual device processing, and also point out recent trends. We first discuss how such devices are fabricated. We give evidence how the properties of thin hydrogenated amorphous silicon (a-Si:H) films can be tuned and exploited to fabricate so-called passivating contacts. The contacts are the key to high-efficiency HJT solar cells, as they enable very high operating voltages, approaching the theoretical limits, and yield small temperature coefficients. With this approach, an increasing number of groups are now reporting devices with conversion efficiencies well over 20% on n-type wafers, with Panasonic leading the field with 24.7%. Exciting results have also been obtained on p-type wafers. Despite these high voltages, important efficiency gains can still be made by optimizing the fill factor and optical design. This requires improved understanding of carrier transport across device interfaces and reduced parasitic absorption in HJT solar cells. For the latter, several strategies can be followed: Short-wavelength losses can be reduced by replacing the front a-Si:H films with wider-bandgap window layers, such as silicon alloys or even metal oxides. Long-wavelength losses are mitigated by introducing new high-mobility TCO’s such as hydrogenated indium oxide, and also by designing new rear reflectors. Optical shadow losses caused by the front metalisation grid are significantly reduced by replacing printed silver electrodes with fine-line plated copper contacts, leading also to possible cost advantages. The ultimate approach to minimize optical losses is the implementation of back-contacted architectures, which are completely devoid of grid shadow losses and parasitic absorption in the front layers can be minimized irrespective of electrical transport requirements. The validity of this approach was convincingly demonstrated by Panasonic, Japan in 2014, reporting on an interdigitated back-contacted HJT cell with an efficiency of 25.6%, setting the new single-junction c-Si record. Finally, given the virtually perfect surface passivation and excellent red response of HJT solar cells, we anticipate

these devices will also become the preferred bottom cell in ultra-high efficiency c-Si-based tandem devices, exploiting better the solar spectrum. Such tandem cells have the potential to overcome the fundamental single-junction limit of silicon solar cells (29.4%). Combining HJT cells with recently emerging perovskite technology for top cell fabrication appears to be particularly appealing to extend the learning curve of silicon-based photovoltaics.

Tutorial III: Effects of disorder in semiconductors

Martin Stutzmann und Matthias Wuttig – TU München und RWTH Aachen, Germany

Disorder can play a prominent role in semiconductors, affecting a wide range of properties including both optical and electronic properties. This tutorial will review different types of disorder from simple defects to the disorder observed in amorphous semiconductors. Interesting enough, the consequences of disorder do not only depend upon the type of disorder, they are also strongly influenced by the type of electronic orbitals, which govern the corresponding properties. Hence, it is possible to realize amorphous TCO materials, which reveal a conductivity closely resembling their crystalline counterpart with the same stoichiometry. On the other hand, disorder in crystalline semiconductors with a different bonding, yet comparable density of charge carriers at the Fermi energy can turn these materials into insulators. In this tutorial, we will hence carefully review the impact of the different types of disorder and bonding and their impact on the resulting properties.

Tutorial IV: Theory and simulation for structurally disordered materials

David Drabold – Ohio University, United States of America

The primary challenge for the modeler in our area is faithfully representing the disorder -- making a realistic computer model. I will briefly

describe the standard methods, such as Molecular Dynamics and attempts to directly "invert" experimental data into a model

using techniques like Reverse Monte Carlo. These are examples of what I have called the "Simulation Paradigm" and the "Information Paradigm". An obvious goal is to attempt to unite these approaches and formulate one method that yields a model that is at once in accord with experimental information and a suitable minimum of a potential energy

functional [1].

A striking indication of the power of simulation is provided by the phase-change memory materials. Here, it is possible to simulate in exquisite detail the key processes of amorphization and crystallization [2]. With this work, realistic atomistic simulation, experiments and devices have made direct contact, and enabled new lines of inquiry. Such is the simulator’s usual stated goal: now it has finally been met for a complex and important material.

Tools exist that allow non-experts to undertake some of this modeling. Many glasses can be modeled by straightforward approaches: creation of an equilibrated liquid, followed by a simulated quench. I also point out that some ab initio codes are surprisingly straightforward to use, and will even run on relatively modest machines, at least for small (ca. 200 atom) models. Such simulations are within the capability of anyone that has a week to spend with a practicing group, the software and hardware needed.

Of course many key properties of real materials are determined by the structure. The vibrational modes, electronic structure, optical and transport properties are examples. One topic of interest is charge carrier

transport. Here, the approach required varies with the question asked. Standard non-equilibrium Green's function codes may be used for I-V

Characteristics [3], and the celebrated Kubo formula from linear response theory is suitable for many applications, including estimates of the temperature dependence as for IR imaging (e.g. for night vision), an application that I briefly describe [4].

As time allows, I will also present a method for simplified first principles modeling of the interaction of solids with light. A byproduct of any first principles simulation is a collection of occupied and unoccupied single-particle levels (Kohn-Sham orbitals). If we treat these as quasiparticle states, it is possible to explore light-induced structure changes and approach problems like light-induced metastability [5].

[1] D. A. Drabold, Eur. Phys. J. B 68 1 (2009).

[2] J. Hegedus and S. R. Elliott, Nature Materials 7 399 (2008).

[3] K. Stokbro et al., Ann. NY Acad. Sci. 1006 212 (2003).

[4] T. Abtew et al., Phys. Rev. B 76 045212 (2007).

[5] D. A. Drabold et al. in Photo-induced metastability in amorphous semiconductors, A. V. Kolobov, Ed., Wiley-VCH, Berl

in, pp 260-276 (2003).

Conference Program

PROGRAM ICANS26 - MONDAY, 14TH SEPTEMBER 2015

		Brüssel		Berlin 1		Berlin 2
9:30 – 10:00		**Opening remarks** **R. Carius (Chair of ICANS 26) & H. Bolt (Member of the board of FZJ)**				
10:00 – 10:20	Chair: Sigurd Wagner	**Mott Lecture:** *What has Bonding Done for Us?* **John Robertson, ID 278**				
10:20 – 10:40						
10:40 – 11:00		**Coffee break**				
11:00 – 11:20	Session: IGZO & TFTS, Chair: Manuela Vieira	*Solution-deposited oxide TFTs and backplanes* **Robert Street, ID 111**	Session: Nanostructures, chair: Thomas Niehaus	*Transrotational microcrystals and nanostructures discovered by TEM in crystallizing amorphous films and a new model of amorphous state* **Vladimir Kolosov, ID 218**	Session: Characterization, chair: Stephen Reynolds	*Subbandgap absorption spectroscopy of solar cell materials* **Jakub Holovsky, ID 205**
11:20 – 11:40		*Analysis of Degradation Phenomenon in a-IGZO TFTs under High Power Stress Condition* **Seok-Woo Lee, ID 46**		*Copper Sulfide Nanoparticles as Absorber for Photovoltaic Application* **Jan Flohre, ID 246**		*Lifetime measurements on poly-crystalline silicon thin films on glass utilzing photoluminescence* **Sven Kühnapfel, ID 99**
11:40 – 12:00		*SiOx Thin-film Hydrogen Diffusion Barriers for High-performance Flexible Transparent IGZO TFTs and Circuits* **Alireza Tari, ID 107**		*Optimizing the growth of ZnO nanowires by chemical bath deposition for energy applications* **George Syrrokostas, ID 233**		*Thickness of amorphous silicon thin films for heterojunction solar cells measured by Raman spectroscopy on textured silicon wafers* **Martin Ledinsky, ID 149**
12:00 – 12:20		*Effect of Top gate bias on Fermi position, photo current and NBIS instability in dual gate a-IGZO TFTs Delwar* **Hossain Chowdhury, ID 142**		*Role of a-Si:H in Lateral Growth of Silicon Nanowires* **Jan Kocka, ID 15**		*Multifrequency EPR Studies on µc-SiC:H films for photovoltaic applications* **Oleksandr Astakhov, ID 178**

12:20 – 14:00	**Lunch break**					
		Brüssel				
14:00 – 14:40	**Chair: John Robertson**	**Keynote Lecture:** Recent Progress of Nanocrystalline Semiconductor-Based Inorganic/Organic Hybrid Solar Cells **Sang Il Seok**				
		Brüssel		**Berlin 1**		**Berlin 2**
14:50 – 15:10	**Session: Devices I, chair: Markus Schubert**	*Inkjet-printed nano materials for stretchable electronic system* **Yongtaek Hong** (invited talk)	**Session: Chalcogenides & transport, chair: Richard Curry**	*The question of photogenerated charge carrier recombination in a-Se* **Oleksandr Bubon, ID 214**	**Session: 2D Materials, chair: tba**	*Electronic properties of CVD Graphene capped with p and n-type doped amorphous silicon* **Arezki Hakim, ID 193**
15:10 – 15:30				*Modeling of Nucleation and Growth in Crystallization of Phase Change Materials* **Fatemeh Tabatabaei, ID 11**		*Atomistic simulation of amorphous graphene: A particle-swarm-assisted first-principles approach* **Taehoon Lee, ID 164**
15:30 – 15:50		*Solar Cells for self-sustainable intelligent packaging* **António Vicente, ID 202**		*Drift in Amorphous Chalcogenides: Challenge and Opportunity for Novel Computing Architectures* **Martin Salinga, ID 181**		*Facile, large area growth of mono- and few-layer MoX2 (X: S, Se, Te) with high catalytic performance by controlled chalcogenation of a molybdenym foil* **Spyros Yannopoulos, ID 221**
15:50 – 16:10		*Reduction of Bubble Defects and Prevention of Wafer Edge Peelings in SADP Stack* **Lihong Xiao, ID 8**		*Transient Photoconductivity in Coplanar vs. Sandwich Device Structure: Bulk and Surface Time-of-Flight Experiments on a-Se Detectors* **Safa Kasap, ID 25**		*Complementary Inverter by Mo-based Chalcogenide Nanosheet Channels: a Few Layer α-MoTe2 and MoS2* **Atiye Pezeshki, ID 61**

16:10 – 16:30		Coffee break				
		Brüssel		Berlin 1		Berlin 2
16:30 – 16:50	Session: Organics & Perovskites, chair: Jarvist Frost	*Towards ultra-high efficient photovoltaics with perovskite/crystalline silicon tandem devices* **Stefaan De Wolf, ID 220**	Session: Sensors, chair: Yongtaek Hong	*Silicon Thin Film Photodetectors for Multi-channel Fluorescence Detection in a Microfluidic Point-of-Care Testing Device* **Marcel Berner, ID 69**	Session: Stability, chair: Arno Smets	*Change of recombination rates of electrons at radiative defects in hydrogenated amorphous silicon with annealing of photo-created dangling bonds of silicon* **Chisato Ogihara, ID 21**
16:50 – 17:10		*From Amorphous Silicon/Organic to Perovskite/Crystalline Silicon Hybrid Multi-Junction Solar Cells* **Steve Albrecht, ID 242**		*Microcrystalline Silicon Photodiode for Near Infrared Light Detection* **Alireza Khosropour, ID 183**		*The effects of air exposure and water treatment on the minority carrier diffusion lengths and sub-bandgap absorption in highly crystalline microcrystalline silicon thin films* **Günes, ID 147**
17:10 – 17:30		*Integration of large area Graphene in Semitransparent Perovskite Solar Cells* **Felix Lang, ID 56**		*Thin-film silicon MEMS and NEMS* **Joao Conde, ID 275**		*Comparative Study of the Stability of Amorphous Zinc Tin Oxide Thin Film Transistors with Different Tin Compositions under Positive Bias Stress* **Kham Niang, ID 251**
17:30 – 17:50		*Real-time characterization of the phase change in CH3NH3PbI3 perovskite materials upon exposure to humid air* **Hiroyuki Fujiwara, ID 49**				

		Berlin 3
18:15 – 20:00		Postersession I

Name	Title	ID
Leonid Skatkov	Influence of surface properties on electrochromic properties of Nb2O5 amorphous films	3
Hajime Shirai	Chemical Mist Deposition of PEDOT:PSS on Textured c-Si for Efficient c-Si/PEDOT:PSS Heterojunction Solar Cells	5
Kenta Masumori	Characterization of a-Si:H/PEDOT:PSS Interface for Efficient Si Thin-Film Solar Cells	6
Amir Fath Allah	Some transport properties of P3HT:PCBM thin films	10
Mark Khenkin	Structural and photoelectric properties of femtosecond laser-modified a-Si:H films	12
Bozena Jarzabek	Heat treatment effect on the optical properties of iodine-doped polyazomethine thin films	23
Andrey Kazanskii	Electrical Bandgap of Low-Bandgap Polymer and Polymer:Fullerene Bulk Heterojunction	27
Anatoly Popov	Structural and chemical modification of diamond like silicon-carbon films	29
Jun Xu	Microstructures and carrier transport properties of nanocrystalline silicon thin films	32
Vachagan Avanesyan	Optical spectroscopy of a new polymer structure of the azomethine base with an inclusion of a metal center	36
Junkang Wang	Microcrystalline silicon thin films with SiF4/H2 chemistry by MDECR-PECVD	42
Alfonso Torres Jacome	25x25 µm microbolometer fabrication process using polymorphous silicon-germanium films (pm-SixGey:H) as thermo-sensing material	43
Ling Xu	Plasmon resonance-induced photoluminescence enhancement of CdTe/CdS quantum dots thin films	47
Yoon Jong-Hwan	Growth of poly-Si film from amorphous silicon-rich oxide using Al film as a catalyst	55
Samir Meziani	Compositional study by SIMS and RBS of oxidized silicon nitride thin films prepared by PECVD	60
Theophillus Muller	Effect of additional electron acceptor in hybrid ZnO:P3HT:PCBM spin-coated films for photovoltaic application	63
Veljko Jankovic	Nonequilibrium Electrical Transport in Materials with Localized Electronic States	66
Vera Kudouarova	EPR and Raman Studies of a-Si1-xCx :H<Er> Films Doped with Erbium from Er(pd)3 Polymer	67
Tamihiro Gotoh	Effects of annealing on the carrier concentration of SnS films	82
Martin Kostejn	Preparation of thin silicon layers highly doped with manganese by reactive pulsed laser deposition	84
Tomas Syrovy	Optical, electrical and morphological study of PEDOT:PSS single layers spin coated with various secondary doping solvents optimized for printed electronics	89
Clive Oliphant	Accurate characterisation of the thickness and structural properties of nanocrystalline silicon synthesised by hot-wire chemical vapour deposition	90
Sergey Khmel	Synthesis of hydrogenated amorphous silicon suboxide films by the gas-jet electron beam plasma CVD method	91
Marushka Sendova-Vassileva	Transition metal oxides as hole transport layers in organic solar cells	92
Dulce Murias	Effect of the substrate temperature on the plasma texturing process of c-Si wafers for black silicon SC	101

Name	Title	ID
Giovanni Landi	Comparison of the charge carrier mobility of the Zn(OC)2 organic compound as a function of the electric field orientation	119
Gabrielle Jost	Stability aspects of hydrogen-doped indium oxide	121
Andrew Paolo Cadiz Bedini	Trisilane-Based Liquid Precursor for the Preparation of a-Si:H Thin Films	132
Asha Yadav	Persistent photoconductivity studies in a-Si:H/nc-Si:H thin film super lattice	134
Alika Khare	Effect of O2 content on third order Nonlinear Optical properties of PLD deposited SiOx thin films	136
Mukesh Singh	Variable range hopping conduction in thermally reduced graphene oxide thin films	137
Himanshu Jha	X-ray Photoelectron Spectroscopy Studies on Cubic Silicon Carbide Thin Films Prepared by HWCVD	146
Yurong Zhou und Fengzhen Liu	Energy Band Structure of Co Heavily Doped Silicon	148
Mehmet Günes	Evidence for four different midgap defect distributions in hydrogenated amorphous silicon thin films obtained from the dual beam photoconductivity method	150
Elizaveta Konstantinova	Paramagnetic States in Amorphous, Polymorphous and Nanocrystalline Silicon	153
Thomas Dittrich	Dependence of modulated surface photovoltage of CH3NH3PbI3 prepared from CH3NH3I:PbCl2 solution on toluene dripping and annealing temperature	158
Zhongyuan Ma	The investigation of atomic migration during the segregation of nc-Si in annealed Si-rich SixN/SiyN multilayers	162
Ekaterina Terukova	Research and development center enabling HJT in Russia	167
Rubens Martins Cunha Junior	Sputtered high c-axis oriented aluminum nitride obtained at room temperature	171
Maria Elisia Armas Alvarado	Influence of AlN crystallinity on SAP waveguides	179
Ulrich Wilhelm Paetzold	Nanoscale Analysis of Resonant Coupling to Waveguide Modes in Periodically Nanopatterned Thin-Film Solar Cells	189
Taylor Grueser und Martin Kordesch	Aluminum and Beryllium induced crystallization of free standing amorphous Silicon thin films	197
Peter Pikna	Passivation Effect of Water Vapour on Thin Film Polycrystalline Silicon Solar Cells	211
Lamia Laidoudi	Optical, structural and electrical properties of a-Si:H thin films elaborated by DC magnetron sputtering at different polarizations of the substrate holder	212
Rachid Ayouchi	Raman Spectroscopy and XRD of Ferroelectric Domains in Ceramisc and in PLD-Deposited Na0.5K0.5NbO3 Films	216
Roberto Ambrosio	Study of the effects of annealing and deposition time on the Chemical Bath-deposited CuS Thin Films at room temperature	222

Name	Title	ID
Zhaoyun Ge	High external quantum efficiency n-SiNW/PEDOT:PSS solar cell	223
Kluska Stanislawa	"The grain boundary passivation of microcrystalline mc-Si by SiNx:H deposited by PECVD technique"	224
Manuel Pomaska	Unintentional doping in n-type microcrystalline silicon carbide thin-films	226
Jürgen Hüpkes	Influence of Atmosphere on Damp Heat Degradation of ZnO:Al	227
Ronghua Lu	Improved Efficiency of Silicon Nanoholes/Gold Nanoparticles /Organic Hybrid Solar Cells Due to Localized Surface Plasmon Resonance	231
Katerina Govatsi	Influence of the ZnO nanowire dimensions on the photoelectrocatalytic properties for water splitting	238
Aspasia Antonelou und Spyros N. Yannopoulos	Laser processing of SiC: From graphene-coated SiC particles to 3D graphene froths	239
Daniel Dorow-Gerspach	Transport in thin transparent oxides: Nb-doped TiO2 compared to conventional TCOs	245
Wolfhard Beyer	Laser annealing of hydrogenated amorphous silicon	252
Fabio Ferri	Metal-induced crystallization by homogeneous insertion of metallic species in amorphous silicon and germanium	253
Stefan Muthmann	Substrate Independent Control of the Thin Film Silicon Crystallinity	255
Christopher Arendse	Nano-structural features of a-Si:H grown by reverse-hydrogen profiling during hot-wire CVD	256
Florian Köhler	Charge carrier mobility in Aluminium doped microcrystalline silicon carbide films	260
Rachid Amrani	Properties of hydrogenated silicon thin films deposited near the nanocrystalline amorphous transition region from argon diluted silane plasma.	261
Philippe Czaja	Assessment of computational methods for the optical characterization of aSi:H	264
Pascal Kaienburg	Understanding the relation between fill factor and thickness in organic solar cells	267
Xiangbo Zeng	Enhanced quantum efficiency of NIP microcrystalline silicon solar cells by hydrogen plasma treatment on the initial intrinsic active layer	268

PROGRAM ICANS26 - TUESDAY, 15TH SEPTEMBER 2015

		Brüssel		Berlin 1		Berlin 2
9:00 – 9:20	**Chair: Uwe Rau**	**Keynote Lecture:** *Gas phase synthesis of semiconductor nanoparticles and their electronic and plasmonic properties* **Uwe Kortshagen**				
9:20 – 9:40						
9:40 – 10:00		**Coffee break**				
10:00 – 10:20	**Session: Si particles, chair: Martin Stutzmann**	*Silicon nanocrystal thin films for solution-cast electronics* **Willi Aigner, ID 18**	**Session: Organic homo/hetero junction, chair: Jenny Nelson**	*Singlet Fission – Using Organic Semiconductors and Nanocrystals to Break Efficiency Limits in Photovoltaics* **Neil Greenham, ID 286** (invited talk)	**Session: Alloys, chair: Wolfhard Beyer**	*Disordered Materials by Design* **David Drabold, ID 14** (invited talk)
10:20 – 10:40		*Fabrication and photovoltaic properties of Si quantum dots/SiC multilayers* **Yunqing Cao, ID 50**				
10:40 – 11:00		*Understanding the formation of crystalline-core and amorphous-shell Si Nanowires and their length limiting factor* **Rajiv Dusane, ID 157**		*Charge Carrier Separation in (Organic) Solar Cells and the Selectivity of Electrodes* **Uli Würfel, ID 169**		*Doped microcrystalline silicon oxides for silicon-based solar cells: Optoelectronic properties, chemical- and structural composition* **Andreas Lambertz, ID 70**
11:00 – 11:20		*Inverse quantum confinement in luminescent Silicon quantum dots* **Thomas Niehaus, ID 277** (invited talk)		*Extremely thin and robust interconnecting layer providing 76% Fill Factor in tandem polymer solar cell* **Alberto Martinez Otero, ID 250**		*Electrical and optical properties of long-throw magnetron sputtered Zinc oxynitride thin films* **Anna Reinhardt, ID 155**
11:20 – 11:40				*Enhanced stability of P3HT/polycrystalline silicon hybrid solar cells* **Matthias Zellmeier, ID 58**		*Universal Medium-Range Order of Amorphous Metal Oxides* **Kengo Nishio, ID 114**
11:40 – 12:00		*Silicon nanocrystals for future electronics and photonics* **Shunri Oda, ID 282** (invited talk)		*Stability of Crystalline Si/3,4-polyethylenedioxythiophene (PEDOT) Heterojunction Solar Cells* **Hajime Shirai, ID 4**		*Light emission efficiency and dynamics in a-SiNx:O films study by time resolved and temperature dependent photoluminescence spectroscopy* **Zhang Pengzhan, ID 22**
12:00 – 12:20				*Hybrid photovoltaic structures based on organic semiconductors and inorganic plasma deposited layers* **Svetlana Mansurova, ID 33**		*Optical conductivity tuning and dielectric response in amorphous BexZnyO thin films* **Jebreel Khoshman, ID 20**

		Brüssel		Berlin 1		Berlin 2
12:20 – 14:00		Lunch break & IAC meeting				
14:00 – 14:20	Session: SHJ I, chair: Masaki Shima	*Hydrogenated amorphous silicon doping by plasma immersion ion implantation for a-Si:H/c-Si heterojunction solar cells* **Tristan Carrere, ID 135**	Session: TFS solar cells I, chair: Virginia Chu	*High efficiency single-, double- and triple- junction silicon based thin film solar cells* **Xiaodan Zhang, ID 280** (invited talk)	Session: Transport, chair: Jan Kočka	*New insights into the modulated photocurrent technique using 2D full numerical simulations* **Raphaël Lachaume, ID 152**
14:20 – 14:40		*Characterization of a-Si:H/c-Si heterojunction by temperature dependent modulated photoluminescence* **Ming Xu, ID 204**				*Response Time Measurements and Photocarrier Life Time Distributions in Zno-Based Thin Films and Nanowires* **Reinhard Schwarz, ID 215**
14:40 – 15:00		*Valence band offset and hole transport at the crystalline silicon/amorphous silicon suboxide heterojunctionSolar Cells for self-sustainable intelligent packaging* **Martin Liebhaber, ID 73**		*Light Management in Flexible Thin-Film Solar Cells on Transparent Plastic Substrates* **Karen Wilken, ID 194**		*Opto-electronic properties measured by transient microwave conductivity in PLD-deposited ZnO-based thin films and nanowires* **Marinus Kunst, ID 217**
15:00 – 15:20		*The amorphous / crystalline interface: a computational point of view* **Robert de Groot, ID 247** (invited talk)		*Thin film silicon photovoltaic cells on paper for flexible indoor applications* **Hugo Aguas, ID 200**		*Amorphous semiconductor mobility limits* **Kevin Stewart, ID 184**
15:20 – 15:40				*Fast deposition of triple junction solar cells with intrinsic amorphous silicon-germanium layers deposited by hot wire chemical vapor deposition* **Leon Willem Veldhuizen, ID 102**		*Correlating the density of states with charge transport in conjugated polymers – A study of poly(9,9-dioctylfluorene) using transient photocurrent measurements and drift-diffusion modeling* **Xingyuan Shi, ID 271**
15:40 – 16:00		Coffee break				

PROGRAM ICANS26 - TUESDAY, 15TH SEPTEMBER 2015

		Brüssel		Berlin 1		Berlin 2
16:00 – 16:20	**Session: SHJ II, chair: Stefaan de Wolf**	*Atomic Scale Study on Interface of Amorphous-Silicon/Crystalline-Silicon* **Hideki Matsumura, ID 126**	**Session: Organics I, chair: Nenad Vukmirovic**	*Novel Approaches to Improve Optical Absorption and Carrier Extraction of Organic Photovoltaic Cells* **Wallace Choy, ID 284** (invited talk)	**Session: Electrochemistry, chair: Jan-Willem Schüttauf**	*Modeling thin film silicon based integrated water-splitting devices* **Jan-Philipp Becker, ID 74**
16:20 – 16:40		*Charge carrier separation at photoactive interfaces: the role of (de)localized defects* **Martin Rohrmüller, ID 240**				*Hybrid photoelectrochemical-photovoltaic devices for water splitting based on silicon wafer hetero-junctions and thin-film silicon multi-junctions* **Arno Smets, ID 266**
16:40 – 17:00		*Interfaces in (p) a-Si:H/(n) c-Si heterojunctions: influence of (i) a-Si:H buffer layer and front electrode on capacitance-temperature dependencies and strong inversion layer* **Olga Maslova, ID 201**		*Hot charges speed up non geminate recombination in polymer-based solar cells* **Jona Kurpiers, ID 235**		*Spectral matching in high-voltage multi-junction thin-film silicon solar cells* **Steve Reynolds, ID 191**
17:00 – 17:20		*Ion energy bombardment measurements and simulations from a low temperature VHF PECVD SiH4-H2 discharge in the a-Si:H to µ-c-Si transition regime* **Kees Landheer, ID 237**		*The Role of Polymer Purification in Optical and Electrical Properties in Indacenodithiophene-co-benzothiadiazole: Fullerene Solar Cells* **Derya Baran, ID 213**		*Light-Driven Vectorial Ion Transport: Using Interdigitated Back-Contact Semiconductors and Organic Photovoltaics for the Photoelectrochemical Generation of Drinking Water from Seawater* **Shane Ardo, ID 228** (invited talk)
17:20 – 17:40		*Ion bombardment on a-Si/c-Si interface : detrimental or affordable?* **Jérôme Meixenberger, ID 173**		*Molar Mass versus Polymer Solar Cell Performance: Highlighting the Role of Homocouplings* **Tim Vangerven, ID 199**		

		Berlin 3
18:15 – 20:00		Postersession II

Name	Title	ID
Kenta Masumori	Improved photovoltaic performance of Si/organic heterojunction solar cells using ferroelectric polymers	7
Naser Qamhieh	Optical and Electrical Characterization of Co Doped Ge-Sb-S Films	13
Celine Durniak	Structural and physical properties of GexAsySe1-x-y glasses	30
Keiji Itoh	Short and medium range order in Sb-Se glass	35
Vachagan Avanesyan	Photodielectric properties of polycrystalline naturally disordered layers of red lead	40
Ayodele Odo	Small angle X-ray scattering study of silicon nanoparticles embedded in different polymeric binders	41
Marina Sparvoli	Characterization of ITON thin film grown by Evaporation for sola cell application	45
Ling Xu	Pulse Voltage Induced Phase Change Characteristic of the ZnxSbyTez Phase-change Prototype Memory Device	51
Peng Lu	Photoluminescence behaviors of undoped and Phosphorous doped nanocrystalline Si/SiO2 multilayers	52
Linwei Yu	Radial tandem junction Si thin film Solar Cells with advanced junction materials and design	53
Franscious Cummings	Post-synthesis HF treatment of chemically etched Si nanowires for effective removal of surface oxides: investigation by means of electron energy loss near edge fine structure	57
Sergey Kozyukhin	Isothermal crystallization of GST225 amorphous thin films and estimation of information reliability of PCM cells.	64
Fan Zhao	0.25 THz MOSFET Direct Detectors in 0.18 µm CMOS Technology with On-Chip Antennas	72
Rongping Wang	Effect of the elemental substitution on threshold behaviours in Ge-As(Sb)-Se glasses	77
Félix Urbain	High performance photoelectrochemical devices based on multijunction thin film silicon solar cells	79
Nikola Prodanovic	Nature of Charge Transport in Nanocrystal Solids	83
Vladislav Dřínek	Catalyst-free growth of silicon nanowires using Low Temperature Chemical Vapor Deposition	85
Yu Linwei	Radial hetero-junction silicon thin film solar cells built over copper oxide nanowires with a high open-circuit voltage	88
Andreas Paulke	Recombination Dynamics in Perovskite Solar Cells probed by Time-Delayed-Collection-Field (TDCF) Experiments	94
Oleg Prikhodko	Electronic properties of amorphous DLC films embedded with platinum nanoparticles	95
Henriette Gatz	Silicon heterojunction solar cell passivation with nanocrystalline silicon oxide emitters	96
Willem Veldhuizen	Advanced light trapping in hydrogenated amorphous silicon-germanium/silicon tandem solar cells	100
Ana-Maria Teodoreanu	Extraction of minority charge carrier diffusion length by the grain-boundary light-beam-induced current method – a simulation based analysis of the measurements	103
Rituraj Sharma	Photo-induced non-linearity in binary pnictogen chalcogenide Sb2Se3 nanowires	104
Peter Schlupp	Room temperature fabricated amorphous oxide heterodiodes on glass and flexible substrates	106
Francisco Bomfim	Optical amplifier based on Yb 3+/Er3+ codoped GeO 2-PbO pedestal type waveguide	110

Name	Title	ID
Miguel Dominguez	Physically-based simulation of ZnO TFTs: Separating the source/drain contact resistance contribution from the DOS	116
Junyi Yang	X-ray irradiation induced hole lifetime change in stabilized a-Se photo-conductive films	117
Andrej Čampa	Optical design aspects for 15% micromorph solar cell	118
Rasha Khoury	Innovative point-contacting technique for thin-film silicon solar cells	123
Miguel Dominguez	Spin-on Glass as gate dielectric for solution-processed Thin-film Transistors	125
Zhongyuan Ma	The evolution of deep depletion behavior for nc-Si floating gate memory during the thermal post-treatment based on 0.13 um technology	127
Pamella Marques de Arruda	Methods to remove “nano-remnants” on top of the TiO2 nanotubes	128
Jan Mock	Electrical Conductivity Studies of Hematite (α-Fe2O3) indicate Phase Transition to Magnetite (Fe3O4) already at 400 K.	131
Pavel Calta	Silicon quantum dots formation in annealed a-SiOxNy:H single layers and a-Si/SiO2 multilayers grown by PECVD: Structural and photoluminiscence properties	138
Janis Teteris	Optical field induced mass transport in amorphous chalcogenide and azobenzene containing polymers	141
Chao Zhang	Impact of TCO front Side Texture on the Voc of a-Si:H Solar Cells	143
Federico Ventosinos	Adapting Characterization Techniques for High Voc Thin-Film Tandem Solar Cells	151
Solomon Nwabueze Agbo	Development of thin-film silicon-based triple-junction solar cell and its photoelectrochemical application	156
Petr Lazarenko	Electrophysical properties of Ge2Sb2Te5 thin films for memory devices	160
Takashi Itoh	Built-in potential in Amorphous Silicon Solar Cells by Kelvin Force Microscope	163
Kousaku Shimizu	Evaluation of Absorption-edge Properties of a- $InGaZnO_4$ by Oxygenation or Hydrogenation using PYS/IPES	165
Luis Guillermo Gerling	Silicon heterojunction solar cells with Hole-Selective-Layers based on Transition-Metal-Oxides	166
Rene A. Castro	Dielectric relaxation in (Ge28.5Pb15.0S56.5)100-xFex glassy systems	168
Sergey Kozlov	Rare-earth and Nb Doping of TiO2 Nanocrystalline Mesoscopic Layers for High-efficiency Dye-sensitized Solar Cells	172
Elizaveta Konstantinova	Phototransfer of Electrons between Bacterial Reactionary Centers and Mesoporous Titania	174
Lalhriat Zuala	Thermal and structural studies of CdSe nanorods synthesized by solvothermal process	175
Joel Molina	Electronic Conduction and Resistive Switching of Metal-Insulator-Metal Devices based on Ultra-Thin HfO2 after Thermal Annealing	187
Fadila Serdouk	Determination of gap-states distribution in Cl doped a-Se from transient photocurrents using Laplace transform technique	188

Name	Title	ID
Ulrich Wilhelm Paetzold	Development of perovskite solar cells with nanophotonic front electrodes for improved light incoupling	190
Rana Biswas	Nano-photonic Organic Solar Cell Architecture for Advanced Light Trapping with Dual Photonic Crystals	192
Akshatha Mohan	Effect of inter-electrode distance and power on the size and crystallinity of gas phase nanoparticles in Plasma Enhanced Chemical Vapor Deposition	195
Ruifeng Yang	Large area superstrate amorphous solar modules on lightweight flexible plastic	196
Vladimir Smirnov	High stabilized efficiency single and multi-junction thin film silicon solar cells	198
Jiri Stuchlik	"Vacuum combined technological methods for deposition of hydrogenated silicon thin films with embedded nanoparticles"	203
Aliaksei Vetushka	Design of electrical junctions by self-assembled monolayer of carborane-thiols dipoles	206
Manuela Vieira	VIS/NIR wavelength selector based on a multilayer pi'n/pin a-SiC:H optical filter	209
Paula Louro	Transmission of signals using white and visible LEDs for VLC applications	210
Ju-Young Cho	Thin-film mechanics for understanding the phase-change kinetics of amorphous Ge2Sb2Te5 doped with Al, C, N and Bi	230
Jona Kurpiers	Charge carrier dynamics in PbS quantum dot solar cells	236
Pedro Alpuim	Graphene field-effect transistors for biosensing applications	244
Michael Smeets	Enhancing short‐circuit current densities by nanophotonic grating structures at the rear contact of electrically flat silicon heterojunction solar cells	263
Akira Nakanishi	Device simulations of CH3NH3PbI3 perovskite / heterojunction crystalline silicon monolithic tandem solar cells using an n-type a-Si:H/p-type µc-Si1-xOx:H tunnel junction.	269
Evgeniy Baranov	Influence of synthesis temperature on the morphology of the silicon oxide nanowires synthesized with tin catalyst	270
Florian Maier	Impact on the electro-optical properties of very rapid, highly selective laser heating of a solar cell front contact composed of textured ZnO:Al and p-SiO_x:H	272
Takehiko Nagai	The nanostructure and light-induced degradation of a-Si:H solar cells produced by expanding thermal plasmas	273

PROGRAM ICANS26 - WEDNESDAY, 16TH SEPTEMBER 2015

		Brüssel				
9:00 – 9:20	Chair: Bob Street	**Keynote Lecture:** *Charge Transport and Recombination in Colloidal Nanocrystal Solids* **Vanessa Wood**				
9:20 – 9:40						
9:40 – 10:00	Coffee break					
		Brüssel		**Berlin 1**		**Berlin 2**
10:00 – 10:20	Session: Polysilicon/ growth, chair: Klaus Lips	*Material properties of buried dielectric layers for solar cells using liquid phase crystallised silicon on glass* **Sonya Calnan, ID 93**	Session: Modelling & simulation, chair: Urs Aeberhard	*Simulation Insights into Electronic Properties of Disordered Organic Semiconductors* **Nenad Vukmirovic, ID 65** (invited talk)	Session: Chalcogenides, chair: Jean-Yves Raty	*Formation and Study of Nanotube Structure in Chalc. Glasses to Improve Speed, Reliability and Lifespan of Non-Volatile Memristive Memory* **Maria Mitkova, ID 9**
10:20 – 10:40		*Influence of inhomogeneities on the low-temperature photoluminescence spectra of microcrystalline silicon* **Sven Burdorf, ID 182**				*Heat sink optimization for GST memory cells* **Anatoly Popov, ID 28**
10:40 – 11:00		*Five-fold symmetries in the multiple twinning found in p-type microcrystalline silicon alloys grown from hexamethyldisiloxane* **Farah Haddad, ID 115**		*Hopping charge transport in a spatially correlated exponential density of states* **Sergei Novikov, ID 75**		*Non-equilibrium doping of amorphous chalcogenide materials and devices* **Richard Curry** (invited talk)
11:00 – 11:20		*Laser patterning of amorphous silicon thin films deposited on flexible and rigid substrates* **Pedro Alpuim, ID 243**		*Density of Localized State Distribution Near the Valence Band in Stabilized a-Se Using Interrupted Field Time of Flight Measurements with Long Interruption Times* **Cyril Koughia, ID 113**		
11:20 – 11:40		*Advances in liquid phase crystallized silicon on glass: growth, electronic properties and solar cell concepts* **Daniel Amkreutz, ID 276** (invited talk)		*Glass polymorphism in amorphous germanium probed by first-principle computer simulations* **Massimo Celino, ID 257**		*Plasmon assisted changes in chalcogenide glass – gold nanostructures* **Istvan Csarnovics, ID 98**
11:40 – 12:00				*Multi-phonon processes in nanocrystal-solids* **Deniz Bozyigit, ID 265**		*Processes of silver photodiffusion into Ge-chalcogenides probed by neutron reflectivity technique* **Yoshifumi Sakaguchi, ID 124**

13:00 – 22:00	**ICANS 26 Conference Excursion to Monschau** Departure: 13:00 pm Return to Aachen: 21:00 pm Arrival in Aachen: 22:00 pm

PROGRAM ICANS26 - THURSDAY, 17TH SEPTEMBER 2015

		Brüssel				
9:00 – 9:20	Chair: Dieter Neher	**Keynote Lecture:** *Molecular factors influencing charge carrier recombination at donor-acceptor interfaces for organic photovoltaics* **Koen Vandewal, ID 281**				
9:20 – 9:40						
9:40 – 10:00	**Coffee break**					
		Brüssel		**Berlin 1**		**Berlin 2**
10:00 – 10:20	Session: SHJ III, chair: Koen Vandewal	*Technological Progress in HIT(R) - on the long way towards the limit* **Masaki Shima, ID 285** (invited talk)	Session: Organics II, chair: Neil Greenham	*Exciton Diffusion Length in Small Molecules* **Bernard Siegmund, ID 161**	Session: Phase change materials, chair: Martin Salinga	*Designing new Phase Change Materials via Disorder and Stoichiometry* **Matthias Wuttig, ID 2**
10:20 – 10:40				*Charge Separation in Hydrogenated Amorphous Silicon and Conjugated Polymers probed by Transient EPR* **Klaus Lips, ID 39**		*Non-isothermal analysis of crystallization kinetics in Ge2Sb2Te5 thin films for PCM application* **Sergey Kozyukhin, ID 145**
10:40 – 11:00		*Hydrogen-doped In2O3 with high mobility and high transparency prepared by atomic layer deposition for silicon heterojunction solar cells* **Yinghuan Kuang, ID 241**		*Understanding enhanced light harvesting of a conjugated polymer* **Michelle Vezie, ID 225**		*Crystallization in the canonical phase-change material Ge2Sb2Te5 : a memory effect in GST-225* **Robert Jones, ID 59**
11:00 – 11:20		*Light Management in Silicon Heterojunction Solar Cells via Implementation of Nanocrystalline Silicon Oxide Films and Nano-Imprint Textures* **Alexei Richter, ID 130**		*Analytical model for voltage-dependent photo and dark currents in bulk heterojunction organic solar cells* **M. Zahangir Saleheen, ID 262**		*Stability and Aging of Phase Change Materials: An Ab Initio* **Jean-Yves Raty, ID 279** (invited talk)
11:20 – 11:40		*Formation of void-rich network structures in a-SiO:H layers prepared by PECVD* **Sato Masanori, ID 48**		*Identifying the correct recombination models in Organic Solar Cells through the use of 'Semiconductor'-simulations* **Ilaria Cardinaletti, ID 139**		

11:40 – 12:00	**Session: SHJ III**	*Thermally evaporated MoO3 thin films: Structural and optical properties and application in solar cells* **Pavel Calta, ID 62**	**Session: Organics II**	*Relating material properties to charge recombination in organic heterojunction solar cells* **Jenny Nelson, ID 288** (invited talk)	**Session: Phase change materials**	*Crystallization of Phase-Change Materials from First-Principles Simulations* **Ronneberger, ID 259**
12:00 – 12:20		*Optimization of nanocrystalline silicon oxide emitters as window layer for HIT solar cells* **Luana Mazzarella, ID 87**				*Ab initio simulation of the atomistic mechanism of the effect of nitrogen doping on the crystallization behaviour of the phase-change memory material, Ge2Sb2Te5* **Elliott, ID 81**
12:20 – 14:00	**Lunch break**					
		Brüssel		**Berlin 1**		**Berlin 2**
14:00 – 14:20	**Session: Perovskite, chair: Thomas Kirchartz**	*Device Physics and Stability of Perovskite Solar Cells* **Vikram Dalal, ID 19**	**Session: Solar materials & cells, chair: Rudi Brüggemann**	*Radial heterojunction Si hierarchical nanowires solar cells with 16.3% conversion efficiency* **Fengyou Wang, ID 37**	**Session: Growth & properties of nanostructures, chair: Shunri Oda**	*Quantum confinement and light trapping effects in nanoporous Ge* **Daniela Cavalcoli, ID 24**
14:20 – 14:40		*Organo-lead Halide Perovskite based Direct X-ray Detectors* **Shreetu Shrestha, ID 144**		*First experimental demonstration of tandem radial junction solar cells* **Soumyadeep Misra, ID 105**		*Correlative microscopy of nanostructures for solar cells* **Antonin Fejfar, ID 44**
14:40 – 15:00		*The dynamic solid-state physics of hybrid halide perovskites* **Jarvist Frost** (invited talk)		*Interface tuning in heterojunction solar cells with ion irradiation* **Olivier Plantevin, ID 16**		*Nanoparticles embedded in hydrogenated amorphous silicon thin layers* **Zdenek Remes, ID 177**
15:00 – 15:20				*Low temperature formation of epitaxial emitter by RF-PECVD using SiF4/H2/Ar gas mixtures* **Ronan Léal, ID 180**		*Effect of diluent gas on silicon oxide nanowires synthesis from a free jet of monosilane–diluent gas mixture activated by electron-beam plasma* **Sergey Khmel, ID 80**

PROGRAM ICANS26 - THURSDAY, 17TH SEPTEMBER 2015

15:20 – 15:40			Session: Solar materials & cells	*Defect-Sensitive Electrical Properties of Hydrogenated Microcrystalline Silicon-Carbon Alloys* **Sofia Gaiaschi, ID 54**	Session: growth & properties of nanostructures	*Annealing and oxygen role in the structural, optical and electrical properties of nc-SiOxNy* **Martina Perani, ID 120**
15:40 – 16:00				*On Defects and Interface Passivation of Thin Crystallized Silicon Absorbers for Next Generation Solar Cells on Glass* **Natalie Preissler, ID 71**		*Low temperature plasma epitaxy. How does it work?* **Pere Roca Cabarrocas, ID 254**
16:00 – 16:20	**Coffee break**					
		Brüssel		**Berlin 1**		**Berlin 2**
16:20 – 16:40	Session: Voids & Hydrogen, chair: David Drabold	*Hydrogen Incorporation, stability and release effects in thin film silicon* **Wolfhard Beyer, ID 283** (invited talk)	Session: Devices II, chair: João Conde	*Integration of hydrogenated amorphous silicon thin-film photodetectors in microfluidic biosensors* **Denis Santos, ID 109**	Session: Methods & Materials, chair: Ruud Schropp	*Modulation of Si Nanocrystals Photoluminescence by Local Field Management Using Gold Grating* **Denis Zhigunov, ID 232**
16:40 – 17:00				*Optical switching device using organic heptazole photovoltaic cell and its application of operating organic field effect transistork* **Junyeong Lee, ID 133**		*Electron spin resonance and photoluminescence from silicon nanostructures in SiOx thin films* **Zaki Saleh, ID 129**
17:00 – 17:20		*Voids in hydrogenated amorphous silicon: A first-principles approach* **Partha Biswas, ID 38**		*Optical signal processing and diversity techniques for data error detection and correction using a-SiCH technology* **Manuela Vieira, ID 208**		*BornAgain software - Simulating and fitting X-ray and neutron small-angle scattering at grazing incidence* **Celine Durniak, ID 31**
17:20 – 17:40		*p-type silicon oxide as doping source for bifacial silicon solar cells* **Prabal Goyal, ID 76**				*Thin film of semiconducting clathrate with group IV elements* **Fumitaka Ohashi, ID 207**
17:40 – 19:00	**Break**					
19:00 – 23:00	**ICANS26 Conference Banquet Location: Krönungssaal im Aachener Rathaus (Coronation Hall in the town hall)**					

		Brüssel		Berlin 1		Berlin 2
9:00 – 9:20	Chair: Friedhelm Finger	**Keynote Lecture:** *Progress and challenges in a-Si:H based solar cells* **Takuya Matsui, ID 274**				
9:20 – 9:40						
9:40 – 10:00	Coffee break					
10:00 – 10:20	Session: TFS solar cells II, chair: Xiaodan Zhang	*Triple- and quadruple-junction thin-film silicon solar cells* **Jan Willem Schüttauf, ID 176** (invited talk)	Session: Oxides & chalcogenides, chair: Matthias Wuttig	*Excitation fluence dependent nanosecond transient absorption in a-Ge25As10Se65 thin film* **Aarsh Kumaran, ID 97**	Session: Devices III, chair: Pedro Alpuim	*FDTD simulation of a-Si:H ring resonator* **Alessandro Fantoni, ID 154**
10:20 – 10:40				*Structure of Ge15Sb20S65-XSeX glasses characterized by Raman and high-resolution x-ray photoelectron spectra* **Siwei Xu, ID 108**		*Deposition and characterization of BST thin films for RF MEMS applications* **Marcus Vinicius Pelegrini, ID 185**
10:40 – 11:00		*Consideration of defective regions in optical modelling of thin-film silicon solar cells* **Martin Sever, ID 78**		*Preparation, structure and switching properties in GaTe and Ga2Te3 amorphous thin films* **Mihai Popescu, ID 112**		*Suitability of oxide based (ZnO, CoGaO, and ZnGaO) semiconductor materials for low temperature solid oxide fuel cells as a potential electrolyte* **Musa M. Can, ID 258**
11:00 – 11:20		*Modify the Schottky Contact between SnO2:F and P-a-SiC:H by Carbon Dioxide Plasma Treatment* **Tiantian Li, ID 34**		*Metal oxide substrate dependent HOMO-LUMO transitions in layers of conjugated molecules* **Thomas Dittrich, ID 170**		
11:20 – 11:40		*Effective Current Matching Modulation for High-Performing Micromorph Tandem Solar Cells* **Lisha Bai, ID 86**		*Evaluations of Stress Induced Instabilities of Amorphous Oxide Semiconductors using reflection CPM and their relations with TFT instabilities* **Kousaku Shimizu, ID 159**		
12:00	Closing announcement (room Brüssel)					

ABSTRACTS

ID 2 - Oral

Designing new Phase Change Materials via Disorder and Stoichiometry

**M. Wuttig*[1]
[1]*RWTH Aachen, Aachen, Germany*

Phase change media utilize a remarkable property portfolio including the ability to rapidly switch between the amorphous and crystalline state, which differ significantly in their properties. This material combination makes them very attractive for data storage application in rewriteable optical data storage, where the pronounced difference of optical properties between the amorphous and crystalline state is used. This unconventional class of materials is also the basis of a storage concept to replace flash memory. This talk will discuss the unique material properties, which characterize phase change materials. In particular, that only a rather small group of materials utilizes resonant bonding, a particular flavour of covalent bonding, which can explain many of the characteristic features of phase change materials. This insight is employed to predict systematic property trends and to explore the limits in stoichiometry for such memory applications. Subsequently, it will be shown that disorder in certain phase change materials is a second turning knob for the properties of crystalline phase change materials. It will be demonstrated how this concept can be used to tailor the electrical and thermal conductivity of phase change materials.

ID 3 - Poster

Iunfluence of Surface Properties on the Electrochromic Properties of Nb2O5 Amorphous Films

**L. Skatkov[1], V. Gomozov[2], S. Deribo[2]*
[1]PCB "Argo", Beer Sheva, Israel
[2]NTU "Kharkov Polytechnical Institute", Electrochemistry, Kharkov, Ukraine

The question of the correlation between the oxide surface morphology and electrochromic process (ECP) efficiency can be resolved on the basis of the theory according to which dispersion of the system is considered as an active thermodynamic variable that can shift the direction of the process (including, in case of massive phase) ensuring its efficient progress. At the same time development of the surface, which increases the dispersion of the system, causes growth of concentration of point defects (vacancies), just as it takes place at temperature increase. In regards to ECP, this means that development of oxide surface, which leads to an increase in concentration of oxygen vacancies, being predominant type of defects in WO_3 and Nb_2O_5 , can not only intensify ECP flow but also activate it at conditions at which it hasn't previously been observed.In the present survey for the purpose of experimental verification of possibility of ECP activation in amorphous niobium pentoxide by changing of the morphology of oxide surface it has been developed a method of producing of amorphous Nb_2O_5 films possessing developed surface.It is known that the anodic oxide film (AOF) on aluminum can be produced with a porous surface in electrolytes which etch oxides. Thus, oxide layers produced in an electrolyte containing etching ingredient - hydrofluoric acid (HF) is considered as the key object of study in this work.The applied method of niobium oxidation allows obtaining of amorphous films of Nb_2O_5 with apparent ECP, as a result of oxide surface development. The resulting oxide layers can withstand not less than 10^6 cycles of staining - bleaching, as well as long-term storage without any signs of degradation.Given results support the decisive role in the ECP oxide surface. Detection of correlations between surface morphology and ECP efficiency contributes to optimization of Nb_2O_5 electrochromic amorphous films producing technique, by means of both anodic oxidation and vacuum condensation, which reveals prospects of niobium pentoxide application in electrochromic display devices.

.

ID 4 - Oral

Stability of Crystalline Si/3,4-polyethylenedioxythiophene (PEDOT) Heterojunction Solar Cells

*Q. Liu[1], R. Ishikawa[1], K. Ueno[1], *H. Shirai[1]*
[1]Saitama Univeristy, Graduate School of Science and Engineering, Saitama, Japan

Today, crystalline-silicon (c-Si) pn junction solar cells show a power conversion efficiency η of 23~24%. But it necessitates a high temperature process of ~1000˚C to make a good pn junction. Alternate approach is the hydrogenated amorphous silicon (a-Si:H)/c-Si heterojunction, used in the heterojunction with intrinsic thin layers (HIT) solar cells. A η of 25.7% has been established using back-contact and back-junction principle. However, the deposition of a-Si:H use a plasma-enhanced chemical vapor deposition (PE-CVD) process of a SiH_4 at a temperature of substrate of 200˚C. It is also difficult to tune the valence and conduction band offset at the a-Si:H/c-Si interface and to control the thickness of intrinsic and doped layers precisely.

Recently, there has been considerable interest in c-Si/organic heterojunction solar cell using the organic conductive polymer such as Poly(3,4-ethyenedioxythiphene)poly(styrenesulfonate) (PEDOT:PSS) that blocks electrons but passes holes. This is because the single junction of c-Si/PEDOT:PSS works as a photovoltaic device without using pn junction and transparent conductive oxide layer such as indium tin oxide (ITO) and ZnO:Al. η has reached at 12-13% with a short-circuit current density J_{sc} of 30 mA/cm^2 and an open-circuit voltage V_{oc} of 0.52 V, and a fill factor *FF* of 0.7 in the spin-coated PEDOT:PSS/c-Si heterojucntion solar cell. η further increased up to 15.4% using AR coating of TiO_2. Thus, we termed this type of solar cell as a c-Si heterojunction with organic thin-layer (HOT) solar cell. However, PEDOT:PSS is a strong acid with PH=2. Thus, long-term stability for air storage and light exposure is serious problem to overcome.

In the present paper, we demonstrate the potential of PEDOT:PSS/c-Si heterojunction solar cells. In addition, we present the effect of the p-toluenesulfonic acid (PTSA) and dimethyl sulfoxide (DMSO) treatment on spin-coated PEDOT:PSS to improve the stability for air storage. The conductivity increased up to 3000 S/cm by removal of PSS from PEDOT:PSS. A PEDOT/c-Si heterojunction solar cell exhibited a η of 13% with better stability even in a 30-nm-thick PEDOT.

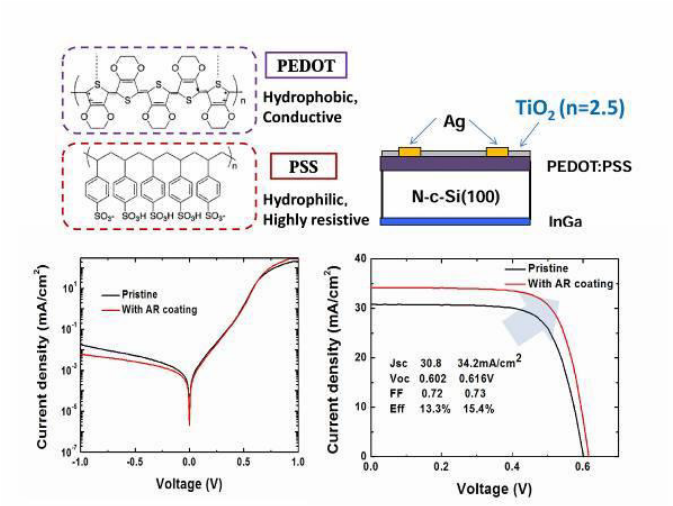

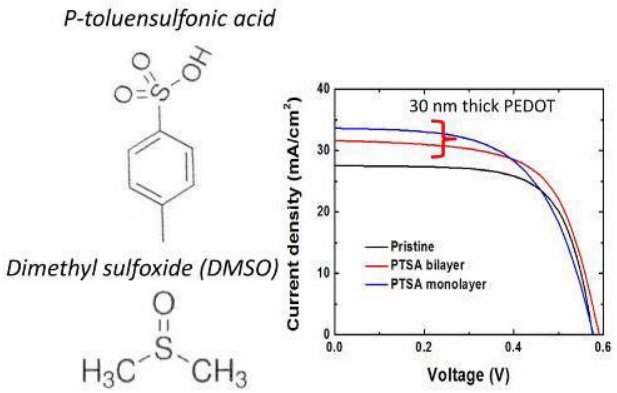

ID 5 - Poster

Chemical Mist Deposition of PEDOT:PSS on Textured c-Si for Efficient c-Si/PEDOT:PSS Heterojunction Solar Cells

*T. Ohki[1], K. Ichikawa[1], R. Ishikawa[1], K. Ishikawa[1], *H. Shirai[1]*
[1]Saitama Univeristy, Graduate School of Science and Engineering, Saitama, Japan

Chemical mist deposition (CMD) of negatively charged mist of poly(3,4-ethylenedioxythiophene):poly(stylenesulfonate) (PEDOT:PSS) was investigated with flow rate of nitrogen, substrate bias, and substrate temperature as variables for efficient crystalline Si (c-Si)/organic heterojunction solar cells. The high-speed camera and differential mobility analysis (DMA) characterizations revealed that average size and flux of PEDOT:PSS mist depend on the polar solvent, atomization ultrasonic vibration frequency and substrate bias. The film deposition rate increased with substrate bias V_s when V_s impressed on positive to a mesh pole at substrate temperature T_s of 30-50˚C, whereas film deposition hardly occurred on negatively bias supply, suggesting that the negatively charged mist mainly contribute to the film deposition. The uniform deposition of PEDOT:PSS films was realized on textured c-Si substrate by adjusting V_s and T_s up to a ~100 nm thickness. The adhesion to c-Si of PEDOT:PSS was improved conspicuously using the CMD with a negatively charged mist precursor more than a spin coat method. The CMD c-Si(1-3Ω·cm)/PEDOT:PSS heterojunction solar cell device on textured c-Si(100) showed a short-circuit current density of 37-40 mA/cm^2 with a relatively high open-circuit voltage of 0.5V more than that of spin-coated device. These findings originate from the improved adhesion and uniformity of PEDOT:PSS on textured c-Si substrate using the CMD with negatively charged mist. However, further increase of film thickness promoted preferentially the pillar growth of PEDOT:PSS.

In this paper, we demonstrate the effect of V_s on the transport and sticking process of PEDOT:PSS mist on flat and texture c-Si substrate using high-speed camera and difference mobility analyser, and Fourier-transform infrared total attenuation reflection spectroscopy (FTIR-ATR) for efficient PEDOT:PSS/c-Si solar cells.

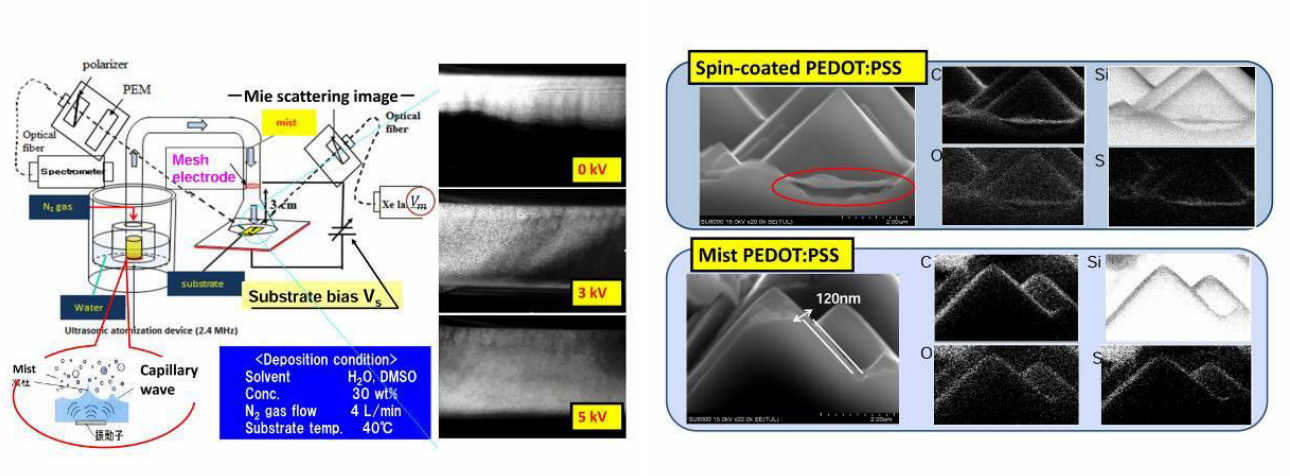

ID 6 - Poster

Characterization of a-Si:H/PEDOT:PSS Interface for Efficient Si Thin-Film Solar Cells

*K. Masumori[1], R. Ishikawa[1], K. Ueno[1], *H. Shirai[1]*
[1]Saitama university, Department of Engineering Functional Material Engineering Department, Saitama Prefecture Saitama City, Japan

Today, highly B-doped hydrogenated amorphous carbon and microcrystalline silicon carbon (a-SiC:H, µc-SiC:H) films by plasma-enhanced chemical vapor deposition (PE-CVD) of a SiH_4,CH_4 and B_2H_6 mixture have been used as a window layer in the a-Si and µc-Si:H thin-film solar cells. However, the doping efficiency of B atom in Si network is not sufficient and these films show optical absorption in the visible region with increasing defects.

To this aim, we attempted the use of spin-coated organic conductive polymer Poly(3,4-ethyenedioxythiphene)poly(styrenesulfonate) (PEDOT:PSS) as a p-layer for super-straight and substrate structured a-Si:H and µc-Si:H thin-film solar cells consisting of ITO/PEDOT:PSS/i/n and AZO/n/i/PEDOT:PSS structures, respectively. The commercialized PEDOT:PSS(Clevios PH1000) was used as a starting material using MeOH, dimethyl sulfoxide (DMSO) as a solvent at 1000 rpm for 1 min. followed by thermal annealing at 140°C for 30 min to remove residual solvent. A 350-nm-thick Si:H films were fabricated by rf PE-CVD of a SiH_4 and H_2 mixture at a T_s of 200-250°C. The a-Si:H/PEDOT:PSS interface was studied using spectroscopic ellipsometry (SE) taking optical anisotropy into consideration. The spectra analysis was performed using a Tauc-Lorentz model and a Drude model. The optical transmittance of PEDOT:PSS was superior to that of B-doped a-Si:H and a-SiC:H. The higher short-circuit current density was obtained in the pin structure, whereas both V_{oc} and FF decreased markedly. On the other hand, the relatively high J_{sc} was obtained without decreasing V_{oc} and FF values for the nip structure device. These differences originate from the increased optical absorption of PEDOT in the visible region and decrease in refractive index *n* and thickness during the deposition of a-Si:H on PEDOT:PSS. The *n* and *k* spectra of PEDOT:PSS on a-Si:H were explained without any interface layer and void fraction. These results imply that spin-coated PEDOT:PSS is also a possible material for p-layer for Si thin-film solar cells. We will present the a-Si:H/PEDOT:PSS interface using SE and Fourier-transform infrared total attenuation spectroscopy (FTIR-ATR).

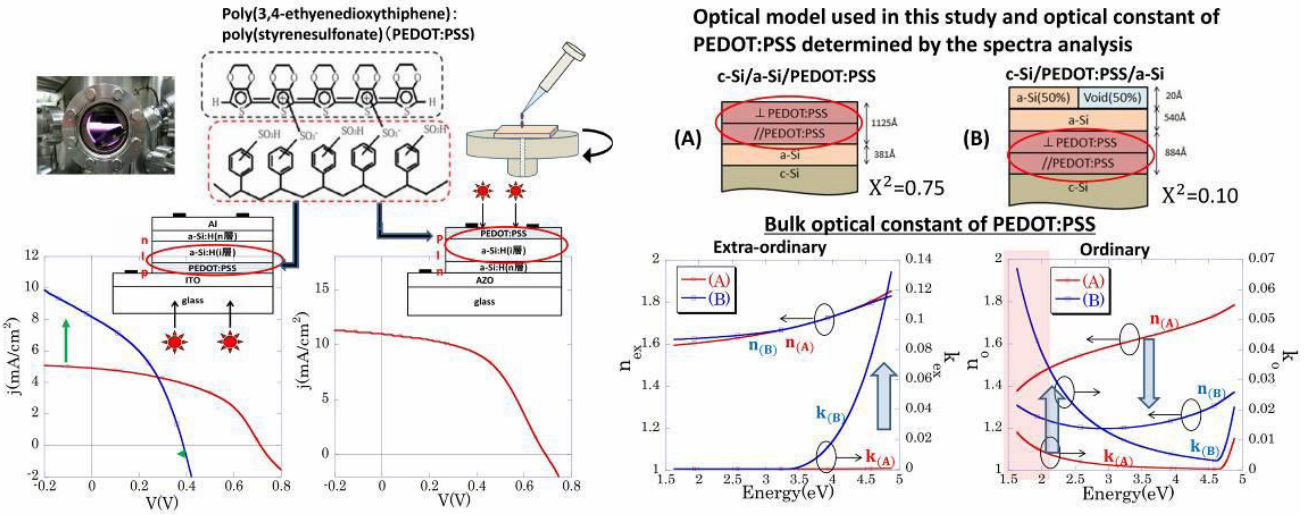

ID 7 - Poster

Improved photovoltaic performance of Si/organic heterojunction solar cells using ferroelectric polymers

**K. Masumori[1], Q. Liu[1], R. Ishikawa[1], K. Ueno[1], *H. Shirai[1]*
[1]Saitama university, Department of engineering functional material engineering department, Saitama prefecture Saitama city, Japan

Recently, efficient crystalline- (c-)Si/Poly(3,4-ethylenedioxythiophene):poly(styrenesulfonate)-(PEDOT:PSS) heterojunction solar cells with a power conversion efficiency η of 11-13% have been extensively studied by adding several polar solvents and nanometer-sized guest materials. The Schottky barrier, fabricated by depositing a metal with a high work function on n-type c-Si, may be an alternative to p-n junctions. As is the case for p-n junctions, the potential barrier has a built-in electric field that can separate electrons and holes, generating a high photocurrent. However, the barrier that impedes the recombination of electrons at the anode is relatively low, resulting in a saturation current density that is typically much higher than that of p-n junction diodes. This is due to an insufficient electric field at the c-Si/organic interface and poor charge extraction. As a result, the open-circuit voltage V_{oc} is limited to 520-550 mV, which corresponds to half the band gap energy of c-Si. To further increase V_{oc}, a higher built-in field at the interface is required. However, these effects have not yet surpassed the V_{oc} of 750 mV obtained by c-Si/hydrogenated amorphous silicon (a-Si:H) heterojunction (HIT) solar cells.

In this paper, we demonstrate the improved photovoltaic performance of c-Si/PEDOT:PSS and a-Si:H/PEDOT:PSS heterojunction solar cells with a vinylidene fluoride-tetrafluoroethylene copolymer P(VDF-TeFE) ferroelectric (FE) polymer layer using a large internal electric field provided by a permanent electrical polarization due to strong dipole moment of hydrogen and fluorine atoms within polymer chain. The effect of inserting an ultrathin layer of P(VDF-TeFE) at the c-Si and a-Si:H/PEDOT:PSS interface of Si/PEDOT:PSS heterojunction solar cells is demonstrated. P(VDF-TeFE) is a highly resistive material that exhibits a large, permanent, internal polarization electric field by poling of molecular dipole among the polymer chains. Because of these properties, performance can be enhanced in the c-Si/PEDOT:PSS heterojunction solar cells by adjusting the thickness of the FE layer and subsequent poling process. Inserting a 3-nm-thick FE layer increases the η from 10.2% to 11.4% with a short-circuit current density J_{sc} of 28.8 mA/cm^2, a V_{oc} of 0.54 V, and a fill factor FF of 0.69. Subsequent poling of the FE layer under a reverse DC bias stress increased η up to 12.3% with a J_{sc} of 29.7 mA/cm^2, a V_{oc} of 0.58 V, and an FF of 0.71. The obtained results confirm that the spontaneous polarization of the FE layers is responsible for the enhancement of η, and that the polarization-based enhancement works if the FE layer is highly crystalline. These findings originate from efficient charge extraction to the electrodes and a suppression of non-radiative recombination at the c-Si/PEDOT:PSS interface. The effect of the FE layer insertion on the front Si/PEDOT:PSS and rear Si/PEDOT:PSS/metal interfaces and dc bias poling is discussed in terms of orientation polarization of dipole moment of FE layer.

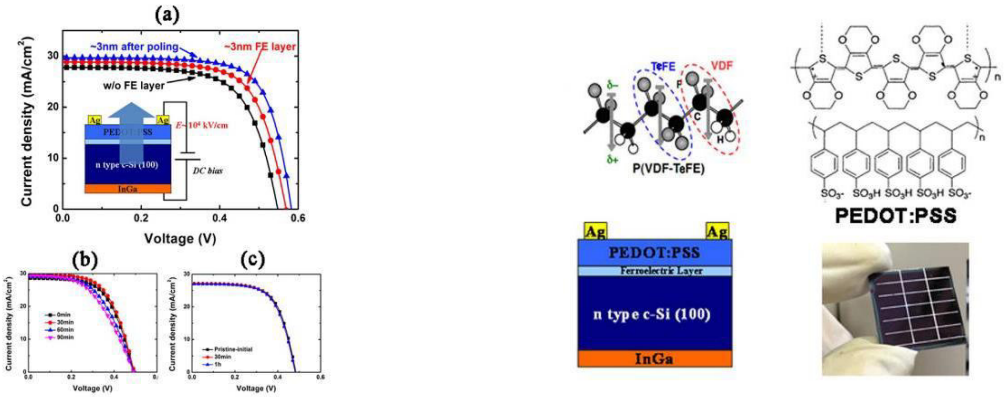

ID 8 - Oral

Reduction of Bubble Defects and Prevention of Wafer Edge Peelings in SADP Stack

*L. XIAO[1], Y. HUANG[1], J. XU[1], J. ZHOU[1], B. ZHANG[1]
[1]SMIC, Technology Research & Development, Shanghai, China

Before EUV becomes the mainstream technology to shrink feature sizes below 40 nm, Double Patterning Lithography (DPL) is considered to be the only feasible alternative for sub-40nm technology nodes. Among all the double patterning strategies, Self-Aligned Double Patterning (SADP) has attracted the highest interest due to its robustness against overlay errors, and currently it has been widely used in 3x nm NAND FLASH specific applications, such as AA (Active Area), CG (Control Gate) and Metal.1/ Metal.2 interconnects.

In this paper, a unique bubble defect caused by double-layer Advanced Patterning Films (APF®) and its suppression methods are presented. Bubble defects mostly located at wafer edge and they could easily kill the yield. The root cause analysis using wafer edge/ bevel inspection tool along with KLA Ellipsometry for stress measurements revealed that the bubble defect source was the stress incompatibility among layers especially at wafer edge, which further led to film peelings. For yield improvement, film stack was optimized to suppress defects and consequently prevent film peelings.

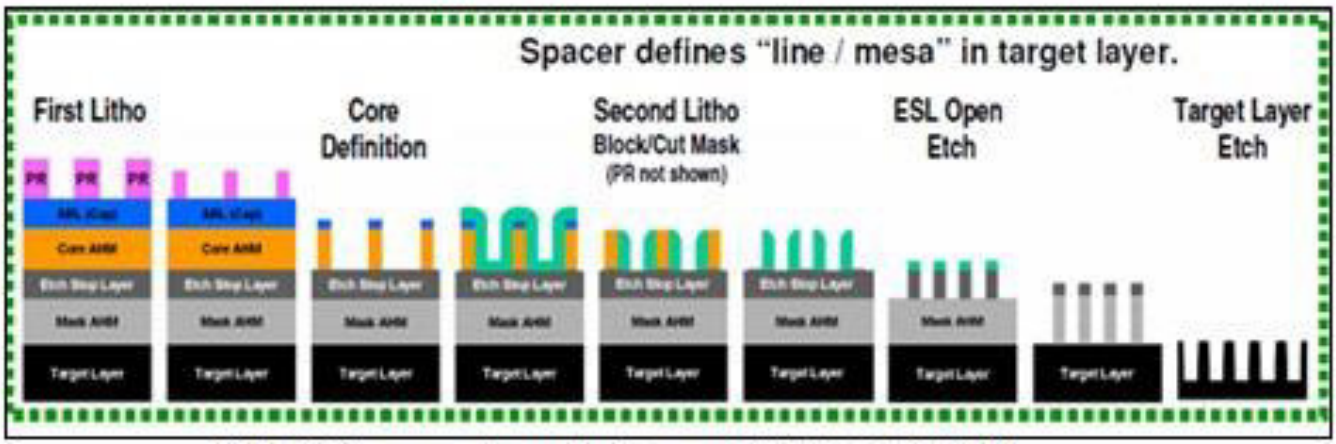

SADP flow cartoon in 3x nm NAND FLASH

ID 9 - Oral

Formation and Study of Nanotube Structure in Chalcogenide Glasses to Improve Speed, Reliability and Lifespan of Non-Volatile Memristive Memory

**M. Mitkova[1], M. R. Latif[1], D. Tenne[2], P. Davis[3], W. Knowlton[3]*
[1]Boise State University , Electrical and Computer Engineering, Boise, ID, United States
[2]Boise State University, Department of Physics, Boise, United States
[3]Bise State University, Materials Science and Engineerign, Boise, United States

Programmable metallization cell memristors are among the most promising emerging technology for nonvolatile memory.These devices consist of an oxidizable active (e.g. Ag or Cu, etc.) and an electrochemically inert (e.g. W, Pt, etc.) metal electrodes; sandwiched in-between is an amorphous oxide, chalcogenide, or halide film (active film), which serves to transport the metal cations. An application of positive voltage to the oxidizable electrode leads to the formation of a metallic filament at the opposite electrode. It ultimately bridges the two electrodes and thus defines the low (ON state) resistance of the memory cell. The filament is dissolved by applying a voltage of the opposite polarity which returns the cell to a high (OFF state) resistance. These devices are also known asConductive Bridge RAM (CBRAM) because of the nature on how they operate and their inclusion in integrated circuits. A core reason for performance failure of these devices is due to the silver ions distribution between the electrodes as they bridge from one side to another. The distribution of the bridge is usually completely random due to the nature of the active film in which it develops, and over time it loses continuity and the device fails.

Chalcogenide glasses are the best material for the CBRAM active film since they supply electrons for the fast growth of the conductive bridge. In this work we present our data related to formation of nanotube structures within the chalcogenide glass films, which confine the path of the conductive bridge resulting in reliable CBRAM cell performance while increasing the desired endurance period. What's more, this new design offers an increase in cell speed, while consuming less power. The reason being direct spanning of the bridge between the two electrodes and avoiding the unnecessary branches within the bridge, which aids in shorter and faster formation of the bridge.

The theory of the nanotubes growth is studied and the conditions of their formation are established, based on the flow of atoms or molecules (vapor flux) in a gas phase that impinge on a substrate under some angle, which results in a nanotube morphology of the deposited material due to shadowing. The angle of incidence controls the tilt of the nanotubes and hence affects the degree of shadowing and thus their size. An empirical equation is derived which describes the nanotube growth in Ge-chalcogenide glasses. The active films, investigated in this work are materials from the Ge_xSe_{100-x} (where x=20, 30, 40) and Ge_xe_{100-x} (where x = 20,50) systems. The composition of the films and its dependence upon the deposition conditions is studied with EDS. The structure is examined by Raman and XRD spectroscopies. These methods prove the presence of short range order and lack of long range order of the network which is important for the retention of the OFF state performance of the cell. This structure aids in nanotube organization of the active films' macrostructure, which confines the bridge growth. Its formation is studied with SEM and AFM.

A process flow for devices fabrication has been created, which proved through a Comsol Spectraphysics simulation that electric field distribution and the energy density are highly concentrated in the nanotube structure and the adjacent interfaces resulting in bridge formation through the nanotubes. Electrical testing of the memristive CBRAM cells yielded an endurance more than 10^6 cycles and retention more than 10^5 hours.

ID 10 - Poster

Some transport properties of P3HT:PCBM thin films

*A. Fath Allah[1], *C. Longeaud[1], J. Schmidt[2], M. El Yaakoubi[3], S. Berson[4], N. Lemaitre[4]*
[1]GEEPS, Gif sur yvette, France
[2]IFIS-Litoral, Santa Fe, Argentina
[3]TFSC Instrument, Palaiseau, France
[4]CEA LITEN, INES, Le bourget du lac, France

During the last decade organic polymers have received a considerable attention for their potential application in solar energy conversion. Conversion efficiencies are now of the order of 10% and researches are still going on to increase this figure. One of the important parameter controlling the thin active layer quality is the ambipolar diffusion length L_d that determines the ability of the carriers to be separated and eventually collected after their generation. Is it possible to apply the well known technique of Steady State Photocarrier Grating (SSPG) to organic blends? How is the L_d parameter reflected in the solar device behavior?

In this paper we present some transport measurements performed on different blends of P3HT:PCBM. In particular, we have focused on the estimate of L_d using the SSPG technique that proves to be very efficient for semi-insulating inorganic thin films as hydrogenated amorphous silicon. Different blends of P3HT:PCBM (weight ratio 1:2, 1:1, 1:0.6, 1:0.3) with a thickness of the order of 200 nm have been deposited on glass at INES, kept in nitrogen atmosphere during transportation, fitted with two parallel electrodes 1 mm apart and subsequently maintained under vacuum to avoid air contamination. Dark conductivity, photoconductivity and diffusion length were measured at room temperature.

The 1:2 sample presented a high resistivity and was not photoconductive. For the other films, we have observed an increase of the conductivity and photoconductivity accompanied by a decrease of L_d from 170 nm to 90 nm with the decrease of the proportion of PCBM in the film. Transport properties of the 1:1 blend were also studied as function of temperature. Besides, we have investigated on the influence of the contacts on the transport properties and found that the response time to a perturbation of the samples fitted with aluminum contacts could depend on the blend proportion. Finally, in this communication we compare the transport properties we have found with the electrical properties (J_{sc}, FF) of the devices achieved with the same active blends.

The two promising blends for device application are the 1:0.6 and 1:1. However, though the 1:0.6 presents a lower L_d than the 1:1 (140 nm instead of 170 nm) its higher photoconductivity results in better device performances.

ID 11 - Oral

Modeling of Nucleation and Growth in Crystallization of Phase Change Materials

**F. Tabatabaei[1], M. Apel[2], E. Brener[1]*
[1]Research center Jülich, Jülich, Germany
[2]ACCESS e.V, Aachen, Germany

Chalcogenide materials like GeSeTe and AgInSbTe showing phase change properties are suitable for the use in non-volatile rewritable memory devices. Their crystallization mechanism in the course of switching is known to be nucleation dominated or growth dominated, respectively. To obtain a quantitative understanding of the kinetics of writing and erasing data, it is essential to gain insights into the energy transport and phase boundary movement during the phase transformation. We applied phase field modeling as a continuum simulation technique in order to study rapid crystallization processes in AgInSbTe. The simulation model is adapted to the experimental conditions used for measurements of crystallization rates by a laser pulse technique. Simulations are performed for substrate temperatures close to the melting temperature of AgInSbTe down to low temperatures when an amorphous state is involved. Different growth regimes are identified by calculating crystallization velocity as a function of undercooling. We discussed the role of interface mobility on solidification kinetics by determining the mobility as a function of temperature. We extended our work by adding a nucleation model to the simulation of crystallization. The modeling was done according to the nucleation rate calculations based on classical nucleation theory for different viscosity models. The crystallization times in a simulation when a nucleation model is included with a growth-dominated crystallization were compared. Furthermore crystallization with a single grain or multiple grains were investigated at different substrate temperatures and subsequently different undercoolings for non-isothermal and transient conditions.

ID 12 - Poster

Structural and photoelectric properties of femtosecond laser-modified a-Si:H films

**M. Khenkin[1], R. Drevinskas[2], M. Beresna[2], O. Kon'kov[3], P. Forsh[1,4], P. Kazansky[2], A. Kazanskii[1]*
[1]Lomonosov Moscow State University, Moscow, Russian Federation
[2]University of Southampton, Southampton, United Kingdom
[3]Ioffe Physicotechnical Institute, St. Petersburg, Russian Federation
[4]National Research Centre "Kurchatov Institute", Moscow, Russian Federation

Femtosecond laser processing of hydrogenated amorphous silicon (a-Si:H) has been proposed as a promising technique for thin film solar cells fabrication. It have been demonstrated that laser treatment succeeds in both increasing the absorption and stability of solar cells parameters. That was achieved due to surface texturing and partial crystallization of a-Si:H films. However no significant improvement in operating solar cells efficiency has been demonstrated so far. To address this issue we studied structural transformations following the femtosecond laser treatment of a-Si:H films as well as photoelectric properties of the obtained material. The use of wide range of treatment parameters (such as laser fluence, wavelength, scanning geometry and post-processing of the films) allowed to reveal and explain specific properties of the laser-modified films.

One of the major advantages of laser micromachining is precise localization of produced modifications. Selection of laser wavelength and fluence allows to control the thickness of crystallized region as well. We obtained uniform crystallites distribution along the film's thickness in case of laser pulses with quanta energy below the mobility gap of a-Si:H. In the opposite case two-layer structures of nanocrystalline hydrogenated silicon (nc-Si:H) on top of a-Si:H were formed upon the laser processing. In both cases obtained films represents a mixed-phase material with crystalline volume fraction growing up to 80% with the increase of laser fluence used for the treatment.

Once crystalline volume fraction exceeds the percolation threshold (which is around 16% for randomly distributed nanocrystals) films dark conductivity increases in 3-5 orders of magnitude.Unexpectedly, spectral dependences of absorption coefficient measured by constant photocurrent method does not show any signs of crystallinity until the highest laser fluences reached.This implies that nc-Si:H part of the film does not contribute effectively to the total photoconductivity of the film. This is, in our point of view, one of the possible explanation for low performance of solar cells based on such material.Analyzing hydrogen bands in films' Raman spectra we concluded that hydrogen concentration in studied films dramatically decreases after their exposure to laser radiation. In turn, this leads to the increase of defects concentration, in particular at the nanocrystals grain boundaries, and consequently degrades photoconductivity of modified part of the samples. We have shown that post-hydrogenation (keeping in H plasma) of the films allows to restore partially their hydrogen content and increase the contribution of nc-Si:H into measured photoconductivity in case of uniform distribution of crystalline phase inside the film. Whereas for the two-layer films dark conductivity is governed by nc-Si:H part while photoconductivity is determined by a-Si:H even after the post-hydrogenation procedure.

ID 13 - Poster

Optical and Electrical Characterization of Co Doped Ge-Sb-S Films

*N. Qamhieh[1], *S. Mahmoud[1], I. Mousa[1], M. Al Shaer[1]*
[1]UAEU, Physics, Al ain, United Arab Emirates

Thin films of amorphous germanium antimony sulfide ($Ge_{30}Sb_{10}S_{60}$) doped with cobalt (Co) have been deposited on glass substrates by thermal evaporation technique. The composition and amorphous structure of as deposited films have been characterized by X-ray diffraction and energy dispersive X-ray analysis (EDX) techniques. Optical transmission spectra measured by UV-VIS spectrophotometer showed that Co-doped $Ge_{30}Sb_{10}S_{60}$ have 2.0 eV optical forbidden energy gap. Raman spectroscopy was used to characterize the composition and phase structure of the prepared film, and shows a wide band spectrum from 300 to 410 cm^{-1} centered at 355 cm^{-1}. The Raman shift peaks at 325 cm^{-1} and 350 cm^{-1} are assigned to the bond-stretching mode Sb-S and Ge-S, respectively. The capacitance and conductance versus voltage measurements were performed at different temperatures. The results show a slight increase in the capacitance with temperature and it reaches a maximum value around 150 °C, and eventually it becomes negative. This behavior is interpreted in terms of the nucleation-growth process and the thermally activated conduction process with measured activation energy of 0.79 eV. This value of activation energy together with the measured optical gap indicates that the Fermi level is unpinned in the middle of the gap that could be attributed to gap states induced by cobalt doping.

ID 14 - Oral

Disordered Materials by Design

**D. Drabold[1], P. Biswas[2], K. Prasai[1], A. Pandey[1]*
[1]Ohio University, Physics and Astronomy, Athens, United States
[2]University of Southern Mississippi, Physics and Astronomy, Hattiesburg, United States

An ideal approach to materials modeling would enable one to impose constraints into the modeling process yielding models with desired structural, optical, electronic or other features. In this talk, we begin with a new method for predicting structures with a prescribed optical gap. Here, we utilize Hellmann-Feynman forces associated with eigenvalues and deliberately modify the structure to push these eigenvalues away from a desired optical gap. The method has been demonstrated for tight-binding models for silicon and carbon systems, and extensions to *ab initio* calculations are underway. In addition, we have further developed our "Experimentally Constrained Molecular Relaxation" (ECMR) method[1] to enforce structural constraints: namely that a computer model should satisfy experimental structural measurements in addition to being a suitable minimum of an accurate energy functional. We will discuss a new force-biased Monte Carlo method, and compare to ECMR. Examples will include amorphous silica and silicon.

[1] P. Biswas, D. Tafen and D. A. Drabold, *Experimentally Constrained Molecular Relaxation: The Case of $GeSe_2$* , Phys Rev B **71** 054204 (2005); *Topics in the theory of amorphous materials*, European Physical Journal B **68** 1 (2009).

ID 15 - Oral

Role of a-Si:H in Lateral Growth of Silicon Nanowires

*J. Kocka[1], M. Muller[1], J. Stuchlik[1], H. Stuchlikova[1], A. Fejfar[1]
[1]Institute of Physics, ASCR, Department of Thin Films and Nanostructures, Prague 6, Czech Republic

Electronic and optoelectronic industry urgently needs [1] the development of nanoscale devices that could enable new functions and/or greatly enhanced performance of the current technology. Self-positioned/aligned silicon nanowires (SiNWs) represent important building block for future three-dimensional (3D) integrated Si technology. There are two basic problems, related to top-down fabrication of Si nanostructures from starting bulk crystalline Si: high temperatures and complicated lithographic processing. Devices using large area or plastic substrate are automatically excluded.

The basic bottom-up technique for SiNWs growth is based on vapor-liquid-solid (VLS) process [2] and nanostructured catalytic metal [3], until recently mainly Au. It has been demonstrated that the use of plasma-enhanced chemical vapor deposition (PECVD) can lead to SiNWs formation [4] and substantial decrease of the processing temperature [5]. Although further research is needed to optimize nucleation and SiNWs orientation, the SiNWs grown with In as catalytic metal have been successfully applied to PV solar cells [6].

The discovery of formation of one-dimensional (1D) SiNWs by In-Plane Solid-Liquid-Solid (IPSLS) growth, based on amorphous silicon (a-Si:H) [7], is an important step for new nanoscale devices. For example FET structure, for which In mediated 1D SiNW has been prepared, is a real breakthrough [8].

In this paper we present our results, related to IPSLS formation of SiNWs. Catalytic metal partly remains in SiNWs and so it is important to test its influence on the function of devices and to test another metals. We have tested Pb as a new catalytic metal, but when the similar conditions to In case [7] (substrate temperature for a-Si:H layer about 100°C) have been used, there has been no 1D growth for Pb. However, when we changed plasma parameters and process temperature for a-Si:H layer to about 350°C, clear 1D SiNWs have been formed with Pb as catalyst, see Fig. 1. On the other hand at these conditions In mediated 1D SiNWs growth failed.

There is a large space of technological parameters for further optimization. Our recent results indicate that the key parameter is the quality of a-Si:H, used for IPSLS process. Comparison of a-Si:H, prepared at two different technological conditions mentioned above proved that for example hydrogen content (13 versus 7 %), conductivity and other properties are different, playing probably important role in IPSLS formation of 1D SiNWs for a given catalytic metal.

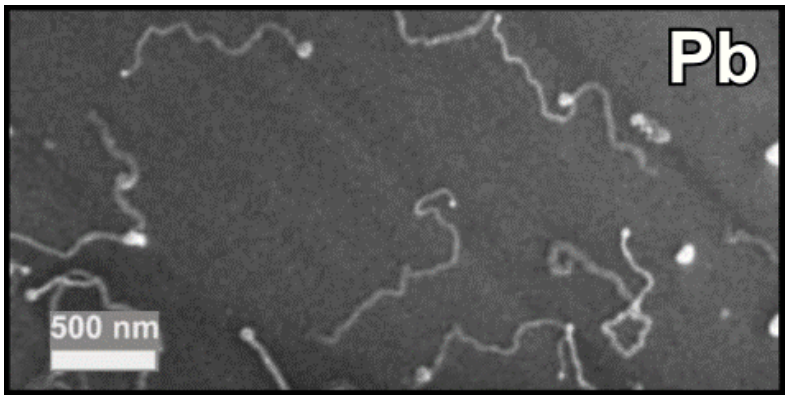

Illustration of one-dimensional SiNWs (Silicon Nanowires) prepared by Pb as a catalytic metal mediated IPSLS (In-Plane Solid-Liquid-Solid) growth, based on amorphous silicon (a-Si:H).

[1] ITRS, International Technology Roadmap for Semiconductors, 2013 edition: http://www.itrs.net
[2] R.S. Wagner and W.C. Ellis, *Appl. Phys. Lett.* 4, 89-90 (1964).
[3] V. Schmidt, J.V. Wittemann, S. Senz, U. Gosele, *Adv. Mat.* 21, 2681-2702 (2009).
[4] S. Hofmann, C. Ducati, R.J. Neill, S. Piscanec, A.C. Ferrari, J. Geng, R.E. Dunin-Borkowski, and J. Robertson, *J. Appl. Phys.* **94**, 6005 (2003). doi:10.1063/1.1614432.
[5] J. Cervenka, M. Ledinsky, J. Stuchlik, H. Stuchlikova, S. Bakardjieva, K. Hruška, A. Fejfar, and J. Kocka, *Nanotechnology,* **21**, 415604 (2010). doi:10.1088/0957-4484/21/41/415604.
[6] S. Misra, L. Yu, W. Chen, and P. Roca i Cabarrocas, *J. Phys.D: Appl. Phys.* 47,393001 (2014)
[7] L. Yu, P.-J. Alet, G. Picardi, and P. Roca i Cabarrocas, *Phys. Rev. Lett.* 102, 125501 (2009).
[8] L. Yu, W. Chen, B. O'Donnell, G. Patriarche, S. Bouchoule, P. Pareige, R. Rogel, A. C. Salaun, L. Pichon and P. Roca i Cabarrocas, *Appl. Phys. Lett.* 99, 203104 (2011)

ID 16 - Oral

Interface tuning in heterojunction solar cells with ion irradiation

**O. Plantevin[1], A. Defresne[1], P. Roca i Cabarrocas[2]*
[1]Université Paris-Sud, CSNSM CNRS, Orsay, France
[2]CNRS - Ecole Polytechnique, LPICM, Palaiseau, France

Silicon heterojunction technology holds great promise for high-efficiency solar cells production on an industrial scale. So-called HIT (Heterojunction with Intrinsic Thin layer) solar cells have reached record conversion efficiencies of 24.7%, and show above 20% energy conversion efficiency at the industrial production level. The appropriate combination of crystalline silicon with different intrinsic and doped hydrogenated amorphous silicon (a-Si:H) thin layers (~10 nm) leads to a photovoltaic device with a rich physical behaviour [1]. In particular, the record values for the open-circuit voltage (V_{oc} up to 750 mV) are related to the good crystalline silicon surface passivation by hydrogenation of the silicon dangling bonds, leading to a reduction of the interface defect density. Several groups have shown that interface passivation represents an actual challenge for HIT solar cell improvement and may be addressed using hydrogen plasma treatment [2]. We explore an alternative option by using the rich possibilities of ion irradiation to directly modify the amorphous/crystalline silicon interface[3]. Ion irradiation with Ar^+ ions at low energy (1-30 keV) allows a controlled modification of the a-Si:H thin layer and its interface with the crystalline silicon substrate. We monitor the changes in optical properties with spectroscopic ellipsometry. The effective lifetime of minority carriers, directly correlated with cell efficiency, is obtained via photoconductance, while the competition between radiative and non-radiative recombination centers is probed using photoluminescence spectroscopy. We show that a fine tuning of ion irradiation parameters at low energy and low fluences associated with proper annealing may lead to interface reordering and passivation improvement, as well as improved robustness of the final solar cell. A possible transfer of this ion irradiation based method on an industrial scale might have an impact on photovoltaic solar cell industry.

[1] *Physics and technology of amorphous-crystalline heterostructure silicon solar cells*, ed. W.G.J.H.M. van Sark, L. Korte and F. Roca, Springer (2012)
[2] A. Descoeudres *et al.*, Appl. Phys. Lett. **99** (2011) 123506 ; M. Mews *et al.*, Appl. Phys. Lett. **102** (2013) 122106
[3] A. Defresne, O. Plantevin, I.P. Sobkowicz, J. Bourçois, P. Roca i Cabarrocas, *Interface defects in a-Si:H/c-Si heterojunction solar cells,* submitted to Nucl. Instr. Meth. Phys. B (IBMM 2014 Conference)

ID 18 - Oral

Silicon nanocrystal thin films for solution-cast electronics

*W. Aigner[1], M. Wiesinger[1], H. Wiggers[2], R. N. Pereira[1,3], M. Stutzmann[1]
[1]Walter Schottky Institut, Technische Universität München, Garching, Germany
[2]Institute for Combustion and Gasdynamics – Reactive Fluids - and CENIDE, Center for Nanointegration Duisburg-Essen, Duisburg, Germany
[3]Institute for Nanostructures, Nanomodelling and Nanofabrication and Department of Physics, University of Aveiro, Averio, Germany

Solution-processed films of semiconductor nanocrystals (NCs) as active layers in thin-film field-effect transistors (FETs) and photovoltaics have been the subject of many studies [1,2]. High-performance devices have been demonstrated using primarily superlattices of II-VI or IV-VI material NCs. Despite their superior electronic properties, these NCs have certain drawbacks concerning environmental issues in large-scale production and control of electronic doping. Here, Si NCs offer a sustainable alternative enabling controlled *n*- and *p*-type doping with P and B, respectively [3]. Recently, a number of studies have demonstrated substantial progress in solution-processed FET technology using intrinsic Si NCs [4], doped Si NCs [5], and Si NC films doped with an electronic coupling agent [6].

In this work, we have carried out a comprehensive study on the morphological and electrical properties of Si NC FETs fabricated using spin-coating and spray-coating deposition methods. By optimizing the deposition method and corresponding parameters we achieved FETs with effective mobilities up to one order of magnitude higher than values reported in the literature [4-6]. The effect of film thickness was investigated studying the electrical characteristics of FETs fabricated in the bottom-gate configuration onto *p*-doped Si wafers with silicon nitride as a dielectric. We studied the current-voltage behavior of the FET structures including hysteresis effects and temperature dependence. The charge transport properties of the Si NC films were found to depend strongly on the morphology and layer thickness and are dominated by percolation effects. We observe a pronounced temperature dependence with space-charge limited current as a dominant transport process for operation close to room temperature. To further investigate the charge transport mechanism, photocurrent measurements were performed to probe conduction in well-defined layers of the Si NC film samples using different light wavelengths. Mixing intrinsic with doped Si NCs was used to tune the doping level in the Si NC films. In this way, we were able to study the contribution of different electronic states (free electron versus localized) to the charge transport.

[1] D. S. Chung, J.-S. Lee, J. Huang, A. Nag, S. Ithurria, D. V. Talapin, Nano Lett. **12**, 1813 (2012)
[2] E. H. Sargent, Nature Photon. **3**, 325 (2009)
[3] R. Lechner, A. R. Stegner, R. N. Pereira, R. Dietmueller, M. S. Brandt, A. Ebbers, M. Trocha, H. Wiggers, M. Stutzmann, J. Appl. Phys. **104**, 053701 (2008)
[4] Z. C. Holman, C.-Y. Liu, U. R. Kortshagen, Nano Lett. **10**, 2661 (2010)
[5] R. Gresback, N. J. Kramer, Nicolaas, Y. Ding, T. Chen, U. R. Kortshagen, T. Nozaki, ACS Nano **8**, 5650 (2014)
[6] R. N. Pereira, J. Coutinho, S. Niesar, T. A. Oliveira, W. Aigner, H. Wiggers, M. J. Rayson, P. R. Briddon, M. S. Brandt, M. Stutzmann, Nano Lett. **14**, 3817 (2014)

ID 19 - Oral

Device Physics and Stability of Perovskite Solar Cells

*V. Dalal[1], H. Abbas[1], R. Kottokkaran[1], B. Ganapathy[1], L. Zhang[1], P. Joshi[1], M. Samiee[1]
[1]Iowa State University, Electrical and Computer Engoineering, Ames, United States

Perovskite solar cells are an important new material system for photovoltaic and light emitting devices. Most devices are made in thin films (~300-400 nm thick films) of polycrystalline materials with grain sizes of 300-500nm. Various material systems are possible, such as methyl-amine (MA)lead iodide perovskites, formamidinium amine lead iodide perovskite, methyl amine lead bromide perovskites etc. In this paper, we discuss the fundamental electronic properties such as shallow and deep defect densities, mobilities, carrier diffusion lengths and device physics of all these materials. All measurements were made in devices, both p-i-n and n-i-p types, with both inorganic and organic heterojunction layers. For n-i-p cells, the n heterojunction was compact TiO2 and the p heterojunction was P3HT. For p-i-n devices, the p heterojunction layer was P3HT and the n heterojunction layer was PCBM. It will be shown that varying the organic material varies the bandgap. MA based Pb iodide materials have a bandgap of 1.57 eV and the FA-based Pb iodide materials have a bandgap of 1.47 eV. The defect densities were measured using capacitance-frequency-temperature techniques. It will be shown that lead-iodide based materials always have a shallow defect at ~0.24 eV and deeper defect at ~0.6 eV. The type of doping was determined using special structures such as pip and nin. It is shown that the perovskite materials are always n type, independently of whether the substrate is p or n type. Mobilities were measured using space charge limited techniques and were found to be in the range of 1 cm^2/V-s. Diffusion length of minority carriers was measured using quantum efficiency vs. voltage at various wavelengths for different thicknesses of the perovskite layer. It was found that the electric field extends throughout the thin (300 nm) perovskite cell, but does not extend throughout a 1000 nm cell. In 300 nm thick cells, the transport is almost entirely by field assisted diffusion. However, in thicker cells, the transport is controlled by field free diffusion, and diffusion length is ~300-500nm. Dark I-V analysis indicates that in p-i-n cells, the current follows a 2 diode model, whereas in n-i-p cells, it does not because of the high resistance of TiO2.

We measured the stability of devices and changes in fundamental properties under full spectrum solar simulation at various intensities. The devices were kept inside a glove box or in a vacuum system filled with pure nitrogen to exclude the influence of moisture and oxygen. It was found that the device performance degraded under light, and the degradation was directly traceable to reductions in minority carrier diffusion lengths.

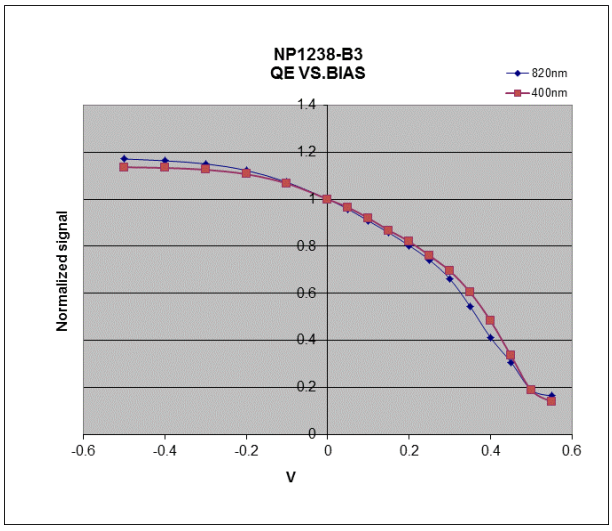

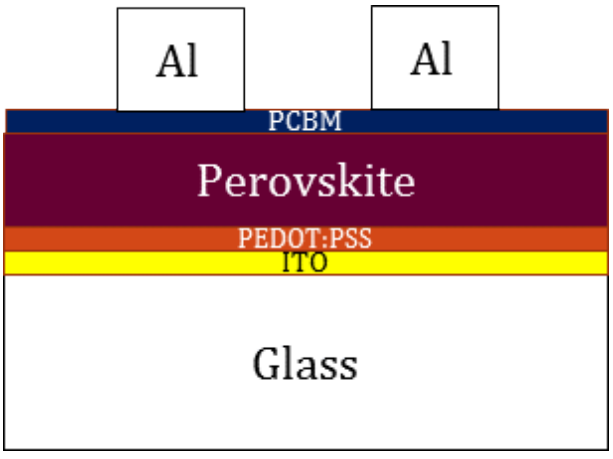

ID 20 - Oral

Optical conductivity tuning and dielectric response in amorphous Be_xZn_yO thin films

*J. Khoshman[1]
[1]Al-Hussein Bin Talal University, Physics, Maan, Jordan

Reactive RF magnetron sputtering was used to grow thin films of Be_xZn_yO on Si (100) substrates at temperature < 52 °C. X-ray diffraction patterns of the films revealed no structure, suggesting the films have an amorphous nature. By using X-ray photoelectron spectroscopy and Rutherford proton elastic backscattering spectroscopy the concentration of Be and Zn atoms were determined to be 4.0% ≤ x ≤ 45.05% and 2.43% ≤ y ≤ 45.0%, respectively. The optical conductivity and the dielectric functions (ε_1 and ε_2) of the amorphous Be_xZn_yO (a-Be_xZn_yO) films were determined in the wavelength range 138 - 1650 nm, using VUV-variable angle spectroscopic ellipsometer measurements, by the analysis of the real and imaginary part of the complex refractive index through the Cauchy-Urbach, Tauc-Lorentz, and Gaussian dispersion models. Changes in the measured of the optical conductivity and the dielectric functions values by changing the Be doping level are described for a-BeZnO alloys. Thus, the amorphous BeZnO films could be used for fabricating excellent amorphous ZnO based electronic and photonic devices.

ID 21 - Oral

Change of recombination rates of electrons at radiative defects in hydrogenated amorphous silicon with annealing of photo-created dangling bonds of silicon

**C. Ogihara[1], M. Ueda[1], K. Morigaki[2]*
[1]Yamaguchi University, Department of Applied Science, Ube, Japan
[2]Hiroshima Institute of Technology, Department of Electrical-System Engineering, Hiroshima, Japan

Light-induced phenomena in hydrogenated amorphous silicon (a-Si:H) have been received much attention for more than 30 years. In a-Si:H, some defects act as radiative recombination centres. The radiative defects are different from dangling bonds of silicon (Si DBs) which act as non-radiative recombination centres. In the study of the light-induced creation of defects in a-Si:H, the radiative defects are also interesting.

The Si DBs created by intense pulsed illumination in a-Si:H at low temperature are partially annealed at room temperature, as has been suggested by our previous results of EPR measurements. The EPR measurements show decrease of the density of photo-created Si DBs at room temperature with a decay time of approximately 48 days[1]. It is also possible to perform PL measurements to obtain the recombination rate at the radiative defects during the decay of the DB density. In this paper we present the lifetime of the defect PL measured at various time after illumination.

The a-Si:H films, prepared in a capacitively coupled glow discharge reactor from a mixture of SiH_4 and H_2, were illuminated by pulsed light of 2.48 eV at low temperature and kept at room temperature after the illumination. The PL of 0.83 eV was measured by means of frequency resolved spectroscopy under excitation by CW light of 1.95 eV at various temperatures in the range of 10 — 200 K. The PL measurements were performed at various time in the range of 24 h - 180 days from the illumination.

The lifetime of the defect PL at low temperature was about 20 μs at 13 days from the illumination and increased to 100 μs at 179 days from the illumination. This change of lifetime is understood as a result of decrease of non-radiative recombination centres with increasing time after the illumination. We have also found that the temperature dependence of the lifetime of the defect PL also changes with the time from the illumination. We will discuss the relation between the density of photo-created Si DBs and the recombination rate at the radiative defects.

[1] C. Ogihara, A. Nakayama, K. Yamaguchi and K. Morigaki, Proc. 6th Int. Conf. Optical, Optoelectronic and Photonic Materials and Applications, Leeds, 2014, in press.

ID 22 - Oral

Light emission efficiency and dynamics in a-SiN_x:O films study by time resolved and temperature dependent photoluminescence spectroscopy

*P. Zhang[1], *K. Chen[1], Z. Lin[1], H. Dong[1], D. Tan[1], W. Li[1], J. Xu[1], X. Huang[1]
[1]nanjing unversity, School of Electron Science and Engineering, nanjing, China

*Author to whom correspondence should be addressed; electronic mail:kjchen@nju.edu.cn

Recently, we have achieved the photoluminescence internal quantum efficiency (PL IQE) from the oxygenated amorphous silicon nitride (a-SiN_x:O) films as high as 60% at peak wavelength of about 470 nm at room temperature, which is much higher than that of Si nanocrystal embedded thin films.[1] The a-SiN_x:O samples were prepared on quartz and p-Si substrates by the PECVD, and then subsequently oxidized in situ by oxygen plasma treatment. The incorporation of oxygen atoms into silicon nitride networks and the related defect states N-Si-O (N_x) in the band gap were confirmed by the results of XPS and EPR measurements, respectively. [2] In the present work, we have performed the time resolved PL (TR-PL) and temperature dependent PL (TD-PL) measurements to investigate the radiative recombination dynamics process through the N-Si-O defect states, and how to enhance the PL efficiency.

The characteristic of TD-PL has been investigated in the equipment of computer-controlled Delta 9023 oven, using a 75w Xe lamp as excitation source. From the temperature dependence of the integrated PL intensities of the a-SiN_x:O samples for temperatures ranging from 8 to 300K, we found that the emission intensities keep stable when the temperature is below 100 K, while the intensities seem to be thermal quenching and decreasing in the temperature range of 100K-300K. Meanwhile, no appreciable PL line shape modifications have been observed under various measurement temperatures. The TD-PL results indicated that the radiative recombination dominates the recombination processes in the low temperature range (Tx:O system, the TR-PL has also been investigated by using a FLS980 (Edinburgh Analytical Instrument) equipped with an EPL375 ps pulse diode laser, and a TCSPC system at room temperature. In the PL time decay spectra, there are two distinct PL decay time, which are a “fast” PL lifetime in the nanosecond magnitude, and a “slow” PL lifetime in the microsecond magnitude. We will also investigate the temperature dependence of the PL lifetimes, to check which decay process is dependent on temperature, therefore we can determine which decay process primarily contributes to the light emission in our a-SiN_x:O films. Based on the luminescent N-Si-O states located in the band gap and the PL decay processes, we explain the PL mechanism and hig h QE in our a-SiN_x:O films.

[1] P. Z. Zhang, K. J. Chen, H. P. Dong, P. Zhang, Z. H. Fang, W. Li, J. Xu, and X. F. Huang, Appl. Phys. Lett. **105**, 011113 (2014).
[2] P. Z. Zhang, K. J. Chen, H. P. Dong, Z.W. Lin, W. Li, J. Xu, and X. F. Huang, to be published.

ID 23 - Poster

Heat treatment effect on the optical properties of iodine-doped polyazomethine thin films

**B. Jarzabek[1], J. Weszka[1,2], B. Hajduk[1], J. Jurusik[1], M. Domanski[1]*
[1]Center of Polymer and Carbon Materials Polish Academy of Sciences, Department of Polymer Materials for Photoelectronics and Non-linear Optics, Zabrze, Poland
[2]Silesian University of Technology, Faculty of Mechanical Engineering, Institute of Engineering and Biomaterials, Gliwice, Poland

Aromatic polyazomethines are conjugated polymers with extended π-system, with alternately imine group CH=N and benzene ring in the main chain. Similarly, as for other conjugated polymers, conductivity and other properties of polyazomethines can be improved by suitable doping or protonating. Our work reports poly(1,4-phenylene-methylenenitrilo-1,4-phenylene-nitrilomethylene) PPI amorphous thin films, obtained by chemical vapor deposition (CVD) method. Iodine (I_2) doping of PPI films have been observed *in situ,* on the base of changes of absorbance spectra during doping process. After doping, the absorption edge shifted to the smaller energy and simultaneously positions of absorption bands changed. Iodine interacting in polyazomethines is *p*-type doping, connected with extracting electron from π-system and a distinct reduction of energy gap, due to polaron states inside the gap. Thermal stability of polymer doped films is important feature in the case of optoelectronic and photovoltaic applications. In our study, thermo-stability of the (PPI+I) film have been investigated on the base of the UV-Vis-NIR transmission *in situ* measurements, during annealing the film, from 25 to 200 °C, with a step of 25 °C. Changes of absorption coefficient spectra and such absorption edge parameters, as the Urbach energy (E_U) and the Tauc energy gap (E_G), allowed us to obtain the border temperature 100 °C and to observe the thermal releasing process of admixture atoms. A distinct increase of the E_U value at 100 °C is connected with the localized states from the structural defects during the “escape” of iodine atoms. Above 150 °C this process seems to be finished and at 200 °C the absorption coefficient spectrum and the edge parameters are typical for PPI film and the same as after cooling to room temperature. In our work, the UV-Vis-NIR(*T*) spectroscopy is shown as a simple method to obtain the border temperature and to analyze electronic transitions and changes of polymer chain structure (conformation and conjugation) during the heat treatment of polymer doped films.

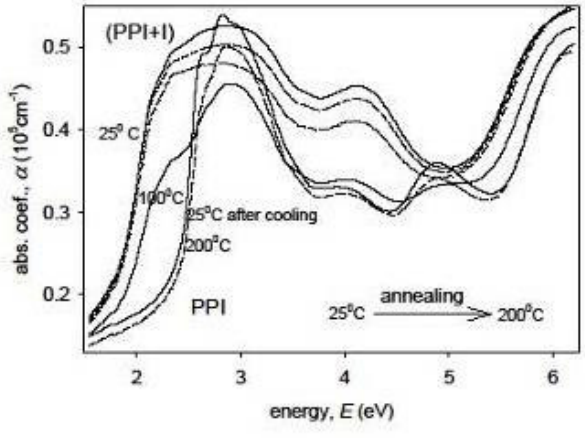

Attachment nr 2.

Absorption coefficient spectra, obtained on the base of *in situ* transmission measurements during annealing of the iodine-doped PPI film; (the special high temperature-controlled equipment of the JASCO V-570, UV-Vis-NIR spectrophotometer have been used).

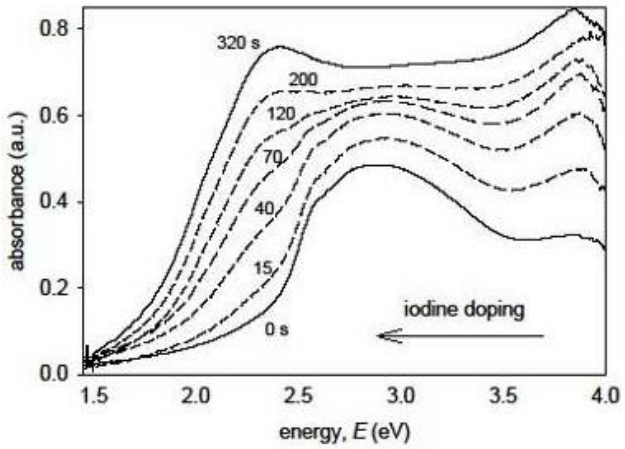

Attachment nr 1.
Absorbance spectra, recorded using OCEAN OPTICS HR400 module spectrometer, during iodine doping process.

ID 24 - Oral

Quantum confinement and light trapping effects in nanoporous Ge

*D. Cavalcoli[1], B. Fraboni[1], G. Impellizzeri[2], L. Romano[2], M. G. Grimaldi[2]
[1]University of Bologna, Physics and Astronomy, Bologna, Italy
[2]CNR-IMM MATIS and Univ of Catania, Physics and Astronomy, Catania, Italy, Italy

Semiconductors containing nanopores have gained a renewed interest as they are able to adsorb and interact with atoms and molecules and can thus be used in several interesting and emerging applications. Ge film and bulk samples, self-implanted with Ge+ ions, have shown to have a sponge-like nanoporous structure [1], as shown in fig.1. Possible applications of porous semiconductors include various novel sensors, solar cells, optoelectronic devices; they can be used for catalysis, biological molecular isolation and purification or electrodes for micro-fuel cells [2 and reference therein].

Optoelectronic characterization of the layers are carried out by Surface Photovoltage (SPV) Spectroscopy, a powerful technique which allows for obtaining detailed information on material optical properties, such as electronic transitions at gap states, and band to band transitions [2,3]. In addition, structural and microscopic analyses have been carried out in order to identify amorphous or crystalline phases and the average size of the nano- pores. Different nanoporous (np) structures have been investigated: crystalline and amorphous np-Ge obtained by implantation of bulk Ge, as well as crystalline and amorphous np-Ge obtained by ion implantation of Ge film grown on Si substrates by molecular beam epitaxy and sputtering. The effect of Au nanoparticles embedded within the nanoporous structure has been also investigated.

Changes in the SPV spectra as a function of ion implantation fluence and annealing treatments have been found and discussed on the basis of the structural properties of the samples [4]. A significant enhancement of the SPV signal in np-Ge samples decorated with Au nanoparticles has been shown, and related to enhanced light trapping effects. SPV spectra of np-Ge thin films show the main peak, which corresponds to band-to-band transitions, significantly blue shifted with respect to the same peak in bulk np-Ge (fig.2). This result has been assigned to a quantum confinement effect occurring at Ge nano-walls separating the nanopores. In addition, a strong enhancement of the SPV signal has been observed due to light confinement effects. Quantum confinement and light trapping effects demonstrated in nanoporous Ge film deposited on Si substrate can be of major interest for future photovoltaic applications of thin film solar cells.

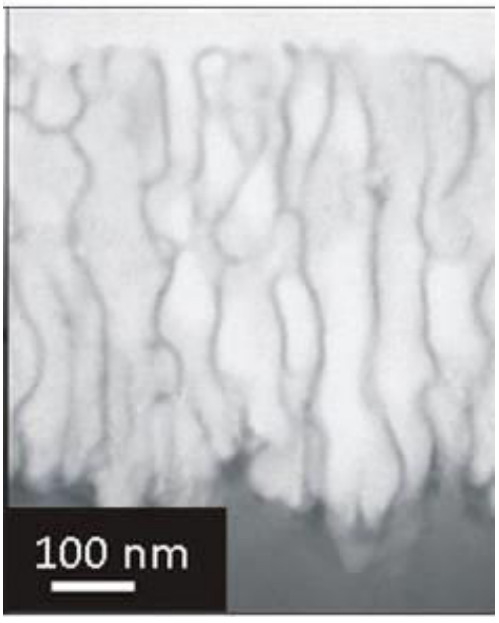

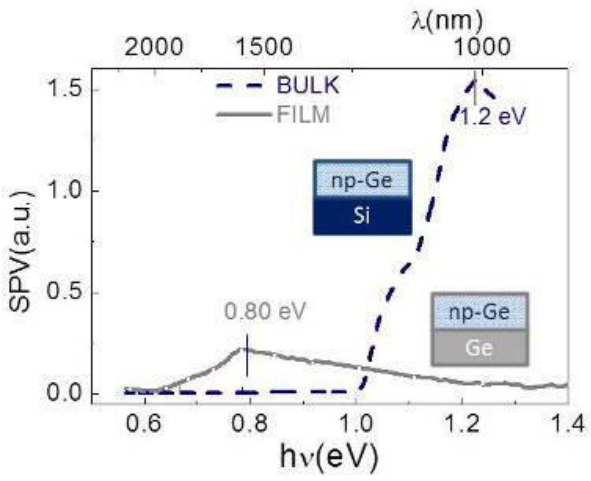

ID 25 - Oral

Transient Photoconductivity in Coplanar vs. Sandwich Device Structure: Bulk and Surface Time-of-Flight Experiments on a-Se Detectors

*D. Hunter[1], *S. Kasap[2], J. Rowlands[1]*
[1]Sunnybrook Research Institute, Toronto, Canada
[2]University of Saskatchewan, Electrical Engineering, Saskatoon, Canada

Stabilized amorphous selenium (a-Se) is currently used in a number of different types of detector structures. In this paper, we examine and contrast the nature of transient photoconductivity exhibited by both coplanar and sandwich structures by the use of so-called "bulk" and "surface" time-of-flight (BTOF and STOF) measurements on stabilized a-Se samples. The samples consisted of a glass substrate (1.1 mm thick) with closely spaced 10.2 to 254 μm gaps between the chromium electrode fingers, themselves 254 μm wide, 0.5 μm thick and 1 cm long, overcoated with a 300 μm layer of stabilised a-Se. STOF measurements were performed using a single pair of chromium electrodes, one at a HV bias, the other connected to a low noise current amplifier. Light from a blue (442 nm) HeCd CW laser was shaped into a narrow line (23 mm wide) and shone in the gap between the two electrodes. The position of the illumination line could be varied in the gap by means of a positioning stage and steering mirrors. The light was pulsed using an AO modulator and the current signal was recorded by a digital oscilloscope. The experiments show that the STOF transient hole photocurrent waveform for holes photoinjected near one electrode and drifting on the surface to the other coplanar electrode is totally different than that observed in sandwich structures, which exhibit the normal BTOF waveform with a clear transit time. Holes drifting in the gap region near the surface diffuse to the surface before transiting to the collecting electrode, and suffer surface trapping so that the resulting STOF photocurrent decays quickly without exhibiting a clear transit time. Experiments and semiquantitative modelling demonstrate that the transient photoconductivity on coplanar device structures are controlled primarily by the diffusion of carriers to the surface and the ensuing trapping, rather than freely drifting along the gap field.

ID 26 - Poster

Current-Voltage (I-V) and Optical Time of Flight (TOF) Measurements of Layered Selenium Structures Comprised of Crystalline Selenium (c-Se) and Amorphous Selenium (a-Se)

*D. Hunter[1], G. Belev[2], *S. Kasap[3], M. Yaffe[1]*
[1]Sunnybrook Research Institute, Toronto, Canada
[2]The Canadian Light Source, Saskatoon, Canada
[3]University of Saskatchewan, Electrical Engineering, Saskatoon, Canada

We report on the electrical and photoconductive properties of electroded selenium film structures comprised of a thick (110-270 μm) stabilised (0.5% As) a-Se layer formed on top of a thin (2-3 μm) trigonal c-Se layer. The c-Se layers were prepared on two different substrate types: HF (1-5%) etched p-type silicon wafer pieces and transparent ITO coated glass slides. The bottom signal contact was made by a connection to the ITO conductive layer, in the case of the glass substrate samples, or by a contact to the degenerate substrate of the silicon samples. The silicon wafer pieces were p-type <100>. The c-Se layers were formed from initially stabilised a-Se layers by photocrystallisation over a period of several weeks at ~ 40° C. The top (x-ray facing) metal electrodes were either sputtered Cr or Au. Measurements were also made using samples lacking the bottom c-Se layer and they serve to illustrate the unique effects caused by the presence of the thin c-Se layers. It is shown that the presence of the c-Se layer suppresses dark current when the samples are positively biased (top metal electrode positive). Conversely the c-Se layer increases the dark current when a negative bias is applied to the top metal electrode. TOF measurements (with optical excitation at 442 nm) show the expected charge carrier transit behaviour (magnitude, mobility, shape) when the c-Se/a-Se samples are pulsed with blue light from the top electrode, but weak or non-existent charge transit behaviour when pulsed from the bottom glass-ITO side. On the other hand, the a-Se samples without the c-Se layer showed the expected weakly dispersive carrier transit electron TOF behaviour when pulsed from either the top or bottom electrode. However hole TOF behaviour was qualitatively different for the glass substrate bottom electrode illumination. Our results from the samples with the c-Se layers indicate that the majority of the dark current resulting when the top metal electrode is positively biased appears to be due to electron injection from the bottom substrate, not hole injection from the top metal electrode.

ID 27 - Poster

Electrical Bandgap of Low-Bandgap Polymer and Polymer:Fullerene Bulk Heterojunction

*V. Malov[1], A. Tameev[1], S. Novikov[1,2], A. Vannikov[1], M. Khenkin[3], *A. Kazanskii[3]*
[1]A.N. Frumkin Institute of Physical Chemistry and Electrochemistry of the Russian Academy of Sciences, Moscow, Russian Federation
[2]National Research University Higher School of Economics, Moscow, Russian Federation
[3]Lomonosov Moscow State University, Moscow, Russian Federation

Many recent successes in organic solar cells have been achieved due to the use of bulk heterojunction (BHJ) which is formed in a polymer composite at the interface between the mutually penetrating phases of an electron-donating semiconducting polymer and an electron-accepting fullerene.

Up to date the physical processes governing the generation, transport and recombination of nonequilibrium charge carriers in the BHJ layer are not completely understood. In particular, there is lack of information on the photoconductivity and absorption on the absorption edge of low-bandgap polymer materials. However the BHJ formation should affect materials properties in the spectral region close to the absorption edge. Yet, accurate measurements in the low-energy spectral region close to the absorption edge are difficult to accomplish due to weak optical absorption of thin films. One of the techniques used to study the absorption edge region in photosensitive materials is constant photocurrent method (CPM). The method allows one to obtain the spectral dependence of the absorption coefficient, α_{CPM}, for optical transitions leading to the photoconductivity.

PCDTBT and PTB7 polymers were used as objects for the study as well as their blends with a fullerene derivative $PC_{71}BM$. The planar electrodes geometry with ohmic contacts allowed us to avoid the nonlinearity of the current-voltage characteristic of solar cell and, therefore, simplified the analysis of experimental data. The measurements of spectral dependences of the photoconductivity show that formation of bulk heterojunction in the blends increases photoconductivity and results in a redshift of the photocurrent edge in the blends compared with that in the neat polymers. Reason for such redshift of the photoconductivity edge is still discussed. In most studies, the reason is assumed to be caused by the generation of charge carriers in the BHJ region via the charge-transfer states, with the energy of formation of the charge-transfer states being lower than that of exciton formation in the individual materials constituting the blend. Obtained from CPM data spectral dependences of α_{CPM} were approximated using Gaussian distribution of density-of-states (DOS) within HOMO and LUMO bands. The approximation procedure allowed us to evaluate from the analysis of their spectra electric band gaps for the studied materials: 1.86 eV and 2.18 eV for PTB7 and PCDTBT, respectively. Moreover, spectra of polymer: $PC_{71}B$ M blends were fitted well by the sum of two Gaussian peaks which reveal both the transitions within the polymer and the transitions involving charge transfer states at the donor-acceptor interface in the BHJ.

ID 28 - Oral

Heat sink optimization for GST memory cells

**A. Popov[1], S. Salnikov[2]*
[1]National Research University , Semiconductor electronics, Moscow, Russian Federation
[2]Institute of Nanotecnology of Microelectronics, Russian Academy of Science, microelectronics, Moscow, Russian Federation

Information recording in the GST phase change memory cells (PCM) is performed by switching between low resistance (ON-state) and high resistance (OFF-state) states. It has been shown earlier [1] that the design of the cell has the most significant impact on the process of switching from ON-state to OFF-state.

This is due the thermodynamics of the processes occurring during the switching pulse. Switching to the ON-state requires the temperature in GST active region to rise up to the crystallization temperature of material (T_{cr}). Switching to the OFF-state requires the temperature to exceed the melting temperature of crystalline phase ($T_{melt} > T_{cr}$). The temperature in the active volume of GTS during the pulse depends on the dissipated power and the efficiency of the heat sink. It should be noted that it is desirable to reduce the dissipated power as the increase in power leads to a sharp decrease in the lifetime of the cells and to an increase in switching to the high-resistance state time. The intensity of the heat removal is determined by the structure of the cell, namely, the size and configuration of the heat sink and its thermal conductivity.

The paper presents the results of theoretical analysis of the dynamics of heat generation and dissipation in the active region during the switching to the OFF-state for the memory cells of various designs. As the equilibrium between the heat generation and dissipation defines the stability of the switching process we have determined the effective area of platinum electrodes that would meet this requirement.

For experimental verification of the results memory cells with platinum electrodes of different sizes for active area (from 10^{-3} μm^2 to $4 \cdot 10^{-2}$ μm^2) were prepared. Switching from OFF-state to ON-state was observed in all cells. However, the switching from ON-state to OFF-state was observed only in cells with minimum size of the platinum electrode which satisfy the condition of heat generation and dissipation equality. Thus, the criterion for sustainable switching of memory cells from ON-state to OFF-state is the relationship between the power dissipation in the active region and the efficiency of the heat sink to guarantee an effective temperature increase above the melting point of the crystalline phase.

The efficiency of the heat sink can be decreased not only by geometrical design choices for electrodes but also by reducing the thermal conductivity of the latter. For example, a 3.5-fold decrease in thermal conductivity of the electrode material (from 70 to 20 W / m • K) increases the minimum allowable contact area by 7.5 times.

[1] Popov A. I., Sal'nikov S. M. and Anufriev Yu.V. Semiconductors, 2015, Vol. 49, pp. 498-503.

ID 29 - Poster

Structural and chemical modification of diamond like silicon-carbon films

**A. Popov[1], A. Barinov[1], M. Shupegin[1]*
[1]National Research University "Moscow Power Engineering Institute" , Semiconductor electronics, Moscow, Russian Federation

Diamond like silicon-carbon films consist of an amorphous carbon (mainly diamond like) network (a-C:H) and an amorphous silica network (a-Si:O). The films allow to introduce a large amount of metals in order to change the material's properties. Metal containing silicon-carbon films were obtained by the simultaneous decomposition of silicon-organic substance and microwave dispersion of metal. High resolution electron microscopy and diffraction experiment have shown that the silicon-carbon matrix remains in the amorphous state and metal as a rule forms nanocrystals of metal carbides. Thus, the metal-containing films are nanocomposites composed of dielectric matrix with nanoscale inclusions of conductive phase. However, chemical modification of silicon carbon films by introduction of metals is not the only way to control their properties. Structural modification - the change of the material structure at a constant chemical composition - can be an effective method of amorphous material properties control as well.

The influence of structural and chemical modification of silicon-carbon films on their electrical properties has been investigated. Structural modification was achieved by changing the conditions of film preparation process, leading to changes in their structure (the magnitude of voltage applied to the substrate holder and partial pressure of argon in the chamber during the film growth. Chemical modification was carried out by incorporating the various metals in films.

Structural modification. It is shown that the variation of the magnitude of voltage at the substrate holder from -150 V to -400 V during the preparation of silicon-carbon films in vacuum leading to a decrease in the conductivity of films on the order of magnitude from 10^{-12} $\Omega^{-1}cm^{-1}$ to 10^{-13} $\Omega^{-1}cm^{-1}$ and to an increase the activation energy of the conductivity from 0.54 eV to 0.84 eV. Adding inert gas (argon) to the vacuum chamber during film growth causes a significant increase in electrical conductivity. Increasing the partial pressure of argon in the chamber from 0 to 10-4 Torr leads to an increase in electroconductivity on 6 orders of magnitude from 10^{-12} Ω^{-1} cm^{-1} to about 10^{-6} Ω^{-1} cm^{-1}.

Chemical modification. Metals (tantalum, tungsten, molybdenum and hafnium) were introduced into the film at an argon partial pressure of 10^{-4} Torr. The dependence of the electrical conductivity on metal concentration in all cases have a similar appearance. There are three areas: at low concentrations of metal transport of charge carriers is carried out in a dielectric amorphous matrix, at high concentrations of the metal conductivity is in the conductive channels of nanocrystals of metal carbides, and the intermediate metal concentrations correspond to the percolation threshold. However, the absolute values of conductivity and concentration of the metal corresponding to the percolation threshold depends on the introduced metal. Conductivity changes by chemical modification reaches 9 orders of magnitude from 10^{-6} Ω^{-1} cm^{-1} to 10^{3} Ω^{-1} cm^{-1}.

Thus, the structural and chemical modification of diamond like silicon-carbon films allows to change their electrical conductivity on 16 orders of magnitude from 10^{-13} Ω^{-1} cm^{-1} to 10^{3} Ω^{-1} cm^{-1}. The report analyzes the reasons of influence of structural and chemical modification on the mechanisms of charge transport in silicon-carbon films.

ID 30 - Poster

Structural and physical properties of $Ge_xAs_ySe_{1-x-y}$ glasses

*C. Durniak[1], R. Wang[2]
[1]Juelich Centre for Neutron Science, Garching, Germany
[2]Australian National University, Centre for Ultrahigh Bandwidth Devices for Optical Systems, Laser Physics Centre, Research School of Physics and Engineering, Canberra, Australia

Chalcogenides are materials containing one or more of the chalcogen elements (S, Se or Te) covalently bonded to semi metallic elements. The wide range of possible chemical compositions and their glass structures have resulted in an increasing number of important applications in electronics and photonics [1]. For example, chalcogenide Ge Sb Te can already be found in Digital Versatile Disks and phase-change access memory (PRAM). Other interesting optical properties like high linear and nonlinear refractive indices and low loss promote chalcogenide glasses as a promising material for optical waveguides. However the performance of glass-based photonics devices always suffers from the structural relaxation intrinsic to disordered materials. Therefore understanding the structure and its correlation with the material's macroscopic properties are essential to the fabrication of high-quality photonic devices.

Here we report on investigations on the structural and physical properties of Ge-As-Se glasses using various characterization techniques, exploring the link between the glass compositions, the mean coordination number, and the materials' properties [2-4].

1. R. P. Wang, Amorphous Chalcogenides: Advances and Applications (Pan Stanford Publishing, Singapore, 2014).
2. R. P. Wang, A. Smith, A. Prasad, D. Y. Choi, and B. Luther-Davies, J. Appl. Phys. **106**, 043520 (2009).
3. W.-H. Wei, R.-P. Wang, X. Shen, L. Fang and B. Luther-Davies, Journal of Physical Chemistry C **117**, 16571 (2013).
4. S.-W. Xu, R.-P. Wang, Z.-Y. Yang, L. Wang and B. Luther-Davies, Applied Physics Express **8**, 015504 (2015).

ID 31 - Oral

BornAgain software - Simulating and fitting X-ray and neutron small-angle scattering at grazing incidence

**C. Durniak[1], M. Ganeva[1], G. Pospelov[1], W. Van Herck[1], J. Wuttke[1]*
[1]Juelich Centre for Neutron Science, Garching, Germany

Grazing incidence small angle scattering (GISAS) is a surface sensitive, non-destructive, technique, which provides statistical information on the vertical but also lateral structures of the investigated samples [1]. It has been increasingly used to characterise deposited or embedded nanoparticles as well as multi-layered thin films [2]. The complex samples' architectures and the wealth of physical effects occurring during such experiments result in a challenging analysis of the experimental data, which therefore requires numerical simulations.

Here we present BornAgain, a multi-platform, open-source project [3]. This software uses Distorted Wave Born Approximation to analyze and fit small angle two-dimensional scattering images for X-ray or neutron scattering at grazing incidence (GISAXS, GISANS). BornAgain provides a generic framework for modelling samples composed of arbitrarily complex multilayers with smooth or rough interfaces, with various shapes and distributions of embedded or deposited nanoparticles. It also offers the option of using polarized neutron or magnetic scattering. Simulations and fits can be controlled through Python scripts. In addition, a growing part of the software's functionality is also available through a Graphical User Interface.

Diverse examples of GISAXS and GISANS (see fig.1) illustrating the broad range of features covered by BornAgain will be presented and discussed.

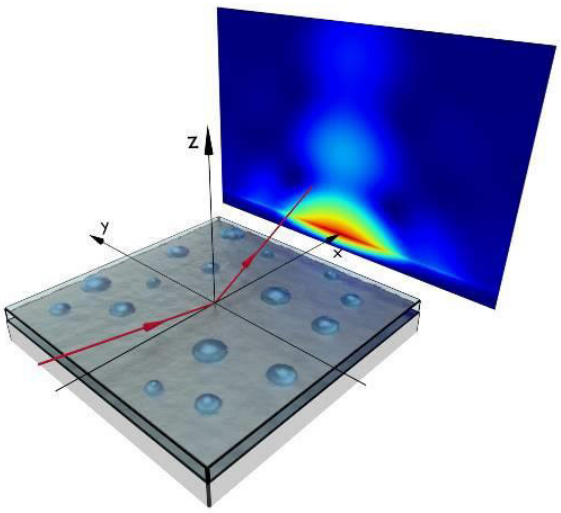

GISAS experimental layout. The detector image was generated with BornAgain using a sample made of a polydisperse distribution of gold half-spherical nanoparticles embedded in a layer of diindenoperylene (DIP) sitting on a SiO_2 substrate. The DIP layer presented some roughness for its interface with air.

[1] G. Renaud, R. Lazzari, F. Leroy, Probing surface and interface morphology with Grazing Incidence Small Angle X-Ray Scattering, Surface Science Reports 64, 255 (2009)
[2] C. Frank et al, Analysis of island shape evolution from diffuse x-ray scattering of organic thin films and implications for growth, Phys. Rev. B 90, 205401 (2014)
[3] bornagainproject.org

ID 32 - Poster

Microstructures and carrier transport properties of nanocrystalline silicon thin films

*D. Shan[1], Y. Ji[1], *J. Xu[1], K. Chen[1]*
[1]Nanjing University, Nanjing, China

Nanocrystalline silicon (nc-Si) thin film, as an important optoelectronic material, has attracted much interest since it can be used in many kinds of devices such as thin film transistor, thin film solar cells as well as memories. In order to further improve the device performance, it is crucial to understand the fundamental carrier transport characteristics in nc-Si thin films together with the microstructural and electrical properties. In this work, hydrogenated amorphous Si thin films were prepared by plasma-enhanced chemical vapor deposition technique. As-deposited samples were then thermally annealed at various temperatures (> 800℃) to obtain nanocrystalline Si film. The microstructures of films before and after annealing were characterized by Raman and cross-sectional TEM techniques which revealed the formation of nc-Si with size less than 10 nm. It was found that both optical and electronic properties were significantly changed after annealing. Room temperature conductivity is increase by over two orders of magnitude and temperature-dependent conductivity measurement indicates the thermally activated conduction mechanism dominant the transport process in nc-Si films. In order to further understand the carrier transport behaviors in nc-Si films, the temperature-dependent Hall measurements were performed in the temperature range from 300K to 550K. It is interesting to find that the Hall mobility increases as the temperature increases and then decreases with the temperature further increasing. The role of grain boundaries on the changes in Hall mobility is discussed. This work is supported by the ‘973 Program’ (2013CB632101), NSFC (No. 61036001 and 11274155) and PAPD.

ID 33 - Oral

Hybrid photovoltaic structures based on organic semiconductors and inorganic plasma deposited layers

**S. Mansurova[1], A. Kosarev[1], I. Cosme Bolañes[1], A. Olivares Vargas[1], H. Martinez[1], H. Martinez[1]*
[1]INAOE, Optics, Tonantzintla, Mexico

Small molecule and polymer based organic semiconductors (OS) have been extensively studied during past decade for photovoltaic (PV) applications due to the possibility for tailoring their optoelectronic properties, mechanical flexibility and ease of scaling up for industrial production. The typical organic PV structure comprises a transparent conductive oxide as anodic electrode, a conductive polymer film of PEDOT:PSS (poly(3,4-ethylenedioxythiophene) polystyrene sulfonate) as hole transporting layer (HTL), an active layer that is the blend of p and n material (one of the most used is the polymer-fullerene blend P3HT(poly(3-hexylthiophene):PCBM (phenyl-C61-butyric acid methyl ester)), and, finally, a layer of aluminum as metal cathode. Recently, polymer based technology has shown wide margins of improvement in terms of energy conversion efficiency, reaching values above 10%. However, the low absorption of OS in IR region of spectra and low mobility of charge carriers in these materials remains a limiting factor for organic solar cells performance. On the other hand, PV solar cells based on plasma deposited materials (Si:H, SiGe:H, SiC:H, etc.) are rather well developed devices fabricates commercially. Efficiency of single p-i-n device is about 10% (for 1 cm^2 area) and it is about 13% for triple junction. Plasma deposition is low temperature technology (conventionally in the range 100-250 ºC). Plasma deposition at T180 ºC is compatible to both plastic substrates and organic semiconductors used in device structures. This compatibility of OS technology with low T plasma deposition, together with some complementary properties of both classes of materials, makes promising study of hybrid devices.

We present results on study of hybrid PV structures fabricated with organic semiconductors and plasma deposited films (PDF). Configurations of PV cells studied are as follow: 1) hybrid structures: ITO-(p-SiC:H)-OS(P3HT:PCBM)-(n-Si:H)-Al (type A), ITO-OS(PEDOT)-(i-Si:H)-(n-Si:H)-Al (type B), ITO-OS(PEDOT)- OS(P3HT:PCBM)-(i-Si:H)- (n-Si:H)-Al (type C), ITO-(p-SiC:H)-OS (P3HT:PCBM)-(i-Si:H)-(n-Si:H)- Al (type D); 2) reference structures: OS PV cell ITO-PEDOT-(P3HT:PCBM-Al), PDF PV cell ITO -(p-SiC:H)-(i-Si:H)-(n-Si:H). Both OS and PDF in the structures studied were fabricated under the same deposition conditions, substrate temperature was T_s=160 C for PDF. Organic films were deposited by spin coating while plasma deposited films by PE CVD technique in 3-chamber cluster tool from "MVSystem Inc." OS films were annealed at the same temperature either during fabrication PV cell with PDF, or separately in vacuum conditions. The structures were characterized by measurements of current-voltage (I-V) characteristics in dark and under illumination. Spectral characteristics of the devices were measured in extended range of signal (about 5 orders of value) in order to use sub-gap signal for intrinsic" layers diagnostic and signal for short wavelengths for frontal interface characterization. We observed significant changes in characteristics of hybrid structures in comparison to those for reference (both OS and PDF) cells, e.g. the highest value of open circuit voltage U_{oc} =0,73 V was observed in Type C structures while short circuit current density was the highest J_{sc}= 5.87 mA/cm^2 in the Type B structures. The structures were also characterized by different values for series R_s and shunt R_{sh} resistances. Finally, the comparative analysis of our experimental data against those reported in literature is presented.

ID 34 - Oral

Modify the Schottky Contact between SnO_2:F and P-a-SiC:H by Carbon Dioxide Plasma Treatment

*T. Li[1], X. Zhang[1], F. Wang[1], J. Ni[1], D. Zhang[1], J. Sun[1], C. Wei[1], S. Xu[1], G. Wang[1], Y. Zhao[1]
[1]University Nankai, Institute of Photo-electronic Thin Film Device and Technique, TianJin, China

The contact property between SnO_2:F (FTO) and p-a-SiC:H plays an important role in affecting the performance of a-Si:H solar cell. However, the instabilities of FTO substrate in hydrogen plasma dramatically restricted the improvement of FTO/p contact properties. In this paper, the CO_2 plasma treatment of FTO has been introduced to increase the work function and then decrease the hole potential barrier in the p-a-SiC:H side, which consequently increases the V_{oc} and *FF* of a-Si:H solar cells. The photoluminescence (PL) spectra of FTO indicated three main emission bands--one weak emission band around 417.2nm and two strong emission bands around 515.6 and 632.3nm, respectively. These emission bands can be attributed to the radiative recombination from oxygen vacancies and surface states of FTO. The CO_2 plasma treatment sufficiently reduces the oxygen vacancies and surface states by the de-doping effect, the work function of FTO was increased from 4.16eV to 4.34eV. Furthermore, the CO_2 plasma treatment promoted the chemisorption of oxygen species and thus affected the surface polarity of FTO substrate, which enhanced the nucleation density of p-a-SiC:H during the initial growth. From the FTO-p contact measurement results, the performance enhancement of schottky contact is attributed to form the high quality interface between FTO surface and p-a-SiC:H. The a-Si:H solar cells with Al back reflector were prepared by plasma enhanced chemical vapor deposition (PECVD) on the Asahi U type FTO substrate. The CO_2 plasma treatment substantially improves the V_{oc} of a-Si:H solar cells from 915mV to 990mV and *FF* from 67.7% to 74.4%, respectively.

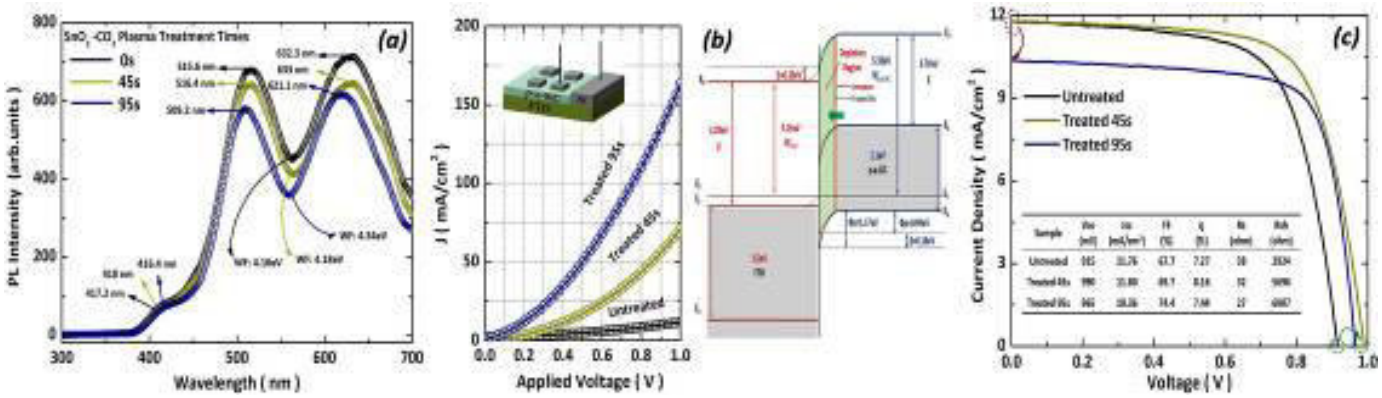

ID 35 - Poster

Short and medium range order in Sb-Se glass

**K. Itoh*[1]
[1]*Okayama University, Okayama, Japan*

Antimony selenide glasses have attracted significant interest because of their electronic and optical properties. A detailed understanding of such materials requires information on the short and medium range structure. However, there is very little information about the atomic structure of Sb-Se glass. In this work, pulsed neutron diffraction measurements were performed to investigate the atomic structure of Sb_xSe_{1-x} binary glasses (x=0, 0.05, 0.1, 0.2 and 0.25). The Fourier transformation of the structure factors of the momentum transfer of 300 nm^{-1} give detailed information of the nearest-neighbor configuration. The pair distribution functions for Sb_xSe_{1-x} glasses has well-resolved two peaks in the nearest-neighbor region. These peaks were attributed to the Se-Se and Sb-Se nearest-neighbor correlations, respectively. The coordination numbers of Sb and Se were calculated from the pair distribution functions. The results indicate that Sb are coordinated by three Se and Se are two-coordinated. In order to elucidate the medium range structure, reverse Monte Carlo simulation was used under the constraint of the nearest-neighbor coordination The most likely model for the network structure contains Sb-$(Se\text{-}Se_{1/2})_3$ units which are linked to one another.

ID 36 - Poster

Optical spectroscopy of a new polymer structure of the azomethine base with an inclusion of a metal center

*V. Avanesyan[1], A. Rakina[1]
[1]Herzen State Pedagogical University of Russia, Physical Electronics, St.Petersburg, Russian Federation

Nowdays the special attention is drawn by metalpolymeric complexes where as an environment of the metal center or azomethine ligands (Schiff's bases) which unlike other types of high-molecular composites possess rather simple manufacturing techniques, stable phase structure and thermal stability are used. Besides the included metal center the specified materials contain the MeN_2O_2 and NH groups, benzene rings and also branched systems of π couplings. Unlike purely organic compounds such systems have great opportunities for management of their properties at the expense of a variation of electronic structure of the metal center. At synthesis of the modern materials of nanoelectronics possessing a wide range of certain optical, electric and photo-electric characteristics, an actual task is inclusion in polymeric matrix of particles of metal of the nanometer size at the molecular level. Thus there is an opportunity formations the new polymeric materials materials with the high conductivity level for the formations of the additional carbon communications between phenyl rings.

The results of the measurement of optical density of the metalpolymeric film created on the basis of an azometin of Saltmen at inclusion of the metal center - nickel and nanotubes of platinum are presented. The studied samples were received by method of electrochemical synthesis of polymeric layer with the content of nickel on the carrying-out substrate with a film of dioxide of tin and the subsequent sedimentation of particles of platinum in a polymer matrix. Growth of the formed film was controlled at different stages of process of polymerization. For carrying out measurements of optical density of samples of a metalpolymeric film the one-beam spectrophotometer was used. Spectral dependences of optical density of a film of structure of poly-[Ni (Saltmen)]/Pt were received in the field of lengths of waves λ = 200 - 400 nanometers under normal conditions of measurement and after preliminary heat treatment of the same sample.

Absorption of light in UF-area of a range is connected, generally with a chemical structure of film-forming substances, the strongest absorption nonsaturated bounds that is connected with existence in them which are easily excited π-электронов possess. Values of optical density of the studied samples under normal conditions are higher than measurement, than after carrying out their preliminary heat treatment which, apparently, intensifies thermal fluctuations of macromolecules and, besides, leads to strengthening of intermolecular interactions. Thus there is a rupture and reorganization of communications in system of π couplings take place. Optical properties of polymers, first of all, are connected with their chemical composition and a molecular structure. The analysis of the experimental results presented in other works shows that preliminary heat treatment changes structure of material, value of width of the forbidden zone and allows to reveal groups of defects, steady against annealing. Supramolecular structure of polymer it is very sensitive to the thermal treatment allowing to increase sharply mechanical properties of polymeric material and considerably to expand area of its practical application.

In the polymeric composites under study the increased concentration of the delocalized polarons is established. The observed shift of a range of optical density in long-wave area as a result of heat treatment can be caused by expansion of a zone of π electrons delocalization in the structure and resulting in greater electroactivity of polymer.

ID 37 - Oral

Radial heterojunction Si hierarchical nanowires solar cells with 16.3% conversion efficiency

*F. Wang[1,2,3,4], X. Zhang[1,2,3,4], Y. Jiang[1,2,3,4], T. Li[1,2,3,4], Y. Zhao[1,2,3,4]
[1]Nankai University, Institute of Photo-electronics Thin Film Devices and Technique, Tianjin, China
[2]Nankai University, Key Laboratory of Photo-electronics Thin Film Devices and Technique of Tianjin, Tianjin, China
[3]Nankai University, Key Laboratory of Photo-Electronic Information Science and Technology of Ministry of Education (Nankai University), Tianjin, China
[4]Nankai University, Collaborative Innovation Center of Chemical Science and Engineering (Tianjin), Tianjin, China

The reason for these boosting advantages of nanostructure is owing to a great potential in improving both optical and electrical properties of the solar cells for its unique architectures. The vertically aligned Si nano-arrays are known as strong reflection suppressed, and the orthogonal separation in directions between sunlight irradiation and diffusion of minority carriers are conducive to the carrier diffusion over a short distance to the p-n junction, and can be extracted with minimal recombination within the bulk of the silicon materials.

However, in order to exploit these advantages in practice, there still exists the key aspect to be considered and design challenges yet to be addressed. In particular, the ultrahigh surface area as prolonging the length of nanostructure is always along with increasing surface defects density which generally results a high recombination velocity (S_{it}). Although photoexcited carriers can rapidly be transported to the junction interface, it easily trapped by the high density surface defects before being collected by the external circuit. The electrical advantages of radial junction architecture were sacrificed by the high S_{it} and thus lead to the performance deterioration.

Here, we report a radial p-n heterojunction solar cell based on hierarchical nanowires (NWs) with a conversion efficiency of 16.3 %. The light management using the random dual-period Micro-Nano structures shows excellent photo-harvesting characteristics. We adopt the wide bandgap intrinsic hydrogenated amorphous silicon (i-a-Si:H) as the passivation layer and highly boron doped a-Si: H (p-a-Si: H) as the emitter layer to demonstrate the concept of radial heterojunction, and specially focused on the interface engineering of the devices.

In order to reduce the surface defects density of the substrates, hydrogen plasma pre-treatment and chemical polishing etching treatment with organic aqueous solution have been applied to avoid the inhomogeneous a-Si:H deposition, metal residual contamination in the high density nanostructures and excessive carrier trapping centers caused by a high density of surface defects. Thus, compared with the planar structure heterojunction solar cell, the Si heterojunction nanostructure solar cell improved photocurrent density without loss in the open-circuit voltage and fill factor, resulting in an overall increase in efficiency by 28.3 %. By employing the concurrent improvements for the Si NWs structure heterojunction solar cell interface passivation, the external quantum efficiency at short wavelength (@ 400 nm) have been remarkable enhanced to 61 %. An open-circuit voltage of *611 mV*, fill factor of *71.7 %*, short current density of *37.1 mA/cm^2*, and a conversion efficiency of *16.3 %* for Si heterojunction nanostructure solar cell have also been achieved.

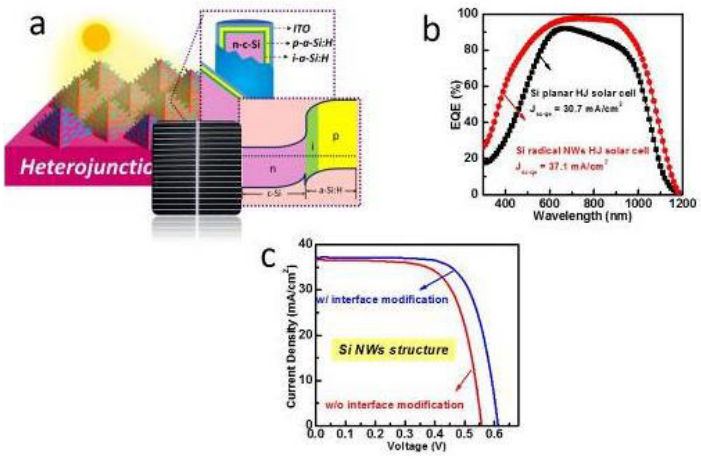

ID 38 - Oral

Voids in hydrogenated amorphous silicon: A first-principles approach

**P. Biswas[1], D. Drabold [2], S. Elliott[3]*
[1]The University of Southern Mississippi, Physics and Astronomy , Hattiesburg, United States
[2]Ohio University, Physics and Astronomy, Athens (OH), United States
[3]University of Cambridge, Department of Chemistry , Cambridge, United Kingdom

Recent experiments on *a*-Si:H samples (deposited by means of an expanding thermal plasma) using infrared absorption spectroscopy suggest that the microstructure of *a*-Si:H at high concentration of H (14% and above) is dominated by voids, whereas vacancies play a dominant role at low concentration [1]. Motivated by this observation, we address the problem by developing a hydrogenation scheme that jointly employs experimental infrared data and *ab initio* simulations. The microstructure of *a*-Si:H is addressed with particular emphasis on the shape and the size of the voids at high concentration (of hydrogen). The size, shape, and the volume distribution of the voids are determined by constructing the convex hull of the regions surrounding the voids. We demonstrate the existence of a useful correlation between the presence of large irreducible rings (decorated with H atoms) and the voids in network [2, 3]. The results from this approach are compared to the ones that are obtained using a Gaussian approximation of the atomic surfaces.

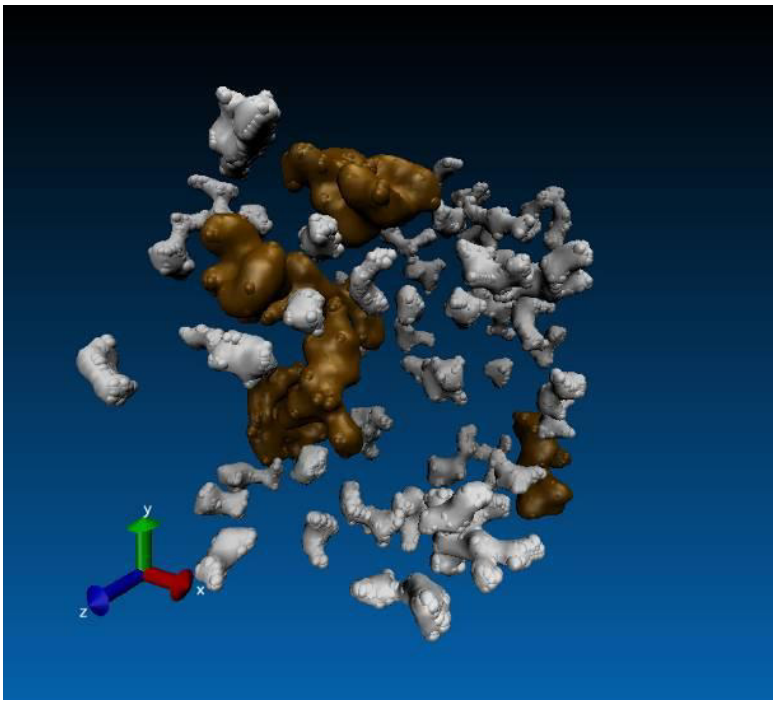

Distribution of voids in a model with 14% H. Void regions are shown as a grey surface with hypothetical void particles on the surface of the voids. Few large voids are shown in color (saddle brown)]

ID 39 - Oral

Charge Separation in Hydrogenated Amorphous Silicon and Conjugated Polymers probed by Transient EPR

**K. Lips[1], J. Behrends[2]*
[1]Helmholtz-Zentrum Berlin für Materialien und Energie, Berlin Joint EPR Laboratory, Berlin, Germany
[2]Freie Universität Berlin, Fachbereich Physik, Berlin, Germany

Using transient electron paramagnetic resonance (trEPR) and electrically detected magnetic resonance (EDMR) spectroscopy we analyse and compare the process of free charge carrier generation and separation in polymer:fullerene and hydrogenated amorphous silicon (a-Si:H). In both types of materials charge transport and recombination is dominated by local disorder. One of the main advantages of trEPR spectroscopy is that it is possible to follow the charge separation process on a nanosecond to millisecond time scale and, at the same time, identify the microscopic origin of the participating paramagnetic states through their EPR signatures. While trEPR has previously been applied to polymer:fullerene blends, no reports so far are available for a-Si:H although many of the models used to describe transport and recombination in organic semiconductors originate from a-Si:H. Here, we will shed light on one of the still open questions after over 40 years of intensive a-Si:H research: the role of excitons and spin-correlated geminate states in the charge separation process. We present a first direct experimental proof for the existence of excitons and spin-correlated (geminate) electron-hole pairs in a-Si:H through the observation of their unique trEPR signatures. We compare the observations to recent results achieved on prototypical P3HT:PCBM blends where, prior to dissociation of photogenerated excitons into separated charges, bound polaron pairs form at the donor/acceptor interface [1].

The trEPR spectrum of undoped a-Si:H at T=80K immediately following photoexcitation reveals the signature of a more than 20mT broad signal that can be modelled by a nearly axially symmetric S=1 exciton with a Gaussian-broadend exciton size distribution centered at 5Å. Simultaneously with the exciton we also observe spin-correlated (geminate) electron-hole pairs that unambiguously can be distinguished from long-lived uncorrelated electron and holes trapped in bandtail states since their spin state population strongly deviates from Boltzmann equilibrium. This proves that both constituents of each charge carrier pair originate from the same excitation process (exciton). These geminate pairs evolve into separated electrons and holes on time scales beyond one µs at low temperatures. Both, the spin-correlated geminate e-h pair as well as the separated charge carriers trapped in tail states are represented by their well known *g* values, g_e=2.0044 and g_h=2.01, as known from LESR.

The experimental results will be discussed within the scope of a tentative model for charge carrier excitation, separation and recombination, where excitons contribute to the generation of free charges through an Auger three particle process.

[1] J. Behrends, A. Sperlich, A. Schnegg, T. Biskup, C. Teutloff, K. Lips, V. Dyakonov and R. Bittl, *Direct detection of photoinduced charge transfer complexes in polymer fullerene blends*, Phys. Rev. B, **2012** (85) 125206.

ID 40 - Poster

Photodielectric properties of polycrystalline naturally disordered layers of red lead

**V. Avanesyan[1]*
[1]Herzen State Pedagogical University of Russia, Physical Electronics, St.Petersburg, Russian Fed.

Research of photodielectric effect (PDE), as well as measurement of dielectric properties, allows to receive data on behavior of the charge carriers with a limited possibility of movement in photoconductive material. Besides, research of this effect is an informative additional contactless method of measurement of photoconductivity in variation electric fields that has great potential opportunities when designing a number of elements of optoelectronics. The considered phenomenon is perspective for physical properties the photosensitive ferroelectric materials. Manifestation of PDE was found for a number of the photosensitive semiconductor connections used in solid-state electronics CdS, CdTe, ZnO, SbSJ, etc. In work results of studying of PDE are given in the lead minium Pb_3O_4, which high-resistance and rather photosensitive semiconductor material possessing the considerable potential of practical application in optoelectronics and nonlinear optics, and also being model object for structural researches in fundamental physics. Studying of PDE was carried out on Pb3O4 layers with binding substance which are rather photosensitive, high-resistance and also, thanks to considerable density, possess low values of a tangent of angle of dielectric losses. The photocapacitor structures created on the glass substrate covered with SnO_2 films in the way described above represented heterogeneous layers. The variation of material of electrodes had no essential impact on the obtained experimental data. Light excitement revealed significant increase in value of capacity of capacitor structures on the basis of Pb_3O_4. PDE was shown in the studied photoconductive layers without existence of an additional dc electrical field.

In the field of low frequencies and high level of light excitement dispersive recession is more noticeable, and the photocapacity is well divided with its dark value. With increase of frequency this distinction decreases and it is practically leveled in high-frequency area irrespective of illumination level. The established nature of frequency dispersion of dielectric coefficients can be explained with polarization of a spatial charge which represents the electric heterogeneity arising in material and leading to dielectric losses. To the probable mechanisms which are the cornerstone of formation of a spatial charge as it was already noted above, processes of polarization of equilibrium carriers of a charge under the influence of electric field, polarization of the photogenerated carriers of a charge and their injection from electrodes can belong. Influence of the created spatial charge becomes noticeable only at low frequencies when its dielectric response answers an identical phase of change of the applied field. The last explains the fact of reduction of experimental values of photocapacity with increase of frequency of measuring tension. As at the lit sample in addition to the equilibrium there are also photocarriers, it is possible to expect that at all frequencies where polarization of a spatial charge prevails, values of capacity at illumination have to be above the corresponding dark values. Besides, with increase of frequency the spatial charge is formed in smaller quantity that leads to reduction of dielectric losses and values of a photocapacity. In this case, we can assume that with increasing light intensity is generated a growing number of charge carriers, which leads to an increase in the total space charge. Significant displacement of the field of dispersion to the higher frequency range by increasing the intensity of illumination give reason to believe that the observed change in the conductivity is determined by the PDE (or rather its increase in inhomogeneous material), that is, there is a manifestation of the second type of PDE. If you change the frequency of the alternating field applied to the structure on the basis of photodielectric Pb_3O_4, we observed the change of illumination range corresponding to the maximum value of the relative steepness of the luxury-voltage characteristics, with adequate photosensitivity coefficient.

The character frequency and spectral dependences along with thermal activation of PDE leads to the conclusion that a certain proportion of the effect may be due to the presence of easily polarizable centers, in particular, electron traps and the formation of space charge in the bulk semiconductor. The problem of PDE interpretation is due to the complexity of identifying the exact phase of the samples Pb3O4 in their natural propensity to disordering. It can be assumed that further research PDE may

provide additional information about the mechanisms of polarization and conductivity in high-oxide photoconductors.

ID 41 - Poster

Small angle X-ray scattering study of silicon nanoparticles embedded in different polymeric binders

*A. Odo[1], D. Britton[2], M. Harting[2], G. Gonfa[3]
[1]Federal University Oye-Ekiti, Physics, Oye-Ekiti, Ekiti State, Nigeria
[2]University of Cape Town, Physics, Cape town, South Africa
[3]Haramaya University, Physics, Dire Dawa, Ethiopia

The structural and interfacial properties of inclusion of P-typed silicon nanoparticles in two classes of polymeric binders (1) a soluble polymers, and (2) a polymerizing monomers was investigated using small angle x-ray (SAXs) technique. The soluble polymers were cellulose acetate butyrate (CAB), and commercial quality low density polystyrene foam (PS). The polymerizing monomer binders were a commercial acrylic printing base (ACR), and refined linseed oil (LIN). Analysis of the obtained SAXs result using the Gunier scheme suggests that the dispersion of the powders in the different binders consisted of a broad distribution of size heterogeneities, one in which the cluster mass is not uniform but varies over a size distribution in the range 69 to 74nm. Further analysis using Porod's law revealed that the ACR, CAB and PS based composite resulted in a surface fractal structures while the LIN based composite gave a characteristic mass fractal with the size of the basic particles ranging from 61nm to 74nm in agreement with the Gunier analysis, while the size of the aggregate clusters ranges from 338 to 370nm. Analysis of the deviation from porods law from the SAXs data reveal that the all of the binder formed a difussed interface with the embedded silicon powder except the LIN based composite sample which exhibited a two-phase systems with electron density inhomogeneity.

ID 42 - Poster

Microcrystalline silicon thin films with SiF_4/H_2 chemistry by MDECR-PECVD

**J. Wang[1], P. Bulkin[1], J.- C. Dornstetter[1], E. V. Johnson[1]*
[1]Ecole Polytechnique, Palaiseau, France

When used as the active layer in PIN solar cells, microcrystalline silicon (µc-Si:H) films deposited from a SiF_4/H_2 chemistry in a RF-PECVD reactor showed excellent performance: a defect density as low as $5.1x10^{14}$ cm^{-3} was achieved, a solar cell efficiency of 9.2 % was obtained (with V_{OC} = 536mV), and even with a 5.5 µm fully-crystallized i-layer, an EQE at 800 nm of as high as 73 % was achieved. However, limited by the plasma density, these results are achieved at a low deposition rate (< 4 Å/s). Motivated to improve the deposition rate while maintaining the excellent properties, we ask: can this chemistry be transferred to the Matrix Distributed Electron Cyclotron Resonance (MDECR)-PECVD system, which has previously achieved high µc-Si:H deposition rates with the SiH_4/H_2 chemistry?

In this study, undoped µc-Si:H films were deposited on Corning Eagle glass from a SiF_4/H_2 mixture using a MDECR-PECVD reactor. A microwave power supply (2.45 GHz) controlled the plasma density, and a 13.56 MHz RF biasing of the substrate electrode was used to independently modify the ion bombardment energy (Ei) at the growth surface by tuning the self-bias voltage (V_{bias}). Ex-situ spectroscopic ellipsometry (SE) and Raman spectrometry (at 633 nm) were used to characterize the optical and microstructural properties of the films. Optical emission spectroscopy (OES) was used to investigate the plasma during the deposition process.

Firstly, a series of films were deposited by varying the V_{bias}, from 50 V (floating potential) to -15 V. The other deposition parameters were kept constant: substrate temperature =135 °C, gas flow SiF_4/H_2 = 35/120 sccm, gas pressure Pr_{gas} = 7 mTorr, microwave power P_{MW} = 1250W and deposition time t_d = 600 s. For the whole range of V_{bias}, a deposition rate within the range of 8 - 9 Å/s was achieved for the films. Raman spectroscopy measurements showed that V_{bias} greatly influenced the films growth. A clear threshold for the films microstructural properties could be observed: when E_i is low (V_{bias} > 20V), films are crystalline phase dominated and its fraction X_C slightly increased (from ~65% to 80%) with the increase of E_i. Once E_i exceeding the threshold, signal of amorphous component becomes pronounced sharply (V_{bias} = 15 V gives 64% X_C and V_{bias} = 10 V gives only 20%). When E_i is even higher, the films become completely amorphous. Curiously, the SE spectra acquired show that while all films deposited with V_{bias} > 20V have similar X_C, the film density was greatly modified by the E_i, and actually shows a greater value when V_{bias} is above floating potential.

Motivated to further explore the deposition window for µc-Si:H films, a second series of films were deposited with different substrate temperatures: 108 °C, 125 °C and 147 °C, keeping all other deposition parameters constant as above, and additionally maintaining V_{bias} = 20 V. The global trend of the deposition rate is just slightly going down from 8.9 Å/s at 108 °C to 8.1 Å/s at 147 °C. However, both SE and Raman measurement show a huge variation in the materials' microstructure with increasing substrate temperature. At 108 °C, the film was fully amorphous with single broad peak near 480 cm^{-1} in the Raman spectra and no shoulder-like peaks in the SE spectra. Then, X_C increases with the increase of substrate temperature and reaches a high level of 80 %, just as in the first sets of experiments at 135 °C.

Generally, within ECR systems, the plasma potential V_{pl} is several volts higher than the V_{bias}, and most ions will arrive at the surface with $E_i=q^*(V_{pl}-V_{bias})$ after passing the almost collisionless sheath (assuming mostly singly charged ions). In other words, the threshold of V_{bias} = 20 V approximately corresponds to E_i = ~35 - 40 eV. OES acquired during these processes shows us that the emissive states of Si^* and SiF^* are two of the dominant species observed, species for which the silicon bulk displacement threshold energies are 38 and 43eV respectively (as calculated by Brice *et al.* (1989)), and therefore supporting this origin for the lack of crystallinity at higher IBE. Knowing that the threshold for surface displacement for Si^+ and SiF^+ are both ~11 eV, ions striking the µc-Si:H films with low E_i could transfer energy to the

surface and heat it up continuously, providing denser films as well as increased X_C, until elevated E_i begins to amorphize the film. This indicates that relatively high substrate temperature is required to achieve high X_C at such high deposition rate, but that local heating by low energy ions can be helpful in this regard.

In addition to these results, more efforts to characterize the µc-Si:H films using AFM, SIMS, and electrical measurements (for activation energy, carrier life time) are underway and will be reported.

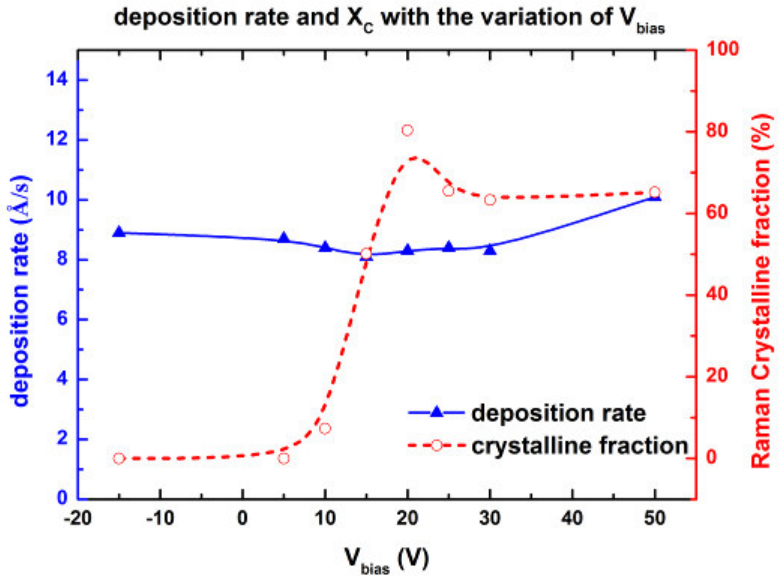

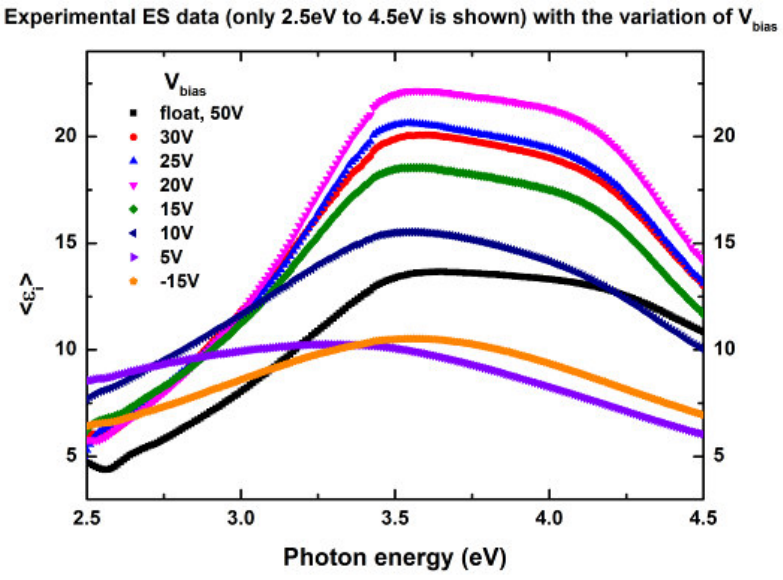

ID 43 - Poster

25x25 µm microbolometer fabrication process using polymorphous silicon-germanium films (pm-Si_xGe_y:H) as thermo-sensing material

**C. Calleja Gomez[1], M. Moreno Moreno[1], P. Rosales Quintero[1], *A. Torres Jacome[1]*
[1]INAOE, Electronics, Tonantzintla, Puebla, Mexico

In the fabrication of uncooled resistive microbolometers, the material properties that one wishes to obtain for the thermo-sensing material are a high temperature coefficient of resistivity (TCR) and low conductivity for obtaining the highest responsivity, detectivity, noise equivalent temperature difference (NETD) and low1/f noise characteristic. The most popular materials that are optimized for these applications are a-Si:H and a-SiGe:H, however not always all these requirements are fulfilled. We completed the deposition and characterization of hydrogenated polymorphous silicon-germanium films (pm-Si_xGe_y:H) deposited by plasma enhanced chemical vapor deposition (PECVD), using a standard 13.56MHz frequency. We found that those films have high values of activation energy (Ea=0.71eV), thermal coefficient of resistivity (TCR=9.1%K-1) and room temperature conductivity (σ_{RT}=2.32E-6Ω-1cm-1), which are superior characteristics than those of microbolometers based on a-Si:H and a-SiGe:H films contained in very large commercial Infrared Focal Plane Arrays (IRFPAs). With these films we fabricated microbolometers of 25x25 mm of area with I and L type isolation legs and these are compared with those fabricated with an optimized a-SiGe:H thermo-sensing material.

ID 44 - Oral

Correlative microscopy of nanostructures for solar cells

**A. Fejfar[1], M. Hývl[1], M. Müller[1], Z. Hájková[1], P. Pikna[1], A. Vetushka[1], M. Ledinský[1], J. Červenka[1], J. Kočka[1], S. Misra[2], L. Yu[2], M. Foldyna[2], P. Roca i Cabarrocas[2], C. Becker[3], T. Itoh[4], M. Kratzer[5], C. Teichert[5]*
[1]Institute of Physics, Academy of Sciences of the Czech Republic, Department of Thin Films and Nanostructures, Prague, Czech Republic
[2]CNRS, Ecole Polytechnique, LPICM, Palaiseau, France
[3]Helmholtz Zentrum Berlin, Berlin, Germany
[4]Gifu University, Gifu, Japan
[5]Montan Universitaet, Leoben, Austria

Radial junctions (RJs) based on silicon nanowires (NW) are examples of modern nanostructured solar cell designs with excellent light trapping and efficient photogenerated charge collection. Low temperature process has been used to prepare conformal p-i-n radial junctions using a random matrix of Si NWs grown by vapour-liquid-solid mechanism in plasma enhanced chemical vapour deposition [1]. Considerable influence of irregularities (e.g. SiNW lengths, orientations, shapes and mutual interactions) on the local photovoltaic performance can be expected. Direct measurements of these effects require microscopic techniques that would provide information on photoresponse of individual cells. This is possible using a conductive atomic force microscopy (C-AFM) with a conductive cantilever which serves as a contact to individual radial junctions [2].

Identification of the origin of variations of local photoresponse requires correlating its maps with other observations, e.g. with scanning electron microscopy. We have developed a procedure (see Fig. 1) for correlative microscopy using nanoindents as position markers [3], which is applicable to various types of nanostructures for photovoltaic solar energy conversion and which serves as a tool for investigating the role of disorder in nanostructured solar cells.

Indents by a Vickers tip were done by Helmut-Fisher GmbH PicoDentor HM500 with the applied maximum force of 300 mN. Groups of three indents arranged in a form of a right angled triangle with 20 mm sides were prepared to provide a local coordinate system for an accurate navigation on the sample in a nearby area. The indents can be easily observed in optical microscopes, e.g. the Leica integrated into the Renishaw InVia Raman microscope.

Samples of RJ based on Si NWs [1] were used to study the local photoresponse, under the illumination by 592 nm LED light, by Kelvin force microscopy (KFM). Maps of the surface potential were observed using ACCESS-EFM nose type cantilevers with Pt/Ir coating, the force constant k = 3.8 N/m and the resonance frequency f = 68 kHz at 3 mm/s scan speed. A Bruker Icon AFM was used in the PF mode to observe both the topography and the local conductivity maps by C-AFM.

An example of the results is shown in Fig. 2 in an area close to the indent (located in top right corner of images). A selected area in the images containing several RJs is highlighted by circles.

The identification of the same nanostructure in various maps is facilitated by the shapes of individual RJs, but the same procedure can be used even for totally featureless structures, for example thin films of solid-phase crystallized silicon [3]. The procedure can be used to identify the same location on various samples before and after different technological operations. For instance, we have used the indent markers to select an area of carbon nanowalls samples prepared by hot-wire chemical vapour deposition on crystalline Si wafers and study local electronic properties [3].

Here we will report the latest results of the correlation of the local (photo)current and surface (photo)potential with the features observed by SEM and by the confocal optical microscopy. We will also discuss the precision of the correlation procedure and possible issues.

We conclude that correlating microscopy techniques using nanoindent triplets for marking the local coordinate system on the sample surfaces with a sub-micrometer precision can help in understanding of the influence of the disorder in nanostructured solar cells.

This work was partly funded by the projects of the Czech Science Foundation (14-15357S, 13-25747S, 13-12386S), AS CR (M100101216 and M100101217), Ministry of Education, Youth and Sports (LM2011026 and 7AMB14ATE004) and OeAD-WTZ (# CZ SP 04/2014). The work at LPICM was partly supported by Solarium project ANR-14-CE05-0005 and PLATOFIL ANR-14-CE26-0020.

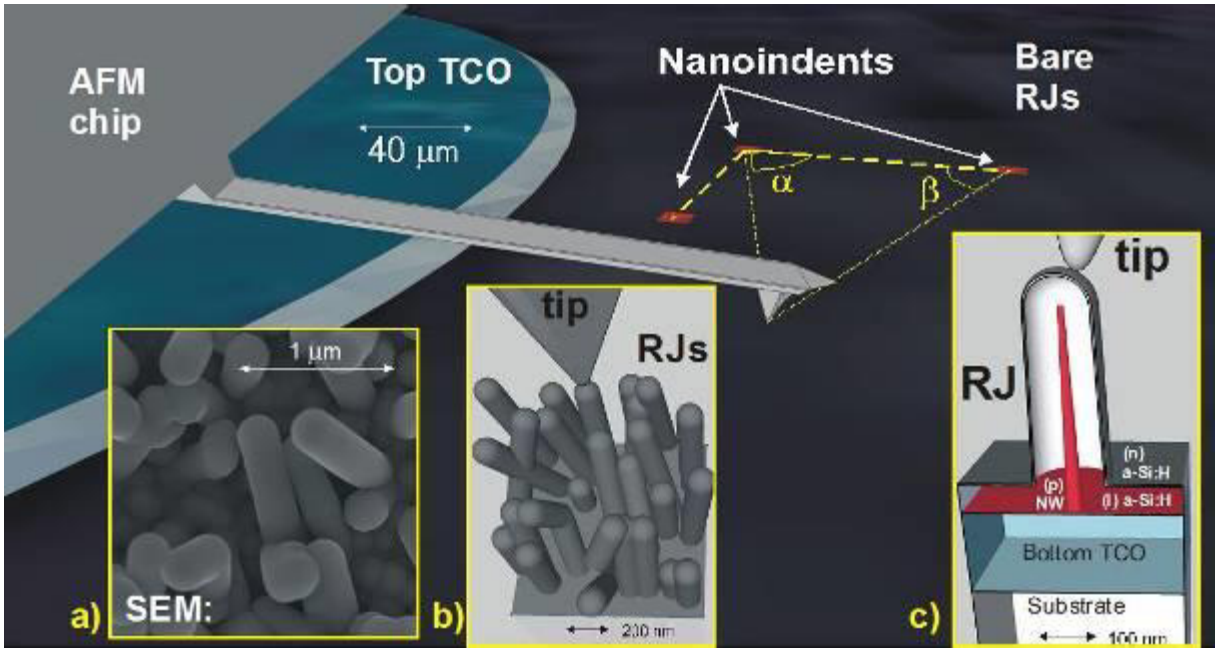

Scheme of the correlated microscopic measurements of solar cells with radial junction (RJ) based on Si nanowires (NW). Orientation on the sample is provided by three nanoindents which are enlarged and highlighted by the red colour for clarity. Circular top TCO contact is shown in blue below the AFM chip with the 200 mm long cantilever. Insets: a) SEM image in the area without the top TCO shows the disorder of the RJs. b) Zoom of the tip - RJs junction. c) Cross section of the RJ contacted by the AFM during the C-AFM measurement.

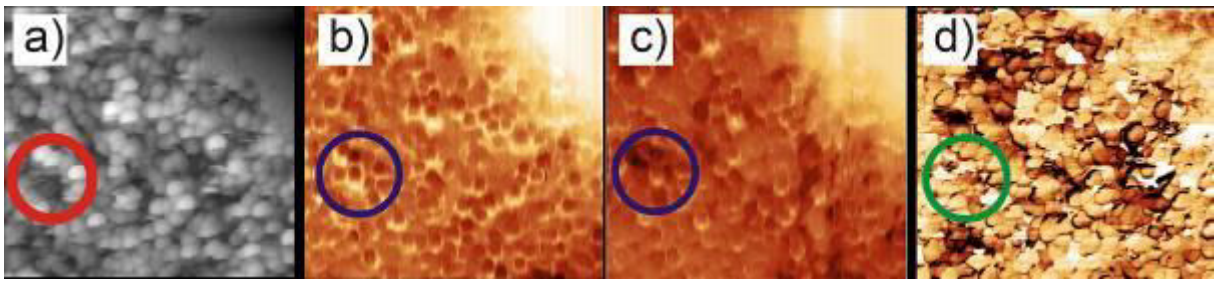

Correlative microscopy of 5x5 mm2 area of RJ on Si nanowires: a) morphology, b) KFM without illumination, c) KFM illuminated by 592 nm LED, and d) C-AFM images.

[1] S. Misra, L. Yu, W. Chen, M. Foldyna, P. Roca i Cabarrocas “A review on plasma-assisted VLS synthesis of silicon nanowires and radial junction solar cells”, J. Phys. D: Appl. Phys. 47 (2014) 393001.
[2] A. Fejfar et al., “Microscopic measurements of variations in local (photo)electronic properties in nanostructured solar cells”, Sol. Energ. Mat. Sol. Cells. 119 (2013) 228.
[3] A. Fejfar et al., “Correlative microscopy of radial junction nanowire solar cells using nanoindent position markers”, Sol. Energ. Mat. Sol. Cells, 135 (2015) 106.

ID 45 - Poster

Characterization of ITON thin film grown by Evaporation for sola cell application

**M. Sparvoli[1], R. Onmori[2], I. Abe[2], A. Lopes[2]*
[1]UFABC, CMCC, São Paulo, Brazil
[2]Escola Politécnica USP, PSI, São Paulo, Brazil

The oxynitrides of many metals have been investigated during the last decade. Indium tin oxide (ITO) is an n-type degenerate semiconductor with a band gap that varies between 3.2 and 4.0 eV. Recently it was obtained a new oxide type that combines ITO and nitrogen: the indium-tin-oxynitride (ITON). The incorporation of nitrogen into the film could improve further the optical and structural properties of the ITON films and thus making ITON film an ideal transparent and conducting material for opto-electronic applications.

The deposition of oxide and oxynitride thin films is generally performed in plasma-containing systems like sputtering and pulsed-laser deposition systems. In this work, ITO film were fabricated by evaporation and nitrogen was incorporated by PECVD (plasma-enhanced chemical vapor deposition) technique (300 °C), forming ITON film. The substrate was p-type silicon wafer with 0.5 mm thickness. The thin film was measured with Raman, SEM (Scanning Electronic Microscopy), Hall effect analysis, IxV analysis and RBS (Rutherford Back Scattering). RBS spectra showed the presence of nitrogen. The objective was to confirm that nitrogen was incorporated in ITON film. In fact, it was verified. Furthermore, this material has interesting properties that make it useful in optoelectronic area. It could be used in solar cells or UV sensors.

The spectral response, quantum efficiency and responsivity were estimated for sample. In the case of measurements of quantum efficiency, the greater response is seen in the near infrared region. The solar cell fabricated in this work have a higher sensitivity between 850 and 1050 nm.

By studying these electrical properties is possible to reach conclusions about the application of these materials in sensors in the infrared region as well as solar cells.

ID 46 - Oral

Analysis of Degradation Phenomenon in a-IGZO TFTs under High Power Stress Condition

**S.- W. Lee[1,2], P. J. Jeon[1], K. Choi[1], S.- W. Min[1], H. Kwon[1], Y.- G. Chang[2], S. H. Nam[2], C. Kim[2], B. Lee[2], K.- S. Park[2], S. Im[1]*
[1]Yonsei University, Physics and Applied Physics, Seoul, Korea, Republic of
[2]LG Display, R&D Center, Paju, Korea, Republic of

TFT degradation phenomenon encountered in short channel bottom gate a-IGZO TFTs with etch stopper layer (ESL) under high applied power condition ($V_G = V_D$) leading to self-heating was studied. Negative shift with slight sub-threshold swing (SS) degradation was observed in the initial stage of stress period followed by positive shift with more SS degradation.

To understand the causes of the slight and more SS degradation with stress time, trap density-of-states were measured on stressed TFT samples by photo-excited charge-collection spectroscopy (PECCS) and time-dependent recovery was measured as well; it was found that shallow level-trap states were generated during the first stage of stress and mainly deep level-trap states were generated in the later stage, and also found that the generated trap states were positioned asymmetrically between the source (S) and drain (D) with stress time.

To find out the origin of the two directional threshold voltage shift (ΔV_{th}) with stress time, ΔV_{th} dependence on TFT dimension was studied: the shorter gate length the more negative shift in the first stage of stress. From the result, we conclude that short channel effect might be involved in the degradation and propose degradation models explaining the two directional V_{th} shift under such a high power stress condition; the holes (generated by impact-ionization under high lateral field) trapped at the back interface between the active and the ESL would lower the source/channel barrier, resulting in negative shift of V_{th} and drain current (I_D) increase which would cause device self-heating in return. In the early stage of stress, such feedback-assisted self-heating is weak yet, so that the negative V_{th} shift by hole trapping can be observed, however, in the later stage of stress the feedback-assisted channel heating gets more serious particularly in short channel device so as to cause thermionic electron emission from the active to gate insulator (GI), which leads to electron trapping into GI. As a result, the electron trapping overrides the hole trapping effects, switching the negative V_{th} shift to a positive side.

In conclusion, the combination of hot carrier effect and self-heating in channel was responsible for the degradation; the initial negative shift is likely to originate from hole trapping at the back interface induced by hot electron impact ionization in short channel TFT, and the trapped holes would lower source barrier to result in drain current (I_D) increase and device self-heating which causes thermionic electron emission into GI eventually leading to the positive shift in the later stage.

ID 47 - Poster

Plasmon resonance-induced photoluminescence enhancement of CdTe/CdS quantum dots thin films

*H. Wang[1], *L. XU[1], R. Zhang[1], Z. Ge[1], W. Zhang[1], F. Yang[2], J. Xu[1], Z. Ma[1], K. Chen[1]*
[1]Nanjing University, Nanjing, China
[2]Anhui University, School of Electronics and Information Engineering, Anhui, China

Hybrid structures containing semiconductor quantum dots and metal nanoparticles have attracted great interests and may find potential applications in opto-electronic devices. In this letter, we investigated photoluminescence (PL) intensity can be enhanced by using Au nanoparticles (NPs) of various sizes and shapes with different localized surface plasmon resonance (LSPR) bands. The Au NPs/CdTe/CdS core-shell QDs nanocomposite films were fabricated by layer-by-layer self-assembly method. The morphology of the Au NPs/QDs nanocomposite films were characterized using a scanning electron microscope (SEM), which revealed CdTe/CdS nanocrystals solids were uniformly distributed on the Au NPs monolayer. PL spectra showed that PL intensity of nanocomposite films were boosted after we had incorporated Au nanospheres(NSs) or nanorods(NRs) into the films. The Au NRs incorporation resulted in a slightly higher PL enhancement comparison with that of the samples with Au NSs. Absorption spectra showed the Au NPs incorporation increased the absorption of QDs. Results of time-resolved PL spectroscopy, revealed that the photoluminescence lifetime at the emission peak of CdTe/CdS core-shell QDs was 8.7ns, while in the presence of Au NSs and NRs, the lifetime decreased to 7.6 ns and 6.5 ns, respectively. We thought this was attributed to localized surface plasmonic effects of the Au NPs. The results of our experiments of Au NPs/QDs nanocomposite films suggest that these films are promising candidates for LED and laser devices applications.

ID 48 - Oral

Formation of void-rich network structures in a-SiO:H layers prepared by PECVD

*M. Sato[1], S. King[2], *H. Fujiwara[1]*
[1]Gifu University, Gifu, Japan
[2]Intel, Hillsboro, United States

Recently, crystalline silicon (c-Si) heterojunction solar cells that incorporate hydrogenated amorphous silicon oxide (a-SiO:H) layers are attracting wide interest, as the detrimental Si epitaxial growth of an intended amorphous layer on the c-Si can be suppressed in a-SiO:H/c-Si structures [1]. Nevertheless, despite the progress for the development of high-efficiency a-SiO:H/c-Si solar cells, the network structure of a-SiO:H alloys is not understood well. In this study, by applying spectroscopic ellipsometry (SE) and infrared attenuated total reflection spectroscopy (ATR), we characterize the variation of the a-SiO:H local network structure with the O content. As a result, we found that the formation of $SiH_2(O_2)$ and $SiH(O_3)$ bonding states in the a-SiO:H leads to the void-rich structure in a-SiO:H.

The a-SiO:H layers were prepared by PECVD at 180 °C using different gas flow ratios of $z=[CO_2]/([SiH_4]+[CO_2])$. With increasing z, the O content increases from 9.5 at.% (z=0.2) to 32.2 at.% (z=0.8). Figure 1 shows the ε_2 spectra of the a-SiO:H layers determined by SE. It can be seen that the onset of the light absorption ($\varepsilon_2>0$) shifts toward higher energy with z by the increase in the band gap. However, the amplitude of the ε_2 peak reduces rapidly with z due to the microvoid formation in the amorphous network [2]. Figure 2 shows the ATR spectra of the a-SiO:H layers (open circles) and the results of the peak deconvolution analysis (solid lines). In the a-Si:H (z=0.0), the SiH mode at 2000 cm^{-1} is dominant, but the SiH peak reduces with increasing z and the SiH_2 stretching mode increases drastically. At higher z conditions, the peak amplitude of the $SiH_2(O_2)$ and $SiH(O_3)$ modes increases, together with the formation of the C=O (1700 cm^{-1}) in the a-SiO:H. We find that the reduction of the ε_2 peak amplitude in Fig. 1 shows almost perfect correlation with the generation of the $SiH_2(O_2)$ and $SiH(O_3)$. Accordingly, the porous a-SiO:H network structure can be attributed to the reduced Si-Si bond density due to the formation of the local $SiH_2(O_2)$ and $SiH(O_3)$ bonding states.

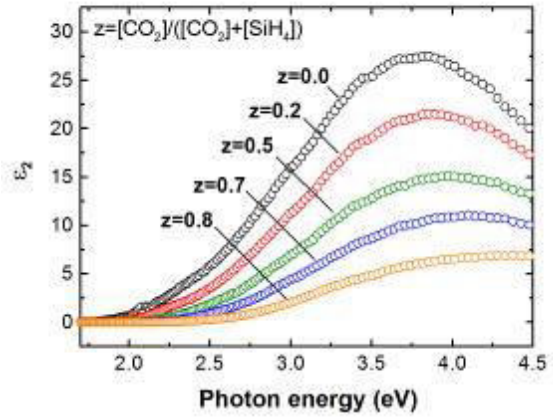

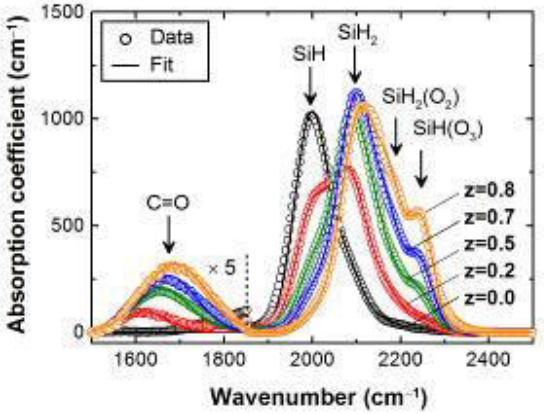

[1] H. Fujiwara, T. Kaneko, and M. Kondo, Appl. Phys. Lett. 91 (2007) 133508.
[2] S. Kageyama, M. Akagawa, and H. Fujiwara, Phys. Rev. B 83 (2011) 195205.

ID 49 - Oral

Real-time characterization of the phase change in $CH_3NH_3PbI_3$ perovskite materials upon exposure to humid air

M. Shirayama[1], T. Miyadera[2], T. Sugita[2], D. Murata[1], S. Hara[1], M. Chikamatsu[2], *H. Fujiwara[1]
[1]Gifu University, Gifu, Japan
[2]AIST, Tsukuba, Japan

Recently, organic-inorganic hybrid perovskite ($CH_3NH_3PbI_3$) solar cells are attracting increased interest, leading to rapid progress toward improving the conversion efficiency, and the highest efficiency now exceeds 20%. Nevertheless, although the perovskite solar cells exhibit excellent solar cell characteristics, the perovskite material has a serious drawback; the $CH_3NH_3PbI_3$ phase is quite unstable in a humid air environment. In this study, by applying real-time spectroscopic ellipsometry, we have characterized the structural change of the perovskite layer in humid air. As a result, we found rapid formation of PbI_2 crystal phase in the surface region upon exposure to humid air due to desorption of CH_3NH_3I from $CH_3NH_3PbI_3$ perovskite layers.

We prepared quite thin $CH_3NH_3PbI_3$ layers (40 nm) on ZnO-coated crystalline Si substrates by a laser evaporation technique in which PbI_2 and CH_3NH_3I source materials are heated by an infrared laser (808 nm). This process allows us to prepare ultra-smooth $CH_3NH_3PbI_3$ layers with roughness of only 5 nm. The change in the optical properties upon air exposure (45% relative humidity) was characterized by real-time ellipsometry.

Figure 1 shows the variation of the layer thickness observed after the air exposure of the $CH_3NH_3PbI_3$ layer. It can be seen that the layer thickness reduces rapidly from 45 nm to 39 nm in the initial 3 hr, followed by the gradual reduction that continues up to 28 hr. The dielectric functions obtained during the air exposure show that (i) visible light absorption decreases gradually and (ii) the intensity of a PbI_2 transition peak at 4.5 eV increases during the air exposure. In particular, the ε_2 peak at 4.5 eV increases rapidly within 2 hr after the air exposure, indicating that the PbI_2 phase formation occurs mainly from the surface region. The x-ray diffraction spectra in Fig. 2 confirm the phase transition from $CH_3NH_3PbI_3$ to PbI_2 upon exposure to humid air. The above result reveals the rapid desorption of the CH_3NH_3I from the $CH_3NH_3PbI_3$ surface, which in turn leads to the formation of the PbI_2 crystal phase. Accordingly, the suppression of CH_3NH_3I desorption from the perovskite surface is a key to achieve long-term stability in hybrid perovskite solar cells.

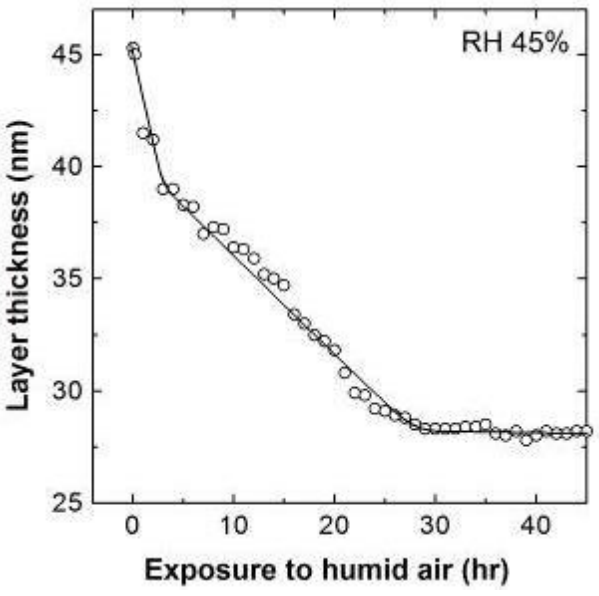

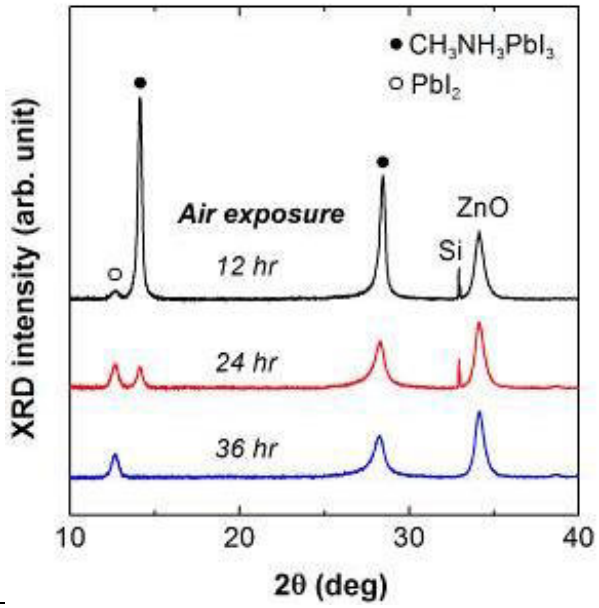

ID 50 - Oral

Fabrication and photovoltaic properties of Si quantum dots/SiC multilayers

**Y. Cao[1], Y. Zhai[1], W. Li[1], J. Xu[1], K. Chen[1]*
[1]Nanjing University, Nanjing, China

Recently, Si quantum dots (Si QDs)/crystalline Si heterojunction solar cells have attracted much attention because they can efficiently match a broad solar spectrum via band engineering, due to the quantum size effect. It has been reported that the spectral response range of Si QDs-based solar cell device was shift with changing the dot size [1, 2]. In the present work, hydrogenated amorphous Si(a-Si:H)/SiC multilayers were grown on both p-type (1-3 Ω•cm) and p^+-type (~ 0.005 Ω•cm) Si wafers by plasma enhanced chemical vapor deposition (PECVD) system. The thickness of a-Si:H and amorphous SiC layer was designed to be 4 nm and 2 nm, respectively. Si QDs/SiC multilayers were formed by annealing the as-deposited samples at 900℃ for 1 hour. The microstructures of samples before and after annealing were examined by Raman spectroscopy, which revealed the crystallization of a-Si after thermal annealing. Phosphorus-doped a-Si film was then deposited to get solar cell device structures. The p-i-n cell had the short current density of 24.1 mA/cm^2 and the power conversion efficiency (PCE) of 6.28% [3]. It was found that the spectral response in the short wavelength region is obviously enhanced after formation of Si QDs, which suggested that the Si QDs is helpful for improving the cell performance. In order to further understand the role of Si QDs, the external quantum efficiency (EQE) spectra of cell devices deposited on P and P^+-Si substrates were measured and compared. It was found that the spectral response of p^+-i-n cell is limited in the wavelength region from 300 nm to 900 nm with the short current density of 9.87 mA/cm^2, which mainly reflects the contribution to the photocurrent from the Si QDs. Furthermore, nano-patterned light trapping structures were used to reduce the optical loss and the corresponding power conversion efficiency is improved.

This work is supported by NSFC (No.11274155 and 61036001) and “973 Program” (2013CB632101).

ID 51 - Poster

Pulse Voltage Induced Phase Change Characteristic of the $Zn_xSb_yTe_z$ Phase-change Prototype Memory Device

*R. Li[1], *L. XU[1], R. Lu[1], T. Wu[1], Z. Ge[1], Z. Ma[1], J. Xu[1], K. Chen[1]*
[1]Nanjing University, Nanjing, China

$Zn_xSb_yTe_z$ thin films are deposited on quartz or glass substrates by electron beam evaporation technique in an ultra-high vacuum. A prototype phase change memory device using ZST thin film was fabricated. The current-voltage test result of the device shows the threshold voltage of ZST531 is 2.4V, which is similar to that of pure $Ge_2Sb_2Te_5$. It can be found that the phase change device of ZST film performs several reading and writing circles and the on/off ratio is nearly 10 times under pulse voltage. The device also shows better switching performances in both SET and RESET process than that of the device using $Ge_2Sb_2Te_5$ film. The results of in situ resistance measurements indicate that, the increase of crystalline temperature (~300 ^oC) and the higher 10 years data retention temperature (~191 ^oC) in ZST were observed. From absorption spectra, the optical band gap of amorphous ZST films is 1.2eV, which is 0.3eV wider than that of pure GST. After annealing at 260 ^oC and 400 ^oC, the optical band gaps of crystalline ZST is 0.7eV and 0.4eV, which are 0.1eV and 0.2eV narrower than that of pure $Ge_2Sb_2Te_5$ thin films respectively.

ID 52 - Poster

Photoluminescence behaviors of undoped and Phosphorous doped nanocrystalline Si/SiO_2 multilayers

**P. Lu[1], W. Mu[1], W. Shao[1], W. Li[1], J. Xu[1], K. Chen[1]*
[1]Nanjing University, Nanjing, China

The study on optical properties of nanocrystalline Si (nc-Si) is currently an interesting topic because it can be applied in many kinds of Si-based optoelectronic devices, such as light emitting diodes and all-Si tandem solar cells. So far, much attention has been attracted on the light emission from un-doped nc-Si materials. However, the influences of dopants on the luminescence behaviors have not been fully understood. In our present work, un-doped and phosphorous-doped (P-doped) nc-Si/SiO_2 multilayers were fabricated in a conventional PECVD system by annealing amorphous Si/SiO_2 or P-doped amorphous Si/SiO_2 multilayers. The structures and photoluminescence behaviors were studied and compared. It was found that crystallization of a-Si sublayers occurred when the annealing temperature exceeds 800℃. With increasing the annealing temperature from 800℃ to 1000℃, the emission centered at 890nm becomes stronger and stronger accompanying with the increased crystallization. However, it is interesting to find the subband emission band centered at around 1200nm in P-doped multilayers after annealing at 800℃, which was not observed in un-doped ones. With increasing the annealing temperature, the intensity of subband emission is gradually reduced meanwhile the emission band around 890nm which is usually observed in un-doped multilayers appears. In order to further understand the luminescence behavior of P-doped multilayers, the changes of PL with varying the P doping concentration was studied. It was found that the PL intensity is enhanced with increasing the P doping concentration and the possible light emission mechanism was briefly discussed. Our results indicate that the luminescence behaviors can be affected by introducing the P dopants which can induces the emission with the suitable wavelength for optical interconnections. This work was supported by “973 project” (2013CB632101) and NSFC (No. 11274155).

ID 53 - Poster

Radial tandem junction Si thin film Solar Cells with advanced junction materials and design

*L. YU[1,2], S. Qian[1], S. Misra[2], J. Lu[1], Z. YU[1], J. Xu[1], J. Wang[1], K. Chen[1], Y. Shi[1], P. Roca i Cabarrocas[2]
[1]Nanjing University, National Laboratory of Solid State Microstructures and School of Electronics Science and Engineering, Nanjing University, Nanjing, China
[2]Ecole Polytechnique/CNRS, LPICM, Palaiseau, France

Silicon thin film solar cells are low-cost, light-weight and environment-friendly photovoltaics, with no fundamental limitation in material supply to reach a Tera-Watt scale deployment. However, in competition with other thin film technologies based on CIGS or CdTe material compounds, a higher conversion efficiency is critical to revive the Si-based thin film technology as a competitive and economic photovoltaics. Structural optimization in planar hydrogenated amorphous Si (a-Si:H) or nanocrystalline Si (nc-Si:H) thin film solar cells has always been limited by a coupled light absorption length and carrier separation distance. In contrast, a nanostructured 3D framework or nanowire-based radial junction architecture brings in exciting opportunities to decouple the optical and electric dimensions, and thus indicate a new and promising route towards a high performance Si thin film solar cells. Our recent progresses in single radial junction a-Si:H thin film solar cells [1-4], built over a matrix of random SiNWs grown via a low temperature plasma-enhanced vapor-liquid-solid (VLS) process, have demonstrated a power conversion efficiency of 9.2% [1,5]. Most importantly, thanks to a thinner absorber layer thickness in the single radial junction cells, the carrier collection distance is greatly shortened, leading to a stronger built-in electric field and a largely improved stability against Staebler Wronski (SW) degradation [6], from typically 15% in planar junctions to only 6% in radial junctions [1].

However, the application of advanced junction materials and tandem solar cell concept in *nanowire-based radial junction* architecture requires a whole new thinking of the structural design, which is critical to fulfill the potentials of nano-structured photovoltaics. Based on a comprehensive knowledge of the multilayer junction materials, we will first demonstrate and assess, in both experimental and theoretical manners, the potential of hydrogenated amorphous Si (a-Si:H) thin film solar cells in a single radial junction configuration. Then, we continue to propose an advanced tandem radial junction (TRJ) structure, with radially stacking a-Si:H/nanocrystalline Si (nc-Si:H) PIN junctions (as schematically illustrated in Figure 1a), and show that a balanced photo-current generation with short circuit current density of J_{sc}=14.2 mA/cm^2 can be readily achievable, while reducing the *expensive* nc-Si:H absorber thickness from 1~3 m (in planar tandem cells) to only 120 nm in TRJ cells (see Figure 1b and 1c for the simulated EQE responses and absorption spectra of a planar or radial tandem junction). These results combined could indicate a clearly-charted route towards future high performance Si thin film photovoltaics with stable power conversion efficiency above 15%.

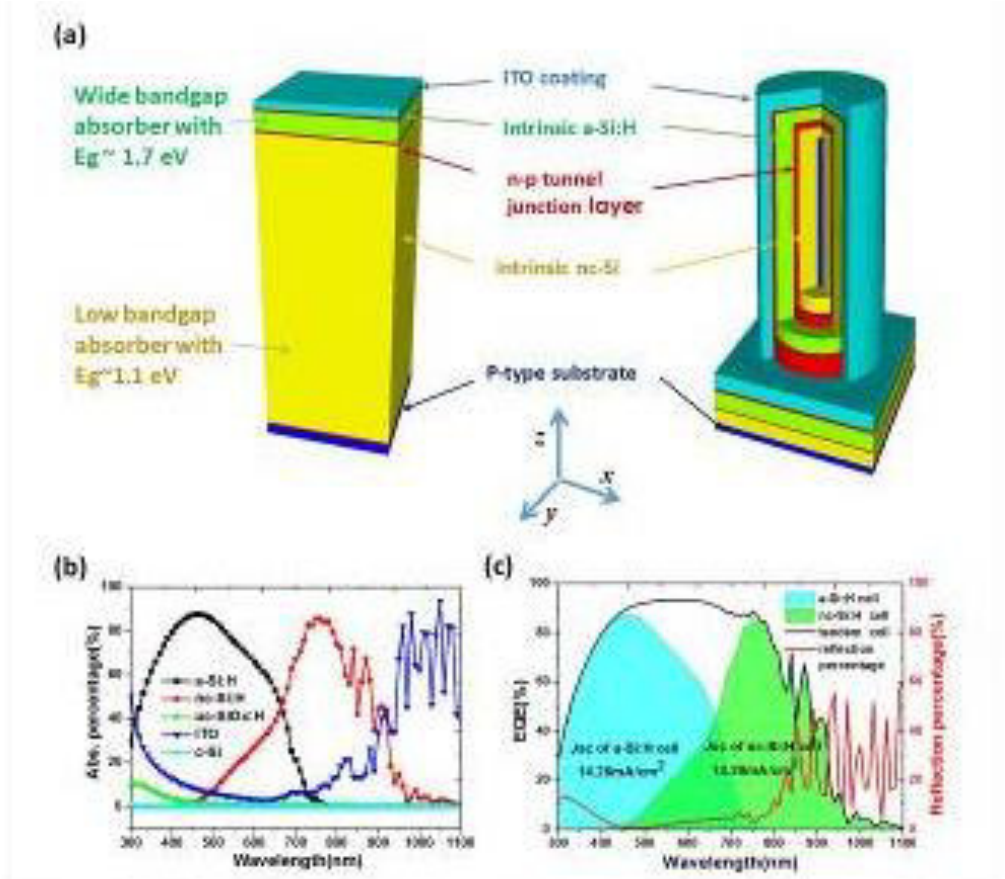

Figure 1: (a) Schematic illustrations of the planar and tandem radial junction solar cells; (b) and (c) provide the absorption (in different material layers) and the balanced EQE response realized in a tandem radial junction solar cell.

[1] S. Misra, L. Yu, M. Foldyna, P. Roca i Cabarrocas, High efficiency and stable hydrogenated amorphous silicon radial junction solar cells built on VLS-grown silicon nanowires, SOL. ENERG. MAT. SOL. C., 118 (2013) 90-95.
[2] L. Yu, F. Fortuna, B. O'Donnell, T. Jeon, M. Foldyna, G. Picardi, P. Roca i Cabarrocas, Bismuth-Catalyzed and Doped Silicon Nanowires for One-Pump-Down Fabrication of Radial Junction Solar Cells, Nano Lett., 12 (2012) 4153-4158.
[3] L. YU, B. O'Donnell, M. Foldyna, P. Roca i Cabarrocas, Radial Junction Amorphous Silicon Solar Cells on PECVD Grown Silicon Nanowires, Nanotechnology, 23 (2012) 194011.
[4] L. Yu, L. Rigutti, M. Tchernycheva, S. Misra, M. Foldyna, G. Picardi, P. Roca i Cabarrocas, Assessing individual radial junction solar cells over millions on VLS-grown silicon nanowires, Nanotechnology, 24 (2013) 275401.
[5] S. Misra, L. Yu, M. Foldyna, P. Roca i Cabarrocas, New Approaches to Improve the Performance of Thin-Film Radial Junction Solar Cells Built Over Silicon Nanowire Arrays, Photovoltaics, IEEE Journal of, 5 (2015) 40-45.
[6] D.L. Staebler, C.R. Wronski, Reversible conductivity changes in discharge-produced amorphous Si, Appl. Phys. Lett., 31 (1977) 292-294.

ID 54 - Oral

Defect-Sensitive Electrical Properties of Hydrogenated Microcrystalline Silicon-Carbon Alloys

*S. Gaiaschi[1], N. Puspitosari[1], C. Longeaud[1], M.- E. Gueunier-Farret[1], E. Johnson[2]
[1]GeePs, Gif sur Yvette, France
[2]LPICM, Palaiseau, France

Thin film silicon multi-junction solar cells are still limited by the light-induced degradation of the amorphous materials they employ. A significant breakthrough could be achieved with new stable material systems having electrical properties similar to those of hydrogenated amorphous silicon or amorphous silicon germanium alloys. Hydrogenated microcrystalline silicon-carbon alloys (µc-$Si_{1-x}C_x$:H) could be promising candidates, as their effective band gap can be controlled through carbon incorporation. When deposited by standard Radio Frequency (RF) - Plasma Enhanced Chemical Vapour Deposition they are characterized by the presence of silicon crystallites embedded in an amorphous silicon-carbon matrix. Extensive structural characterizations revealed that process parameters have a strong influence on the microstructural properties of this mixed-phase material. As microstructure may play a significant role on the defect-related properties, the impact of the independent variation of a selected range of deposition parameters has been studied using several photo-current methods.

In this work, we focused on µc-$Si_{1-x}C_x$:H thin films deposited by standard (13.56 MHz) RF-PECVD at 285 °C, using a highly H_2-diluted silane and CH_4 gas mixture. To study the influence of deposition conditions, three sets of samples were deposited. First, the variation of the CH_4 flow rate was investigated, as the microcrystallinity of the alloys is deteriorated by the presence of carbon-based precursors in the gas phase. Then, the addition of very few sccm of SiF_4 to the gas mixture was tested, as the presence of atomic fluorine leads to materials with a higher crystalline volume fraction. Finally, the variation of the RF-power density was investigated, as it is reported that the crystalline volume fraction of the alloys can be increased by decreasing such parameter. Three photo-current methods: Modulated Photo-Current, Fourier Transform Photocurrent Spectroscopy and Constant Photocurrent Method, were used for the investigation of the evolution of the density of states (DOS) in the forbidden band gap.

Analysis of our results showed that for all silicon-carbon alloys (both µc and amorphous) the DOS is characterized by exponential band tails and some deep defects that, in the case of a-Si:H, have been linked to dangling bonds. All photo-current methods highlighted that the amorphization induced by the variation of both CH_4 flow rate and RF-power density, leads to an increase in the deep defects and a broadening of the band tail. This is also true for materials made with the addition of SiF_4 to the gas mixture, despite the improvement in crystallinity. Experimental results were completed by numerical simulations to match µc-$Si_{1-x}C_x$:H properties to consistent defect models.

The use of photo-current methods for the investigation of defect-related electrical properties highlighted the strong impact of the microstructure on the performance of µc-$Si_{1-x}C_x$:H. It was shown that the most promising route for the development of this new class of materials for photovoltaic applications is the use of low RF-power densities, which result in large grain size, good photo-response and low density of states. Moreover, the combination of several photo-current methods proved to be an efficient approach for the investigation of the DOS of µc-$Si_{1-x}C_x$:H thin films, over the whole forbidden band gap, giving a reliable tool for the assessment of possible defect models.

ID 55 - Poster

Growth of poly-Si film from amorphous silicon-rich oxide using Al film as a catalyst

**Y. Jong-Hwan[1]*
[1]Kangwon National University, Department of Physics, Chuncheon, Korea, Republic of

Polycrystalline silicon (poly-Si) thin films have great potential for electronic and photovoltaic applications such as thin film transistors and solar cells. In particular, they are now drawing attention as a promising alternative for achieving solar cells with both high conversion efficiency and low production cost. Poly-Si thin films can be grown by a range of techniques. Specifically, Al-induced crystallization (AIC), in which Al thin film is used as a catalyst and poly-Si films are formed via layer exchange process, has great potential for fabricating poly-Si films suitable for photovoltaic applications because the resulting poly-Si films feature large grains and a high preferential orientation. As a consequence, a variety of studies to heighten the usability of AIC process, such as annealing conditions, thickness ratio of Al and Si layer, and interfacial oxide layer between Al and Si, have been extensively performed.

In this work we report for the first time the formation of poly-Si thin film from amorphous silicon-rich oxide (SiO_x: 0x films were grown by a conventional PECVD method using a mixture of N_2-diluted SiH_4 (5%) and N_2O gases. SiO_x/Al/glass layered structures were annealed below the eutectic temperature (~577°C) of Al/Si binary system. TEM, ED, and EDX analyses clearly show the appearance of poly-Si layer with large grains after annealing. Furthermore, the resulting poly-Si films show a high preferential (111) orientation as analyzed by XRD spectroscopy. Raman spectroscopic analyses demonstrate that the crystallization is much faster than that of a conventional layer structure of a-Si/Al/glass. Possible explanations for the formation of poly-Si layer in the SiO_x/Al/glass structures are presented.

ID 56 - Oral

Integration of large area Graphene in Semitransparent Perovskite Solar Cells

*F. Lang[1], M. A. Gluba[1], S. Albrecht[1], J. Rappich[1], N. H. Nickel[1], B. Rech[1]
[1]Helmholtz-Zentrum Berlin, Institut für Silizium Photovoltaik, Berlin, Germany

Commonly, the hybrid perovskite methylammonium lead iodide ($CH_3NH_3PbI_3$) is used as absorber in single junction solar cells. However, because of its high absorption strength, sharp absorption onset, and the remarkable low sub-band gap absorption (1) it is of interest for implementation as high band-gap absorber in tandem solar cells. In combination with crystalline silicon tandem efficiencies beyond 30% are proposed (1). However, both a monolithic integration and a four terminal tandem solar-cell design require the development of a highly transparent electrode for the perovskite top solar cell. Promising approaches such as lamination of a silver nanowire mesh (2), poly(3,4-ethylenedioxythiophene) polystyrene sulfonate layers (3), or carbon nanotube networks (4) have been developed, recently. Unfortunately, these electrodes cause a considerable amount of parasitic absorption. On the other hand, sputtering of transparent conductive oxides is delicate since it requires a meticulous control of the process and an additional buffer layer to minimize damage of the organic hole-transport material (1).

In this study, we present the use of macroscopic graphene as highly transparent electrode for semi-transparent perovskite solar cells. Macroscopic graphene hereby is prepared by catalytic decomposition of methane on copper foil within a CVD process (5, 6) with sizes exceeding 1 cm^2 and transferred onto the hole conductor 2',7,7'-tetrakis-(N,N-di-4-methoxy-phenyl-amino)-9,9'-spirobifluorene (spiro-OMeTAD). Such electrodes based on graphene combine excellent optical transmission (T) of 97.4 % with a sheet resistance of 100 W/$\int$ (7), while being fully compatible to solution processing of perovskite solar cells. Solar cells with implemented macroscopic graphene, glass/FTO/TiO_2/$CH_3NH_3PbI_3$/spiro-OMeTAD/graphene, exhibit open circuit voltages that are comparable to that of devices with a standard gold electrode. An optical transmission of around 60 % for the wavelength range below the optical band gap of the perovskite absorber is achieved for such semitransparent cells. At the moment this sub-band gap transmission is limited by parasitic absorption in the FTO substrate and spiro-OMeTAD layer. Single light-pass efficiencies of 6.2 % are achieved with graphene electrodes compared with 10.2 % on the gold reference. Superior light management of semi-transparent graphene versus gold electrodes is observed in an internal quantum efficiency (IQE) analysis, showing that the parasitic absorption is reduced in semitransparent devices. Therefore, highly transparent graphene electrodes implemented in semitransparent perovskite solar cells are a game changer in the development of perovskite/silicon tandem solar cells.

(1) Löper P et al. *Phys. Chem. Chem. Phys.*, p. 1619. (2014)
(2) Bailie CD et al. *Energy Environ. Sci.* 8, p. 956. (2014)
(3) Jiang F et al. . 23(3), p. 3748. (2015)
(4) Li Z et al. *ACS Nano*. 8(7), p. 6797. (2014)
(5) Li X et al. *Science*. 324(5932), p. 1312. (2009)
(6) Gluba M a. et al. *Appl. Phys. Lett.* 103(7), p. 073102. (2013)
(7) Bae S et al. *Nat. Nanotechnol.* 5(8), p. 574. (2010)

ID 57 - Poster

Post-synthesis HF treatment of chemically etched Si nanowires for effective removal of surface oxides: investigation by means of electron energy loss near edge fine structure

**F. Cummings[1,2], S. Nqgoloda[2], T. Muller[2], G. Malgas[2], C. Arendse[2]*
[1]University of the Western Cape, Electron Microscope Unit, Bellville, South Africa
[2]University of the Western Cape, Department of Physics, Bellville, South Africa

Arrays of one-dimensional silicon nanowires (SiNWs) synthesized by means of metal-assisted chemical etching (MaCE) show great potential for application in photovoltaics as both a vectorial transport medium for photon-generated charge carriers, as well as anti-reflection of incoming light rays for improved light absorption. Optimization of both the opto-electronic and structural properties of these materials is thus important to realize their full potential. During typical MaCE synthesis the incorporation of O^{2-} from the native electrolyte solution, as well as post-synthesis ambient surface oxidation, lead to the formation of an amorphous Si_xO_y encapsulation layer, which effectively introduces an undesirable wide bandgap insulating layer, screening the crystalline Si structure.

In this work a post-synthesis HF treatment of the SiNW array, for the removal of these surface oxides, is introduced. Scanning and transmission electron microscopy show that the HF treatment introduces no adverse structural features within the SiNWs, with average diameters of 50 nm and lengths up to 20 µm obtained after 80 minutes of etching. Scanning transmission electron microscopy-coupled energy dispersive x-ray spectroscopy (STEM-EDS) shows an oxygen concentration of less than 1 at% for post HF treatment compared to 5% of the as-synthesized nanowire array.

STEM-coupled electron energy loss spectroscopy shows that the HF treatment yields no significant change in the electron energy loss near edge fine structure (ELNEFS) and hence the Si electronic structure across the diameter of the nanotube. Rather, an evolution of the surface Si-H bond concentration is noted from the ELNEFS post HF treatment, which corroborates the effective removal of Si-O, as noted from the STEM-EDS results. This indicates further passivation of the dangling surface Si with H^- from the HF. Selected area electron diffraction patterns collected along the [012] zone axis show that the diamond crystal structure of the SiNWs is not affected by the HF treatment, with a lattice constant a = 0.527 nm recorded, which is in good agreement with that obtained from the bulk x-ray diffraction result of 0.542 nm.

ID 58 - Oral

Enhanced stability of P3HT/polycrystalline silicon hybrid solar cells

*M. Zellmeier[1], S. Kühnapfel[1], J. Rappich[1], N. H. Nickel[1]
[1]Helmholtz-Zentrum Berlin, Institut für Silizium-Photovoltaik, Berlin, Germany

Hybrid solar cells combining crystalline silicon (c-Si) and polymers are a promising approach for the reduction of production costs while maintaining the good performance expected from wafer based devices. In recent years, a strong scientific interest led to a steep increase in performance. Hybrid devices easily exceeded 10 % efficiency with the material combinations PEDOT:PSS[1] and P3HT[2]. These values become even more appealing since the formation of these junctions is achieved by low temperature solution processing. To further reduce the costs of polymer/c-Si hybrid solar cells the single crystal wafer has to be replaced by thin-film polycrystalline silicon.

In this study, we present the realization of this concept. The thin-film silicon absorber is prepared directly on glass. The 10 µm thin amorphous silicon (a-Si) layer was crystalized by a liquid phase process. By moving a line shaped laser across the substrate, the a-Si film is molten and subsequently recrystallizes forming a large-grained polycrystalline material[3]. The active interface is passivated by methyl groups bonded to the silicon in a one-step grafting process[4, 5] before spin coating 20 nm P3HT as an emitter and applying the contacts on the same side. The 620 nm thick TI/Al absorber contact is placed outside the 610nm thick MoO_3/Au emitter contact, which defines the active area of 0.64 cm². The resulting inverted device structure was illuminated from the glass side. The measured open circuit voltage, short current density, and fill factor amounted to V_{OC} = 552 mV, j_{SC} = 23.93 mA cm^{-2} and FF = 49.8 %, respectively. This resulted in a power conversion efficiency of η = 6.6 %.

For comparison, wafer-based hybrid solar cells with a conventional stacked structure (Al back contact/c-Si/P3HT/semitransparent Au front contact) were fabricated. They exhibited a superior performance. The solar cell parameters amounted to V_{OC} = 617 mV, FF = 72.6 %, η = 9.2 %.

The inverted device structure has strong advantages nonetheless. External quantum efficiency measurements exhibit an influence of the organic layer on the current generated in the silicon. The high absorption coefficient of P3HT leads to parasitic absorption in the emitter layer, which is avoided in the inverted devices. In combination with the semitransparent metal front contact, a current density of only j_{SC} = 20.6 mA cm^{-2} was achieved in the wafer cells. In addition, the inverted device structure exhibits a significantly improved long-term stability in ambient conditions. While the conventional stacked devices lose their photoactive properties within one day, the inverted devices do not exhibit degradation even after one month. The thick metal anode provides a self-encapsulation for the active layer, making the inverted device structure a promising design towards commercialization of hybrid solar cells.

[1] S. Jeong, E.C. Garnett, S. Wang, Z. Yu, S. Fan, M.L. Brongersma, M.D. McGehee, and Y. Cui, Nano Lett. 12, 2971 (2012).
[2] S. Avasthi, S. Lee, Y.-L. Loo, and J.C. Sturm, Adv. Mater. 23, 5762 (2011).
[3] S. Kühnapfel, N.H. Nickel, S. Gall, M. Klaus, C. Genzel, B. Rech, and D. Amkreutz, Thin Solid Films 576, 68 (2015).
[4] V. V. Brus, M. a. Gluba, X. Zhang, K. Hinrichs, J. Rappich, and N.H. Nickel, Phys. Status Solidi Appl. Mater. Sci. 211, 843 (2014).
[5] F. Yang, K. Roodenko, R. Hunger, K. Hinrichs, K. Rademann, and J. Rappich, (2012).

ID 59 - Oral

Crystallization in the canonical phase-change material $Ge_2Sb_2Te_5$: a memory effect in GST-225

**R. O. Jones[1], J. Akola[2], J. Kalikka[3]*
[1]Forschungszentrum Jülich, PGI-1, Jülich, Germany
[2]Tampere University of Technology, Tampere, Finland
[3]Singapore University of Technology and Design, Singapore, Singapore

Phase-change materials are chalcogenide alloys that are ubiquitous in the world of rewritable optical storage media, including DVD-RW and Blu-ray Disc. Nanosized bits in a thin polycrystalline layer are switched reversibly and extremely rapidly between amorphous and crystalline states by laser irradiation or resistive heating. Crystallization of amorphous bits is the time-limiting process in the write/erase cycle and has been the subject of much speculation. We have studied the process in amorphous $Ge_2Sb_2Te_5$ (GST) using four extensive (460 atoms, up to 5 ns) density functional/molecular dynamics simulations at 600 K. This phase change material is a rare system where crystallization can be simulated without adjustable parameters over the physically relevant time scale. Crystallization is accompanied by an increase in the number of "ABAB squares" (A: Ge, Sb; B: Te), percolation, and the occurrence of low-frequency localized vibration modes. A sample with a history of order crystallizes completely in 1.2 ns, but ordering in others was less complete, even after 5 ns, and can lead to more than one crystalline cluster, i.e. a polycrystalline material. The amorphous starting structures without "memory" display phases (>1 ns) with sub-critical nuclei (10-50 atoms) ranging from nearly-cubical blocks to strings of ABAB squares and AB bonds extending across the cell. Percolation initiates the rapid phase of crystallization and is coupled to the directional p-type bonding in metastable GST. Cavities play a crucial role, and the final ordered structure is distorted face-centered-cubic with a sublattice containing predominantly Te atoms. These extremely extensive calculations demonstrate that much shorter simulations on smaller samples can lead to qualitatively incorrect findings.

ID 60 - Poster

Compositional study by SIMS and RBS of oxidized silicon nitride thin films prepared by PECVD

*S. Meziani[1], A. Moussi[1], L. Mahiou[1], R. Outemzabet[2]
[1]Centre de Recherche en Technologie des Semi-conducteurs pour l'Energétique, DDCS, Algiers, Algeria
[2]USTHB, Algiers, Algeria

Stoichiometric silicon nitride (SiN) thin films were grown on multicristalline silicon (mc-Si) by Plasma Enhanced Chemical Vapour Deposition (PECVD) at temperature 380°C and flow gas ratio R = 6 for ammoniac (NH_3) and silane (SiH_4) gaz mixture. After a deposition process, these films were oxidized in dry oxygen ambient at 950°C. Then thermal annealing at different annealing temperature was made. Secondary ion Mass Spectroscopy (SIMS) and Rutherford Backscattering Spectroscopy (RBS) were employed for analyzing quantitatively chemical composition and stoichiometry in oxide/nitride (ON) stacked films. The effect of annealing temperature on the chemical composition of ON structure is investigated. It is shown that high-oxygen contents exist on the surface. Indeed, this is due to the oxidation growth effect on nitride. It was observed that after oxidation and annealing SiN, we have found thickness of 0.037 µm, 0.069 µm for SiO_2 and SiN, respectively, with the presence Si_2O_2N thin film with thickness of 0.006 µm.

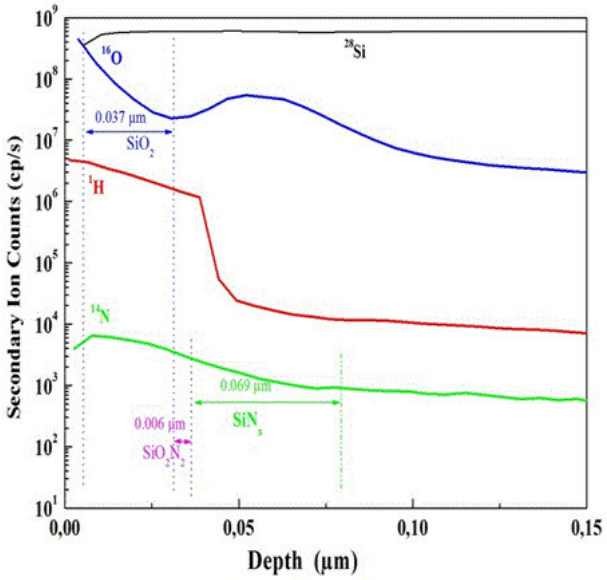

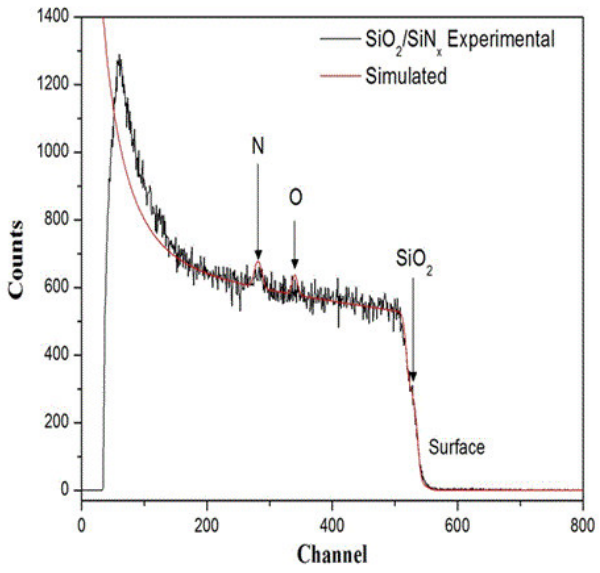

ID 61 - Oral

Complementary Inverter by Mo-based Chalcogenide Nanosheet Channels: a Few Layer α-$MoTe_2$ and MoS_2

*A. Pezeshki[1,2], S. H. Hosseini Shokouh[2], S.- W. lee[2], S. Im[2]
[1]Yonsei university, physics, Seoul, Korea, Republic of
[2]Yonsei University, Institute of Physics and Applied Physics, seoul, Korea, Republic of

Two-dimensional (2D) layered nanomaterials for semiconductor channel have recently been attracting great attentions from researchers in many possibilities of future applications such as high speed electronics, flexible electronics, and immunity of short channel effects in scale-down transistors. Transition-metal dichalcogenides (TMDs) are well-known type of 2D nanomaterial with the common formula MX_2, where M is a transition metal element from group IV-VII (M = Mo, W, Nb, Re, and so on) while X is a chalcogen element (X = S, Se, Te). In general, M atoms are sandwiched between X atoms to form a single layer, and each layer can be stacked together via van der Waals forces, which make 2D TMDs easily cleaved by scotch tape, or other similar techniques. Among TMD families with ultra-thin layers, molybdenum disulfide (MoS_2), tungsten dislenide (WSe_2), and molybdenum ditelluride (α-$MoTe_2$) are semiconductors with their bandgaps of more than 1 eV; depending on their layer numbers, the band gap ranges from 1 eV to 1.8 eV while their band gap properties changes from indirect to direct type as their layer number decreases to monolayer. The band gap of $MoTe_2$ is almost the same as that of silicon, which forecasts that $MoTe_2$ may become a candidate to be used along with silicon although further study must be followed in this regard.

In the present study, we demonstrated high performance heterogeneous but Mo-based complementary (Mo-based CMOS) inverters which take α-$MoTe_2$ as a p-type channel for a patterned back gate FET and MoS_2 as n-channel for the other FET in the inverter. Our p-channel FET with nanosheet α-$MoTe_2$ showed much higher ON-current than previously reported ambipolar $MoTe_2$ FETs, since we used a properly-deep work function metal, platinum (Pt), for S/D contact. As a result, our Mo-based CMOS device with nanosheet channels demonstrated high CMOS performances in switching dynamics and electrostatic behavior; high voltage gain of ~ 12 and 60 μs switching delay at longest were displayed at a few volts. (The switching speed measurements were limited by our equipment (up to only 1 kHz) but we regard that much higher switching speed must have been guaranteed from our CMOS inverter.)

ID 62 - Oral

Thermally evaporated MoO_3 thin films: Structural and optical properties and application in solar cells

*P. Calta[1], G. Yang[2], D. Deligiannis[2], O. Isabella[2], P. Šutta[1], M. Zeman[2]
[1]University of West Bohemia, New Technologies-Research Centre, Plzen, Czech Republic
[2]Delft University of Technology, Photovoltaic Materials and Devices – ESE, Delft, Netherlands

Transition metal oxide semiconductors have attracted attention during the last few years as they show a wide variety of optical, electrical and magnetic properties and provide good opportunities for technological applications. In this contribution, thin-film molybdenum trioxide (MoO_3) was investigated and used as an effective hole injection layer in silicon heterojunction solar cells. We synthesized thin films of MoO_3 via thermal evaporation (molybdenum (VI) oxide powder, purity of 99.5%, evaporated from alumina boat) at room temperature under an operating pressure of 10^{-6} mbar. Single layers (up to 200-nm thick) were prepared simultaneously on Corning glass and Si substrates. The influence of different deposition rates (0.02 - 0.4 nm/s) and post-deposition annealing (air atmosphere at various temperatures in the range of 200 - 500 °C) on the structure, chemical binding configuration and optical properties of MoO_3 films was studied. The structure of MoO_3 was characterized by means of X-ray diffraction (XRD), Raman, Fourier Transform Infrared (FTIR) and UV-Vis spectroscopy and spectroscopic ellipsometry (SE) measurements. The as-deposited films were transparent and light blue in colour. The XRD studies revealed that the as-deposited films had amorphous structure. The presence of absorption peaks in FTIR spectra in the range between 850 and 1000 cm^{-1} highlights the formation Mo-O bonds (stretching vibration modes). Deposited films exhibited a high optical transmittance (>80%) in the visible range, while the absorption edge was observed at 400 nm. The optical band gap and the refractive index of the films, formed at room temperature, were 3.02 eV and 2.03, respectively. The electrical conductivity and the activation energy (evaluated from the Arrhenius plots) of as-deposited films were about 9×10^{-8} S/cm and 0.45 eV, respectively. Finally, we used transparent MoO_3 as a hole-injection layer in flat silicon heterojunction solar cells (1cm^2 area of the device). The best cell showed performance with a fill factor of 0.67, a short circuit current of 36 mA/cm^2, an open-circuit voltage of 677 mV, and a conversion efficiency equal to 16.5%.

ID 63 - Poster

Effect of additional electron acceptor in hybrid ZnO:P3HT:PCBM spin-coated films for photovoltaic application

**T. Muller[1], T. A. Ramashia[1], D. Motaung[2], F. Cummings[3], G. Malgas[1], C. Oliphant[4], C. Arendse[1]*
[1]University of the Western Cape, Physics, Bellville, South Africa
[2]Council for Scientific and Industrial Research, National Centre for Nano-Structured Materials, Pretoria, South Africa
[3]University of the Western Cape, Electron Microscope Unit, Bellville, South Africa
[4]National Metrology Institute of South Africa, Pretoria, South Africa

The power conversion efficiency (PCE) of organic photovoltaics (OPVs) is influenced by the choice of electron acceptor material, the structure of the polymer, the morphology of the film, the interfaces between the layers, and the ratio between the electron acceptor material and the polymer. In order to become competitive with conventional silicon based PV cells, the limited efficiencies of OPVs need to be improved. As such, the low mobility of charge carriers caused by the short exciton diffusion length in the active layer needs to be enhanced. In this regard attempts to incorporate inorganic semiconductors into organic blends in hybrid organic solar cells, in various configurations, have so far been promising.

In this work ZnO nanoparticles were mixed into the poly (3-hexylthiophene) (P3HT):[6,6]-phenyl-C61-butyric acid methyl ester (PCBM) blend, and used as additional acceptors of electrons. The thermo-gravimetric analyses revealed improved thermal stability of P3HT upon incorporating ZnO in the polymer matrix. The photovoltaic properties demonstrated that the addition of ZnO nanoparticles in the P3HT:PCBM bulk-heterojunction increases the PCE from a baseline of ~1.0 % in the P3HT:PCBM system to 1.7% in the ZnO:P3HT:PCBM ternary system. Upon loading ZnO nanoparticles in the P3HT:PCBM matrix to a 2:1:1 ratio, the PCE decreases, due to a large phase separation between the polymer, PCBM and ZnO induced by ZnO agglomerations, which resulted in increased surface roughness of the active layer.

ID 64 - Poster

Isothermal crystallization of GST225 amorphous thin films and estimation of information reliability of PCM cells.

*S. Kozyukhin[1,2], A. Sherchenkov[3], A. Babich[3], Y. Vorobyov[4], N. Vishnyakov[4], O. Boytsova[1]
[1]Kurnakov Institute of General and inorganic Chemistry of RAS, Moscow, Russian Federation
[2]Tomsk State University, Department of Chemistry, Tomsk, Russian Federation
[3]National Research University of Electronic Technology, Faculty of Intellectual Technical Systems , Zelenograd, Moscow, Russian Federation
[4]Ryazan State Radio Engineering University, Ryazan, Russian Federation

Chalcogenide compounds of Ge-Sb-Te system are currently in use as materials for the phase-change memory (PCM) application, and one of the most promising among them is $Ge_2Sb_2Te_5$ (GST225) composition.Clarification of the various aspects of isothermal crystallization phenomena is an important scientific and practical task as these issues are directly related with the reliability of data storage in the PCM devices based on this material. In this study we investigated the isothermal crystallization process of amorphous films and found correlation of experimental results with the estimated information reliability.

Thin films were prepared by thermal evaporation of pre-synthesized polycrystalline material on the c-Si substrates. The pressure in the chamber during the deposition was 10^{-4}Pa, the maximum temperature of evaporator was 900K. The structures of synthesized materials and thin films were investigated by XRD. The composition of thin films was determined by Rutherford Backscattering Spectroscopy (RBS) and Energy Dispersive X-Ray Analysis (EDXRA). Isothermal crystallization of thin films was carried out in an inert atmosphere at varying time-temperature regimes: ΔT=423-493K, Δt=15-180 min. The choice of these regimes was based on the earlier published data and our preliminary experiments. We also used for crystallization of amorphous films laser irradiation at room temperature. For this purpose we used laser (λ = 532 nm, P = 13 mW), the beam diameter is of about 5μm, exposure time is a few seconds. This allowed us to compare the two processes of phase transition: in isothermal conditions and external influences. We used the complex of methods to determine the evolution of the amorphous thin films: 2θ scan (thin film XRD, Rigaku), DSC-50 (Shimadzu), AFM (Solver Pro NT-MDT), SEM (JEOL), Raman spectroscopy and optical microscopy (NTEGRA Spectra NT MDT).

The presence of crystalline phase in thin film was determined by the appearance of reflexes in X-Ray spectrum, changes in the Raman spectrum, and increasing of the reflectance and roughness (R_{ms}) of thin film. It was found that noticeable crystallization begins for the temperature range of 423-453K after the annealing during several hours, whereas at T=453K and above it crystallization process happen almost immediately, and after 30 min. of heat treatment thin film became completely crystalline. The time-temperature regimes were also identified in which the films were crystalline only partly. The correlation between the experimental data and results of the calculations of information reliability of PCM cells was revealed. For this purpose we used the approach proposed in [1] according to which information reliability of the RESET state can be estimated on the basis of Kolmogorov model, and taking into account the size of PCM cell and percolation threshold (P_{th} = 0.3) also.

Comparison of the Raman spectra of GST225 amorphous thin film, crystalline thin film after thermal annealing and thin film after laser irradiation showed that the strongest changes were observed after laser irradiation (Fig.1). As these results indicate, the process of phase transition is dependent on the driving force of the process and its nature.

Thus, we have examined an isothermal crystallization of GST225 amorphous thin films and compared obtained results with the calculations of reliability of data storage in PCM cells.

The study was supported by RFBR (14-03-00314).

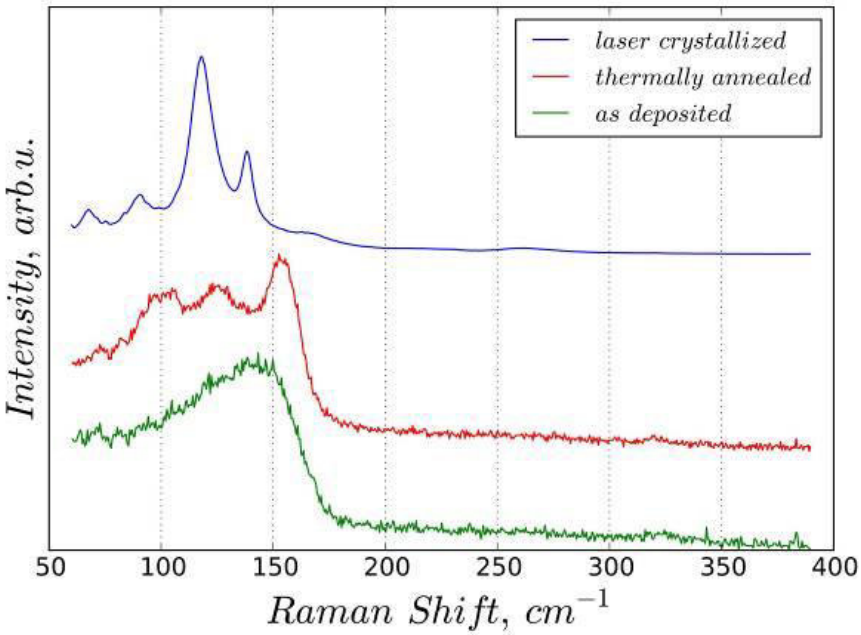

Fig.1. Variations in the Raman spectrum of GST225 thin film with different methods of crystallization

[1] K.N. Egarmin, E.N. Voronkov, S.A. Kozyukhin. Inorg. Mat., 2013, 49 (9), 878.

ID 65 - Poster

Simulation Insights into Electronic Properties of Disordered Organic Semiconductors

*N. Vukmirovic[1], M. Mladenovic[1]
[1]Institute of Physics Belgrade, Belgrade, Serbia

Organic semiconducting materials exhibit complex atomic structures with a lack of periodicity that lead to charge carrier localization which, in turn, strongly affects electronic transport properties of these materials. To understand charge carrier localization and electronic transport in organic semiconductors, simulations that take into account the details of the atomic structure of the material are of utmost importance. Computational methods that can be used to simulate the electronic properties of organic semiconductors are reviewed and an overview of some results that have been obtained from such simulations is given. Using these methods the effects of static disorder, thermal disorder and interfaces between domains are investigated and the microscopic origin of these effects is identified. It is shown that in strongly disordered conjugated polymer materials the main origin of the localization of charge carrier wave functions is disordered long-range electrostatic potential. In ordered polymers, thermal disorder of main chains leads to wave function localization. In small molecule based organic semiconductors, grain boundaries introduce localized trap states at the points where electronic coupling is the strongest. It is also demonstrated that detailed atomistic simulations are necessary for quantitative and sometimes even qualitative description of charge mobility in organic materials.

[1] M. Mladenović and N. Vukmirović, Adv. Funct. Mater. (2015), DOI: 10.1002/adfm.201402435

ID 66 - Poster

Nonequilibrium Electrical Transport in Materials with Localized Electronic States

**N. Vukmirovic[1], V. Jankovic[1]*
[1]Institute of Physics Belgrade, Belgrade, Serbia

A broad range of disordered materials contain electronic states that are spatially well localized. In this work we studied the electrical response of such materials to external terahertz electromagnetic field [1]. We obtained expressions for nonequilibrium terahertz conductivity of a material with localized electronic states and weak electron-phonon or electron-impurity interaction. The expression is valid for any nonequilibrium state of the electronic subsystem prior to the action of external field. It gives nonequilibrium optical conductivity in terms of microscopic material parameters and contains both coherences and populations of the initial electronic subsystem's density matrix. Particularly, in the case of incoherent nonequilibrium state of the electronic subsystem, the optical conductivity is entirely expressed in terms of the positions of electronic states, their nonequilibrium populations, and Fermi's golden rule transition probabilities between the states. The same mathematical form of the expression is valid both in the case of electron-phonon and electron-impurity interaction. Moreover, our result for the nonequilibrium optical conductivity has the same form as the expressions previously obtained for the case of equilibrium. Our results are expected to be valid at sufficiently high frequencies, such that the period of the external field is much smaller than the carrier relaxation time. We apply the derived expressions to two model systems, a simple one-dimensional Gaussian disorder model and the model of a realistic three-dimensional organic polymer material obtained using previously developed multiscale methodology [2]. We note that the simple one-dimensional model captures the essential features of the mobility spectrum of a more realistic system. Furthermore, our simulations of the polymer material yield the same order of magnitude of the terahertz mobility as previously reported in experiments.

[1] V. Janković and N. Vukmirović, Phys. Rev. B 90, 224201 (2014).
[2] N. Vukmirović and L.-W. Wang, Nano Lett. 9, 3996 (2009).

ID 67 - Poster

EPR and Raman Studies of a-$Si_{1-x}C_x$:H<Er> Films Doped with Erbium from $Er(pd)_3$ Polymer

*V. Kudouarova[1], A. Troitskii[2], A. Smirnov[1]
[1]A.F.Ioffe Physical-technical Institute, physica of semiconductors, St-Petersburg, Russian Federation
[2]Lomonocov Moscow State University, physica, Moscow, Russian Federation

The electron paramagnetic resonance (EPR) has been studied in a-$Si_{1-x}C_x$:H<Er> films doped with erbium from the $Er(pd)_3$ polymer. The technique used to obtain a-$Si_{1-x}C_x$:H<Er> films combined the high-frequency decomposition of a mixture of gases $(SiH_4)_a + (CH_4)_b$ with the simultaneous sputtering of an Er-containing complex compound $Er(pd)_3$.

The content of CH_4 in the gas mixture (parameter *b*) was varied from 0 to 70%. The fabrication conditions of the films and their composition were described in detail in [1]. The goal of the present study was to determine the density of dangling bonds in order to elucidate the mechanism of excitation and quenching of the Er-related photoluminescence in a-$Si_{1-x}C_x$:H<Er>.

The EPR in a-$Si_{1-x}C_x$:H<Er> has been extensively studied . It was found that an increase in *x* leads to a more pronounced porosity of the films and higher density of dangling bonds. The novelty of the present study consists in that a nonmonotonic variation of the density of dangling bonds is observed in doping of a-$Si_{1-x}C_x$:H (introduction of Er from the $Er(pd)_3$ compound).

The EPR spectra show a broad signal with g = 2.005 and width of 8 Gs. According to published data, this signal can be attributed to dangling bonds of silicon in the amorphous phase. It was found that the spin density N_s varies nonmonotonically with the composition of the gas mixture. An increase in the content of CH_4 in the gas mixture leads first to a three-orders-of-magnitude decrease in the spin density and then to its increase (at CH_4 > 40%). These data are in good agreement with the results of Raman studies.

On the basis of the results obtained in the study, it is possible to choose the range of gas mixture compositions (b < 40%) in which introduction of Er from the $Er(pd)_3$ complex leads to ordering of the matrix of amorphous silicon and, as a consequence, to a decrease in the density of dangling bonds of silicon. Presumably, Er present in the local environment of oxygen heals dangling bonds of silicon and reduces the porosity of films. For these compositions of a-$Si_{1-x}C_x$:H<Er>, an increase in intensity is observed for the Er-related photoluminescence (1.54 μm) at room temperature.

[1] V. Kh. Kudoyarova, V. A. Tolmachev, and E. V. Gushchina, *Fiz. Tekhn. Poluprovodn*. **47**, 353 (2013).

ID 68 - Poster

Nonequilibrium Electrical Transport in Materials with Localized Electronic States

*V. Jankovic[1], *N. Vukmirovic[1]*
[1]Institute of Physics Belgrade, Scientific Computing Laboratory, Belgrade, Serbia

A broad range of disordered materials contain electronic states that are spatially well localized. In this work we studied the electrical response of such materials to external terahertz electromagnetic field [1]. We obtained expressions for nonequilibrium terahertz conductivity of a material with localized electronic states and weak electron-phonon or electron-impurity interaction. The expression is valid for any nonequilibrium state of the electronic subsystem prior to the action of external field. It gives nonequilibrium optical conductivity in terms of microscopic material parameters and contains both coherences and populations of the initial electronic subsystem's density matrix. Particularly, in the case of incoherent nonequilibrium state of the electronic subsystem, the optical conductivity is entirely expressed in terms of the positions of electronic states, their nonequilibrium populations, and Fermi's golden rule transition probabilities between the states. The same mathematical form of the expression is valid both in the case of electron-phonon and electron-impurity interaction. Moreover, our result for the nonequilibrium optical conductivity has the same form as the expressions previously obtained for the case of equilibrium. Our results are expected to be valid at sufficiently high frequencies, such that the period of the external field is much smaller than the carrier relaxation time. We apply the derived expressions to two model systems, a simple one-dimensional Gaussian disorder model and the model of a realistic three-dimensional organic polymer material obtained using previously developed multiscale methodology [2]. We note that the simple one-dimensional model captures the essential features of the mobility spectrum of a more realistic system. Furthermore, our simulations of the polymer material yield the same order of magnitude of the terahertz mobility as previously reported in experiments.

[1] V. Janković and N. Vukmirović, Phys. Rev. B 90, 224201 (2014).
[2] N. Vukmirović and L.-W. Wang, Nano Lett. 9, 3996 (2009).

ID 69 - Oral

Silicon Thin Film Photodetectors for Multi-channel Fluorescence Detection in a Microfluidic Point-of-Care Testing Device

*M. Berner[1], R. Rothemund[1], U. Hilbig[2], S. Vollmer[1], M. B. Schubert[1], G. Gauglitz[2]
[1]University Stuttgart, Institute for Photovoltaics, Stuttgart, Germany
[2]University Tübingen, Institute for Phyisical and Theoretical Chemistry, Tübingen, Germany

Fluorescence spectroscopy is widely used in analytical chemistry, bioanalytics and medicine. By monitoring fluorescence in a direct test format with no need for time-consuming replication methods, like the polymerase chain reaction (PCR), the European NANODEM consortium pursues to demonstrate a miniaturized Point-of-Care Testing (POCT) device for quasi-continuous post-surgical control of critical immunosuppressant concentrations [1]. Amorphous silicon (a-Si:H) based thin film photodetector arrays contribute to miniaturizing the POCT device and to integrating multi-analyte fluorescence detection with appropriate microfluidic chips. A peculiar challenge arises from the very low fluorescence signals of the specific labels, which are suited for monitoring the desired targets in the dialysate samples of the POCT device [1]. Therefore ultimate sensitivity of the photodetectors and efficiency of the optical excitation and detection paths are needed to discriminate the low fluorescence signals generated inside the microfluidic channel against the excitation and corresponding stray light. In contrast to the more common excitation rejection by angle-selective interference filters, this contribution focuses on optimizing multi-channel a-Si:H photodiode arrays for fluorescence monitoring by employing angle-independent absorption filters for excitation cut-off. Our properly tailored photodiodes present an external quantum efficiency $EQE_{\text{cut-on}}$ = 52.4 % at the filter cut-on wavelength $\lambda_{\text{cut-on}}$ = 645 nm and $EQE_{\text{em,peak}}$ = 31.3 % at the fluorescence emission peak wavelength $\lambda_{\text{em,peak}}$ = 675 nm. Operating the diodes with bias voltages down to -5 V, the external quantum efficiency can be boosted to $EQE_{\text{cut-on}}$ = 59.7 % and $EQE_{\text{em,peak}}$ = 34.8 %. Due to the low dark current density $J_{\text{dark}} \leq 10^{-10}$ Acm^{-2}, the four photodiodes per detector chip, with 1 mm^2 area each, allow the sensing of fluorescence intensities $I_f \leq 1$ nWcm^{-2}. Laser excited fluorescence measurements of the carboxylic acid dye Dyomincs DY-636 (diluted with purified water to a molar concentration c = 1.31 µM) in the microfluidic channel evince the suitability of the multi-channel photodetector chips for the NANODEM test format.

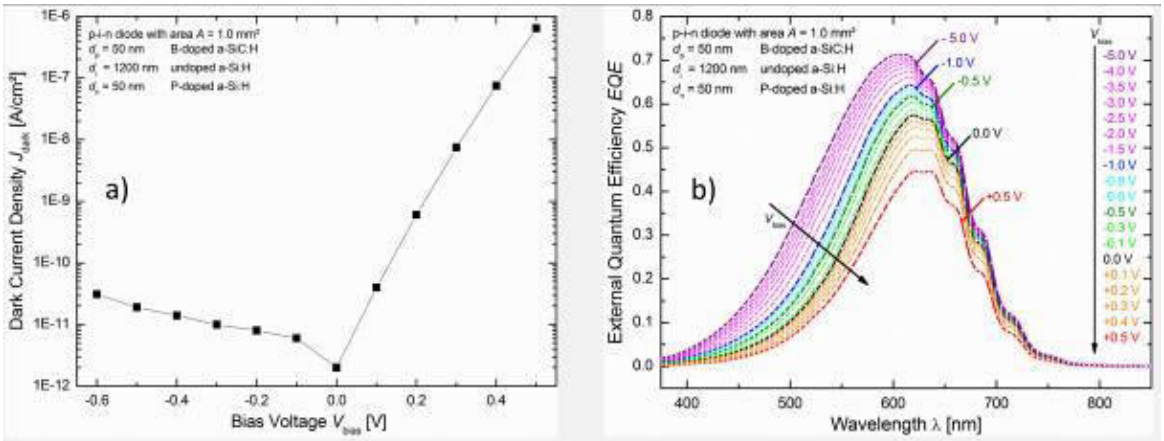

Fig.1. Characteristics of the a-Si:H p-i-n diode with an intrinsic layer thickness d_i = 1200 nm and with an area A = 1.0 mm². (a) Dark current density J_{dark} and b) external quantum efficiency EQE of the p-i-n diode for different forward and reverse bias voltages V_{bias}.

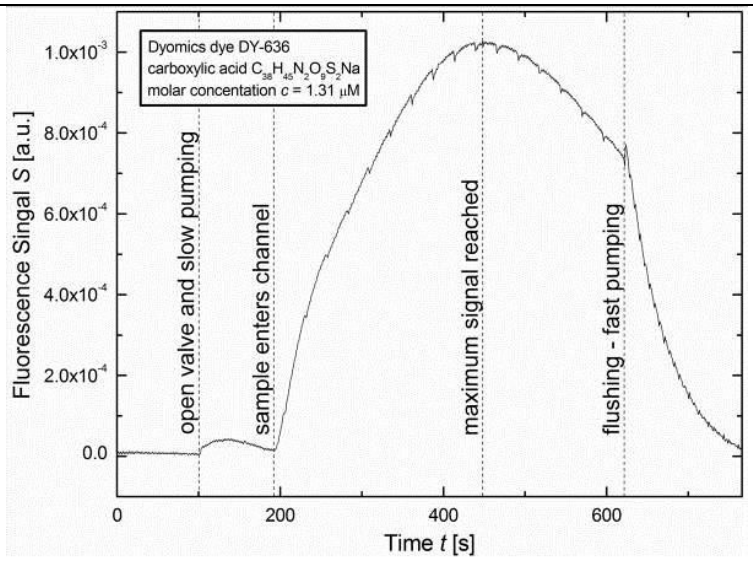

Fig. 2 shows one full fluorescence measurement cycle in the NANODEM test format using the here developed a-Si:H diodes as detectors. The sample is a dilution (with purified water) of the dye DY-636 by the vendor Dyomics GmbH with a molar concentration c = 1.31 µM. Before the sample injection, the flow channel is idle and shows a constant base line around S = 0. The valve to access the flow channel opens at $t \approx 100$ s and the pump starts injecting the sample with slow pumping speed. The fluorescent signals measured before the actual sample enters the flow channel at $t \approx 193$ s are due to dye remainders of previous measurement cycles in the microfluidic system. The fluorescence signal S reaches its maximum at $t \approx 448$ s. At $t \approx 622$ s the flushing procedure is started by assigning a faster pump rate. At $t \approx 766$ s the measurement cycle ends.

[1] http://nanodem.ifac.cnr.it

ID 70 - Oral

Doped microcrystalline silicon oxides for silicon-based solar cells: Optoelectronic properties, chemical- and structural composition

*A. Lambertz[1], V. Smirnov[1], S. Moll[1], M. Bär[2,3], D. Starr[2], R. Wilks[2], A. Heidt[4,5], M. Luysberg[4], B. Holländer[6], F. Finger[1]
[1]Forschungszentrum Jülich GmbH, IEK5-Photovoltaik, Jülich, Germany
[2]Renewable Energy, Helmholtz-Zentrum Berlin für Materialien und Energie GmbH, Berlin, Germany
[3]Institut für Physik und Chemie, Brandenburgische Technische Universität Cottbus Senftenberg, Cottbus, Germany
[4]Peter Grünberg Institute (PGI-5), Forschungszentrum Jülich GmbH, Jülich, Germany
[5]Carl Zeiss Microscopy GmbH, Oberkochen, Germany
[6]Peter Grünberg Institute (PGI-9), Forschungszentrum Jülich GmbH, Jülich, Germany

Doped microcrystalline silicon oxide (µc-SiO_x:H) layers with high transparency and appropriate conductivity have demonstrated to improve the performance of silicon based solar cells. We prepared p-type µc-SiO_x:H films using plasma enhanced chemical vapour deposition (PECVD), which is fully compatible with the production process of both wafer based hetero junction and thin-film silicon solar cells. The present study investigates the relationship between the oxygen content in the films, measured by Rutherford backscattering spectroscopy (RBS), and the material properties such as optical band gap, refractive index, conductivity, and crystalline volume fraction. The microscopic structure is imaged using high resolution transmission electron microscopy (HRTEM) of sample cross-sections. Furthermore, the distribution of the silicon in the films is shown by cross-sectional energy filtered transmission electron microscopy (EFTEM) images, and the Si chemical environment studied using hard X-ray photoelectron spectroscopy (HAXPES). With these techniques, we investigated a series of boron doped samples ranging from microcrystalline silicon (µc-Si:H) (without additional oxygen) to oxygen-rich samples of amorphous silicon oxide (a-SiO_x:H), showing a significant decrease in dark conductivity, crystalline volume fraction, refractive index together with a strong increase in transparency with increasing oxygen content. For mixed compositions, the conductivity at a given optical band gap is strongly improved due to the presence of µc-Si:H in the a-SiO_x:H matrix. The doped crystalline Si regions are mainly responsible for the electronic charge transport, while the amorphous silicon oxide matrix maintains a high optical band gap. From the HAXPES measurements we find two dominant chemical binding configurations Si^0 (Si) and Si^{4+} (SiO_2). Furthermore, the distribution of the silicon in the films is in a branch-like structures in growth direction as shown by cross-section EFTEM images taken from the crystalline Si plasmon energy. Accordingly elongated crystalline silicon grains are identified in HRTEM images. These results reveal the relationship between the optoelectronic properties and the chemical and structural composition of the doped µc-SiO_x:H. Optimal p-type µc-SiO_x:H films for the application in thin-film silicon solar cells with an optical band gap of $E_{04} = 2.4$ eV, a conductivity of 5×10^{-6} $(\Omega cm)^{-1}$ have an oxygen content of 40% with silicon regions in branch-like structures in growth direction and two dominant chemical binding configurations (Si and SiO_2).

ID 71 - Oral

On Defects and Interface Passivation of Thin Crystallized Silicon Absorbers for Next Generation Solar Cells on Glass

**N. Preissler[1], O. Gabriel[1], S. Calnan[1], D. Amkreutz[2], B. Stannowski[1], B. Rech[2], R. Schlatmann[1]*
[1]Helmholtz-Zentrum Berlin für Materialien und Energie GmbH, PVcomB, Berlin, Germany
[2]Helmholtz-Zentrum Berlin für Materialien und Energie GmbH, Institute for Silicon Photovoltaics, Berlin, Germany

Solar cells based on liquid-phase crystallized silicon (LPC-Si) absorbers on glass substrates are a promising recent development, because they combine a high material quality comparable to multi-crystalline silicon wafers with a reduced thickness of only 5-20 µm. The performance of these cells is strongly influenced by defects in the silicon absorber as well as by the passivation at the interface towards the silicon-dielectric intermediate layer (IL) stack which is in between the glass and the absorber. An increase in cell performance is achieved with a hydrogen plasma passivation (HPP) treatment which saturates defects in the material.

In this context we show our results on the effect of the HPP on the IL/absorber interface region in LPC-Si solar cells on glass. Furthermore, we report on our investigations of important parameters of the IL/absorber interface region such as the density of fixed charges in the IL stack as well as the interface defect density.

We prepared LPC-Si solar cells with different IL stacks based on amorphous silicon oxide a-SiO_x, silicon nitride a-SiN_x and silicon oxynitride a-SiO_xN_y deposited by plasma enhanced chemical vapor deposition (PECVD) or physical vapor deposition on 3.3 mm thick Borofloat glass substrates. The 10 µm thick n-type silicon absorbers, which were grown using either PECVD or electron beam evaporation, were crystallized with a cw laser and were subsequently passivated with a hydrogen plasma.

The positive effect of passivating defects with hydrogen depends strongly on the nature of the IL/absorber interface, indicating that HPP mainly improves this interface rather than the LPC-Si bulk quality. Based on capacity-voltage measurements parameters such as the density of fixed charges in the IL stack as well as the interface defect density were visualized. We performed current-voltage and Suns-V_{oc} measurements on test-cell structures to determine the open circuit voltage V_{oc} and the short circuit current density J_{sc}. Voltage dependent photoluminescence measurements gave further insight into the defect structure in the IL/absorber interface region.

ID 72 - Poster

0.25 THz MOSFET Direct Detectors in 0.18 µm CMOS Technology with On-Chip Antennas

*F. Zhao[1], L. Mao[1], W. Guo[1], P. He[1]
[1]University TianJin, TianJin, China

Detectors working at terahertz frequency range have been reported by many papers, and the application in imaging has been received a great deal of attention for low cost. But the cost is not low enough for commercial applications because of the Si-lens. This paper presents a lens-free 0.25 THz terahertz imaging detector implemented in a low-cost 180 nm CMOS process technology. Due to the appropriate impedance characteristics of the differentially driven antenna, broadband detector operation centered around 0.1 THz～10 THz could be achieved. Each detector unit can detect an incident carrier with 100-Hz～20-MHz amplitude modulation. This is the first time that 0.25 THz CMOS active imaging results without a lens are presented. At 309-Hz modulation frequency, the detector achieves a noise equivalent power (NEP) of 166 and a responsivity (Rv) of 800 front-side illumination. The detector responded at the frequency from 0.205 THz to 0.260 THz when the V_{GS}=0.238 V, V_{DS}=0 V. These results pave the way towards high sensitivity focal plane arrays in silicon for terahertz imaging.

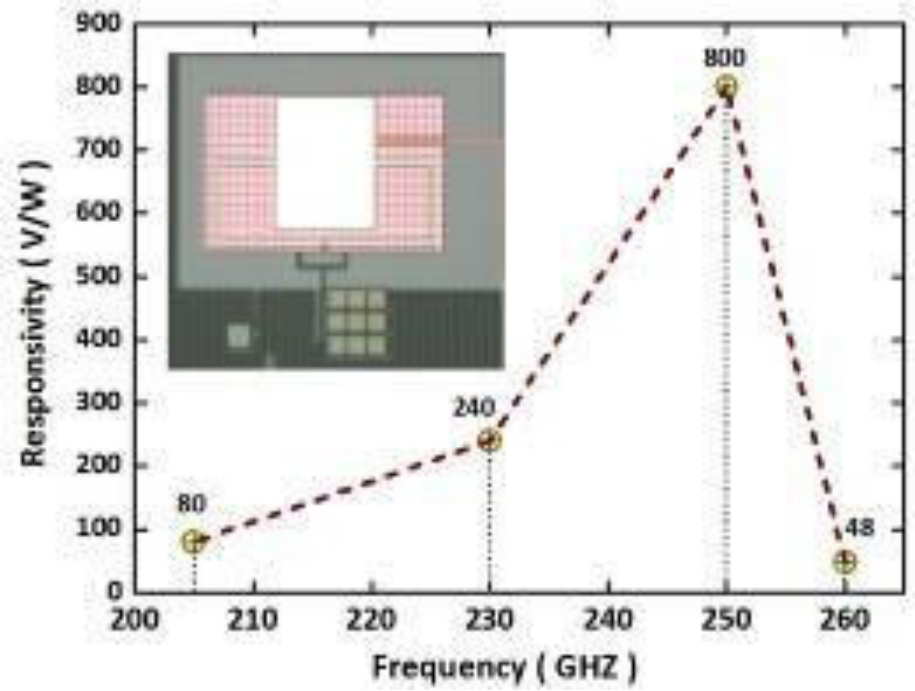

ID 73 - Oral

Valence band offset and hole transport at the crystalline silicon/amorphous silicon suboxide heterojunction

*M. Liebhaber[1], M. Mews[1], T. F. Schulze[1], B. Rech[1], L. Korte[1], K. Lips[1]
[1]Helmholtz-Zentrum Berlin, Institute of Silicon Photovoltaics, Berlin, Germany

The high potential of silicon heterojunction (SHJ) solar cells is reflected in the record efficiency of 25.6% for silicon based photovoltaics reported by Panasonic in 2014 [1]. One possibility to further improve conventional SHJ cell performance is to reduce current losses due to parasitic light absorption in the thin amorphous layers at the front side, by using wider band gap materials, such as a-SiO_x:H [2,3]. Larger band gaps result in increasing valence band offsets (ΔE_V) at the hole contact. In this report we will investigate the hole transport across the silicon oxide layer for various band gap energies and hence different ΔE_V.

For this systematic study thin layers ranging from pure intrinsic a-Si:H to near-stoichiometric a-SiO_2 were grown by varying the SiH_4/CO_2 precursor gas mixtures during chemical vapor deposition. A continuous increase of ΔE_V starting from 270 meV for the a-Si:H/c-Si to 4.3 eV for the a-SiO_2/c-Si heterointerface was measured by *in-system* photoelectron spectroscopy (cf. Fig. 1 [4]).

Furthermore, (p)a-Si:H/(i)a-SiO_x:H/(n)c-Si HJ solar cells, with intrinsic a-SiO_x:H passivation layers deposited using the same parameter sets, were fabricated. We report a linear decrease of the fill factor for increasing ΔE_V in the range of 0.27 - 0.85 eV (cf. Fig. 2). The reason is an increase of the barrier height for holes at the (i)a-SiO_x:H/(n)c-Si HJ and a simultaneous change of the hole transport mechanism from thermionic emission to defect-assisted tunneling processes across the junction. Our results are compared and discussed with modeling studies [5].

We arrive at the conclusion that a-Si:H alloys with ΔE_V higher than 420 meV are unsuitable for the application as hole contacts in SHJ solar cells. Nevertheless, it is demonstrated that clearly larger barrier heights can be tolerated if a stack of high band gap material and a material with lower band gap, forming a „staircase“ of band offsets is being used.

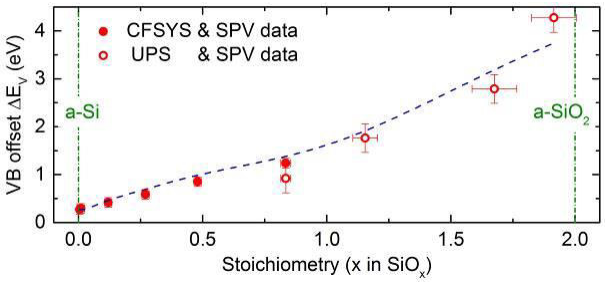

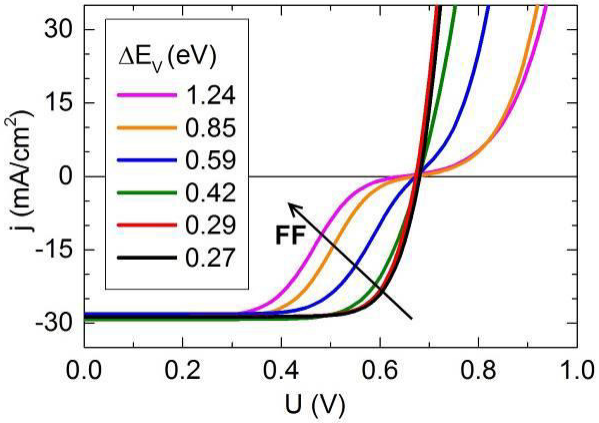

[1] K. Masuko et al., IEEE J. Photovolt. 4, 1433 (2014).
[2] K. Ding et al., Phys. Stat. Solidi 6, 193 (2012).
[3] J. Seif et al., J. Appl. Phys. 115, 024502 (2014).
[4] M. Liebhaber et al., Appl. Phys. Lett. 106, 031601 (2015).
[5] A. Kanevce and W. K. Metzger, J. Appl. Phys. 105, 094507 (2009).

ID 74 - Oral

Modeling thin film silicon based integrated water-splitting devices

*J.- P. Becker[1], F. Urbain[1], V. Smirnov[1], U. Rau[1], J. Ziegler[2], B. Kaiser[2], W. Jaegermann[2], F. Finger[1]
[1]Forschungszentrum Jülich , IEK5 - Photovoltaics, Jülich, Germany
[2]TU Darmstadt, Institute of Materials Science, Darmstadt, Germany

The generation of hydrogen by conversion of sunlight into chemical energy is considered a promising route to storing solar energy in the form of a chemical fuel to replace fossil fuels in the future. Integrated solar water-splitting devices present an elegant approach for the technical realization of this process. Such devices utilize semiconductor photoelectrodes which either use solid/liquid junctions or so-called buried (solid/solid) junctions, i.e. photovoltaic cells, to generate a photovoltage above approx. 1.6 V. This voltage is necessary to drive the anodic oxygen evolution reaction (OER) and the cathodic hydrogen evolution reaction (HER) at separate locations in the device and to account for additional overpotential losses.[1]

One of the few systems which, so far, were proven suitable for efficient solar water-splitting without additional bias is based on silicon thin-film solar cells.[2] The combination of hydrogenated amorphous silicon (a-Si:H) and microcrystalline silicon (µc-Si:H) thin films in multijunction solar cells allows for both an efficient utilization of the solar spectrum and the generation of a sufficient photovoltage.[3]

Compared to considerable efforts to find and optimize suitable (photo-)electrochemically active electrode materials, the design of the integrated device and other system parameters such as the electrolyte (ion species, pH, concentration), the operating temperature and the pressure within the reactor have received relatively little attention. Therefore, in this study we modeled integrated photovoltaic-electrochemical systems in terms of an equivalent circuit aiming to minimize the losses in the total device structure. Losses may occur due to optical losses in the photoelectrode, overpotential losses due to slow kinetics at the electrodes, or series resistances in the electrolyte to name but a few. The simulated current-voltage behavior of the integrated device showed very good agreement with measurements. Thereby, the model allows for a prediction of the efficiency of photovoltaic-biased water-splitting devices based on the individual parameters and the performance of the components (photoelectrode, electrolyte, catalysts for HER and OER). The optimized system in this study featuring a triple junction thin film silicon based photocathode in combination with platinum and ruthenium oxide catalysts for the HER and OER, respectively, operated in an alkaline electrolyte exhibited a very high solar-to-hydrogen efficiency of 9.5%. Here, Si thin-film multijunction photocathodes were used as a well performing model system. However, the methodology is also applicable to devices based on other photovoltaic materials such as III-V semiconductors or chalcopyrites.

1. J. Rongé, T. Bosserez, D. Martel, C. Nervi, L. Boarino, F. Taulelle, G. Decher, S. Bordiga, and J. a Martens, *Chem. Soc. Rev.*, 2014, **43**, 7963-81.
2. R. Rocheleau, E. Miller, and A. Misra, *Energy & Fuels*, 1998, **0624**, 3-10.
3. F. Urbain, K. Wilken, V. Smirnov, O. Astakhov, A. Lambertz, J.-P. Becker, U. Rau, J. Ziegler, B. Kaiser, W. Jaegermann, and F. Finger, *Int. J. Photoenergy*, 2014, **2014**, 1-10.

ID 75 - Oral

Hopping charge transport in a spatially correlated exponential density of states

*S. Novikov[1]
[1]A.N. Frumkin Institute of Physical Chemistry and Electrochemistry, Moscow, Russian Federation

Characteristic feature of amorphous organic materials is a long range spatial correlation of the random energy landscape [1]. Correlation arises because of the influence of the molecules having permanent dipole or quadrupole moments. Spatial correlations provide particular field dependence of the carrier drift mobility $\mu(E)$ in organic materials [2]. Typically, in organic materials the density of states (DOS) has a Gaussian form. Yet, there is a mechanism capable to produce an almost exponential DOS $\rho(U) \propto \exp(U/U_0)$, $U < 0$ even in organic materials [3]. This very DOS is typical for chalcogenide glasses as well. Until now the charge transport in the correlated exponential DOS is not studied. A possible dependence of the energy correlation function on distance is poorly known for amorphous materials with exponential DOS.

For the case of nondispersive transport with $\alpha = kT/U_0 > 1$ one can obtain an exact solution for the 1D case. The simplest relations can be obtained for the close vicinity of the transition to the dispersive regime $\alpha \to 1$. For example, for the power law dependence $C(r) \propto 1/r^n$ of the correlation function of the random energy the carrier drift mobility depends on applied electric field E as $\mu \propto E^n$ for moderate E. This very form of the correlation function is typical for amorphous organic materials, but usually in such materials the Gaussian DOS takes place leading to drastically different dependence $\mu(E)$ [1]. For the short range correlation having characteristic length a we have $\mu \propto \exp(eaE/kT)$.

We also discuss an approximate treatment of the dispersive transport with $\alpha < 1$. In the limit of weak E the mobility depends on the thickness L of the transport layer as $\mu \propto L^{1-1/\alpha}$, exactly as in the case of the multiple trapping model of charge transport. However, in comparison to the multiple trapping model, the dependence of μ on E is much stronger. For example, for the short range correlation $\mu \propto E^{1/\alpha-1}\exp(eaE/\alpha kT)$. For the power law correlation function the dependence $\mu(E)$ is rather complicated.

Our results indicate that the reliable information about the spatial dependence of the random energy correlation function in amorphous materials with the exponential DOS should be very desirable. This information could give us a possibility to calculate the corresponding mobility field dependence and test predictions of the theory.

[1] S.V. Novikov, A.V. Vannikov, J. Phys. Chem. C **113**, 2532 (2009).
[2] S.V. Novikov, D.H. Dunlap, V.M. Kenkre, P.E. Parris, A.V. Vannikov, Phys. Rev. Lett. **81**, 4472 (1998).
[3] F. May, B. Baumeier, C. Lennartz, D. Andrienko, Phys. Rev. Lett. **109**, 136401 (2012).

ID 76 - Oral

p-type silicon oxide as doping source for bifacial silicon solar cells

*P. Goyal[1,2], E. Urrejola[1], J. Hong[1], D. Daineka[2], E. Johnson[2], P. Roca i Cabarrocas[2]
[1]Air Liquide, Jouy-en-Josas, France
[2]LPICM-CNRS, Palaiseau, France

Bifacial solar cells offer a high potential to increase the efficiency of industrial silicon solar cells while reducing their cost by combining fabrication steps through co-diffusion. However, the dopant source layers deposited on silicon wafers must sustain high temperatures (~1000°C) during the solar cell fabrication. In this work we explore whether p-type silicon oxide layers (p-SiOx:H) deposited by PECVD using a non-conventional precursor can be used as a p-type dopant source and a passivation layer in bifacial silicon solar cells.

The p-SiOx:H layers were deposited using Hexamethyldisiloxane ($O[Si(CH_3)_3]_2$, HMDSO) as the Si-O source for the layers. To diffuse the B into the crystalline silicon wafer, the layers were subjected to a one-step thermal diffusion, and in another experiment to a two-step thermal diffusion (with an intermediate temperature). Optical and bond-configuration properties were studied with Spectroscopic Ellipsometry and Fourier Transform Infrared (FT-IR) spectroscopy, respectively, before and after thermal diffusion. The diffusion of boron inside c-Si bulk was studied with Electrochemical Capacitance Voltage (ECV) measurements.

As deposited, the p-SiOx:H layers passivate the silicon wafers, giving them an effective lifetime of 800 µs, but the layers peel off when subjected to a one step thermal diffusion. However, in the two-step process, the layers are thermally stable and can survive a higher temperature (1050°C). The higher thermal stability allows for acceptable dopant diffusion into the wafer. With FT-IR measurements, we show that the p-SiOx:H layers densify after thermal diffusion, and some structural changes in the layer - such as dissociation of $Si-CH_3$ bonds - are also observed. It was possible to control the doping profile inside c-Si bulk with the thickness of layers and the time of thermal diffusion.

One-step diffusion profile leads to a fast out diffusion of hydrogen and to the formation of pinholes which damage the layers. On the contrary, using a two-step annealing process, the effusion is gradual and the layers remain attached to the silicon surface. These layers can be used as an effective dopant source and applied to bifacial silicon solar cells. Solar cell results will be presented during the conference.

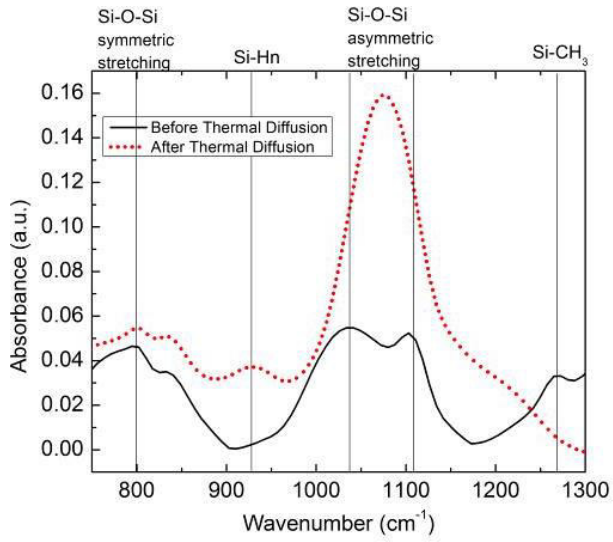

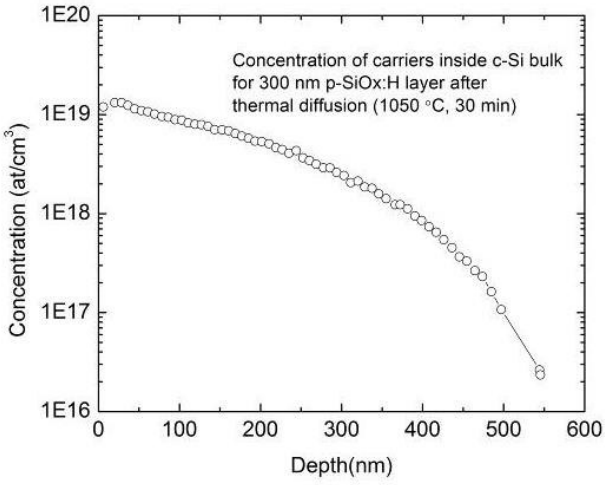

ID 77 - Poster

Effect of the elemental substitution on threshold behaviours in Ge-As(Sb)-Se glasses

**R. Wang*[1]
[1]*Australian National University, Laser Physics Centre, Canberra, United Kingdom*

Threshold behaviours in chalcolgenide glasses with covalent bonds have been intensively investigated. In most cases, physical parameters of the glasses exhibit a transition at the glass with a mean coordination number (MCN, defined as a sum of products of abundance of constituent atoms valency) of 2.4, and this comes from an under-constrained “floppy” network to an over-constrained “rigid” phase. Another transition at MCN =2.67 has also been reported, which represents a topological change from a 2-D to 3-D “stressed rigid” phase. In the present context, we investigated the effect of the elemental substitution of As by Sb on threshold behaviours in Ge-As(Sb)-Se glasses. Through systematic measurements of various physical parameters like glass transition temperature, density, refractive index, and optical bandgap, we found that, while the transition thresholds at 2.4 and 2.67 were verified in Ge-As-Se with ideal covalent network, the replacement of As by Sb can induce the change of the transition thresholds. Further structural characterisation using Raman and x-ray photoelectron spectra confirmed that, the threshold behavior of the physical properties in the $Ge_xSb_{10}Se_{90-x}$ glasses can be traced to demixing of networks above the chemically stoichiometric composition.

ID 78 - Oral

Consideration of defective regions in optical modelling of thin-film silicon solar cells

*M. Sever[1], J. Krč[1], M. Topič[1]
[1]University of Ljubljana, Faculty of Electrical Engineering, Ljubljana, Slovenia

Texturing of the interfaces of thin-film silicon solar cells has proven to bring significant increase in J_{SC} of the cells due to longer average path of light through the absorptive layers. However, textures of the substrates that comprise narrow valleys result in shading during deposition of amorphous or nanocrystalline layers material and in formation of structural and electronic defective regions of less dense material. Since these regions deteriorate external electrical characteristics (V_{OC}, *FF*) of the device, the gain of the efficiency due to the improved optical properties is often negated. In addition, since the textures are not ideally translated to subsequent interfaces during the deposition due to non-conformal layer growth, the analysis of initial texture alone is not enough to predict and guarantee defect-less growth of subsequent layers.

In this contribution, previously developed non-conformal model of layer growth is used to trace the texture morphology throughout the deposition of *a*-Si:H and *μc*-Si:H layers in thin-film solar cell devices:. Therefore, not only initial substrate texture, but also the changing texture during the deposition can be analysed for potential of defective region occurrence. Thus, defective regions emerging at later stages of the deposition can also be anticipated. This enables inclusion of additional criteria within the optimisation procedure that discards the detrimental substrate textures already in the phase of the design rather than after the fabrication of the prototype cells. The procedure for detection of defective regions will be presented in combination with fully 3-D optical modelling of single and tandem devices, performed in COMSOL Multiphysics software. Directions will be shown for choice of the textures or their modification in order to avoid electrical deterioration while still improving optical properties and efficiency of final single-junction and tandem devices.

ID 79 - Poster

High performance photoelectrochemical devices based on multijunction thin film silicon solar cells

*F. Urbain[1], V. Smirnov[1], J.- P. Becker[1], U. Rau[1], J. Ziegler[2], F. Yang[2], B. Kaiser[2], W. Jaegermann[2], F. Finger[1]
[1]Forschungszentrum Jülich GmbH, IEK-5 Photovoltaik, Jülich, Germany
[2]TU Darmstadt, Darmstadt, Germany

We report on the application of multijunction solar cells in photoelectrochemical devices for hydrogen production. Hydrogen, as a storable chemical fuel, can be generated through photoelectrolysis of water, a chemical reaction which requires potentials, i.e. photovoltages over 1.5 V to run autonomously. The solar-to-hydrogen (STH) efficiency is determined by the photocurrent at the respective required voltage. It is therefore important to develop solar cells which can cover up a wide photovoltage range in combination with high photocurrents. This high photovoltage/high photocurrent tradeoff can be solved by multijunction solar cells made of amorphous (a-Si:H) and microcrystalline (µc-Si:H) silicon.

We investigated a-Si:H/µc-Si:H and a-Si:H/a-Si:H tandem junction, a-Si:H/µc-Si:H/µc-Si:H and a-Si:H/a-Si:H/µc-Si:H triple junction, and a-Si:H/a-Si:H/µc-Si:H/µc-Si:H quadruple junction solar cells, which provide open-circuit voltages V_{oc} ranging from 1.5 to 2.8 V and maximum power voltages V_{mpp} from 1.3 to 2.5 V, along with initial efficiencies up to 13.6 %. The performance and stability of the solar cells as photocathodes was investigated in an integrated photovoltaic-biased electrosynthetic cell (PV-EC) device configuration. We demonstrate that this device configuration in combination with the broad range of available photovoltages presents a useful toolbox for the investigation of additional PV-EC parameters, such as different counter electrodes, catalysts or electrolyte solutions and related stability or degradation issues. The latter ones comprise in particular two major mechanisms, which we investigated in more detail: Light-induced degradation (LID) of the integrated solar cell and electrochemical degradation of both electrodes during PV-EC operation.

LID was measured under AM 1.5 illumination up to 1000 hours for the solar cells. We integrated both, initial and degraded cells in the PV-EC device configuration and particularly evaluated to what extend degradation in V_{mpp} and J_{mpp} influences the STH.

The electrochemical performance and stability of the PV-EC device was evaluated by means of potentiostatic measurements as a function of different metal catalysts and electrolyte concentrations, respectively. With an a-Si:H/a-Si:H/µc-Si:H solar cell in initial state and Pt as hydrogen evolution reaction catalyst we achieved a record STH efficiency of 9.5%.

ID 80 - Oral

Effect of diluent gas on silicon oxide nanowires synthesis from a free jet of monosilane-diluent gas mixture activated by electron-beam plasma

*S. Khmel[1], E. Baranov[1], A. Zamchiy[1]
[1]Istitute of Thermophysics, Siberian Branch of RAS, Laboratory of rarified gases, Novosibirsk, Russian Federation

Nanowires of various materials are promising candidates for the creation of nanoelectronic devices due to their small size, low power consumption, and unique physical properties. In particular, silica nanowires have good photoluminescence properties and may be used for creation of the optoelectronic devices. Therefore, a study of the synthesis of silica nanowires, including oriented arrays of nanowires, and a study of the nanowire properties, including the creation of the solar cell, is an actual problem.

Silicon oxide nanowires were synthesized from mixture monosilane with gas diluent (hydrogen, helium, argon) by gas-jet electron beam plasma CVD method. Oxygen was supplied directly into the vacuum chamber. The synthesis was carried out on c-Si substrate with micrometer-sized particles of Sn catalyst. The process of nanowire synthesis on the substrate with the catalyst consists of three stages: heating up to operating temperature, treatment by gas diluent plasma and the actual growth of nanowires. SEM observations show that this method provides different morphologies of system “catalyst particle - nanowires” for different gas diluents. Oriented arrays of nanowire bunches (“microropes”) were synthesized in the area corresponding of the jet axis from mixture monosilane-hydrogen [1-3]. Every particle of catalyst produces large number of curved shape nanowires with mean diameter about 15 nm. The EDS (energy dispersive spectroscopy) revealed that the synthesized nanowires were composed of silicon and oxygen, and quantitative analysis showed that the atomic ratio of Si:O was 1:2.4. These silicon oxide nanowires were produced at low temperature about 320°C and with growth rate about 25 nm/s. When one used helium as gas diluent, chaotic arrays of silicon oxide nanowire bunches were synthesized. The EDS revealed that the atomic ratio of Si:O was 1:2.15. We observed cocoon-like nanostructures of silicon oxide nanowires, when one used mixture argon with monosilane. The EDS showed that the atomic ratio of Si:O was 1:0.53. The influence of the concentration of silane in the mixture on the morphology of system “catalyst particle-nanowires” at a constant flow of argon was investigated. Decrease of the silane concentration has transformed the morphology from the cocoon-like nanostructures to oriented array of “microropes”. Possible growth model has been suggested in order to explain the results. Silicon oxide nanowires probably were synthesized by VLS (“vapor-liquid-solid”) mechanism via catalyst-on-bottom mode, where multiple nanowires grow simultaneously from the surface of one catalyst drop. Apparently, nonuniform heating of the catalyst particles due to directed plasma flow leads to the preferential growth of nanowires on one side of the particles and synthesis of oriented array. This work was supported in part by the Russian Foundation for Basic Research (gr. #15-08-05394-a)

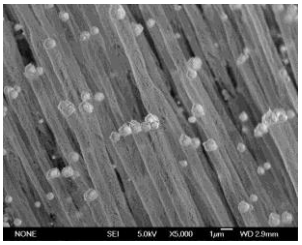

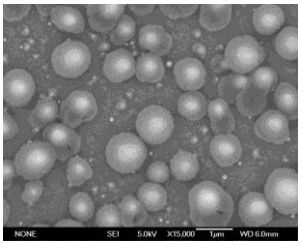

1. Khmel S.Ya., Baranov E.A., Zamchiy A.O., Proc. 28th European Photovoltaic Solar Energy Conference, France, Paris, 2013, p. 395-398.
2. Baranov E.A., Zamchiy A.O., Khmel S.Ya., Tech. Phys. Lett., 2013, vol. 39, p.1023-1025.
3. Zamchiy A.O., Baranov E.A., Khmel S.Ya., Physica Status Solidi C, 2014, vol. 11, p. 1397-1400.

ID 81 - Oral

Ab initio simulation of the atomistic mechanism of the effect of nitrogen doping on the crystallization behaviour of the phase-change memory material, $Ge_2Sb_2Te_5$

**S. Elliott[1], T.- H. Lee[1]*
[1]University of Cambridge, Chemistry, Cambridge, United Kingdom

We describe the effect on the crystallization behaviour of the canonical phase-change memory material, $Ge_2Sb_2Te_5$ (GST), of the incorporation of a few atomic % of the dopant, nitrogen, using *ab initio* molecular-dynamics simulations. The experimentally observed crystal-grain 'refinement' (reduction in size) on nitrogen doping is revealed to be due to the topological hindering of cryatal growth at the atomic level by the incorporation of nitrogen dopants due to the difference in atomic coordination of the dopant species and the host atoms. Extended (~ns) simulation runs of large models of GST:N using templated (heterogeneous) crystallization have been used to reveal this atomic-scale behaviour for the first time.

ID 82 - Poster

Effects of annealing on the carrier concentration of SnS films

*T. Gotoh[1], K. Yazawa[1]
[1]Gunma University, Maebashi, Japan

The optical band gap of Tin Sulfide (SnS) is close to the optimum value of 1.5 eV for solar cell applications. In addition, SnS has high optical absorption coefficient of the order of 10^5 cm^{-1}. These properties indicate that SnS is suitable material for solar cell, however, the achieved conversion efficiency of SnS solar cells is very low so far[1)]. The reason of the low efficiency remains unclear, however, the control of carrier properties in semiconductors is quite important for improving device performance. In the present work, we prepared thermally evaporated SnS thin films and investigated the change of carrier concentration induced by thermal annealing treatments.

SnS films were deposited onto glass slide at room temperature by vacuum evaporation of the SnS powder. The vacuum chamber was evacuated down to 1×10^{-3} Pa. During the evaporation, the temperature of substrates was not controlled. The film thickness was 50 - 200 nm. The incorporation of S or Sn was achieved by diffusing S or Sn during annealing in S vapor (S annealing) or annealing of glass/Sn/SnS/glass system (Sn annealing). Electrical resistivity and Seebeck coefficient were measured for the samples after S or Sn annealing. Figure 1 shows the effects of annealing on the carrier concentration of SnS films. Carrier concentration of thermal annealed SnS was normalized by the reported value of ~1.7×10^{15} cm^{-3} [1)]. Increase of carrier concentration may be caused by the increase of Sn vacancy in SnS films.

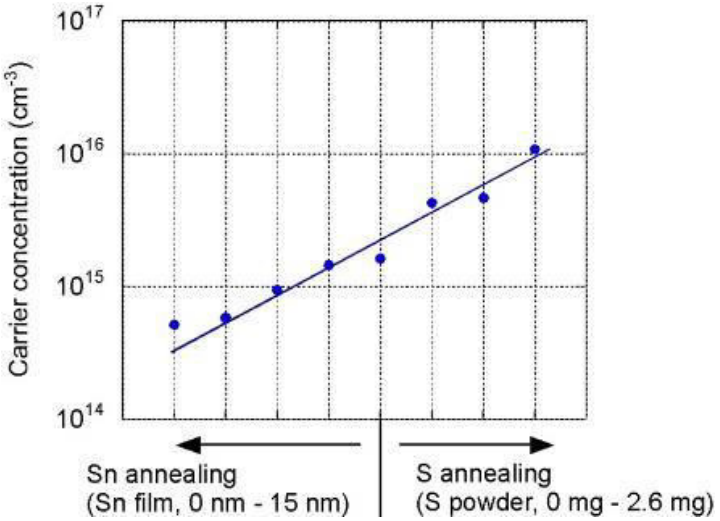

1) K. T. R. Reddy, N. K. Reddy, and R. W. Miles, Sol. Energy Mater. Sol. Cells 90, 3041 (2006).

ID 83 - Poster

Nature of Charge Transport in Nanocrystal Solids

**N. Vukmirovic[1], N. Prodanovic[1]*
[1]Institute of Physics Belgrade, Belgrade, Serbia

Colloidal quantum dot supercrystals are nanostructured materials which appear very promising in potential optoelectronic applications and for fundamental study of electronic transport properties in condensed matter physics. Recent fabrication of high quality supercrystals with relatively strong inter-site electronic coupling and high size monodispersity enabled high carrier mobilities that slightly decrease with increasing temperature. Due to such temperature behaviour it is believed that band transport is present in such materials.

We performed detailed calculations of electron-phonon interaction in colloidal quantum dot supercrystals that allowed us to identify the nature of charge carriers and the electrical transport regime [1]. We found that in experimentally relevant CdSe nanocrystal solids, electron-phonon interaction is sufficiently strong that small polarons localized to single dots are formed. Charge-carrier transport occurs by small polaron hopping between the dots with mobility that decreases with increasing the temperature. While such a temperature dependence of mobility is usually considered as a proof of band transport, we showed that the same type of dependence occurs in the system where transport occurs by small polaron hopping.

[1] N. Prodanović, N. Vukmirović, Z. Ikonić, P. Harrison, and D. Indjin, J. Phys. Chem. Lett. 5, 1335 (2014).

ID 84 - Poster

Preparation of thin silicon layers highly doped with manganese by reactive pulsed laser deposition

*M. Kostejn[1], V. Drinek[1], R. Fajgar[1]
[1]Institute of Chemical Process Fundamentals of the CAS, v.v.i., Department of Analytical and Material Chemistry, Prague 6, Czech Republic

Silicon with a high doping concentration of manganese is frequently studied for its potential magnetic properties. This type of material is referred as a possible ferromagnetic semiconductor up to the room temperature. The origin of this behaviour is still unclear. For deep study of this material it is necessary to prepare a stable oxygen free silicon-manganese compound.

The high concentration of manganese in silicon is achievable only due to highly non-equilibrium preparation methods. In our group we propose usage of a reactive pulsed laser deposition (PLD) technique as a universal method for preparation of highly homogenous manganese doped silicon compound with the manganese concentration above 30%. An arrangement of our experiments consists of ArF excimer laser (193nm), evacuated reaction chamber with a quartz entrance window, a manganese target and silane (SiH_4) as a background gas under low pressure. Focused laser pulse with high fluence efficiently sputters the manganese target. Evaporated manganese ions interact with silane molecules and prepared material is deposited onto various substrates in a form of thin layer. The interaction occurs under highly non-equilibrium conditions where temperature decreases by 10^4 K/s.

To evaluate initial conditions, high resolution emission spectroscopy was used. Scanning electron microscopy (SEM) with energy dispersive X-ray spectroscopy (EDS), X-ray photoelectron spectroscopy (XPS), Raman spectroscopy and high-resolution transmission electron microscopy (HRTEM) were used to characterize properties of the Mn-Si layers prepared.

EDS measurement of material prepared by the reactive PLD revealed presence of silicon with high concentration of manganese which can by varied from 30 to 60 at. % based on silane pressure (0.5 to 8 Pa) and target to substrate distance.

Manganese is an element which is very likely oxidised. XPS was used in order to study elemental composition and chemical states of a superficial layer. Mn 2p 3/2 line was observed as the most intense signal. On the surface oxide abundant layer has occurred due to air exposure. In the spectra a broad peak centred at 642 eV occurs. After etching there was revealed a sharp peak at 638.9 eV which was identified as Mn-Si bond. Due to the same position of the silicide peak and elemental manganese it is not possible to distinguish between them. The peak corresponding to oxidised manganese almost disappeared, which evidence only for surface oxidation.

Mn-Si bonding was proved by Raman spectroscopy, HRTEM imaging and diffraction measurements. Raman spectra showed no peaks corresponding to crystalline or amorphous silicon. In HRTEM images there is homogenous layer without any sign of Mn or Si separation. Diffraction spectra show broad reflections which were best assigned to MnSi or Mn_5Si_3in the most cases.

Preliminary electrical measurements show that conductivity of the layers is approximately 10 times higher than that of intrinsic silicon and it increase with temperature.

We present a robust method for preparation of manganese silicides in form of thin layers with Mn concentration from 30 to 60 at. %. The prepared layers are homogenous, amorphous or containing crystallites smaller than 3 nm. Electron diffraction showed broad reflections corresponding to manganese silicides; however, complete solving of the structure requires supplementary analysis. Manganese in our samples is not bonded to oxygen atoms, except superficial layer exposed to air. Electrical conductivity measurements of our samples show semiconducting properties.

ID 85 - Poster

Catalyst-free growth of silicon nanowires using Low Temperature Chemical Vapor Deposition

*V. Dřínek[1], M. Klementová[2], R. Fajgar[1]
[1]Institute of Chemical Process Fundamentals, Prague, Czech Republic
[2]Institute of Physics, Prague, Czech Republic

Majority of deposition techniques for preparation of silicon nanowires (SiNWs) anticipate using of metal seed for the growth initialisation via vapor-liquid-solid (VLS) approach. However, those metals - especially most used Au - act as deep level traps for free charge carriers resulting in deteriorated properties of micro- and optoelectronic SiNW components. Removing of the metal caps on the SiNW tips means to use HF solution or another etching agent with consecutive annealing. As it was shown in literature [1], even after this procedure gold residues were detected in SiNW bodies. The solution bases on avoiding metal seeds and applying catalyst-free approach. Although very few works have been published dealing with this approach, the possible benefit has an important impact on SiNW technology.

We deposited SiNWs onto molybdenum and iron substrates using low pressure chemical vapor deposition (LPCVD). During the experiment the temperature was fixed at 500 °C a the pressure approximately at 150 Pa. Several analytical techniques were used for characterisation of SiNW deposits: scanning electron microscopy (SEM), high resolution transmission electron microscopy (HRTEM), energy dispersive X-ray analysis (EDX), Raman spectroscopy and selected area electron diffraction (SAED).

Deposition of silane on molybdenum and iron substrates yielded thick grown films. According to the SEM micrographs, some nanowires are more than 20 microns long and about 100 nm thin.

SiNWs are composed of a core and a jacket. The crystalline core is very thin (sometimes barely visible as in Image 1), usually only about 10 nm in diameter. However, it is clearly discernible in the electron diffraction. The NWs grow in the direction of the Si crystalline core. The composition of amorphous jacket was not clear from the EDS analysis. It is obvious that there is a thin layer of silicon oxide on the surface of NW; however, to decide whether the rest of the NW jacket is composed of amorphous oxide or amorphous silicon, amorphous silica was added to the sample, and the electron diffraction of the NW was compared to the one of silica. The Process Diffraction software was used to integrate diffraction patterns and produce diffraction profiles (Image 2). The first broad maxima of silica and NW do not overlap, which suggests that the NW jacket is composed of amorphous silicon rather than amorphous silicon oxide. This fact is further corroborated by the fact that the maximum corresponds to the distance of (111) planes of Si.

We succeeded to grow SiNWs on molybdenum and iron substrates without using any external or internal metal or non-metal seeds. As those seeds are or may be a source of problems in production and/or applications, we anticipate that this fabrication is attractive enough to develop this approach for any kind of substrate.

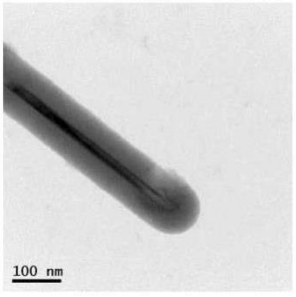

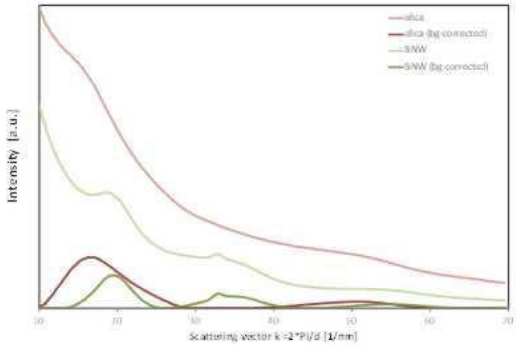

[1] Dupré L, Buttard D, Leclere C, Renevier H, Gentile P. Gold contamination in VLS-grown Si nanowires: Multiwavelength anomalous diffraction investigation. Chem Mater 2012; 24:4511-16

ID 86 - Oral

Effective Current Matching Modulation for High-Performing Micromorph Tandem Solar Cells

*L. Bai[1], B. Liu[1], J. Fang[1], Q. Huang[1], B. Li[1], D. Zhang[1], J. Sun[1], C. Wei[1], Y. Zhao[1], X. Zhang[1]
[1]Institute of Photo Electronics thin Film Devices and Technology of Nankai University, Tianjin, China

We report our latest progress on improving the performance of pin-type a-Si:H/μc-Si:H tandem solar cells in this paper. After adjusting the material quality of intrinsic layers and optimizing the device architecture of μc-Si:H single-junction solar cells, we then applied them as bottom component cells in a-Si:H/μc-Si:H tandem solar cells based on metal organic chemical vapor deposited (MOCVD) boron-doped zinc oxide (ZnO:B) substrates. For improving the current output of μc-Si:H bottom component cell and achieving a better current matching between the component cells, two major approaches were applied and compared. The first one is to elevate the crystalline volume fraction of the μc-Si:H intrinsic layers to reduce the band gap, thereby expanding the absorbable wavelength range, the other one is to enlarge the thickness of the μc-Si:H intrinsic layers. By comparing the two optimization approaches, we concluded that the current output in μc-Si:H bottom component cells can be more effectively improved by modifying the thickness of μc-Si:H bottom solar cells in comparison to the crystalline volume fraction. As a result of this work, an initial efficiency of 13.65% of pin-type a-Si:H/μc-Si:H tandem solar cell was successfully achieved with a component current of 13.69 mA/cm^2 in the a-Si:H and μc-Si:H sub-cells

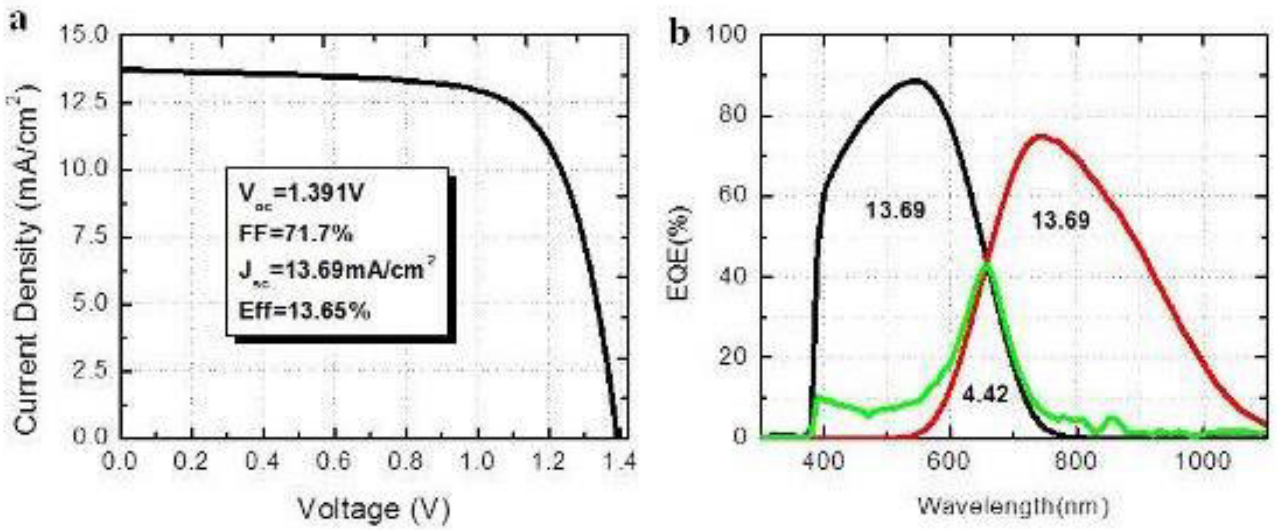

ID 87 - Oral

Optimization of nanocrystalline silicon oxide emitters as window layer for HIT solar cells

*L. Mazzarella[1], S. Kirner[1], O. Gabriel[1], L. Korte[2], B. Stannowski[1], B. Rech[2], R. Schlatmann[1]
[1]Helmholtz-Zentrum Berlin, PVcomB, Berlin, Germany
[2]Helmholtz-Zentrum Berlin, Institute for Silicon Photovoltaics, Berlin, Germany

In this study we developed a p-doped hydrogenated nanocrystalline silicon oxide ((p)nc-SiO_x:H) emitter window layer for silicon heterojunction solar cells. We investigated the material properties of several layers deposited under varying plasma enhanced chemical vapor deposition (PECVD) conditions and addressed the issues that have to be taken into account when nanocrystalline layers of a few tens of nanometers are used: (a) incubation layer/initial stage of growth, (b) bulk material electrical/optical trade-off and (c) contact to the front TCO. So far, our best cell with optimized nc-SiO_x:H growth conditions has a conversion efficiency exceeding 20 % on a textured wafer.
Silicon wafer based heterojunction solar cells with intrinsic thin-hydrogenated amorphous ((i)a-Si:H) silicon layer (HIT) structure have demonstrated a conversion efficiency of 24.7 % [1] The HIT device concept combines low temperature fabrication processes, typically performed by PECVD, which lead to well passivated silicon surfaces, permitting open circuit voltages of 750 mV [1].

The p-doped nc-SiO_x:H layers are deposited by RF PECVD technique using SiH_4, H_2, TMB and CO_2 as process gases and varying the PECVD conditions (RF power, gas pressure and hydrogen dilution). For layer characterization, the emitter materials are deposited on glass substrates and characterized by means of spectrophotometry and Raman spectroscopy. Devices with (p)nc-SiO_x:H emitters are fabricated on random pyramids textured FZ n-type wafers (3 Ωcm, 270 µm, and crystal orientation). The emitter surface is passivated by 6 nm of intrinsic a-Si:H and a stack of (i)a-Si:H/(n)a-Si:H is deposited as passivation and BSF layers on the back side. To complete the device, a stack of 80 nm ZnO:Al and 200 nm Ag is deposited on the non-illuminated side by DC sputtering and the front is covered with 80 nm of TCO (In_2O_3:Sn, ITO) and a metallic grid (10 nm Ti and 1500 nm Ag). The devices are characterized using a class AAA+ solar simulator with dual-source illumination under standard test conditions (25°C), illumination dependent open-circuit voltage (Suns-V_{oc}), external quantum efficiency (EQE) and absorptance measurements (1-total reflection).

In this work, we show that it is possible to improve the light incoupling at the front side of silicon heterojunction solar cells by minimizing reflection losses and parasitic absorption of the window emitter layer. Although an optimized (p)a-Si:H emitter layer is only a few nanometers thick (~10 nm), it absorbs a significant amount of incoming light parasitically [3]. Furthermore, its refractive index is unfavorably close to or even higher than that of the crystalline silicon wafer, which leads to increased reflection at the front side. We have recently demonstrated that a short circuit current density (J_{sc}) above 40 mA/cm^2 can be reached, by employing amorphous silicon oxide containing doped silicon nanocrystallites as emitter. This two phase material is typically referred to as micro- or nanocrystalline silicon oxide, nc- or µc-SiO_x:H) and due to its tunable optical properties, it allows to form a stack with a refractive index *n* grading from silicon to the ambient air and thus minimizes the reflection losses [4]. The lower parasitic absorption, compared to an a-Si:H emitter, permits to fully take advantage of the antireflection effect by depositing a thicker emitter (~ 30 nm) [4] that is also required to reach a suitable crystallinity F_c within such a layer. Fig. 1 (a-c) shows 1-R and EQE spectra measured on solar cells with selected emitter layers (*n* and F_c vs. H_2/SiH_4 ratio in the inset). A short circuit current density ($J_{sc\text{-}EQE}$) of 40 mA/cm^2 was measured, i.e. an improvement of 2 % if compared to nc-SiO_x:H emitters with higher *n* and up to 4 % with respect to standard emitters (10 nm of (p)a-Si:H). We also show an approach to reduce the incubation layer thickness and reach a faster nc-SiO_x:H growth by means of plasma treatments. The passivation quality is monitored by measuring QSSPC both for standard a-Si:H and nc-SiO_x:H emitters. Finally, the interface between the (p)nc-SiO_x:H emitter and the front TCO is changed by inserting a nc-Si:H contact layer with variable thickness in order to address the poor fill factor displayed in Fig. 2.

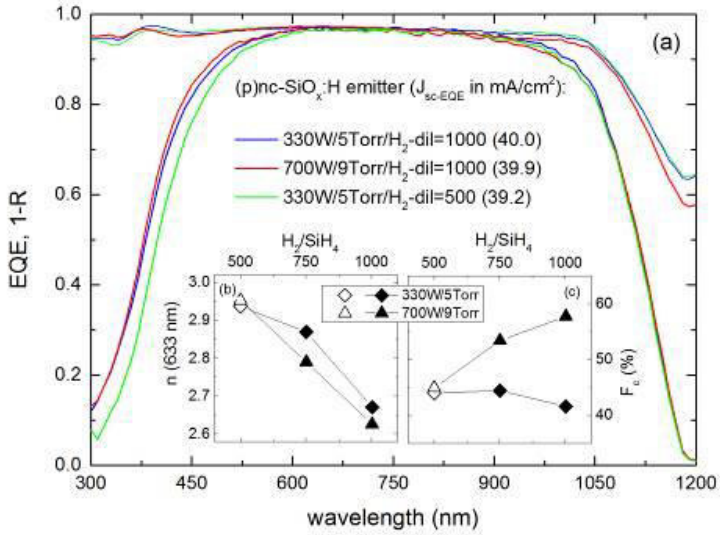

Fig. 1: EQE and 1-R as a function of wavelength for the best cells on textured wafers with three different (p)nc-SiO_x:H emitters (30 nm) deposited at different PECVD conditions. Refractive index n and Raman crystallinity F_c as function of H_2/SiH_4 ratio are shown in the inset.

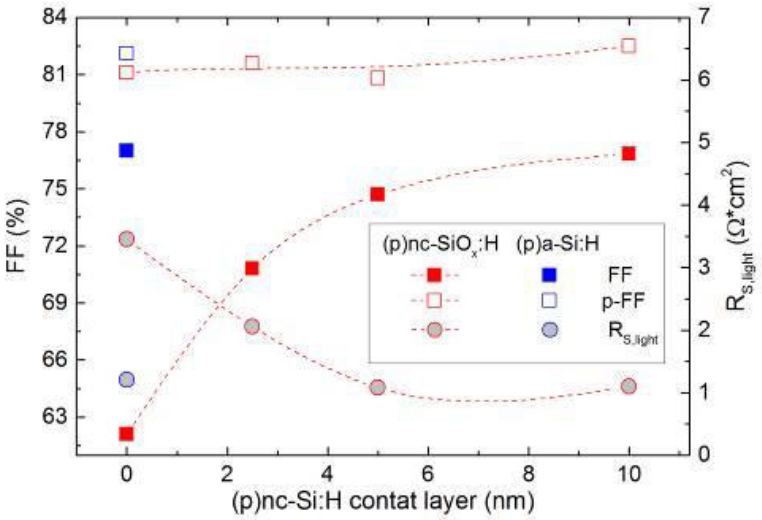

Fig. 2: Fill factor, pseudo Fill factor and series resistance for the best cells on textured wafers with (p)nc-SiO_x:H emitters (~ 30 nm thick) as function of (p)nc-Si:H contact layer (nominal thickness). Blue symbols represent results for reference cells with standard p-aSi:H emitter (~10 nm).

[1] M. Taguchi, A. Yano, S. Tohoda, K. Matsuyama, Y. Nakamura, T. Nishiwaki, K. Fujita and E. Maruyama, IEEE Journal of Photovoltaics, 1 (4), 96-99 (2013)
[2] K. Masuko, M. Shigematsu, T. Hashiguchi, D. Fujishima, M. Kai, N. Yoshimura, T. Yamaguchi, Y. Ichihashi, T. Mishima, N. Matsubara, T. Yamanishi, T. Takahama, M. Taguchi, E. Maruyama, and S. Okamoto, IEEE Journal of Photovoltaics, 6 (4), 1433-1435 (2014)
[3] Z.C. Holman, A. Descoeudres, L. Barraud, F. Zicarelli Fernandez, J. P. Seif, S. De Wolf, and C. Ballif, IEEE Journal of Photovoltaics, 1 (2), 7-15 (2012)
[4] L. Mazzarella, S. Kirner, B. Stannowski, L. Korte, B. Rech, and R. Schlatmann, Applied Physics Letters 106, 023902 (2015)
[5] P. Cuony, D. T. L. Alexander, I. Perez-Wurfl, M. Despeisse, G. Bugnon, M. Boccard, T. Söderström, A. Hessler-Wyser, Advanced Material, (24), 1182-1186 (2012)

ID 88 - Poster

Radial hetero-junction silicon thin film solar cells built over copper oxide nanowires with a high open-circuit voltage

*Q. Shengyi[1], *L. Jiawen[1], Y. Zhongwei[1], Y. Linwei[1,2], X. Jun[1], W. Junzhuan[1], X. Ling[1], S. Yi[1], C. Kunji[1], C. Pere Roca [2]
[1]Nanjing University, National Laboratory of Solid State Microstructures and School of Electronics Science and Engineering, Nanjing, China
[2] Ecole Polytechnique, LPICM, France, France

Radial junction solar cells constructed over a matrix of nanowires (NWs) framework has been widely investigated as a promising 3D architecture that will not only boost the light harvesting performance of thin film solar cells, but also allow a new control dimension to optimize the junction design for achieving a fast carrier separation and better stability against lasting sunlight exposure. This concept has been explored and proven effective in our recent works in hydrogenated amorphous Si (a-Si:H) thin film radial junction solar cells deposited over p-type doped SiNWs, where a high open circuit voltage of Voc=0.92 V and an power conversion efficiency of 9.2% [1,2].

In parallel, p-type semiconductor of copper oxide (CuO) has become a popular thin film material for exploring a type of c-Si/CuO heterojunction solar cells[3,4]. But, the potential of a radial heterojunction thin film Si/CuO solar cell has never been explored so far. Actually, the p-type CuO nanowires could serve as both an ideal 3D framework and a p-type electrode in a p-i-n Si radial junction solar cell. Meanwhile, the acquired knowledge of the a-Si/CuO interface is also critical for the optimization of a c-Si based CuO heterojunction solar cell.

In this talk, we will report a novel p-type copper oxide nanowires (CuO NWs)/a-Si:H thin film solar cells, which can be fabricated conveniently in a large-area thin film process, with a full compatibility of the conventional low-T a-Si:H thin film procedure. We show that a highly conformal coating can be easily achieved among the long CuO nanowires matrix by a PECVD thin film deposition, and a simple CuO NW/a-Si:H/n-a-Si:H radial junction cell exhibits an unexpected high open-circuit voltage of Voc=740 mV (see Figure 1 for the J-V curve and the SEM images of the as-deposited radial junction cells). We carry out also a series of parametric investigation in terms of the length, density and surface passivation of the CuO NWs, which will be addressed in a more systematic way in our presentation.

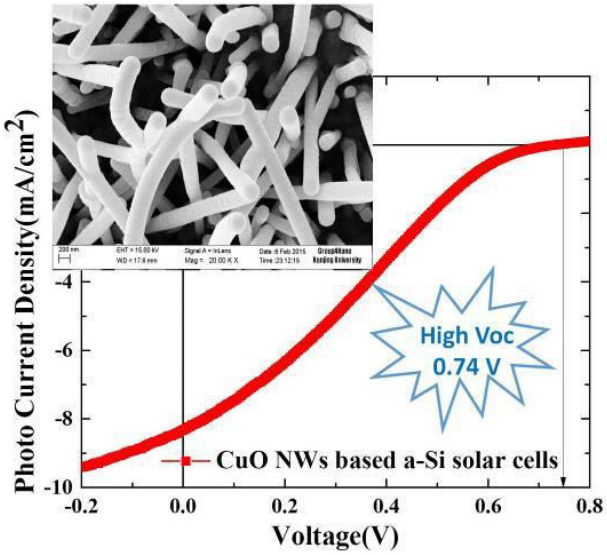

Figure 1. Current density - voltage (J-V) curve and a SEM image of the radial junction a-Si:H/CuO NW solar cells in the top in-set

[1] S. Misra, L. Yu, M. Foldyna, P. Roca i Cabarrocas, High efficiency and stable hydrogenated amorphous silicon radial junction solar cells built on VLS-grown silicon nanowires, SOL. ENERG. MAT. SOL. C., 118 (2013) 90-95.
[2] S. Misra, L. Yu, M. Foldyna, P. Roca i Cabarrocas, New Approaches to Improve the Performance of Thin-Film Radial Junction Solar Cells Built Over Silicon Nanowire Arrays, Photovoltaics, IEEE Journal of, 5 (2015) 40-45.
[3] S.H. Lee, M. Shin, S.J. Yun, J.W. Lim, CuOx/a-Si:H heterojunction thin-film solar cell with an n-type µc-Si:H depletion-assisting layer, Progress in Photovoltaics: Research and Applications, (2015).
[4] S. Masudy-Panah, G.K. Dalapati, K. Radhakrishnan, A. Kumar, H.R. Tan, E. Naveen Kumar, C. Vijila, C.C. Tan, D. Chi, p-CuO/n-Si heterojunction solar cells with high open circuit voltage and photocurrent through interfacial engineering, Progress in Photovoltaics: Research and Applications, (2014).

ID 89 - Poster

Optical, electrical and morphological study of PEDOT:PSS single layers spin coated with various secondary doping solvents optimized for printed electronics

*T. Syrovy[1], *P. Janicek[2], J. Mistrik[2], K. Palka[3], P. Hawlova[1], L. Kubac[4], M. Klanjšek Gunde[5]*
[1]University of Pardubice, Faculty of Chemical Technology, Department of Graphic Arts and Photophysics, Pardubice, Czech Republic , [2]University of Pardubice, Faculty of Chemical Technology, Institute of Applied Physics and Mathematics, Pardubice, Czech Republic, [3]University of Pardubice, Faculty of Chemical Technology, Department of General and Inorganic Chemistry, Pardubice, Czech Republic, [4]Center for Organic Chemistry s.r.o., Rybitví, Czech Republic, [5]National Institute of Chemistry, Ljubljana, Slovenia

Poly(3.4-ethylenedioxythiophene):poly(styrenesulfonate) (PEDOT:PSS) is one of the most promising conducting polymers for industrial applications such as Light Emitting Diodes, Light Emitting Capacitor, Photovoltaic Cells and sensors, organic transistors, batteries, etc. [1-3] due to its high electrical conductivity and good optical transparency in the visible spectral region and good environmental stability. Owing to these properties (PEDOT:PSS) has become one of the most important and widely used transparent electrode layers in polymer based and organic electronic devices.

Films of PEDOT:PSS can be easily processed from aqueous dispersions by spin coating or by printing or coating techniques. Development of PEDOT:PSS preparation process requires various characterization techniques as a feedback for tuning specific properties of final layers. We report on characterization study of a series of spin coated single layers of PEDOT:PSS with properties varied by using different secondary dopants. To avoid possible problems with dependency of quality/properties of printed layers, the spin coating technique was used as a standard method for fabrication of smooth, homogeneous layers.

Spectroscopic ellipsometry used for optical characterization of single layers of PEDOT:PSS films is capable to determine optical constants (refraction index *n*, extinction coefficient *k*) and thickness of the layer via suitable model. Anisotropic model was used with different in plane and out of plane properties due to lasagna like inner structure of the layer reported in literature [4]. From Drude term used for in plane optical constants evaluation optical conductivity can be determined. Example of measured (for angle of incidence 70°) and modeled ellipsometry parameters Ψ and Δ as a function of photon energy for one of the PEDOT:PSS single layer are in Fig. 1 where squares are experimental values of Ψ, dashed line shows modeled values of Ψ, circles are experimental values of Δ and full line shows modeled values of Δ. Results of optical (measured by spectroscopic ellipsometry, UV-VIS and Raman spectroscopy), electrical (DC conductivity) and morphological (AFM, profillometry) properties of these PEDOT:PSS films will be presented and compared together with previously published results [5-6] with the emphasis to optimize preparation of PEDOT:PSS single layers for printed electronics.

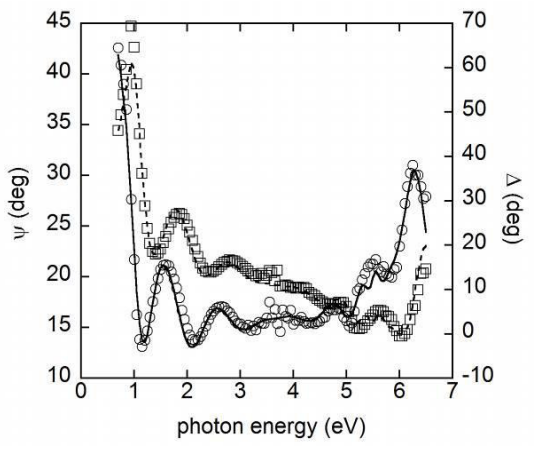

[1] M. Granström, M. Berggren, O. Inganäs: Science 267 (1995) 1479-1481.
[2] A. Dhanabalan, et al.: Adv. Funct. Mater. 11 (2001) 255-262.
[3] D. Setiadi, Z. He, J. Hajto, T. D. Binnie: Infrared Physics and Technology 40 (1999) 267-278.
[4] A. M. Nardes, M. Kemerink, R. A. J. Janssen, J. A. M. Bastiaansen, N. M. M. Kiggen, B. M. W. Langeveld, A. J. J. M. van Breemen, and M. M. de Kok: Advanced Materials 19 (2007) 1196-1200.
[5] M. Losurdo, K. Hingerl: Elipsometry at the Nanoscale. Springer-Verlag Berlin Heidelberg 2013. ISBN 978-3-642-33955-4.
[6] L. A. A. Pettersson, F. Carlsson, O. Inganäs, H. Arwin: Thin Solid Films 313-314 (1998) 356-361.

ID 90 - Poster

Accurate characterisation of the thickness and structural properties of nanocrystalline silicon synthesised by hot-wire chemical vapour deposition

*C. Oliphant [1], R. Pepenene[1,2], T. Muller[2], W. Jordaan[1], F. Cummings[2], C. Arendse[2]
[1]NMISA , Materials Characterisation , Pretoria, South Africa
[2]University of the Western Cape, Physics, Cape Town, South Africa

The reliable characterisation of nanostructured materials is important for understanding the relationship between the nanostructure and the corresponding properties. In the case of nanocrystalline silicon (nc-Si:H), which has been identified as a cheap and more stable alternative to amorphous and monocrystalline silicon based solar cells, the film thickness and chemical state is important from an application point of view as it influences the material structure and optoelectronic properties (e.g. absorption and conductivity). An accurate measurement of the nanostructural properties of nc-Si:H is challenging, given the complex microstructure (voids, crystallinity, amorphous fraction) that varies as a function of depth within the film. In this study, we report on the accurate determination of the film thickness, optical response and nanostructural properties of nc-Si:H synthesised by hot-wire chemical vapour deposition.

The fgures show the cross-sectional SEM image and TOFSIMS examination. The nc-Si:H film thickness amounted to 1464 nm ± 10 nm. This value was then compared to thickness value deduced from the TOFSIMS depth profile at the time before the onset of the substrate surface oxide. The values from TOFSIMS (~ 1450 nm) corresponded well with that deduced from SEM (~ 1460 nm) and UV-VIS interference analysis (~ 1470 nm). Interestingly, the so-called incubation layer from which the nanocrystals are reportedly grown from amounted to ~ 190 nm (from SEM), comparing well with the value determined from the TOFIMS SiH signal (~ 180 nm). This is to be expected given the fact that the incubation layer has typically a highly dense, porous amorphous silicon structure.

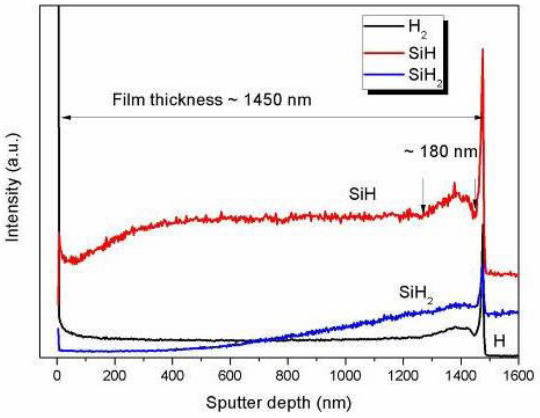

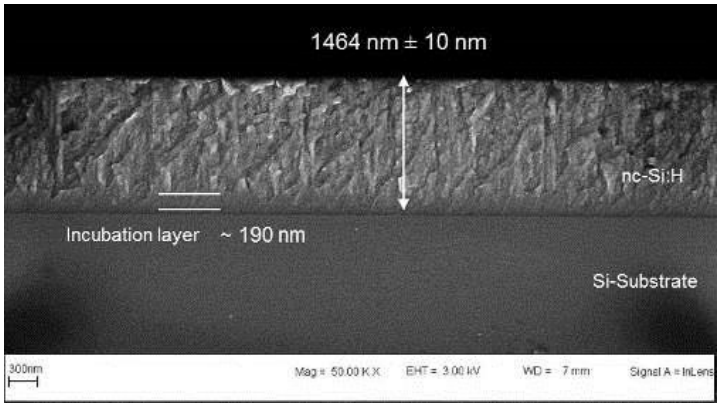

ID 91 - Poster

Synthesis of hydrogenated amorphous silicon suboxide films by the gas-jet electron beam plasma CVD method

**S. Khmel[1], E. Baranov[1], A. Zamchiy[1], M. Buyko[1]*
[1]Novosibirsk State University, Physics department, Novosibirsk, Russian Federation

Hydrogenated amorphous silicon suboxide (a-SiOx:H) has been widely used in solar cells as buffer and window layers and an intrinsic absorber layer. Silicon suboxide films can be prepared by various methods, such as plasma enhanced chemical vapor deposition (PECVD), hot wire chemical vapor deposition (HWCVD), very high frequency PECVD and radio frequency PECVD.

In this paper, the a-SiOx:H films were obtained by gas-jet electron beam plasma chemical vapor deposition method. This method provides high deposition rates of silicon films for solar cells with low energy consumption in a standard vacuum chamber [R. G. Sharafutdinov, S. Ya. Khmel, V.G.Shchukin et al, Solar Energy Materials & Solar Cells 89, 99 (2005)].

The experiments were carried out in a vacuum chamber pumped off by a forevacuum pump. The processing gas was a mixture of silane and argon. The $R=G(Ar)/G(SiH_4)$ was changed from 19 to 109 at a constant flow rate of silane. Oxygen was supplied directly into the vacuum chamber. Substrate temperature was 260 C. The chamber was equipped with a forevacuum electron gun with a plasma cathode. This gun generated an electron beam with 1.6 keV energy and about 70 mA current. Hydrogenated amorphous silicon suboxide thin films were prepared on Corning Eagle XG substrates and crystalline silicon wafers. The thicknesses of the synthesized films were about 850 nm.

The structural properties of the films were investigated by Raman spectroscopy.

Fourier transformed infrared (FTIR) spectroscopic studies were performed to obtain hydrogen and oxygen concentration in the films synthesized on c-Si wafers. With R increasing oxygen concentration in the films decreases from 40 to 12.5 at.%. The higher the gas jet density, which is determined by argon flow rate, the less oxygen is supplied to the jet axis from the background gas. The hydrogen content in the films was 3 - 8 at.%.

Optical transmission spectra were recorded for investigation optical properties and thickness measurement of the films with help of PUMA code on Corning Glass XG. It is known the band-gap of a-SiOx:H films strictly depend on varying oxygen content of the samples. Obtained values of the optical band gap decrease from 2 to 1.77 eV with the R increasing due to the decrease of oxygen content in the film.

The deposition rate increases from 0.6 to 2 nm/sec with R increasing. Generally, increasing the argon flow rate during an electron beam activation leads to the formation of a large number of high-energy secondary electrons. These electrons have an energy higher than the silane dissociation threshold, which leads to activation of more silane-containing radicals and thus increases the deposition rate of film.

This work was supported in part by the Russian Foundation for Basic Research (grant#15-08-08334-a)

ID 92 - Poster

Transition metal oxides as hole transport layers in organic solar cells

**M. Sendova-Vassileva[1], H. Dikov[1], G. Popkirov[1], P. Vitanov[1], V. Gancheva[2], G. Grancharov[2]*
[1]CL SENES, BAS, Sofia, Bulgaria
[2]Institute of Polymers, BAS, Sofia, Bulgaria

Solar cells with polymer based active layers are the subject of intensive research because of their potential to be inexpensive, flexible and have a short energy payback time. However they still have a number of problems connected with their efficiency and stability. In this contribution an attempt is made to improve the series resistance and current collection of bulk heterojunction polymer solar cells based on P3HT:PCBM and PCDTBT:PCBM. Thin transition metal oxide layers MoO_3 and WO_3 are applied as hole transport layers in conventional and inverted bulk heterojunction polymer solar cells and compared with PEDOT:PSS, which is commonly applied. The MoO_3 and WO_3 films are deposited by magnetron sputtering from MoO_3 and WO_3 targets. The oxidation state of the metal ions, the optical and structural properties of the films are studied and compared by measuring their IR, optical absorption, Raman and photoluminescence spectra. The current collection efficiency and series resistance of the obtained solar cells are compared by determining their current-voltage characteristics, spectral response as well as using impedance spectroscopy.

ID 93 - Oral

Material properties of buried dielectric layers for solar cells using liquid phase crystallised silicon on glass

**S. Calnan[1], O. Gabriel[1], S. Ring[1], B. Stannowski[1], R. Schlatmann[1,2]*
[1]Helmholtz-Zentrum Berlin, PVcomB, Berlin, Germany
[2]Hochschule für Technik und Wirtschaft (HTW) Berlin, Umwelttechnik/Regenerative Energien, Berlin, Germany

Liquid phase crystallisation (LPC) of amorphous silicon by use of a moving laser beam exposures one side of the substrate to temperatures above the melting point of silicon for such a short time that glass can be used for this purpose, even though the glass melting point is well below that of silicon. However, a dielectric interlayer (IL) stack separating the glass substrate and the LPC-Si absorber, is necessary to prevent diffusion of contaminants from the glass and to passivate the buried surface of the silicon. We show that the chemical composition of the last dielectric material in the IL stack, adjacent to the LPC-Si strongly affects the short circuit photocurrent density and the open circuit voltage of solar cells using LPC-Si absorbers. A comparison of different silicon dielectrics grown by plasma enhanced chemical vapour deposition showed that when the N-H and Si-H bond densities in the a-SiO_xN_y:H layers increased, their passivation quality improved. The best passivation as measured by Suns-V_{oc} and spectral response measurements on solar cells, with the highest N-H content in the passivating a-SiO_xN_y:H layer, yielded V_{oc} and J_{sc} values of 560 mV and 19.5 mA/cm², respectively, with a 4.3 µm thick p-type LPC-Si absorber. Since aluminium oxide AlO_x has been proven to provide excellent passivation of p-type silicon, this possibility was also explored for LPC-Si on glass. First results are shown for the replacement of the a-SiO_xN_y:H by AlO_x grown by atomic layer deposition.

ID 94 - Poster

Recombination Dynamics in Perovskite Solar Cells probed by Time-Delayed-Collection-Field (TDCF) Experiments

*A. Paulke[1], S. D. Stranks[2], T. J. K. Brenner[1], H. J. Snaith[2], D. Neher[1]
[1]University, Physics, Potsdam, Germany
[2]University, Physics, Oxford, United Kingdom

Time-Delayed-Collection-Field (TDCF) experiments are applied to working organometal halide perovskite ($CH_3NH_3PbI_{3-x}Cl_x$) solar cells with different device architectures. In TDCF, charges generated by a nanosecond optical pulse are extracted by a reverse voltage pulse. Thereby, the delay between the photoexcitation and the extraction is tuned over a wide range, with a minimal delay of 10 ns. This allows to probe the temporal evolution of the photogenerated charges and quantify nongeminate recombination losses in the device. For comparison, the charge carrier dynamics of all-organic polymer bulk heterojunction devices (P3HT:$PC_{61}BM$ and PTB7:$PC_{71}BM$) with similar performance is studied under comparable illumination conditions. We find that the predominant recombination mechanism in perovskite solar cells is very different from that of the organic cells. In particular, while the charge carrier dynamics in the all-organic cell can be described by purely bimolecular recombination with a time and fluence independent recombination coefficient, the dynamics in mesoporous-TiO_2/Perovskite/Spiro-OMeTAD and planar PEDOT:PSS/Perovskite/PCBM devices is characterized by a slow-down of the recombination rate over several microseconds.

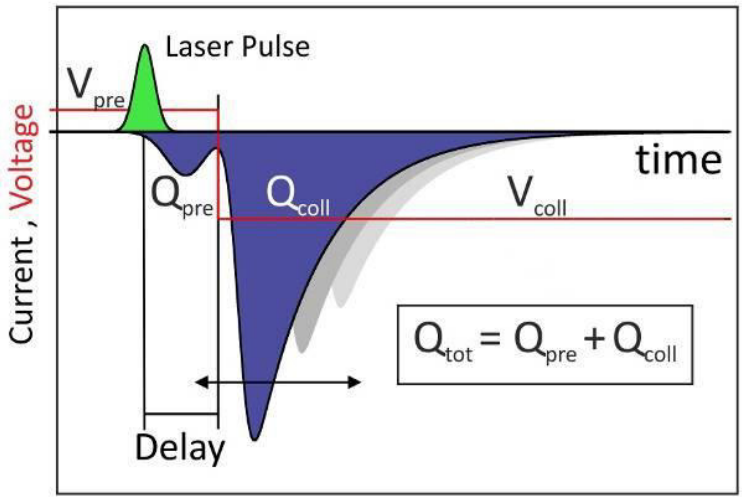

By varying the delay of the extraction voltage pulse V_{coll} with respect to the photoexcitation the recombination of charge carriers in a working solar cell can be studied.

ID 95 - Poster

Electronic properties of amorphous DLC films embedded with platinum nanoparticles

**S. Mikhailova[1], *O. Prikhodko[1], N. Manabaev[1], N. Guseynov[1], S. Maksimova[1], E. Daineko[1], Y. Mukhametkarimov[1]*
[1]al-Farabi Kazakh National University, Physical-Technical, Almaty, Kazakhstan

In this report the results of electronic properties and structure study in amorphous diamond-like carbon films with platinum nanoparticles (a-C:H<Pt> films) are presented. The films were produced by ion-plasma magnetron sputtering of combined polycrystalline graphite-metal target. The sputtering process was produced in hydrogen and argon gas mixture. The films were deposited on quartz and silicon substrates. The content of platinum impurity in the carbon matrix was changed from 0 to 9 at. %. Concentrations of metal impurity in the films were alternated by change of platinum and graphite area relation in the combined target.

Platinum embedding in a-C:H films lead to increase in their conductivity. Impurity influence on the conductivity of a-C:H<Pt> films substantially depends on the films deposition temperature. It was found that conductivity of amorphous a-C:H<Pt> films deposited at a temperature of 200°C results in substantially by 13 orders of magnitude more than that of pure films. The most significant increase of a-C:H<Pt> films conductivity occurs at the Pt concentration lied in the range from 3 to 7 at.%. Transmission electron microscopy (TEM) showed the presence of isolated particles in the a-C:H<Pt> films. The diameter of particles weakly changed with a rise of a metal content, and it was ~5 nm.

One of the important peculiarity of a-C:H<Pt> films optical properties was the appearance of absorption peak in the visible range of the optical absorption spectra. The absorption peaks in spectra of the a-C:H<Pt> films situated in the range from 495 to 498 nm. The intensity of the peak rose with increase of platinum content in the films. It is supposed that the absorption peaks are the result from surface plasmon resonance on metal nanoparticles in the a-C:H<Pt> films. Sizes of particles were determined from resonance absorption spectra, and these results were in a good agreement with TEM results.

Modeling of the resonance absorption procedure with use of Mie theory for the isolated metal particles imbedded in the dielectric matrix provides good coincidence with our experiment.

A part of the research was carried out in framework 4608/GF4 grant of Ministry of Education and Science of Kazakhstan Republic.

ID 96 - Poster

Silicon heterojunction solar cell passivation with nanocrystalline silicon oxide emitters

**H. Gatz[1], J. K. Rath[2], W. M. M. Kessels[1], R. E. I. Schropp[1]*
[1]Eindhoven University of Technology, Eindhoven, Netherlands
[2]Utrecht University, Utrecht, Netherlands

Silicon heterojunction (SHJ) solar cells are well known for their remarkably high efficiency. To increase the front side transmission of conventionally bifacially contacted SHJ solar cells we implement p-type nanocrystalline silicon oxide (nc-SiO_x:H(p)) as a wide band gap emitter layer. Promising characteristics for the emitter layer function of an optimized nc-SiOx:H(p) material, grown by radio frequency plasma enhanced chemical vapor deposition were observed. A necessity for high efficiency SHJ solar cells are high open circuit voltages, requiring excellent surface passivation of the crystalline silicon wafer interface. The passivation properties of layer stacks consisting of intrinsic amorphous silicon (a-Si(i)) and p-type nanocrystalline silicon oxide are investigated and the influence of the nc-SiO_x:H(p) layer is analyzed. One of the lingering question is how the hole and electron diffusion/transport is facilitated at a heterojunction with a wide difference in band gap using silicon oxide emitter. The effect of the of a-Si(i) layer thickness and the annealing temperature of the novel layer stack on the minority carrier lifetime are evaluated, yielding in an optimized passivation.

The result show that life time critically depends on the a-Si(i) layer thickness and a sharp drop in the life time with a-Si(i) layer thinner than 3 nm is seen. The buffer a-Si(i) layer creates the discontinuity in the conduction band at the amorphous-crystalline silicon interface [1], which serves to reduce the recombination in the mixed phase nanocrystalline silicon oxide p-layer. The annealing studies of the a-Si(i)/nc-SiO_x(p) layer stack on the c-Si wafer confirms the deleterious effect of the annealing temperature above 150°C, the deposition temperature of the nanocrystalline silicon oxide p-layer, presumably due to the competing effects of interface passivation and out-diffusion of hydrogen. One of the important findings of this study is that the adverse effect is only noticeable for thick a-Si(i) layer.

[1] M. W. M. van Cleef, J. K. Rath, F. A. Rubinelli, C. H. M. van der Werf, R. E. I. Schropp, and W. F. van der Weg, J. Appl. Phys. 82, (1997) 6089

ID 97 - Oral

Excitation fluence dependent nanosecond transient absorption in a-$Ge_{25}As_{10}Se_{65}$ thin film

*P. Khan[1], R. Sharma[1], *A. Kumaran Nair Valsala Devi[1]*
[1]IISER Bhopal, India, Department of Physics, Bhopal, India

Chalcogenide glasses (ChG) consists of S, Se or Te are an important class of amorphous semiconductors, distinguished itself from other inorganic amorphous semiconductors by their unique photosensitivity depicted in terms of chemical, physical and structural changes upon illumination with bandgap/sub-bandgap light [1, 2]. In this article, we report nanosecond (ns) laser induced broad transient absorption (TA) spanning of ~ 150 nm near the bandgap region of a-$Ge_{25}As_{10}Se_{65}$ thin film. The rapid timing response and full reversibility of TA have great potential for applications in fast optical switching device.

$Ge_{25}As_{10}Se_{65}$ thin film of thickness ~1.0 μm was deposited on microscopic glass substrate by conventional thermal evaporation technique. In our experiments, TA was studied using pump-probe set up in cross beam configuration. Nanosecond laser pulses of wavelength 532nm were used as pump beam whereas Xenon Arc lamp (120 W) was used for producing white probe beam (200-1000 nm). Delay between pump and probe beam was created using digital delay generator. In order to study the intensity dependent TA, the intensity of the pump beam was varied from 37mJ/cm^2 to 75mJ/cm^2 [3, 4].

Upon pump beam excitation, ΔA (a measure of TA) spectra spreads over a broad wavelength range of 470-610 nm for different probe delays. Interestingly, rise of ΔA is instantaneous with pump excitation and decays gradually however, the recovery was not fully complete within our experimental time window of 5 μs. TA in our sample occurs due to the transient change in the amorphous network through bond rearrangements by self trapped excitons. Interestingly, decay kinetics of TA becomes faster at longer wavelengths as compared to shorter wavelengths which provide direct evidence that the trapped exciton posse's longer life time in deep than in shallow traps. Excitation fluence dependent study reveals TA exhibits a quadratic dependence on laser dose indicating that the effects are originating from two-photon process. Further, decay time constant scales a linear relationship with excitation fluence which signifies that TA decays faster at lower fluence.

The authors thank Department of Science and Technology (Project no: SR/S2/LOP-003/2010) and council of Scientific and Industrial Research, India, (grant No. 03(1250)/12/EMR-II) for financial support.

[1] P. Khan, A. R. Barik, E. M. Vinod, K. S. Sangunni, H. Jain and K. V. Adarsh, Coexistence of fast photodarkening and slow photobleaching in $Ge_{19}As_{21}Se_{60}$ thin film, Opt. Express **20**, 12416 (2012).
[2] P. Khan, H. Jain and K. V. Adarsh, Role of Ge5As ratio in controlling the light-induced response of a-$Ge_xAs_{35-x}Se_{65}$ thin films, Sci. Rep. **4**, 4029 (2014).
[3] P. Khan, T. Saxena and K. V. Adarsh, Nanosecond light induced, thermally tunable transient dual absorption bands in a-$Ge_5As_{30}Se_{65}$ thin film, Sci. Rep. **4**, 6573 (2014).
[4] P. Khan, T. Saxena and K. V. Adarsh, Tailoring between network rigidity and nanosecond transient absorption in a-$Ge_xAs_{35-x}Se_{65}$ thin films, Opt. Lett. **40**, 768 (2015).

ID 98 - Oral

Plasmon assisted changes in chalcogenide glass - gold nanostructures

*I. Csarnovics[1], P. Nemec[2], M. Veres[3], K. V. Adarsh[4], A. Bonyár[5], S. Molnár[1], S. Kökényesi[6]
[1]University of Debrecen, Department of Experimental Physics, Debrecen, Hungary
[2]University of Pardubice, Department of Graphic Arts and Photophysics, Faculty of Chemical Technology, Pardubice, Czech Republic
[3]HAS, Institute of Solid State Physics and Optics, Budapest, Hungary
[4]Indian Institute of Science Education and Research, Physics, Bhopal, India
[5]Budapest University of Technology and Economics, Department of Electronics Technology, Budapest, Hungary
[6]University of Debrecen, Department of Electrical Engineering, Debrecen, Hungary

Different effects like photo-darkening and bleaching, local expansion and contraction, bond breaking and rearrangement, atomic movements take place in amorphous chalcogenides under near band-gap illumination. These processes are essential for the development of amplitude-phase optical recording and memory devices, fabrication of photonic elements. Shrinking dimensions towards nanophotonic applications requires investigation of sub-wavelength structures, which nowadays are often connected with plasmonic effects. Since the photo-induced electron-hole generation, defect creation or modification and atomic motions are the basic for structural changes in chalcogenide layers, these processes can be influenced by plasmon fields. Metals as Au, Ag and Cu are widely used for surface plasmon resonance experiments, not in the last place because of the manifestation of optical resonances in the visible spectral region. The localized surface plasmon resonance is rather easily observed in nanometer-sized metallic structures and widely used for measurements, sensing, in semiconductor devices and even in optical data storage. Gold nanoparticles on silica glass substrate satisfy the conditions for surface plasmon resonance in the green-red spectral range, where the chalcogenide glasses have the the highest sensitivity.
Gold nanoparticles deposited on silica glass substrate and covered by amorphous chalcogenide film satisfy the conditions of efficient surface plasmon resonance. In this work the additional plasmon-related effects on the laser-induced optical, surface and structural changes in the created samples were investigated. The films were analyzed with various methods (Raman Spectroscopy, Atomic Force Microscopy (AFM) and Energy Dispersive X-Ray Spectroscopy (EDS)) in order to determine the influence of the irradiation on the structure, surface topography and elemental composition. It was established that the gold nanostructures influence and enhance the optical, structural and volume changes and promote the exciton generation in gold nanoparticles/chalcogenide layer structure.
The experimental results support the importance of localized electric fields in photo-induced transformation of chalcogenide glasses as well as suggest new approaches to improve the performance of these optical recording media. Results may be utilized for direct, micrometer- or submicron size geometrical and optical pattern formation and used also for further development of the explanations of these effects in chalcogenide glasses.
The work is supported by the project TÁMOP-4.2.2.A-11/2/KONV-2012-0032, which is co-financed by the European Union and European Social Fund. Financial support from the Czech Science Foundation (Project No. 15-02634S) is greatly acknowledged.

ID 99 - Oral

Lifetime measurements on poly-crystalline silicon thin films on glass utilzing photoluminescence

*S. Kühnapfel[1], J. Huang[2], A. Teal[2], P. Sonntag[1], D. Amkreutz[1], S. Gall[1], B. Rech[1]
[1]Helmholtz-Zentrum Berlin für Materialien und Energie, Institut für Silizium-Photovoltaik, Berlin, Germany
[2]University of New South Wales, Sydney, Australia

The fabrication of thin-film multicrystalline silicon solar cells by liquid-phase crystallization (LPC) is a promising emerging technology. In the last years it has been demonstrated that a high-quality silicon absorber material can be produced on glass substrates by a single crystallization scan using either a continuous wave laser (Dore et al., 2012) or an electron beam (Amkreutz et al., 2011). With open circuit voltages well above 620 mV (Haschke et al., 2014) a material quality of commercially available multicrystalline wafers (Yang et al., 2013) has been reported. In order to improve the material quality, further characterization is required. However, reliable methods used in wafer technology are not as straight forward for silicon thin films on glass and failed to deliver results in the past due to the small material thickness and insufficient material quality. In this work we use a 10 µm thick state of the art LPC solar cell which was electrically characterized by measuring both, current voltage characteristic and spectral response. The same cell was used for photoluminescence (PL) imaging and transient PL measurements. The PL image was measured at an LED excitation of 530 nm with an excitation intensity of 1 sun with the system described in ref. (Teal et al., 2014). Transient PL was done with a 200 µm² spot of a 532 nm pulsed laser using an InGaAs detector and suitable filters. Due to the high material quality we observe a clear inter band luminescence for both systems. The PL imaging clearly reveals a grain structure. The transient PL was measured at various position across the cell. The effective minority carrier lifetime was then extracted from the resulting transients and compared to the local PL-imaging intensity. We found a proportionality between both measurements. The resulting calibration factor was used to calculate a lifetime mapping from the measured PL intensity image. Assuming a proportionality of minority carriers mobility and the HALL measured majority mobility, an effective diffusion length mapping was derived. The obtained diffusion length of 14 ± 2 µm is slightly higher than the value gained by evaluating the spectral response (11 ± 1 µm). Thus it is shown that electrical properties of the material can be extracted in early stages of the device preparation which is standard in wafer technology but has not been available for poly silicon thin film solar cells so far.

Amkreutz, D., Müller, J., Schmidt, M., Hänel, T., Schulze, T.F., 2011. Electron-beam crystallized large grained silicon solar cell on glass substrate. Prog. Photovolt. Res. Appl. 19, 937-945. doi:10.1002/pip.1098
Dore, J., Evans, R., Eggleston, B.D., Varlamov, S., Green, M.A., 2012. Intermediate Layers for Thin-Film Polycrystalline Silicon Solar Cells on Glass Formed by Diode Laser Crystallization. MRS Online Proc. Libr. 1426, 63-68. doi:10.1557/opl.2012.866
Haschke, J., Amkreutz, D., Korte, L., Ruske, F., Rech, B., 2014. Towards wafer quality crystalline silicon thin-film solar cells on glass. Sol. Energy Mater. Sol. Cells 128, 190-197. doi:10.1016/j.solmat.2014.04.035
Teal, A., Dore, J., Varlamov, S., 2014. Photoluminescence imaging of thin film silicon on glass. Sol. Energy Mater. Sol. Cells 130, 1-5. doi:10.1016/j.solmat.2014.06.024
Yang, Y.M., Yu, A., Hsu, B., Hsu, W.C., Yang, A., Lan, C.W., 2013. Development of high-performance multicrystalline silicon for photovoltaic industry. Prog. Photovolt. Res. Appl. n/a-n/a. doi:10.1002/pip.2437

ID 100 - Poster

Advanced light trapping in hydrogenated amorphous silicon-germanium/silicon tandem solar cells

*L. W. Veldhuizen[1], Y. Kuang[1], K. H. M. van der Werf[2], R. E. I. Schropp[1]
[1]Eindhoven University of Technology, Applied Physics, Eindhoven, Netherlands
[2]Energy research Center of the Netherlands, Eindhoven, Netherlands

The energy conversion efficiency of a hydrogenated amorphous silicon (a-Si:H) thin film solar cell can be significantly increased when it is combined with narrow band gap semiconductors in a multijunction solar cell. This is often accomplished by choosing hydrogenated microcrystalline silicon (µc-Si:H) and/or hydrogenated amorphous silicon-germanium (a-SiGe:H) als narrow-band gap material. As a direct-band gap semiconductor, a-SiGe:H has particularly high absorption coefficients for photon energies that are higher than the band gap. An active layer of a-SiGe:H in a thin film solar cell can therefore be made approximately one order of magnitude thinner compared to a layer made out of an indirect band gap material as µc-Si:H, even without the use of extensive light trapping techniques. Nevertheless, the lower ambipolar diffusion length of a-SiGe:H with respect to unalloyed a-Si:H and µc-Si:H limits the layer thickness to values for which light trapping is essential. Moreover, a thin active layer is desired for amorphous silicon alloys in order to mitigate light induced degradation by the Staebler-Wronski effect.

In contrast to µc-Si:H, the amorphous nature of a-SiGe:H makes it easier to use light scattering substrates with relatively high aspect ratio features, as structural and electronic properties of the material are less likely to be compromised. In addition, conformal layer growth on such substrates can be realized even at high deposition rates, when hot wire chemical vapor deposition (HWCVD) is used as the deposition method.

In this work we study the suitability of various light scattering substrates for a-SiGe:H/a-Si:H tandem cells with substrate (*n-i-p*) configuration. The a-SiGe:H bottom cells are made by HWCVD instead of the more conventional method of plasma enhanced chemical vapor deposition (PECVD) and have an exceptionally narrow optical band gap of 1.37 eV. We test and compare random and periodic textures created with nanoimprint lithography and textures consisting of solution-grown ZnO nanorods. Additionally, we demonstrate the potential of double textured substrates consisting of a rough transparent conductive oxide on a smoother silver back reflector (fig. 1). This concept enables excellent light trapping by the dielectric features, while reducing the parasitic plasmonic absorption in the moderately textured silver back reflector.

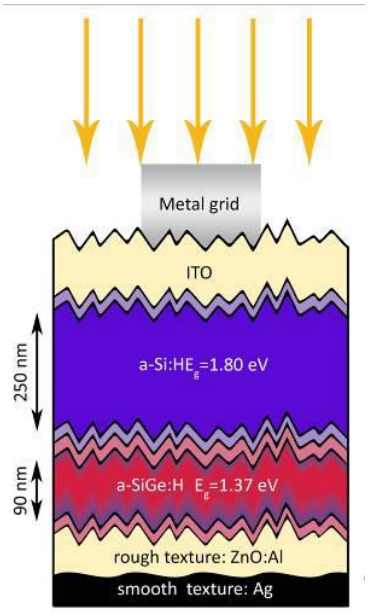

ID 101 - Poster

Effect of the Substrate Temperature on the Plasma Texturing Process of c-Si Wafers for Black Silicon Solar Cells

*D. Murias[1], M. Moreno[1], C. Reyes-Betanzo[1], A. Torres[1], R. Ambrosio[2], P. Rosales[1]
[1]INAOE, Electronics, Puebla, Mexico
[2]BUAP, Electronics, Puebla, Mexico

In this work we present the study of the effect of the substrate temperature on the formation of pyramid like structures on crystalline silicon (c-Si) wafers, in a plasma texturing process. The optimized substrate temperature used during the plasma process has resulted on the formation of well defined pyramid like structures as is done by wet processes. Moreover, the textured c-Si wafers have very low diffuse reflectance values, as low 2%, which are much more lower than those obtained by we texturing processes based on KOH and NaoH.

SF_6 and O_2 gas mixtures have been used in the plasma for texturing the surface of c-Si wafers in a Reactive Ion Etching (RIE) system. The surface morphology of the textured c-Si wafers has been characterized using scanning electron microscopy (SEM), atomic force microscopy (AFM) and the reduction of the reflectance of the c-Si surfaces has been studied using a spectrophotometer (Perkin Elmer) in the range of 400 - 700 nm, which provides diffused reflectance.

Our results demonstrate that plasma texturing processes produce a complete black silicon surface, which is of interest for hetero junction solar cells, since the use of deionized water (DI) and wet chemicals for texturization are suppressed from the cells fabrication process.

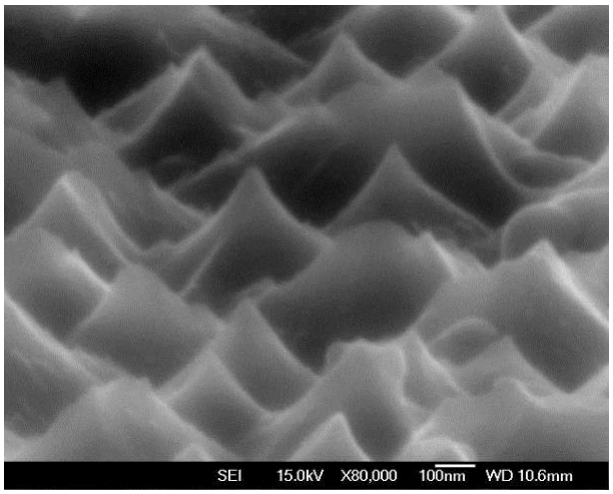

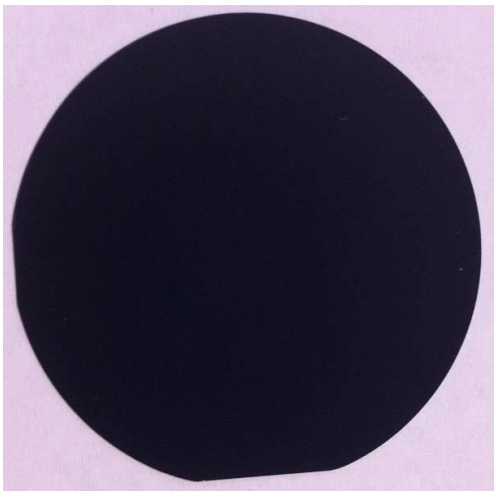

ID 102 - Oral

Fast deposition of triple junction solar cells with intrinsic amorphous silicon-germanium layers deposited by hot wire chemical vapor deposition

*L. W. Veldhuizen[1], K. H. M. van der Werf[2], Y. Kuang[1], R. E. I. Schropp[1]
[1]Eindhoven University of Technology, Applied Physics, Eindhoven, Netherlands
[2]Energy research Center of the Netherlands, Eindhoven, Netherlands

In multijunction thin film silicon solar cells, hydrogenated microcrystalline silicon (µc-Si:H) is often the material of choice as narrow-band gap absorber. Unfortunately, the considerable thickness required for the µc-Si:H layer to absorb enough light, combined with the low deposition rate that is necessary for µc-Si:H to be of satisfactory electronic quality, lead to deposition times often exceeding 45 minutes for a single layer. This leads to high manufacturing costs, making it harder for the thin film silicon based solar cell technology to compete with other photovoltaic industries. An alternative narrow-band gap material to be reconsidered is hydrogenated amorphous silicon-germanium (a-SiGe:H). Like hydrogenated amorphous silicon (a-Si:H), a-SiGe:H is a direct band gap semiconductor, which allows the absorber layer to be approximately one order of magnitude thinner than that of µc-Si:H. The conventional plasma enhanced chemical vapor deposition (PECVD) technique used for deposition of a-SiGe:H however, has commonly led to reduced material quality of films when the germanium content was increased to reach a narrow band gap (< 1.5 eV).

Therefore, in recent work we have studied and optimized a-SiGe:H films deposited by hot wire chemical vapor deposition (HWCVD). We demonstrated that even films with germanium concentrations over 60% and optical band gaps lower than 1.4 eV have excellent material properties for the use as active layers in thin film solar cells. This enables us to use a-SiGe:H instead of µc-Si:H in tandem and triple devices without compromising the IR-response of the solar cells. Moreover, these layers are deposited at a high rate of 0.5 nm/s.

We present a-SiGe:H/a-SiGe:H/a-Si:H triple junction solar cells of which all absorber layers are deposited with HWCVD. These layers have a combined thickness of less than 400 nm and are deposited within 16 minutes in total, thus creating a significant economic advantage with respect to conventional multijunction solar cells. The initial energy conversion efficiency of these solar cells is higher than 10% and we discuss the stability of the solar cells using light soaking experiments.

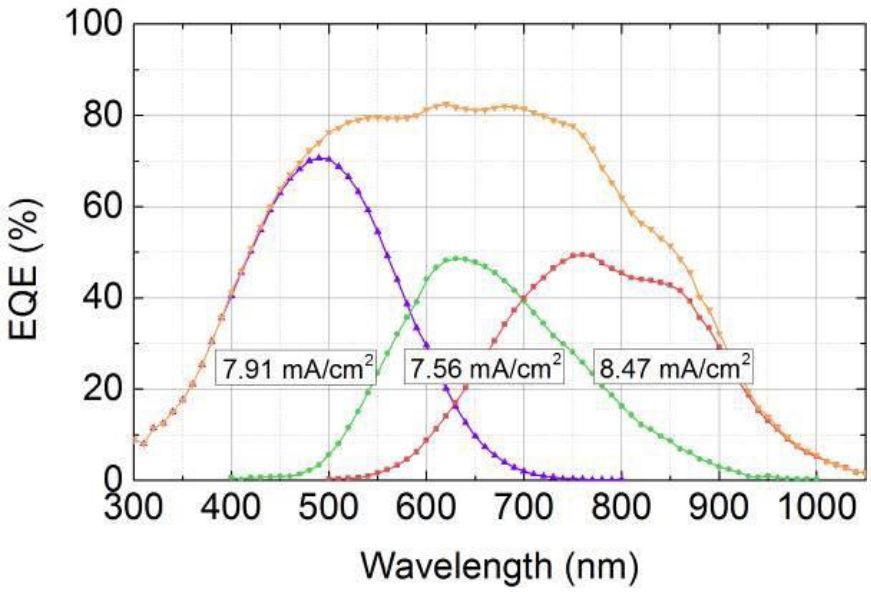

ID 103 - Poster

Extraction of minority charge carrier diffusion length by the grain-boundary light-beam-induced current method - a simulation based analysis of the measurements

*A.- M. Teodoreanu[1], *O. Gref[1], R. Leihkauf[1], H. Lohrke[1], M. Kittler[2], C. Boit[1], F. Friedrich[1]*
[1]Technische Universitaet Berlin, Semiconductor Devices, Berlin, Germany
[2]Joint Lab IHP/BTU, BTU Cottbus, Cottbus, Germany

The charge carrier lifetime and accordingly the diffusion length in polycrystalline semiconductor materials is known to be detrimentally influenced by disordered interfaces like grain boundaries (GBs). The GB light-beam-induced-current (GB-LBIC) technique allows for the extraction of the minority charge carrier diffusion length in unprocessed polycrystalline materials [Palm1994]. This measurement method is based on the GB itself acting as a charge collector. A spatially-resolved light-beam-induced-current can thus be measured even without a collecting p-n junction or Schottky contact, and without biasing the sample [Palm1994] and refs. therein.

In this contribution we present a simulation based analysis of measured GB-LBIC line scans on bonded silicon wafers, which feature “model grain boundaries” [Kittler2008]. The experiments were performed with three different LBIC measurement setups with laser wavelengths of 532 nm, 633 nm, and 1064 nm, respectively. The 2D simulations where performed with the numerical device simulator Sentaurus TCAD, which is based on the drift-diffusion model for charge carrier transport. Here the coupled set of differential equations - the Poisson equation and the continuity equations for electrons and holes - is solved for the discretized mesh points within a model sample containing a grain boundary that separates two crystalline silicon grains. The simulations allow for the understanding of 2D effects caused by surface recombination, illumination with different wavelengths and contact type (ohmic or Schottky) on the GB-LBIC line scans. Thus, the accuracy of the extracted bulk minority carrier diffusion length will be analyzed with regard to the above specified effects.

Indeed, the performed GB-LBIC measurements show at the shortest wavelength of 532 nm a strong influence of surface effects that requires a particularly good surface passivation for extracting a meaningful diffusion length. This effect is diminished for illumination with a wavelength of 1064 nm. However, imperfections in the ohmic character of the contacts can also render the line scan in the vicinity of the GB unsuitable for the diffusion length extraction. The simulation shows that measuring at a distance of roughly six times the diffusion length from the GB can present a solution to this dilemma. However, the local current at said location is a few orders of magnitude lower than the maximum current (~ 1 to 100 nA), which is obtained close to the GB. Thus, the signal might be lost in noise depending on the setup. Finally, we have found that due to the reduced spot size in LBIC measurements, special care has to be taken in regard to the illumination intensity in order to maintain the sample in low injection. For the 1064 nm wavelength this condition is more easily achieved due to the low absorption coefficient of silicon for this wavelength.

Keeping the discussed conditions in mind, GB-LBIC is a versatile method to extract a meaningful minority charge carrier diffusion length from polycrystalline material.

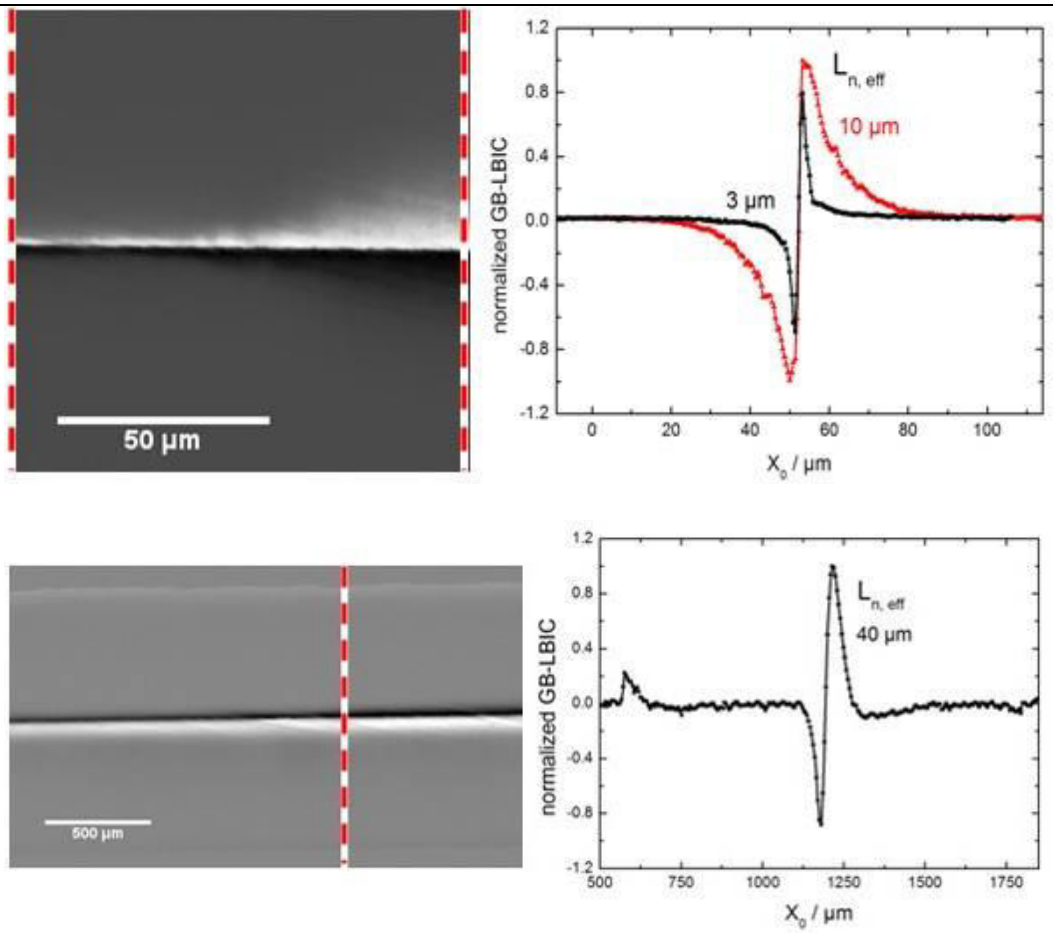

[Kittler2008] M. Kittler, M. Reiche, T. Arguirov, T. Mchedlidze, W. Seifert, O.F. Vyvenko, T. Wilhelm, X. Yu, Dislocations in Silicon as a Tool to be Used in Optics, Electronics and Biology, Solid State Phenomena, Vols. 131-133 (2008) 289-292.
[Palm1994] J. Palm, D. Steinbach, H. Alexander, Local Investigation of the Electrical Properties of Grain Boundaries, Materials Science and Engineering B24 (1994) 56-60.

ID 104 - Poster

Photo-induced non-linearity in binary pnictogen chalcogenide Sb_2Se_3 nanowires

*R. Sharma[1], R. K. Yadav[1], P. Khan[1], A. KV[1]
[1]IISER Bhopal, Physics, Bhopal, India

Group V-VI binary pnictogen chalcogenides have garnered considerable interest owing to their exotic thermoelectric and optoelectronic properties. Amongst these, antimony selenide (Sb_2Se_3) has shown great potential due to its narrow band gap and high thermoelectric coefficient. Moreover it can be easily crystallized into high aspect ratio 1-d structures which makes it ideal for semiconductor interconnects. In this article, we report nanosecond (ns) laser induced non linear absorption in Sb_2Se_3 nano wires. High value of non-linear absorption coefficient (600 cm/GW) essentially forsees novel applications of these 1-d nanostructures in optical limiting technologies.

1-d Sb2Se3 nanostructures were prepared by hydrothermal reduction. Briefly, a precursor solution of antimony chloride ($SbCl_3$) was prepared by stirring 0.15 g of $SbCl_3$ in 20 mL water. During continuous stirring, 20 mL glycol was added. Now, 0.13 g of Se powder and 0.2 g $NaBH_4$ was added in the solution. After 15 mins of stirring the entire solution was transferred into a 50 mL teflon lined stainless steel autoclave and kept in a hot air oven at 180^0C for 72 h. The black precipitate was then washed several times ethanol and distilled water. The scanning electron microscope (SEM) images show high aspect ratio nano wires ranging from 100-150 nm radius and few micrometers in length. X-ray diffractometry (XRD) data reveal orthorhombic phase (JCPDS Card, No. 15-0861) of the synthesysed nano wires. Prominent Raman bands corresponding to heteropolar Sb-Se bond vibrations in the $SbSe_{3/2}$-pyramides occur at 188 cm^{-1} and Sb-Sb bonds in Se_2Sb-$SbSe_2$ structural units appear at 252 cm^{-1} which are in agreement with reported data. UV Vis absorption data indicate a direct band gap of ~1.35 eV which in accordance with the literature.

Non linear behavior of Sb_2Se_3 nano wires dispersed in distilled water was studied by open aperture z-scantechnique. Second Harmonic (532 nm) from a Q-switched Nd: YAG laser with 5 ns pulse width and 10 Hz repetition rate was used as excitation at an energy of 250 µJ per pulse (~150 GW cm^{-2}). The laser beam was focused on to the sample by a plano-convex lense of focal length 50 cm. The transmitted intensity through the signal was recorded as a function of the sample position was measured using piezo photodiodes. The non-linear behavior of Sb_2Se_3 nano wires is evident by a dip in the normalized transmission at the focus. The non-linear absorption coefficient was obtained to be 600 cm/GW as determined by fitting the intensity dependent transmission equation using MATLAB. In conclusion, the z-scan measurements of Sb_2Se_3 nanowires shows their highly non linear behavior which can be a combination of two photon absorption and excited state absorption processes.

ID 105 - Oral

First experimental demonstration of tandem radial junction solar cells

*S. Misra[1], M. Foldyna[1], I. Florea[1], L. Yu[1], P. Roca i Cabarrocas[1]
[1]Ecole Polytechnique, LPICM-CNRS, Palaiseau, France

Silicon nanowires (SiNWs) provide an effective research platform for developing a new generation of low-cost and high efficiency solar cells owing to their enhanced light trapping and anti-reflection effects. By decoupling the light absorption and carrier collection directions, SiNWs permit to use very thin intrinsic layers for PIN radial junction thin film solar cells. This provides a higher built in field and hence a better separation of carriers. Simultaneously, ultra-thin absorber layers minimize the light-induced degradation of hydrogenated amorphous silicon (a-Si:H) solar cells [1]. By optimizing the density of radial junctions and replacing the top n-type a-Si:H by a more transparent hydrogenated microcrystalline silicon oxide (n-type µc-SiOx:H), we have managed to achieve an initial efficiency of 9.2% with just 100 nm thick intrinsic a-Si:H [2]. The thickness of the active material can also be verified thanks to transmission electron microscope images of transversal cross-sections prepared using a focused ion beam.

As we are using a low-temperature plasma-assisted vapour-liquid-solid method to grow our silicon nanowires on ZnO:Al coated corning glass substrates, we do not have any control over their orientations. Consequently, one might assume that it would be impossible to achieve the current matching in tandem solar cells fabricated on such “wild” structures. Nevertheless, we have successfully combined hydrogenated polymorphous silicon (pm-Si:H) and a-Si:H absorbers in a tandem radial junction solar cell, which to the best of our knowledge is the first demonstration of such device. The structure of our tandem solar cell is ITO/n-type µc-SiOx:H/intrinsic pm-Si:H/p-type µc-SiOx:H/ n-type µc-SiOx:H /intrinsic a-Si:H/p-type a-Si:H/p-type SiNW/ZnO:Al/Cg, as shown schematically in Fig. 1 (a). The corresponding scanning electron microscope image is provided in Fig. 1 (b). Moreover, by varying thicknesses of the active materials we have also managed to achieve a good current matching, as shown in Fig. 2. Along with an open circuit voltage of 1.5 V and a fill factor of 60.3%, we have achieved a power conversion efficiency of 6.5% for a cell area of 0.126 cm^2.

The next step is to improve the performance by optimizing various interfacial layers and also to explore the feasibility of combining other materials (a-SiGe:H and µc-Si:H) for the tandem radial junctions. The radial junctions have an excellent potential to reduce the material consumption and hence the deposition time. In combination with a minimal light-induced degradation they open a new direction for silicon thin film solar cells.

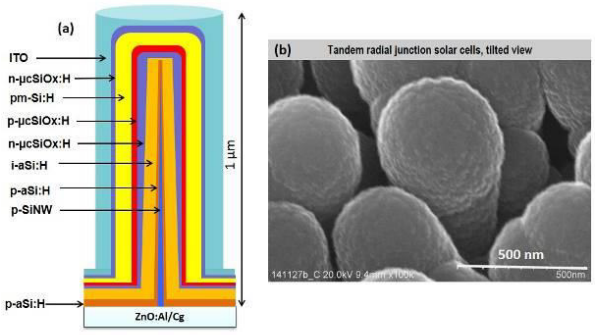

Fig. 1: (a) Schematic diagram of the fabricated tandem radial junction solar cells. (b) Corresponding scanning electron microscope image (using a 30° tilted stage).

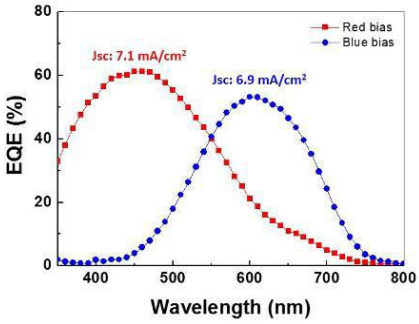

Fig. 2: External quantum efficiency of silicon nanowire based tandem radial junction solar cell measured under an appropriate bias illumination. Top cell is made of pm-Si:H (red curve), while a-Si:H is used for the bottom cell (blue curve). Despite inhomogeneous deposition and random tilt of the silicon nanowires a good current matching can be achieved.

[1] S. Misra, L. Yu, M. Foldyna, and P. Roca i Cabarrocas, SOLMAT, 118, 90-95, 2013.
[2] S. Misra, L. Yu, M. Foldyna, and P. Roca i Cabarrocas, IEEE JPV, **5** (1), 40-45, 2015.

ID 106 - Poster

Room temperature fabricated amorphous oxide heterodiodes on glass and flexible substrates

*P. Schlupp[1], H. von Wenckstern[1], M. Grundmann[1]
[1]Universität Leipzig, Institut für experimentelle Physik II, Leipzig, Germany

The use of abundant materials and low temperature fabrication, preferrably at room temperature (RT), can greatly reduce the cost of semiconductor devices. The latter further enables the usage of flexible materials as substrates. In this contribution, we present our investigations on heterodiodes consisting of the amorphous oxides zinc tin oxide (ZTO, *n*-type) and zinc cobalt oxide (ZCO, *p*-type), which show promising semiconducting properties even though they are fabricated at RT [1,2]. Both semiconducting thin films were fabricated by pulsed laser deposition (PLD). The conductivity can be easily controlled by the oxygen pressure in the chamber during the deposition.

Room temperature fabricated all amorphous oxide *n*-ZTO/*p*-ZCO heterodiodes will be presented [3]. To enhance the rectification of the diodes, an ultrathin insulating ZTO layer was introduced at the heterointerface leading to bipolar diodes with a rectification of more than six orders of magnitude. The ideality factors of these improved diodes are about 2 while they bunch around 1.2 for the heterodiodes without intinsic layer. Both diode structures will be compared and the conduction mechanism will be derived from temperature-dependend current voltage measurements.

These heterodiodes are also fabricated on flexible polyimid substrates and show similar properties like the diodes on rigid glass substrates. The stability against bending will be dicussed with focus on the bending radius and the number of bending events.

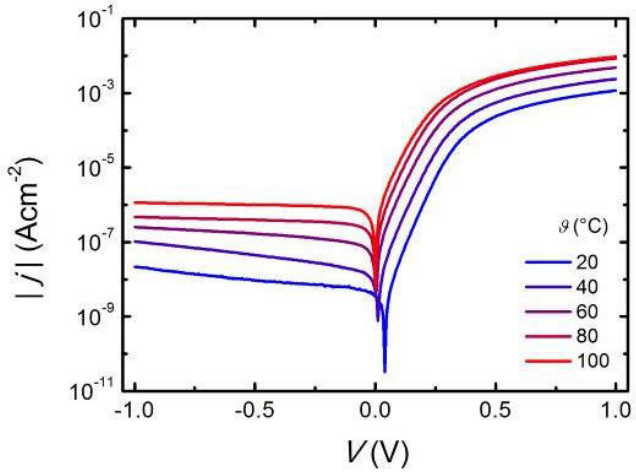

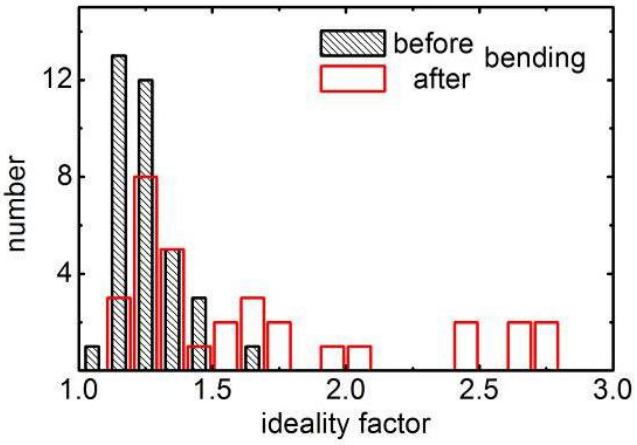

[1] P. Schlupp, H. von Wenckstern and M. Grundmann, *MRS Proceedings* **1633**, 101-104 (2014).
[2] F.-L. Schein, M. Winter, T. Böntgen, H. von Wenckstern and M. Grundmann, *Applied Physics Letters* **104**, 022104 (2014).
[3] P. Schlupp, F.-L. Schein, H. von Wenckstern and M. Grundmann, *Advanced Electronic Materials* **1**, 1400023 (2015).

ID 107 - Oral

SiO_x Thin-film Hydrogen Diffusion Barriers for High-performance Flexible Transparent IGZO TFTs and Circuits

*A. Tari[1], W. S. Wong[1,2]
[1]University of Waterloo, Department of Electrical and Computer Engineering, Waterloo, Canada
[2]University of Waterloo, Electrical and Computer Engineering, WATERLOO, Canada

Amorphous InGaZnO (IGZO) thin-film transistors (TFTs) are a promising transparent-metal oxide semiconductor for large-area electronics due to its high optical transparency and field-effect mobility (μ_{FE}) compared to conventional amorphous silicon (a-Si:H)-based devices. The IGZO amorphous structure possesses better carrier transport uniformity with high carrier mobility compared to polycrystalline Si films. These unique advantages have attracted increased interest and rapid development of these oxide semiconductors over the past decade. Unfortunately, this materials system is extremely sensitive to plasma damage, especially hydrogen in plasma-enhanced chemical vapor deposition (PECVD), resulting in increased channel conductivity that reduces the on/off ratios and hinders the fabrication of IGZO-based circuits. In this study, a SiO_x-based hydrogen barrier layer was implemented to minimize hydrogen diffusion into the active TFT region during PECVD processing.

In order to study the effect of the hydrogen plasma and oxide diffusion barrier on TFT performance, bottom-gate TFTs were fabricated on SiN_x and thermal oxide gate dielectrics. A 50 nm IGZO layer was deposited using RF sputtering at room temperature for the active layer. IGZO intrinsic layers deposited directly on SiN_x typically resulted in high conductivity IGZO channel layers. X-ray photoelectron and photoluminescence spectroscopy showed an increase in hydrogen-induced oxygen vacancies for the IGZO films deposited onto SiN_x compared to films on thermal oxide suggesting the hydrogen in the PECVD gate dielectric was responsible for the increased IGZO conductivity. To test this theory further, two different passivation layers were implemented to investigate the effect of hydrogen plasma damage on the active channel region. In the first set, fabricated TFTs were passivated with a 300 nm PECVD SiN_x deposited directly on the TFT back-channel. These TFTs did not show any switching characteristics while the intrinsic channel layer transformed into a conductive layer after nitride deposition. In order to protect the backchannel region from hydrogen plasma damage, a 30 nm SiO_x buffer layer was deposited by electron-beam deposition onto the intrinsic IGZO channel followed by a 270 nm 150°C PECVD SiN_x to form a bilayer SiN_x/SiO_x passivation layer over the TFT. The completed fully encapsulated TFTs had an on/off ratio of > 10^6, threshold voltage of ~1V and m_f of ~7.5 cm^2/V.sec. Using the oxide barrier in a similar manner at the IGZO/SiN_x gate-dielectric interface (forming a IGZO/SiO_x/SiN_x stack) resulted in TFTs having improved threshold voltage of ~5 V and on/off ratios of > 10^6 on flexible substrates, suggesting the efficacy of the SiO_x layer as a hydrogen diffusion barrier. We will also discuss the fabrication of flexible IGZO transparent pixel compensation circuits using this novel diffusion barrier structure and present the circuit operation under applied mechanical strain.

TFT I-V characteristics before backchannel passivation

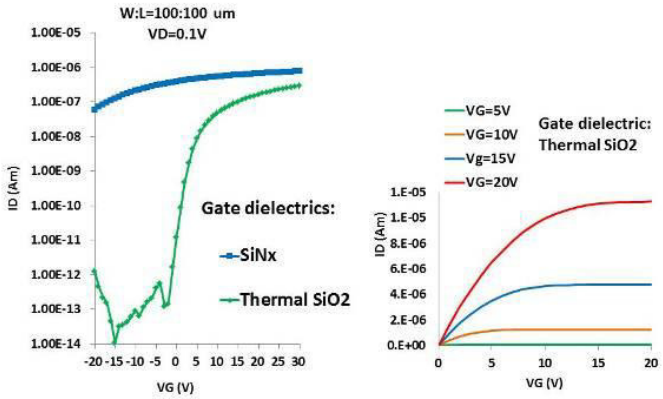

TFT I-V characteristics after backchannel passivation and Top contact deposition

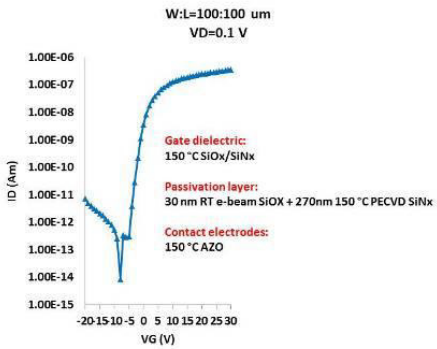

ID 108 - Oral

Structure of $Ge_{15}Sb_{20}S_{65-X}Se_X$ glasses characterized by Raman and high-resolution x-ray photoelectron spectra

*S. Xu[1], L. Wang[1], R. Wang[2]
[1]Beijing University of Technology, physics, Beijing, China
[2]Australian National University, physics, Canberra, Australia

It is well known that, Ge-Sb-Se glasses usually exhibit higher nonlinearity than Ge-As-Se but both Se-based glasses are too soft with lower laser damage threshold. One of the solutions is to partly place Se by S but this will be at the expense of the linear and nonlinear optical properties. Therefore in the paper we explore the dependence of structure and physical properties on the Se-content in $Ge_{15}Sb_{20}S_{65-X}Se_X$ (with x=0, 16.25, 32.5, 48.75 and 65) in order to screen the best compositions for the applications in photonics. We found that, while the density and refractive index of the glasses decrease with decreasing Se content, the laser damage threshold increases with increasing S-content. Raman scattering and high-resolution x-ray photoelectron spectra (XPS) were further employed to understand their structural origins. Through the evolution of the different structural units in the glasses, it was concluded that, the heteropolar bonds (Ge-Se/S, Sb-Se/S) were dominated in these glasses, and Ge is prior to bond with Se rather than S. With the increase of chalcogen Se/S molar ratio, the number of the Se-related chemical bonds (Ge-Se, Sb-Se and Se-Se) increases and that of S-related chemical bond (Ge-S, Sb-S and S-S) decreases gradually.

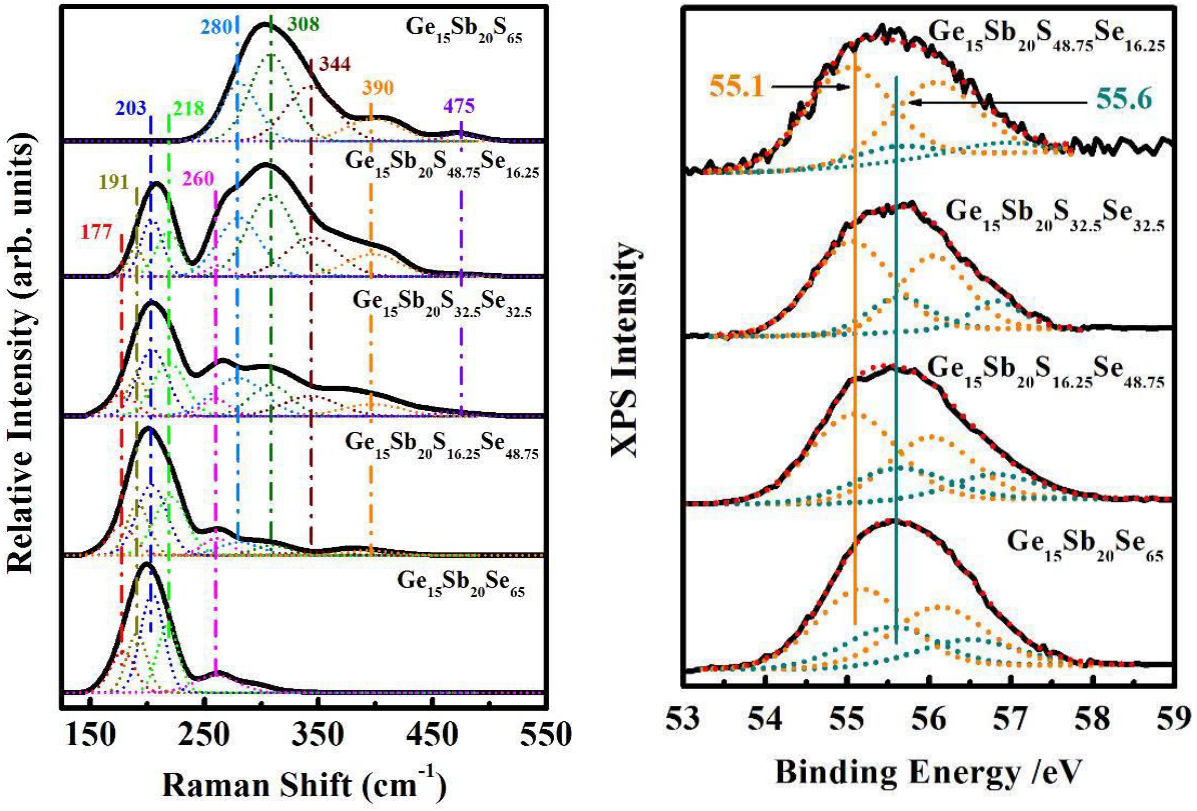

ID 109 - Oral

Integration of hydrogenated amorphous silicon thin-film photodetectors in microfluidic biosensors

*D. R. Santos[1,2], C. R. Pedrosa[1], R. R. G. Soares[1,2], N. Madaboosi[1], H. Muller-Landau[1], V. Chu[1], J. P. Conde[1,2]
[1]INESC Microsistemas e Nanotecnologias and IN-Institute of Nanoscience and Nanotechnology, Lisboa, Portugal
[2]Instituto Superior Técnico - University of Lisbon, Department of Bioengineering, Lisboa, Portugal

The integration of sensor systems in lab-on-chip (LoC) devices is a critical and rewarding step towards the development of high-throughput sensing systems, and also towards the development of tissue-, organ- and organism-on-chip miniaturized systems for biomedical, toxicological and drug development studies. This work focuses on the development of thin-film silicon photodetectors on glass substrates and their application towards high sensitivity fluorescence, chemiluminescence and colorimetric-based imagers and biosensors in microfluidic LoC systems. These photodetectors are integrated with microfluidic devices which allow the manipulation of minute quantities of fluids in microfabricated channels with dimensions typically in the range of 10-100 µm. The thin-film photodetectors are also used in direct imaging of cells for applications in biotechnology, for disease detection and for cell culture monitoring. Perpendicular *p-i-n* photodiodes and parallel intrinsic a-Si:H photoconductors were microfabricated as sensors and integrated with the microfluidic LoC platform.

The photodiode sensor is a vertical stack with back contact in aluminum deposited by magnetron sputtering over a cleaned glass substrate, patterned by direct writing photolithography (DWL) and wet chemical etching. The a-Si:H *p-i-n* junction is deposited by rf-PECVD and mesa junctions with lateral dimensions between 5 and 200 µm are defined by DWL followed by reactive ion etching (RIE). Silicon nitride (SiNx) is deposited by rf-PECVD to passivate the lateral walls of the junction, and a via is opened by lift-off to allow electrical contact between the p+-a-Si:H layer and the transparent top contact made of indium tin oxide (ITO) deposited by magnetron sputtering and defined by lift-off. A silicon nitride (SiNx) layer is deposited by rf-PECVD as a protective layer and vias are opened by lift-off at the contact pads to allow the wire bonding with the aluminum contacts. The microfabrication process of the a-Si:H photoconductors is simpler than that described above for the photodiodes. Parallel aluminum electrodes are defined by DWL followed by a deposition via rf-PECVD of the intrinsic a-Si:H. The a-Si:H layer is then defined by RIE into islands with interelectrode distances that can be controlled between 100 nm and several mm. A SiNx passivation layer is deposited as described for the photodiodes (Figure 1-A and 1-B).

The current-voltage (*I-V*) characteristics of the photosensors were measured at room temperature in the dark and under illumination (calibrated photon flux $\Phi_{(\lambda=510nm)}$ ~10^{14} $cm^{-2}.s^{-1}$). The photoconductor exhibits a dark conductivity and photoconductivity at λ = 510 nm of σ_{dark} = 5.1 x 10^{-9} $S.cm^{-1}$ and $\sigma_{\lambda=510nm}$ = 2.6 x 10^{-6} $S.cm^{-1}$, respectively. The sensor photoresponse was also measured with both photodetectors showing a linear photocurrent dependence with the incident photon flux Φ in the range of Φ~1 x 10^{7} $cm^{-2}.s^{-1}$ to Φ~1 x 10^{14} $cm^{-2}.s^{-1}$. (Figure 1-C).

The fabrication of the polydimethylsiloxane (PDMS) microchannels involved the production of a SU- 8 mold using a hard mask of sputtered and patterned aluminum on glass and the fabrication of PDMS microfluidic devices by a molding process.

To demonstrate the application of the integrated biosensor systems (integrated thin-film photosensors and surface functionalized microfluidic platform), results will be presented for experiments of miRNA and DNA hybridization, prostate specific antigen (PSA) immunoassays and harmful food and feed contaminant ochratoxin-A (OTA) immunoassays using fluorescently and enzymatically-labeled antibodies. The target analytes were quantified using either a competitive or sandwich immunoassay for

mycotoxins and PSA or a hybridization assay for miRNA by flowing the intended solutions sequentially, intercalated with washing steps with an appropriate stringency (Figure 2).

This work demonstrates the concept of a bioassay platform using PDMS-based microfluidics, with integrated optical detection based on thin-film silicon photodetectors on a glass substrate. The sensor integration allows significant gain in the efficiency of the capture of the emitted light, and the development of a truly miniaturized, portable multiplex biosensing platform. The incorporation of thin-films photosensors allows for an on-chip real-time data acquisition without the requirement of a bulky external setup, improving the point-of-care applicability and the speed of detection as well as reducing the cost for a detection analysis, thus providing fast and reliable on-chip results. The use of photosensors as an optoelectronic detection method of biomolecules in microfluidic on-chip applications is thus a promising approach towards a fully integrated hand-held detection device.

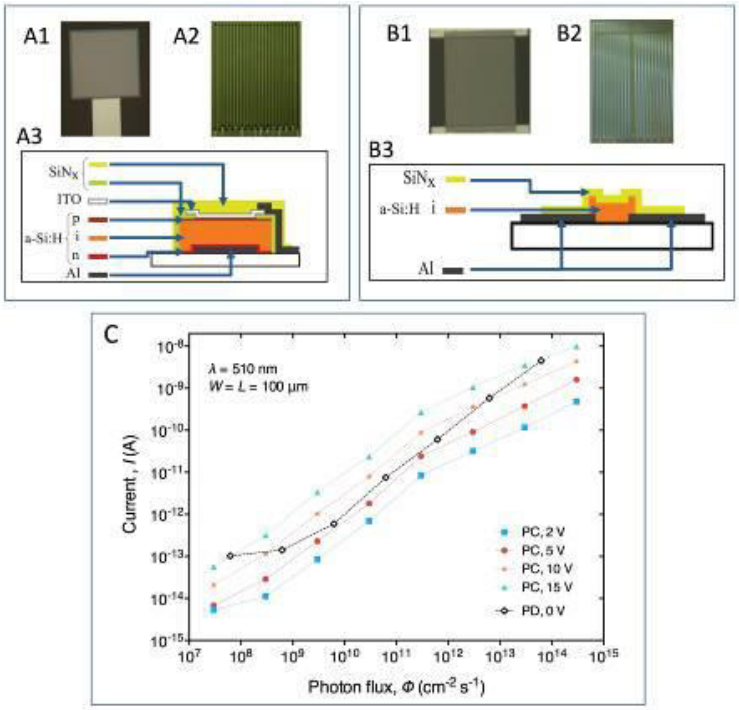

Figure 1 - Photosensors details. (A1) Microfabricated 100 µm photodiode and (A2) 24 sensors die wire bonded to a PCB. (A3) Schematic photodiode cross-section (not to scale). (B1) Microfabricated 100 µm photoconductor and (B2) 24 sensors die wire bonded to a PCB. (B3) Schematic photoconductor cross-section (not to scale). (C) Photoresponse comparison between photoconductor sensors (PC) at different values of bias voltage and photodiode (PD).

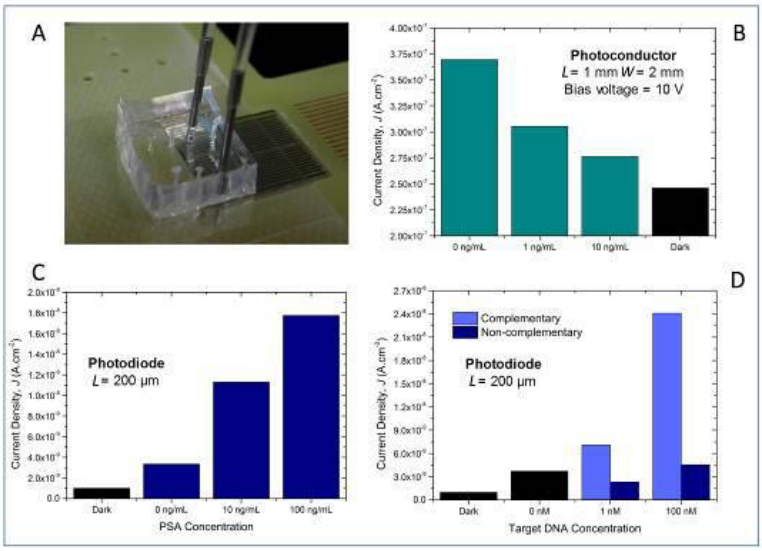

Figure 2 - (A) Photograph of the photosensors integration with the microfluidic platform. Integrated Lab-on-Chip chemiluminescence results of microfluidic (B) competitive immunoassay for mycotoxin OTA, (C) prostate specific antigen (PSA) sandwich immunoassays and (D) DNA hybridization experiment.

ID 110 - Poster

Optical amplifier based on Yb^{3+}/Er^{3+} codoped GeO_2-PbO pedestal type waveguide

**F. Bomfim[1], D. da Silva[2], V. Del Cacho[2], L. Kassab[2], M. Alvarado[1], M. Alayo[1]*
[1]Escola Politécnica da Universidade de São Paulo, Engenharia de Sistemas Eletrônicos, São Paulo, Brazil
[2]Laboratório de Tecnologia em Materiais Fotônicos e Optoeletrônicos, Faculdade de Tecnologia de São Paulo, São Paulo, Brazil

The present work reports on results of Yb^{3+}/ Er^{3+} codoped GeO_2-PbO pedestals waveguides for optical amplifier applications. Among the photonic glasses of interest PbO-GeO_2 glasses are promising materials for waveguide amplifiers due to some of their important characteristic such as high linear refractive index (~2.0), low phonon energy (around 700 cm^{-1}) when compared to silicate glasses and large transmission window (0.4 to 5 µm). When only Er^{3+} ions are present in optical waveguides, the pumping at 980 nm is not efficient; however this problem can be alleviated by the addition of Yb^{3+} which is an efficient sensitizer of Er^{3+} ions that normally provides strong luminescence at 1.5 µm. Also, the higher index core enhances the confinement factor of the optical field, which is a favorable characteristic for the development of narrower waveguides as a thinner cladding can be used. For pedestal waveguides the reactive ion etching occurs before the core definition, representing an alternative method for achieving the lateral confinement in optical waveguides fabricated with silicon technology and with advantages over rib waveguides which normally uses more complex etching procedures. Pedestal waveguides based on Yb^{3+}/Er^{3+} codoped PbO-GeO_2 thin films were produced in a silicon wafer using conventional microelectronics procedures: chemical cleaning, thermal oxidation, optical lithography, plasma etching and sputtering deposition. Scanning Electron Microscopy (SEM) was performed in order to observe the resulting structure of the pedestal-type waveguides. The concentration of Er^{3+} and Yb^{3+} were determined by Rutherford Backscattering Spectrometry (RBS) and Particle Induced X-Ray Emission (PIXE) analysis. Optical characterizations were performed to determine propagation losses in the visible (VIS) and infrared (IR) regions using the “top view” technique. Propagation losses around 2.5 dB/cm and 1.5 dB/cm were obtained at 632 and 1068 nm, respectively, for waveguides width in the 20 - 100 µm range. Gains of 6.0 dB and 4.0 dB, at 1530 nm, for waveguides width of 80 and 14µm, respectively, and a pump power inside the waveguide of 100 mW, at 980nm, were measured. These results show the possibility of using pedestal type waveguides as optical amplifiers with appreciable advantages over rib waveguides. In addition the present study also has the purpose of filling the lack of results in the literature related to Yb^{3+} /Er^{3+} codoped germanate waveguides for optical amplifiers applications.

ID 111 - Oral

Solution-deposited oxide TFTs and backplanes

*R. Street[1], T. N. Ng[1], R. Lujan[1], T. Lee[2]
[1]Palo Alto Research Center, Palo Alto, United States
[2]Samsung Fine Chemicals, Suwon, Korea, Republic of

The high mobility of the metal oxide semiconductors enables their use for OLED displays or high speed LCD switching. Solution deposition methods of fabrication are attractive for low cost manufacturing and so there is interest in the formation of the oxide semiconductors from solution. InGaZn oxide semiconductor TFTs with various metal compositions, processed from solution by the sol-gel method using metal nitride precursors are described. The sol-gel films were annealed in the range 350-500 °C in ambient air and processed TFTs were annealed at 180°C. The solution deposited IGZO and IZO TFTs have mobility values of up to 20-30 cm^2/Vs. High mobility was obtained for devices using a lithography-defined etch stop structure, while lift-off gave slightly lower mobility and a back channel etch process gave substantially lower mobility. The difference is presumably related to etching damage of the channel.

The solution oxide TFTs exhibit bias stress effects similar to the sputtered oxides. The highest mobility sol-gel devices have positive bias stress comparable to sputtered oxide TFTs. The negative bias illumination stress (NBIS) effect is also present in the TFTs. The turn-on voltage of the TFTs varied quite widely and is largely controlled by a low temperature anneal. The mobility, stress and annealing properties can be explained by a common model involving the thermal generation of self-compensating donor and acceptor states, taking into account the position of the Fermi energy in the device. The model suggests that the densification of the sol-gel oxide material by a high temperature anneal increases the defect formation energies and steadily reduces the defect density.

Metal oxide TFT backplanes have been fabricated with 200 micron pixel size to explore the technology for x-ray imaging application. The devices used sputtered oxide TFTs, a-Si p-i-n photodiodes, both deposited on a flexible plastic substrate with process temperature below 200°C. High performance x-ray imaging was demonstrated.

ID 112 - Oral

Preparation, structure and switching properties in GaTe and Ga_2Te_3 amorphous thin films

**M. Popescu[1], F. Sava[1], A. Velea[1], A. Lőrinczi[1], I. D. Simandan[1], A. C. Galca[1], G. Socol[2], F. Jipa[2], M. Zamfirescu[2], E. Matei[1], V. Braic[3], A. Kiss[3], L. Ion[4]*
[1]National Institute of Materials Physics, Magurele, Romania
[2]National Institute for Laser, Plasma and Radiation Physics, Magurele, Ilfov, Romania
[3]National Institute for Research and Development in Optoelectronics, Magurele, Ilfov, Romania
[4]Faculty of Physics - University of Bucharest, Magurele, Ilfov, Romania

Amorphous thin films of GaTe and Ga_2Te_3 have been prepared by pulsed laser deposition (PLD). The structural and optical properties have been investigated by X-ray diffraction (XRD), extended X-ray absorption fine structure (EXAFS), scanning electron microscopy (SEM), atomic force microscopy (AFM) and ellipsometry. The effect of femtosecond laser irradiation was investigated as a function of laser power. The electrical switching effect in both types of films was studied.

ID 113 - Oral

Density of Localized State Distribution Near the Valence Band in Stabilized a-Se Using Interrupted Field Time of Flight Measurements with Long Interruption Times

*C. Koughia[1], A. Reznik[1], C. Allen[1], R. Johanson[1], S. Kasap[1]
[1]University of Saskatchewan, Electrical and Computer Engineering, Saskatoon, Canada

After a long domination in xerography [1], and much research in the seventies and the eighties, there has been a renewed research interest in the DOS distribution for amorphous selenium (a-Se) due to its recent commercialization as a photoconductor in flat panel X-ray imaginers [2] as well as its use in the Harpicon, a super sensitive TV video tube that is based on avalanche multiplication [3]. However, despite decades of investigations, the DOS distribution in a-Se still remains a controversial subject of interest. A general consensus on the DOS distribution in the upper half of the mobility gap is that it is not a monotonically decaying function but exhibits certain peaks whose exact positions are still being discussed [4-7]. However, the DOS distribution in the lower part (closer to valence band) has been even more controversial. There have been different points of view that have led to both monotonic and non-monotonic DOS distributions [8-11]. More recently, DOS distributions with features have been based on the analysis of steady state photoconductivity [12] and transient photocurrents [7] measured on samples with coplanar electrodes. However, these results may be compromised by holes diffusing to the surface of a-Se, which is well known to deeply trap holes [13]; the latter phenomenon has been confirmed by surface time-of-flight (TOF) transient photoconductivity measurements [14]. In contrast, bulk TOF transient photocurrents measured on sandwich device structures over wide field and temperature ranges indicate a monotonically decreasing DOS from the valence band edge E_v into the mobility gap up to about 0.55 eV [15]. In the present paper we investigate hole transport in stabilized a-Se films using conventional TOF and IFTOF experiments with interruption times up to 600 ms. A distinct advantage of IFTOF measurements is that one can monitor the average "free" hole concentration $p(t)$ (= $p(x,t)$ averaged over the thickness of the sample L) at a given location x_1 in the sample inasmuch as the applied field is removed at a certain time t_1 for an interruption period of t_i. At time $t_1 + t_i$, the field is reapplied and the recovered photocurrent i_2 at $t = t_1 + t_i$ is measured with respect to the original photocurrent i_1 at $t = t_1$. The stabilized a-Se that was investigated here is a-Se alloyed with As (0.2 - 0.7%) and then doped with Cl at ppm level; that is, it has a composition that is typical for use in a-Se detector applications. The experimental results are interpreted by the comparison of experimental photocurrent transients with numerical and Monte-Carlo simulations of multiple trapping hole transport for different DOS models; and their agreement with a featureless DOS distribution is confirmed.

1. J. Mort, *The Anatomy of Xerography* Its Invention and Evolution, McFarland & Company, Inc, Jefferson, North Carolina, 1989
2. S. Kasap et al., Sensors, 11, 5112 (2011).
3. S.O. Kasap, J. A. Rowlands, S.D. Baranovskii, and K. Tanioka, *J. Appl. Phys.,* 96, 2037 (2004)
4. H.-Z. Song, G.J. Adriaenssens, E.V. Emelianova and V.I. Arkhipov, *Phys. Rev.*, B59, 10607 (1999)
5. K. Koughia et al., *J. Non-Cryst. Solids,* 338-340, 569 (2004)
6. K. Koughia, Z. Shakoor, S. O. Kasap, J. M. Marshall, J. Appl. Phys. 97, 033706 (2005)
7. F. Serdouk, M.K. Benkhedir, Physica B, 459, 122 (2015) and references there in
8. M. Abkowitz, Philos. Mag. Letts, 58, 53 (1988)
9. H. Naitoet al., *J. Non-Crystalline Solids,* 114, 112 (1989)
10. K. Koughia, S. O. Kasap, J. Non-Cryst. Solids, 352, 1539 (2006)
11. F. Serdouk, M.K. Benkhedir, Physica B, 459, 122 (2015) and references there in
12. N. Qamhieh et al., J. Phys. CM, 16, 3827 (2004)
13. S.O. Kasap, J. Electrost. 22, 66 (1988)
14. D. Hunter, MSc Thesis," Digital Radigraphy by Laser Scanned Readout of Amorphous Selenium",University of Toronto, 1996
15. S. Kasapet al., J. Mater. Sci. Mater. Electron. 2015 (in press)

ID 114 - Oral

Universal Medium-Range Order of Amorphous Metal Oxides

*K. Nishio[1], T. Miyazaki[1]
[1]National Institute of Advanced Industrial Science & Technology, Tsukuba, Japan

Exploring universal features hidden behind disordered materials has been a challenge of materials science. The random-sphere-packing (RSP) structure, which is characterized by the existence of plenty of pentagonal- bipyramid structures, is one of the most successful models to describe the atomic structure of disordered monatomic materials such as liquids of face-centered-cubic (fcc) metals, hexagonal-close-packed (hcp) metals, body-centered-cubic (bcc) metals, and rare gases. Pentagonal bipyramid structures are also found in rare-gas and colloid glasses.

In this presentation, by generalizing the dual-sphere-packing structure of crystalline metal oxides (CMOs), we propose that the structure of amorphous metal oxides (AMOs) can be regarded as a dual-random-sphere-packing (Dual-RSP) structure, which is a superposition of the RSP structure of metal and that of oxygen [1,2]. Our ab initio molecular dynamics (AIMD) simulations show that metal and oxygen sublattices of amorphous HfO2, ZrO2, TiO2, In2O3, Ga2O3, Al2O3, Cu2O, and Li2O have plenty of pentagonal bipyramid structures, which proves the validity of our Dual-RSP model and provides hard evidence of the universality of pentagonal medium-range order of AMOs irrespective of detailed chemistry.

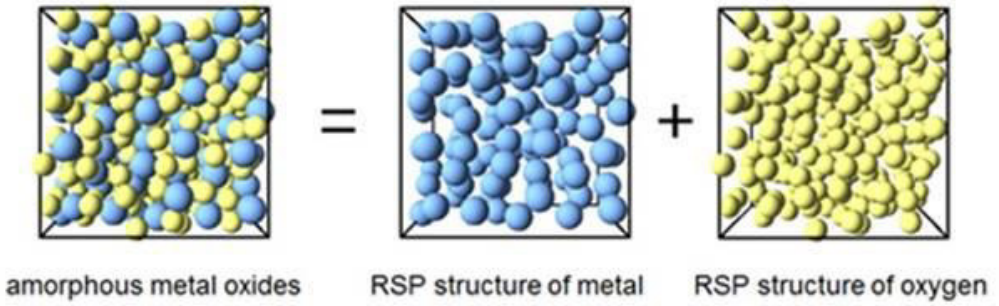

Dual-RSP structure.

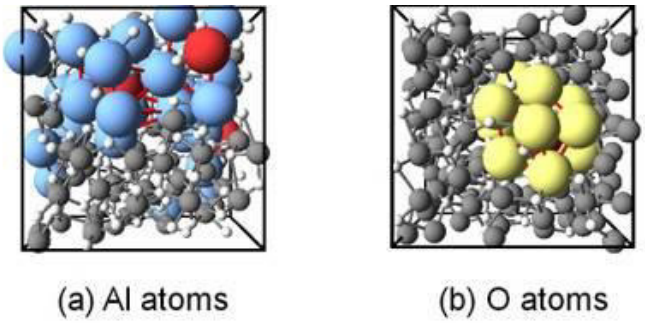

Icosahedral packings of (a) Al and (b) O atoms found in amorphous Al_2O_3.

[1] K. Nishio, T. Miyazaki, and H. Nakamura, Phys. Rev. Lett. 111, 15502 (2013).
[2] K. Nishio, T. Miyazaki, and H. Nakamura, Trans. Mat. Res. Soc. Japan, accepted.

ID 115 - Oral

Five-fold symmetries in the multiple twinning found in p-type microcrystalline silicon alloys grown from hexamethyldisiloxane

*F. Haddad[1], P. Goyal[2,1], J. Hong[2], E. Johnson[1], J.- L. Maurice[1], P. Roca i Cabarrocas[1]
[1]LPICM, CNRS, Ecole Polytechnique, Palaiseau, France
[2]Air Liquide, Centre de Recherche Paris Saclay, Jouy-en-Josas, France

Doped microcrystalline silicon oxide (µc-SiO_x:H) has attracted scientific interest for applications in solar cells as it can enhance absorption of light in the active material. The most common gas precursor used to obtain doped µc-SiO_x:H is CO_2 or N_2O mixed with SiH_4, H_2 and a doping agent. In this study, we use hexamethyldisiloxane ($C_6H_{18}OSi_2$, HMDSO) as a new way to introduce oxygen in microcrystalline silicon deposited at 150°C by radio frequency glow discharge in a plasma-enhanced chemical vapor deposition (PECVD) reactor containing SiH_4, H_2, HMDSO and 2% B_2H_6 in Ar. A non-negligible amount of carbon was also found in the deposited material. The quality of the layers is strongly dependent on the deposition conditions.

What is the influence of increasing the HMDSO flow and the RF power on the optical and structural properties of the films? How is the crystalline fraction changing? Is there a modification in the microstructure and elemental composition?

To check the structure of the deposited layers, we first analyzed them by spectroscopic ellipsometry (SE), from which we estimated the crystalline fraction using optical modeling based on Bruggeman's effective medium approximation. Then, we prepared sample cross sections, by the tripod polishing technique and ion milling, for a thorough investigation by transmission electron microscopy (TEM), including high resolution images (HRTEM), diffraction patterns and electron energy loss spectroscopy (EELS) for chemical analysis.

At low HMDSO flow, the layers have microcrystalline structure. As we increase HMDSO flow, their crystalline fraction decreases until they become completely amorphous at 1.2 sccm of HMDSO (see attached figures). This might be explained by amorphization due to a larger content of oxygen and carbon incorporation during film growth. Discussion of the effect of plasma power on the growing layers is also presented.

Interestingly, the layers display cyclic twinning, where the diffraction patterns reveal a five-fold symmetry; we observe five grains rotated by approximately 71° around. They have a structure similar to the decahedral structures frequently observed in the case of Au nanoparticles [1]. We systematically found this five-fold symmetry in HMDSO samples, but never in samples grown without HMDSO.

HMDSO is an easy to handle oxygen source that enables us to control the crystalline fraction, which decreases while increasing HMDSO flow. The microstructure of the layers shows interesting multiple twinning around axis.

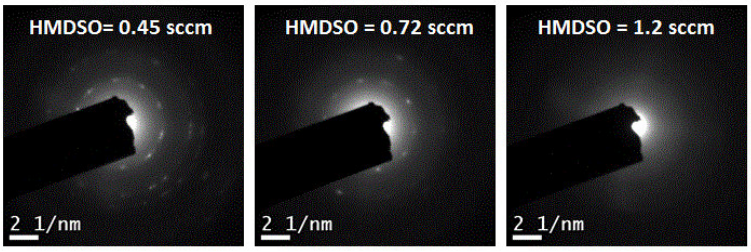

Diffraction patterns of the deposited layers. The crystalline fraction is decreasing when HMDSO flow increases.

[1] Esparza, R.I ; Rosas, G.II; Valenzuela, E.III; Gamboa, S.A.III; Pal, U.IV; Pérez, R.I , Revista Matéria, v. 13, n. 4, pp. 579 - 586, 2008

ID 116 - Poster

Physically-based simulation of ZnO TFTs: Separating the source/drain contact resistance contribution from the density of states

**M. Dominguez[1], S. Alcantara[1], J. Luna[1], R. Ambrosio[2], S. Soto[1]*
[1]Benemerita Universidad Autonoma de Puebla (BUAP), CIDS, Puebla, Mexico
[2]Benemerita Universidad Autonoma de Puebla (BUAP), FCE, Puebla, Mexico

Currently, one of the bottlenecks in oxide Thin-film Transistor (TFTs) technologies is the material science and modeling of the devices. Since to modeling the electrical performance of the devices, it is necessary to know the approximated distribution of defects in the gap of the semiconductor (active layer), typically the so-called density of states (DOS) [1]. First, the material science in oxide semiconductors is still not completely understood. Second, the calculation of the DOS in semiconductors materials is a complex work, since the extracted DOS reflects contributions of the main interfaces in the TFT (metal-semiconductor and insulator-semiconductor). Typically, in order to extract a realistic DOS, the TFTs need to be free of parasitic effects related to low-quality interfaces (high contact resistance, gate leakage current effects, etc.). However, usually, having a metal-oxide semiconductor contact without interface states is difficult. Also, matching the semiconductor and metal work functions is nearly impossible [2]. Although some methods have been reported to extract approximately the DOS, they require complex calculations and do not consider the contact resistance contribution into the DOS [3, 4]. The contact resistance reduces the on-current, affect the off-current, the on/off-current ratio and masks the real value of the electron mobility. Moreover, even some authors have reported a better subthreshold slope by improving the contact resistance [5]. Since the DOS is calculated from the electrical characteristics of the TFTs, for the above reasons, easily one can attribute some of the contact resistance effects to the DOS, resulting in an inaccurate modeled DOS and hence, an inaccurate modeled device. On the other hand, the advantage of using physically-based simulators is that they provide information that is difficult or impossible to measure. Moreover, one can incorporate the necessary parameters in order to enable (simulate) the contribution of the different interfaces in the device (fixed oxide charge density, interface charge density, high contact resistance, etc.). Using a physically-based simulator, the density of states DOS is modeled to reproduce the experimental electrical characteristics of ZnO TFTs fabricated by Ultrasonic Spray Pyrolysis at 200°C. A comparison between the modeled DOS considering the contact resistance and disregarding it is also presented. The contact resistance was extracted from the ZnO TFTs by the extrapolation of the width-normalized contact resistance (RcW) (obtained from the linear region of Ids vs Vds) for different channel lengths and gate voltages Vgs. This was included into the simulation, in order to separate the metal-semiconductor interface contribution from the DOS. The simulated data, using both modeled DOS, reproduces well the experimental transfer characteristic. However, as expected, a higher density of acceptor-like states is necessary to compensate the contact resistance contribution where this last was neglected. The use of physically-based simulation can be useful to model the DOS of Oxide semiconductor films in TFTs by reproducing the experimental data, even in TFTs with low-quality interfaces.

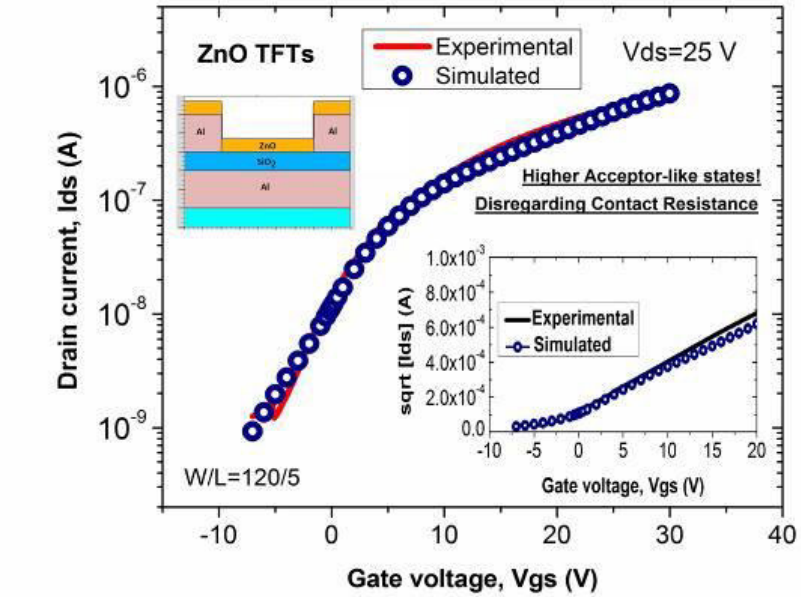

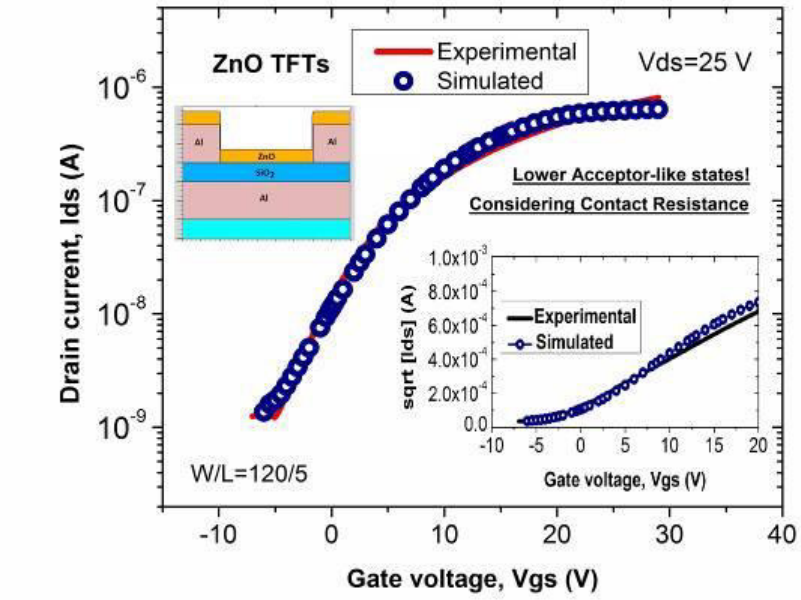

[1] A. Nathan et. al., J. Display Technol., 10, 917 (2014).
[2] H. Morkoc et. al., Zinc Oxide, Wiley-VCH, (2009). [3] M. Bae et. al., IEEE Electron Devices Lett., 33, 399 (2012).
[4] S. Bubel et. al., J. Appl. Phys., 113, 234507 (2013).
[5] F. Chen et. al., Electrochem. Solid-State Lett., 10, H186 (2007).

ID 117 - Poster

X-ray irradiation induced hole lifetime change in stabilized a-Se photo-conductive films

**J. Yang[1], M. Bradley[2], S. Kasap[3]*
[1]University of Saskatchewan, Biomedical Engineering, Saskatoon, Canada
[2]University of Saskatchewan, Physics and Engineering Physics, Saskatoon, Canada
[3]University of Saskatchewan, Electric Engineering, Saskatoon, Canada

Experiments were conducted to examine the dose and dose rate effects on the hole lifetime (or deep trapping time) in stabilized a-Se photo-conductive films due to X-ray irradiation. Interrupted-Time-of-Flight (IFTOF) measurements were performed on several Cl-doped and As-alloyed a-Se (stabilized a-Se) X-ray photo-conductive films after X-ray irradiation. The samples were prepared by the vacuum deposition of a-Se layers onto either Al or ITO substrates. The top contact was a semitransparent gold electrode.The maximum dose was~10Gy (into the a-Se films).Different dose rates were applied during the irradiation to examine the effect of x-ray intensity. After irradiation, the samples were rested in the dark. The time evolution of the hole lifetime was monitored while the sample gradually recovered towards its unirradiated state. The dose rate difference does not result in a significant change in the X-ray induced hole lifetime decrease for a given amount of dose. Within experimental errors, we find the drop in the hole lifetime depends on the accumulated dose rather than the dose rate itself. The x-ray induced reduction in the hole lifetime is believed to be due to x-ray induced formation of deep traps. The recovery of the hole lifetime was examined under different electric fields and temperature. The hole lifetime recovery was observed to be a thermally activated process and the time evolution was modelled by using a stretched exponential recovery.

ID 118 - Poster

Optical design aspects for 15% micromorph solar cell

*A. Čampa[1], J. Krč[1], *M. Sever[1], M. Meier[2], F.- J. Haug[3], M. Topič[1]*
[1]University of Ljubljana, Ljubljana, Slovenia
[2]Forschungszentrum Jülich, IEK5 Photovoltaik, Jülich, Germany
[3]Ecole Polytechnique Fédérale de Lausanne, Neuchâtel, Switzerland

In the field of thin-film solar cells, boosting up the efficiency is of great importance in order to keep the thin-film technologies in competition to conventional c-Si technology and to make it commercially more attractive.

In this work we have focused on thin-film a-Si:H/µc-Si:H (micromorph) solar cells, where matched short-circuit current of the top (a-Si:H) and bottom (µc-Si:H) solar cell is of great importance. A cell with the lower current limits the overall performance of the tandem micromorph solar cell.

In Figure 1, the results of the best micromorph solar cell are summarized [2]. In the figure the sum of matched short-circuit current density (J_{SC}) of top a-Si:H cell (J_{SC_top}) and of J_{SC} of bottom µc-Si:H cell (J_{SC_bottom}) is shown. The experimental results are well below the 15% efficiency. However, by inspecting the best optical performance (J_{SC}) and best electrical performance (open circuit voltage - V_{OC}, fill factor - FF) we see the 15% efficiency might be already in reach. The multiplication of best values V_{OC}*FF*J_{SC} (1.407 V *78.7%*13.6 mA/cm^2) already results in 15% efficiency. However, best measured values show the interplay between electrical and optical performance, i.e. the electrical performance degrades with better optical performance and vice versa.

By means of 3-D rigorous optical simulations using COMSOL Multiphysics we will show how to furtherly improve the optical performance of micromorph solar cells. For the optimization the micromorph structure deposited on LPCVD ZnO with 220 nm thick top cell and 1200 nm thick bottom solar cell was considered (base solar cell). In Table 1 the calculated short-circuit current density in top and bottom cell are presented for the each optimization step. Each optimisation step gradually improves the performance of the solar cell and are (in order of appearance in Table 1): (1) introduction of nano imprinted layer, (2) multifunctional intermediate layer (n-SiOx), (3) replacing the back n-mc-Si:H layer with a n-SiO$_x$ layer, (4) antireflective coating, (5) low absorbing p-a-SiC:H layer, (6) optimised double texture and (7) current matching step by thickness change. By considering all 7 steps we can reach the 15 mA/cm^2 of matched current, grey line in Figure 1. All the steps will be analysed and feasibility of introducing them into the solar cell production will be discussed in details.

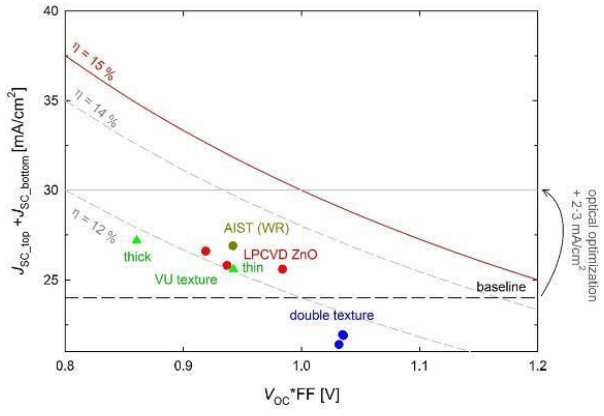

Fig. 1: The optical (J_{SC}) versus electrical (V_{OC} *FF) performance graph for micromorph a-Si/µc-Si solar cells and obtained maximal values.

Table 1: Short circuit current of 220 nm/1200 nm thick tandem solar cells deposited on LPCVD ZnO substrate for different optimisation steps.

Step	base	1	2	3	4	5	6	7
J_{SC_top} [mA/cm^2]	12.1	12.8	13.0	13.0	13.5	14.0	14.1	15.0
J_{SC_bottom} [mA/cm^2]	12.0	12.4	12.8	13.1	13.5	13.7	15.7	15.0
Matched $J_{SC\_top} + J_{SC\_bottom}$	24.0	24.4	25.6	26.0	27.0	27.4	28.2	30.0

[1] A. Kolodziej and Staebler-Wronski, effect in amorphous silicon and its alloys, Opto-Electron. Rev. 12 (2004), p. 21.

[2] M.A. Green, K. Emery, Y. Hishikawa, W. Warta, E.D. Dunlop, Solar cell efficiency tables (version 45), Prog. Photovolt. Res. Appl. 23 (2015) p.1.

ID 119 - Poster

Comparison of the charge carrier mobility of the $Zn(OC)_2$ organic compound as a function of the electric field orientation

**G. Landi[1], A. Veysel Tunc[2,3], A. De Sio[3], H.- C. Neitzert[1]*
[1]Università degli Studi di Salerno, Fisciano, Italy
[2]TUBITAK MAM, Kocaeli, Turkey
[3]Institute of Physics, Oldenburg, Germany

The synthesis and the characterization by means of elemental and thermal analyses and infrared spectroscopy of a new type of small molecule, $Zn(OC)_2$, has been investigated. Devices based on a small molecules have the potential to combine the capability of high-density devices with low power consumption and can be fabricated with simple deposition techniques, such as spin-coating, ink-jet printing and drop-casting. In this work the Zn-complex contains the carbazole hole transporter unit and the oxadiazole electron transporter unit which are covalently bonded by a bridging Zn-atom. In order to analyze the electrical properties of the organic thin films, a heterodiode test structure with the organic emitter deposited by solution-processing on top of a crystalline silicon base has been fabricated. Good rectification behavior has been observed for both heterostructures, independent of the silicon substrate doping type, confirming that the metal-organic layer can act both as electron or hole-conductor. The hole transport and the dielectric properties have been evaluated by capacitance and current-voltage measurements. In addition, the small molecules have used as active layer in an organic diode and in an organic field effect transistor (OFET) in order to evaluate the charge carrier mobility as a function of the electric field orientation. In the vertical structure (organic diode) the dominating electrical conduction mechanism for holes is the trap-controlled space charge limited current, where the hole mobility μ^{diode}_h is influenced by the electric field E and obeys to the equation:

$$\mu^{diode}_h(E) = \mu_0 \times \exp[\gamma(E)^{0.5}].$$

By the fitting procedure performed on the linear part of the curve in Fig. 1 the values of the mobility at zero electric field $\mu_0 = 2.78 \times 10^{-9}$ cm^2 V^{-1} s^{-1} and $\gamma = 2.35$ cm$^{-0.5}$ V$^{-0.5}$ have been obtained. In addition, the small molecules have used as active layer in an organic field effect transistor (OFET). In Fig. 2 the output characteristics of the OFET with the $Zn(OC)_2$ as active layer for different gate voltage V_g values are shown. The value of the hole mobility extracted for the planar structure are $\mu^{OFET}_h = 1.09 \times 10^{-9}$ cm^2 V^{-1} s^{-1} and $V_{th} = 57$ V, where V_{th} is the threshold voltage. The high value of the V_{th} suggests a low crystallinity of the thin organic film and the low values of the holes mobility, proportional to ~ 10^{-9} cm^2 V^{-1} s^{-1} for both the device structures, are due to the high density of traps in the organic films which reduce drastically the charge flow in the organic devices.

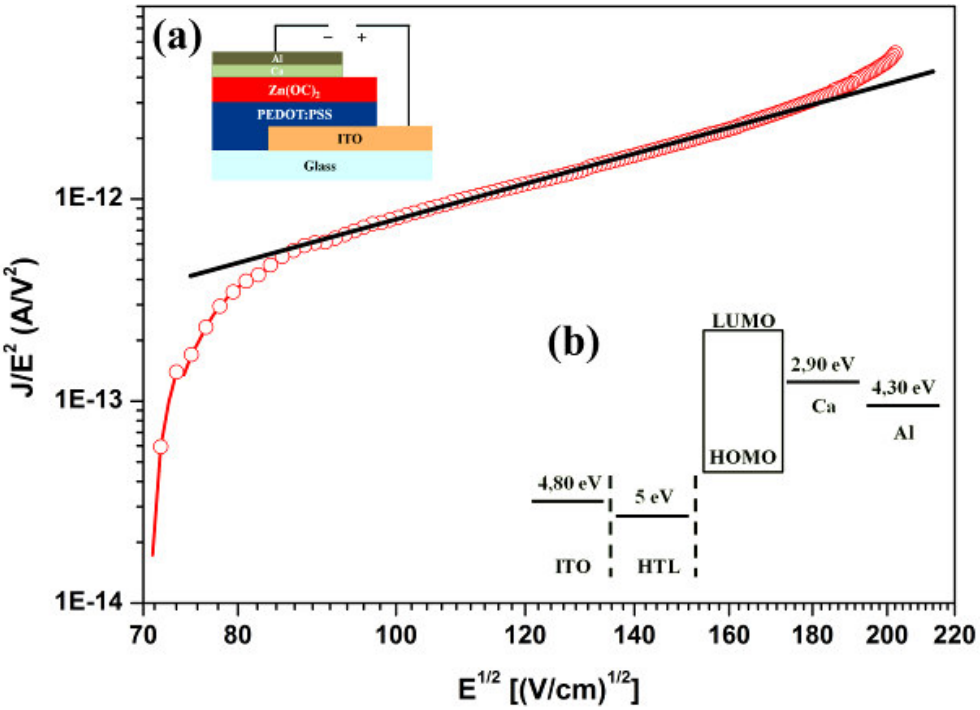

Space-charge limited current characteristics (see straight line) for an organic diode with Zn(OC)2 as active layer. In inset (a) the cross section of the device and in inset (b) the band diagram structure of the diode are shown. The energy levels are referred to the vacuum level.

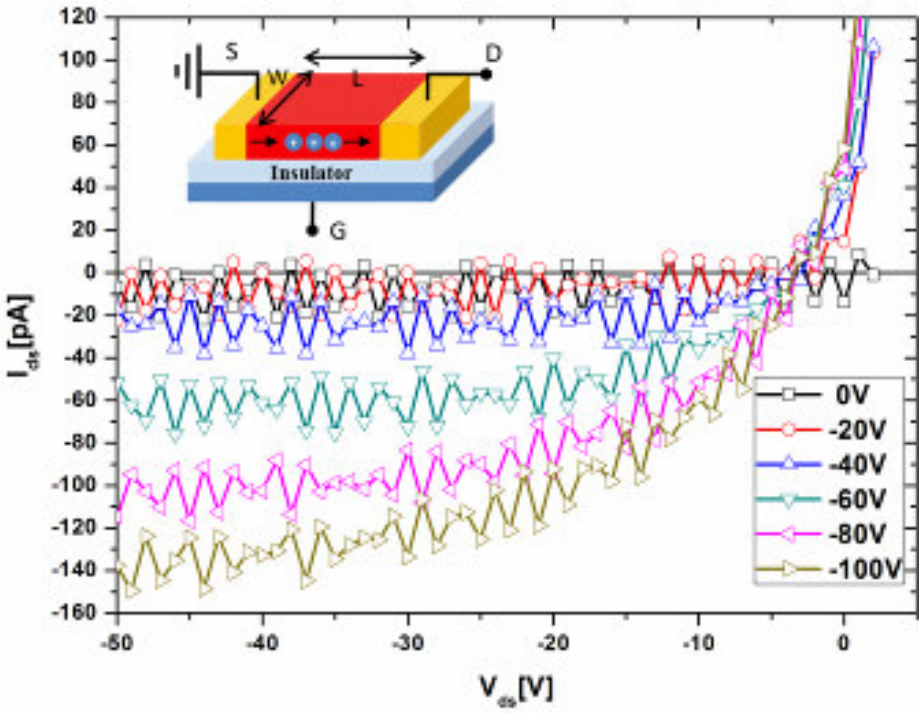

Output characteristics for different gate voltages for the organic field effect transistor with Zn(OC)2 active layer. In the inset the schematic illustration of the device, where S, D and G are the source, the drain and the gate terminal respectively, is shown.

ID 120 - Oral

Annealing and oxygen role in the structural, optical and electrical properties of nc-SiO_xN_y

*M. Perani[1], N. Brinkmann[2], A. Hammud[2], D. Cavalcoli[1], B. Terheiden[2]
[1]University of Bologna, Bologna, Germany
[2]University of Konstanz, Konstanz, Germany

Research in the renewable energy field is mandatory to provide alternatives to fossil fuels in energy production and photovoltaics is very promising as solar energy is widely distributed. Moreover, the related technology is nowadays easily available, it can be integrated with buildings and presents limited environmental issues. Silicon Oxi-Nitride (SiO_xN_y) thin films have been characterized in view of the application in thin-film solar cells as well as in wafer based silicon solar cells, like Silicon HeteroJunction (SHJ) solar cells. Material properties like optical and electronic properties of the film, composition and structure of the nanocrystals have not been studied yet. In addition, the role of deposition conditions and precursor gas concentrations on these properties is also not clear. The results presented in the contribution aim to clarify several aspects concerning nc-SiO_xN_y film properties.

SiO_xN_y thin films have been deposited by plasma enhanced chemical vapor deposition and subsequently annealed to increase the crystalline fraction. The process of nanocrystal formation have been investigated through structural, compositional and optical methods, such as Fourier transform infra-red, Raman and energy dispersive X-ray spectroscopy. The morphology and the local conductivity of the layers have been measured by Atomic Force Microscopy (AFM). The crystallization of SiO_xN_y layers with respect to the annealing time and the N_2O dilution ratio during deposition have been studied, as well as the influence of these two parameters on the properties of the layers.

The results show that during annealing the material undergoes a phase transition from a homogeneously distributed material in terms of Si-Si and Si-O-Si bonds towards a two phase material consisting of Si-rich and O-rich clusters. Both phase separation and increase of crystalline fraction upon annealing could be responsible for the measured increase of the conductivity. In particular, oxygen-rich clusters are likely related to the less conductive paths observed by current-AFM. An increase of N_2O dilution causes an enhancement of crystal disorder, revealed through a decrease of the crystalline fraction and an increase of the lateral correlation length.

The layers exhibit very high conductivity σ_{dark}, low activation energy E_a and high Tauc gap E_{Tauc}, very interesting characteristics for their application in Si-based heterojunction solar cells, where low parasitic absorption and high conductivity are required. In particular, the films deposited with low N_2O dilution (R_{N2O}=9%) and annealed for 3 h at 800°C show optimal performances for photovoltaic applications: σ_{dark} = (44 ± 4) S/cm, E_{Tauc}=(2.5 ± 0.1) eV, E_a=(1.85 ± 0.09) meV and χ= (88 ± 2)%, whereas for the application in SHJ solar cells the formation of nc-SiO_xN_y should be carried out directly during deposition of the layer by adjusting the deposition parameters accordingly.

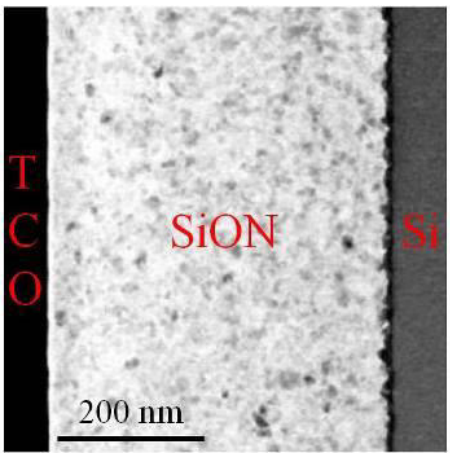

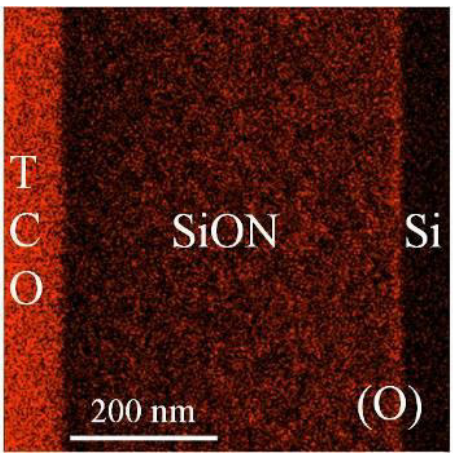

ID 121 - Poster

Stability aspects of hydrogen-doped indium oxide

*G. Jost[1], A. Hamri[1], J. Hüpkes[1]
[1]Forschungszentrum Jülich GmbH, IEK-5 Photovoltaik, Jülich, Germany

Transparent conductive oxides play an important role as contact layers in various opto-electronic devices such as solar cells or LEDs. Whilst crystalline materials e.g. zinc oxide (ZnO), tin oxide (Sn_2O_3) or tin doped indium oxide (ITO) have already been vastly investigated and applied [1] hydrogen doped indium oxide (In_2O_3:H) entered the scene a while ago as a new material with a superior trade-off between electrical and optical performance. In_2O_3:H is commonly deposited at room temperature via sputter deposition using an In_2O_3 target and water vapor as hydrogen source [2]. Its initial state is amorphous and provides good TCO properties. However, a short annealing step leads to the crystallization of the film. The crystalline phase exhibits outstanding optical and electrical properties. Carrier mobilities between 98-130 cm^2/Vs have been reported for charge carrier densities in the range of 1.4-1.8 x 10^{20} cm^{-3} [3]. This combination leads to highly conductive layers with high NIR transparency due to very low free carrier absorption making it attractive as front contact layer in silicon based solar cells. The successful integration into silicon heterojunction [4] and micromorph thin-film silicon solar cells [5] have already been reported. Furthermore, the versatility of In_2O_3:H make the material an ideal candidate for low temperature processes on plastic foils for flexible applications.

This paper addresses two stability aspects of In_2O_3:H in the deposition and the application phase. In the first part we will demonstrate the successful substitution of the commonly used water vapor by hydrogen as process gas. The results underline that the electrical and optical performance using the new process is on equal level with the conventional approach (see also Fig. 1). However, a great benefit of working with hydrogen gas as dopant source is the stability and reproducibility of the new process as standard mass flow controllers can be used to adjust the gas mixture more accurately.

In the second section we will present the results of degradation tests of amorphous as well as crystalline In_2O_2:H. We use a standard damp heat degradation test (85°C, 85% relative humidity) that is also applied in PV module certification. Hall measurements (see also figure 2) clearly show that both material phases, amorphous and crystalline, change under the influence of damp heat. The specific resistance increases with increasing damp heat duration and there appears to be no saturation after the standard testing time of 1000h. Although the resistivity increases for both material phases the behavior is different in detail. In the crystalline material the charge carrier density and mobility decrease slowly over time. In the amorphous material on the other hand the carrier density drops rapidly while the carrier mobility is increasing. X-ray diffraction shows a crystallization process during the damp heat degradation tests which could be the explanation for the increased mobility. However, the rapid carrier density loss is compensating the marginal win in carrier mobility. We will discuss these differences in detail.

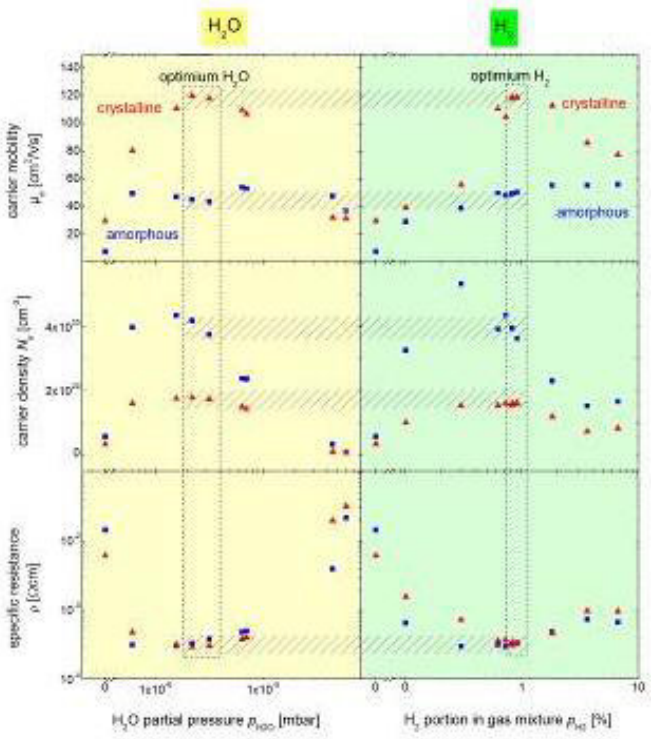

Fig. 1: Electrical properties extracted from HallI measurements of layers with H_2O (left) and H_2 (right) as dopant source. Achieved carrier concentrations, mobilities and specific resistance value are similiar for both preparation methods. The hatched areas indicate the optimimum level.

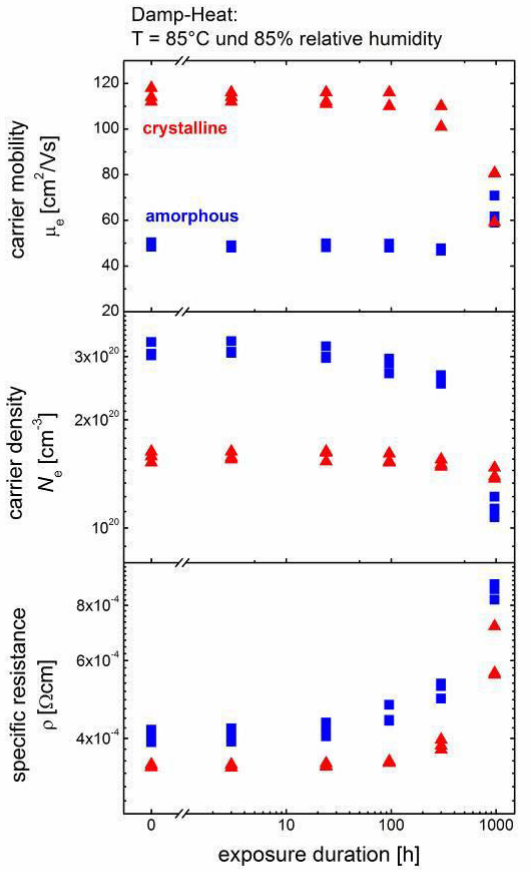

Fig. 2: Electrical properties extracted from Hall measurements as a function of damp heat exposure duration for as-deposited (blue) and annealed (red) In_2O_3:H thin films.

[1] H. Liu, V. Avrutin, N. Izyumskaya, Ü. Özgür, H. Morkoç, Superlattices and Microstructures 48/5 (2010) 458.
[2] T. Koida, M. Kondo, K. Tsutsumi et al.; Journal of Applied Physics 107, 033514 (2010).
[3] T. Koida, H. Fujiwara, M. Kondo; Japanese Journal of Applied Physics Express Letter Vol. 46 No. 28 pp. L685-687 (2007).
[4] T. Koida, H. Fujiwara and M. Kondo, Applied Physics Express 1 (2008) 041501.
DOI: 10.1143/APEX.1.041501 DOI: 10.1143/APEX.1.041501
[5] C. Battaglia, L. Erni, M. Boccard, et al., Journal of Applied Physics 109, 114501 (2011).
DOI: 10.1063/1.3592885

ID 123 - Poster

Innovative point-contacting technique for thin-film silicon solar cells

*R. Khoury[1], E. Johnson[1], D. Tondelier[1]
[1]Laboratoire de physique des interfaces et couches minces(LPICM)-CNRS-Ecole polytechnique, palaiseau cedex, France

The passivated emitter with rear locally diffused (PERL) cell has remained one of the most efficient monocrystalline-silicon photovoltaic cell designs in the lab and in production through the use of point contacts. However, point contacts have never been used on thin-film silicon solar cells, because forming the openings with a nanometer scale would be very expensive if done with existing techniques. We explore if an alternative technique could make such an application feasible.

The innovative technique presented is nano-scale contacting by using nanoparticles (NPs) of polystyrene as a mask. The challenge is to provide effective point contacts, usually done by expensive lithography or laser processing, but by using this far less expensive method. The 50nm diameter NPs are first dispersed onto a crystalline silicon test substrate by spin coating, using undiluted and deionized-water-diluted solutions. An annealing of the substrate is done after spin coating, varying the temperature from 0°C to 120°C in steps of 30°C. The samples are characterized by SEM and AFM techniques, in order to analyse the dispersion of NPs on the surface of the substrate.

Before dilution with deionized water, closely packed particle films were obtained, unsuitable for our application. After dilution, homogenously distributed individual NP's were obtained, with only a few observed agglomerations. Particle densities of about ~40-100/μm^2 were obtained, which would give an average distance to a contact of ~50-100 nm, well below the diffusion length in thin-film silicon solar cells. The diluted-solution samples were then annealed to observe changes in the NPs. Whereas well-attached NPs could be observed for all annealing temperatures at and below 90°C, it was difficult to observe the NPs on the sample annealed at 120°C. This is probably due to the melting of the NPs at a temperature around 100°C.

The study has shown that a disperse layer of NPs suitable to achieve point contacting at a nanoscale can be achieved. It should be taken into account that the temperature of the subsequent deposition process shouldn't exceed 100°C in order to ensure that the NPs will not be melted before being used as a mask. The next steps, to be presented at the conference, include deposition of a thin insulating and passivating layer on top of the NP's, followed by NP removal, and the subsequent deposition of a nano-scale point contact layer.

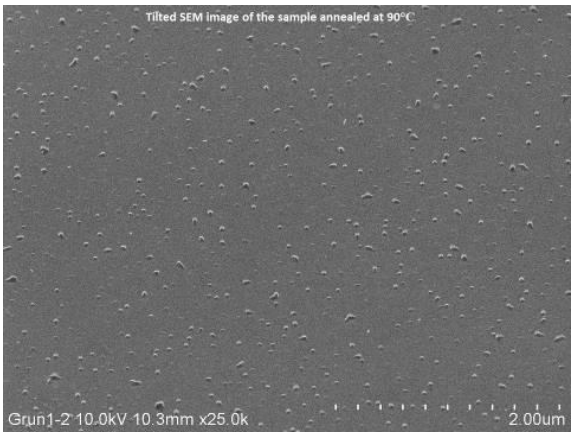

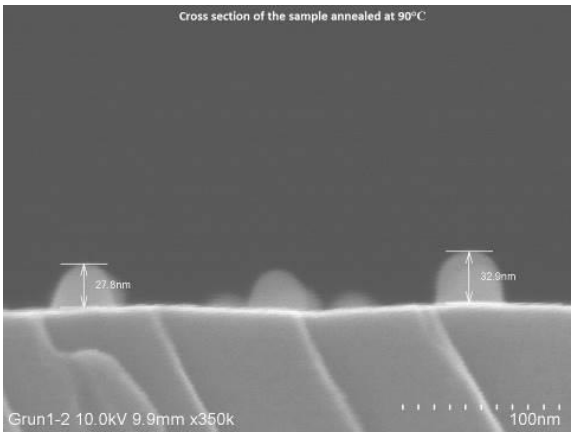

ID 124 - Oral

Processes of silver photodiffusion into Ge-chalcogenides probed by neutron reflectivity technique

**Y. Sakaguchi[1], H. Asaoka[2], Y. Uozumi[2], Y. Kawakita[2], T. Ito[2], M. Kubota[2], D. Yamazaki[2], K. Soyama[2], G. Sheoran[3], M. Mitkova[3]*
[1]Comprehensive Research Organization for Science and Society, Research Center for Neutron Science and Technology, Tokai, Japan
[2]Japan Atomic Energy Agency, Tokai, Japan
[3]Boise State University, Department of Electrical and Computer Engineering, Boise, United States

Silver photo-diffusion is one of the attractive phenomena observed in amorphous chalcogenide films which exhibit various photo-induced changes related to structural metastability. It is interesting to investigate the mechanism to know why and how silver diffuses into the chalcogenide layer and there have been a number of reports on the phenomena. According to several studies using Rutherford backscattering (RBS), the “diffusion” is unique to show a step-like profile of silver concentration in contrast to a usual diffusion in which the concentration gradually decreases as a function of distance from the silver layer. Although RBS is a powerful technique to clarify concentration profiles of constitutional elements, *in situ* studies under light exposure was not successful because silver diffusion was taken place also by a strong He^+ ion beam, which was used for time-resolved measurement to get enough statistics in a short time. Therefore, it is desirable to use a proper probe beam which does not affect silver diffusion and to realize such *in situ* studies. Recently, we have carried out time-resolved neutron reflectivity measurements of Ag/Ge-S films using pulsed neutron beam with a time-of-flight technique [1]. Neutron reflectivity is a useful technique to reveal the layer structure in a multi-layer film as well as X-ray reflectivity. Since strong X-rays such as synchrotron radiation can induce silver diffusion, use of neutrons is safer approach without inducing silver diffusion by the probe beam itself. In fact, our neutron reflectivity measurements demonstrated that neutrons do not affect silver diffusion. Also, it turned out from the measurements that a metastable Ag-rich layer was firstly formed after starting a light exposure, and then, silver diffused from the metastable Ag-rich reaction layer to chalcogenide layer (Ag-poor reaction layer) almost fixing the position of the interface. This is in contrast to a previously proposed model, which suggests a progression of a diffusion front.

In this presentation, we discuss the processes of silver diffusion into chalcogenide films based on our recent measurements and analytical results of neutron reflectivity for Ag/a-Ge_xS_{1-x} (x=0.2, 0.33, 0.4) films. From the recent measurements, we confirmed that the position of the interface (Ag-rich reaction layer/ Ag-poor reaction layer) was almost fixed and the silver ions seem to go to the other layer by overcoming the potential barrier at the interface. This would indicate the presence of two types of Ag ions in Ag-Ge-S system (Ag ions in the network and mobile Ag ions) as the previous *ab initio* simulations of the system has shown that there are least diffusive and most diffusive Ag atoms [2]. The first diffusion process, in which the Ag-rich reaction layer is formed, will also be discussed on the basis of our recent measurements and analysis with shorter time-resolution.

[1] Y. Sakaguchi, H. Asaoka, Y. Uozumi, et al., Can. J. Phys. 92 (2014) 654.
[2] De N. Tafen, D. A. Drabold and M. Mitkova, Phys. Rev. B 72 (2005) 054206.

ID 125 - Poster

Spin-on Glass as gate dielectric for solution-processed Thin-film Transistors

*M. Dominguez[1], M. Moreno[2], J. Luna[1], S. Alcantara[1], P. Rosales[2], R. Ambrosio[3], S. Soto[1]
[1]Benemerita Universidad Autonoma de Puebla (BUAP), CIDS, Puebla, Mexico
[2]National Institute for Astrophysics, Optics and Electronics (INAOE), Electronics, Puebla, Mexico
[3]Benemerita Universidad Autonoma de Puebla (BUAP), FCE, Puebla, Mexico

Dielectric materials obtained at low temperature have received great attention for their use on flexible and large-area electronics as gate dielectric. In order to meet the requirements for a good gate dielectric, this film must have good insulating properties and low charge-trapping rate at low electric fields, and should form a high-quality interface with the semiconductor layer (dielectric-semiconductor interface). Solution-processed dielectric films have found a potential research in thin-film Transistors where vacuum-based dielectric deposition techniques commonly suffer of high manufacturing cost and their incompatibility with large area deposition. In this respect, silicon oxide films (SiO_2) deposited by Spin-On Glass (SOG) at low temperatures results very attractive [1, 2]. The advantages of SOG include a low defect density in the films deposited, low process cost, excellent for planarization applications, filling gaps and smoothing the surface with multiple coatings. SOG is an interlevel insulator that is supplied in liquid form. The SOG solution forms an arrangement of silicate polymers with a Si-O structure, these polymers are in an alcohol solvent system. The refractive index of the films produced from diluted SOG are close to those of thermally grown SiO_2. The SiO_2 films from SOG diluted with deionized water were used in MOS capacitors using p-type silicon wafers. The dielectric constant k, obtained from the measurements of the C-V curves of the MOS capacitors was approximately 4.1. The use of SOG as gate dielectric in solution-processed thin-film transistors by Ultrasonic Spray Pyrolysis is demonstrated.

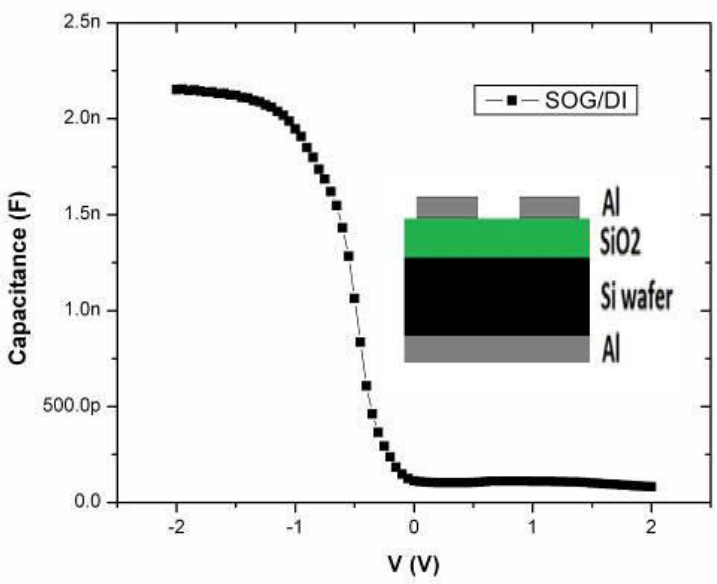

[1] M. Dominguez et. al., Thin solid films, 520, 5018 (2012). [2] M. Dominguez et. al., Mater. Res. Soc. Symp. Proc., 1436, K05-01 (2012).

ID 126 - Oral

Atomic Scale Study on Interface of Amorphous-Silicon/Crystalline-Silicon

**H. Matsumura[1], K. Higashimine[1], K. Koyama[1], K. Ohdaira[1], S. Yokoyama[1]*
[1] Japan Advanced Institute of Science and Technology, Nomi, Japan

Hetero-junction of amorphous-silicon (a-Si) and crystalline-silicon (c-Si) is important for solar cells and passivation of c-Si surface. Therefore, we investigate the features of a-Si/c-Si interface by atomic scale observation using scanning transmission electron microscope (STEM) with a spatial resolution of 0.08 nm, which demonstrates even the position of Si atoms at interface. We also investigate the surface recombination velocity (*SRV*) using micro-wave photo-conductive decay (micro-PCD) method and the interface state density. The samples, prepared by both Cat-CVD (Hot Wire CVD) and PECVD, have silicon- nitride (SiNx)/a-Si/c-Si stacked structures, since it is convenient to measure both *SRV* and interface state density.

The maximum possible *SRV* (*SRV*$_{max}$) evaluated by neglecting recombination inside the bulk c-Si was 5 cm/s for PECVD sample and 1.5 cm/s for Cat-CVD sample. The transition width from c-Si to a-Si at the interface is 1.8 nm for PECVD and only 0.6 nm for Cat-CVD, although the similar width for thermally grown gate SiO_2/c-Si interface with state density of $1x10^{10}$ $eV^{-1}cm^{-2}$, which is believed as one of the best interfaces, is about 1.0 nm. The transition width observed in STEM expresses the interface roughness, and the larger roughness means the larger interface area. Thus, if intrinsic real state density of a-Si/c-Si interface is decided, the effective interface state density should proportional to atomic scale real interface area, and so, *SRV*$_{max}$ should be inversely proportional to the width of transition layers. The experimental results appear to clearly verify this relationship.

The interface state density implies that the defects at a-Si/c-Si interface may be generated for every 10^5 to 10^6 Si atoms in c-Si surface and the ratio of defects to Si atoms at interface appears smaller than gate SiO_2/c-Si interface when a-Si is prepared by Cat-CVD. Cat-CVD a-Si/c-Si may be one of the ideal interfaces.

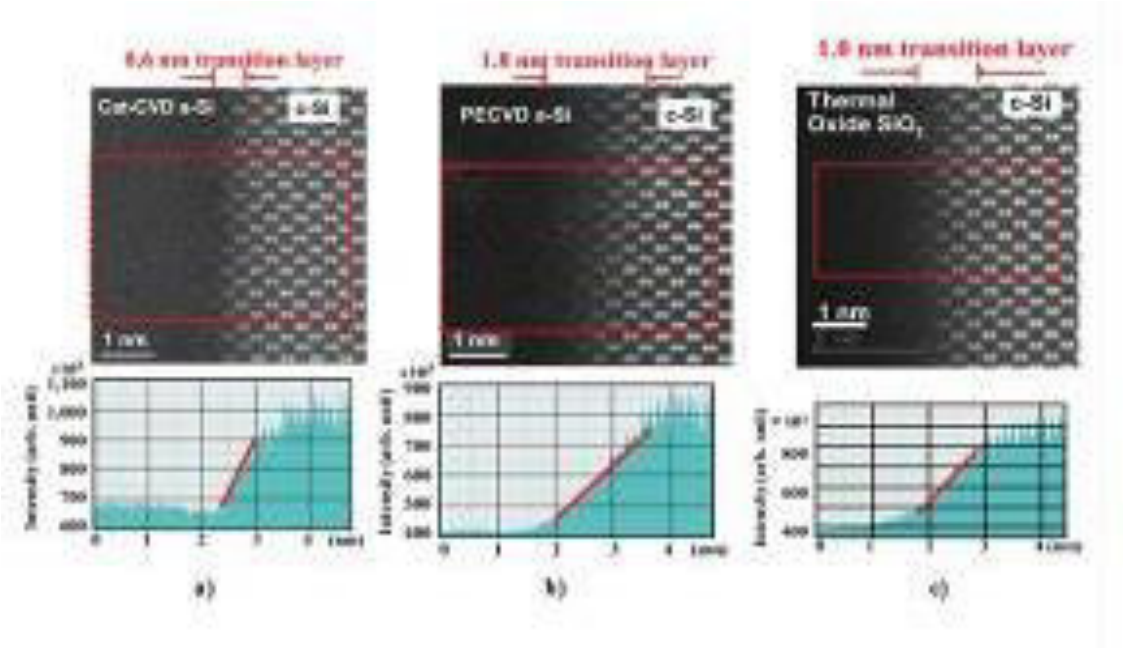

ID 127 - Poster

The evolution of deep depletion behavior for nc-Si floating gate memory during the thermal post-treatment based on 0.13 um technology

*Z. ma[1], J. yu[1], X. huang[1], K. chen[1], Y. shi[1], X. jiang[1], G. wu[2], Y. zhang[2], L. wang[2], L. xu[1], J. xu[1], W. li[1], D. feng[1]
[1]Nanjing University, Nanjing, China
[2]Semiconductor Manufacturing International Corporation, Shanghai, China

Nc-Si floating gate memory has recently attracted great interest as the flash memory candidate of next generation due to the faster programming/erasing speed, higher storage density and lower power. The discrete and size-controllable nc-Si embedded structure can inhibit the lateral leakage current and improve the retention properties [1-3]. However for the nc-Si floating gate memory to be scalable down to nanoscale sizes, the endurance of traditional SiO_2 tunnel layer is faced with challenge during the write/erase programming process. The electrical properties especially uniformity of the SiO_2 needs to investigate because the inherent defects at the Si/SiO_2 interface will result in oxide charging, increasing gate leakage current and reducing threshold voltage of gate dielectric breakdown. Therefore the uniformity at the SiO_2/Si interface becomes vital important for improving the performance of nc-Si floating gate memory. Although the deep depletion in the MOS structure is of use for the characterization of the interface properties, the relationship between uniformity of SiO_2/Si interface in nc-Si floating gate MOS structure and deep depletion phenomena at inversion stage are less reported.

Here in order to monitor the interfacial properties of nc-Si dots floating gate MOS structure post-treated by step-by-step rapid thermal annealing, which is designed to simulate the thermal process for fabrication of nc-Si floating gate memory unit in the 0.13 um product line, we carried out the research of deep depletion behavior from nc-Si dots floating gate MOS structure by using C-V measurement. The evolution of deep depletion behavior was observed after step-by-step RTA. It is found that the interfacial property for SiO_2/Si is improved obviously after step-by-step thermal post-treatment. Base on the analysis of the deep depletion behavior at different gate bias, we found that the novel interface property for SiO_2/Si is a key for the realization of the long endurance of 10^5 for nc-Si floating gate memory.

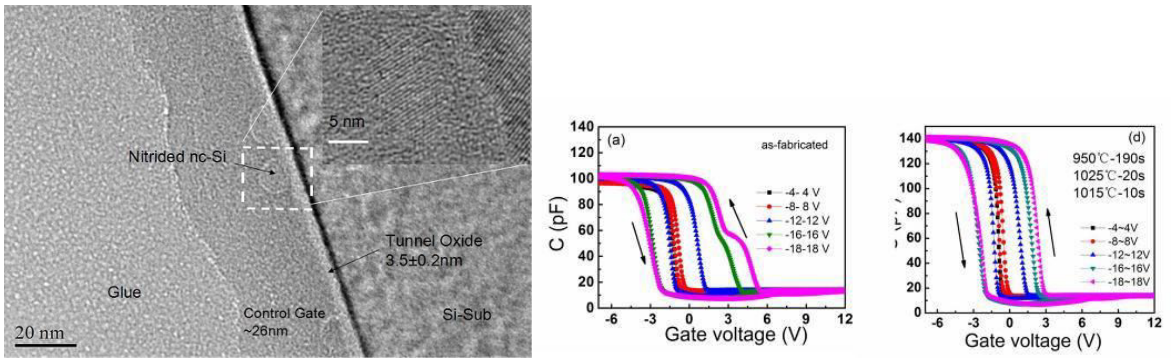

[1]T. Y. Chiang, Y. H. Wu, W. C. Y. Ma, P. Y. Kuo, K. T. Wang, C. C. liao, C. R. Yeh, W. L. Yang, T. S. Chao, IEEE Electron Device Lett. **57**, 1895(2010).
[2]S. Miyazaki, K. Makihara, M. Ikeda, Thin Solid Films. **517**, 41(2008).
[3]S. Tiwari, F. Rana, H. Hanafi, A. Hartstein, EF. Crabbe, K. Chan, Applied Physics Letters. **68**,1377 (1996).

ID 128 - Poster

Methods to remove "nano-remnants" on top of the TiO_2 nanotubes

*P. Marques de Arruda[1], G. Zeca Monteiro[2], *K. Franklin Albertin Torres[2], I. Pereyra[1]*
[1]University of Sao Paulo, Sao Paulo, Brazil
[2]Universidade Federal do ABC, Centro de Engenharia, Modelagem e Ciências Sociais Aplicadas, Santo André, Brazil

The purpose of this work is the production of free-remnants TiO_2 nanotube arrays. During the anodization process, bundles of clumped remnants (known as nanograss) could be produced at the tube top. This is a critical issue for many applications, because the nanograss affects the infiltration of materials, exciton transport and recombination in TiO_2 nanotube solar cells. In this work, four methods to eliminate nano-remnants are studied: (1) etching with a buffered hydrofluoric acid (BHF) solution, (2) chemical mechanical polishing (CMP) with Al_2O_3 particles, (3) positive photoresist based sacrificial layer method and (4) post-synthesis bath in the anodization solution. The nanostructures were characterized by scanning electron microscopy (SEM) to analyze the tubes morphology. Preliminary results are shown in the SEM images in figure 1 below, obtained using the sacrificial layer method.

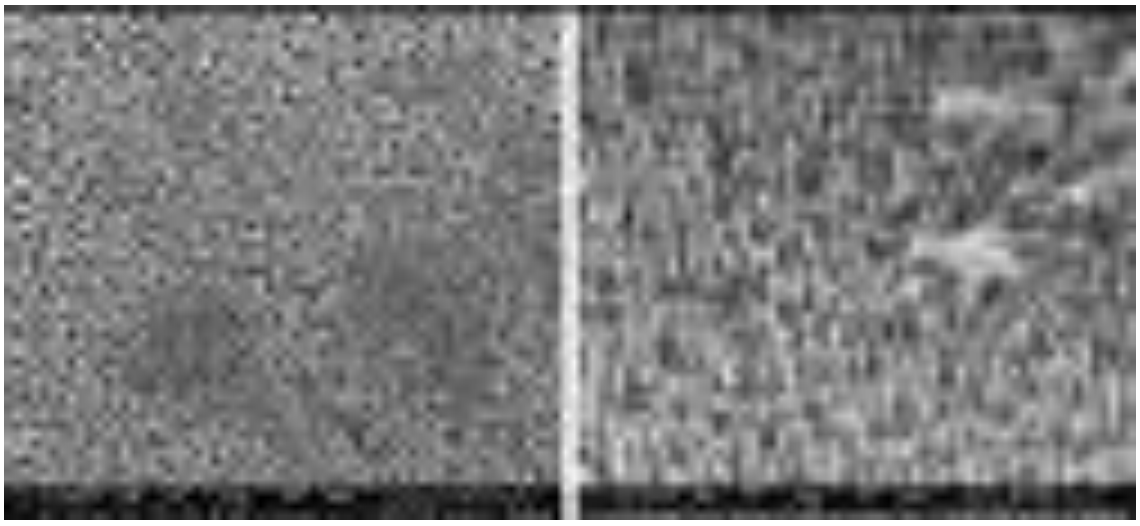

SEM images of the surface structures obtained with sacrificial layer method.

ID 129 - Oral

Electron spin resonance and photoluminescence from silicon nanostructures in SiO_x thin films

*Z. Saleh[1,2], S. Ilday[3], B. Altuntaş[3,4], R. Turan[2]
[1]Arab American University-Jenin, Physics, Jenin, Palestine
[2]Middle East technical University, Physics, Ankara, Turkey
[3]Bilkent University, Physics, Ankara, Turkey
[4]Turkish Aerospace Industries , Ankara, Turkey

*ABSTRACT*_Nanostructured silicon in the form of silicon quantum dots embedded in a matrix of amorphous silicon (a-Si), silicon nitride (SiNx) or silicon oxide (SiOx) have gained considerable interest in emitting and photovoltaic devices. These materials combine the lower processing cost of a-Si and the higher efficiency and probably the stability of crystalline silicon. Nanostructured silicon exhibits extensive and efficient photoluminescence and a band gap that may be tunable by the host matrix. However, a working structure for both applications remains far from optimum and the stability is still questionable. In this work, we investigate local structure, defects and stability of silicon nanostructures embedded in SiO_2 matrix. These nanostructures maybe disconnected in the form of quantum dots or connected in the form of "quantum sponge". Three silicon rich oxide (SRO) samples with different oxygen contents (x = 0.57, 1.01, 1.19) were prepared by co-sputtering from Si and SiO_2 targets and annealing at 1100 C in N_2 environment for one hour. The three samples were deposited at room temperature on quarts and Si substrates for various measurements. Raman spectroscopy (RS), photoluminescence (PL) and electron spin resonance (ESR) measurements conducted on these samples in the as-grown, furnace-annealed (1100 C, N_2, 1 hour), and aged (one year at room conditions) states, reveal major changes associated with the nanostructure formation upon annealing but negligible changes due to aging. The dark ESR signal associated with neutral dangling bonds increases with increasing Si content but the small feature typically associated with the e'-center, barely visible in the as-grown state, becomes a prominent component in annealed state. Raman spectra decomposed into narrow and broad components show the crystalline fraction (narrow component) to increase with decreasing oxygen content while the weak PL spectrum is greatly enhanced by increasing oxygen fraction. These results will be discussed and compared for the as-grown, annealed and aged states as functions of oxygen content.

ID 130 - Oral

Light Management in Silicon Heterojunction Solar Cells via Implementation of Nanocrystalline Silicon Oxide Films and Nano-Imprint Textures

**A. Richter[1], F. Lentz[1], M. Meier[1], K. Ding[1]*
[1]Forschungszentrum Jülich, IEK-5, Photvoltaics, Jülich, Germany

Excellent light management is essential to increase the amount of light being captured in the absorber of silicon heterojunction solar cells in order to obtain a high photoelectric current. Three possible ways to achieve this are improving the cell anti-reflectance, increasing the light path through the absorber material, and minimizing the parasitic losses in the other layers. The former two goals can be realized via surface texturing and the latter by using highly transparent materials. In this study, we focus on implementing hydrogenated nanocrystalline silicon oxide (nc-SiO_x:H) in combination with front side nano-imprint textures in silicon heterojuction solar cells. Nc-SiO_x:H offering a unique combination of high conductivity and high transparency is perfectly suited as an alternative wide-gap doped layer to minimize parasitic absorption. At the same time, nano-imprint technology provides a way to realize various textures on “flat” silicon solar cells without inevitably promoting recombination at the absorber interface by enlarging the surface area and increasing the number of defect states. We show by a systematic investigation how the interplay between the imprinted layer and the underlying thin films of the silicon heterojunction based solar cell affects the generated current. Ultimately, we demonstrate very high current densities and efficiencies beyond 20% without wet-chemically texturing the Si-wafer by combining the benefits of the highly transparent nanocrystalline silicon oxide layers and the favourable properties of the nano-imprint technology.

ID 131 - Poster

Electrical Conductivity Studies of Hematite (α-Fe_2O_3) indicate Phase Transition to Magnetite (Fe_3O_4) already at 400 K.

*J. Mock[1], B. Klingebiel[1], F. Köhler[1], M. Nuys[1], J. Flohre[1], S. Muthmann[1], C. Leidinger[1], O. Thimm[1], R. Carius[1]
[1]Forschungszentrum Jülich, IEK-5, Jülich, Germany

Hematite (α-Fe2O3) nanoparticles (NPs) show great potential for application as absorber material in multi-junction solar cells due to their suitable band gap accompanied by high absorption coefficients. Additionally, hematite is a highly promising photoanode material for photoelectrochemical solar water splitting due to its chemical stability, band structure and abundance. However, the pure hematite phase is required to overcome surface recombination for both applications. In this study we investigated the temperature dependent electronic transport properties of hematite NP layers. A successively increasing electrical conductivity for annealing temperatures above 360 K under vacuum condition is observed. We interpret the increased conductivity as percolating transport through magnetite shells surrounding the hematite NPs, i.e. the results indicate a continuous material conversion of hematite into magnetite (Fe3O4). This phase transition is confirmed by Raman spectroscopy for annealing temperatures above 600 K. The theoretical conversion temperature of hematite as bulk material into magnetite is around 1000 K under vacuum annealing. The results therefore indicate a significantly reduced conversion temperature of the NP surface region as compared to the NP bulk. Due to the continuous conversion of the NP surface into the higher conductive magnetite phase, we are able to tune the conductivity of the NP layer over seven orders of magnitude. Electrons are identified as the majority charge carriers by thermoelectric power measurements. The size and shape of the NP's remains unchanged during the annealing process as confirmed by Scanning Electron Microscopy. Photothermal deflection spectroscopy measurements show an additional narrow band gab material absortion for subsequently annealed samples under nitrogen atmosphere. Using synthetic air during the annealing process, we are also able to reverse the phase transition and the conductivity drops close to its initial value. The present study shows the importance of controlling temperature and atmosphere when hematite is processed, since the structural phase of iron oxide can change on a nanometer scale.

ID 132 - Poster

Trisilane-Based Liquid Precursor for the Preparation of a-Si:H Thin Films

**A. P. Cadiz Bedini[1], S. Muthmann[1], F. Finger[1], R. Carius[1]*
[1]Forschungszentrum Jülich, IEK-5, Jülich, Germany

The preparation of solution-based silicon electronics from liquid oligosilanes is an attractive low-cost alternative to conventional technologies such as gas-phase thin film preparation methods and crystalline silicon technology. Some of the major disadvantages associated with solution-based methods, however, are the high cost and scant commercial availability of the precursor monomers. With this in mind, we developed a liquid silicon hydride precursor based on trisilane (Si_3H_8, TS), which constitutes a more economic starting material compared to those currently being used in the literature. Due to its industrial relevance, trisilane is readily available in large quantities and at high purity.

Low-volatility, high molecular weight hydridosilanes (-$(SiH_x)_n$-) are prepared from TS in a cyclooctane solution at ambient pressure under inert atmosphere by means of a novel method involving a combination of sonication and ultraviolet irradiation. The resulting -$(SiH_x)_n$- are cast as thin films on glass and c-Si substrates via spin coating and subsequently pyrolytically converted into hydrogenated amorphous silicon (a-Si:H).

The initial polymerisation process is studied using gas chromatography-mass spectrometry (GC-MS). The microstructure factor of the a-Si:H thin films, as calculated using Fourier transform infrared spectroscopy (FTIR), is found to be ~0.8, indicating a void-rich morphology. In addition, photothermal deflection spectroscopy (PDS) is used to study the optical absorption and defect density of the films, revealing a well-defined band edge and a rather high subgap absorption of ~10^2 cm^{-1} indicating a dangling bond defect density of ~10^{17} cm^{-3}.

ID 133 - Oral

Optical switching device using organic heptazole photovoltaic cell and its application of operating organic field effect transistor

*J. Lee[1], S. R. A. Raza[1,2], S. Im[1]
[1]Yonsei University, Physics and Applied Physics, Seoul, Korea, Republic of
[2]University of Azad Jammu and Kashmir, Physics, Muzaffarabad, Korea, Republic of

Optoelectronics and photonics can be possible application field based on organic semiconductor, and recent progress has been significantly developed by various types of devices such as organic photodiode, photovoltaic and phototransistor. In this context, several optical switching operations are proposed by organic photovoltaic cell. The cell is based on Schottky rectifying contact between p-type small molecule organic semiconductor, heptazole ($C_{26}H_{16}N_2$), and low work function electrode of Al. Transparent electrode of ITO is employed for light input. The single heptazole photovoltaic cell can generate ~0.3 V as open circuit voltage under blue light, but recovery process turns out to be slow. The two photovoltaic cells are connected in series, and the fast recovery process can be achieved by making short recombination step. Consecutive positive and negative voltage signal can be also induced using the consecutive light inputs. This converted voltage signals can turn on heptazole based organic field effect transistor as gate voltage. The voltage signal from photovoltaic cell and the current signal from connected transistor can be amplified by forming tandem structure. In addition, the basic optical Boolean logics such as NOT, OR, AND are demonstrated. We believe these proposed functions can provide new approaches for organic optoelectronics and photonics.

ID 134 - Poster

Persistent photoconductivity studies in a-Si:H/nc-Si:H thin film super lattice

*A. Yadav[1], *P. Agarwal[2,1]*
[1]IIT Guwahati, Center for Energy, Guwahati, India
[2]IIT Guwahati, Department of Physics, Guwahati, India

The electronic properties of undoped a-Si:H/nc-Si:H super lattice structures have been investigated by photoconductivity measurements. Multilayered structures consisting of 2 and 5 period each of alternating layers of a-Si:H and nc-Si:H were deposited on corning 1737 glass substrate, keeping the total thickness of films constant at 700 nm by Hot wire chemical vapor deposition (HWCVD) technique. Dark & photo conductivity and Persistent Photoconductivity (PPC) are measured in coplanar geometry using Ag paste as electrodes.To ensure contact to all layers, the super lattice structures were scratched before making the electrodes. Quite interestingly room temperature persistent photoconductivity (PPC) has been observed in these undoped a-Si:H/nc-Si:H super lattice structures. In PPC current does not fall back to initial dark value after switching off the illumination, instead it shows a slow exponential decay. The decay kinetics of the PPC is well described by single exponential function $I=I_o exp^{-t/\tau}$ in our case. Electric field as well as light intensity dependence of photoconductivity and PPC is also measured. The photo current varies linearly with applied field. However, the extent of PPC reduces with the increase in applied field. Similarly when the light intensity is high, PPC is more compared to low illumination intensities. Further the PPC is more when number of periods is more even when the total thickness of the samples remains the same.

In multilayer structures different band gaps and intrinsic conductivity of a-Si;H and nc-Si:H layers result in band bending at the interfaces. When sample is illuminated, the photo carriers are generated which can move along the depth due to band bending at interfaces and also in lateral direction due to external fields. Carriers trapped in the interface states are likely to be responsible for observed PPC. When the external field is high the carrier are swept in lateral direction and small PPC is observed. Similarly when the light intensity is less, less carriers are generated allowing a few of carrier to move to other layer than sweeping away in lateral direction and small PPC is observed. When number of periods is more, more interfaces are created and individual layer thickness is less resulting in higher PPC.More results on single layer and super-lattice structures will be presented during the conference.

Acknowledgement: Authors acknowledge the fruitful discussions with Professor S.C. Agarwal, Professor Emeritus, IIT Kanpur.

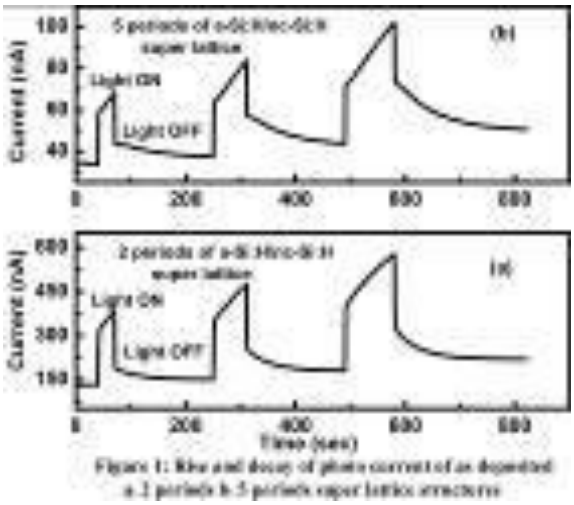

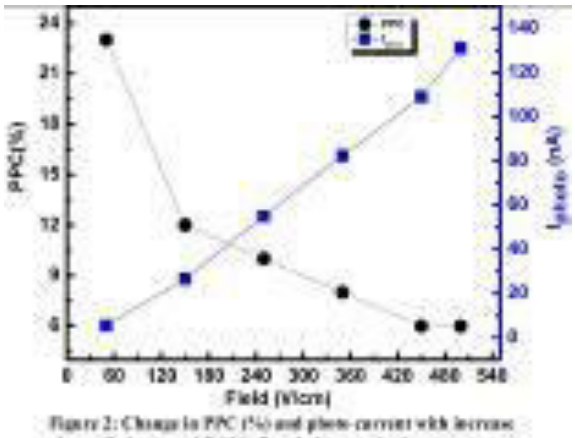

ID 135 - Oral

Hydrogenated amorphous silicon doping by plasma immersion ion implantation for a-Si:H/c-Si heterojunction solar cells

*T. Carrere[1,2], A.- S. Ozanne[1], D. Muñoz[1], J.- P. Kleider[2]
[1]CEA - INES, Le Bourget-du-Lac, France
[2]GeePs, CentraleSupélec, Univesité Paris-Sud, Sorbonne Universités UPMC Univ Paris 6, Gif-sur-Yvette, France

In the frame of the photovoltaic market competition, there is a major need of increasing cells efficiency while decreasing their manufacturing costs. Rear contacted silicon heterojunction solar cells have already proven their capability to reach efficiencies as high as 25.6% *(Masuko et al., IEEE J. of Photovoltaics, 2014)*. However their manufacturing process is not yet cost competitive because of the need of numerous steps to pattern the rear side in interdigitated n- and p-type contacts.

Doping the amorphous silicon layers using ion implantation through a mask seems very attractive to simplify the manufacturing process. Thanks to the last developments of plasma immersion ion implantation (PIII), allowing very shallow implantation depth, doping of the very thin a-Si:H layer has now become possible with a perspective of limited damage of the a-Si:H/c-Si interface *(Torregrosa et al., Surf. Coat. Technol., 2004)*.

Therefore, our research is focused on using the PIII process to achieve highly doped (n)a-Si:H layers (conductivity > 10^{-4} Ω^{-1} cm^{-1}) while keeping an efficient c-Si surface passivation (open circuit voltage V_{OC} > 700 mV). Thus, one needs to understand: **(i) How PIII modifies the material and the electric properties**, and **(ii) what is the effect of post-implantation annealing with regards to the electric properties.**

To our knowledge, this is the first study focusing on ion implantation doping of a-Si:H thin layers applied to silicon heterojunction solar cells technology (i.e. which focuses on both the a-Si:H layer conductivity and the a-Si:H/c-Si interface passivation).

(i)a-Si:H layers of various thicknesses are deposited by RF PECVD on glass and on both sides of n-type float-zone double side polished c-Si substrates. Once they have been PIII implanted and annealed, glass and c-Si samples are dedicated to conductivity and passivation (effective lifetime/implied V_{OC} by QSSPC) measurements, respectively. c-Si samples also undergo spectroscopic ellipsometry (SE), SIMS and FTIR measurements to characterize the material changes. The experimental process flow is introduced in Figure 1.

The energy-over-thickness ratio is found to control the passivation loss caused by ion implantation. Under 25±5 V/nm, there is almost no passivation loss upon ion implantation. Above 25±5 V/nm, the passivation is destroyed. In Figure 2, the electrical properties of the experiment batch having the highest conductivities are displayed versus the layer thickness and the implantation energy for a dose of 10^{16} cm^{-2}. Conductivities after implantation are clearly energy-dependent: for the same dose, a higher energy leads to a higher conductivity. Finally a 30 min annealing at 300°C fully restores the passivation but decreases the conductivity by 2 to 3 orders of magnitude.

From SIMS and FTIR measurements, the hydrogen content decreases upon the 300°C annealing. Less hydrogen results in a density of states increase in the a-Si:H layer which is likely to hinder the displacement of the Fermi level towards the conduction band that is targeted by addition of P atoms. Therefore, the hydrogen loss is believed to be responsible of the conductivity decrease upon annealing. These material changes are also correlated with the optical band gap and the compact and disorder parameters evolution obtained from SE measurements.

FTIR measurements confirm that the hydrogen bonding configuration explains the passivation evolutions previously described. Upon implantation, there is an increase in the SiH_2 bonds compared to the SiH

ones. Upon annealing, the SiH_2 bonds proportion is decreased. As for gas phase doped a-Si:H layers, the SiH_2 configuration controls the passivation quality *(Wang et al., Phys. Chem. Chem. Phys., 2014)*.

The passivation recovery upon annealing is found to take place through two distinct regimes. A first mechanism recovers quickly the passivation (4.3 mV/min at 150°C) up to a threshold. The recovery rate and the threshold reached during the first 15 min of annealing both increase with the annealing temperature. A 300°C annealing is able to fully recover the interface damages by this mechanism. However, such regime is temperature activated and takes place above 100°C only. After 15 min of annealing, a slower regime, temperature-independent (~0.6 mV/min) becomes predominant.

We investigated the doping of thin a-Si:H layers by PIII with the aim of simplifying the rear contacted silicon heterojunction solar cells manufacturing. Upon ion implantation, the passivation is damaged above a given energy-over-thickness ratio. However, an appropriate annealing fully recovers the passivation properties thanks to a hydrogen bonding reconfiguration from SiH_2 to SiH. High implantation energies promote the dopant activation and results in higher conductivities. However, the 300°C annealing decreases significantly the as-implanted layer conductivity. Finally, it is found that there are two mechanisms controlling the passivation recovery.

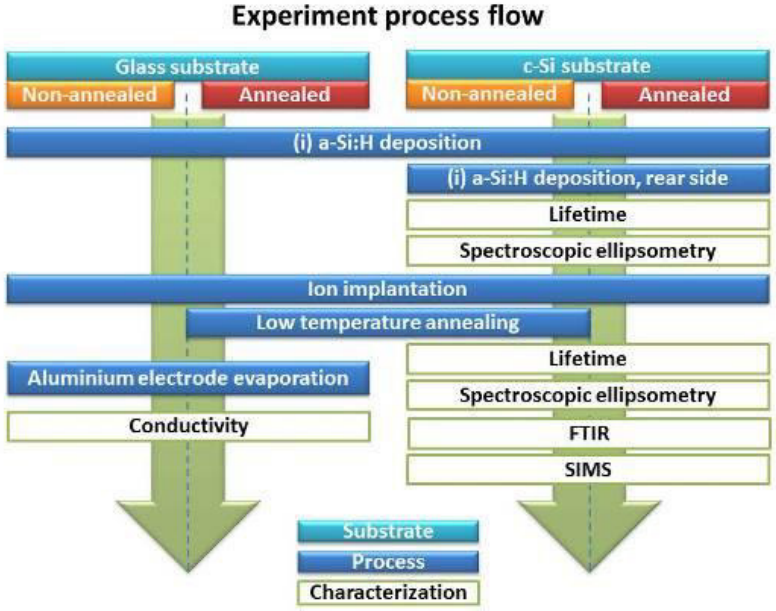

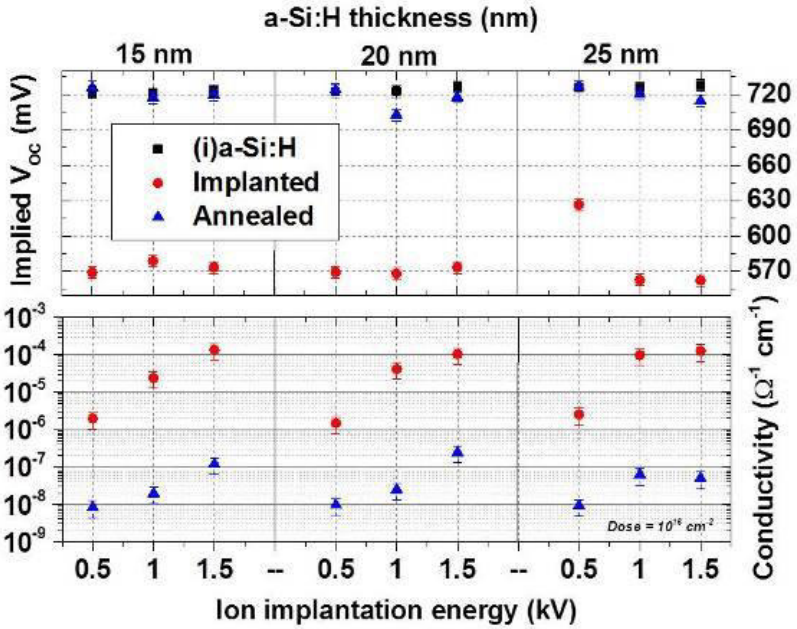

ID 136 - Poster

Effect of O_2 content on third order Nonlinear Optical properties of PLD deposited SiO_x thin films

P. P. Dey[1], **A. Khare*[1]
[1]*Indian Institute of Technology Guwahati, Physics, Guwahati, Assam, India*

Nonlinear optical properties of materials have been used for various applications such as optical switching, optical limiting, harmonic generation and information storage. The non-linear optical (NLO) susceptibility in nanoscale dimensions is enhanced due to manifestations of quantum size effects. In this paper, linear and nonlinear optical absorption and refraction coefficient of the nanostructured SiO_x thin films are reported. Films were deposited by Pulsed Laser Deposition (PLD) technique using Q-switched Nd: YAG laser (532 nm) onto fused silica substrate at substrate temperature of 400 ^{0}C by varying the O_2 pressure in the range of 5×10^{-5} to 0.5 mbar. All the thin films show characteristic XRD peaks, Fig. 1, for the Si (111), Si (220) and Si (311) planes at around 2θ ~ 28.45˚, 47.37˚ and 56.2˚, respectively confirming the formation of nc-Si. The crystallite sizes within the films were found to be around 20 nm and nearly independent of O_2 pressure. It is observed that the intensity of these peaks gradually increased with decreasing O_2 pressure. EDX spectra exhibit the increase in oxygen content with increasing O_2 pressure in SiO_x films. Linear absorption coefficients (α) and refractive indices (n) were estimated from UV-Vis-NIR transmission spectra. Refractive indices of the films were found to vary from 4.54 - 1.68 (within λ ~1000 nm to 3000nm) with the increase in O_2 pressure in the range of 5×10^{-5} to 0.5 mbar, respectively. The non linear absorption coefficient (β) and nonlinear refractive index (n_2) of all the films were estimated by Z scan technique using a cw-He-Ne laser. The Fig 2 (a) and (b) show the open and closed Z-scan spectra of SiO_x thin film deposited at an O_2 pressure of 5×10^{-5} mbar. The open Z scan spectrum, Fig 2(a) depicts strong reverse saturation absorbtion and so was observed for all the films. The value of β estimated from the open z scan data for the SiO_x films was observed to be decreasing from 22.5 cm/W to 4.6 cm/W, with increase in O_2 pressure from 5×10^{-5} to 10^{-2} mbar. The normalized transmission profile for closed Z scan spectrum, Fig 2(b) shows a transmittance minimum (valley) prior to focus followed by a transmittance maximum (peak) after focus for this film as well as for other films. This valley-peak signature observed in all the SiO_x films indicates the presence of self focusing property, which corresponds to positive nonlinear refractive index, n_2. The n_2 for the SiO_x films was observed to be decreasing from 34.8×10^{-5} cm^2/W to 4.96×10^{-5} cm^2/W, with increase in O_2 pressure from 5×10^{-5} to 10^{-2} mbar. The significantly large nonlinear optical absorption and refraction coefficients were observed in the SiO_x films deposited via PLD as compared to that of a bulk Si and SiO_2. This can be attributed to limitations imposed by the quantum size effects of nc-Si within SiO_2 matrix. In smaller dimension, the oscillator strength enhances and interaction of the local electric field of the light with nc-SiO_x becomes stronger. The detailed results and explanations for the variations of third order non-linear coefficients with O_2 pressure will be presented in full manuscript. We acknowledge DRDO, New Delhi, India (project no. ERIP/ER/07003/30/M/01/1138) for providing the PLD chamber.

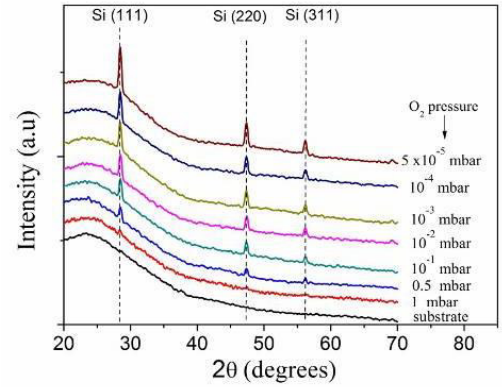

Figure 1. XRD spectra of the substrate and PLD SiO_x thin films fabricated at different ambient O_2 pressure.

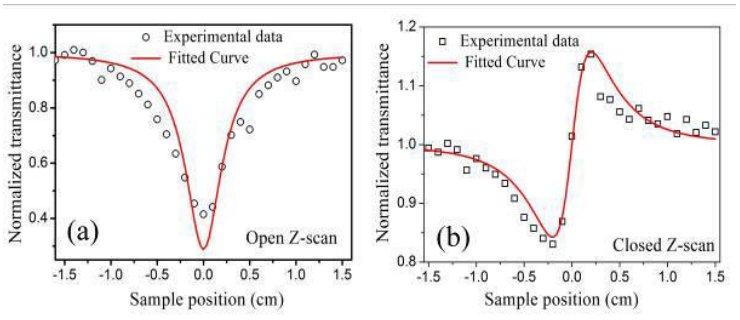

Figure 2. (a) open and (b) closed Z-scan of SiO_x film deposited at 5×10^{-5} mbar O_2 pressure.

ID 137 - Poster

Variable range hopping conduction in thermally reduced graphene oxide thin films

*M. Singh[1], *P. Agarwal[1]*
[1]IIT Guwahati, Department of Physics, Guwahati, India

Temperature dependent electrical conductivity of thermally reduced graphene oxide (rGO) thin films was measured from 270 to 40 K. Thin films were made on quartz substrates using drop casting method with thickness of~ 60 nm and were annealed in vacuum at three different temperatures 130, 300 and 400 °C for 1h. Room temperature electrical conductivity of pre-annealed graphene oxide is ~ 0.6, 20.5, 22.3 S/cm respectively for pre-annealing temperature of 130, 300 and 400 °C. Conductivity of rGO is found to decrease with decreasing temperature, and at 40K, the measured values are 0.2, 2.8, 5.5 S/cm respectively. Electrical conductivity data is analyzed using resistance curve derivative analysis (RCDA) [1, 2]. It is observed that conduction mechanism in rGO films pre-annealed at 300 and 400 °C follow Mott variable range hopping (VRH) , where T_0 and d are the characteristic temperature and dimensionality of hopping process respectively. From RCDA analysis, the observed value of p is 0.19 and 0.27 for the films pre-annealed at 300 and 400 °C respectively, which is close to p = 1/4, and corresponds to 3D-VRH in the temperature range 250 - 80 K. Below 80 K, the conductivity was found to decrease much more rapidly in comparison to that higher temperature. This is due to increase in hopping distance with decrease in temperature down to 40 K, as indicated in figure 1. Mott VRH conduction process was not observed for rGO pre-annealed at 130 °C. The reason of not observing VRH in rGO pre-annealed at 130 °C could be the presence of excess amount of oxygen containing functional groups, as discussed earlier in ref. [3]. These oxygen containing functional groups make the channel for the conduction of electron even at low temperature.

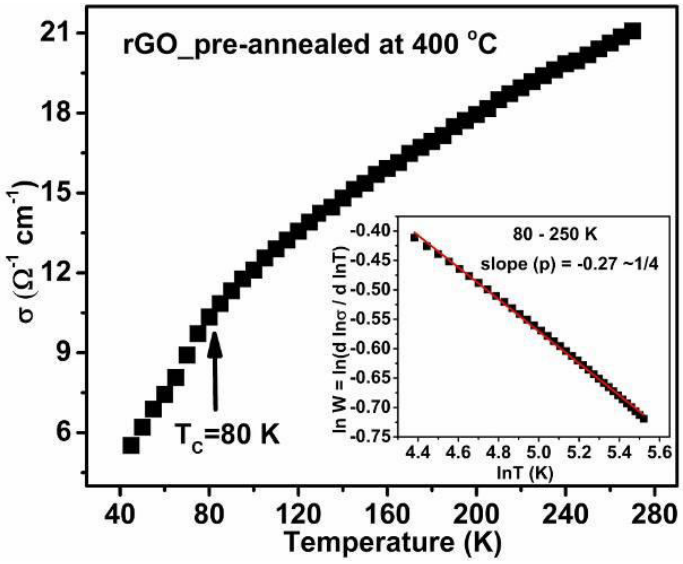

1. C. Chuang, R.K. Puddy, H. De Lin, et al. Solid State Communications **152** (2012) 905 - 908.
2. D. Joung, S.I. Khondaker, Physical review B **86** (2012) 235423.
3. M. Singh, A. Yadav, S. Kumar, P.Agarwal, Applied Surface Science **326** (2015) 236-242.

Acknowledgements: Authors would like to thank Prof. S. Ravi from Dept. of Physics, IIT Guwahati, India for providing low temperature He^4cryostat facility and his students for helping in measurements.

ID 138 - Poster

Silicon quantum dots formation in annealed *a*-SiO_xN_y:H single layers and *a*-Si/SiO_2 multilayers grown by PECVD: Structural and photoluminiscence properties

*P. Calta[1], *S. Agbo[2], P. Šutta[1], R. Medlín[1], M. Netrvalová[1], J. Savková[1]*
[1]University of West Bohemia, New Technologies-Research Centre, Plzen, Czech Republic
[2]Forschungszentrum Jülich GmbH, Institut für Energie- und Klimaforschung (IEK-5), Jülich, Germany

Silicon nanostructures embedded in dielectric matrix have interesting possible applications in new photovoltaic devices where they could be used as absorbers (multi-band gap approach). Variation in band-gap of thin film silicon-based materials through the use of quantum confinement in Si quantum dots is cheap and very promising route towards the third generation of silicon photovoltaic devices such as all-Si based tandem solar cells with high efficiency. These novel thin film fabrication usually involve a high-temperature post-deposition annealing.

In this study, we report on synthesis and characterization of silicon quantum dots formed by thermal annealing of *a*-SiO_xN_y:H single layers and *a*-Si:H/SiO_2 multilayers prepared by plasma enhanced chemical vapor deposition (PECVD). *A*-SiO_xN_y:H single layers were deposited from gas mixture of silane and nitric oxide (($[N_2O]/[SiH_4]$ = 1). Multilayers were grown by alternating deposition of hydrogenated amorphous silicon sublayers (from SiH_4) and silicon dioxide sublayers ($[N_2O]/[SiH_4]$ = 20) with varying sublayer thickness. Size-controlled silicon nanocrystals have been fabricated by step-by-step thermal annealing post-deposition treatment (up to 1100°C) of these as-deposited single- and multilayers. The influence of post-deposition thermal treatment on the microstructural (by TEM and XRD), chemical bonding configuration (by FT-IR and Raman microscope), optical (by spectroscopic ellipsometry and UV-VIS spectroscopy) and photoluminiscence (PL) properties of these formed nanostructures in the amorphous embedding matrix were studied and the experimental results are presented and discussed.

We are able to show the different stages of the nanostructure formation in single- and multilayers and the evolution of the sizes and the crystallized mass fraction. FT-IR spectroscopy indicated the chemical composition of SiO_xN_y single layers was dominated by silicon suboxide containing silicon-nitride and silicon-hydrogen bonds. From analysis of the Si-O-Si stretching band vibrations between 1000 and 1150 cm^{-1} in single- and multilayers, we have found that this peak frequency, integration area and FWHM are dependent on temperature. During annealing, the shift of the Si-O-Si vibration to higher wavenumbers is attributed to a reordering in the films toward an increased SiO_2 bonding configuration resulting from the precipitation of silicon. The disappearance of the hydrogen related bonds indicates the hydrogen effusion. For the both kind of as-deposited and annealed films, Raman spectra showed a band approximately at 480 cm^{-1}, related to amorphous silicon and a band at around 517 cm^{-1}, related to nanocrystallite silicon, respectively. The crystalline mass fractions (exceeding 50%) and structural order of nc-Si is compared with XRD and TEM measurements. Over 1000°C, both kind of annealed samples showed the *c*-Si diffraction peaks, which became narrower with increasing temperature. From the width of the Si peaks, the mean size of Si nano-crystallites and their dependence on temperature was determined. The formation of Si-ncs is corroborated by TEM, which demonstrate the appearance of silicon nano-crystals that are 5-15 nm (multilayers) and up to 10 nm (single layers) in size. Room-temperature photoluminescence (PL) excited by the 325 nm line exhibits peaks between 700-900 nm associated with the nanocrystal formation. The PL intensity of SiO_xN_y single layers is significantly enhanced by a high-temperature annealing at 800°C. It is induced by the increase of the number of nc-Si and oxygen-related defects saturated by Si-O-Si within the Si/SiO_2 interface. PL intensity reaches a maximum in Si/SiO_2 multilayers at 900°C which is lower than those needed for single layers. The peak position and intensity of the main emission band in the PL spectra strongly depend on the Si layer thickness. We will describe the nano-crystal dimension and photo-luminescence as a function of the superlattice layer thickness, and annealing conditions, to understand the crystallization proces.

ID 139 - Oral

Identifying the correct recombination models in Organic Solar Cells through the use of 'Simiconductor'-simulations

*I. Cardinaletti[1], J. Liesenborgs[2], J. Drijkoningen[1], S. Bertho[1], T. Vangerven[1], D. Schreurs[1], W. Maes[1,3], J. D'Haen[1], F. Van Reeth[2], J. V. Manca[1,4]
[1]Hasselt University, IMO-IMOMEC, Diepenbeek, Belgium
[2]Hasselt University -tUL - iMinds, EDM, Diepenbeek, Belgium
[3]IMEC vzw, Associated lab IMOMEC, Diepenbeek, Belgium
[4]Hasselt University, XLab, Diepenbeek, Belgium

In this work a new - free and easy-to-use - simulation tool 'Simiconductor' [1] is introduced for the simulation of current/voltage curves in organic solar cells. Similar to the works of e.g. [2] and [3], simulations of organic solar cells in 'Simiconductor' are based on drift-diffusion equations. These drift-diffusion equations can be solved in either a 1D or 2D situation (in the latter case with periodic boundary conditions) by discretizing them on a grid. The use of the technique by Scharfetter and Gummel [4] to calculate currents allows very accurate calculations when using even a small amount of grid points in each direction.

With 'Simiconductor', simulations can be programmed by diversifying a number of material dependent parameters, as well as by selecting specific recombination methods for the generated electron-hole pairs, or by choosing different approaches in the search for an equilibrium situation. Required inputs can be collected in most cases through experiments and literature, although full active layer characterization is not always attainable.

We note that the choice of some of the materials' characteristics (e.g. charge carrier mobility) is of paramount importance for an appropriate simulation.

Comparing Simiconductor-simulations using several recombination models with experimental curves, offers the possibility to infer which mechanism is most likely to take place in the active layer of the studied solar cells. Here this methodology will be applied for the high-efficiency material system Poly[[5-(2-ethylhexyl)-5,6-dihydro-4,6-dioxo-4H-thieno[3,4-c]pyrrole-1,3-diyl][4,8-bis[(2-ethylhexyl)oxy]benzo[1,2-b:4,5-b']dithiophene-2,6-diyl]]:[6,6]-Phenyl C71 butyric acid methyl ester (PBDTTPD:$PC_{71}BM$). In particular, we focus on the change of Fill Factor induced by the implementation of the various recombination mechanisms. Identifying the correct cause of performance loss is crucial in order to develop appropriate solutions and methodologies towards the control and minimization of the phenomenon.

[1] 'Simiconductor' by J. Liesenborgs,http://research.edm.uhasselt.be/jori/simiconductor/
[2] LJA Koster, ECP Smits, VD Mihailetchi, and PWM Blom. Device model for the operation of polymer/fullerene bulk heterojunction solar cells. Physical Review B, 72(8):085205, 2005.
[3] K Maturova, SS Van Bavel, MM Wienk, RAJ Janssen, and Martijn Kemerink. Morphological device model for organic bulk heterojunction solar cells. Nano letters, 9(8):3032-3037, 2009.
[4] D.L. Scharfetter and H.K. Gummel. Large-signal analysis of a silicon read diode oscillator. IEEE Transactions on Electron Devices, 16(1):64-77, 1969.

ID 141 - Poster

Optical field induced mass transport in amorphous chalcogenide and azobenzene containing polymers

*J. Teteris[1]
[1]Institute of Solid State Physics, University of Latvia, 8 Kengaraga Str., LV-1063, Riga, Latvia

teteris@latnet.lv

The direct surface patterning of amorphous chalcogenide(As-S, As-S-Se, As-Se and Ge-Se systems)and azobenzene containing organic glass films induced by polarization direction modulated optical field was studied. A single light beam polarization direction modulation and focusing, and two coherent beam interference patterns were used for optical-field formation with high intensity gradient. Under intensive illumination the formation of relief structures on the surface of amorphous films due to lateral mass transport regarding the light propagation direction has been observed [1].

The influence of the amorphous film thickness, recording laser wavelength in the spectral range of (375 nm - 671 nm), grating period, recording light intensity and polarization state on the relief formation process in amorphous chalcogenides films was evaluated and compared with the measurements in azo-benzene containing low molecular organic glass films . The best efficiency of surface relief grating (SRG) formation was observed with ($+45^0$, -45^0) and (RCP, LCP) polarized beam combinations, which involve primarily variation in linearly polarized state across the film - parallel and perpendicular regarding the grating vector [2]. The relief grating profile on amorphous films was analyzed by means of atomic force microscope (AFM).

A strong relationship between SRG and polarization holographic grating formation was observed. It is known that polarization gratings can be recorded in a material which possesses photo-induced birefringence and dichroism. Therefore a detailed study of a photo-induced birefringence and changes of optical properties in studied films was performed.

The phase relationship between the exciting light field and the resulting surface deformation was studied. It was observed that the peak of the SRG on chalcogenide films was formed at the position of p-polarization state in the polarization modulation pattern. It was shown that the efficiency and direction of mass movement is determined by a value and sign of photoinduced birefringence in amorphous films. This fact is crucial to infer the direction of the forces to form the SRG.

The photoinduced dielectrophoretic model of the direct recording of surface-relief on amorphous films based on the photoinduced softening of the matrix, formation of defects with enhanced polarizability, and their drift under the optical field gradient forces has been discussed [3].

The possibilities in practical application of photoinduced direct surface patterning in lithography and fabrication of diffractive optical elements will be inspected.

[1] U.Gertners, J.Teteris, Optical materials, 32 (2010) 807-810.
[2] M.Reinfelde, J.Teteris, E.Potanina, Canadian Journ. of Physics, 92, (2014) 659-662.
[3] J.Teteris, M.Reinfelde, J.Aleksejeva and U.Gertners, Physics Procedia, **44** (2013) 151-158.

ID 142 - Oral

Effect of Top gate bias on Fermi position, photo current and NBIS instability in dual gate a-IGZO TFTs

**M. D. H. Chowdhury[1], M. Chun[1], E. Lee[1], J. Jang[1]*
[1]Kyunghee University, Information Display, Seoul, Korea, Republic of

Amorphous Indium Gallium Zinc Oxide (a-IGZO) based thin film transistors (TFTs) are the most comparable devices for switching operation in high resolution display industries, considering low cost process, high filed effects mobility (μ_{fe}), lower threshold voltage (V_{TH}) and subthreshold swing (SS) [Ref.1]. The drawback of such devices are the device uniformity in broad area and degradation of performances under negative bias illumination stress (NBIS). The uniformity issue could be solvable by using a dual gate a-IGZO TFT structure [Ref.2], which has additional top gate metal on a conventional bottom gate inverted staggered TFTs. Transfer characteristics and device performances of dual gate a-IGZO TFT has reported elsewhere [Ref.2]. In our investigation, we observed that top gate bias amplitude and polarity plays a big role on V_{TH} and μ_{fe}, calculated from bottom gate sweep. Top gate voltage actually modulate the Fermi level position of a-IGZO, which influence to control the generation of photo induced electron-hole pair as well as NBIS induced V_{TH} shift. It is well known that NBIS in a-IGZO TFTs make a negative transfer shift due to the formation of positive charges (by transition of V_O to V_O^+/V_O^{2+} and/or hole traps) at interfaces/IGZO bulk [Ref. 1 & 3]. We observed that positive bias at top gate show less photo current generation as well as less V_O^+/V_O^{2+} generation, compared with negative top gate bias. For metal oxide based phototransistor [Ref. 4], we can easily improve the performances by controlling the top gate voltage. It also gives a simple solution to suppress the NBIS instability in all metal oxide based TFTs.

[1] M. D. H. Chowdhury, P. Migliorato and J. Jang: Appl. Phys. Lett. 102, (2013) 143506.
[2] M. Mativenga, S. An, and J. Jang, IEEE Electron Device Lett. 34, (2013) 1533.
[3] H. Oh, S. M. Yoon, M. K. Ryu, C. S. Hwang, S. Yang, and S. H. K. Park, Appl. Phys. Lett. 97 (2010) 183502.
[4] A. Nathan, S. Lee, S. Jeon, and J. Robertson, Journal of Display Technology, 10, (2014) 917.

ID 143 - Poster

Impact of TCO front Side Texture on the V_{oc} of a-Si:H Solar Cells

*C. Zhang[1], M. Meier[1], T. Merdzhanova[1]
[1]IEK-5, jülich, Germany

Previous investigations of single- or multi-junction solar cell devices deposited on top of different transparent conductive oxides (TCO) front textures pointed out differences in terms of electrical and optical properties. Regarding the short-circuit current density of a-Si:H solar cells high performances were achieved for double textured ZnO:Al and APCVD SnO_2:F front TCOs. This is driven by the, particularly for a-Si:H solar cells, highly suitable light scattering provided by the respective texture. Especially for double textured ZnO:Al, which contains smaller and steeper crater structures in combination with an improved transparency, high conversion efficiencies of 11% initial were achieved for a-Si:H solar cells. However, in this work the focus is on the electrical performance for solar cells deposited on various textures. Solar cells deposited on top of double textured ZnO:Al show a reduced V_{oc} of approximately 30 mV. Also, when depositing solar cells on top of APCVD SnO_2:F and LPCVD ZnO:B front textures a lower V_{oc} is measured comparing to flat textures. Very rough morphologies can influence the electrical properties of a solar cell. Commonly, a reduction of V_{oc} especially for µc-Si:H solar cells is attributed to the formation of cracks occurring due to microcrystalline growth on very steep structures. However, such cracks are not observed in a-Si:H solar cells. One aspect of this work is to investigate the formation of defective-regions and recombination processes that are related to the front side topography.

It was found that the reduction of V_{oc} in a-Si:H thin film solar cells deposited on very rough front textures are mainly due to defective regions in the first 100 - 200 nm of the bulk material. When increasing the i-layer thickness it was seen that the “nanocracks” in the absorber layer partially heal out. Still, the bulk material include defective areas within the first 200 nm leading to higher reverse bias saturation current density J_0 and also a lower V_{oc}. In a-Si:H solar cells with thicker i-layers the negative impact of the rough front contact becomes less insignificant.

Solar cells deposited on differently textured front TCOs show differences in terms of the V_{oc}. Reasons for the deterioration of voltage seen for very rough front textures are discussed based on a series of a-Si:H single junction solar cells deposited on six different front contacts and various i-layer thickness.

ID 144 - Oral

Organo-lead Halide Perovskite based Direct X-ray Detectors

**S. Shrestha[1], G. Matt[1], H. Azimi[1], M. Richter[1]*
[1]Friedrich-Alexander-University (FAU) Erlangen-Nürnberg, Materials for Electronics and Energy Technology (i-MEET), Erlangen, Germany

Organo-lead halide perovskite has emerged as a cost effective and high performance light harvesting material for solar cells. Over a short period of time, solar cells with power conversion efficiencies comparable to that of crystalline Si solar-cells have been realized. This success can be attributed to the high absorption coefficient in visible, low binding energy, high carrier mobility and long carrier diffusion length. In addition to these physical properties, the heavy element lead in the material results in a high X-ray absorption coefficient and thus makes it an ideal candidate for X-ray detection. Here we demonstrate for the first time, the generation of primary photo-current in a solution processed Methylammonium lead iodide based photo-detector under X-ray exposure. The achieved X-ray sensitivity is up to 25 µC mGy^{-1} cm^{-3} (1). This value is already comparable to the current state of the art.

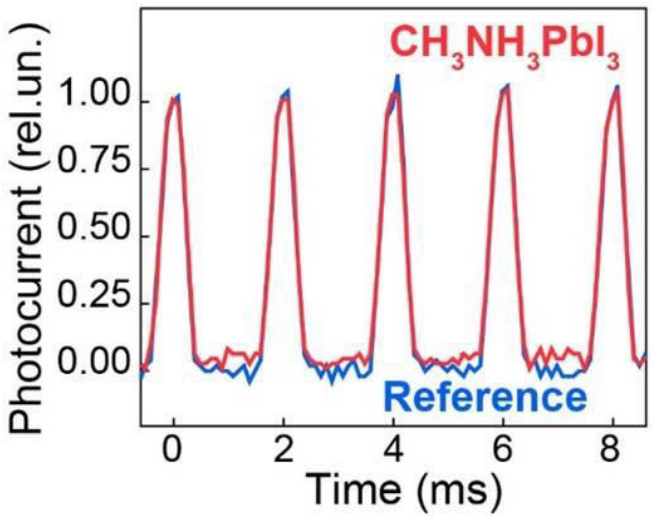

Figure: Time-resolved primary photocurrent under 50 Hz pulsed X-ray exposure. The Methylammonium lead iodide detector is shown in red and a reference commercial silicon detector sensitized with cerium doped ytterbium aluminium garnet (YAG:Ce) scintillator is shown in blue.

(1) Detection of X-ray photons by solution-processed organic-inorganic perovskites Sergii Yakunin, Mykhailo Sytnyk, Dominik Kriegner, Shreetu Shrestha, Gebhard J. Matt, Moses Richter, Hamed Azimi, Christoph Brabec , Julian Stangl, Maksym Kovalenko and Wolfgang Heiss, submitted

ID 145 - Oral

Non-isothermal analysis of crystallization kinetics in $Ge_2Sb_2Te_5$ thin films for PCM application

*A. Sherchenkov[1], *S. Kozyukhin[2], A. Babich[1], P. Lazarenko[1], S. Timoshenkov[1], O. Boytsova[2]*
[1]National Research University of Electronic Technology, Moscow, Russian Federation
[2]Kurnakov Institute of General and Inorganic Chemistry of the Russian Academy of Sciences, Moscow, Russian Federation

Currently active investigations of phase change memory (PCM) are carried out. Chalcogenide compounds on the pseudo-binary line $GeTe$-Sb_2Te_3 are considered to be perspective for PCM application, and most promising among them is $Ge_2Sb_2Te_5$ (GST225). One of the problems of the PCM technology is connected with the necessity of decreasing the data processing time (write time is 100 ns [1]) to the level comparable with that of the Random Access Memory (~10-50 ns [2]).

Concept of PCM is based on rapid reversible amorphous-to-crystalline phase-change processes. Crystallization kinetics is sufficiently at least on the order of magnitude slower than formation of amorphous state [2]. So, crystallization process determines the data processing rate of the PCM cell which strongly motivates investigation of the mechanism and kinetics of crystallization. The main purpose of this study was to investigate the thermal properties, mechanism and kinetics of crystallization for GST225 thin films.

GST225 thin films were prepared by thermal evaporation of synthesized material. The pressure in the chamber during the deposition was 10^{-4} Pa, and the substrate temperature does not exceed 50°C. The structures of synthesized materials and thin films were investigated by XRD. The composition of thin films was determined by Rutherford Backscattering Spectroscopy (RBS) and Energy Dispersive X-Ray Analysis (EDXRA). Atomic force microscope (NT-MDT SolverPro) was used for the investigation of the characteristic features of the film morphology. Differential scanning calorimetry (DSC-50, Shimadzu) at 8 different heating rates in the range of 5 - 90°C/min was used to examine thermal properties and thermally induced transformations.

To determine kinetic triplet for crystallization process of GST thin films we proposed method which is based on joint use of model-free and model-fitting methods [3]. This allowed us to estimate activation energy and pre-exponential factor as the functions of conversion, and determine reaction model.

According to RBS and EDXRA thin films have composition of $Ge_2Sb_2Te_5$ with accuracy of ± 5%. XRD study showed that the synthesized materials had a trigonal structure, while as-deposited films were amorphous. A number of heat effects was revealed for as-deposited films by DSC. Exopeak in the range 130-190 °C is due to the crystallization of amorphous phase.

The iso-conversional model-free method of Ozawa-Flynn-Wall [4,5] was used to determine the dependence of effective activation energy on conversion. It was found that effective activation energy gradually decreases with the increase of conversion (Fig. 1). This result indicates that crystallization of GST225 film is a complex process consisting of two parallel processes - nucleation and crystalline growth. Contribution of the first process gradually decreases, while of the second increases. In this case, activation energy at the initial moment corresponds to the activation energy of nucleation, while in the end - to the activation energy of crystalline growth. The use of Coats - Redfern approach [6] showed that the most probable models describing crystallization process are the second and third order reaction models. Determined kinetic triplet was used for the estimation of possible data processing and storage times of the PCM cell. It was found that GST225 films can provide the data processing time of the PCM cell about nanoseconds (Fig. 2).

According to AFM as-deposited films have island-like structure, however mean height of the islands does not exceed 1 nm. Crystallization of the thin film at 150°C is accompanied by the increase of mean height nearly on the order of magnitude. We suppose that island-like structure promote nucleation on the film surface.

Thus, in this study thermal properties, mechanism and kinetics of crystallization for GST225 films were investigated. The model of GST film crystallization is proposed. Obtained kinetic parameters for GST225 films allowed predicting data processing and storage times of the PCM cell. It was found that GST225 thin film can provide the data processing time of the PCM cell about nanoseconds.

This study was supported by Ministry of Education and Science of RF (project ID: RFMEFI57814X0085).

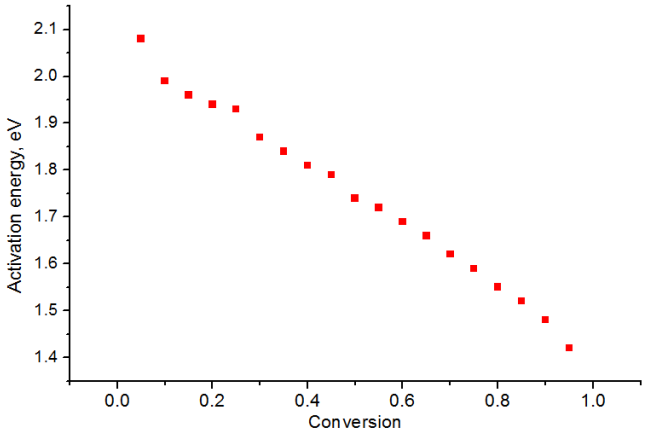

Fig. 1. Effective activation energy of crystallization for GST225 thin film

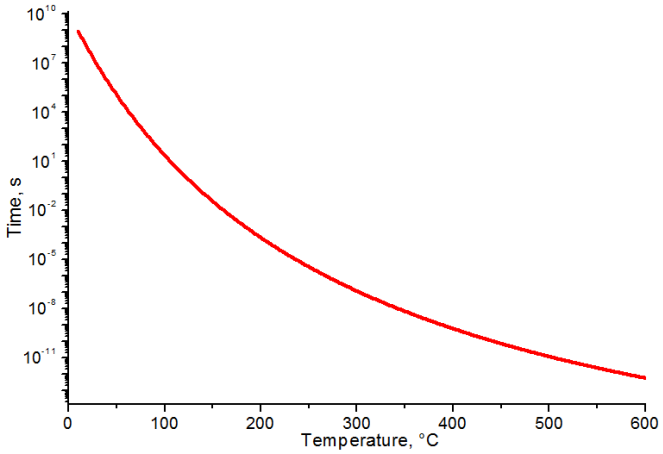

Fig. 2. Temperature dependence of crystallization times for GST225 film

[1] Kryder M.H., Kim C.S. IEEE Transactions on magnetics. 2009, 45(10), pp.3406-3413.
[2] Burr G.W., Breitwisch M.J., Franceschini M., Garetto D., and et al. Journal of Vacuum Science and Technology B. 2010, 28(2), pp.223-262.
[3] Sherchenkov A., Kozyukhin S., Babich A. J. Therm. Anal. Calorim. 2014, 117(3), pp. 1509-1516.
[4] Flynn J.H., Wall L.A. Polym. Lett. 1966, 4, pp. 323-328.
[5] Ozawa T. Bull. Chem. Soc. Jpn. 1965, 38(11), pp. 1881-1886.
[6] Coats A.W., Redfern J.P. Nature. 1964, 201, pp.68-69.

ID 146 - Poster

X-ray Photoelectron Spectroscopy Studies on Cubic Silicon Carbide Thin Films Prepared by HWCVD

*H. Jha[1], A. Yadav[2], M. Singh[1], S. Kumar[3], P. Agarwal[1]
[1]Indian Institute of Technology Guwahati, Department of Physics, Guwahati, India
[2]IIT Guwahati, Center for Energy, Guwahati, India
[3]RRCAT, Indus Synchrotron Utilization Division, Indore, India

Cubic Silicon Carbide (3C-SiC) is a promising material for various optoelectronic and electronic devices, due to its unique physical and chemical properties, such as high breakdown field, high thermal conductivity, high saturated drift velocity and chemical inertness for most of the chemicals. However, preparation of device quality stoichiometric thin film of 3C-SiCat low substrate temperature is challenging task. In recent years, hot wire chemical vapour deposition (HWCVD) technique has emerged as a promising technique to deposit SiC thin films at relatively low substrate temperature. This technique has several advantages like high gas-decomposition efficiency, large area fabrication, high deposition rate etc. over other conventional chemical vapour deposition techniques. However, the chemical composition and bonding states of deposited 3C-SiC films are strongly dependent on the different process parameters used for deposition. X-ray photoelectron spectroscopy (XPS) is most reliable technique for the determination of elemental chemical composition and bonding (electronic) states at thin film surface. In this paper, we report the studies on compositional and electronic states properties of 3C-SiC films using XPS. A series of 3C-SiC films are deposited on corning 1737 glass substrate in a load lock based HWCVD chamber. Hydrogen diluted Silane (SiH_4, 10% in H_2) and Methane (CH_4) was used as precursor gases. All the deposition parameters such as substrate temperature, Silane flow rate, Methane flow rate and filament temperature were kept constant at 350 °C, 20 SCCM, 2 SCCM and 1900 °C respectively, while process pressure were varied from 2-5 mbar. The films were initially characterized by XRD and Raman scattering to find out the microstructural nature of films. After that angle integrated XPS experimental station with MgKα (1256.3 eV) x-ray source were used to record the XPS spectra. The measurements were done on samples stored in ambient conditions for couple of months and before scan, the top surface of the samples was etched by sputtering with 1KV Ar+ ions for 15 minutes. All the 3C-SiC films have similar wide and narrow scan XPS spectra as shown in Figure 1. The peaks present in the spectra are the signature of different binding energy (BE) states of elements of Si (2p), Si (2s), C (1s), O (1s) and O (KLL) at ~ 100, 150, 285, 532 and 740 eV respectively. However, no trace of any contamination of filament material (Tungsten (W)) is observed in these films as the peak near 245 eV corresponding to W $4d_{5/2}$ state is absent. The presence of O (1s) peak (532eV) in all the films is possibly due to residual oxygen in the growth chamber. To find out exact quantitative estimation of all the elements present in the films, the narrow scan spectrum was deconvoluted into several different components (peaks) assuming that each peak consist of Gaussian/Lorentzian sum function. All the narrow scan spectra of 3C-SiC films are fitted with Gaussian/Lorentzian sum functions after removing background by the Shirley subtraction method. The Si_{2p} spectrum near ~100 eV was deconvoluted into two components (peak) corresponding to BE of Si-C and O-Si-C at ~100.3 and ~101.8 eV respectively as shown in Figure 2. Similarly, the C_{1s}spectrum is deconvoluted into two peaks corresponding to BE of C-Si and C-C/C-H at 282.9 and 284.6 eV respectively. The XPS analyses confirm that the films deposited ≤ 3 mbar of chamber pressure are nearly stoichiometry with almost equal share of silicon and carbon with significant amount of oxygen. However, as process pressure increases above 3 mbar, 3C-SiC films become carbon rich. More detailed results will be presented during conference. The work reported here is supported by BRFST, India.

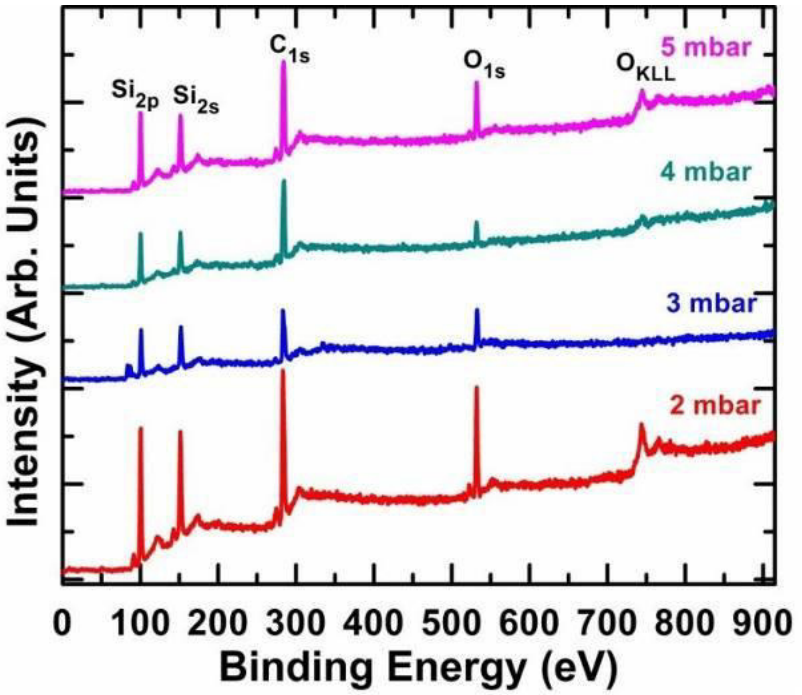

Figure 1: XPS wide scan spectra of 3C-SiC films deposited at process pressureof 2- 5 mbar.

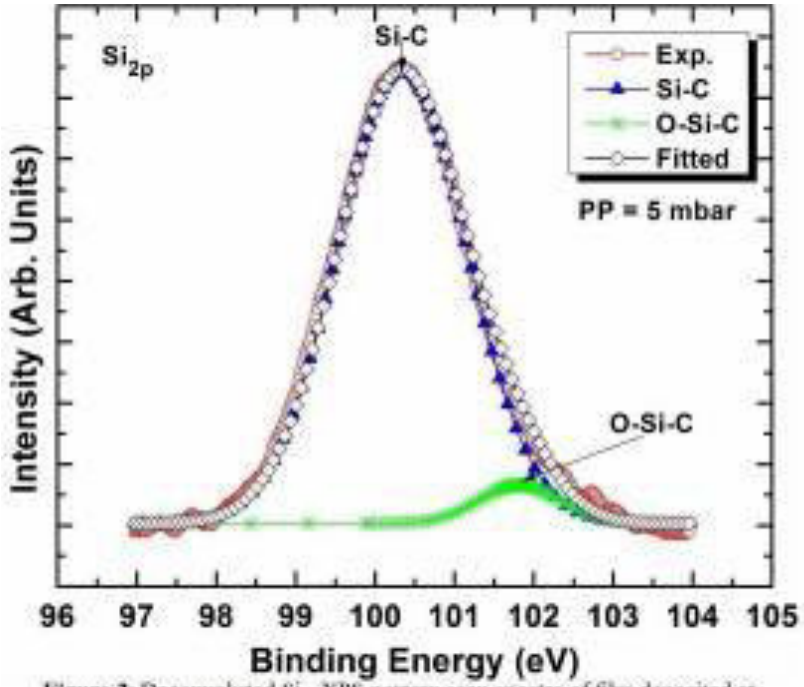

Figure 2: Deconvoluted Si_{2p} XPS narrow-scan spectra of film deposited at process pressure (PP) of 5 mbar

ID 147 - Oral

The effects of air exposure and water treatment on the minority carrier diffusion lengths and sub-bandgap absorption in highly crystalline microcrystalline silicon thin films

*M. Günes[1], G. YILMAZ[1], V. SMIRNOV[2], F. FINGER[2], R. Brüggemann[3]
[1]Mugla Sitki Kocman University, Physics, Mugla, Turkey
[2]Forschungszentrum Juelich, IEK-5, Juelich, Germany
[3]Carl von Ossietzky University of Oldenburg, Physics, Oldenburg, Germany

Highly crystalline thick (> 1 µm) microcrystalline silicon films having slightly n-type conductivity with Fermi level position 0.24 - 0.34 eV from the conduction band edge were deposited by VHF-PECVD on rough glass substrates at 200 °C. Using rough glass substrates allows us to investigate samples of up to 1500 nm thickness which would otherwise peel off from the substrate after the various treatment steps. Temperature dependent dark conductivity, σ_{dark}, steady-state photoconductivity(SSPC), σ_{ph}, steady-state photocarrier grating (SSPG), and dual beam photoconductivity (DBP) methods were used to detect the reversible and irreversible changes created by long term exposure to (a) room ambient and (b) to five hours de-ionised (DI) water at 353K. Standard measurement procedures [1] were carefully applied for reliable characterization of metastable changes at room temperature and in high vacuum. SSPC and SSPG measurements were performed using He-Ne laser light with different intensities. DBP measurements were carried out using ac monochromatic light with energy between 0.6 eV and 2.2 eV and a dc bias light with different intensity [1]. Ag parallel electrodes were evaporated on the sample with 0.05 cm width and 0.5 cm length and a dc voltage in the Ohmic region was applied between the electrodes during the measurements. Probe measurements were performed at 300K and in high vacuum with pressure of 1-2x10^{-6} mbar.

The samples were first characterized after one and a half year exposure to room ambient and then annealed at 430 K to remove the metastability effects. It was found that σ_{dark} (300K) increased by more than two orders of magnitude while σ_{ph} increased within a factor of 2 to 4 after the annealing process. The sub-bandgap absorption coefficient at 0.9 eV increased by a factor 2, indicating an increase in the density of occupied defect states below the dark Fermi level, which is also accompanied with the reduction in the minority carrier diffusion length, L_D, by approximately 50 nm after the annealing. As a method of an accelerated creation of the metastable state or permanent degradation, annealed samples were exposed to DI water. Then, samples were cooled to 300K and placed in high vacuum cryostat. Time dependent dark conductivity at 300K was monitored in vacuum as previously described [1] until it reached to a constant value before applying the measurements under light described above. After the DI-water treatment; there was no significant change in σ_{dark}(300K) of the samples from that of annealed state. However, σ_{ph} increased more than one order of magnitude from the annealed state value measured before the treatment and the relative sub-bandgap absorption coefficient at 0.9 eV decreased by the same factor, indicating a significant decrease in the density of occupied bulk defect states located below the Fermi level. In addition, the minority carrier diffusion length, L_D, improved significantly between 50 nm to 150 nm. After the annealing of DI water treated samples at 430K, such changes caused by the DI water treatment were found to be irreversible since no significant changes were detected in the measured parameters of the samples.

We investigated two types of effects: (a) long term exposure to ambient air which is reversible and accompanied with an increase in the absorption coefficient and reduction in L_D after annealing and (b) DI water treatment which is irreversible upon annealing and decreases absorption coefficient and increases L_D. The differences in behavior are discussed in terms of the effects of band banding and relative changes in the Fermi level position and defect distributions.

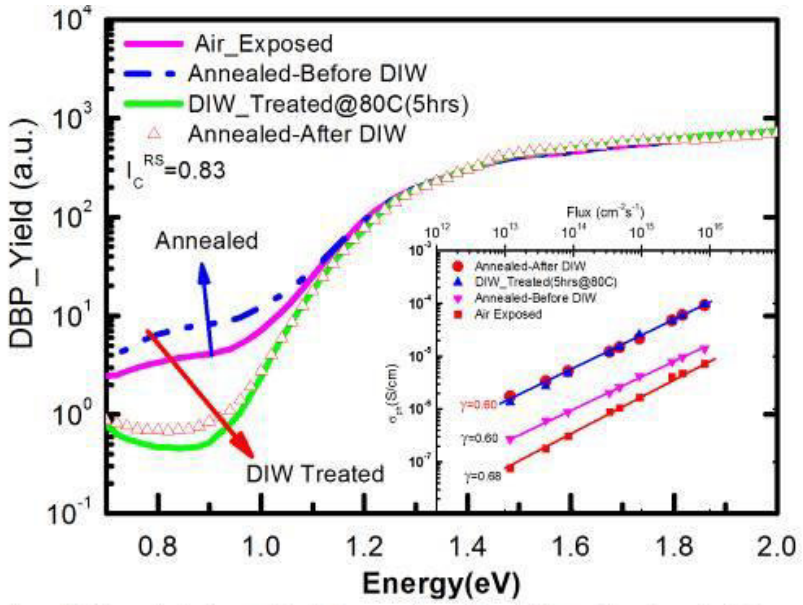

Caption: DBP and photoconductivity spectra after different treatments (Gunes et al.)

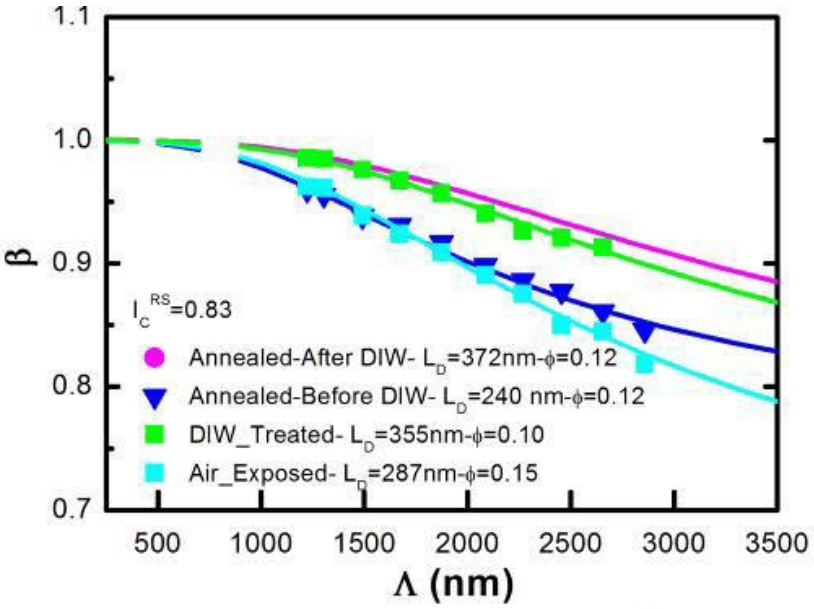

Caption: SSPG evaluation and determination of the diffusion length L_D(Gunes et al.)

1. M. Günes, H. Cansever, G. Yilmaz, H.M. Sagban, V. Smirnov, F. Finger, R. Brüggemann, Canadian Journal of Phys. 92: 768-773 (2014), dx.doi.org/10.1139/cjp-2013-0630.

ID 148 - Poster

Energy Band Structure of Co Heavily Doped Silicon

*Y. Zhou[1], F. Liu[1], M. Zhu[1]
[1]University of Chinese Academy of Sciences, Beijing, China

Introducing an intermediate band (IB) in the forbidden band gap of a semiconductor has been proposed as a means of fabricating high efficiency solar cells and infrared detectors. Solar cells with optimized band gap and intermediate band present efficiencies of up to 63.3% in ideal conditions. Heavily doping of deep level impurities into a semiconductor has been recognized as one approach to achieve the IB material.

In this paper, Co supersaturated Si samples were prepared by ion implantation and pulse laser melting (PLM). HRTEM measurements indicate that no Co clusters can be observed in the PLM treated Co implanted Si layer. X-ray absorption spectroscopy shows that Co is neither agglomerated nor oxidized. Photoelectron spectroscopy shows that the Co highly doped Si samples transit from semiconductor to metal with the increase of the Co concentration. X-ray emission and absorption spectroscopy indicate that high Co doping results in a slightly shift of the valence band edge and the appearance of energy states in the band gap. And, it is difficult to determine the energy band gap now. The energy band structure obtained from the first principle calculation is consistent with the experimental observations.

ID 149 - Oral

Thickness of amorphous silicon thin films for heterojunction solar cells measured by Raman spectroscopy on textured silicon wafers

**M. Ledinsky[1], Z. Hájková[1], A. Vetushka[1], A. Tomasi[2], B. Paviet-Salomon[2], S. De Wolf [2], C. Ballif[2], A. Fejfar[1]*
[1]Institute of Physics CAS, Thin films and nanostructures, Prague, Switzerland
[2]Ecole Polytechnique Fédérale de Lausanne (EPFL), Photovoltaics and Thin Film Electronics Laboratory, Neuchatel, Switzerland

Due to the high passivation quality of hydrogenated amorphous silicon (a-Si:H) layers, crystalline silicon (c-Si) heterojunction (SHJ) solar cells have already reached very high conversion efficiencies in the last years [1]. Optimization of the back-contacted solar cell concept by Panasonic, Japan [2], led to the current world record conversion efficiency for silicon based solar cells of 25.6 %.

The actual processing of back-contacted SHJ devices requires to accurately pattern the electron- and hole-collecting regions at the rear of the device into two interdigitated combs, made out of p- and n-type a-Si:H. The individual fingers of these combs have typical width of 1 mm or less. In an earlier work, we reported on the patterning of such p- and n-type a-Si:H interdigitated fingers through in situ shadow masking in the PECVD reactor [3]. The thickness of the amorphous doped combs depends among others on mask dimensions. But even if this thickness and overall shape of the combs are important for final cell performances like V_{OC} and FF [3]; there is no easy way how to measure them. Spectroscopic ellipsometry, used to determine a-Si:H thickness on rough substrates, lacks the needed spatial resolution. Scanning electron microscopy on sample cross-section may be used for this purpose, but it is highly time-consuming and impractical. Therefore we propose to use a novel approach based on Raman micro-spectroscopy.

Raman spectroscopy is a widely used method for characterization of silicon thin films. Broad Raman band at 480 cm^{-1}, signature of the a-Si:H structure, may be used for evaluation of amorphous silicon quantity. But due to the sharp Raman c-Si related band at 520 cm^{-1}, the amorphous signal from ~10 nm thick films is hard to detect. Therefore we calculate the a-Si:H film thickness from decreasing absolute intensity [4] of c-Si Raman band. The decrease is caused by the absorption of the excitation laser and the back-scattered c-Si Raman signal in the upper lying a-Si:H film. In order to increase the sensitivity of this technique we used 442 nm excitation laser which is highly absorbed in a-Si:H. In this case the detection limit of this method is well below 1 nm (see Fig. 1) and its spatial resolution is limited by the optical resolution of the used optical set-up (down to 500 nm). Raman absorption based method for evaluation of extremely small thicknesses of a-Si:H films was tested on shadow mask-patterned a-Si:H fingers deposited on both rough and flat c-Si wafers, for use in back-contacted SHJ solar cells [3]. For flat wafers we could compare the Raman based thickness with profilometer or SEM measurements and we found an extremely good correlation.

Raman absorption based measurement method is not restricted to the SHJ samples but it may be used for all thin absorbing films prepared on a Raman active substrate.

This work was partly funded by the projects of the Czech Science Foundation (14-15357S) and Ministry of Education, Youth and Sports of the Czech Republic (LM2011026).

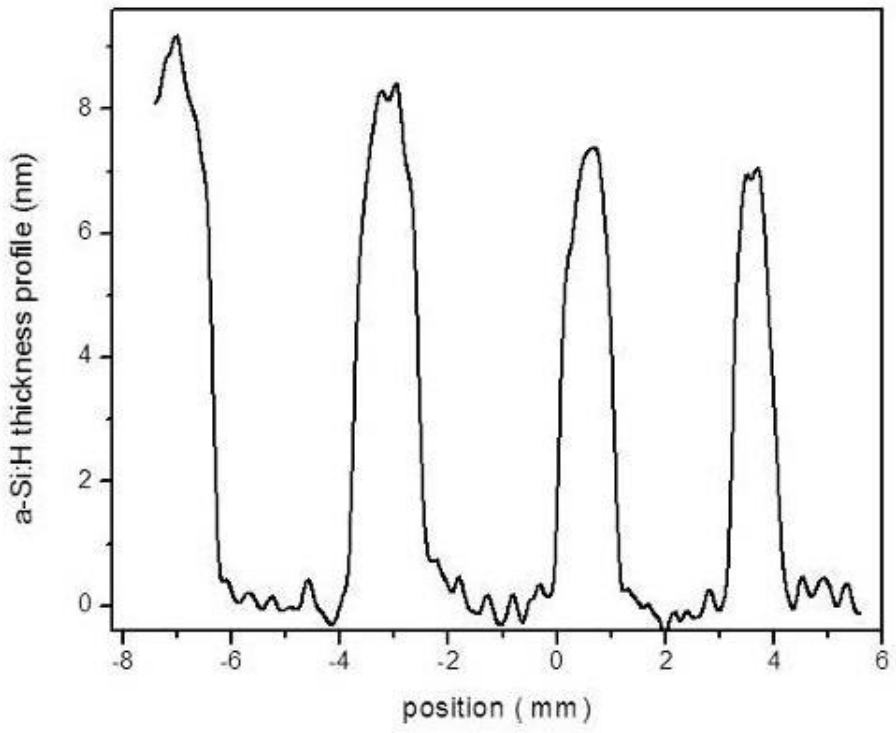

Thickness profile of four a-Si:H fingers on c-Si substrate proves high sensitivity of the proposed Raman absorption based technique. Thickness of the a-Si:H layer decreases with decreasing fingers width.

[1] M. Taguchi, A. Yano, S. Tohoda, K. Matsuyama, Y. Nakamura, T. Nishiwaki, K. Fujita, and E. Maruyama, "24.7% Record Efficiency HIT Solar Cell on Thin Silicon Wafer", IEEE Journal of Photovoltaics, 4, 2014, 96-99.
[2] K. Masuko, M. Shigematsu, T. Hashiguchi, D. Fujishima, M. Kai, N. Yoshimura, T. Yamaguchi, Y. Ichihashi, T. Mishima, N. Matsubara, T. Yamanishi, T. Takahama, M. Taguchi, E. Maruyama, and S. Okamoto, "Achievement of More Than 25% Conversion Efficiency With Crystalline Silicon Heterojunction Solar Cell", IEEE Journal of Photovoltaics, 4, 2014, 1433-1435.
[3] A. Tomasi, B. Paviet-Salomon, D. Lachenal, S. Martin De Nicolas, M. Ledinsky, A. Descoeudres, S. Nicolay, S. De Wolf, and C. Ballif, "Photolithography-free interdigitated back-contacted silicon heterojunction solar cells with efficiency >21%" in *Photovoltaic Specialist Conference (PVSC), IEEE 40th*, 2014, 3644-3648.
[4] M. Ledinský, E. Moulin, G. Bugnon, K. Ganzerová, A. Vetushka, F. Meillaud, A. Fejfar, and C. Ballif, "Light trapping in thin-film solar cells measured by Raman spectroscopy", Applied Physics Letters, 105, 2014.

ID 150 - Poster

Evidence for four different midgap defect distributions in hydrogenated amorphous silicon thin films obtained from the dual beam photoconductivity method

*M. Günes[1], J. Melskens[2], Y. Mohammadian[2], A. H. M. Smets[2], C. R. Wronski[3]
[1]Mugla Sitki Kocman University, Physics, Mugla, Turkey
[2]Delft Technology of University, Delft, Netherlands
[3]Pennsylvania State University, University Park, PA, United States

Although extensive research has been carried out on the Staebler-Wronski effect [1] for the last four decades, there is still no well-defined picture of the defects in the bandgap of hydrogenated amorphous silicon (a-Si:H). In this study, high-quality undoped hydrogenated amorphous silicon thin films were studied using steady-state photoconductivity (SSPC), steady-state photocarrier grating (SSPG), dual beam photoconductivity (DBP) and optical transmission methods in the light soaked and annealed states. Light soaking was carried out under AM1.5 white light illumination and annealing was performed at 410 K for several hours. SSPC and SSPG measurements were done using He-Ne laser light under diffferent intensities. DBP measurements were carried out using different dc bias light intensities and simultenously measured optical transmission spectrum was obtained from the back of samples using a pyroelectric detector. The absolute absorption coefficient spectrum, $a(hn)$, was calculated from the raw DBP and optical transmission spectra using the Ritter-Weiser optical equations [2]. All measurements were performed in a high vacuum cryostat at a pressure of $2\text{-}3\text{x}10^{-6}$ mbar and a dc voltage in the Ohmic region was applied between coplanar aluminum contacts that are deposited on the a-Si:H film, which in turn was deposited by PECVD using a hydrogen-to-silane gas flow rate ratio fo 10 at low power and low pressure.

The derivative of the subgap absorption coefficient, $\mathrm{d}(a(hn))/\mathrm{d}E$, was taken to calculate the relative densities of electron occupied gap states, $kN_{gap}(hn) = (hn)(\mathrm{d}(a(hn))/\mathrm{d}E) + a(hn)$, and the occupied valence band tail states were subtracted. The resulting electron occupied midgap states were deconvoluted into four different Gaussian distributions with well-defined energy positions. It was found that the peak energy positions of these Gaussian distributions labelled as C, B, A, and X states following previously defined nomenclature [3,4] were at the photon energies of 1.24 eV, 1.11 eV, 0.90 eV and 0.77 eV , respectively. The peak energy positions of these Gaussian distributions are consistent with the results recently obtained from FTPS measurements [3]. There is no significant change in the peak energy positions of these defect states in the light soaked state. However, their relative densities increase in different amounts, where the densities of C and B states increase twice as much as the A states. The density of X states located in the middle of the bandgap was the lowest in the annealed state, however the relative increase in its density was found to be the highest after light soaking. In addition, the change in the occupation of each Gaussian distribution was controlled by increasing the intensity of the dc bias light in the DBP measurement as the quasi Fermi levels move towards the band edges. It was found that the density of occupied C states was almost unchanged even at the highest dc bias light used for DBP measurements. However, occupied density of A states increases substantially and that of B states drastically decreases and even become completely unoccupied in the soaked state under the highest dc bias light condition. The occupation of X states in the soaked state increases in the same way as the A states, however, there is almost no change in its occupation in the annealed state for the highest dc bias light intensity. The corresponding steady-state photoconductivity, s_{photo}, and minority carrier diffusion length, L_D, obtained from the SSPG measurement change consistently, where s_{photo} decreased by a factor 20 and L_D decreased from 211 nm to 148 nm after light soaking.

[1] D.L. Staebler and C.R. Wronski, Appl. Phys. Lett. **31**, 292 (1977).
[2] D. Ritter and K. Weiser, Opt Commun. 57, 336 (1986).
[3] J. Melskens et al. Solar Energy Materials and Solar Cells, vol. 129, p.7081 (2014).
[4] L. Jiao and C. R. Wronski, Mat. Res. Soc. Symp. Vol. 1066, p.A04-05 (2008).

ID 151 - Poster

Adapting Characterization Techniques for High Voc Thin-Film Tandem Solar Cells

*F. Ventosinos[1], B. Fakes[1], E. V. Johnson[1]
[1]LPICM, Palaiseau, France

To compete with the market standard of low-cost per Watt crystalline silicon solar cells, thin-film silicon devices must display a great leap forward in their power conversion efficiency. Multijunction devices - from the micromorph concept up to three and four junction devices - have proven to be able to reach higher efficiencies, meaning that characterization techniques for these complex structures are needed to fully understand and optimize them. In this work we focus on two techniques developed to extract the individual open circuit voltages (V_{oc}) of tandem devices, as well as their sub-cell current voltage (IV) characteristics. These were developed to work on the micromorph cell, the subcells of which have limited regions of overlapping photoresponse due to very different band gaps. However, it is not known if such techniques will work in tandem structures consisting of very high V_{oc} structures, such as device stacks using amorphous silicon oxide/polymorphous silicon (a-SiO:H/pmSi:H), and hydrogenated amorphous silicon(a-Si:H)/ pm-Si. These novel structures have proven to suffer from less light induced degradation (LID), which is one of the main drawbacks of devices using a-Si:H. The presence of similar band gaps (difference below 150mV in both cases) and overlapping external quantum efficiencies (EQEs) above 500nm implies that some changes have to be done in order to make these characterization techniques work.

A V_{oc} separation technique, proposed by Holovsky et al, uses two different light sources to make a mapping of the total voltage developed while using different light intensities. A mathematical procedure allows access to the individual voltage curves, from where V_{oc} may be recovered. As also developed by Holovsky et al, an IV separation technique uses the response of individual subcells to fix the working voltage of one of the subcells at its V_{oc} by the use of a selective illumination, and thus by measuring an IV curve by setting the current and recording the developed voltage of the whole tandem structure, one obtains information about the unfixed subcell. Both techniques exploit the non-overlapping EQE to induce a fixed voltage or current in only one of the subcells. For high V_{oc} devices made with a-SiO:H/pm-Si:H and a-Si:H/pm-Si:H, there is only one region with non-overlapping EQE, so both techniques must be adapted to rely mostly on one light source**.** Also the presence of small series resistance (R_s) complicates the use of the IV separation technique, (for which R_s=0 is typically assumed).
The IV separation technique was applied to a-SiO:H/pm-Si:H and a-Si:H/pm-Si:H tandems by assuming the individual V_{oc} of subcells. A numerical technique was used to extract both curves through the use of a blue laser (400nm) alone. Samples with low R_s presented reliable results, but the presence of higher R_s leads to errors. To improve the procedure, we will include R_s in the formulas that are used in this technique. An accurate measure of the V_{oc} of subcells is also needed. A procedure will be shown to adapt the technique to the occurrence of only one non-overlapping region of the EQE.
Characterization techniques for obtaining information about individual subcells in tandem structures are important to achieve better optimizations and more insight of the material properties. In this presentation we present how to adapt two of these techniques to be used in high V_{oc} tandem structures such as a-SiO:H/pm-Si:H and a-Si:H/pm-Si:H.

ID 152 - Oral

New insights into the modulated photocurrent technique using 2D full numerical simulations

*R. Lachaume[1], C. Longeaud[1], J.- P. Kleider[1]
[1]GeePs | Group of electrical engineering - Paris, UMR CNRS 8507, CentraleSupelec, Univ Paris-Sud, Sorbonne Universités, UPMC Univ Paris 06, F91192, Gif sur Yvette CEDEX, France

The modulated photocurrent (MPC) technique has proved to be a powerful tool to investigate the density of localized states (DOS) in the bandgap of disordered semiconductor thin films. In previous works two regimes were identified: the high frequency (HF) regime where the MPC is determined by the trapping and release of carriers producing a significant phase shift of the MPC relative to the excitation, and the low frequency regime (LF) where the MPC is determined by the recombination of carriers with a very low phase shift [1]. Each regime was analysed in order to describe the phase shift and amplitude of the MPC and to reconstruct the DOS from the frequency and temperature dependence of these quantities [2]. However, these analyses relied on a simplified analytical treatment of the transport equations. In particular, it was assumed that all physical quantities under light (like the generation rate, the free carrier concentrations, etc.) were homogeneous within an effective depth related to the light absorption. This means that the true profiles of generation rate, carrier densities were not considered.

We here present for the first time the full calculation of the MPC without any simplifying assumption using 2D numerical simulations. This calculation is compared to the previous analyses of the MPC. Particular emphasis is put on the transition between the HF and LF regimes and on the DOS reconstruction in both regimes.

It is demonstrated that the reconstruction in the HF regime works very well. However very strong errors can occur in the transition between the HF and BF regimes and in the reconstruction of the DOS from the LF regime. Our simulation results also nicely explain the previously observation that the dependence of the reconstructed DOS upon the dc light flux was weaker than predicted by the simplified analytical approach. We show that the approximate analytical approach underestimates the phase shift values in the LF regime (Figure 1). This discrepancy increases with ad (a being the absorption coefficient and d the sample thickness) and can yield to errors of more than a factor of 10 in the DOS reconstructed from the LF formulas (Figure 2). This is interpreted by the contribution to the MPC originating from regions in the sample that are deeper than 1/ a from the illuminated surface and that are not working in the recombination regime, thus adding a non negligible contribution to the phase shift.

In conclusion, this work is an original extension of the MPC analysis. It brings new insights into the physics of the modulated photocurrent allowing one to avoid misinterpretations of experimental data such as overestimated reconstructed DOS values.

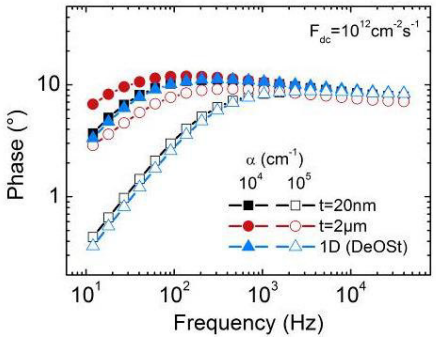

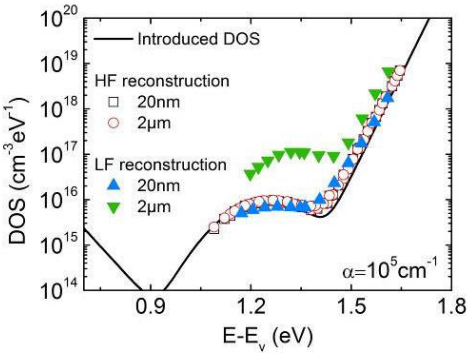

[1] C. Longeaud and J.-P. Kleider, Phys. Rev. B 45 (1992) 11672.
[2] M.-E. Gueunier, C. Longeaud and J.-P. Kleider, Eur. Phys. J. Appl. Phys. 26 (2004) 75.

ID 153 - Poster

Paramagnetic States in Amorphous, Polymorphous and Nanocrystalline Silicon

**E. Konstantinova[1,2], A. Emelyanov [2], P. Kashkarov[1,2]*
[1]M.V. Lomonosov Moscow State University, Physics , Moscow, Russian Federation
[2]Russian Research center "Kurchatov Institute", Moscow, Russian Federation

Recent investigations indicate that Si based materials such as hydrogenated amorphous (a-Si:H), polymorphous (pm-Si:H) and nanocrystalline (nc-Si) silicon are promising in microelectronics, solar energy field and biomedicine [1,2]. Paramagnetic states are defects in the structure of a-Si:H, pm-Si:H, nc-Si limiting their electrical transport and as a rule a photoluminescence. Therefore it is very important to know their nature and concentration in order to estimate the prospects of application of these materials in the field of solar energy and biomedicine. It is also interesting to compare how the structure of samples influences on the properties of their defects.

All details of the sample preparation were published in [3,4]. EPR spectra were detected by the standard Bruker EPR spectrometer ELEXSYS-500 (X-band, sensitivity is around ~10^{10} spin/G). The measurements were made at 300 K. The samples were illuminated in situ with a 100 W tungsten lamp.

EPR signal observed in a-Si:H has g = 2.0055 and concentration is about 10^{15} cm^{-3}. It is due to Si dangling bonds according literature data [1]. Paramagnetic states in pm-Si:H can be attributed to the electrons trapped in the states in the conduction band tail of the system of Si nanocrystals (g_1=1.9980, g_2=1.9885, g_3=1.9790). It is not possible to exclude the presence of Si dangling bonds in these samples. Probably they have a negligibly small amount in comparison with the concentration of trapped electrons reaching values ~ 10^{19} cm^{-3}. Thus it has been shown that the introduction of a small fraction of nanocrystals into the amorphous silicon films nonadditively changes the electronic properties of the material. The parameters (g_{per}= 2.0082, g_{par}=2.0024) of the observed EPR signal in nc-Si samples are characteristic of so-called P_b centers, which are the dangling bonds of silicon at the Si/SiO_2 interface [2]. Their concentration was about 10^{17} cm^{-3}. In vacuum we have detected a saturation effect of microwave absorption but only for nc-Si samples. Furthermore, absorption of microwave radiation by P_b centers was saturated also in air under illumination. «Strange» behavior of defects in nc-Si can be explained by their interaction with paramagnetic oxygen molecules (dipole-dipole mechanism of interaction) adsorbed on a sample surface. Under illumination a transition of triplet oxygen (ground state) in excited singlet state takes place. Therefore a concentration of paramagnetic oxygen decreased at the nc-Si surface. In turn, this caused an increase in the relaxation time of P_b centers, as a result of this, the EPR signal amplitude decreased (the saturation effect). Therefore, properties of defects are very sensitive to the structure of the samples, i.e. amorphous, polymorphous and nanocrystalline silicon.

Acknowledgement: This work was supported by the Ministry of Education and Science of the Russian Federation (no 14.604.21.0085; Identification number RFMEFI60414X0085).

[1] Stegner A.R., Pereira R.N., K.Klein, Physica B. 401-402, 541 (2007).
[2] O. Bisi, S. Ossicini, L. Pavesi, Surf. Sci. Rep. 38, 1 (2000).
[3] A. V. Emelyanov, E. A. Konstantinova, P. A. Forsh, A. G. Kazanskii, E. I. Terukov, N. A. Bert, S. G. Konnikov, P. K. Kashkarov, JETP Letter. 97, 8, 466 (2013).
[4] E. A. Konstantinova, V. A. Demin, V. Yu. Timoshenko, and P. K. Kashkarov, JETP Letters. 85, 1, 59 (2007).

ID 154 - Oral

FDTD simulation of a-Si:H ring resonator

**A. Fantoni[1,2], P. Pinho[1], J. M. Ferreira[1], P. Louro[1,2], M. Vieira[1,2,3]*
[1]ISEL, Instituto Superior de Engenharia de Lisboa, ADEETC, Lisbon, Portugal
[2]UNINOVA-CTS, Caparica, Portugal
[3]FCT-UNL, DEE, Caparica, Portugal

Silicon photonics is a very promising technology for the next future photonic integration platform, mainly because of the possibility of producing high index contrast waveguide structures and the possibility of taking profit from the well established CMOS fabrication technology, allowing a good integration in a single chip between photonic and the electronic components [[i]]. For these applications it is necessary to develop novel, highly integrated and CMOS compatible devices and, among other devices, micro-ring resonators have been found to be a very flexible structure that has been used in optical filtering, add-drop, multiplexing, dispersion compensation and bio-sensing applications[[ii]]. Hydrogenated amorphous silicon (a-Si:H) can be deposited at CMOS-compatible low temperature using PECVD technique, and could be considered as a promising candidate to enable an easy back-end integration with standard microelectronics processes. Within this application context a few examples of passive waveguides structures and ring resonator structure based on a-Si:H have been demonstrated during the recent years.[[iii],[iv]]

In this work we present an analysis based on simulation obtained with the Finite Difference Time Domain (FDTD) method. This method solves the Maxwell equation following an iterative scheme in space and time without any major physical approximation. The dispersive properties of a-Si:H are described by following the a double Lorentz model (LL model) for the electrical permittivity [[v]]. The subject of our analysis is the simulation of an a-Si:H ring resonator deposited onto a SiO_2 substrate. The configuration of this simulation domain reproduces the possible fabrication of a photonic layer on top of an electronic microchip, following the CMOS process and before the encapsulation. The photonic structure is studied in the simple notch filter configuration and as an add-drop device for wavelengths in the near infrared region.
According to our model, the refraction index of a-Si:H varies between 3 and 4 at the wavelength of 1550 nm, depending on the material properties, while the refraction index of the SiO_2 substrate is about 1.5, ensuring a good vertical optical confinement. The waveguide properties are analyzed in term of light confinement and dispersion. It is reported a spectral analysis aimed to relate light wavelength, curvature radius and material properties. Special attention is given to the standard telecom wavelengths windows of 850, 1300 and 1500 nm and to the possibility of implementing a WDM multiplexing scheme. The rings configuration has been chosen as close as possible to the real dimension that should be requested in real photonic chips. Waveguide width varies between 0.3 and 0.7 mm, while the ring radius is in the range of 2-5 mm. The coupling distance between the straight waveguide and the ring structure is also evaluated in term of coupling efficiency, power dispersion and wavelength filtering properties. This study represents a preliminary step toward the realization of a-Si:H photonic structures by means of PECVD deposition onto SiO_2 substrates.

[i] Bahram Jalali and Sasan Fathpour, *Silicon Photonics*, Jo. of Lightwave Tech., vol. 24, no. 12(2006)
[ii] D.G. Rabus, *Integrated Ring Resonators*, Springer-Verlag Berlin Heidelberg (2007)
[iii] S.Rao; C. D'addio, F.G.. Della corte, *All-optical modulation in a CMOS-compatible amorphous silicon-based device*, Journal of the European Optical Society - Rapid publications, Europe, v. 7, jun. (2012)
[iv] Zhang, Z. et al., *High-quality-factor micro-ring resonator in amorphous-silicon on insulator structure*, ECIO'08 Eindhoven - Proceedings of the 14th European Conference on Integrated Optics and Technical Exhibition, Contributed and Invited Papers, 329-332 (2008).
[v] Fantoni, Alessandro, and Pedro Pinho. "*FDTD simulation of light propagation inside a-si: H structures.*" MRS Proceedings. Vol. 1245. Cambridge University Press, 2010.

ID 155 - Oral

Electrical and optical properties of long-throw magnetron sputtered Zinc oxynitride thin films

*A. Reinhardt[1], H. Frenzel[1], H. von Wenckstern[1], M. Grundmann[1]
[1]Universität Leipzig, Leipzig, Germany

Amorphous oxide semiconductors (AOS) such as amorphous In-Ga-Zn-O (a-IGZO) have attracted much attention as channel material for thin-film transistors due to their comparatively large electron mobility (> 10 cm^2/Vs) already achieved by low-temperature fabrication methods. However, a mobility being considerably higher than 10 cm^2/Vs cannot be achieved in such multi-metal compounds due to potential fluctuations within the conduction band that arise from the random distribution of the different cations. A promising approach to further increase carrier mobility in AOS is the formation of a single-metal compound with multiple anions like zinc oxynitride (ZnON) suppressing such potential fluctuations [1]. We have deposited ZnON thin films on glass substrates using a long-throw magnetron sputtering system. The thin films were radio-frequency sputtered at room temperature from a metallic zinc target (purity: 99.99 %) in a reactive atmosphere consisting of Ar (gas flow: 10 sccm), N_2 (gas flow: 100 sccm) and O_2 (gas flow: 1 − 4 sccm). In order to obtain amorphous, semiconducting ZnON thin films the O_2 partial pressure was varied by adjusting the O_2:N_2 ratio as well as the total gas pressure in the range between 10^{-3} and 10^{-2} mbar.

The electrical properties of the as-deposited films were determined by Hall-effect measurements at room temperature using the four-point probe van der Pauw technique. At a total gas pressure of 4×10^{-3} mbar in the sputtering chamber and a O_2:N_2 ratio of 1:100 we obtained *n*-type semiconducting thin films with carrier concentrations of about 10^{18} cm^{-3} and Hall mobilities up to 25 cm^2/Vs. At higher O_2:N_2 ratios the thin films become transparent and insulating with resistivities larger than 10^4 Ωcm. Therefore, at a constant O_2:N_2 ratio of 1:100 the deposition pressure was varied. With increasing pressure the resistivity increases as depicted in Fig. 1(c). The structure of the thin films was determined by means of X-ray diffraction that confirmed the formation of a ZnO phase at higher pressures as well as larger O_2:N_2 ratios leading to insulating films. However, the semiconducting thin films are X-ray amorphous as desired (see Fig. 1(b)). Furthermore, Hall-effect measurements revealed decreasing electron concentrations with increasing deposition pressure for the amorphous *n*-type semiconducting thin films with electron mobilities of 20 − 25 cm^2/Vs (cf. Fig. 1(d)). Fig. 1(a) depicts the transmittance spectra of the films measured with a double-beam spectrometer. It turns out that the higher the deposition pressure the higher is the transparency of the films in accordance with the formation of ZnO. For the amorphous and semiconducting thin films an enhanced absorption of light in the entire visible spectral range is observed with an average transmittance around 50%. The optical band gaps were estimated from the Tauc model. The amorphous thin films revealed a strongly reduced band gap of 1.3 eV. This decrease in band gap value is properly due to the formation of Zn-N bonds which have smaller ionicity than Zn-O bonds.
In conclusion, by adjusting the O_2 flow rate and the deposition pressure we are able to deposit amorphous high-mobility ZnON thin films which are promising to realize high-performance thin-film transistors.

[1] Y. Ye *et al.*, *J. Appl. Phys.*, **106**, 074512 (2009)

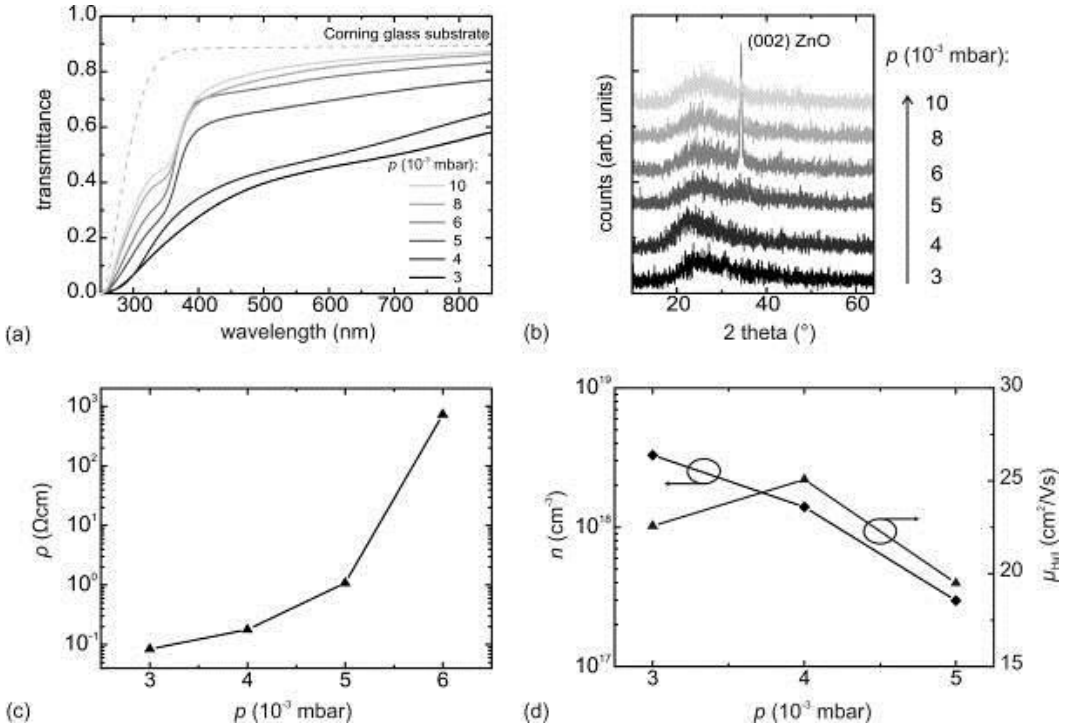
Corning glass substrate
transmittance
wavelength (nm)
p (10⁻³ mbar):
10
8
6
5
4
3
(a)
(002) ZnO
counts (arb. units)
2 theta (°)
(b)
p (Ωcm)
p (10⁻³ mbar)
(c)
n (cm⁻³)
μHall (cm²/Vs)
p (10⁻³ mbar)
(d)

ID 156 - Poster

Development of thin-film silicon-based triple-junction solar cell and its photoelectrochemical application

*S. N. Agbo[1], O. Astakhov[1], T. Merdzhanova[1], S. Yu[2], H. Tempel[2], H. Kungl[2], R.- A. Eichel[2], U. Rau[1]
[1]Forschungszentrum Julich, Institute of Energy and Climate Research-IEK-5 (Photovoltaics), Julich, Germany
[2]Forschungszentrum Julich, Institute of Energy and Climate Research-IEK-9 (Fundamental Electrochemistry), Julich, Germany

Development and popularization of various portable electronic devices as well as improvements of their energy efficiency raises interest in a photovoltaic (PV) power source for indoor and outdoor operations which could cover the power needs of such devices or at least supplement it.

This kind of PV power source should be integrated with a storage battery, be scalable, thin, lightweight, cost-effective and, taking into account potential popularity, environmentally friendly. These requirements are optimally fulfilled by thin-film solar cells (TFSC) based on hydrogenated amorphous (a-Si:H) and microcrystalline (µc-Si:H) silicon. TFSC have the advantage of covering wide range of voltages - open-circuit voltage may vary from 0.5 V for µc-Si:H solar cell and exceeding 3 V for quadruple junction devices combining a-Si:H and µc-Si:H absorbers. Among these, triple cells reach over 12% initial efficiency with open-circuit voltage of 1.8-2 V. This voltage allows merging triple-junction TFSC with efficient secondary battery system in an integrated PV/battery solution providing power for outdoor and indoor operations of autonomous portable devices.

In this work, we used a battery with LFP (Lithium iron phosphate) cathode against LTO (Lithium titanate) anode and a glass fiber separator soaked with LP30 (DMC:EC 1:1 1M LiPF6, dimethylene carbonate: ethylene carbonate) electrolyte for the combination with the triple-junction TFSC. The materials for the battery were selected because of their high stability against over-charging and availability as commercial sheets with graphite and binder. The voltage of the battery cell of 1.93 V is given by the difference of the cathode potential, 3.43 V (vs. Li/Li^+) and the anode potential of 1.5V (vs. Li/Li^+) and matches perfectly to the output of a triple TFSC with a-Si:H/µc-Si:H/µc-Si:H absorber layers. Both electrodes of the battery cell are relatively cheap and made of nontoxic and abundant elements, which leads to realistic upscaling possibilities.

In our report we present the development of both solar cell and battery for the integrated device, as well as the behavior of the PV/battery combination in different illumination conditions.

ID 157 - Oral

Understanding the formation of crystalline-core and amorphous-shell Si Nanowires and their length limiting factor

**R. DUSANE[1], A. Soam[1]*
[1]IIT Bombay, Met. Eng. & materials Science, Mumbai, India

As-grown Silicon Nanowires exhibit crystalline-core amorphous-shell structure with a taper along the growth direction. It is also observed that the length of the Nanowires gets limited for a given size of the Sn nanoparticle used as template and the operating conditions. The hot wire process generally enables the production of a large amount of atomic hydrogen during the dissociation of the silane source gas. Earlier observations indicated that this atomic hydrogen played a crucial role in modifying the size and shape distribution of the Sn nano-template even leading to the complete etching of the Sn particle thus stopping of further growth of the nano-wire. However our experiments show clearly that the migration of Sn along the higher surface tension wall of the Si nanowire leads to its redistribution and complete loss from the growing tip of the nanowire so that it is not available for further growth as per the liquid vapor-solid mechanism. Subsequently then amorphous silicon starts depositing on the side wall of the nanowire leading to the crystalline-core and amorphous -shell structure. However we see a positive aspect of this structure for Lithium ion battery application where the amorphous part could accomodate the stresses during charging and discharging and the core could provide electrical transport as well as mechanical stability. Additionally one can control the diameter of the crystalline core and the thickness of the amorphous shell desirably by the process conditions.

ID 158 - Poster

Dependence of modulated surface photovoltage of $CH_3NH_3PbI_3$ prepared from CH_3NH_3I:$PbCl_2$ solution on toluene dripping and annealing temperature

*T. Dittrich[1,2], P. Prajongtat[1,2], A. Naikeow[1,2], M. Arunchaya[2]
[1]Helmholtz-Center Berlin for Materials and Energy, Berlin, Thailand
[2]Kasetsart University, Department of Materials Science, Bangkok, Thailand

The research addresses the influence of toluene dripping and annealing temperature on the perovskite phase formation from CH_3NH_3I:$PbCl_2$ solution, on decomposition and on the electronic properties of $CH_3NH_3PbI_3$.

A CH_3NH_3I:$PbCl_2$ (molar ratio 3:1 in DMF) solution was spin coated onto Mo coated glass substrates. During the spin coating, half of the samples were dripped with toluene. Pairs of un-dripped and dripped samples were annealed at 60, 100, 120 and 140°C for one hour in a nitrogen filled glove box. The as-deposited and annealed samples were characterized by modulated surface photovoltage (SPV) spectroscopy (spectral range from the near infrared to the ultra-violet range). The change of the sign, onset-energies and heights of SPV signals were analyzed.
The onset of $CH_3NH_3PbI_3$ with energy at about 1.5 eV (band gap of $CH_3NH_3PbI_3$) was present for the as-deposited and annealed samples independent of annealing temperature and dripping or no dripping. The highest SPV signal related to $CH_3NH_3PbI_3$ was observed for the dripped sample after annealing at 120°C. An onset energy at about 3 eV, which is related to the absorption gap of $CH_3NH_3PbCl_3$, was detected for the as-deposited un-dripped sample and for the dripped and un-dripped samples annealed at 60°C. An additional onset energy at about 3.4 eV has been distinguished for the as-deposited un-dripped and for the dripped and annealed at 60°C samples.

Only one onset energy related to the band gap of $CH_3NH_3PbI_3$ was observed for the un-dripped sample annealed at 100°C and for the dripped sample annealed at 100 and 120°C.

The sign of the SPV signals of $CH_3NH_3PbI_3$ changed from positive to negative for annealing temperatures above 100°C (without toluene dripping) or 120°C (with toluene dripping). The change of the sign of the SPV signals was accompanied by the appearance of an onset-energy at about 2.3 eV which is related to the formation of PbI_2. In addition, an onset energy appeared at about 2.8 eV for the un-dripped samples annealed at 120 and 140°C. The behavior of the phase angle showed the existence of several mechanisms of modulated charge separation and relaxation.

Coexisting onset energies related to $CH_3NH_3PbI_3$ and $CH_3NH_3PbCl_3$ gave evidence for phase separation instead of formation of a $CH_3NH_3PbCl_xI_{3-x}$ phase. Further, dripping increased the technological window for the formation of a single phase (in relation to the onset-energies) $CH_3NH_3PbI_3$ layer. For samples prepared without (with) toluene dripping, the decomposition of $CH_3NH_3PbI_3$ set almost on at 120°C (140°C).

ID 159 - Oral

Evaluations of Stress Induced Instabilities of Amorphous Oxide Semiconductors using reflection CPM and their relations with TFT instabilities

**K. Shimizu[1,2], H. Takeyama[1,2], Y. Ohno[1,2]*
[1]Nihon University, Department of E&E, Narashino, Japan
[2]Nihon University, Department of E&E, Narashino, Japan

Amorphous indium-gallium-zinc or indium-tin-zinc compound oxides have attracted particular attention for thin-film-transistor application as a channel material. The stable operation against the gate bias, thermal stress, and light-induced stress are rather difficult to achieve. Although it has been intensively studied in the world, it is still unresolved.

The device instabilities in a-IGZO and a-ITZO have been investigated by reflection constant photocurrent method in TFT structure (W/L=7.8mm/0.3mm). The TFT was fabricated on the glass substrate. 100nm-think of the active layer of TFT was deposited by DC sputtering method. 20nm-thick silicon dioxide film as a passivation was deposited onto the back channel.

The optical band gap of a-IGZO and a-ITZO is 3.02 and 2.95eV, respectively. 1.4-1.7eV of broad state and 2.3-2.4eV state from the conduction band edge are observed in as-fabricated TFT for both the samples. These both the states disappear by thermal annealing at 350C in air for one hour and appear again in both the sample when illumination stress or constant negative gate-bias stress is applied. On the other hand, 1.4-1.7eV broad state also appears when over the band gap energy illumination is irradiated. These phenomena correspond to negative Vt shifts, and are observed in both a-IGZO and a-ITZO-TFTs and strongly depend on gate insulator materials.

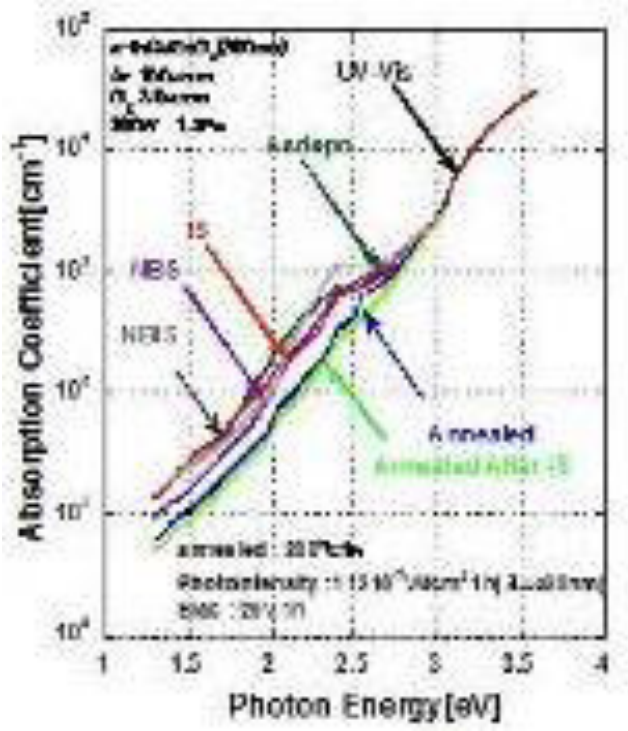

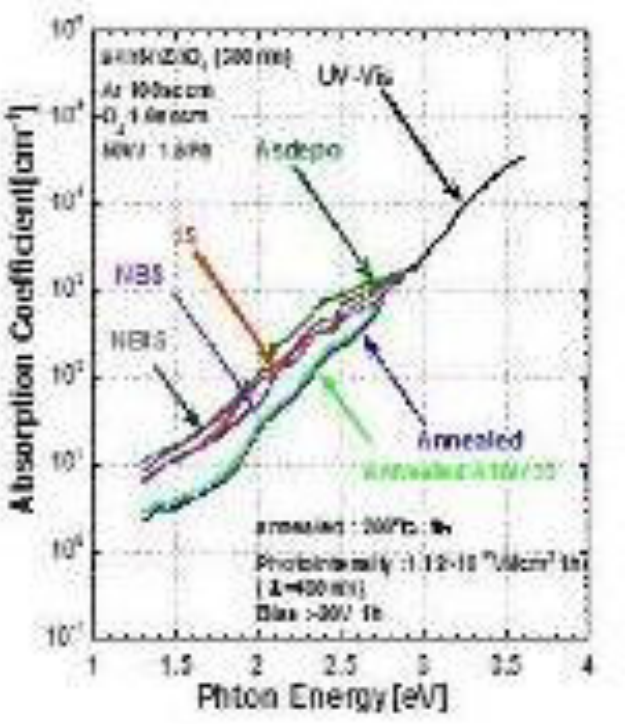

ID 160 - Poster

Electrophysical properties of $Ge_2Sb_2Te_5$ thin films for memory devices

*P. Lazarenko[1], S. Kozyukhin[2], A. Sherchenkov[1], A. Babich[1], H. P. Nguen[3], S. Timoshenkov[1], A. Shuliatyev[1], D. Terekhov[1], *A. Yakubov[1]*
[1]National Research University of Electronic Technology, Zelenograd, Russian Federation
[2]Kurnakov Institute of General and Inorganic Chemistry of the Russian Academy of Sciences, Moscow, Russian Federation
[3]Industrial University of Ho Chi Minh City, Ho Chi Minh, Viet Nam

Currently nonvolatile memory devices are actively developed. However, the most widespread flash technology has two tough problems: limited cyclability and scaling issue [1]. So, the development of alternative nonvolatile memory technologies is actual problem now. Phase change memory (PCM) operated by electrical impulse is one of the main candidates for a new generation of memory devices [1]. Chalcogenide semiconductor $Ge_2Sb_2Te_5$ (GST225) is considered to be most perspective for PCM application [1,2]. But many questions related to the electrical properties are still open [3,4]. For example mechanisms of dc conduction in the PCM materials are still to be clarified [4]. Therefore, the aim of this work is to investigate electophysical properties, in particular energy diagrams and mechanisms of charge carriers transport in thin films of $Ge_2Sb_2Te_5$.

The initial $Ge_2Sb_2Te_5$ was synthesized with using of quenching technique. Thin films were prepared by thermal evaporation in vacuum of the synthesized GST225. The composition of thin films was studied by Rutherford backscattering spectroscopy (RBS) and Energy Dispersive X-Ray Analysis (EDXRA). According to RBS and EDXRA deposited thin films have composition of $Ge_2Sb_2Te_5$ with accuracy of ± 5%. The structures of synthesized materials, and amorphous and polycrystalline structures thin films were investigated by X-ray diffraction (2Θscan). The thicknesses of GST225 films were detected with using of atomic force microscope (AFM), and were in the range from 100 to 150 nm.

The research system on the basis of KEITHLEY 6486 and a voltage control unit NI6008 was used for investigation of the current-voltage characteristics (CVC) and temperature dependencies of resistivity of planar structures by DC measurements. The stand based on the Agilent E3647A, HP 34401A, and DTI 1000 was used for measurements of thermoelectric power, Seebeck coefficient and type of conductivity. Experimental set-up based on G5-61 generator, oscilloscope LeCroy WaveRunner 44xi with active probe ZS-1000 was used for the pulse measurement and investigation of switching effect on the vertical structures. The spectrophotometer (Cary 5000, λ = 400-2500 nm) was used for estimation of band gap (E_g) and Urbach energy (E_0).

The measurements of resistivity for GST225 thin films showed that the phase transformation is accompanied by the drastic decrease of resistivity in the range from 120 to 170 °C. Ratio of the resistivities of amorphous and crystalline states exceeds 10^3, which is important for the reliable work of PCM cells.

CVC of the amorphous planar samples from room temperature to 100 °C were obtained. The experimental data for GST225 amorphous thin films indicate the existence of three regions with different I-V dependences. Modification of I-V dependencies with increasing applied field strength are connected with the change of the dominating charge carrier transport mechanism.

It was determined that holes are majority carriers in the investigated thin films and activation energy of conductivity (0.29 eV) is close to the middle of the mobility gap (0.61 eV). Urbach tails of localized states exist in the band gap. The energy diagram for GST225 thin film is presented in the Figure 1.

For modelling of the dependences of σ versus 1/kT we used two-channel transport model proposed by P.Nagels [5], according to which conductivity is caused by the transport of charge carriers by the delocalized states of the valence band and localized states of the valence band tail. So, for the

description of the model the sum of two exponents characterizing the charge transport by these states was used.

Switching effect with memory in thin films was investigated by DC and pulse measurements. A region of negative differential resistance is observed. Threshold voltage, delay time, transition time due to the transformation from OFF to ON state and recording time were determined.

Thus, in this study electrophysical properties of GST225 thin films were investigated. It was shown that transport mechanism based on the two-channel model has a good correlation with experimental results.

This work was supported by the Ministry of Education and Science of Russian Federation (FPP, project ID: RFMEFI57514X0096).

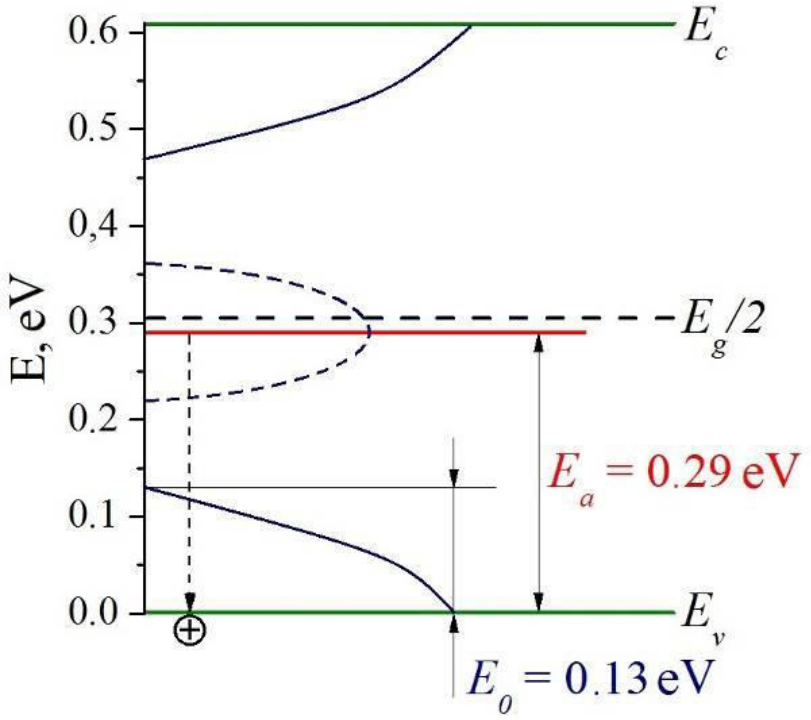

Figure 1 - Energy diagram for GST225 thin film.

[1] Burr, G. W. Breitwisch, M. J. Franceschini, M. Garetto, D. and et al.: Journal of Vacuum Science and Technology B. 28(2) (2010) 223- 262.
[2] Raoux, S. Wełnic, W. and Ielmini, D.: Chem. Rev. 110 (2010) 240-267.
[3] N. A. Bogoslovskiy and K. D. Tsendin: Semiconductors 46 (2012) 559-590.
[4] Nardone, M. Simon, M. Karpov, I. V. and Karpov, V. G.: Journal of Applied Physics 112 (2012) 071101.
[5] Nagels P., Callaerts R. and Denayer M.: Proc. 5th Int. Conf. Amorphous and Liquid Semiconductors, London (1973) 867.

ID 161 - Oral

Exciton Diffusion Length in Small Molecules

*B. Siegmund[1], C. Körner[1], K. Leo[1], K. Vandewal[1]
[1]Institut für Angewandte Photophysik, Technische Universität Dresden, Dresden, Germany

The photo-current of organic solar cells is the result of a multi-step process. It includes the generation and diffusion of excitons as well as their separation into free charge carriers, their transport to the electrodes, and their final extraction. Cascade structures of neat absorber layers have recently proven to be a convincing concept for efficient exciton harvesting with power conversion efficiencies comparable to those of tandem devices. Enhanced diffusion lengths of excitons would provide further improvements in terms of higher short-circuit currents.

In this work, we study the exciton diffusion length of several organic semiconductors. For this purpose, a series of solar cells with varying absorber thickness is investigated in terms of photo-current measurements and modelling of the optical field distribution. This approach allows distinguishing between the exciton diffusion length and the charge-carrier-extraction efficiency.

ID 162 - Poster

The investigation of atomic migration during the segregation of nc-Si in annealed Si-rich Si_xN/Si_yN multilayers

*X. jiang[1], *Z. ma[1], H. yang[1], W. li[1], L. xu[1], J. xu[1], K. chen[1], X. huang[1], D. feng[1]*
[1]Nanjing University, Nanjing, China

The multilayered silicon nanocrystal (nc-Si) film has been utilized in many research areas due to its novel structure and improved characteristic for silicon-based devices. Compared to single layer film, the multilayered nc-Si has some advantages such as controllable size of Si cluster and confinement effect of quantum dots [1]. In order to achieve band gap engineering of nc-Si for its application in photonic and photovoltaic devices, the multilayer structure of SiO_x/SiO_2 was used to control the size, density distribution and even the orientation of the nc-Si [2, 3]. Furthermore, enhancement in light emission efficiency of silicon nanocrystal light emitting diode was obtained by the multilayered Si_xN/Si_yN structure, which was attributed to the strong confinement of carriers in the multilayers [4]. Recently we found that unipolar and electrode-independent resistive switching effects can be realized in the annealed Si-rich SiN_x/SiN_y multilayers with high on/off ratio of 10^9 [5]. The break-and-bridge evolution of nc-Si pathway is the origin of resistive switching memory behavior. The size and density distribution of nc-Si embedded in sublayer with different ratio of Si/N is the key for the formation of nc-Si pathway in SiN_x/SiN_y multilayers. However, the migration mechanism of Si and N atoms during the formation of nc-Si in annealed Si-rich Si_xN/Si_yN multilayers was not clear, which is needed to ascertain.

In this paper, an interesting atomic migration was investigated during the formation of nc-Si in a silicon-rich Si_xN/Si_yN multilayer film after thermal annealing. XPS analysis revealed that the Si or N atoms migrated from the annealed sublayers with low concentration to the ones with high concentration. The driving force of the migration of Si or N atoms was further confirmed using Raman and HRTEM measurement. It is found the atomic migration between annealed sublayers was related with the driving force of nc-Si crystallization rate, which was determined by the level of the supersaturation in silicon nitride. Through the atomic migration during the formation of nc-Si in annealed Si-rich Si_xN/Si_yN multilayers, nc-Si quantum dot multilayers with controllable size can be obtained, which has potential application in the next generation Si-based nonvolatile memory.

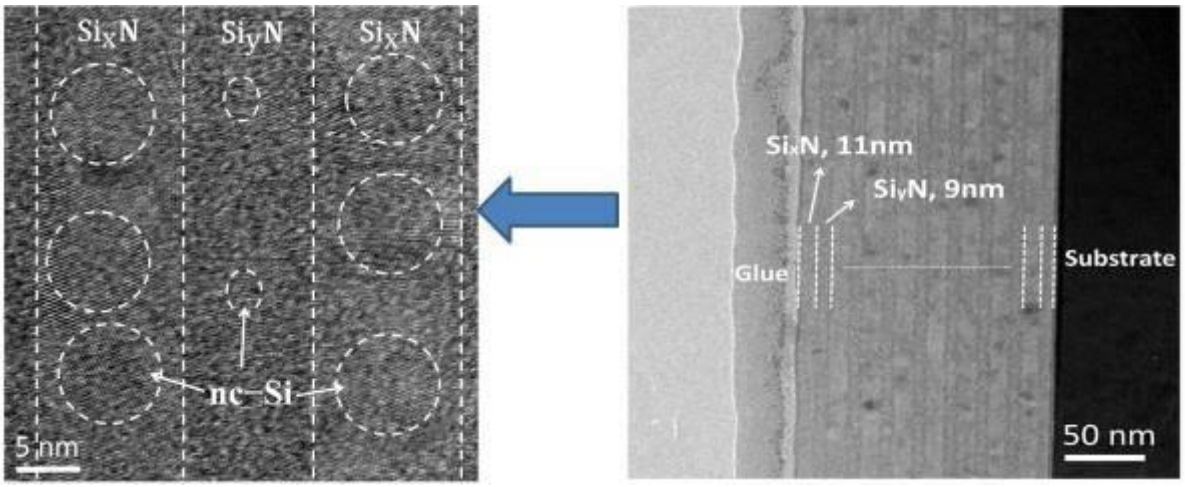

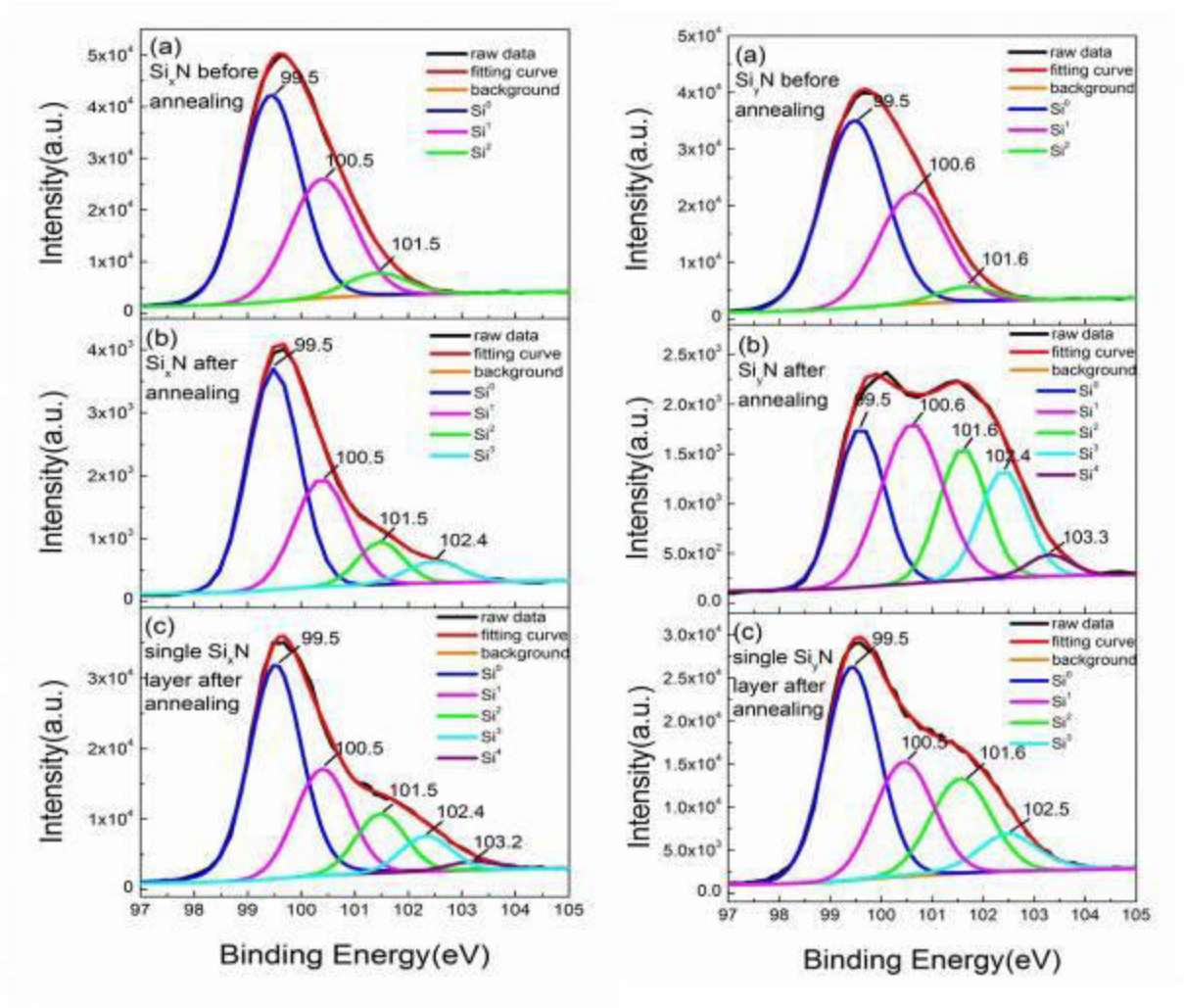

[1] L. Tsybeskov, K. D. Hirschman, S. P. Duttagupta, M. Zacharias, P. M. Fauchetd, Appl. Phys. Lett. **72**, 1(1998)
[2] G.F. Grom, D.J. Lockwood, J.P. McCaffrey, H.J. Labbe, P.M. Fauchet, B. White Jr, J. Diener, D. Kovalev, F. Koch, L. Tsybeskov, Nature **407**, 358 (2000)
[3] R.P. Nalini, L. Khomenkova, O.Debieu, J. Cardin, C.Dufour, M. Carrada, F.Gourbilleau, Nanoscale Research Letters **7**, 124(2012)
[4]C. Huh, K.H. Kim, B.K. Kim, W. Kim, H. Ko, C.J. Choi, G.Y. Sung, Adv. Mater **22**, 5058(2010)
[5] X.F Jiang, Z.Y. Ma, H.F Yang, J. Yu, W. Wang, W.P.Zhang, W. Li, J. Xu, L. Xu, K.J. Chen, X.F. Huang, and D. Feng, Journal of Applied Physics **116**, 123705 (2014)

ID 163 - Poster

Built-in potential in Amorphous Silicon Solar Cells by Kelvin Force Microscope

**T. Itoh[1], T. Ito[1], H. Kuriyama[1], S. Nonomura[1]*
[1]Gifu University, Dept. of Electrical, Electronic and Computer Engineering, Gifu, Japan

In silicon thin film solar cells, microcrystalline materials such as hydrogenated microcrystalline silicon (μc-Si:H) are used as photo-absorption layer and doped layer materials. The μc-Si:H has hetero-structure composed of amorphous silicon (a-Si), crystalline Si grains, and grain boundaries. Typical Si thin film solar cells are prepared on glass substrates coated with textured transparent conductive oxide (TCO). Therefore the local properties in Si thin film solar cells would be different due to above effects. In this work, the local Built-in potential in a-Si:H solar cells was studied by Kelvin force microscope (KFM).

Structure of a-Si:H solar cells used in this work were Asahi U-type substrate/n-type μc-Si:H/i-type a-Si:H/p-type a-$Si_{1-X}C_X$:H.

Difference between surface potential on n-type μc-Si:H and that on pin a-Si:H solar cell would correspond to built-in potential in a-Si:H solar cells. So, we measured surface potential images on n-type μc-Si:H films and pin a-Si:H solar cells deposited on Asahi U-type substrates by KFM. Then, the difference between average of surface potential on n-type μc-Si:H and that on pin a-Si:H solar cell increased from 0.26V to 0.77V with increasing built-in potential from 0.61V to 1.30V. Based on this result, built-in potential was able to be evaluated from difference between surface potential on n-type μc-Si:H films and that on pin a-Si:H solar cells by KFM. However, the difference between surface potential on n-type μc-Si:H films and that on pin a-Si:H solar cells by KFM were smaller than the built-in potential. The KFM measurements were conducted in air. Therefore, this could be related to oxidization of free surface of the samples.In the surface morphology images for pin a-Si:H solar cells deposited on Asahi U-type substrates, large convex grains were observed. The large grains would be related to the textured surface of Asahi U-type substrates. In the surface potential images for pin a-Si:H solar cells deposited on Asahi U-type substrates, the surface potential distribution was observed. The surface potential on the large convex grains was smaller than that in the region between the large convex grains. Using above method, the local built-in potential was able to be evaluated in a-Si:H solar cells. Therefore, the difference between the surface potential on large convex grains for pin a-Si:H solar cells deposited on Asahi U-type substrates and that for n-type μc-Si:H films deposited on Asahi U-type substrates was obtained. The difference between the surface potential in the region between the large convex grains for pin a-Si:H solar cells deposited on Asahi U-type substrates and that for n-type μc-Si:H films deposited on Asahi U-type substrates was also obtained. Both of the difference in surface potential on large convex grains and in the region between the large convex grains increased with increasing the built-in potential. The difference in surface potential on the large convex grains was smaller than that in the region between the large convex grains. The difference between the surface potential on the large convex grains and that in the region between the large convex grains in a-Si:H solar cells with large built-in potential was smaller than that with small built-in potential. This result suggests that the properties in a-Si:H solar cells would be affected by the local properties in a-Si:H solar cells.

Acknowledgments: This work was supported partially by SENTAN, JST.

ID 164 - Oral

Atomistic simulation of amorphous graphene: A particle-swarm-assisted first-principles approach

*T. Lee[1], P. Biswas[1,2], S. Elliott[1]
[1]University of Cambridge, Cambridge, United Kingdom
[2]The University of Southern Mississippi, Physics and Astronomy, Hattiesburg, United States

We present a new approach to model structural properties of amorphous graphene using a population-based, particle-swarm approach in conjunction with a first-principles total-energy functional [1]. The variation of the total energy as a function of the planar density of the models is studied in an effort to predict the equilibrium density for amorphous graphene using models consisting of a few hundred of atoms. Structural properties of the models have been characterized by calculating the pair-distribution function, the bond-angle distribution function, and the statistics of the ring-size distribution. The atomic-scale character of the models is examined by calculating the Delaunay triangulation, the Mermin order parameter, and the ring statistics for the amorphous networks. The nature of various exotic defect configurations appearing in the network is discussed with reference to recent electron-irradiation studies [2].

[1] Computational Intelligence: Concepts to Implementation, Russell C. Eberhart and Yuhui Shi (Morgan Kaufmann, First Edition, 2007)
[2] J. Kotakoski, A.V. Krasheninnikov, U. Kaiser, and J.C. Meyer, PRL **106,** 105505 (2011)

ID 165 - Poster

Evaluation of Absorption-edge Properties of a- $InGaZnO_4$ by Oxygenation or Hydrogenation using PYS/IPES

**K. Shimizu[1], S. Zhang[1], D. Komatsu[1]*
[1]Nihon University, Department of E&E, Narashino, Japan

Amorphous indium-gallium-zinc oxide thin film transistors have attracted a great deal of interest for their use in large area organic light-emitting diode displays due to their high field-effect mobility and low temperature processing capability. Above all the bias stability and on environment resistance is an extremely important for device application.

In this study, we report the results on the absorption-edge of amorphous semiconductors using Photoelectron Yield Spectroscopy and Inverse PhotoEmission Spectroscopy. A-IGZO film and a-Si:H film were deposited on the glass substrate by DC and AC sputtering method. In order to find the change in surface electronic structure, the a-IGZO film was performed hydrogenation and oxygenation.

We have found that hydrogenation and oxygenation greatly affect the surface. The change in surface electronic state and the photoelectron yield slope are reflected on the signal shift and the slope, respectively(Fig.1). We have also found that the slope of the signal has a strong correlation with the quality factor calculated from Tauc plot.

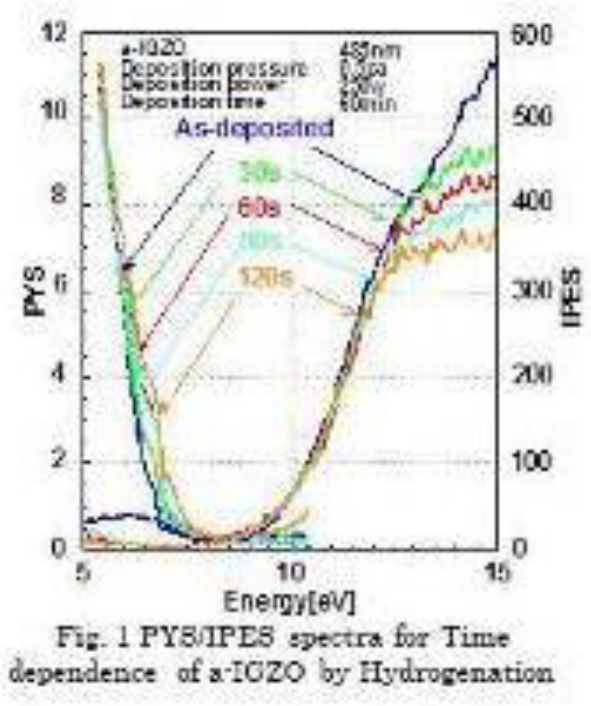

Fig. 1 PYS/IPES spectra for Time dependence of a-IGZO by Hydrogenation

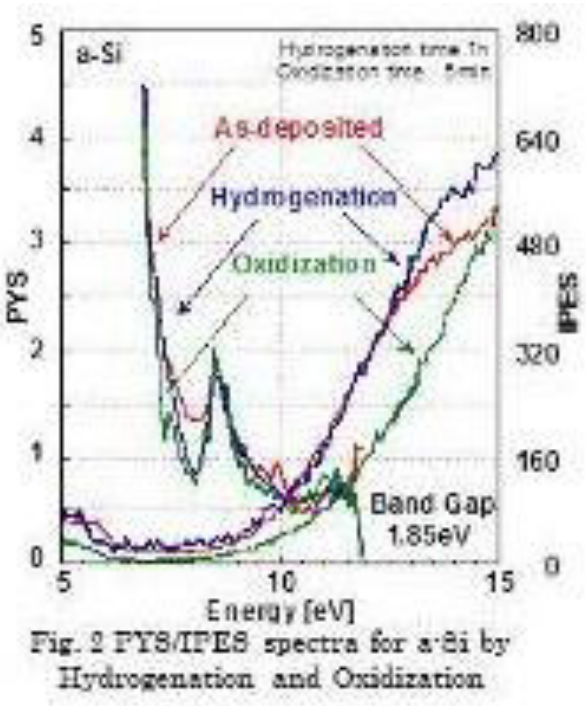

Fig. 2 PYS/IPES spectra for a-Si by Hydrogenation and Oxidization

ID 166 - Poster

Silicon heterojunction solar cells with Hole-Selective-Layers based on Transition-Metal-Oxides

*L. G. Gerling[1], A. B. Morales[1], P. Ortega[1], J. Puigdollers[1], C. Voz[1], R. Alcubilla[1]
[1]Universitat Politecnica de Catalunya, Enginyeria Electronica, Barcelona, Spain

The last years much effort has been devoted by the photovoltaic community to find crystalline silicon (c-Si) solar cell technologies with reduced manufacturing costs for a higher competitiveness. Such cost reduction could be accomplished by using very thin wafers or lower-quality substrates, but in any case low-temperature fabrication processes would be desirable. The silicon heterojunction (SHJ) concept is definitely the most successful solution to achieve high-efficiency c-Si solar cells at low temperature processing. Namely, Panasonic has demonstrated the possibility to achieve record efficiencies of 24.7% on very thin n-type c-Si substrates [1]. Nevertheless, the highly-developed deposition systems used to obtain the hydrogenated amorphous silicon (a-Si:H) layers have an impact on the final cost of this technology.On the other hand, selective electron and hole transport layers have been widely studied in organic semiconductor devices either for better carrier injection or extraction. These organic materials have recently attracted much attention to substitute the doped layers of hybrid devices based on silicon, owing to their low-temperature and solution-based processability. Thus, such hybrid solar cell structures could be in the way towards a more cost-effective photovoltaic technology. Focusing on organic hole transport layers (HTL), polyethylene dioxythiophene:polystyrene sulfonate (PEDOT:PSS) [2] and a variery of p-type polymers [3] have already been used to replace the p-doped a-Si:H layer in different hybrid solar cell structures. However, these organic materials typically suffer from low conductivity, moderate transparency and important instability issues. Another problem, which could be particularly important for heterojunction solar cells, is the limited endurance of organic layers to a later sputtering of transparent conductive oxide (TCO) electrodes.

Alternatively, layers of transition metal oxides (TMO) have already demonstrated excellent hole injection and extraction properties in organic devices. Many reports can be found in the literature of interface engineering with TMOs, such as molybdenum oxide (MoO_3), tungsten oxide (WO_3) or vanadium oxide (V_2O_5). Besides, a higher stability has been found for these inorganic materials compared to HTLs based on organic polymers [4]. However, only a few studies on the incorporation of TMO layers into hybrid devices based on silicon have been reported to date [5]. Particularly, first heterojunction solar cells based on n-type c-Si wafers with a MoO_3 emitter were referenced very recently [6]. The wide band gap of TMOs is also well-suited to achieve a high short circuit current in these devices, as the optical absorption of the window layer at short wavelengths can be significantly reduced. The potential of this novel solar cell concept has been demonstrated by a high conversion efficiency of 18.8% [7].

In this work, we investigate the incorporation of different TMOs (MoO_3, WO_3, V_2O_5) as the emitter of n-type c-Si solar cells. Besides, owing to their hole selectivity character, we show that layers of these TMOs can be also used to contact the rear electrode of p-type c-Si solar cells. Our preliminary devices fabricated on flat c-Si wafers have reached a conversion efficiency of about 13% when the TMO is used as an emitter, and over 15% when it is incorporated at the rear contact. In our opinion, there is still much room for improvement by optimizing interface passivation for a higher V_{oc} and using textured substrates to increase the J_{sc} value.

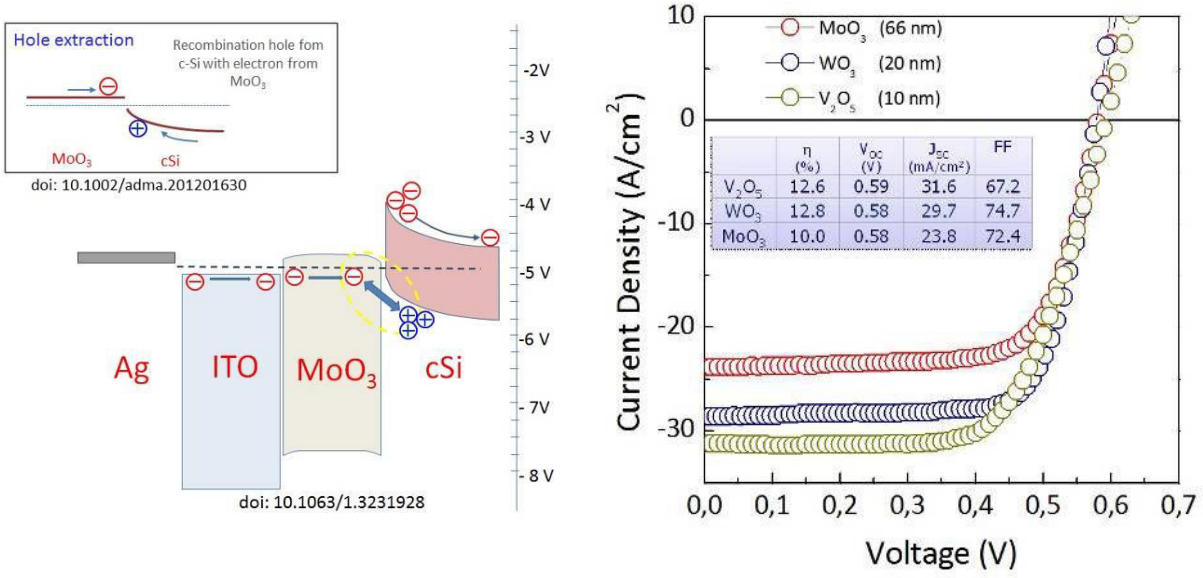

[1] M. Taguchi, A. Yano, S. Tohoda, K. Matsuyama, Y. Nakamura, T. Nishiwaki, K. Fujita, and E. Maruyama, “24 . 7 % Record Efficiency HIT Solar Cell on,” vol. 4, no. 1, pp. 96-99, 2014.
[2] K. A. Nagamatsu, S. Member, S. Avasthi, J. Jhaveri, and J. C. Sturm, “A 12 % Efficient Silicon / PEDOT : PSS Heterojunction Solar Cell Fabricated at < 100 ◦ C,” vol. 4, no. 1, pp. 260-264, 2014.
[3] S. Avasthi, S. Lee, Y.-L. Loo, and J. C. Sturm, “Role of majority and minority carrier barriers silicon/organic hybrid heterojunction solar cells.,” *Adv. Mater.*, vol. 23, no. 48, pp. 5762-6, Dec. 2011.
[4] Y. Sun, C. J. Takacs, S. R. Cowan, J. H. Seo, X. Gong, A. Roy, and A. J. Heeger, “Efficient, air-stable bulk heterojunction polymer solar cells using MoO(x) as the anode interfacial layer.,” *Adv. Mater.*, vol. 23, no. 19, pp. 2226-30, May 2011.
[5] S. Il Park, S. Jae Baik, J.-S. Im, L. Fang, J.-W. Jeon, and K. Su Lim, “Towards a high efficiency amorphous silicon solar cell using molybdenum oxide as a window layer instead of conventional p-type amorphous silicon carbide,” *Appl. Phys. Lett.*, vol. 99, no. 6, p. 063504, 2011.
[6] C. Battaglia, X. Yin, M. Zheng, I. D. Sharp, T. Chen, S. McDonnell, A. Azcatl, C. Carraro, B. Ma, R. Maboudian, R. M. Wallace, and A. Javey, “Hole Selective MoO_x Contact for Silicon Solar Cells.,” *Nano Lett.*, vol. 14, no. 2, pp. 967-71, Feb. 2014.
[7] C. Battaglia, S. M. de Nicolás, S. De Wolf, X. Yin, M. Zheng, C. Ballif, and A. Javey, “Silicon heterojunction solar cell with passivated hole selective MoOx contact,” *Appl. Phys. Lett.*, vol. 104, no. 11, p. 113902, Mar. 2014.

ID 167 - Poster

Research and development center enabling HJT in Russia

*E. Terukova[1,2], D. Andronikov[1,2], S. Abolmasov[1], A. Abramov[1,2], E. Terukov[1,2], D. Orekhov[1], A. Semenov[1], I. Nyapshaev[1,2], K. Emtsev[1], A. Kukin[1,2]
[1]R&D TF TC, Solar department, Saint-Petersburg, Russian Federation
[2]Ioffe Institute RAS, Saint-Petersburg, Russian Federation

This paper presents research and development center established in Saint-Petersburg the goal of which is to develop and promote photovoltaic technology in Russia. R&D Center of Thin Film Technologies in Energetics under Ioffe Institute LLC (TFTC) [1] is the R&D unit of Hevel Solar company [2] - a breakthrough project of Renova group [3] and Russian Corporation of Nanotechnologies [4]. The company provides end-to-end alternative energy services starting from design and production of PV modules to integration and operation of PV systems as a sustainable alternative to conventional sources of electricity. Hevel's PV plant located in Novocheboksarsk (Chuvash Republic, Russia) started its trial production in June 2014 and will reach full capacity of 700 000 modules per year in the second half of 2015.

Research works of the R&D center include fundamental and application research in different areas as follows: silicon thin film and silicon heterojunction technologies, amorphous silicon flexible solar cells, research of new materials and development of new technological processes, exploratory research for application of thin films in existing and emerging technologies, new PV components employment and testing, terrestrial monitoring of PV modules in different climatic regions of Russia, scaling of technologies and transferring of new technologies to the production facility, recycling of gases and materials used in PV production. Most of the TFTC activities are accomplished in close collaboration with academic and industrial partners in Russia and abroad. TFTC also provides training of highly skilled professionals in PV industry together with educational institutions.

The most recent achievements of the TFTC team is development of transfer roadmap of silicon heterojunction solar cells for the fab in Novocheboksarsk. During this project together with scientific and industrial partners a batch of cells with size of 156x156 mm^2 has been produced using pilot line and laboratory equipment. All the cells showed high uniformity in efficiency with the best ones having 20,4% efficiency value. In the nearest future TFTC will launch chemical laboratory for development of texturing procedure for silicon wafers that will enable further development of heterojunction solar cells.

[1] www.tf-tc.ru
[2] www.hevelsolar.com
[3]www.renova.com
[4]www.rusnano.ru

ID 168 - Poster

Dielectric relaxation in $(Ge_{28.5}Pb_{15.0}S_{56.5})_{100-x}Fe_x$ glassy systems

**R. A. Castro[1], N. I. Anisimova[1], G. I. Grabko[1,2]*
[1]Herzen State Pedagogical University of Russia, Electronic Physics, Saint-Petersburg, Russian Federation
[2]Transbaikal State University, Chita, Russian Federation

Study of many classes of materials (polymers, liquid insulators, chalcogenide glassy semiconductors) indicates the existence of relaxation spectra with significant deviations from classical Debye dispersion. These deviations are interpreted in terms of the concepts about diffuse dielectric spectrum, which can be due both to the presence of relaxators with somewhat different (but similar) relaxation times and to the interaction between different relaxators. Such relaxators are generally atoms, molecules, groups of atoms, structural defects, etc.; they can form a continuous spectrum of relaxation times. Concerning glassy systems, it is well known that D^+ and D^- centers with negative correlation energy can play the role of such defects, which exchange electrons during charge transport and accumulation. Analysis of the $Ge_{28.5}Pb_{15.0}S_{56.5}$ system by thermoactivation spectroscopy at temperatures T from 260 K to 280 K revealed the existence of defect states with activation energy of 0.43 eV and concentration of ~10^{16} cm^{-3}.

In this paper, we report the results of studying the spectrum of relaxators for the $(Ge_{28.5}Pb_{15.0}S_{56.5})_{100-x}Fe_x$ glassy systems and calculations of the energy distribution of the density of charged defects, which are responsible for long-term isothermal relaxation in this semiconductor.

The $(Ge_{28.5}Pb_{15.0}S_{56.5})_{100-x}Fe_x$ layers with thickness d ~ 1.0μm were obtained by method of joint-frequency atomization of the glass $Ge_{28.5}Pb_{15.0}S_{56.5}$ and the modifier Fe onto silicate substrate at pressure of $8x10^{-3}$ mm Hg in the argon atmosphere. All samples had a sandwich configuration with aluminum electrodes and a contact area 15.0 ± 0.3 mm^2. The dielectric parameters were measured in the frequency range of 10^{-2} to 10^5 Hz and in the temperature range of 250 K to 350 K by using a High-Resolution Dielectric Analyzer (Novocontrol Concept 81). The empirical data were sufficient fitted using the Havriliak-Negami approximation. The temperature dependence of the relaxation parameters is discussed.

Based on the experimental data we have calculated the relaxation time distribution function and its main parameters. The found specific features of this function reveal its structural sensitivity (which can be used in further study of the electronic properties) and confirm the existence of non-Debye dispersion in studied systems at low frequencies. It is established that the density of states of the localized charged defect exponentially decreases with increasing the spacing from the bottom of the conduction band.

ID 169 - Oral

Charge Carrier Separation in (Organic) Solar Cells and the Selectivity of Electrodes

**U. Würfel[1,2], M. Sessler[1], M. Kohlstädt[1,2], M. Unmüssig[1]*
[1]Fraunhofer Institute for Solar Energy Systems, Freiburg, Germany
[2]University of Freiburg, Materials Research Center FMF, Freiburg, Germany

Among other requirements such as high conductivity and high transparency or reflectivity the electrodes in a solar cell should also provide selectivity for the charge carriers generated in the photoactive layer in order to extract the “right” type of charge carrier and to block the “wrong” one. The ideal selectivity of the contacts is given when the electron contact exchanges only electrons with the photoactive layer and the hole contact only holes. If however the selectivity is not sufficient, a part of the photogenerated charge carriers will be lost by surface recombination and the power output of the device will be reduced.

It could recently be shown - independent of the exact device configuration of a solar cell - that the essential requirement for efficient separation of photogenerated charge carriers and thus for selectivity is a very low electron (hole) conductivity in the vicinity of the hole (electron) contact [1].

In order to realize a high degree of selectivity and thus to minimize surface recombination in organic solar cells charge carrier selective layers are used between the photoactive layer and the electrode. These layers (e.g. PEDOT:PSS, TiOx, ZnO, WoOx, MoOx) often comprise a rather large band gap and thus can block the “wrong” type of charge carrier quite efficiently. However, interface states within the band gap at the interface between these layers and the photoactive absorber can still act as recombination centers. Another way to achieve charge carrier selectivity is to use polar (organic) molecules manipulating the work function of the electrode.

We used cheap and easy-to-process organic molecules with dipole moments which alter the effective work function of the electrode. It will be shown that the induced strong increase (decrease) of the electron (hole) concentration in the adjacent photoactive layer is the main reason for the enhanced selectivity. The latter can be observed in an increased open-circuit voltage Voc for different active layers. We performed scanning Kelvin probe microscopy as well as UPS measurements and found a corresponding shift of the surface potential. A theoretical model was set up and the results of the numerical simulations are in full accordance with the experimental data. Interestingly, DFT-calculations prove that the energy levels of the dipole molecules are not suited to conduct charge carriers from the photoactive layer to the electrode. Using a tunneling mechanism in our model, it is found that there is no necessity to assume preferential tunneling for electrons. Their accumulation due to the lowered work function is sufficient to explain the observed behavior.

These findings will be complemented by data obtained from crystalline silicon solar cells.

[1] Würfel, U. Cuevas, A. & Würfel, P. Charge Carrier Separation in Solar Cells, *IEEE J. Photovoltaics* 5, 461-469 (2015).

ID 170 - Oral

Metal oxide substrate dependent HOMO-LUMO transitions in layers of conjugated molecules

**T. Dittrich[1], S. Fengler[1], M. Rusu[1]*
[1]Helmholtz-Center Berlin for Materials and Energy, Berlin, Germany

The research addresses the influence of a metal oxide substrate on the onset energy and electronic disorder of the HOMO-LUMO transition in C_{60}, ZnPc and ZnPc:C_{60} layers.

Layers of C_{60}, ZnPc and ZnPc:C_{60} were deposited by organic vapor phase deposition (OVPD) onto indium tin oxide (ITO), aluminum doped zinc oxide (AZO) and TiO_2 coated glass substrates. The layers were investigated by modulated surface photovoltage (SPV) spectroscopy (spectral range from the near infrared to the ultra-violet). As remark, SPV is a method with much higher sensitivity and spectral resolution compared to photo electron spectroscopy. Heights, phase angles and onset-energies of SPV signals as well as characteristic exponential tails were analyzed.

Photo-generated electrons were preferentially separated towards the external surface for all layers deposited onto ITO and for ZnPc deposited onto AZO. In contrast, photo-generated electrons were preferentially separated towards the metal oxide surface for C_{60} deposited onto AZO and for all layers deposited onto TiO_2 excepting ZnPc:C_{60} for higher photon energies.

The largest SPV signals were measured for ZnPc:C_{60} layers deposited onto ITO and AZO substrates and for C_{60} deposited onto TiO_2.

Transitions related to charge transfer complexes and to HOMO-LUMO gaps were distinguished. The dominant onset energies depended on the metal oxide substrate: C_{60} (1.677, 1.681 and 1.608 eV for ITO, AZO and TiO_2, respectively), ZnPc (1.443, 1.40, 1.464 eV for ITO, AZO and TiO_2, respectively) and ZnPc:C_{60} (1.458, 1.483, 1.48 eV as well as 0.956, 1.11, 0.985 eV for ITO, AZO and TiO_2, respectively). The characteristic energies of the exponential tails amounted for C_{60} to 45, 50 and 54 meV for ITO, AZO and TiO_2, respectively, for ZnPc to 107, 84, 88 meV for ITO, AZO and TiO_2, respectively and for ZnPc:C_{60} to 57, 60, 65 meV for ITO, AZO and TiO_2, respectively.

Polarization of conjugated molecules at metal oxide interfaces has a strong influence on the onset energies of the HOMO-LUMO gaps. In addition, the morphology at metal oxide / conjugated molecules interfaces seems to influence the electronic disorder in HOMO-LUMO bands and related transitions.

ID 171 - Poster

Sputtered high *c-axis* oriented aluminum nitride obtained at room temperature

*R. Martins Cunha Junior[1], *M. V. Pelegrini[1], K. Franklin Albertin Torres[2], I. Pereyra[1]*
[1]University of Sao Paulo, Electrical Engineering, Sao Paulo, Brazil
[2]UFABC , CECS, Sao Paulo, Brazil

Piezoelectric materials, in particular aluminum nitride (AlN), have become very attractive for MEMS applications, because of their mechanical and electrical response. In this work we present a study about the fabrication and characterization of AlN thin films obtained by r.f. Reactive Magnetron Sputtering.

Here we report the effect of the deposition parameters, such as r.f. power density, temperature and pressure deposition, on the morphological, structural and electrical properties of AlN thin films. This study aims to use the produced thin film as piezoelectric element in devices such as actuators and sensors.

The AlN thin films are characterized by Fourier Transform Infrared Absorption technique (FTIR) and X-ray diffraction. d_{33} piezoelectric coefficient was estimated by the capacitive method proposed by Mahmoud et. al [1], through its geometrical dimensions variation.

This study allowed us to produce high oriented [002] AlN thin films at room temperature from a pure Al target with a piezoelectric coefficients d_{33} around 4 pm/V correlated to the crystalline orientation of the film.

[1] M. Al Ahmad and R. Plana, IEEE Microw. Wirel. Components Lett. **19**, 140 (2009).

ID 172 - Poster

Rare-earth and Nb Doping of TiO_2 Nanocrystalline Mesoscopic Layers for High-efficiency Dye-sensitized Solar Cells

**S. Kozlov[1], L. Larina[1,2], A. Nikolskaia[1], M. Vildanova[1], A. Vishnev[1], O. Shevaleevskiy[1]*
[1]Institute of Biochemical Physics RAS, Solar Photovoltaics, Moscow, Russian Federation
[2]Chungnam National University, Chemical Engineering, Daejeon, Korea, Republic of

Thin mesoscopic TiO_2 layers fabricated from TiO_2 nanocrystals are widely used for constructing next-generation dye-sensitized solar cells (DSSCs). Recently we have shown that the power conversion efficiency of DSSCs can be sufficiently improved if the mesoscopic layers were prepared using Nb-doped TiO_2 nanocrystals [1].

In this research we have prepared Nb and rare-earth-doped TiO_2 nanocrystalline layers, using the europium (Eu), yttrium (Y) and samarium (Sm) ions. Mesoscopic doped and undoped TiO_2 layers were fabricated from the appropriate colloidal suspensions prepared by the sol-gel method with doping concentrations ranging from 0 - 10 wt.%. The structure and morphology characterizations of the prepared samples were provided using XRD, TEM and SEM measurements which have shown a uniform distribution of the doped atoms in the bulk of TiO_2 nanocrystals.

A series of DSSCs based on doped TiO_2 layers was prepared and the properties of the photovoltaic cells were obtained including the measurements of IPCE in the wavelength range 350 - 1100 nm, I-V characteristics and PV cell performance under AM1.5 illumination (1000 W/m^2). The best DSSCs, based on Nb-doped and Eu-doped TiO_2 layers, have shown the energy conversion efficiencies ~ 9% that is nearly 20% higher than that observed in the undoped samples.

We have found that the increase in doping concentration to a level ~ 2.5 - 3.5 wt.% for both Nb and rare-earth doped samples tends to improve the DSSC conversion efficiency, while the further increase in doping concentration decreases the efficiency.

We discuss the effects, caused by doping, by the creation of shallow donor levels belowTiO_2 conduction band that improves the conductivity of the layer. To prove this we have provided the EPR measurements of both doped and undoped samples that revealed the creation of spin-containing defects with *g*-value ~ 1.98 in doped TiO_2 which results in increasing the electronic conductivity.

[1] N.A. Tsvetkov, L.L. Larina, O. Shevaleevskiy, E.A. Al-Ammar, and B.T. Ahn, Prog. Photovolt: Res. Appl. 20, 904 (2012)

ID 173 - Oral

Ion bombardment on a-Si/c-Si interface : detrimental or affordable?

*J. Meixenberger[1], G. Wahli[1], *D. Lachenal[1], D. Bätzner[1], W. Frammelsberger[1], B. Legradic[1], P. Papet [1], B. Strahm[1]*
[1]Meyer Burger Research AG, Hauterive, Switzerland

Silicon heterojunction is seen as the next solar cell technology to achieve efficiencies in the 24% range at the mass production level. This is supported by the recent very high efficiencies reported at the research level by many groups and companies achieving more than 23%. The highest of them being a 24.7 % cell reported by the pioneers in Si-HJT, Panasonic Corporation. Moreover, integrating silicon heterojunction contacts into an inter-digitated back contacted (IBC) scheme, efficiencies can be even higher than 25% as also reported by Panasonic.

In terms of efficiency capability, there is no doubt that Si-HJT is the leading technology. However, these cells have to be produced under mass production conditions and therefore using low cost deposition techniques. The previously reported record cells have been produced using so called “low damage” deposition techniques such as very high frequency (VHF) PECVD deposition of amorphous silicon and ion plated transparent conductive oxides (TCO) for the front and back electrical contacts. However, these techniques have some cost drawbacks. VHF requires very special and expensive reactor design in order to circumvent the layer uniformity in large reactors [] and ion plating equipment have very high running costs.

The question is then the following: can these techniques be replaced by more industrially compatible technologies even if these are considered to have higher ionic bombardment on the growing film? Namely, can VHF be replaced by radio-frequency (RF) excitation and ion plating by magnetron sputtering that are both well-known method for low cost production?

This contribution will demonstrate that the use of RF PECVD deposition can lead to very high c-Si passivation quality with surface recombination velocities in the range of 1 cm/s and discuss the ion bombardment during deposition of a-Si thin films. More interestingly, the impact of sputtering on c-Si surfaces passivated with very thin (10 nm) a-Si layers will be discussed.

As shown recently by Demaurex *et al* [1], magnetron sputtering induces damages of the passivation and this suggests that sputtering is not the method of choice for high performance Si-HJT cells. In this contribution, we will demonstrate that these damages depends on the sputtering apparatus and conditions and that the defects generated by the deposition of the TCO are not only due to ion bombardment and that most of them - if not all of them - can be recovered by a short thermal annealing.

[1] B. Demaurex *et al*, Applied Physics Letters, 101, 171604 (2012)

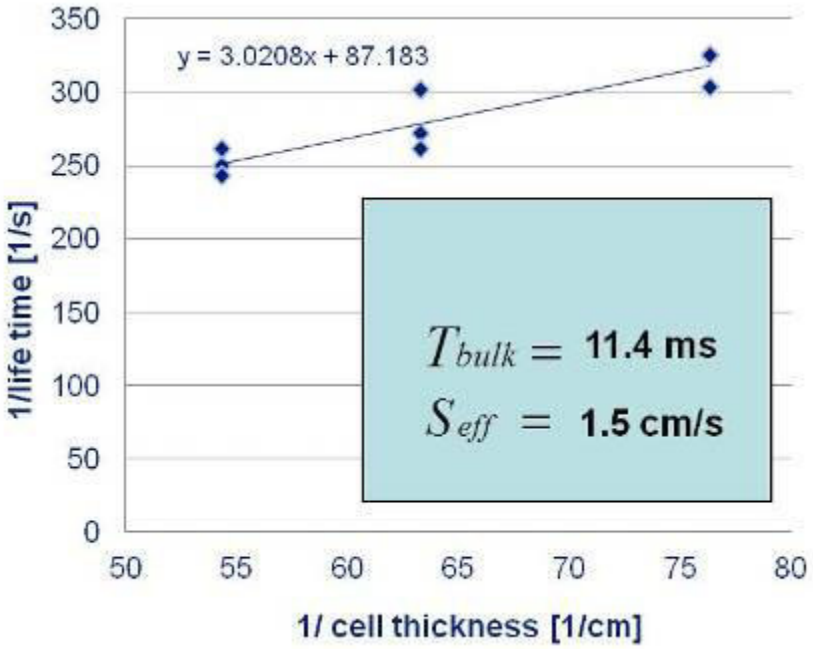

Fig. 1: low surface recombination velocity of c-Si passivated by a-Si deposited under RF excitation.

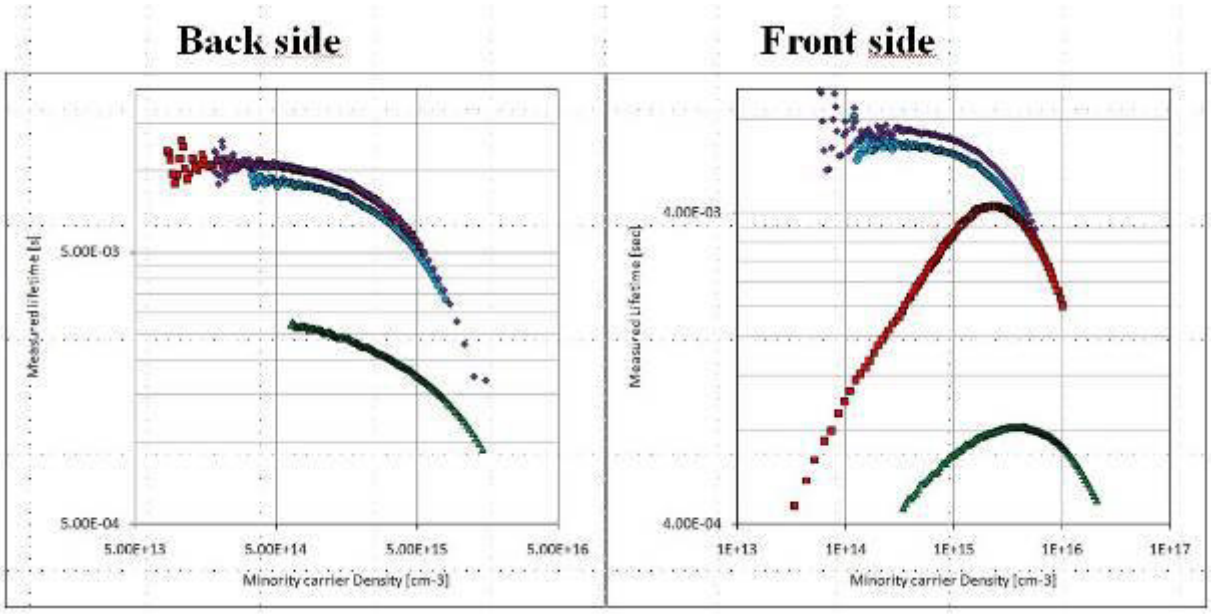

Fig. 2: Lifetime measurements of damage and recovery of passivation after deposition of TCO and thermal annealing. Curves description; passivated wafer (blue), after TCO sputtering (green), after short thermal annealing (red), after TCO removed with HF (purple)

ID 174 - Poster

Phototransfer of Electrons between Bacterial Reactionary Centers and Mesoporous Titania

**E. Konstantinova[1,2], A. Troitskij [1], P. Kashkarov[1,2]*
[1]M.V. Lomonosov Moscow State University, Physics , Moscow, Russian Federation
[2]Russian Research center "Kurchatov Institute", Moscow, Russian Federation

In recent years titania (TiO_2) is often used as an element of gas sensors. Besides, TiO_2 based solar cells are actively developed now. Generalization of these two directions is development of light accumulation devices on the basis of mesoporous TiO_2 with bacterial reactionary centers (natural bioaccumulators of solar energy) incorporated in it [1]. The purpose of this work was studying of paramagnetic properties of mesoporous TiO_2 with Rhodobakter sphaeroides bacteria incorporated in its structure for clarification of a role of TiO_2 matrix defects in processes of charge carrier transfer between the bacterial reactionary centers and conductivity band of titania.

EPR spectra were detected by the standard Bruker EPR spectrometer ELEXSYS-500 (X-band, sensitivity is around ~10^{10} spin/G). The measurements were made at 300 K. The samples were illuminated in situ by a halogen lamp with cut-off filter (λ>680 нм). All details of the sample preparation were published in [2].

It is established that in initial titania the main types of the paramagnetic centers are superoxide radicals; electrons trapped on the oxygen vacancies, Ti_3^+ centers. Illumination of the samples in the visible range didn't influence intensity of the EPR lines. In titania with incorporated protein from Rhodobakter sphaeroides the electrons trapped on oxygen vacancies, Ti_3^+ centers are also detected. It is established that illumination of the samples with protein in the visible range causes a change of EPR line intensity. It can be explained to that the oxygen vacancy defects are recharged as a result of capture of the electron injected from the bacterial reactionary centers into the conductivity band of TiO_2. A transition from non paramagnetic defect state into a paramagnetic state ($V_O + e \rightarrow V_O^-$) takes place. The obtained results can be used for developing new photoelectronic devices on the basis of titania/Rhodobakter sphaeroides protein.

Acknowledgement: this work was supported by the Russian Foundation for Basic Research № 15-29-01185 ofi_m.

[1] Y. Lu, Y. Liu, J. Xu, Sensors. 5, 258 (2005).
[2] E.P. Lukashev, V.A. Nadtochenko, E.P. Permenova, O.M. Sarkisov, A.B. Rubin, Reports of Russsian Science Academy. 415, 5, 696 (2007).

ID 175 - Poster

Thermal and structural studies of CdSe nanorods synthesized by solvothermal process

*L. Zuala[1,2], P. Agarwal[2]
[1]Pachhunga University College, Mizoram University, Physics, Aizawl, India
[2]Indian Institute of Technology Guwahati, Physics, Guwahati, India

CdSe nanostructures such as nanorods, nanoribbons, etc are of great importance for both fundamental research and technical applications. CdSe can exist in cubic and hexagonal phase and the bulk sample has a relatively wide direct bandgap of 1.74 eV at room temperature. However, properties of the nanomaterials such as electrical, optical and thermal properties are largely controlled by the particle size, size distribution and morphologies. Different methods have been employed to synthesize the nanostructures with controlled size and shape. Great efforts have been made to optimize the synthesis process in order to control the morphology and size effectively so as to have the desired properties. Solvothermal synthesis process is one of the most efficient routes to achieve this optimization.

CdSe nanorods samples with wurtzite structure are synthesized by solvothermal process at different reaction time in a mixed solvent of hydrazine hydrate [H_6N_2O], ammonia [NH_3] and deionzed water. Cadmium acetate [$(CH_3COO)_2$ Cd; $2H_2O$] and sodium selenite [Na_2SeO_3] are used as precursors for cadmium and selenium ions respectively. The average crystallite size, lattice strain and dislocation densities are obtained using Williamson Hall plot from the X-ray diffraction (XRD) spectra. The crystallite size and the structural parameters are found to improve with increase in reaction time. Energy dispersive X-ray analysis (EDX) measurements show that the synthesized samples are slightly cadmium rich and the stoichiometry improves with reaction time. Field emission scanning electron microscope (FESEM) images show elongated rod shaped structures with wide distribution in sizes. Samples prepared at longer reaction time are found to have larger grain sizes than samples at lower reaction time. Thermal stability of the nanorods is studied using thermogravimetric analysis (TGA), derivative thermogravimetry (DTG) and differential thermal analysis (DTA). All the samples have high thermal stability without significant weight loss up to 600 °C. Once the thermal decomposition takes place above this temperature, a weight loss of about 35% is observed in all the samples. The kinetics of thermal decomposition studied using Coats-Redfern method shows that the decompositions follow contracting cylinder model, which assumes that nucleation occurs rapidly on the surface of the cylindrical nanoparticles. Thermodynamic parameters involved in the decompositions such as activation energy, change in entropy, enthalpy of activation, and Gibbs free energy are deduced.

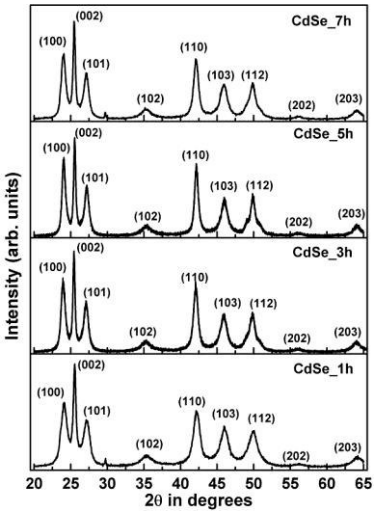

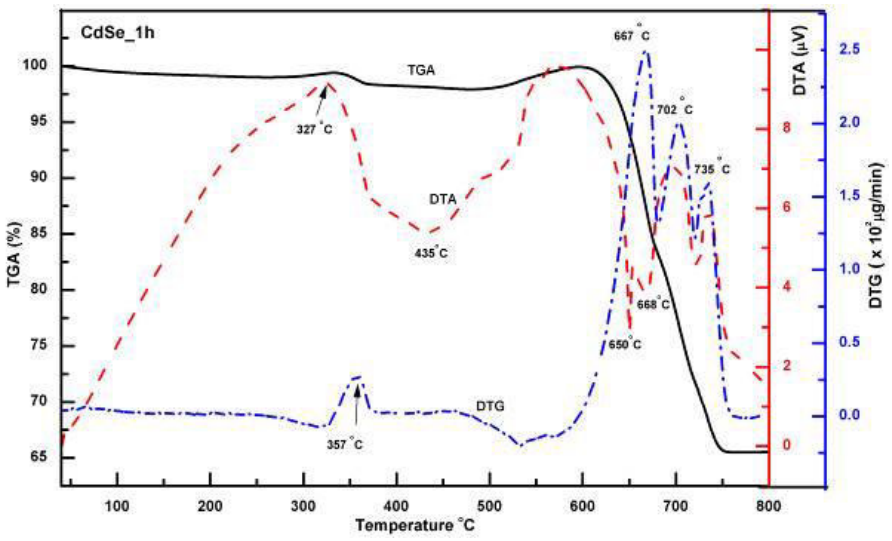

ID 176 - Oral

Triple- and quadruple-junction thin-film silicon solar cells

*J.- W. Schüttauf[1], E. Moulin[1], F. Meillaud[1], F.- J. Haug[1], C. Ballif[1]
[1]EPFL, Neuchâtel, Switzerland

We study thin-film silicon-based solar cells in triple- and quadruple-junction configuration to obtain the highest possible efficiencies for this technology. We will present high-quality component cells for the different relevant materials, i.e. amorphous silicon, amorphous silicon-germanium and microcrystalline silicon, respectively, including their main features such as mixed-phase silicon oxide doped layers and buffer layers. With such component cells, we have already been able to fabricate triple-junction devices with initial efficiencies up to 13.7% and stabilized efficiencies up to 12.8% [1]. Recently, excellent high bandgap amorphous silicon cells have been developed that are very suitable as top cells in both triple- and quadruple-junction devices, and should allow for even higher conversion efficiencies due to an increase in open-circuit voltage of approximately 40-60 mV. The incorporation of these new top cells in triple- and quadruple-junction devices is currently being investigated. Other important features for triple-junction cells include (i) dedicated superstrate structures that allow for better light management, and (ii) a thin intermediate reflector between top and middle cell to reduce the top cell thickness and thereby light-induced degradation. For quadruple-junction cells, we have so far shown a properly working device with an open-circuit voltage as high as 2.57 V, but its initial conversion efficiency was limited to 10.1% due to non-optimized current matching [2]. In principle, quadruple-junction devices should lead to higher efficiencies than triple-junctions, but this has not been demonstrated yet for thin-film silicon technology. We are currently pursuing efficiencies exceeding the ones for triple-junctions in this device configuration and will present our latest results at the symposium. With already available building blocks in our lab, we believe that we should be able to obtain stabilized efficiencies of 13.5% for triple-junction cells and 14% for quadruple-junction devices, respectively. With improved materials such as recently incorporated in TEL Solar's record module, stabilized efficiencies above 14% in triple-junction configuration and up to 15% for quadruple-junction devices should be attainable on cell level. Simulations for quadruple-junction devices have shown efficiencies up to almost 20% [3], but such efficiencies require the fabrication of excellent and highly stable materials with four different band gaps which has not been demonstrated yet. For the moment we believe that triple-junction cells in which the upper two cells consist of amorphous silicon and the bottom two cells of microcrystalline silicon have the highest efficiency potential for the short- and mid-long term. The incorporation of an excellent intermediate reflector between the second and third cell, such as already demonstrated for tandem devices [4], will also be indispensable.

[1] J.-W. Schüttauf *et al.*, IEEE J. Photovolt. 4 (2014), 757.
[2] J.-W. Schüttauf *et al.*, Sol. Energy Mater. Sol. Cells 133 (2015), 163.
[3] O. Isabella *et al.*, Sol. Energy Mater. Sol. Cells 129 (2014), 82.
[4] M. Boccard *et al.*, IEEE. J. Photovolt. 4 (2014), 1368.

ID 177 - Oral

Nanoparticles embedded in hydrogenated amorphous silicon thin layers

**Z. Remes[1], J. Stuchlik[1], T. H. Stuchlikova[1], A. Purkrt[1], R. Fajgar[2], V. Drinek[2], K. Zhuravlev[3], N. G. Galkin[4]*
[1]Institute of Physics, Praha 6, Czech Republic
[2]Institute of Chemical Process Fundamentals CAS, v. v. i., Praha 6, Czech Republic
[3]Rzhanov Institute of Semiconductor Physics, Siberian Branch of the Russian Academy of Sciences, Novosibirsk, Russian Federation
[4]Institute of Automation and Control Processes, Far East Division of the Russian Academy of Sciences, Vladivostok, Russian Federation

Nanoparticles (NPs) embedded in the hydrogenated amorphous silicon (a-Si:H) thin layer modify its optoelectronic properties making this new nanocomposite material suitable for low cost, large area applications such as light emitting diodes (LED). The a-Si:H layer was grown on glass substrates at 250°C at the Institute of Physics in Prague by the radio frequency plasma enhanced chemical vapor deposition (CVD). The deposition of PbS and CdS nanoparticles on a-Si:H surface was achieved ex-situ at the Rzhanov Institute of Semiconductor Physics in Novosibirsk using Langmuir-Blodgett technique. The Reactive Deposition Epitaxy (RDE) in the ultra high vacuum (UHV) chamber was used ex-situ at Institute of Automation and Control Processes in Vladivostok to deposit metal(Mg, Ca, Cr)silicide nanoparticles. Various NPs were also formed in-situ by vacuum evaporation (VE) followed by plasma treatment and by the reactive laser ablation (RLA). The selection of target material, substrate temperature, presence of a background gas, plasma treatment, energy in laser pulse et. give many possibilities how to influence the size and quality of the deposited NPs.

We show how the embedded nanoparticles enhance the optoelectronic properties of thin layers such as optical absobance, the photoluminescence in the visible and near infrared region etc. We evaluate the activation energy of electrical conductivity by the temperature dependence of electrical conductivity (Arrhenius plot). The absorption coefficient is measured by the constant photocurrent method (CPM) and photothemal deflection method (PDS). The Raman spectroscopy is applied for the assessment of the structure of the deposited layers, the electron scanning microscopy (SEM) to visualize the surface and NPs. For the characterization of multilayer diode structures, it is indispensable to measure the I-V curves and the electroluminescence spectra. We acknowledge the projects MEYS KONTAKT II gr. nr. LH12236, pr. LD14011 (HINT COST Action MP1202) & the Czech Science Foundation project GA14-05053S

[1] J. Stuchlík et al., Deposition of Magnesium Silicide Nanoparticles by the Combination of Vacuum Evaporation and Hydrogen Plasma Treatment, JJAP Conf. Proc. 3 (2015) 011301-1 - 011301-5.
[2] Z. Remes et al., Infrared photoluminescence spectra of PbS nanoparticles prepared by Langmuir-Blodgett and laser ablation methods, Acta Polytechnica 54 (2014) 426 - 429.
[3] Z. Remeš et al., The optical spectra of a-Si:H and a-SiC:H thin films measured by the absolute photothermal deflection spectroscopy (PDS), Solid State Phenom. 213 (2014) 19 - 28.
[4] N. G. Galkin et al., Semiconducting CrSi2, Mg2Si and Ca2Si nanocrystallites for solar cells based on hydrogenated amorphous silicon on glass substrates, ICSS-Silicide2014, International conference and summer school on advanced silicide technology 2014, Tokyo University of Science,Katsushika Campus, Tokyo, Japan, July. 19 - 21, 2014
[5] The Ha Stuchliková et al., The Laser ablation as a perspective technique for the deposition of metal-silicide nanoparticles in situ embedded in PECVD of Si:H thin films, ICSS-Silicide2014, International conference and summer school on advanced silicide technology 2014, Tokyo University of Science,Katsushika Campus, Tokyo, Japan, July. 19 - 21, 2014

[6] The Ha Stuchlíková et al., Deposition of modified Si:H thin films with embedded silicide nanoparticles formed by the combination of Vacuum Evaporation and Plasma Treatment, ICSS-Silicide2014, International conference and summer school on advanced silicide technology 2014, Tokyo University of Science,Katsushika Campus, Tokyo, Japan, July. 19 - 21, 2014
[7] N. G. Galkin et al., Technological possibilities of Si:H thin film deposition with embedded cubic Mg2Si nanoparticles, phys. status solidi c 10 (2013) 1712 - 1716.

ID 178 - Oral

Multifrequency EPR studies on µc-Si:C:H films for photovoltaic applications

**O. Astakhov[1], L. Xiao[1], T. Chen[1], M. Fehr[2], B. George[2,3], A. Schnegg[2], K. Lips[2], C. Teutloff[3], F. Finger[1]*
[1]Forschungszentrum Jülich, IEK-5 Photovoltaik, Jülich, Germany
[2]Helmholtz-Zentrum Berlin für Materialien und Energie, Institut für Silizium-Photovoltaik, Berlin, Germany
[3]Freie Universität Berlin, Fachbereich Physik, Berlin, Germany

Microcrystalline silicon carbide alloys (µc-Si:C:H) have attracted attention for photovoltaic applications as a window layer for thin film silicon or crystalline silicon heterojunction solar cells thank to the combination of high transparency and high conductivity. The electrical conductivity of µc-Si:C:H depending on deposition conditions may vary over a very wide range from 10^{-14} S/cm to 1 S/cm without intentional doping and has n-type character. This puzzling behavior suggests unintentional background doping to affect the electronic properties of µc-Si:C:H but the donor has not been identified so far. The films of µc-Si:C:H usually exhibit a high density of paramagnetic centers (10^{18}-10^{19} cm^{-1}) which makes electron spin resonance to be a suitable characterization technique for the electronic properties of this material. Application of EPR is of particular interest for the possible identification of dopants via the hyperfine signature of the paramagnetic dopant states. EPR spectra measured in µc-Si:C:H films deposited over a variety of conditions indeed often show presence of hyperfine-like satellites on the shoulders of the main resonance line at g ≈ 2.003. Neither the central line nor the satellite lines have been clearly identified so far. It has been suggested however that the hyperfine structure may be related to nitrogen impurities. In our study we applied X-band continuous wave EPR, S-band, X-band and Q-band pulsed EPR and ENDOR experiments to resolve the structure of the EPR spectra in µc-Si:C:H and identify spin active impurities in the material tissue. The material was prepared with hot wire chemical vapour deposition from gas mixtures of monomethylsilane with hydrogen at filament temperature of 2000 - 2100 °C and substrate temperature of 250-270 °C on sacrificial metal substrates. The substrates were removed and the material sealed in quartz EPR tubes. It was found that the central line consists of at least two resonance components at g=2.0038 and 2.0027 whereas the satellite structure is a hyperfine pattern related to hydrogen atoms. Therefore formerly proposed interpretation of the satellites as a hyperfine pattern related to nitrogen is disproved. The results of the study contribute to further understanding of the electronic properties of µc-Si:C:H in combination with available and upcoming data on the structure of µc-Si:C:H alloys.

ID 179 - Poster

Influence of AlN crystallinity on SAP waveguides

*M. E. Armas Alvarado[1], E. Gonçalves de Melo[1], I. Pereyra[1], M. I. Alayo Chavez[1]
[1]University of Sao Paulo, Sao Paulo, Brazil

In this work, a comparison between self-aligned pedestal (SAP) optical waveguides utilizing as core layer either highly c-axis oriented or amorphous Aluminum Nitride (AlN) films is presented. The aim of this work is to study the influence of the AlN films crystallinity in the optical characteristics of the waveguides.

The fabrication of a pedestal optical waveguide utilizes an easier procedure compared to the rib waveguide fabrication once it avoids the etching of the core layer, facilitating in this way the utilization of new materials. [1,2].

For the fabrication of these devices, a 0.3µm-thick AlN film was deposited by RF reactive Sputtering technique using a 99.999% purity aluminum (Al) target, and Argon (Ar) and nitrogen (N_2) were used as sputtering and reactive gas, respectively. A related work has found the best parameters to achieve the minimal intrinsic stress, which were used in the present work [3]. The pedestal profile is geometrically defined by etching the thermally grown silicon dioxide lower cladding - before depositing the AlN core layer - using conventional photolithography procedures, followed by plasma etching using CHF_3 and O_2 as reactive gases.

Optical losses characterization were measured in these devices using the top-view technique [4] at a wavelength of 633 nm for pedestal heights of 1.2 µm and with widths varying from 1 to 100 µm. The expected eigenmodes and transmission spectra of these waveguides were also calculated by means of tridimensional simulation techniques. AlN films were examined by X-ray diffraction (XRD) measurements to determine their crystalline structure. Additional characterization techniques such as FTIR spectroscopy and ellipsometry were also used.

[1] Fabrication and characterization of aluminum nitride pedestal-type optical waveguide, M.A. Alvarado, M.V. Pelegrini, I. Pereyra, T.A.A. de Assumpção, L.R.P. Kassab, M.I. Alayo, Canadian Journal of Physics, 2014, 92:951-954, 10.1139/cjp-2013-0587.
[2] Single polarization transmission in pedestal-supported silicon waveguides ,J. Cheng, W. Zhang, Q. Zhou, Y. Wang, Y. Huang, J. Peng, Optical Letters 36 (2011) 1797.
[3] Deposition and characterization of AlN thin films obtained by radio frequency reactive magnetron sputtering, M.V. Pelegrini, M.A. Alvarado, M.I. Alayo, I. Pereyra, Canadian Journal of Physics, 2014, 92:940-942, 10.1139/cjp-2013-0556,
[4] Comparison among various Si_3N_4 waveguide geometries grown within a CMOS fabrication pilot line, Daldosso, N.; Melchiorri, M.; Riboli, F.; Girardini, M.; Pucker, G.; Crivellari, M.; Bellutti, Pierluigi; Lui, A.; Pavesi, Lorenzo, , *Lightwave Technology, Journal of* , vol.22, no.7, pp.1734,1740, July 2004

ID 180 - Oral

Low temperature formation of epitaxial emitter by RF-PECVD using SiF_4/H_2/Ar gas mixtures

*R. Léal[1,2], J.- C. Dornstetter[2], F. Haddad[2], G. Poulain[1], J.- L. Maurice[2], P. Roca i Cabarrocas[2]
[1]TOTAL, Palaiseau, France
[2]Ecole Polytechnique, Palaiseau, France

Thermal stress induced during solar cell manufacturing is responsible for cracks formation in wafers and, in turn, for a reduction of manufacturing yield. This effect is even more critical with thin wafers. Thus, if photovoltaic industry expects to reduce production costs by using thinner wafers, it needs to develop low temperature processes.

Here, we investigate the possibility of replacing the standard high temperature diffusion process by the deposition of a doped silicon epitaxial layer at temperatures below 200°C by radiofrequency (RF) plasma-enhanced chemical vapor deposition (PECVD). Epitaxy in such conditions has already been achieved by using standard silane chemistry. It has been integrated in a homo-hetero junction by Labrune et al. [1] to reach an efficiency of 14.2% but also by inserting a thin highly-doped crystalline layer in heterojunction solar cells [2]. However in spite of a theoretical higher efficiency for the latter [3], it has not yet shown any efficiency improvement. This has been attributed to recombination within the epitaxial layers and at the emitter surface. In this study we explore the SiF_4/H_2/Ar chemistry for epitaxial growth, motivated by high quality µc-Si thin film solar cells obtained using these specific gas mixtures [4].

We obtained a few microns of high quality epitaxy demonstrated by X-ray diffraction (not shown here), where the contribution of the epitaxial layer is very close to the one of the parent wafer and most importantly, a very clean interface between the wafer and the epitaxial layers, as shown by the HRTEM image in Fig. 1. Interestingly, we found that in order to perform epitaxy on c-Si substrates, the plasma conditions have to be tuned to those used for amorphous deposition on glass, where hydrogen is totally depleted in the plasma [4]. We are currently studying phosphorous doping of these layers: an epitaxy breakdown occurs as the PH_3 flow rate increases, as shown in ellipsometry spectra from Fig. 2. However for PH_3=0.5 sccm (minimum flow rate), the good fit of the ellipsometry data obtained with layers composed of 100% poly-Si (large grains poly-Si ellipsometry reference from Jellison) and a roughness of 4 nm, shows that we are already able to deposit n-doped poly-Si. A higher dilution of PH_3 should give better results.

Epitaxial layers grown by RF-PECVD using SiF_4/H_2/Ar have a great potential for manufacturing crystalline solar cells with low temperature processes keeping high efficiency. Problems of doping should be handled by reducing PH_3 gas concentration. Once doped epitaxial layers will be achieved, homojunction solar cells will be manufactured.

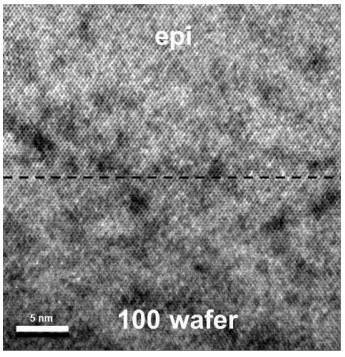

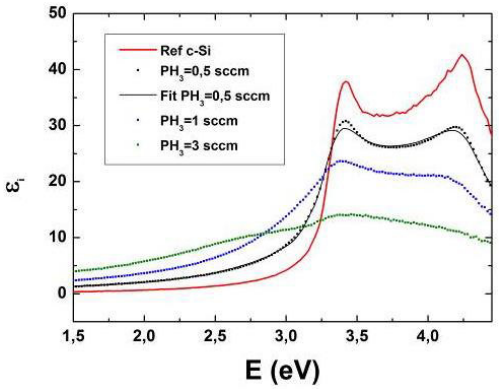

[1] M. Labrune et al., *Thin Solid Films*, 2010.
[2] B. Hekmatshoar et al., *Appl. Phys. Lett.*, vol. 101, no. 10, p. 103906, Sep. 2012.
[3] T. Carrere et al., *J. Renew. Sustain. Energy*, vol. 7, no. 1, p. 011202, Jan. 2015.
[4] J.C. Dornstetter et al., *J. Chem. Phys.*, 2014.

ID 181 - Oral

Drift in Amorphous Chalcogenides: Challenge and Opportunity for Novel Computing Architectures

*M. Salinga[1]
[1]RWTH Aachen University, Aachen, Germany

Memories based on so-called phase change materials are considered to be a highly promising next generation technology. The unique set of properties of those materials enables fast, reliable and durable, non-volatile memory. Research groups have demonstrated an excellent scaling behaviour of phase-change memory and several large-scale memory chips have been produced already demonstrating the outstanding potential of the technology.

However, success in commercializing phase change memory depends on the realization of a crucial feature: multi-level storage, i.e. the representation of several bits of information by multiple distinct levels of resistance in a single memory cell. The major obstacle for this is the resistance increase over time observed in the amorphous state.

It is therefore crucial to understand this temporal decrease of conductivity in amorphous phase change materials on a fundamental level.

To this end different types of phase change materials, i.e. GeTe, GeSbTe and AgInSbTe, are experimentally investigated with respect to the temporal evolution of their low-field resistivity and their dielectric function in the infrared-range. Also the field-dependence of their conductivity is determined and photo-conductivity is measured. The systematic variation of temperature adds another valuable dimension to all investigated physical properties.

A comparative analysis of this comprehensive set of experimental data shows where similarities in the behaviour of different material give rise to general explanations for the drift of the electronic properties. At the same time, the observed discrepancies set clear limits to attempts of farther-reaching generalization implied by literature and instead display the complexity of relaxation effects in these disordered solids.

In conclusion, the experimental evidence on drifting electronic properties in these amorphous semiconductors is discussed with respect to its meaning for novel computing systems including neuromorphic hardware.

ID 182 - Oral

Influence of inhomogeneities on the low-temperature photoluminescence spectra of microcrystalline silicon

*S. Burdorf[1], *R. Brüggemann[1]*
[1]Carl von Ossietzky Universität Oldenburg, Institut für Physik, Oldenburg, Germany

Photoluminescence (PL) from semiconductors can be related with the quasi-Fermi level splitting of the electron-hole-ensemble from which the radiation originates. In microcrystalline silicon solar cells the Jülich group has successfully compared the temperature dependence of the photoluminescence [1,2] with the open-circuit voltage for temperature larger than 100 K. Extending the range to lower temperatures, we have measured quantitative photoluminescence from microcrystalline silicon thin films on quartz between 20 K and 140 K upon excitation with a green laser beam. For the interpretation of the temperature-dependent µc-Si:H PL Planck's generalized law is extended and applied to describe the radiative recombination via band-tail states. This substantial refinement of existing approaches allows for the modeling of temperature-dependent spectra over the entire measured temperature range and furthermore provides access to the quasi-Fermi level (qFL) splitting of electron-hole ensembles in the thin film and furthermore yields quantitative information on band-tail energies.

In crystalline silicon where an increase in the quasi-Fermi level splitting causes only an increase in the overall PL-intensity, while the spectral shape of the spectrum is unaffected. In contrast, the PL-spectra of µc-Si:H differ with varying qFL-splitting both in intensity and shape. Here, the temperature is also an important parameter. The temperature dependence of the experimental PL-spectra cannot be reproduced in a simple modelling approach assuming a constant qFL-splitting to generate a spectrum. For this purpose, the values of the input parameters for the theoretical treatment like density-of-states have been chosen in relation to the structural properties of µc-Si:H. Only by introducing variations of qFL-splitting to represent inhomogeneity in the µc-Si:H film and constructing an overall PL-spectrum that is a superposition from excitation states with different qFL-splittings, the experimental temperature-dependent PL spectra from µc-Si:H can be reconstructed for the entire temperature range. Possible origins of these variations in qFL-splitting are discussed.

1. Merdzhanova, T., Carius, R., Klein, S. & Finger, F., J. Optoelectronics and Advanced Materials 7, 485-489 (2005).
2. Pieters, B., Kirchartz, T., Merdzhanova, T. & Carius, Solar Energy Materials and Solar Cells 94, 1851-1854 (2010).

ID 183 - Oral

Microcrystalline Silicon Photodiode for Near Infrared Light Detection

*A. Khosropour[1], A. Sazonov[1]
[1]University of Waterloo, ECE, Waterloo, Canada

For large area electronics near-infrared (NIR) sensing applications such as display touch sensors and biomedical tissue analysis, microcrystalline silicon photodiode is proposed due to its high absorption coefficient in NIR region. Here, we report on fabrication of a microcrystalline silicon n-i-p photodiode on a glass substrate at temperature of 180 °C with external quantum efficiency (EQE) of 11% at the wavelength of 850 nm. The obtained EQE is almost 3 orders of magnitude higher than the typical EQE value of 0.01% in previously reported amorphous silicon photodiodes at the same wavelength. Our 500µm×500µm microcrystalline silicon photodiodes show dark current of 2.7 nA and photocurrent of 550.9 nA at the wavelength of 850 nm and incident power density of 2.85 mW/cm^2 measured under reverse bias voltage of -1 V resulting in photo/dark current ratio (dynamic range) of 260. The dynamic range of operation of our device is similar to that of hydrogenated amorphous silicon germanium (a-SiGe:H) NIR phototransistors [1]. Hence, microcrystalline silicon photodiodes are highly promising for large area NIR touch sensing applications. Fabrication process, device and pixel circuit design, and readout scheme will also be reported.

[1] Han, Sang Youn; Kyung Sook Jeon; Byeonghoon Cho; Mi Seon Seo; Junho Song; Hyang-Shik Kong, "Characteristics of a-SiGe:H Thin Film Transistor Infrared Photosensor for Touch Sensing Displays," Quantum Electronics, IEEE Journal of , vol.48, no.7, pp.952,959, July 2012.

ID 184 - Oral

Amorphous semiconductor mobility limits

**K. A. Stewart[1], B.- S. Yeh[1], J. F. Wager[1]*
[1]Oregon State University, School of EECS, Corvallis, Oregon, United States

There are more and more reports in the literature of amorphous oxide semiconductor (AOS) thin-film transistors (TFTs) that exhibit an (n-channel) mobility in excess of 100 $cm^2V^{-1}s^{-1}$. The highest AOS (nanocrystalline) mobility actually reported in the literature to date, as far as we know, is 285 $cm^2V^{-1}s^{-1}$ extracted from TFT measurements. However, we are aware of papers submitted for publication in which a mobility in excess of 400 $cm^2V^{-1}s^{-1}$ is claimed. In our opinion, this is ***nonsense***.

We believe that these erroneous mobility claims are a consequence of measurement artifacts associated with employing a leaky gate insulator, not properly accounting for hysteresis, peripheral current flow in an unpatterned-channel TFT, depletion-mode operation, and/or simple incorrect calculation of the mobility.

In order to attempt to restore a bit of rationality into the discussion of AOS TFT mobility, we will present very simple considerations in which we estimate the absolute maximum n-channel (p-channel) mobility to be ~75 $cm^2V^{-1}s^{-1}$ (~15 $cm^2V^{-1}s^{-1}$). However, we also point out that these absolute maximum mobilities are essentially inaccessible in a real TFT structure such that practical upper mobility limits are more likely in the range of ~50 $cm^2V^{-1}s^{-1}$ (~1 $cm^2V^{-1}s^{-1}$) for n-channel (p-channel) operation.

Although these mobility limit estimates were formulated with amorphous oxide semiconductors in mind, we believe that these limits pertain to any class of amorphous semiconductors. General amorphous semiconductor mobility trends will be discussed in the context of covalent and ionic bonding character of the given amorphous semiconductor.

ID 185 - Oral

Deposition and characterization of BST thin films for RF MEMS applications

*M. V. Pelegrini[1], I. Pereyra[1]
[1]University of Sao Paulo, São Paulo, Brazil

The use of ferroelectric materials for applications in tunable devices dates back over 50 years. However, due to the continuous miniaturization of the microwave devices, usually aiming production cost reduction and integration with semiconductor microelectronics, several efforts have been made in the last few years. Among the ferroelectric materials, barium strontium titanate ($Ba_xSr_{1-x}TiO_3$), hereinafter called BST, is one of the most studied materials due to its large electric field tunability, low dielectric loss and the possibility of changing its electrical properties according to the deposition parameters. These characteristics make BST thin films very attractive for the fabrication of passive devices such as phase shifters, oscillators, tunable filters and high-*Q* resonators for communication and radar applications up to 65GHz.

The production of competitive BST based microwave devices generally lies on a material with both high electric field tunability and low dielectric losses. Nevertheless, the production of a material with both properties is very challenging, and often adds production complexity and incompatibility with standard microelectronic process. Another technological issue in the microwave component fabrication employing BST is its deposition on a metal electrode. Due to the high temperature and oxygen atmosphere generally employed on the BST deposition, platinum is one of the most popular electrodes, widely reported in the literature. However this noble material presents thickness and cost limitations. Numerous base metals also can be used as electrodes, significantly reducing the cost (compared with noble metals). Among them, copper has been presented as a good electrode candidate due to its low cost, relative easiness to deposit by low cost processes such as thermal evaporation and electrodeposition, and its high conductivity at microwave frequencies.

In this work BST thin films are produced by RF Sputtering, to be used as tunable element in intelligent phase shifters as shown in figure 1. The basic concept of this device lies on a CPW, where its phase velocity (Vf) and impedance (Z) can be defined by:

$Vf=1/(L*C)^{1/2}$

$Z=(L/C)^{1/2}$

where *L* and *C* are the inductance and capacitance per unit length respectively of the s-CPW, which are directly associated to the material under the waveguide. A more detailed explanation of the device can be seen on its patent [1]. Thus the greater the BST electric permittivity variation the greater the phase variation is. However this change in permittivity also leads to a high impedance mismatch with the other components in the microwave device, such as antennas, splitters and so forth, which generally operate at 50 Ω.

The main focus of this work is to understand and correlate the sputtering deposition parameters to the BST thin film properties deposited directly on copper. Series of samples were prepared varying the Ar and O_2 gaseous mixture, deposition temperature and power density. X-ray diffraction and Rutherford backscattering spectrometry will be performed to physical characterize the material.

The electrical field tunability at 1MHz was already characterized, as seen at figure 2, using parallel plate capacitor. This characterization demonstrates a tunability of 1.25, which is low when compared with the literature, however, as mentioned before, no impedance mismatching with other microwave devices is desired.

In this work the electrical field tunability and dielectric loss at the GHz range using the BST in a well-known microstrip transmission line is reported.

[1] P. Ferrari and G. Rehder, “Ligne de transmission haute fréquence accordable,” Patente internacional n°. WO/2012/032269, Data da publicação 15.03.2012.

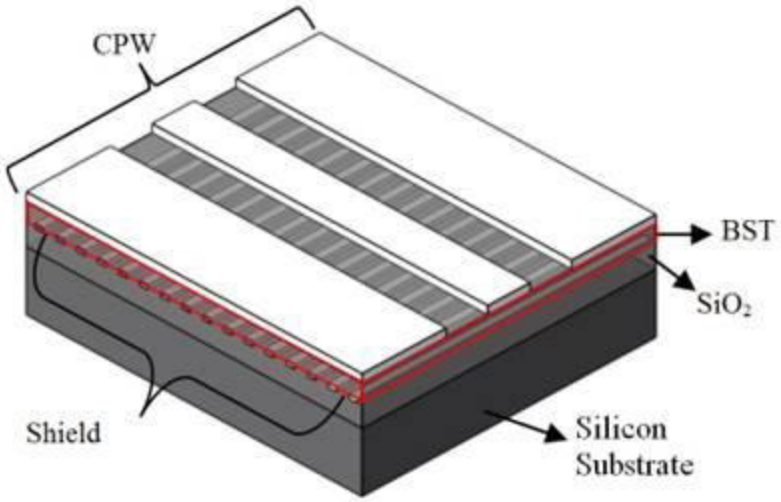

Figure 1 – Ilustration of the phase shifter based on a shielded coplanar waveguide using BST as tunable element.

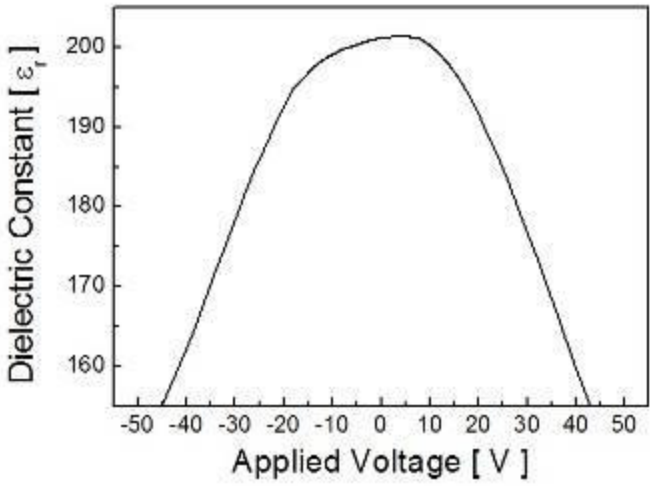

Figure 2 – Electric field tunability at 1MHZ of a parallel plate capacitor fabricated using BST as dielectric.

ID 186 - Oral

Light induced degradation of organic semiconductors - understanding atomistic origins and pathways

*S. Shah[1], *R. Biswas[2]*
[1]Iowa State University, ECpE, Microelectronics Res Ctr, Ames, IA, United States
[2]Iowa State University & Ames Lab, Physics, Ames, IA, United States

One of the most common and widely studied features of amorphous semiconductors is light induced degradation and metastability, typified by the well-known Staebler-Wronski (SW) effect in a-Si:H. Recent experimental studies have observed analogous light induced effects in organic semiconductors, exemplified by light induced degradation of organic solar cell (OSC) characteristics when light soaked in ambient atmosphere. Under light exposure, OSC's demonstrate a continuously decreasing short circuit current (Jsc), open circuit voltage (Voc) and fill factor, with correspondingly increasing densities of states in the gap region.

We seek to understand the fundamental atomistic mechanisms underlying the light induced degradation process in such organic semiconductors, and compare their behavior with amorphous silicon. We focus on the prototypical low band gap donor material PTB7, commonly used in higher efficiency OSCs composed of the donor-acceptor blend PTB7:PCBM71. Since photon absorption occurs in the donor, light induced structural changes in the donor are most likely. As is typical of many organic donors PTB7 consists of an aromatic backbone connected to alkyl chains with bridging oxygen atoms. We utilize ab-initio density functional simulations to elucidate low energy structural rearrangements that can be accessed by light absorption. Two very interesting and unexpected defect pathways are found involving O- and H- induced motion. In the first pathway, local motion of the bridging O atom can occur leading to a defect configuration where the O rebonds within the aromatic backbone, with an defect energy of 2.1 eV and an energy barrier of 2.6 eV, accessible to blue photons. Two C-O bonds in the C-O-C are replaced by the double C=O bond, leaving a C dangling bond with gap states. The formation of gap states agrees with measurement of OSC's. In another defect pathway a H can move from the βC site of the alkyl chain to the αC site of the alkyl chain causing a C=O formation, and C dangling bond formation with gap states, accompanied by cleaving of the polymer. Defect energy is 2.2 eV. Bridging O atoms in the polymer are a central source of instability. The defect energies can also be lowered in the presence of electronic excited states. We examined annealing of these defect states and find annealing can be reversible (as in the SW effect) or irreversible to distorted states - which is a departure from SW effect. While the local motion of H has many analogies proposed for metastabililty in a-Si:H, the role of O is quite different. We compare the defect formation and annealing with experimental light soaking measurements on OSC's and contrast it with the SW effect.

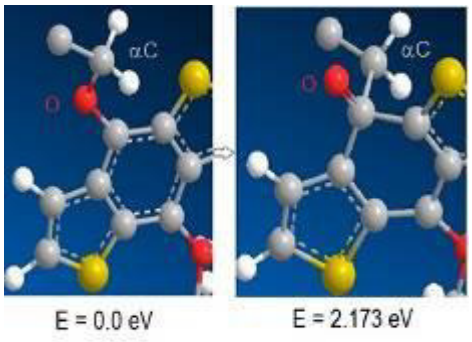

ID 187 - Poster

Electronic Conduction and Resistive Switching of Metal-Insulator-Metal Devices based on Ultra-Thin HfO_2 after Thermal Annealing

**J. Molina[1], R. Valderrama[1], C. Zuniga[1], W. Calleja[1], F. J. De La Hidalga Wade[1], P. Rosales[1], A. Torres[1]*
[1]National Institute of Astrophysics, Optics and Electronics, Electronics, Tonantzintla, Mexico

Metal-Insulator-Metal (MIM) structures based on ultra-thin hafnium oxide with different annealing process were fabricated at low temperatures (low thermal budgets). Their electronic conduction mechanisms and resistive switching characteristics are both compared in order to determine the role of specific temperature and atmosphere conditions of the annealing process on better performance characteristics of these non-volatile emergent memory devices.

For fabrication of these MIM structures, sequential deposition of Al/HfO_2/W staked thin films was done on n-type silicon wafers with resistivity of 5-10 Ω•cm. Tungsten was used as bottom electrode (BE) with 200 nm in thickness and deposited by E-beam evaporator (Temescal BJD-1800 from Edwards) under ultra-high vacuum conditions. After BE deposition, 4 nm of HfO_2 were deposited directly on this metal by ALD (Savannah-S100, from Cambridge Nanotech) at 250°C using H_2O and TDMAH (preheated at 75°C) as chemical precursors. Right after ALD of stoichiometric HfO_2, all the samples were immediately moved back to the e-beam evaporator in order to deposit 400 nm of aluminum which is then used as top electrode (TE). A lithography step was used in order to define devices with area of 3.6e-5 cm^2. After lithography, two annealing conditions were performed on the final MIM devices. First, one sample was subjected to thermal treatment in pure N_2 at 300°C for 60 minutes. A second sample had a thermal treatment in Forming-Gas (H_2/N_2) at 475°C for 30 minutes. A third sample was used as reference; so that no thermal treatment was executed on it (as-deposited sample). Electrical characterization was done using a Semiconductor Device Analyzer (SDA, 2400 from Keithley) in order to obtain capacitance-voltage (C-V at 100 kHz), current-voltage (I-V) and current-voltage-time (I-V-t) characteristics for each MIM structure (at room temperature).

Figure 1 shows the resistive switching characteristics of MIM structures with and without annealing process. Only the first ten resistive switching cycles for each condition are shown. As-prepared sample (left plot) operates in bipolar mode, thus any SET condition, from high resistance state (HRS) to low resistance state (LRS), occurs at positive bias (+1.2V), and all RESET conditions, from LRS to HRS, occur at negative bias (-1.2). Samples annealed in N_2 at 300°C (center plot) show a HRS®LRS transition occurring at higher gate voltages and very low currents, thus allowing wider resistance windows (~2.5 orders of magnitude at +2V). However, large I-V dispersions are observed for the RESET condition. The samples annealed in H_2/N_2 (right plot) have switching characteristics with multiple variations for both SET and RESET. Even though there are some variations in the resistive switching characteristics for all samples, we notice that an exposure of the MIM structure to thermal annealing (in pure N_2 or forming gas) increases both the voltages required for the SET/RESET conditions which is important in order to enhance the endurance characteristics (large voltage windows during continuous SET/RESET cycles) of these devices. For both thermal annealing conditions, the electron conduction mechanisms prior to the transition events during the SET/RESET conditions, also play an important role in order to obtain more uniform conduction characteristics and this is directly related to the resistive switching properties of both devices.

Specific temperature and atmosphere conditions during annealing will directly impact the memory device performance. For the H_2/N_2 annealing, it is thought that a reduction in the concentration of oxygen vacancies (Vo^+, participating in SET/RESET conduction processes) could reduce proper uniformity in the resistive switching characteristics of the MIM devices because of the passivation of Vo^+ by hydrogen. For a N_2 based annealing, more uniform switching conditions are observed only for the SET conditions and this is related to a gradual densification of the HfO_2 film and its interfaces generated at both top and bottom metal electrodes. The electronic conduction mechanisms also play an important role for proper

definition of the SET and RESET conditions in all samples.

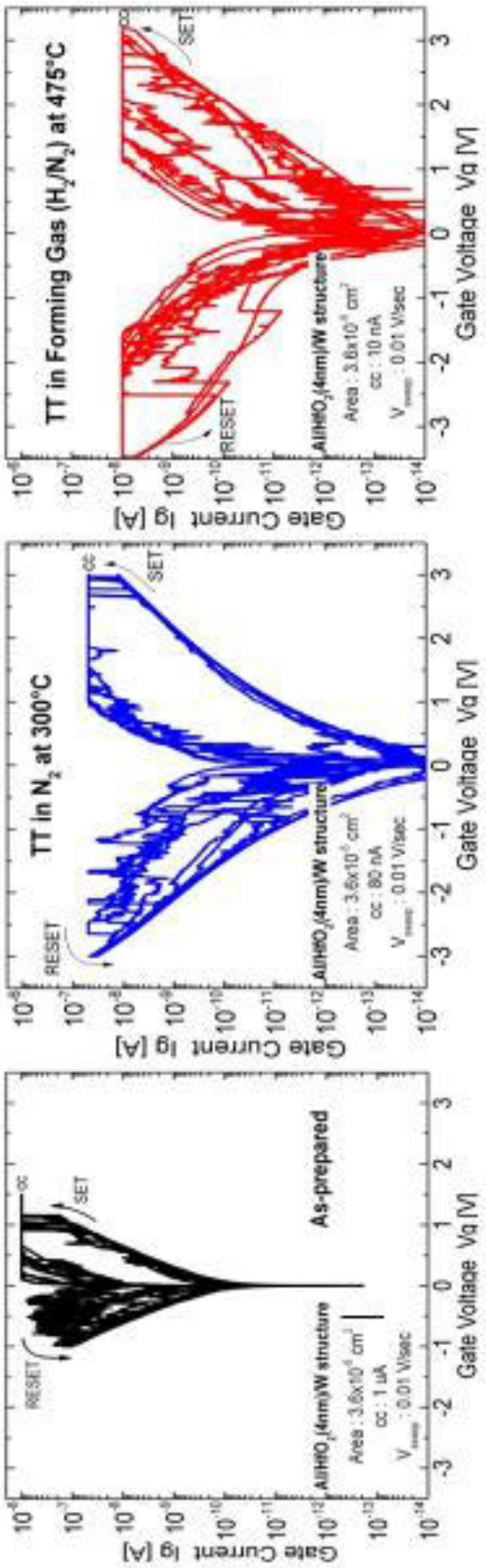

ID 188 - Poster

Determination of gap-states distribution in Cl doped a-Se from transient photocurrents using Laplace transform technique

**M. L. Benkhedir[1], F. Serdouk[1]*
[1]Larbi Tebessi university, Sciences de la matiére, Tebessa, Algeria

Amorphous selenium (a-Se) is used as a photosensitive material in direct digital X-ray imaging and HARP vidicon tubes [1], it was the material of choice in xerography. Because Pure a-Se has a low glass transition temperature of some 40 ◦C, applications make use of so-called stabilized a-Se which contains 0.2-0.5% As and 10-20 ppm of Cl. Cl is added to recover an undesirable decrease in the hole lifetime that accompany the introduction of As in the a-Se lattice [2]. The DOS above the valence band edge in pure a-Se consists of a shallow defect level at ~0.25 eV above Ev and a defect level at ~0.45 eV. The shallow one is connected to a change in the dihedral angle while the deeper is the D^- center in the negative-U model [3]. These image of the DOS is built, essentially, on the transient photoconductivity, TPC and TOF, Cl doping of a-Se in the limit of 20 ppm suppresses the shallow defect and decreases the deep one [4]. This was deduced using the pre-transit technique to interpret the TPC traces, however, Marshall [5] has shown that this technique miscalculates the energy positions of the defects. To solve this problem, the TPC traces in [4] are studied using the high resolution Laplace transform method [7-8]. It was found that the shallow defect level decreases at 12.5 ppm doping with Cl and disappears for 20ppm Cl doping of a-Se. The deep level decreases with Cl doping, the energy position of the defect levels are almost the same as found using the pre-transit technique. The results are used to explain how the Cl recovers the decrease in hole life time that accompanies As doping of a-Se. The decrease of hole life time in As doped a-Se is due to gain of importans of the deep defect level when the shallow one is suppressed while the recovering by Cl Doping is due to decrease of the deep defect level density.

[1] J.A. Rowlands and S.O. Kasap. Phys. Today, **50**, 24 (1997).
[2] S. O. Kasap and C. Juhasz, Photogr. Sci. Eng. **26**, 239 (1982).
[3] M L Benkhedir, M Brinza, G J Adriaenssens and C Main J. Phys.: Condens. Matter **20** 215202 (2008).
[4] M. L. Benkhedir, M. Mansour, F. Djefaflia, M. Brinza and G. J. Adriaenssens Phys. Status Solidi B **246**, 1841-1844 (2009).
[5]J. M. Marshall,C. Main,NATO Science for Peace and Security Series B. Physics and Biophysics, 49-58(2009).
[7] N. Ogawa, T. Nagase and H. Naito, J. Non-Cryst. Solids, **266-269**, 367-371 (1998).
[8] F. Serdouk and M. L. Benkhedir, Physica. B. **459**, 122-128 (2015).

ID 189 - Poster

Nanoscale Analysis of Resonant Coupling to Waveguide Modes in Periodically Nanopatterned Thin-Film Solar Cells

*U. W. Paetzold[1,2], S. Lehnen[1], K. Bittkau[1], U. Rau[1], R. Carius[1]
[1]Forschungszentrum Jülich GmbH , Institute of Energy and Climate Research - Photovoltaics (IEK-5), Jülich, Germany
[2]IMEC v.z.w, Leuven, Germany

In order to advance the widespread of photovoltaic technologies, production and material cost of solar cells need to decrease and energy conversion efficiencies need to increase. For both reasons, advanced light-trapping concepts in solar cells are essential since they increase the absorption of incident sunlight in optically thin absorber layers. In the last decade, the research on nanophotonic light-trapping concepts making use of periodic nanostructures such as photonic crystals, grating couplers or plasmonic gratings has experienced a vast development. These periodically nanopatterned devices exploit light coupling to leaky waveguide modes supported by the absorber layers of the thin-film solar cells.
In the past, the experimental analyses of light coupling to leaky waveguide modes in nanophotonic solar cells has been limited to macroscopic and indirect methods like angular dependent reflectance measurements or external quantum efficiency measurements. In a recent publication, we have presented a new method that enables direct nanoscopic experimental observations of light coupling to individual leaky waveguide modes enhancing light trapping in nanophotonic solar cells [1]. Applying a particular configuration of the scanning near-field optical microscopy (SNOM), we measure the electric field distribution with sub-wavelength resolution at the surface of thin-film solar cells. Thereby we presented the first direct experimental observation of light coupling to an individual leaky waveguide mode in a nanophotonic thin-film solar cell. We provide a self-consistent picture of resonant light coupling, increased photocurrent generation and improvement of the power conversion efficiency in a thin-film silicon solar cell. Beyond this, we present a new detailed study _based on this new method on the polarization dependence of the light coupling to an individual waveguide mode.

[1] U. W. Paetzold, S. Lehnen, K. Bittkau, U. Rau, and R. Carius, “Nanoscale observation of waveguide modes enhancing the efficiency of solar cells.,” Nano letters, vol. 14, no. 11, pp. 6599-605, Nov. 2014.

ID 190 - Poster

Development of perovskite solar cells with nanophotonic front electrodes for improved light incoupling

*U. W. Paetzold[1,2], W. Qiu[2], J. Poortmans[2,3,4], D. Cheyns[2]
[1]Forschungszentrum Jülich GmbH , Institute of Energy and Climate Research - Photovoltaics (IEK-5), Jülich, Germany
[2]IMEC v.z.w, Leuven, Belgium
[3]Katholieke Universiteit Leuven, ESAT-Electa, Leuven, Belgium
[4]Hasselt University, Hasselt, Belgium

The recent fast development of metal halide perovskite solar cells has induced a uniquely fast advancement of this technology. Today, three years after the first reported solid state perovskite solar cell, a maximum power conversion efficiency above 20% has been certified. Thus, despite the unresolved challenges, e.g., the possible low stability of the devices, this technology bears enormous potential. Perovskite solar cells combine uniquely excellent electrical and optical material properties. For organolead halide perovskite (CH3NH3PbI3) diffusion lengths above 100 nm have been reported. At the same time a sharp optical absorption edge at 1.55 eV with absorption depths below 350 nm is found. These material properties allow for close to optimal charge carrier collection even in optically thick absorber layers (≥300 nm). In consequence, perovskite solar cells do not rely strongly on light trapping. However, up to date, their light incoupling is not optimal and new anti-reflective front electrodes need to be developed.

In this contribution, we report on the development and successful implementation of nanophotonic front electrodes in solution processed perovskite solar cells. The nanostructured front electrodes were fabricated by sputtering the ITO front electrode onto a prepatterned transparent substrate. The nanostructures were replicated via the versatile and large-area compatible UV-nanoimprint lithography into a glass-like resist on a glass substrate. Due to the shallow geometry of the employed transparent and conductive nanopatterned front electrodes a straight forward integration into a solution-based baseline process was enabled. The nanophotonic electrodes yield a significantly improved light incoupling. Prototype methylammonium lead iodide perovskite solar cells show an improvement of 5% in short-circuit current density and an improvement from 9.6% to 9.9% in power conversion efficiency compared to the flat reference device. These results are confirmed by three-dimensional electromagnetic simulations.

[1] U. W. Paetzold, W. Qiu, F. Finger, J. Poortmans, and D. Cheyns. “Nanophotonic front electrodes for perovskite solar cells” Applied Physics Letters (accepted April 2015).

ID 191 - Oral

Spectral matching in high-voltage multi-junction thin-film silicon solar cells

*S. Reynolds[1], F. Urbain[2], *V. Smirnov[2]*
[1]University of Dundee, School of Engineering, Physics and Maths, Dundee, United Kingdom
[2]Forschungszentrum Juelich, IEK-5 Photovoltaik, Juelich, Germany

Multi-junction (tandem and triple) thin-film silicon solar cells offer increased PV conversion efficiencies over single cells, through improved utilization of the solar spectrum. However, the series electrical connection inherent in most stacked-cell designs dictates that the cell generating the smallest photocurrent will limit the current in the external circuit. As cells and modules are normally optimised under AM1.5G, variations in the solar spectrum due to weather, seasonal and diurnal effects will change the proportion of current generated by each sub-cell and lead to reduced 'outdoor' solar to electrical conversion efficiencies.

Previously [1, 2], we carried out computer simulations of spectrum matching in 'micromorph' tandem solar cells, comparing a series-connected two-terminal cell with a four-terminal cell in which both sub-cells were considered to be electrically independent. Current loss due to spectral mis-match in a two-terminal cell was found to be partially compensated by an increase in fill-factor, and the nett reduction in annual electrical energy generation, relative to the four-terminal cell, amounts to around 2% under northern European conditions. The present work extends these studies, to investigate spectral dependence in tandem- and triple-junction cells developed to provide increased voltage output for photoelectrochemical (PEC) applications [3, 4].

The simulation utilises a semi-empirical model, with the overall J-V curve obtained by simultaneous solution for each sub-cell under equal-current conditions. Realistic spectral weightings are included through a wavelength-dependent scaling factor applied to the AM1.5G spectrum. To estimate the 'outdoor' efficiency, a statistical distribution of contributions to the total annual electrical energy yield as a function of spectral quality, expressed in terms of average photon energy, is used. The effects of light-induced degradation on the output from multi-junction cells, and differences in maximum power and optimum current matching scenarios, are also considered.

[1] S Reynolds and V Smirnov, *J. Phys.: Conf. Ser.* **398** 012006 (2012).
[2] S Reynolds and V Smirnov, to be presented at EMRS Spring Meeting (Lille, May 11-15 2015).
[3] F Urbain, K Wilken, V Smirnov, O Astakhov, A Lambertz, J-P Becker, U Rau, J Ziegler, B Kaiser, W Jaegermann and F Finger, *Int. J. Photoenergy* **2014** 249317 (2014).
[4] F Urbain, V Smirnov, J-P Becker, U Rau, F Finger, J Ziegler, B Kaiser and W Jaegermann, *J. Mater. Res.* **29** 2605 (2014).

ID 192 - Poster

Nano-photonic Organic Solar Cell Architecture for Advanced Light Trapping with Dual Photonic Crystals

*A. Peer[1], *R. Biswas[2]*
[1]Iowa State University, ECpE, Microelectronics Res Ctr, Ames, IA, United States
[2]Iowa State University & Ames Lab, Physics, Ames, IA, United States

Thin film organic solar cells have demonstrated rapidly increasing efficiencies, but typically absorb less than half of the incident solar spectrum. Absorber layer thicknesses are typically less than 200 nm, to achieve high carrier collection, resulting in incomplete light absorption particularly at longer red and near-IR wavelengths. To increase broad-band light absorption, we rigorously design experimentally realizable solar cell architectures based on dual photonic crystals using scattering matrix simulations.

We find an optimized architecture consists of a polymer microlens at the air-glass interface, coupled with a photonic-plasmonic crystal at the metal cathode on the back of the cell. The micro-lens focuses light on the periodic nanostructure that in turn generates strong diffraction of light. Wave-guiding modes and surface plasmon modes together enhance long wavelength absorption. The optimal architecture has a period of 500 nm for both arrays, resulting in absorption enhancement of 49% and photocurrent enhancement of 58% relative to the flat cell, for nearly lossless metal cathodes [1]. The enhanced absorption approaches the Lambertian limit. Misalignment between the two photonic crystals leads to about 1% loss of performance. Simulations incorporating experimental dielectric functions for metal cathode and ITO, using a real space methodology find the enhancement of 38% for the photocurrent and 36% for the weighted absorption, due to parasitic losses mainly in the metal cathode.

This solar architecture is particularly amenable for fabrication since it does *not* require spin coating of organic layers on corrugated surfaces, but instead requires nano-imprinting an organic layer, followed by metal cathode deposition. We will also discuss approaches for achieving patterning organic absorber layers. Our predicted enhancements also compare well with measurements on simpler microlens based structures, where absorber layers were not patterned. We will discuss higher efficiency donor materials as well. This dual photonic crystal architecture has great potential to achieve >12% efficient single junction organic solar cells, and to control photons by focusing light on nanostructures and plasmonic components.

[1] A. Peer, R. Biswas, Nano-photonic Organic Solar Cell Architecture for Advanced Light Trapping with Dual Photonic Crystals, ACS Photonics 1 (9), 840-847 (2014).

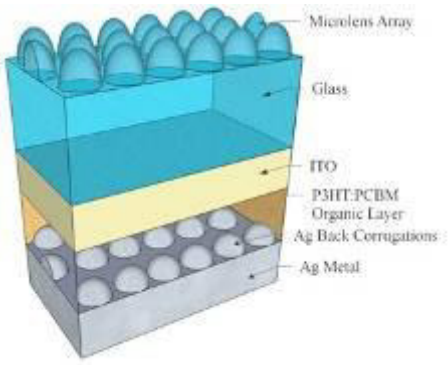

ID 193 - Oral

Electronic properties of CVD Graphene capped with p and n-type doped amorphous silicon

*A. Hakim[1], M. Boutchich[1], D. Alamarguy[1], F. Gunes [1], A. Madouri[1], J. Alvarez[1], P. R. i Cabarrocas[1], J.-P. Kleider[1], Y. Fei[1], Y. Hee Lee[1]
[1]Group of electrical engineering, Paris, Semiconductor Characterization and Modelling group (SCM), GIF SUR YVETTE, Korea, Republic of

There is a strong research effort to replace rare earth ITO (Indium Tin Oxide) with graphene transparent electrode in optoelectronic devices such as solar cells. To achieve this goal, the objectives are on one hand to reduce the resistivity of CVD (chemical vapour deposition) graphene and on the other hand to passivate the interface between graphene and a semiconductor[1][2]. A typical semiconductor indispensable in solar cell heterojunctions is amorphous silicon (a-Si:H). The question that arises is whether a heterojunction composed of CVD graphene and doped a-Si:H would compete with ITO? To address this question, we investigated the transport properties of one monolayer of CVD graphene encapsulated by n or p doped a-Si:H deposited by low temperature plasma CVD.

High quality large-area graphene was synthesized on copper substrates then transferred to (90nm) SiO_2/ Si substrate [3].To study the influence of a capping layer on the charge carrier transport in embedded graphene, 10nm of doped a-Si:H (n-type and p-type) were deposited onto the graphene by PECVD at 100°C. Subsequently, Hall bars were patterned using optical lithography, then Hall and four probe measurements were carried out to evaluate the sheet resistance, charge carrier density and Hall mobility of the encapsulated film. Moreover, confocal micro-Raman spectroscopy using 532 nm line was utilized to investigate the uniformity and the defect density of the graphene before and after a-Si:H deposition.

We observe a change in the carrier density of graphene measured on n and p-type a-Si:H. This yields to a sheet resistance of 1200 Ω/□ for capped graphene for n-type doped a-Si:H whereas it drops to 375 Ω/□ for p-type doped a-Si:H. We can conclude that although the change in carrier density is within the same order of magnitude, it is enough to substantially reduce the sheet resistance of graphene. Indeed, the mobility is more affected by n-type a-Si:H and this can be related to the surface defects. The mobility of graphene transferred on SiO_2 is μ= 1500 cm².V.s comparable to that of graphene capped with p-type a-Si:H. On the other hand, the mobility of graphene capped with n-type a-Si:H drops to μ= 600 cm².V.s. Raman spectroscopy shows that the defect density introduced by the a-Si:H plasma deposition onto graphene is larger under n-doped a-Si:H as indicated by the I_D/I_G ratio that is 0.4 as opposed to 0.2 for graphene under p-type a-Si:H. on the other hand the I2D/IG increases from 0.4 for the p-type a-Si:H to 1.8 for n-type a-Si:H. The increase observed on the p-type sample indicates that this sample has lost holes. Interestingly we note that no dominant scattering mechanism dominates the Hall mobility that remains stable across the whole temperature range (from room temperature down to 4K).

Electrical and Raman spectroscopy measurements have shown a significant difference between n-type and p-type a-Si:H doped silicon capped graphene. We show that graphene capped with p-type a-Si:H undergoes a limited holes transfer increasing its charge carrier density without affecting its mobility (about 1400 cm².V.s). The deposition of n-type a-Si:H on graphene results in a reduced holes density as observed on the I_{2D}/I_G ratio (1.8) ratio and Raman shifts compared to the I_{2D}/I_G ratio on SiO_2 (1.4) [4]. Nevertheless, it suffers from a large defect density as indicated by the I_D/I_G ratio. As a result, the mobility substantially decreases down to μ= 600 cm².V.s. Temperature Field effect transport measurements with heat treatment cycles to investigate the effect of crystallized a-Si:H (strain and electronic properties) on CVD graphene are underway and will be presented at the conference.

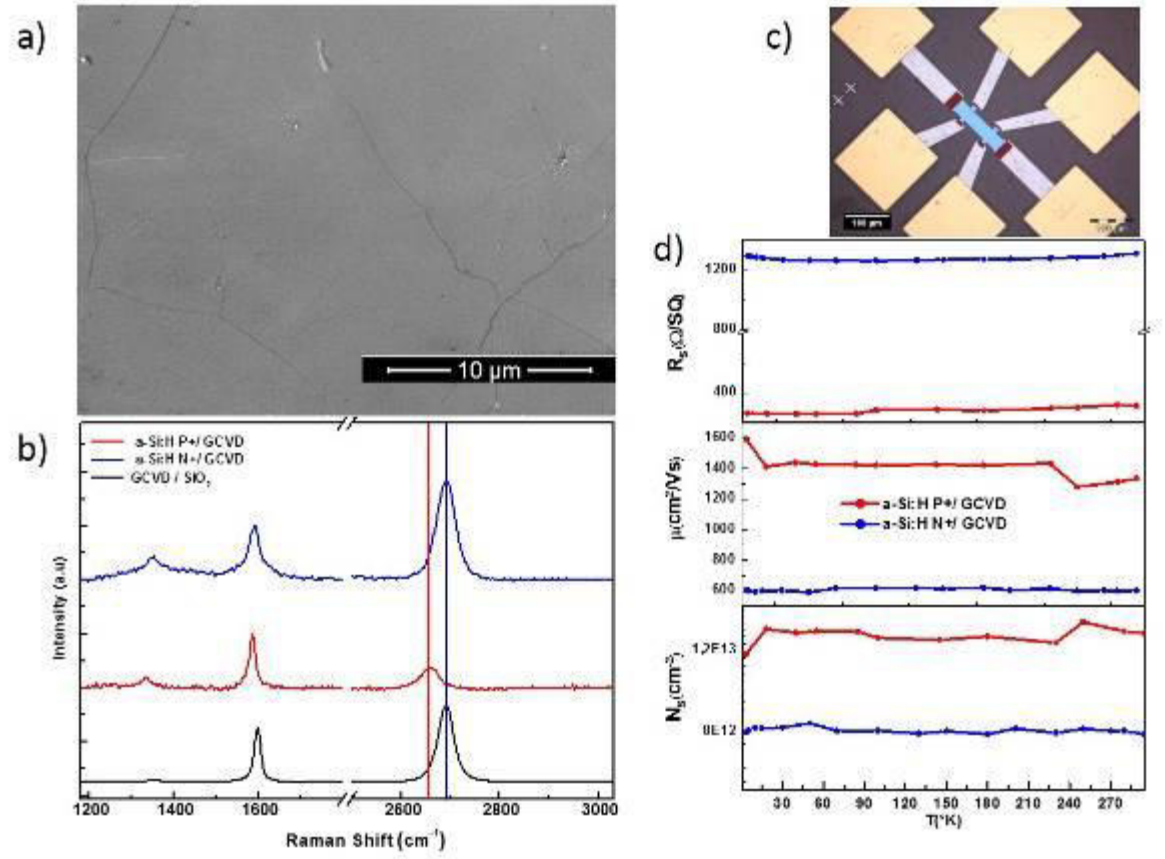

a) SEM image of graphene on SiO2/Si. b) Raman spectra of transferred graphene on SiO2/Si (pristine) and under p and n-type a-Si:H. c) Optical image of Hall bar of the test structure. d) Temperature dependence of sheet resistance, Hall mobility and charge carrier density of CVD graphene on a SiO2 capped with p and n-type a-Si:H.

[1] B.-J. Kim, C. Lee, M. A. Mastro, J. K. Hite, C. R. E. Jr, F. Ren, S. J. Pearton, and J. Kim, "Buried graphene electrodes on GaN-based ultra-violet light-emitting diodes," *Applied Physics Letters*, vol. 101, no. 3, p. 031108, Jul. 2012.
[2] M. A. Gluba, D. Amkreutz, G. V. Troppenz, J. Rappich, and N. H. Nickel, "Embedded graphene for large-area silicon-based devices," *Applied Physics Letters*, vol. 103, no. 7, p. 073102, 2013.
[3] F. Güneş, H.-J. Shin, C. Biswas, G. H. Han, E. S. Kim, S. J. Chae, J.-Y. Choi, and Y. H. Lee, "Layer-by-layer doping of few-layer graphene film," *ACS nano*, vol. 4, no. 8, p. 4595, 2010.
[4] M. Kalbac, A. Reina-Cecco, H. Farhat, J. Kong, L. Kavan, and M. S. Dresselhaus, "The Influence of Strong Electron and Hole Doping on the Raman Intensity of Chemical Vapor-Deposition Graphene," *ACS Nano*, vol. 4, no. 10, pp. 6055-6063, Oct. 2010.

ID 194 - Oral

Light Management in Flexible Thin-Film Solar Cells on Transparent Plastic Substrates

*K. Wilken[1], U. W. Paetzold[1], M. Meier[1], G. Ablayev[1,2], N. Prager[3], M. Fahland[3], F. Finger[1], V. Smirnov[1]
[1]Forschungszentrum Jülich, IEK-5 Photovoltaics, Jülich, Germany
[2]Ioffe Physical-Technical Institute, Physicochemical Properties of Semiconductors, St. Petersburg, Russian Federation
[3]Fraunhofer-Institut für Elektronenstrahl- und Plasmatechnik FEP, Dresden, Germany

Flexible solar cells offer many advantages, such as high throughput production by roll-to-roll manufacturing, versatility regarding shapes and size, and also exceptionally light weight. To minimize costs of the device, flexible transparent polymer substrates such as polyethylene terephthalate (PET) is a convenient alternative. Such polymer substrates are usually temperature sensitive and process temperatures have an upper limit of around 140 °C in the case of PET. This implies additional limitations on applicable light management concepts that must be processed below this temperature. A commonly used approach for improved light management is the insertion of textured surfaces to scatter or diffract the light, thus increasing the optical path length of the light within the absorber layer of a solar cell.

In this study, we investigate two alternative approaches to realize advanced light scattering features on a transparent PET film at low temperature: (1) UV nanoimprint texturing of the substrates and (2) chemical etching of low temperature ZnO:Al layers with suitable properties. By the application of nanoimprint technology an optimized light trapping texture of high temperature ZnO:Al was replicated on the low temperature PET film. Our results demonstrate that the nanoimprint process was successfully applied without deterioration of the total transmittance and resistivity of the substrates covered with ZnO:Al. Furthermore, the light scattering properties of the substrate, evaluated by diffuse transmittance, were significantly improved (from 2 % to 45 % at a wavelength of 500 nm) due to the nanoimprint texture. In the case of wet-chemical etched ZnO:Al front contacts, we investigate the properties with respect to their light scattering abilities after this treatment and the trade-offs between electrical and optical properties of ZnO:Al layers on plastic substrates. The two light management concepts are compared and discussed with respect to the effects on the quantum efficiency and short circuit current density. Our results show that in flexible thin-film silicon solar cells, the short circuit current density can be improved by around 2.5 mA/cm² compared to a flat reference.

ID 195 - Poster

Effect of inter-electrode distance and power on the size and crystallinity of gas phase nanoparticles in Plasma Enhanced Chemical Vapor Deposition

*A. Mohan[1], I. Poulios[1], W. Goedheer[2], R. Schropp[3], J. Rath[1]
[1]Utrecht University, Eindhoven, Netherlands
[2]Dutch Institute for Fundamental Energy Research (DIFFER), Computational Plasma Physics, Nieuwegein, Netherlands
[3]Eindhoven University of Technology (TU/e), Department of Applied Physics, Eindhoven, Netherlands

The synthesis of crystalline silicon nanoparticles (NPs) by plasma enhanced chemical vapour deposition (PECVD) has been amply reported and the properties of the produced particles are very promising for optoelectronics devices. Various parameters such as coupled power, process pressure, gas flow and source gas ratios (SiH_4:H_2) play crucial roles in determining the size and crystallinity of the synthesized particles. One of the less studied parameters for nanoparticle growth is the inter-electrode distance, *d*.

Our study focuses on the effect of power density and d on the size distribution and crystallinity of gas phase grown nanoparticles. Plasma is sustained between the two perforated parallel plate electrodes, the holes of the top (grounded) electrode allow the formed NPs to escape the plasma region and be collected on a substrate. Growth of nanoparticles in a VHF PECVD process was done at *d* of 10 mm and 30 mm, keeping the other parameters constant. A constant power density of 81.24 mW/cm^3 was applied in both the cases. For a larger *d* (case 1), a higher deposition rate was observed and a larger fraction of the total deposited area was crystalline. The crystalline particles have cauliflower structures. However, at a *d* of 10 mm (case 2) only amorphous particles were deposited. These amorphous particles exist as clusters of smaller nanoparticles.

To study the effect of power density, it was tripled in case 2. This resulted in crystalline cauliflower particles along with well-defined amorphous spherical particles (case 3).

The higher deposition rate at the larger *d* may be attributed to larger plasma volume. Although a same power density is applied at smaller *d* only amorphous particles are created. This can be attributed to a lower residence time of the particles in the plasma zone and smaller number of the electron-ion recombination events, leading to reduced particle heating. By tripling the power density crystallization can be achieved as higher power density leads to higher electron temperature which aids in particle heating [1], resulting in more crystalline powders prevalent. We suspect the role of residence time of the particles in the plasma, (where the electron-ion recombinations take place) is more important that the applied power. We also speculate a substantial portion of particle heating also comes from hydrogen abstraction which is higher for greater electrode distances.

The input power plays an important role in deciding whether the resulting particle is amorphous or crystalline. The present study shows that a larger electrode distance and higher power density are more favorable for the formation of crystalline nanoparticles.

[1]. R. Anthony, U. Kortshagen, Phys. Rev. B 80 115407-115412 (2009)

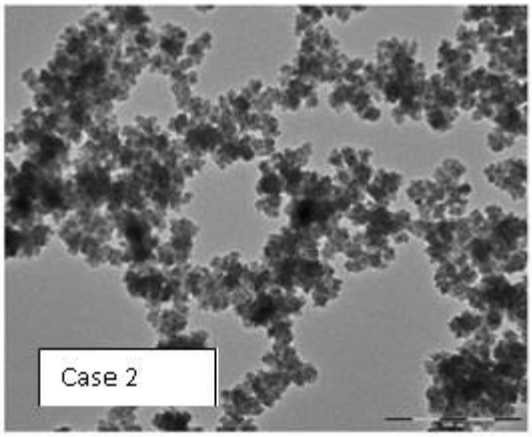
Case 2

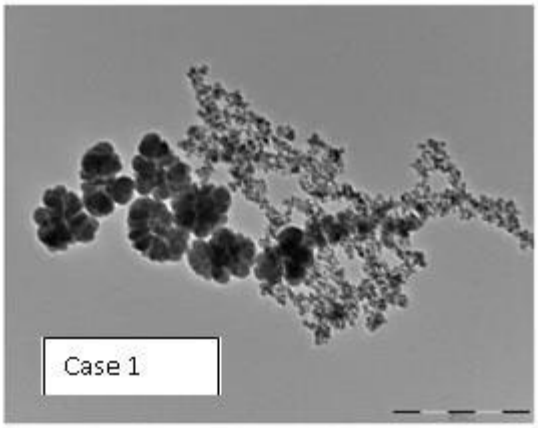
Case 1

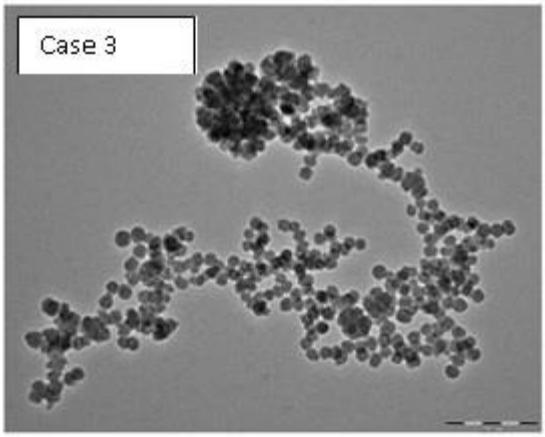
Case 3

ID 196 - Poster

Large area superstrate amorphous solar modules on lightweight flexible plastic

**R. Yang[1], *A. Sazonov[1]*
[1]University of Waterloo, Electrical and Computer Engineering, Waterloo, Canada

Solar cells on lightweight and flexible substrates have advantages over glass or wafer-based photovoltaic devices for portable and extraterrestrial applications. Here, we report on the comparison of fabrication and performance of substrate and superstrate amorphous silicon thin film photovoltaic modules fabricated at maximum deposition temperature of 150 °C on 100 um thick polyethylene-naphtalate plastic films. Each module of 10 cm × 10 cm area consists of 4 pieces of 5 cm × 5 cm submodules which is a-Si:H p-i-n rectangular structures with transparent conducting oxide top electrodes with Al fingers and metal back electrodes. Individual structures are connected in series. The module is calculated to yield about 300 W/kg with output voltage of 15 V under optimized load conditions. Cell structure optimization and fabrication process details will be discussed.

ID 197 - Poster

Aluminum and Beryllium induced crystallization of free standing amorphous Silicon thin films

*T. Grueser[1], A. Zanatta[1], M. Kordesch[1]
[1]Ohio University, Physics and Astronomy, Athens, United States

Differential scanning calorimetry, Raman spectroscopy and x-ray diffraction have been used to determine the temperature at which metal induced crystallization proceeds in free-standing thin films of sputter deposited amorphous silicon (a-Si) and the metals aluminum and beryllium. Free standing bi-layer films have been examined. Films were deposited by DC sputtering in Ar atmosphere on glass slides coated with dried sugar-water solutions. The films were subsequently removed from the substrates by immersion in water. The free-standing films were examined using differential scanning calorimetry (DSC). Co-sputtered alloy films (on glass and quartz substrates) were also prepared for comparison.

Differential scanning calorimetry of free standing Al-aSi films showed a systematic variation of the crystallization peak temperature with Al-Si ratio. The speed of heating broadened the crystallization peak. A Kissinger plot of the peak temperatures and heating rates resulted in a value of the activation energy of 600 kCal/mole. The order of deposition also affected the crystallization temperature, in particular if the vacuum was broken between deposition of the aluminum film and the aSi film. The Al films oxidize due to exposure to the ambient atmosphere. The oxide, which is at the Al-Si interface formed after deposition of the aSi film, results in an approximately 60 C increase in the crystallization peak in the DSC. Therefore, the standard procedure was to deposit the films of both aSi and the metal without breaking vacuum. Film weights used for DSC were between 0.3 and 0.7 mg.

Al-aSi films have been studied extensively with many results published in the literature. Our results for the Al-aSi free standing films are generally consistent with other published results.

A limited number of beryllium -aSi films were studied. Free standing Be-aSi films approximately 200 nm thick (total 0.25-0.3 mg) and with a 1:1 Be:aSi ratio showed a crystallization peak at about 426 C in the DSC. Co-doped Be-aSi films (500 nm thick) were studied using the “staircase” heating method: Films were heated from 200 to 800 C in 50 C steps lasting 15 minutes. A MIC temperature between 650-700 C was determined for three concentrations of Be/aSi (all less than 18% Be) from the observation of the c-Si peak at 520 cm^{-1} in Raman spectra.

Raman spectra showed that a Be-aSi bilayer film deposited on high temperature glass heated to 500 C for 30 minutes in vacuum was not completely crystallized, while in the DSC, the same type of free standing film showed complete crystallization. The crystallization is complete because there was no peak observed when the sample was heated a second time in the DSC.

There is as yet no systematic understanding of metal-induced-crystallization (MIC) of a-Si. Two groups of metals are usually studied, eutectic formers and silicide formers. Be forms a eutectic with silicon at 1085 C; the eutectic temperature is 577 C for Si-Al. There is no known silicide for Be-Si.

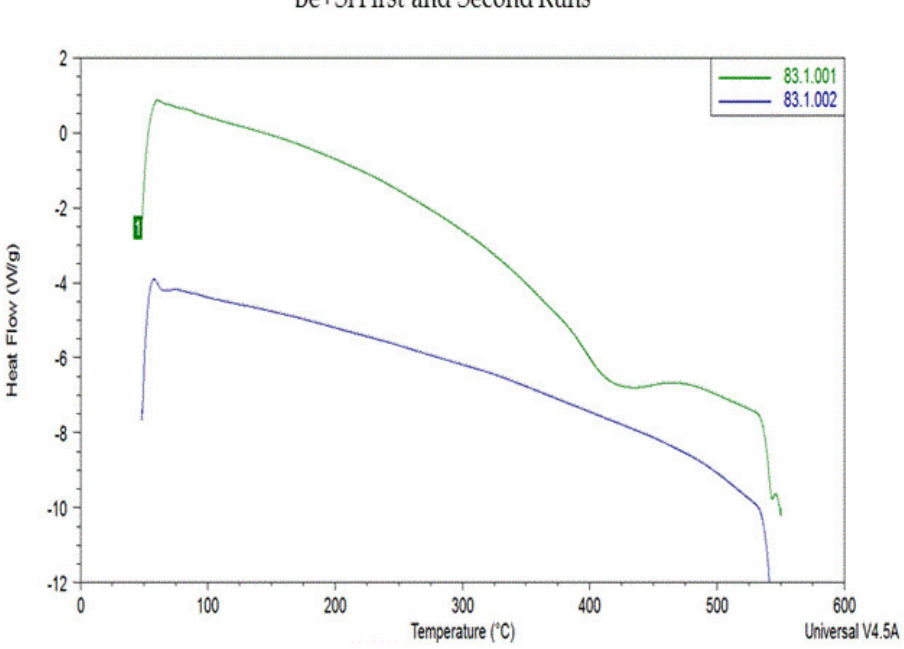

Sample	Speed	Onset (C)	Peak Maximum (C)
83.1.001	10 deg/min	411.19	426.28
83.1.002	10 deg/min	No peak	No peak

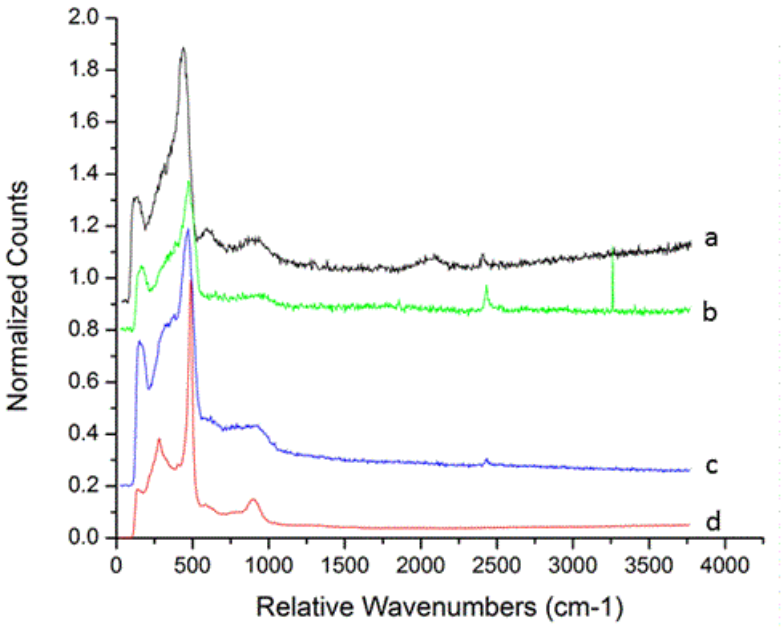

a.) as deposited, b.) heated 30 min at 500 C, c.) laser annealed, d.) laser crystallized.

ID 198 - Poster

High stabilized efficiency single and multi-junction thin film silicon solar cells

*V. Smirnov[1], F. Urbain[1], A. Lambertz[1], F. Finger[1]
[1]Forschungszentrum Jülich GmbH, IEK-5 Photovoltaik, Jülich, Germany

Silicon thin film solar cells are known to suffer from degradation due to prolonged illumination. This degradation process, known as Staebler-Wronski effect, is considered as a major limiting factor for high efficiency devices and usually is associated with the stability of amorphous silicon (a-Si:H) absorber layers, while the microcrystalline silicon (µc-Si:H) absorber is generally more stable. Here we present the development of high efficiency single and multi-junction solar cells, focusing on the stability against prolonged illumination.

Single and multi-junction solar cells were prepared by PECVD at deposition temperatures of 185°C or below. In the case of multi junction devices, we have prepared a-Si:H/µc-Si:H tandem solar cells, a-Si:H/µc-Si:H/µc-Si:H or a-Si:H/a-Si:H/µc-Si:H triple junction solar cells and a-Si:H/a-Si:H/µc-Si:H/µc-Si:H quadruple junction cells. The matching of the current in the sub-cells of the multijunction devices was achieved by variation in the bandgap and thickness of the absorber layer and by implementation of doped microcrystalline silicon oxide (µc-SiO_x:H) layers. Solar cells were investigated by current-voltage (*J-V*) measurements under AM 1.5 illumination (intensity of 1000 W/m^2, class A spectrum), quantum efficiency (QE) and reflectance measurements. Degradation of solar cell was performed at 55 °C in open circuit condition with an intensity of 1000 W/m^2 (class B spectrum) over a period of 1000 hours.

High initial efficiencies were achieved for all types of solar cells: 12.4% in the case of a-Si:H single junction cell and above 13.5% for each type of multijunction cells. The degradation behaviour was evaluated with respect to the thickness and bandgap of the a-Si:H absorber layers. In the case of a-Si:H single junction solar cells, 300 nm was found to be an optimal absorber layer thickness resulting in high stabilized efficiency of 10.3%. Further increase in the thickness of the absorber layer results in the reduction of stabilized efficiency due to stronger degradation in fill factor (*FF*) and short circuit current density (*Jsc*) values. In the case of triple and quadruple junction solar cells, the total thickness of the a-Si:H absorber layers (first and second sub-cells) can be significantly increased above 500nm while keeping the degradation level low (around 10% in efficiency) which is due to compensation of the degradation in *FF* and *Jsc* in the individual sub-cells by current mismatch. While higher bandgap a-Si:H absorber layers show stronger degradation, the stability of multi junction devices can be improved by reduction in the high bandgap a-Si:H layer thickness of the top cell down to around 80 nm. After 1000 hours illumination low degradation values of as little as 5 % from the initial value were found resulting in stabilized of degradation we achieved efficiencies of 11.8% in the case of tandem and triple solar cell, and of 12.1% in the case of quadruple cells.

ID 199 - Oral

Molar Mass versus Polymer Solar Cell Performance: Highlighting the Role of Homocouplings

*T. Vangerven[1], P. Verstappen[2], J. Drijkoningen[1], W. Dierckx[1], S. Himmelberger[3], A. Salleo[3], D. Vanderzande[2], W. Maes[2], J. Manca[4]
[1]Hasselt University / Institute for Materials Research, Material Physics Division, Diepenbeek, Belgium
[2]Hasselt University / Institute for Materials Research, Design and Synthesis of Organic Semiconductors, Diepenbeek, Belgium
[3]Stanford University, Department of Materials Science and Engineering, Stanford, United States
[4]Hasselt University, X-LaB, Diepenbeek, Belgium

Although a strong link between the molar mass of conjugated polymers and the performance of the resulting polymer:fullerene bulk heterojunction organic solar cells has been established on numerous occasions, a clear understanding on the origin of this connection is still lacking. Moreover, the usual description of molar mass and polydispersity does not include the shape of the polymer distribution, although this can have a significant effect on the device properties. In this work, the effect of molar mass distribution on photovoltaic performance is investigated using a combination of structural and electro-optical techniques for the state-of-the-art low bandgap copolymer PTB7. Some of the studied commercial PTB7 batches exhibit a bimodal distribution, of which the low molar mass fraction contains multiple homocoupled oligomer species, as identified by MALDI-TOF analysis. This combination of low molar mass and homocoupling drastically reduces device performance, from 7.0 to 2.7%. High molar mass batches show improved charge carrier transport and extraction with much lower apparent recombination orders, as well as a more homogeneous surface morphology. These results emphasize the important effect of molar mass distributions and homocoupling defects on the operation of conjugated polymers in photovoltaic devices.

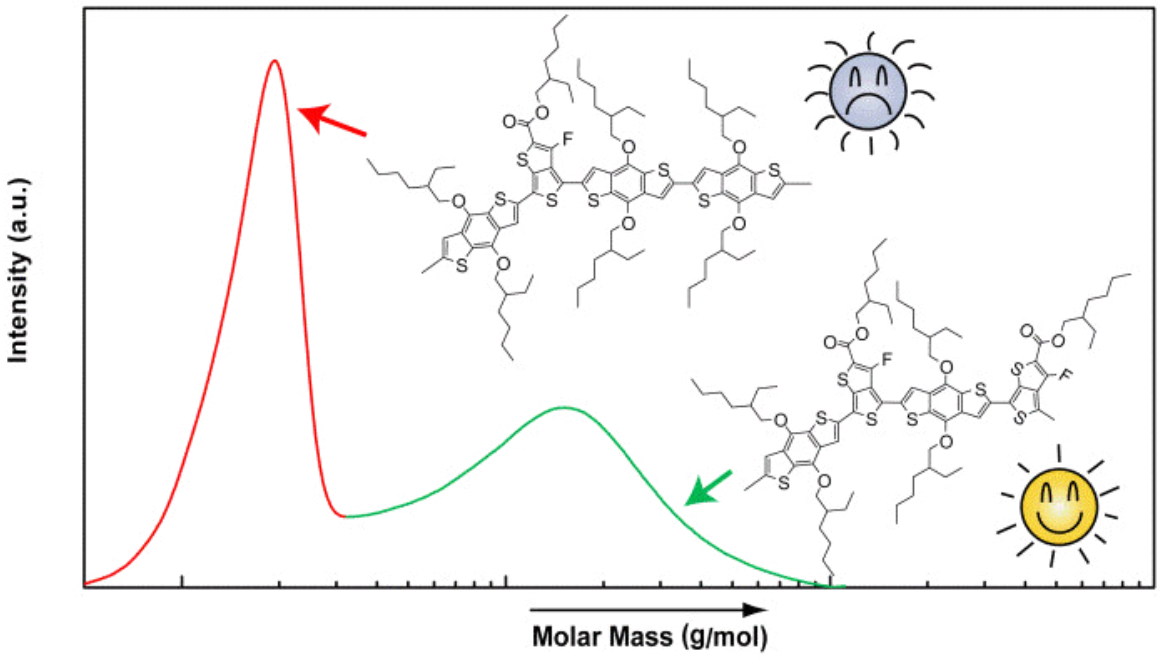

ID 200 - Oral

Thin film silicon photovoltaic cells on paper for flexible indoor applications

**H. Aguas[1], T. Materus[1], A. Vicente[1], D. Gaspar[1], M. Mendes[1], W. Schmidt [2], L. Pereira[1], E. Fortunato[1], R. Martins[1]*
[1]FCT-UNL, CENIMAT/I3N, Caparica, Portugal
[2]Schoeller Technocell GmbH & Co.KG, Osnabrück, Germany

The next-generation of low cost flexible, disposable, portable and potentially wearable electronic systems will require the integration of energy power sources to turn them fully autonomous. These electronic systems are expected to attain a major influence in our future lifestyles, at the levels of communications, logistics, and medicine. For this reason it is highly demanding to develop thin, lightweight, and flexible energy sources with various sizes and shapes and capable of being integrated with such low cost consumer oriented systems. So far, plastic substrates have dominated this technology mostly due to their flexibility, lightweight, durability and widespread usage. However, a major concern with plastics is that they have low thermal durability and a high coefficient of thermal expansion, which frequently becomes an obstacle for the manufacturing processes. High-quality plastics can alleviate these problems, but are expensive, and since the substrate occupies a large portion of the devices, cost effective and environmentally friendly materials are strongly required.

Cellulose paper has excellent mechanical properties, such as flexibility and foldability, and it is a low cost, recyclable, and environmental friendly material. It is chemically and mechanically stable under atmospheric conditions and its surface wetting properties can be easily modified. Moreover, paper is quite stable at elevated temperature. The degradation of cellulose, the major constituent of paper, begins at a temperature above 250 ºC, while its extensive degradation occurs when the temperature is over 300 ºC.

Paper-based photovoltaic (PV) devices are the ideal power source for most of the low cost disposable electronic commodities based on the above-mentioned devices. In addition, they can contribute to the creation of new paradigms concerning light harvesting, including its seamless integration into ubiquitous formats such as window shades, wallpaper, wear, and magazines. Its installation may be as simple as cutting the paper PV to the desired size and then gluing it onto the required surfaces.

However, their fibrous structure makes it quite challenging to fabricate good-performing inorganic PV devices like thin film silicon cells on such substrates. The advances presented here demonstrate the viability of fabricating thin film silicon PV cells on a paper coated with a cast-coating a layer of a hydrophilic mesoporous (HM) material which gives it a smooth finishing. Such layer can, not only withstand the cells production temperature (150 °C), but also provides an adequate paper sealing and surface finishing for the deposition of the cell's layers.

The substances released from the paper substrate were continuously monitored during the cell deposition by mass spectrometry analysis, which allowed adapting the deposition procedures to mitigate any possible contamination from the substrate. In this way, a proof of concept solar cell with a 3.4% cell efficiency (with 41% fill factor, 0.82V open circuit voltage and 10.2mA/cm^2 short-circuit current density) was attained, opening the door to the use of paper as a reliable low cost substrate to fabricate inorganic PV cells for a plethora of indoors applications with tremendous impact in multisectorial fields such as the food, pharmacy and security.

[Accepted for publication in Advanced Functional Materials, 2015]

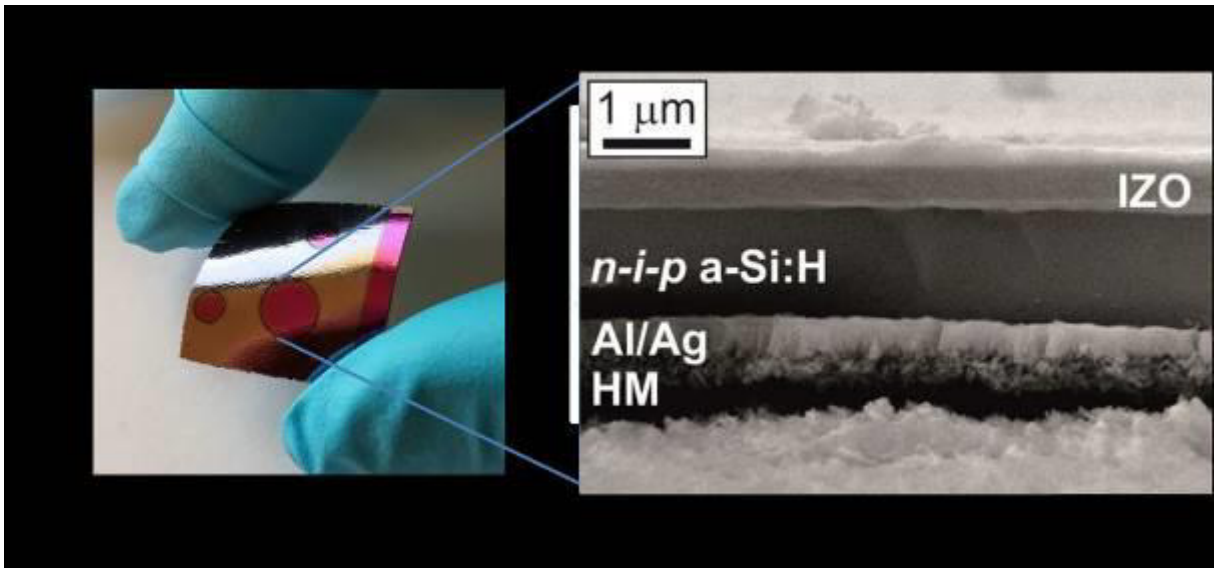
1 μm
IZO
n-i-p a-Si:H
Al/Ag
HM

ID 201 - Oral

Interfaces in (p) a-Si:H/(n) c-Si heterojunctions: influence of (i) a-Si:H buffer layer and front electrode on capacitance-temperature dependencies and strong inversion layer.

*M. Olga[1], L. Raphaël[2], J. Alvarez[2], *J.- P. Kleider[2]*
[1]Keldysh Institute of Applied Mathematics , Moscow, Russian Federation
[2]Laboratoire de Génie électrique et électronique de Paris (GeePs), Gif-sur-Yvette, France

Passivation of the heterointerfaces in order to decrease the recombination is of particular importance in silicon heterojunction solar cells that combine a crystalline silicon (c-Si) absorber with hydrogenated amorphous silicon (a-Si:H) for the emitter and BSF (Back Surface Field) junctions. The so-called field effect passivation is one of the strategies that can be used for this purpose. Indeed, strong electric field and strong band bending in c-Si can decrease the recombination at the interface by repelling one type of carriers. The existence of a strong inversion layer in (n) c-Si at the interface with (p) a-Si:H has been observed in the past years using several kinds of techniques: conductive-probe AFM [1], planar conductance [2], capacitance spectroscopy [3]. For the latter we have shown previously that the temperature dependence of the quasistatic capacitance is much stronger in the presence of a strong hole inversion layer at the c-Si surface. This was obtained from a fully analytical calculation of the capacitance. However, in this calculation the (p) a-Si:H layer on top of the (n) c-Si absorber was assumed to semi-infinite and the (i) a-Si:H buffer layer that is used in real solar cells to decrease the density of interface states was neglected.

We have extended our calculation to take account of both the (i) a-Si:H buffer layer and the finite thickness of the (p) a-Si:H layer. The latter also implies to consider the contacting electrode, usually indium tin oxide (ITO), and its difference in work function with (p) a-Si:H. We have calculated the capacitance as a functionof temperature (C-T) for several sets of parameters where we varied the density of states (DOS) in the (i) a-Si:H layer, the DOS at the Fermi level in (p) a-Si:H, the work function of the electrode, and the thickness of both doped and undoped a-Si:H layers, and we compared the obtained values to that previously obtained under the assumption of semi-infinite (p) a-Si:H and no (i) a-Si:H. We show that the introduction of the (i) a-Si:H layer can yield to slightly larger capacitance values and a weaker slope of the C-T curve especially at low temperature. The effect of the finite thickness of (p) a-Si:H depends on the sign of the difference in work function between the contacting electrode and (p) a-Si:H, $\Delta WF=\Phi_C-\Phi_{p\text{-}aSi:H}$. If $\Delta WF<0$, the same trend is observed as with introduction of the (i) a-Si:H buffer, namely an increase of the capacitance togetherwith a weaker slope at low temperature. This weaker temperature dependence at low temperature is a signature of the disappearance of the strong inversion layer at the c-Si surface. Indeed, introducing the (i) buffer layer implies a weaker band bending in c-Si, while negative DWF implies that a counter-diode develops at the contact/a-Si:H interface. This can extend towards the a-Si:H/c-Si interface (especially if the DOS is not too large in (p) a-Si:H or if its thickness is very small) and also leads to lower band bending in c-Si.

The trends obtained from our new analytical calculations are well reproduced by full numerical simulations. Finally experimental resultsobtained on high efficiency solar cells indicate that the strong holeinversion layer that exists at room temperature tends to disappear below 150 K. This is compatible with previously proposed values of the valence band offset (around 0.4 eV) and reasonable values for the DOS in a-Si:H provided the work function of ITO is large enough ($\Phi_{ITO}>4.8$ eV). We demonstrate that lower values of Φ_{ITO} that can be commonly found in the literature are incompatible with our experimental capacitance data and their temperature dependence.

[1] O. Maslova et al, Appl.Phys.Lett. 97, 252110 (2010)
[2] R. Varache et al., J. Appl. Phys. 112, 123717 (2012)
[3] O. Maslova et al, Appl. Phys. Lett. 103 183907 (2013)

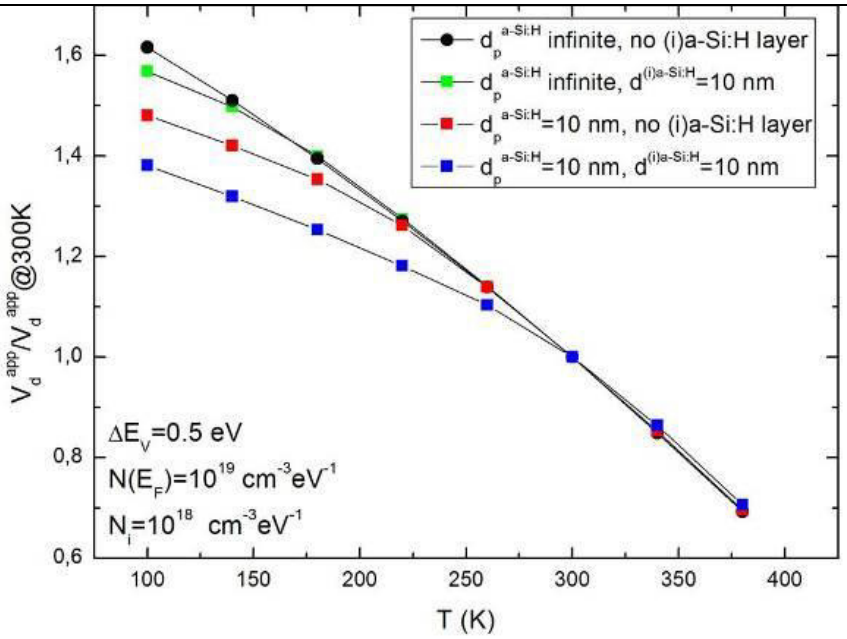

Influence of the (i) a-Si:H buffer layer and the finite thickness of the (p) a-Si:H on temperature dependence of normalized (at 300 K) apparent diffusion potential, V_d^{app}, defined as:

$$V_d^{app}(T) = \frac{qN_d\varepsilon}{2}\left(\frac{1}{C}\right)^2$$

Smaller values/weaker temperature dependence of V_d^{app} correspond to larger values/weaker temperature dependence of the capacitance. This corresponds to the disappearance of the strong inversion layer at the (n) c-Si surface.

ID 202 - Oral

Solar Cells for self-sustainable intelligent packaging

*A. Vicente[1], *H. Aguas[1], T. Mateus[1], A. Araujo[1], A. Lyubchik[1], E. Fortunato[1], R. Martins[1]*
[1]FCT-UNL, CENIMAT/I3N, Caparica, Portugal

Solar energy is doubtless the source of renewable energy that better perspectives has to endow any object with truly autonomous and self-sufficiency performance, which is of particular relevance for the packaging industry where there is a strong demand for solutions to increase food and beverage shelf life, improve the food distribution systems and also to assure food safety as consumers demand. Intelligent packaging can play a central role by allowing owners, vendors and consumers, to have real-time information about the contents and interact with the goods. However, there are significant limitations to what the package can execute which are intimately related to its energy requirements and the cost of the power sources. This can be addressed by a combined use of a small disposable battery, charged by a disposable solar cell, able to work under indoor lighting, but to achieve such energy revolution, the manufacturing cost of solar cells has to be minimized while flexibility and simplified implementation are mandatory conditions. Here, we demonstrate that the paper based packaging material, used in the food and beverage industry, can put us one step closer to this revolution, by providing a flexible, renewable and extremely cheap substrate for the deposition of amorphous silicon (a-Si:H) thin film solar cells with efficiencies of 4% and fill factor of 54%, by plasma enhanced chemical vapor deposition (PECVD) at low temperature.

To achieve this, the fabrication process has to address all the challenges that paper-based substrates pose to solar-cells, namely concerns with roughness, stability under vacuum, plasma and temperature. The fabrication strategy presented here is able to address these challenges by achieving a good compromise between the deposition conditions, indispensable to obtain an homogeneous coverage of the surface and high quality Si active layers, and also by continuously monitoring the process via Optical Emission Spectroscopy (OES) and Mass Quadrupole Spectrometry (MQS), to detect paper degasification and species present in the deposition chamber, essential for a dynamic deposition methodology and assure the reproducibility of solar cells.

The obtained results demonstrate the viability of applying the traditional thin film technology to this original substrate and produce solar cells with the best cost/efficiency relation when compared with other possible substrates used for flexible solar cells. Moreover, such Si thin films take advantage of their good performance at low-light levels, which also makes them highly desirable for cheap mobile indoor applications; thus opening the path towards low cost, lightweight and reliable devices, ideal to be integrated in a wide variety of common day objects and at the same time contribute to a sustainable lifestyle.

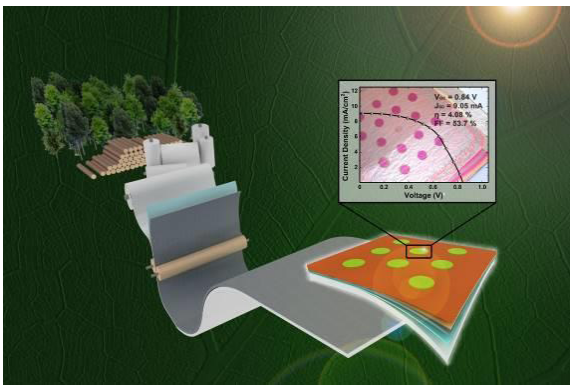

[J. Mater. Chem. A, DOI: 10.1039/c5ta01752a]

ID 203 - Poster

Vacuum combined technological methods for deposition of hydrogenated silicon thin films with embedded nanoparticles

**J. Stuchlik*[1]
[1]*Institute of Physics, Thin films and Nanostructures, Praha, Czech Republic*

The photoluminescence of thin films and electroluminescence of diode structures based on amorphous (a-Si:H) and microcrystalline (µc-Si:H) hydrogenated silicon have been studied only sporadically due to the very low quantum efficiency of energy transfer. The process is very difficult to detect at room temperature and higher levels of emitted light at low temperatures has no applicable usage. PECVD technique alone probably cannot bring new surprising results. The basic problem is it is not possible to transport some needed elements in the form of gases or vapors of some liquids into the vacuum reaction chambers. For new quality of Si:H thin films we develop new (combined) technological procedures, which allows the integration of convenient nanoparticles of different semiconductors into the Si:H structures. Those methods are a combination of:

PECVD and Reactive Deposition Epitaxy (RDE)

PECVD and Reactive Laser Ablation (RLA)

PECVD and Laser Treatment (LT)

PECVD and Vacuum Evaporation and Plasma Treatment (VE+PT)

The promising results, namely the electroluminescence of diode structures based on hydrogenated silicon achieved by the application of the mentioned methods, will be introduced.

ID 204 - Oral

Characterization of a-Si:H/c-Si heterojunction by temperature dependent modulated photoluminescence

*M. XU[1,2,3,4,5], M. Boutchich[1,2,3,4,5], I. Sobkowicz[6,7], J. Alvarez[1,2,3,4,5], R. Brüggemann[1,2,3,4,5], P. Roca i Cabarrocas[6,7], J.- P. Kleider[1,2,3,4,5]
[1] Génie électrique et électronique de Paris, Gif sur Yvette, France
[2]CentraleSupelec, Gif sur Yvette, France
[3]Université Paris-Sud, Orsay, France
[4]Sorbonne Universités, Paris, France
[5]Université Pierre et Marie CURIE, Paris, France
[6]Laboratoire de Physique des Interfaces et des Couches Minces, Total Joint Research Team, Palaiseau, France
[7]Total New Energies, Paris La Défense, France

Recombination at the heterointerfaces has to be reduced in order to enhance the performance of silicon heterojunction (HETs) solar cells. It has been proposed that this can be done through enhanced field effect passivation or by decreasing the density of interface states. However, there is still only a poor knowledge of the effective recombination paths and on its temperature dependence. Here modulated photoluminescence (MPL) has been applied to investigate the passivation quality of the various interfaces of a-Si:H/c-Si heterojunctions. The temperature dependence of the minority carrier lifetime has been determined between 300 K and 50 K.

To address the problem, we studied various samples with the following configuration: (p)a-Si:H/ (i)a-Si:H / (n)c-Si /(i)a-Si:H/ (n+) a-Si:H HETs with different thicknesses of the intrinsic passivation layer. The samples are n-type c-Si wafer with p-type a-Si:H emitter on front surface. The intrinsic a-Si:H layers are 5, 10, 20 and 50nm thick. The back surface is passivated with the same (i) a-Si:H/ (n) a-Si:H stack. In order to characterize these samples and extract the minority carrier lifetime we have developed a temperature dependent MPL technique. The samples are embedded into a temperature controlled cryostat from 300 K down to 50 K and illuminated by a 785nm laser with an excitation equivalent to one sun. Our work is complemented by a full numerical simulation of the HET structure in order to interpret the experimental data. For the recombination model, we consider deep defects introduced by dangling bonds at the interface or in the bulk, and we also take account of the level introduced by the phosphor dopants located 45 meV below the conduction band.

The experimental results show that with decreasing temperature the lifetime of the minority carriers decreases for all the samples. The overall decrease in the lifetime is less than a factor of 10 for a change from 300 K to 100 K and with a further decrease in lifetime towards 50 K, as is found in all the samples. The recombination rate through defects in the heterojunction, both in the volume and at the interface, changes as function of temperature, and leads to a characteristic profile of the temperature dependence. We propose, supported by rigorous numerical simulations, that this dependence can be interpreted by considering the collaborate effects of both the shallow defects, eg. dopants in the wafer, and deep defects, that is, the dangling bonds at the silicon interface and recombination centers in the bulk. The role of the (i)a-Si:H layer thickness on the band-bending and related interface recombination will be explored.

ID 205 - Oral

Subbandgap absorption spectroscopy of solar cell materials

*J. Holovsky[1,2], M. Stuckelberger[3,4], T. Finsterle[2], A. Purkrt[1], F.- J. Haug[4], V. Benda[2], M. Bertoni[3], C. Ballif[4]
[1]Instute of Physics, ASCR v. v. i., Optical materials, Prague, Czech Republic
[2]Czech Technical University, Faculty of Electrical Engineering, Prague, Czech Republic
[3]Arizona State University, Defect Lab, Tempe, United States
[4]École Polytechnique Fédérale de Lausanne, PV-lab, Neuchâtel, Switzerland

Low absorption optical spectroscopy is a useful method for the absorber quality evaluation of novel solar cell materials as well as of absorbers incorporated in thin-film silicon devices. We improved our expertise in evaluation of defect density in thin layers by a method correcting for surface defect absorptance [1]. We have used the method to subbandgap absorption of $CH_3NH_3PbI_3$ perovskites as well [2].

In the field of hydrogenated amorphous silicon (a-Si:H), state-of-the-art material reach an absorption coefficient down to 1cm^{-1} at 1.2 eV after light-soaking under standard conditions. The absorption at this energy is related to defects (predominantly dangling bonds); these are mostly light-induced defects created through the Staebler-Wronsky effect.

High-quality a-Si:H was incorporated by co-authors into solar cells to study the effect of absorber-layer thickness on the device performance and its degradation under light soaking [2]. In the present study, we combine the defect absorption with the device properties of a solar cell thickness series, using cutting edge devices and characterization techniques (photothermal deflection spectroscopy and Fourier-transform photocurrent spectroscopy). This allows us to fill the gap between layer quality measurements and device performance, and finally evaluate today's technologically achievable device properties for given defect density and absorber layer thickness.

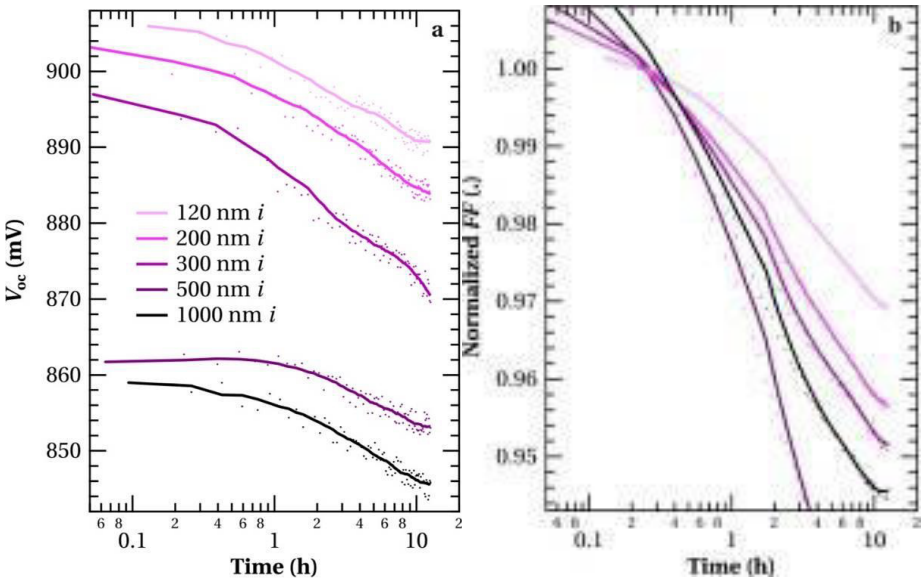

[1] J. Holovský, C. Ballif, Thin-film limit formalism applied to surface defect absorption, Opt. Express. 22 (2014) 31466. doi:10.1364/OE.22.031466.
[2] S. De Wolf, et al., Organometallic Halide Perovskites: Sharp Optical Absorption Edge and Its Relation to Photovoltaic Performance, J. Phys. Chem. Lett. (2014) 1035-1039. doi:10.1021/jz500279b.
[3] M. Stuckelberger, et al., Comparison of amorphous silicon absorber materials: Kinetics of light-induced degradation, Prog. Photovolt. Res. Appl. (2014) n/a-n/a. doi:10.1002/pip.2559.

ID 206 - Poster

Design of electrical junctions by self-assembled monolayer of carborane-thiols dipoles

*A. Vetushka[1], F. Křížek[1], M. Hývl[1], M. Müller[1], M. Ledinský[1], P. Pikna[1], T. Baše[2], J. Kočka[1], A. Fejfar[1]
[1]Institute of Physics ASCR, Thin films and nanostructures, Prague, Czech Republic
[2]Institute of Inorganic Chemistry ASCR, Husinec-Řež, Czech Republic

Electrical junctions of metal-semiconductor (Schottky) or semiconductor-semiconductor (p-n) interfaces have similar diode-type I-V characteristic and represent fundamental elements of most electronic and optoelectronic devices. The interfaces can induce a depletion region (in a semiconductor) with built-in potential (barrier) that blocks the current flow through the interface in one direction. The final characteristics of an electronic device strongly depend on the potential barrier. Therefore the possibility of fine adjustment of an interfacial junction in a desired way is of high importance and is extensively studied. For example, to reduce the undesirable thermionic component of current (for the Schottky junction) a thin insulator layer (1-2 nm) is often placed into the metal-semiconductor interface [1,2].

The Schottky-Mott theory assumes that the Schottky barrier height depends on the work-function of metal and can be adjusted by choosing anappropriate metal substrate. The metal work-function can also be tuned by Self-Assembled Monolayers (SAMs) of oriented dipoles. The use of SAMs is a highly innovative approach to adjust surface properties of metals, metal oxides, and semiconductors [3]. Campbell et al. [4] have used an oriented dipole layer at the silver/organic interface to change the effective Schottky barrier height. They reported that the barrier height could be either increased or decreased over a range of more than 1 eV.
In this work we study the influence of a SAMs of carborane-thiols (1,2-$(HS)_2$-1,2-$C_2B_{10}H_{10}$ and 9,12-$(HS)_2$-1,2-$C_2B_{10}H_{10}$) placed at an interface of a junction. Dicarba-*closo*-dodecaboranes-thiols (often referred to just as carborane-thiols) are rigid and thermally robust molecules with a nearly regular icosahedral structure [5]. Their key properties related to the work are 1) the remarkable ability of the isomeric $C_2B_{10}H_{12}$ clusters to remain intact under a wide range of conditions and 2) relatively large and oppositely oriented dipole moment. We used plasma enhanced chemical vapor deposition to make multilayered silicon thin films (with layers of mc-Si:H or a-Si:H) on SAM-modified silver thin films (~20 nm in thickness) deposited on a differently doped silicon wafers. The changes of the potential barrier were investigated by the photocurrent method and Suns-V_{OC}. Results are compared to the changes of the surface potential induced by the SAM observed by Kelvin probe force microscopy in order to check the applicability of the Schottky-Mott model. This work was supported by the SCIEX program (project 11.206) from the Swiss Universities conference within an established cooperation between the Institute of Inorganic Chemistry ASCR (project nos. GACR-P205100348, ASCR-M200321201) Rez near Prague and EMPA, Dübendorf and by ESF project CZ.1.07/2.3.00/20.0092 (J.H. Inst. Phys.Chem. ASCR). We additionally acknowledge the use of facilities of the Laboratory of Nanostructures and Nanomaterials at the Institute of Physics ASCR in Prague and partial support through project GACR 14-37427G.

[1] R. Wang, M. Xu, P.D. Ye, R. Huang, Schottky-barrier height modulation of metal/In0.53Ga0.47As interfaces by insertion of atomic-layer deposited ultrathin Al2O3, J. Vac. Sci. Technol. B. 29 (2011) 041206. doi:10.1116/1.3610972.
[2] Z. Wu, W. Huang, C. Li, H. Lai, S. Chen, Modulation of Schottky Barrier Height of Metal/TaN/n-Ge Junctions by Varying TaN Thickness, IEEE Trans. Electron Devices. 59 (2012) 1328-1331. doi:10.1109/TED.2012.2187455.
[3] C. Vericat, et al., Self-assembled monolayers of thiolates on metals: a review article on sulfur-metal chemistry and surface structures, RSC Adv. 4 (2014) 27730-27754. doi:10.1039/C4RA04659E.
[4] I.H. Campbell, S. Rubin, T.A. Zawodzinski, J.D. Kress, R.L. Martin, D.L. Smith, et al., Controlling Schottky energy barriers in organic electronic devices using self-assembled monolayers, Phys. Rev. B. 54 (1996) R14321-R14324. doi:10.1103/PhysRevB.54.R14321.
[5] R.N. Grimes, Carboranes, Second Edition, 2 edition, Academic Press, Burlington, MA, 2011.

ID 207 - Oral

Thin film of semiconducting clathrate with group IV elements

**F. Ohashi[1], M. Nomura[1], H. Manjo[1], K. Uehara[1], K. Sumiya[1], T. Kume[1], T. Ban[1], S. Nonomura[1]*
[1]Gifu University, Faculty of Engineering, Gifu, Japan

Semiconductor clathrates are materials composed with cage frameworks of group IV atoms (E = Si or Ge) with inclusion of metal atoms (M) in the cages as a guest. The metal atoms are ionized at room temperature and induce a doping effect to the cage frameworks. Several crystalline structures classified into type I (M_8E_{46}), type II ($M_{24}E_{136}$) and others have been reported so far. In the case of type II clathrate including Na atoms (Na_xE_{136}: x = 0 - 24), the electric property is known to be transferred from metallic to semiconducting by reducing the Na content. According to previous experimental and theoretical studies, [1,2] the clathrate without the guest atoms (the guest free clathrates: E_{136}) are predicted to have a direct bandgap much wider than that of the diamond structures. Such the properties arose interests in applications to optical devices such as photo-absorption materials for solar cells. Since, however, the materials were basically synthesized as powdery shapes, the clarification of the optoelectronic properties and the device fabrications have not been conducted.

In this paper, we report techniques to prepare thin films of Na_xE_{136}. The Na_xE_{136} thin film were synthesized by thermal decompositions of Zintl phase precursor films (NaGe or NaSi) prepared at on Si or Ge (111) substrates.[3] X-ray diffraction and Raman measurements showed evidence of the formation of the clathrate thin films. For the Ge clathrate (Na_xGe_{136}), the films have a crystalline orientation with the (111) plane parallel to the Ge(111) substrate. The optical and electronic measurements using the prepared Si or Ge clathrate are progress in our laboratory.

These research works are conducted as a part of Advanced Low Carbon Technology Research and Development Program (ALCA) funded by Japan Science and Technology Agency (JST).

[1] K. Moriguchi *et al.*, PRB, 62 (2000) 7138.
[2] J. Gryoko *et al.*, PRB, 62 (2000) R7707.
[3] F. Ohashi *et al.*, J. Phys. Chem. Solids, 75 (2014) 518.

ID 208 - Oral

Optical signal processing and diversity techniques for data error detection and correction using a-SiCH technology

*M. Vieira[1], M. A. Vieira[1,2], P. Louro[1,2], V. Silva[1,2]
[1]UNINOVA, CTS, Caparica, Portugal
[2]ISEL, DEETC, Lisbon, Portugal

Optical signal processing and diversity techniques are the driving forces which have allowed a-SiC:H technology to multiply error control capacities. Digital optical systems and optical processors demand an all-optical arithmetic unit to perform different optical arithmetic operations. Various architectures, logical and/or arithmetic operations have been proposed in optical/optoelectronic computing. Effort has been given to the development of all-optical logical functions by using different schemes like optoelectronic devices based on nonlinear micro-ring resonators.

Multilayered Si/C structures based on amorphous silicon technology are reconfigurable to perform WDM optoelectronic logic functions. They have a nonlinear magnitude-dependent response to each incident light wave.In this paper, we exploit the nonlinear property of SiC multilayer devices under wavelength backgrounds to design an optical processor for error detection and correction, that enable reliable delivery of spectral data of four-wave mixing over unreliable communication channels.

The SiC optical processor for error detection and correction is realized by using double pin/pin a-SiC:H photodetector with front and back biased optical gating elements.The operational principle of SiC based switches is discussed. Simulation results confirming the described method are also presented and compared with experimental results.The relationship between the optical inputs and the corresponding digital output levels is established.

Data shows that the background act as selector that pick one or more states by splitting portions of the input multi optical signals across the front and back photodiodes. Boolean operations such as exclusive OR (EXOR) and three bit addition are demonstrated optically with a combination of such switching devices, showing that when one or all of the inputs are present the output will be amplified, the system will behave as an XOR gate representing the SUM. When two or three inputs are on, the system acts as AND gate indicating the present of the CARRY bit. The design of an optical full-adder is presented. Additional parity logic operations are performed by use of the four incoming pulsed communication channels that are transmitted and checked for errors together. As a simple example of this approach, we describe an all optical processor for error detection and correction and then, provide an experimental demonstration of this fault tolerant reversible system, in emerging nanotechnology. An intuitive representation with a 4 bit original string color message and the transmitted 7 bit string, the parity matrix and the encoding and decoding processes are presented. These will provide various functionalities since all-optical logic gates are essential elements for optical signal processors and networks.

ID 209 - Poster

VIS/NIR wavelength selector based on a multilayer pi'n/pin a-SiC:H optical filter

**M. Vieira[1,2,3], M. A. Vieira[1,2], P. Louro[1,2], V. Silva[1,2], A. Fantoni[1,2]*
[1]UNINOVA, CTS, Caparica, Portugal
[2]ISEL, DEETC, Lisbon, Portugal
[3]FCT-UNL, DEE, Caparica, Portugal

LEDs are a very effective lighting technology due to high brightness, long life, energy efficiency and affordable cost. Their use as communication device with a photodiode as receptor has been experienced for many years in hand held devices, to control media equipment, and with higher rates between computational devices. This communication path has been employed in the near-infrared (NIR) range, but due to the increasing LED lighting in homes and offices, the idea to use them for visible light communications (VLC) has come up recently.To enhance the transmission capacity and the application flexibility of optical communication, efforts have to be considered, namely the fundamentals of WDM based on a-SiC:H light controlled filters, when different visible signals are encoded in the same optical transmission path.

In this paper we present a tandem VIS/NIR wavelength selector based on a multilayer a-SiC:H optical filter that requires appropriate near-ultraviolet steady states optical switches to select the desired wavelengths in the VIS-NIR ranges.Spectral response and transmittance measurements are presented and show the feasibility of tailoring the wavelength and bandwidth of a polychromatic mixture of different wavelengths.

The selector filter is realized by using a two terminal double pi'n/pin a-SiC:H photodetector, sandwiched between two ITO contacts that act as biased optical gating elements. Five visible/infrared communication channels (400nm-900nm) are transmitted together, each one with a specific bit sequence. The combined optical signal (MUX signal) is analyzed by reading out the generated photocurrent, under near-UV steady state background applied either from the front, from the back or from both sides.

Results show that the background side and intensity works as a selector in the infrared/visible regions, shifting the sensor sensitivity. Front background enhances the light-to-dark sensitivity of the long and medium wavelength channels and quenches strongly the others. Back background has the opposite behavior; it enhances channel magnitude in short wavelength range and reduces it in the long ones.The optical gain depends mainly on the channel wavelength and to some extent on the lighting intensity. Even across narrow bandwidths, the photocurrent gains are quite different. This nonlinearity allows the identification and decoding of the different input channels in the visible/infrared ranges.This concept is extended to implement a 1 by 5 wavelength division multiplexer with channel separation in the VIS/NIR range and a transmission capability of 24 Kbps. The relationship between the optical inputs and the output signal is established and an algorithm to decode the MUX signal presented.

An optoeletronic model gives insight on the system physics. A numerical simulation, having as input parameters the experimental data, is presented and explains the light filtering properties of VIS/NIR selector.

ID 210 - Poster

Transmission of signals using white and visible LEDs for VLC applications

*P. Louro[1,2], M. Vieira[1,2,3], V. Silva[1,2], M. A. Vieira[1,2]
[1]UNINOVA, CTS, Caparica, Portugal
[2]ISEL, DEETC, Lisbon, Portugal
[3]FCT-UNL, DEE, Caparica, Portugal

Recent developments in LEDs allowed them to be used in environmental lighting and have revealed many advantages over incandescent light sources including lower energy consumption, longer lifetime, improved physical robustness, smaller size, and faster switching. Besides this general lighting application, LEDs are now used in other specific fields such as automotive headlamps, traffic signals, advertising, and camera flashes. However another emerging field of application is inadvanced communications technology due to its high switching rates. Thus,the visible light spectrum is currently being used in the Visible Light Communication (VLC) technology, taking advantage of the lighting infrastructure based on white LEDs. Theseenergy-saving white light sourcesdevices were enabled bythe invention of efficient blue LEDs.

In this paper we propose the use of a multilayered pinpin device based on a-SiC:H to work as a photodetector operating in the pertinent range of operation for VLC (375 nm - 780 nm) using as optical sources while and visible wavelengths LEDs. The device consists of a p-i'(a-SiC:H)-n/p-i(a-Si:H)-n heterostructure with low conductivity doped layers, sandwiched between two transparent contacts. It works as an optical filter in the visible range with tunable spectral sensitivity dependent on both applied bias and type of steady state optical bias (wavelength, intensity and direction of incidence on the device).

Optoelectronic characterization of the device is presented and includes with spectral response, transmittance and I-V characteristics, with and without background illumination. Results show that when the device is biased with front optical steady state light of short visible wavelength (400 nm) superimposed with the pulsed light emitted from the optical transmission sources, it exhibits an increased output current in the long part of the spectrum (550-650 nm), and a reduction of the same photocurrent for the short wavelengths (400-500 nm). An opposite behavior is observed is the wavelength of the background is changed to longer values. A comparison of the performance of white LEDs and visible wavelengths is presented.

Results show that, front background enhances the light-to-dark sensitivity of the medium, long and infrared wavelength channels and quench strongly the low wavelength, depending optical amplification on the background intensity. The change of the impinging side of the steady state illumination produces the reverse effect, as the output photocurrent is enhanced under short wavelength signals and range and strongly reduced it under the long wavelength.

A decoding algorithm for the detection of different optical signals is presented and discussed with a self-recovery error procedure. A capacitive optoelectronic model supports the experimental results and explains the device operation. A numerical simulation will be presented.

ID 211 - Poster

Passivation Effect of Water Vapour on Thin Film Polycrystalline Silicon Solar Cells

**P. Pikna[1], A. Fejfar[1], C. Becker[2]*
[1]Institute of Physics, Department of thin films and nanostructures, Prague, Czech Republic
[2]Helmholtz-Zentrum Berlin für Materialien und Energie GmbH, Berlin, Germany

Water vapour is commonly used as an alternative to a dry oxygen atmosphere for a surface passivation of silicon wafers by creation of a high quality thermal silicon oxide [1]. While surface is the most defective region of a monocrystalline silicon wafer, defects in polycrystalline silicon (poly-Si) thin film, both in the bulk and at the surface, limit the lifetime of free charge carriers. Water vapour can suppress recombination activity of silicon imperfections such as Si/SiO_2 interface, grain boundaries, intra-grain defects, and impurities [2], [3]. Water vapour passivation conditions, e.g. temperature, steam pressure, exposure time, for silicon bulk and surface in polycrystalline silicon thin film solar cells on glass were investigated to determine optimum processing parameters and to better understand the passivation process. Some poly-Si solar cells were treated in a hydrogen plasma to compare a passivation effect of both media.

Polycrystalline silicon (poly-Si) thin film solar cells [4] were prepared on borosilicate glass by CSG Solar [5], [6]. The preparation procedure involved the manufacturing steps illustrated in Fig. 1. For passivation, the samples were exposed to the water vapour in a stainless steel pressure chamber. Passivation parameters, e.g. temperature, steam pressure, exposure time, were tested in the following ranges: 150 - 650°C, 0.1 - 1.1 MPa, 5 - 225 minutes, respectively. Silicon quality and a success of the passivation was assessed by a Suns-V_{OC} method [7].

Variations of the water vapour passivation parameters brought the best result of 360 mV (from the initial value of 220 mV) at the temperature of 450 °C, steam pressure of 0.75 MPa and exposure time of around 100 minutes.

Several passivation media consisting of hydrogen, oxygen and water molecules in different ratio were applied to determine what element or a functional group predominantly deactivate recombination centres in poly-Si. The best improvement was observed due to the pure water vapour, other media (hydrogen gas H_2 (g); mixture of H_2 (g) and steam; boiling 30% H_2O_2) gave worse results. On the base of these experiments with different hydrogen and oxygen concentration, it is assumed that both elements as hydrogen so oxygen participate in the water vapour passivation process and their optimum ratio in the passivation atmosphere is 2:1, respectively.

Passivation effect of the water vapour on the polycrystalline silicon thin film solar cells on glass was investigated and compared with the treatment in the hydrogen plasma. While the water vapour passivation brought the best result of 360 mV (from the initial value of 220 mV), it was still not as high as effect of the plasma hydrogenation which achieved 497 mV. Nevertheless, a clear passivation effect of the water vapour on poly-Si was proved and it could be a suitable low-cost alternative to the hydrogen plasma or an additional passivation supporter.

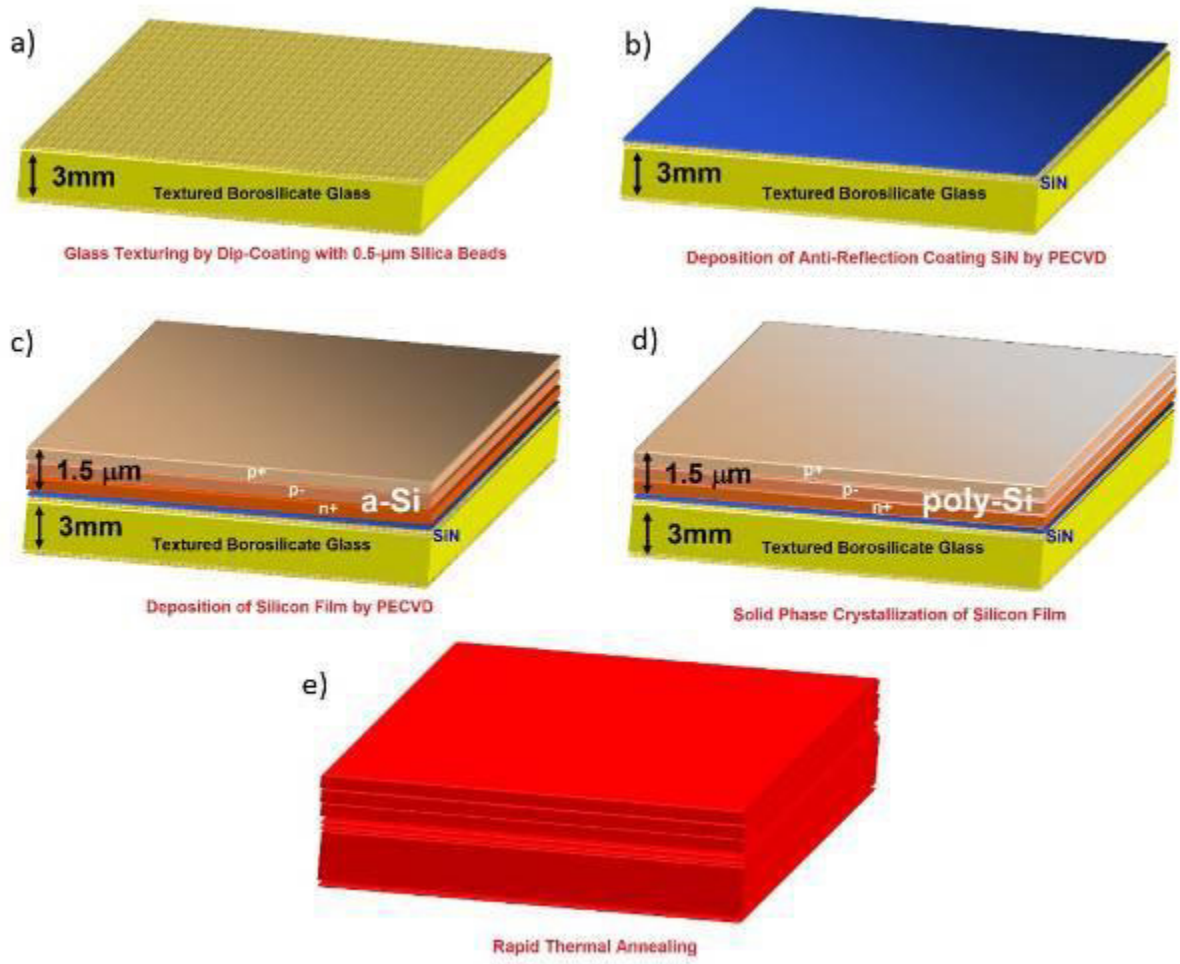

Manufacturing sequence of the thin film polycrystalline silicon (poly-Si) solar cells: a) texturing of borosilicate glass by dipping in bath with glass beads, b) deposition of an anti-reflection coating SiN (65 nm), c) deposition of amorphous silicon n+/p-/p+ structure (50 nm, 1400 nm, 100 nm) d) SPC process to prepare polycrystalline silicon, e) rapid thermal annealing. The scheme is based on [8].

[1] D. Biro, S. Mack, and A. Wolf, "Thermal oxidation as a key technology for high efficiency screen printed industrial silicon solar cells", Proceedings of the 34th IEEE PVSC, Philadelphia, United States (2009).
[2] S. Honda, T. Mates, B. Rezek, A. Fejfar, and J. Kočka, "Microscopic study of the H_2O vapor treatment of the silicon grain boundaries", Journal of Non-Crystalline Solids **354** (2008) 2310.
[3] H. Watakabe and T. Sameshima, "High-Pressure H_2O Vapor Heat Treatment Used to Fabricate Poly-Si Thin Film Transistors", Japanese Journal of Applied Physics (2002) L974.
[4] C. Becker, D. Amkreutz, T. Sontheimer, V. Preidel, D. Lockau, J. Haschke, L. Jogschies, C. Klimm, J. J. Merkel, P. Plocica, S. Steffens, and B. Rech, "Polycrystalline silicon thin-film solar cells: Status and perspectives", Solar Energy Materials and Solar Cells **119** (2013) 112.
[5] M. J. Keevers, "Remarkably effective hydrogenation of crystalline silicon on glass modules", Proceedings of the 22nd European Photovoltaic Solar Energy Conference, Milan, Italy (2007).
[6] M. J. Keevers, T. L. Young, U. Schubert, and M. A. Green, "10% Efficient CSG Minimodules", Proceedings of the 22nd European Photovoltaic Solar Energy Conference, Milan, Italy (2007).
[7] R. A. Sinton and A. Cuevas, "A Quasi-Steady-State Open-Circuit Voltage Method for Solar Cell Characterization", Proceedings of the 16th European Photovoltaic Solar Energy Conference, Glasgow, United Kingdom (2000).
[8] Crystalline Silicon on Glass - Silicon Preparation Process, Germany (2006).

ID 212 - Poster

Optical, structural and electrical properties of a-Si:H thin films elaborated by DC magnetron sputtering at different polarizations of the substrate holder

**L. LAIDOUDI[1], R. Cherfi[1], S. Tata[1], A. Rahal[1]*
[1]University of sciences and technology HOUARI BOUMEDIEN, Department of Physics, Algeirs, Algeria

The hydrogenated amorphous silicon (a-Si:H) is a very attractive material for photovoltaic applications, since its strong absorption in visible light, possibility of deposition on large area and low cost of fabrication.

Thin films of a-Si:H have been elaborated by DC magnetron sputtering at 300°C. For all our samples, the deposition conditions are kept constant (Power of 130 Watts, flow rate of hydrogen at 0.75 sccm, flow rate of argon at 6.38 sccm) except the polarization of the substrate holder which varies between -200 volts and +50 volts.

Infrared absorption spectroscopy gives an estimation of the hydrogen concentration between 7% and 14% from the 640 cm^{-1} absorption peak.

The samples were examined by optical absorption technique to determine the absorption coefficient, the optical gap, the thickness and the refractive index. The thickness of the samples is around of 1.4 m and the deposition rate is in order of 9 A/s. The optical gap increases from 1.63 eV to 1.75 eV and the refractive index increases too from 2.8 to 3.15 when the substrates-holder polarization varies between -200 volts and +50 volts. This augmentation of the polarization is responsible for an increase of the material density.

Dark-conductivity and activation energy are obtained via I-V-T electrical measurements. Photoconductivity is measured under white light of 40mW/cm^2.

The variation of substrates-holder polarization between -200 volts to +50 volts is responsible of a slight decrease of the dark conductivity (measured at 40°C) from $5x10^{-8}$ $(\Omega cm)^{-1}$ to $2x10^{-8}$ $(\Omega cm)^{-1}$ well correlated with the increase activation energy between 0.61 eV and 0.66 eV in the extended conductivity model.

On the other hand, the photoconductivity of all our samples is constant and it is in order of magnitude of 10^{-5} $(\Omega cm)^{-1}$.

The results obtained for our samples deposed at 300°C are compared with a previous works [1] which concerned a-Si:H thin films prepared by the same technique, at the same range of substrate holder polarization and at a deposition temperature of 150°C. This work shows the important influence of the polarization of the substrate holder on the samples prepared at 150°C compared with those prepared at 300°C. In fact, at a temperature deposition of 150°C the material is very resistive (E_g=2.1 eV), and a little photoconductive. A presence of oxygen in the thin films is noted and extremely influenced by the value of the polarization of substrate holder.

The IR measurements of our samples prepared at 300°C show for all the substrates holder polarization that the material is free of oxygen, this loads to good optoelectronic properties and in particular a ratio between the photoconductivity and the conductivity about 3 order of magnitude. These optoelectronic properties vary slightly versus the substrates holder polarization. However, considering the photoconduction properties, for photovoltaic applications, the best material we obtained is prepared at a substrates holder polarization of +50 volts.

[1] A. Benabdelmoumen, R. Cherfi, M. Kechouane, A. Rahal, and T. Mohammed-Brahim, Amorphous Materials New Research (Nova Publ,New York, 2013), pp. 61-71, Chap. 4.

ID 213 - Oral

The Role of Polymer Purification in Optical and Electrical Properties in Indacenodithiophene-co-benzothiadiazole: Fullerene Solar Cells

*D. Baran[1,2], M. Vezie[2], N. Gasparini[3], F. Deledalle[2], J. Yao[2], B. Schroeder[2], H. Bronstein[4], T. Ameri[3], T. Kirchartz[1,5], I. McCulloch[2,6], J. Nelson[2], C. Brabec[3]
[1]Forschungszentrum Julich, IEK-5-PHotovoltaics, Julich, Germany
[2]Imperial College London, London, United Kingdom
[3]Friedrich-Alexander University Erlangen-Nurnberg, Erlangen, Germany
[4]University College London, London, United Kingdom
[5]University of Duisburg-Essen, Duisburg, Germany
[6]King Abdullah University of Science and Technology, Thuwal, United Kingdom

Minimizing the difference between maximum attainable open circuit voltage ($V_{oc,rad}$) (where all the recombination is radiative) and the open circuit voltage will bring the OPV devices to its radiative limit.[1] Furthermore, strategies to simultaneously increase the short circuit current (J_{sc}) of BHJ solar cells will result in high efficiency solar cells. Understanding on the reduced non-radiative recombination paths and strategies to simultaneously increase photocurrent generation will determine the upper limits of OPV technology.

In this report, we describe the role of material purification on energetic losses and photocurrent enhancement in high efficiency indacenodithiophen-*co*-benzothiadiazole (IDTBT): $PC_{70}BM$ bulk-heterojunction (BHJ) solar cells. We investigate the reciprocity relation between photovoltaic quantum efficiency and electroluminescence to explain the reduced energetic losses in highly purified IDTBT-HMw: $PC_{70}BM$ solar cells. In addition, we explain the photocurrent enhancement from non-purified to highly purified IDTBT: $PC_{70}BM$ solar cells by combining electroluminescence spectroscopy (EL), fourier transform photocurrent spectroscopy (FTPS), photo-induced charge carrier extraction by linearly increasing voltage technique (photo-CELIV) and transient photovoltage (TPV) measurements. Highly purified IDTBT-HMw system exhibited reduced non-radiative recombination and higher photocurrent generation among its analogues mainly due to higher electroluminescence emission yield, improved mobility and charge carrier concentration.

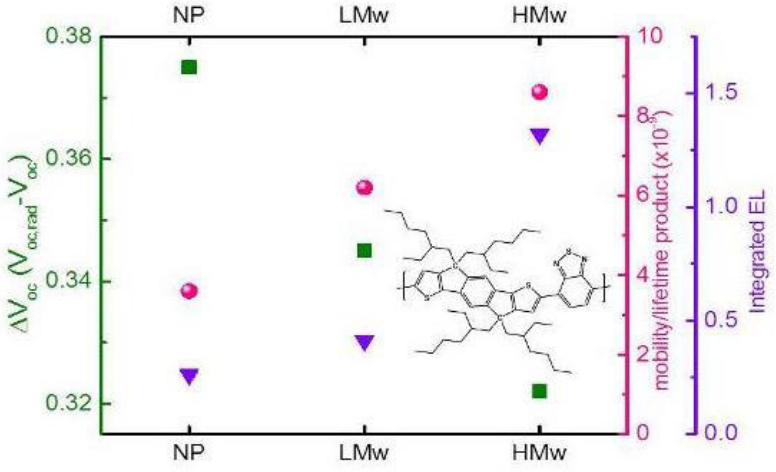

(1) Tvingstedt, K.; Malinkiewicz, O.; Baumann, A.; Deibel, C.; Snaith, H. J.; Dyakonov, V.; Bolink, H. J. Sci. Rep. 2014, 4.

ID 214 - Oral

The question of photogenerated charge carrier recombination in a-Se

**O. Bubon[1], K. Jandieri[2], A. Reznik[3,4], S. Kasap[5], S. Baranovski[2]*
[1]Lakehead University, Chemistry and Material Science, Thunder Bay, Canada
[2]Philipps University Marburg, Department of Physics, Marburg, Germany
[3]Lakehead University, Department of Physics, Thunder Bay, Canada
[4]Thunder Bay Regional Research Institute, Thunder Bay, Canada
[5]University of Saskatchewan, Department of Electrical Engineering, Saskatoon, Canada

Amorphous selenium (a-Se) is a photoconducting material with a set of unique properties many of which do not fit into the conventional notions of amorphous materials. This applies both to charge transport in high electric fields, and to the mechanisms of photogeneration and recombination. Indeed, it was shown that electron-hole pair creation energy (*W*) in a-Se does not follow the general so-called Klein rule for semiconductors. Moreover, it was shown that the value of *W* decreases with the increase in electric field. Although the underlying mechanism for a such dependence remained unclear, it was generally believed that the application of high electric field to a-Se suppresses recombination of photogenerated charge carriers thus improving charge collection and decreasing *W*. Clarification of the effect of electric field on electron-hole creation energy requires Pulse Height Spectroscopy (PHS) and charge collection (CC) experiments over a much broader range of electric fields than it is possible with plain a-Se layers due to the technical complications associated with operating a-Se at electric fields higher than 30 V/μm.

To enable measurements of *W* at high electric fields, we use a modified a-Se HARP (High-gain Avalanche Rushing Photoconductor) structure with pixel electrodes that allows us to apply electric fields up to 100 V/μm. We show that electron-hole pair creation energy *W* decreases linearly with field all the way up to avalanche threshold of 80 V/μm and saturates at ~ 9 eV at higher fields. In addition we measured *W* in a wide range of temperatures (193K - 330 K) and show that it decreases with increasing temperature. Moreover, the higher the electric field, the less pronounced is the temperature dependence of *W*.

Our experimental data clearly confirms previous findings [1] that it is columnar recombination that governs electron-hole creation energy in a-Se. Our results allow us to expand our knowledge on columnar recombination suggested initially by Jaffe [2] to explain the saturation in the field dependence of the charge extraction yield in gases and liquids ionized by α or β particles. We suggest that upon x-ray excitation, the yield of charge extraction from the cylinder (column) created by charge carriers along the track of the primary photoelectron is conditioned by the interplay between the field enhanced drift-driven diffusion escape of carriers from the column and their biomolecular recombination inside the column. We used this theory to account for our experimental data on the dependence of the electron-hole pair creation energy on the electric field and temperature *W*(*F,T*).

1) C.Haugen, S.O.Kasap and J.Rowlands, J. Phys. D: Appl. Phys., **32**, 200 (1999)
2) G.Jaffe, Ann. Phys., Lpz. (Series No 4), **42**, 303 (1913)

ID 215 - Oral

Response Time Measurements and Photocarrier Life Time Distributions in Zno-Based Thin Films and Nanowires

*R. Schwarz[1], R. Ayouchi[1], J. Godinho[1], P. Sanguino[2], R. Franco[2], S. R. Bhattacharyya[3]
[1]Instituto Superior Técnico, Departamento de Física, Lisbon, Portugal
[2]Universidade Nova de Lisboa, Departamento de Química, Caparica, Portugal
[3]Suri Vidyasagar College, Department of Physics, Birbum-Colcatta, India

Steady-state photocurrent spectra in ZnO thin films show a sharp rise near the band gap at 366 nm, but also a decline for the deep UV region due to strong surface absorption. Time-resolved measurements will give access to different recombination processes of photogenerated carriers. The density of defects and their energetic position within the band gap might vary strongly depending on deposition method, film microstructure, sample geometry, contact quality and measurement environment. Here we compare the kinetics of photoinduced conductivity as well as transient photocapacitance in order to study recombination in typically 200 nm thick films of ZnO and in nanowires of 40 to 200 nm diameter. Bulk films and nanowires were prepared by pulsed laser deposition (PLD) and by a wet chemical process, respectively.

PLD was performed using a ZnO target under various background oxygen conditions and sapphire or ITO-coated glass substrates. The substrate temperature was varied between RT and 800 ºC. The targets were ablated with either the IR line at 1064 nm or the 4th harmonic at 266 nm of a Nd:YAG laser.

The UV laser line was then used for excitation of ZnO samples with 5 ns UV pulses to monitor the photocurrent decay. Initial decays show a power law and typical decay times of nano- to microseconds. Strong persistent photoconductivity (PPC) was present at long times in both homogeneous thin films and in ZnO nanowires, with characteristic decay times of up to 400-1000 seconds. Practical problems occurred in vertical readout of sandwich type samples of nanowires deposited on ITO-coated glass, due to shunt currents or inhomogeneous film thickness.

Coplanar measurements, on the other hand, with typically 5 mm long Au contacts at 0.5 mm distance, resulted in easy photocurrent measurements, but led to small photocapacitance values in the low pF range, when excited with a 75 W Xe lamp and controlled by a mechanical shutter. We find that both photocurrent (PC) and photocapacitance (PhotoCap) decays are governed by stretched exponential fit, or, alternatively, by a power law decay. We have looked at the dependence - especially in the long-time range - of the power law exponent as a function of measurement temperature, of light intensity, and of film morphology.

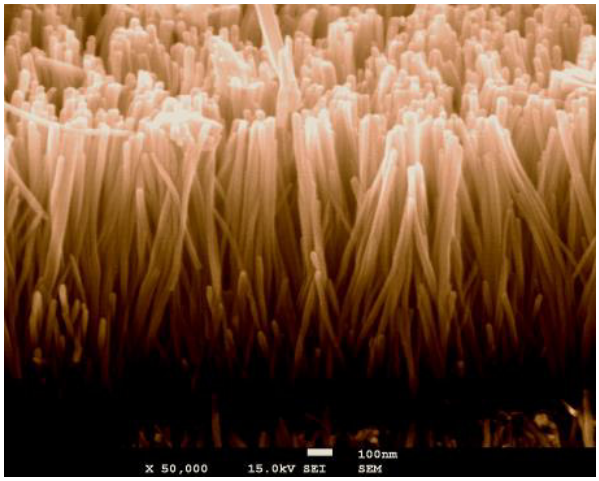

ID 216 - Poster

Raman Spectroscopy and XRD of Ferroelectric Domains in Ceramisc and in PLD-Deposited Na0.5K0.5NbO3 Films

*R. Ayouchi[1], *R. Schwarz[1], L. Santos[2], M. Leal[3], W. Donner[3]*
[1]Instituto Superior Técnico, Departamento de Física, Lisbon, Portugal
[2]Instituto Superior Técnico, Departamento de Química, Lisbon, Portugal
[3]Universitaet Darmstadt, Inst. Materialwissenschaften, Darmstadt, Germany

Lead-free, and therefore environmentally friendly, thin films of sodium-potassium niobate (NKN, Na0.5K0.5NbO3) are optically transparent and show ferroelectric properties. Therefore, they might find applications as active or passive thin surface coatings of solar cell window layers. Thin films of NKN, produced by laser ablation of stoichiometric ceramic targets, have shown an increase of polycrystalline structure and increase in ferroelectric quality, when the substrate temperature is raised from room temperature up to 600 ºC. However, increasing loss of Na and K might occur. We have therefore prepared ceramic targets with excess alcali content. Some ceramics have undergone an additional high-temperature sintering step.

Detailed information of the morphology and structure of both targest and thin films was obtained from confocal Raman spectroscopy. The lateral resolution allowed us to scan domains with submicron precision. The change in film structure observed by SEM is accompanied by a shift of the Nb-O-octaeder stretching mode at an energy of 615 cm-1 , suggesting a change in internal stress of the films. Two further strong peaks [1] present in the ceramic NKN targets at 260 cm-1 and 852 cm-1, are either low in intensity in the films or they do not change position. These results are correlated with XRD diffraction data to identify the possible content of non-stoichiometric NKN components.

The optical quality of the NKN samples was further investigated by optical transmission, revealing a bandgap of near 4 eV with large Urbach tail parameters of up to 200 meV. Finally, we performed second-harmonic generation measurements (SHG) using the 1064 nm line of a pulsed Nd:YAG laser and relating the conversion efficiency to target morphology and thin film deposition parameters.

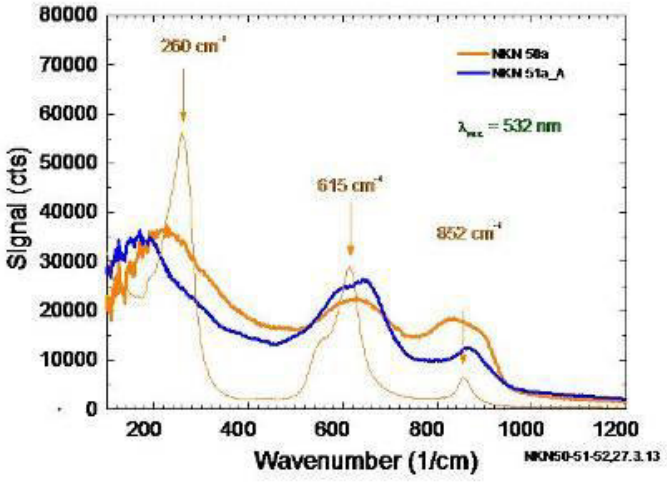

[1] K. Kakimoto, K. Akao, Y. Guo and H. Ohsato, Raman Scattering Study of Piezoelectric (Na0.5K0.5)NbO3-LiNbO3 Ceramics, Jpn. J. Appl. Phys. 44 (2005) pp. 7064-7067.

ID 217 - Oral

Opto-electronic properties measured by transient microwave conductivity in PLD-deposited ZnO-based thin films and nanowires

*M. Kunst[1], R. Ayouchi[2], R. Schwarz[2]
[1]Helmholtzzentrum-Berlin, Dep. Solar Fluids, Berlin, Germany
[2]Instituto Superior Técnico, Departamento de Física, Lisbon, Portugal

ZnO films are of increasing importance for (photo) induced water decontamination and water splitting for hydrogen production. To this purpose optimal (excess) charge carrier transport is essential. In this contribution the optoelectronic properties of ZnO films are investigated by contactless transient photoconductivity measurements, based on Time Resolved Microwave Conductivity (TRMC) method.

ZnO films were prepared by reactive pulsed laser ablation of metallic Zinc target in Oxygen plasma atmosphere using a frequency-doubled Nd:YAG laser, in the temperature range of 400°C to 700°C. Films have been characterized by different methods including X-ray diffraction, Scanning Electron Microscopy, photoluminscence spectroscopy and optical absorption measurements.

Contactless TRMC measurements at a microwave frequency of 30 GHz were induced by short 355 nm light pulses. The TRMC signals due to mobile electrons show an extended decay characterized by a straight line between 100 ns - 1 ms in a double logarithmic representation with a slope of -0.3, possibly due to multiple trapping in an approximately exponential conduction band tail. Up to an excitation density of 3 mJcm-2, the signal is proportional to the excitation density, at higher intensity a faster decay appears between 10 ns - 100 ns accompanied by a sublinear dependence of the signal amplitude on the excitation density. Both effects are probably due to electron-hole recombination in films goverend by dispersive transport.

"Fig-ZnO-old+new.doc"
1.3.2013

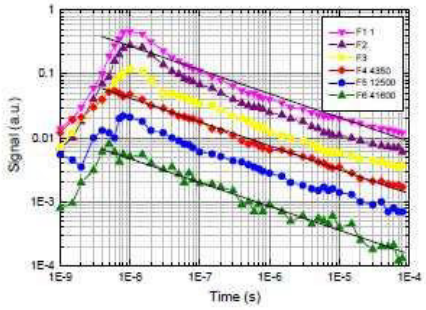

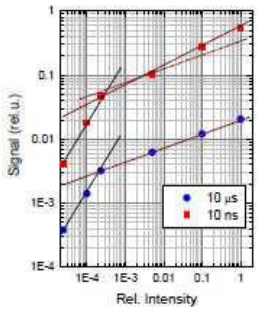

ID 218 - Oral

Transrotational microcrystals and nanostructures discovered by TEM in crystallizing amorphous films and a new model of amorphous state

**V. Kolosov*[1]
[1]*Ural Federal University, Physics Dept., Ekaterinburg, Russian Federation*

As was first discovered for *Se, Te* [1] and later on proved for different films amorphous-crystalline transformation can be associated with rather general unusual phenomenon: strong (up to 300 degrees per micrometer) dislocation independent **regular internal lattice bending** round an axis (or axes) lying in the film plane of the growing crystal. Such **"transrotational" structure** has been revealed and studied (***in situ*** as well*)*, using transmission electron microscopy (TEM) bend-contour technique [2, 3] for the different amorphous films (primary chalcogenides and oxides), prepared by various methods and crystallized in different manner. HREM, correlative AFM-TEM were used in due case to study some details of both initial amorphous and final crystallized areas.

In this paper we describe (on the level from nano- to microscale) different geometries, textures and gradients of lattice orientations, for this unusual microstructure named “transrotational” [4]. Main schemes of internal crystal lattice transrotation geometry with corresponding TEM images below are shown at Fig.1 (left to right: Se, Fe_2O_3, Ta_2O_5, C+Se+C, Sb_2Se_3 with a bar = 1 μm where not specified). In the sense of atom order and energy it can be considered as an intermediate between amorphous and crystalline. It may be one of the reasons of easy transitions in chalcogenide-based films for phase-change memory, which in fact tend to crystallize in such manner. Multiple reversible local transformations “amorphous - transrotational crystalline” observed *in situ* in TEM are presented for *Se-Te* films, films with some of TEM micrographs shown at Fig.2 (see presence and absence of diffraction contrast, bend contours, at the center of left "finger" - initial magnification 10K).

Atomistic mathematical model for the atom positions in "transrotational" single crystal is proposed (based on mathematical instruments of conformal/quasi-conformal transformations of usual set of crystal lattice points to the transrotational one).

Microcrystals and nanostructures with “transrotation” during last years have been eventually recognized/studied in a variety of thin film systems including well-known chalcogen/chalcogenide-based compositions (e.g. [5-6]). We suppose that the role of transrotational crystalline structures (can be recognized directly only by TEM) has been underestimated since corresponding microstructure parameters can strongly influence the phase switching.

Basing on the above results a new hypothetical model of the amorphous state (at least for the film deposits) is proposed: ultra-fine-grained (microcrystalline) structure in which the grains have "transrotational" structure, Fig. 1 (right bottom). Thus the great variety of different transrotational lattice geometries inside fine crystal grains (e.g., complying with different conformal transformations described mathematically for 2D case) in the model corresponds to different amorphous structures hardly distinguished by usual methods but inevitably carrying some distinct physical properties.

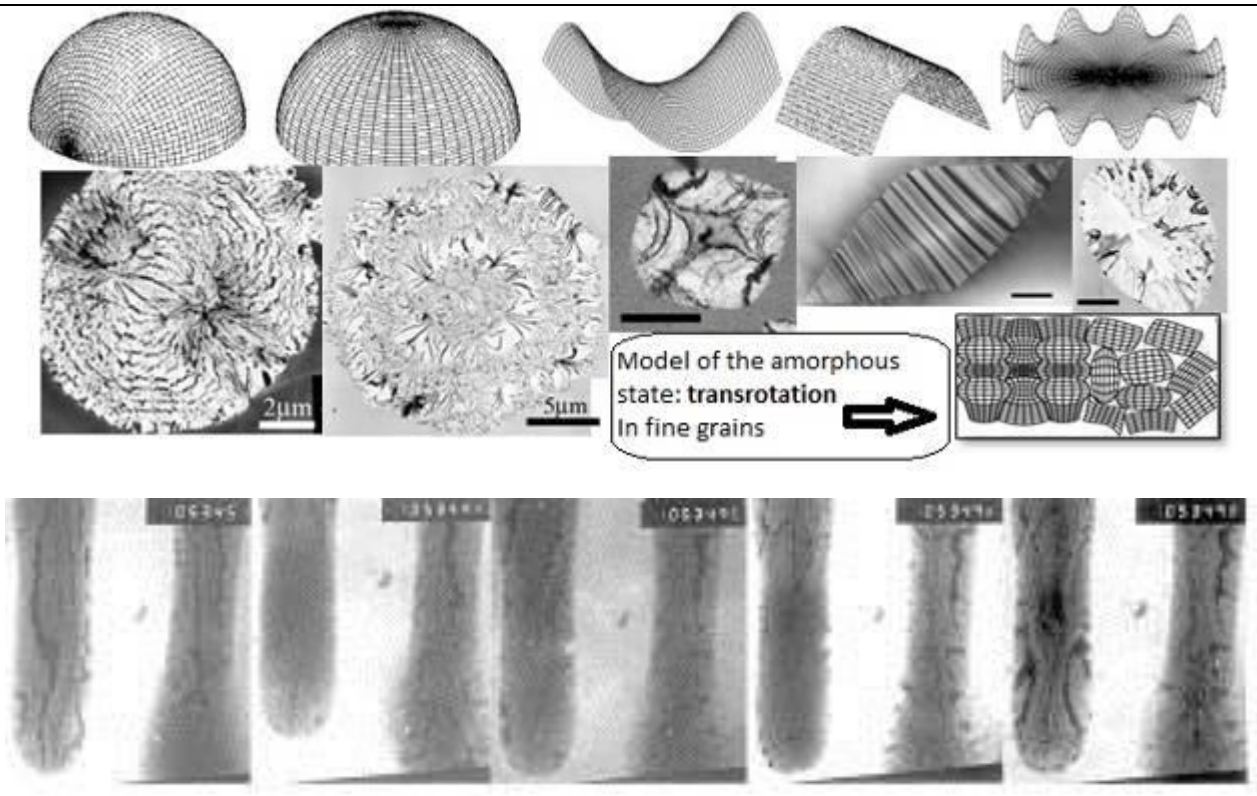

[1] I. E. Bolotov, V. Yu. Kolosov and A.V. Kozhyn, Phys. Stat. Sol. **72a**, 645 (1982).
[2] V. Yu. Kolosov, Proc. XII ICEM, Seattle, **1**, 574 (1990).
[3] I. E. Bolotov and V. Yu. Kolosov, Phys. Stat. Sol. **69a**, 85 (1982)
[4] V. Yu. Kolosov and A. R. Thölen, Acta Mat. **48**, 1829 (2000).
[5] B. J. Kooi, and J. Th. M. De Hosson, J. of App. Phys., **95,** 4714 (2004).
[6] E. Rimini, et. al., J. Applied Physics **105**, p.123502 (2009).

Partially supported by RF Ministry of Education and Science.

ID 219 - Oral

Amorphous Electride to realize OLEDs with Inverted Structure

**H. Hosono[1,2], J. Kim[1], S. Watanabe[3,2], N. Miyakawa[3], T. Toda[1,2], T. Kamiya[1]*
[1]Tokyo Institute of Technology, Materials and Structures Laboratory, Yokohama, Japan
[2]Japan Science and Technology Agency, ACCEL, Kawaguchi, Japan
[3]Asahi Glass, Yokohama, Japan

Electrides are ionic compounds in which electrons serve as anions. First electride material was reported in 1983 by J.Dye who succeeded in crystallizing solvated electrons by using crown ethers. Although a series of organic electride materials were reported since then, the materials research remained almost uncultivated due primarily to their extreme sensitivity to heat and ambient atmosphere. In 2003, we reported stable electride using $12CaO \cdot 7Al_2O_3$ (C12A7) crystal composed of 3-dimensionally connected sub-nanometer-sized cages. C12A7 is, of course, is a typical insulator but can be converted into a metallic conductor and eventually to a superconductor by exchanging oxygen ions as the counter anion with electrons. Subsequently, we found amorphous C12A7 electride (C12A7:e) can be fabricated by melt-quenching or conventional sputtering method. The resulting amorphous C12A7:e contains anionic electrons of $\sim 1 \times 10^{21} cm^{-3}$ and semiconducting properties.

This paper reports realization of OLED with inverted structure using amorphous C12A7:e- as the electron injection layer. Inverted structure is superior to the conventionally used normal type because light can emit without passing through TFTs arrays. This feature is much advantageous for high resolution OLEDs because of high aperture ratio. In particular, this structure is highly demanded now because oxide-TFTs represented by a-IGZO-TFT are promising as the backplane of OLEDs.

The largest obstacle for inverted OLEDs is absence of excellent electron injection materials suitable for this stacking sequence. The currently used materials, LiF + Al, work well for the normal stacking but their performance is much degraded for inverted structure. Here we report that amorphous C12A7:e works as an excellent electron injection material of OLEDs. The inverted type OLED utilizing a-C12A7:e showed the almost the same or slightly better performance than the normal type OLEDs. This result is attributed to the unique properties of a-C12A7:e, i.e., low work function of 3.0eV , chemical inertness and visible transparency.

ID 220 - Oral

Towards ultra-high efficient photovoltaics with perovskite/crystalline silicon tandem devices

*S. De Wolf[1], J. Werner[1], P. Löper[1], A. Walter[1], S.- J. Moon[2], C.- H. Weng[1], J.- H. Yum[2], S. Nicolay[2], J. Bailat[2], M. Filipec[3], M. Topic[3], R. Peibst[4], B. Niesen[1], C. Ballif[1,2]
[1]EPFL, Neuchatel, Switzerland
[2]CSEM, Neuchatel, Switzerland
[3]University of Ljubljana, Ljubljana, Slovenia
[4]ISFH, Hamelin, Germany

Perovskite/crystalline silicon (c-Si) tandem solar cells are one of the most promising approach to reach conversion efficiencies beyond 30% at reasonable additional costs. In these tandem structures, a semi-transparent perovskite cell is either mechanically stacked onto a c-Si bottom cell to form a 4-terminal tandem device or directly processed onto the c-Si cell to form a monolithic (2-terminal) tandem cell. In this work, we discuss the requirements to reach ultra-high efficiencies with such device, identify potential bottlenecks and show the solutions recently developed in our labs towards this performance goal. These include optical simulations (based on experimentally measured optical properties of the perovksite cell layers) and the development of a transparent electrode with high near-infrared transparency, using sputtered transparent conductive oxides. With this, we have produced efficient semi-transparent perovskite solar cells, as well as 4- and 2-terminal perovskite/c-Si tandem cells.

As the efficiency of c-Si solar cells is approaching the practical efficiency limit of 26% [1], novel solutions should be found for Si photovoltaics to become fully competitive with conventional energy sources. One of the most promising approaches lies in combining market-proven silicon solar cell technology with a low-cost wide-bandgap top cell to form a tandem cell. Organic-inorganic halide perovskite solar cells are promising candidates for top cells, showing high efficiencies with simple and cost-effective device fabrication. The combination of perovskite and crystalline silicon absorbers has been shown by calculations to have the potential to reach efficiencies beyond 30% [2,3]. However the necessary technological steps are yet to be precisely defined, in terms of device architecture, materials choice and optical properties of the two sub-cells.

We use optical and device simulations to provide guidelines for layer thickness optimization, for the choice of c-Si bottom cell texturation and to identify the principle requirements for the perovskite top-cell, including high near-infrared transparency, excellent optical outcoupling and cautious choice of the charge transport layers. Indeed, for tandem applications, the perovskite solar cell must be highly transparent at near-infrared wavelengths such that sufficient light is transmitted to the narrower-bandgap bottom cell. The first practical step is thus to replace the metallic rear electrode by a transparent material. Then the semi-transparent top cell can be integrated in tandem device architectures, considering the guidelines given by optical simulations. In monolithic tandem devices, an efficient intermediate layer is required for electrical interconnection and optical coupling. Finaly, the top charge transport layer must be highly transparent.

Tandem solar cells combining two efficient single-junction cells with different optical band gap are promising to overcome the current lab record efficiency of 25.6% [4]. The required excellent near-infrared transparency in the top-cell can be achieved with amorphous transparent conductive oxides, deposited by sputtering, a wide-spread industrial process, compatible with large-scale conventional fabrication. This transparent electrode together with the optical simulations is the key element towards highly-efficient tandem devices.

Optical simulations give optimization guidelines for layer thicknesses and show that minimal parasitic absorption in the top cell is required. We fabricated semitransparent perovskite solar cells with over 10% efficiency, using a sputtered broadband transparent electrode made of amorphous indium zinc oxide. This IZO electrode absorbs less than 3% over the whole spectra range of interest, while maintaining good electrical properties. We avoid sputter damage to the sensitive organic layers by inserting a thin

metal-oxide buffer layer. Our four-terminal devices consisting of the developped NIR-transparent perovskite top cell and an amorphous silicon/crystalline silicon heterojunction (SHJ) bottom cell yield efficiencies of up to 18%. Our current work focuses on the integration of these developments to monolithic tandem solar cells, for which we will discuss J-V and EQE measurements. This work represents a further step towards industrially viable tandem cells with performances beyond the current single-junction silicon record efficiencies.

[1] R. M. Swanson, “Approaching the 29% limit efficiency of silicon solar cells,” in *Proc. 31st IEEE Photovoltaic Specialists Conference, 2005.*, 2005, pp. 889-94.
[2] P. Löper, S.-J. Moon, S. Martin de Nicolas, B. Niesen, M. Ledinsky, S. Nicolay, J. Bailat, J.-H. Yum, S. De Wolf, and C. Ballif, “Organic-inorganic perovskite/crystalline silicon four-terminal tandem solar cells,” *Phys. Chem. Chem. Phys.*, 2014.
[3] M. Filipič, P. Löper, B. Niesen, S. De Wolf, J. Krč, C. Ballif, and M. Topič, "$CH_3NH_3PbI_3$ perovskite / silicon tandem solar cells: characterization based optical simulations", *Optics Express*, submitted Dec 2014 and currently in revision review.
[4] NREL, “NREL Efficiency Chart,” 2015. [Online]. Available: http://www.nrel.gov/ncpv/images/efficiency_chart.jpg.
[5] Z. C. Holman, A. Descoeudres, S. De Wolf, and C. Ballif, “Record Infrared Internal Quantum Efficiency in Silicon Heterojunction Solar Cells With Dielectric/Metal Rear Reflectors,” *IEEE J. Photovoltaics*, vol. 3, no. 4, pp. 1243-1249, 2013.

ID 221 - Oral

Facile, large area growth of mono- and few-layer MoX_2 (X: S, Se, Te) with high catalytic performance by controlled chalcogenation of a molybdenym foil

*A. Antonelou[1], V. Dracopoulos[1], G. Syrrokostas[1], *S. Yannopoulos[1]*
[1]FORTH/ICE-HT, Rio-Patras, Greece

Two-dimensional (2D) crystals have attracted a tremendous amount of research interest over the last decade owing to their unique properties in comparison to their bulk counterparts. The interest is not only academic as 2D crystals exhibit a number of unique phenomena exploitable in various applications. Besides single-atom thick 2D crystals such as graphene, polyhedral thick materials whose layer thickness is dictated by the size of structural unit, i.e. transition metal di-chalcogenides, TMDCs (MoX_2, TaX_2, etc., with X: S, Se, Te) can be prepared in mono- and few-layer thickness by various methods.

Whilst the vast majority of the spectacular properties of TMDCs emerging as the number of monolayers decreases are so far considered adequately understood, vivid interest is focused now on commercialization and viable applications of these materials. Essentially, the prerequisite to achieve this is the facile, reliable and low-cost preparation of substrate-wide films of controlled thickness. Here, we show that preparation of substrate-wide MoX_2 is achievable with easy control down to the monolayer thickness. The growth takes place via soft chalcogenation of commercially available Mo foils without any pretreatment by a process that is scalable to any substrate dimension. The quality of the prepared MoX_2 layers on such flexible substrates is characterized by Field-Emission Scanning Electron Microscopy (FE-SEM), Raman scattering and X-ray photoelectron spectroscopy (XPS). In addition, the catalytic activity of MoX_2 as counter electrodes (CE) has been evaluated demonstrating outstanding performance, similar to that of the more costly Pt-based CEs.

ID 222 - Poster

Study of the effects of annealing and deposition time on the Chemical Bath-deposited CuS Thin Films at room temperature

*R. Ambrosio[1], A. Carrillo[2], M. Moreno[3], E. Lira[2], M. D. L. Mota[2], *D. Murias[3], F. Guerrero[1]*
[1]BUAP, Electronics, Puebla, Mexico
[2]UACJ, Electrical and Computing, Ciudad Juarez, Mexico
[3]INAOE, Electronics, Puebla, Mexico

Chemical bath deposition (CBD) is a simple, reproducible and cost effective technique for fabricating high quality compound semiconductors as metal chalcogenides thin films on different substrates.

In this study, amorphous copper sulfide semiconductor thin films have been deposited on indium tin oxide (ITO) substrates at room temperature by chemical bath deposition (CBD). The effect of the parameters such deposition time and annealing were studied. The thin films deposited were optically, chemically, structurally and electrically characterized.

This work reports the successful deposition of copper sulfide (CuS) thin films on ITO substrates at 27 °C and varying the time of deposition (20, 25, 35, and 40 minutes), using as complexing agents triethanolamine and ammonia. The films were characterized using X- ray diffraction (XRD-Figure 1) and atomic force microscopy (AFM) to understand the CuS structure and topography. The optical band gap was determined from UV-Vis absorption edge. The electrical characterization was carried out in order to obtain the resistance of the material, and the current-voltage characteristics (Figure 2).

For our CuS thin films ,the energy band gap values were in the range from 2.22 to 2.32 eV, the smaller value corresponds to the shorter deposition time. The annealing process modify the roughness of the surface in the obtained thin films. The XPS characterization demostrated that CuS thin films were deposited on the substrate from chemical bath. The resistivity of the films decrease as the thickness increases with values in the range from 95.55 to 16.18 Ω-cm for CuS films without annealing and 1.99 x 10^{-4} to 3.29 x 10^{-5} Ω-cm for annealed samples, those material properties are very attractive for flexible electronics applications at low deposition temperature.

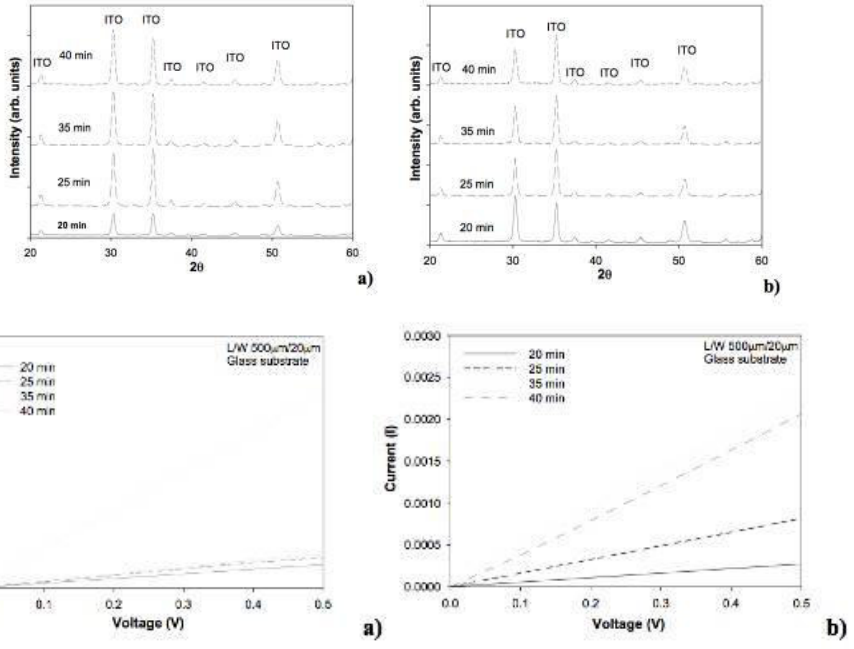

ID 223 - Poster

High external quantum efficiency n-SiNW/PEDOT:PSS solar cell

*Z. Ge[1], *L. Xu[1], W. Li[1], J. Xu[1], Y. Yu[1], W. Su[1], Z. Ma[1], K. Chen[1]*
[1]Nanjing University, Nanjing, China

Silicon nanowires (SiNWs) have been studied in many photoconductive fields owning to their wide absorption spectrum, intensity light absorption and nanometer size effect [1-4]. The hybrid solar cells based on silicon nanowire have attracted much attention for their simply fabrication process and low-cost compared to the conventional p-n Si solar cells, which require high temperature (~1000 °C) processing for ion implantation and dopant diffusion [5.6]. The external quantum efficiency (EQE), which is the percentage of electrons collected per incident photon, can be used as a measure of the efficiency of charge transport given that the following quantities are comparable for a set of devices: (i) incident light intensity; (ii) fraction of light absorbed; (iii) charge collection efficiency at the electrodes, which is mainly given by the choice of electrodes; and (iv) the charge transfer efficiency, as determined from photoluminescence quenching. [7]

We report herein on the effects of different silicon nanowire length and the surface of silicon on the device performance of n-SiNW/PEDOT:PSS hybrid solar cells. The power conversion efficiency (PCE) and external quantum efficiency (EQE) of the SiNW/PEDOT:PSS hybrid solar cells can be optimized by tuning the length of the silicon nanowires and the etching conditions during NW formation. The EQE of over 80% between the wavelengths of 300 and 800 nm was obtained, and with a peak EQE of 86% in the wavelength of 550nm. The optimal short-circuit current density (J_{sc}) of solar cells can reach 33.29mA/cm^2.The PCE of 9.3% is obtained. Scanning electron microscope (SEM) was used to observe the structure of the hybrid solar cells. By controlling nanowire length and the surface of the wafer, we can change the distance on which electrons are transported directly through the thin film device and the density of the surface state, and then gain the optimal condition of fabricating the device. Our approach is a significant contribution to design of high-performance and low-cost inorganic/organic hybrid solar cell.

ID 224 - Poster

The grain boundary passivation of microcrystalline mc-Si by SiN_x:H deposited by PECVD technique

*K. Stanislawa[1], P. Piotr[1]
[1]AGH-University of Science and Technology, Materials Science and Ceramic, Kraków, Poland

One of the key issues for high efficiency silicon solar cells is reducing the surface recombination of charge carriers. Therefore the front surface of cell is covered by passivation layer, for example SiO_2, SiN_x or Al_2O_3. The single amorphous SiN_x:H layer is most often used in production. It can serve as antireflection and passivation layer simultaneously. It is found that as-deposited SiN_x:H layers exhibit an excellent passivation effect on p-and n-type silicon due to the high density bonded hydrogen and/or positive fixed charges. Plasma enhanced chemical vapour deposition process (PECVD) is currently one of the most preferred deposition methods for the SiN:H layers due to a thermal budget lower than the other CVD processes and a high amount of hydrogen in the layer. Because the single SiN_x:H layer requires to find compromise between good optical and passivation properties, application multilayer system composed with two or event three SiN_x:H layers with different refractive index can be more suitable for the high efficiency solar cells. The combination of triple stack system are used as very effective antireflective coatings, in which the main interest is attributed to the bulk and surface defects of silicon passivation.

In this work we investigated the optical and electrical properties of silicon nitride stacks deposited by a large area 13.56 MHz plasma enhanced chemical vapour deposition (PECVD) system. The stack of three SiN_x:H layers with different refractive index were be deposited at 400°C using silane (SiH_4) and ammonia (NH_3) as precursor gases. The chemical composition of the films is modulated by varying the gas flow rate ratio $R=NH_3/SiH_4$. Thanks to spectrophotometric and spectroscopic ellipsometry measurement we have confirmed the suitability of three layer SiN:H stack for antireflection coating. Passivated effects were evaluated by the measurements of effective lifetime using Photoconductance Lifetime Tester WCT-120 (Sinton Consulting). Combination of the antireflection and passivation effects efficiently improves the photovoltaic performance of the crystalline silicon solar cell.

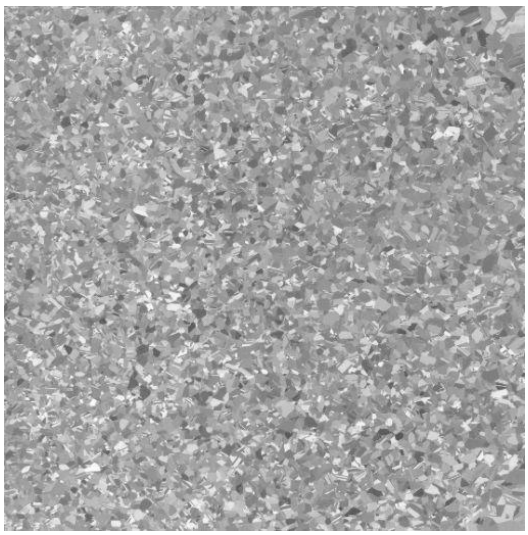

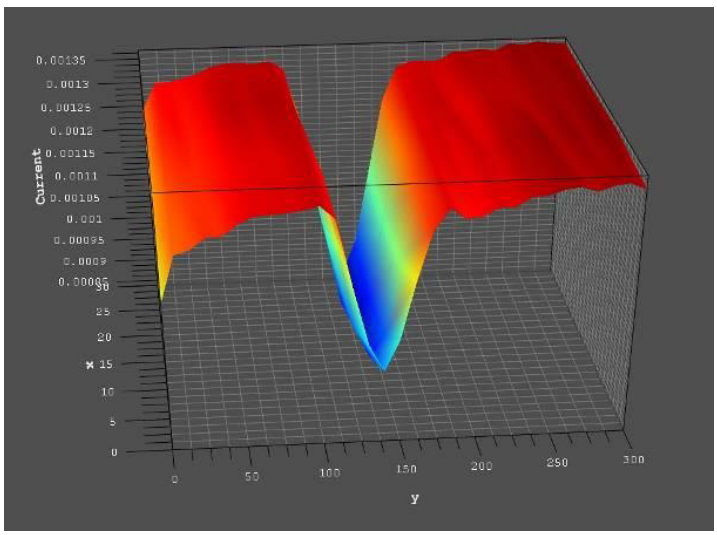

The digital picture of microcrystalline 10 x 10 cm mc-Si wafer and LBIC results after grain boundary investigation performed with 405 nm laser

ID 225 - Oral

Understanding enhanced light harvesting of a conjugated polymer

**M. Vezie[1], S. Few[1], M. Campoy-Quiles[2], I. Meager[3], J. Frost[1], R. S. Ashraf[3], B. Dörling[2], A. Goni[2], I. McCulloch[3], J. Nelson[1]*
[1]Imperial College, Physics, London, United Kingdom
[2]Institut de Ciència de Materials de Barcelona (ICMAB-CSIC), Barcelona, Spain
[3]Imperial College, Chemistry, London, United Kingdom

Increasing polymer absorptivity is a critical parameter for increasing the power conversion efficiency of polymer-based organic photovoltaics given the very low device thickness that is often required for optimum charge collection. We study a series of low bandgap diketopyrrolopyrrole polymers with systematically varied alkyl side chain and molecular weight. The high molecular weight polymers exhibit higher extinction coefficients at low excitation energies than any polymers we have measured previously. Devices made with blends of these polymers with $PC_{71}BM$ exhibit exceptionally high photocurrent densities of 22 mA cm^{-2} and power conversion efficiencies of 8.5%. We investigate the origin of this enhanced absorption through detailed experimental measurements, including ellipsometry and ultraviolet-visible spectroscopy on films and solutions. Furthermore, quantum chemical calculations probe the impact of chemical structure and molecular conformation on oscillator strength, which is proportional to change in dipole moment in the transition and the overlap between the initial and final states. Insights from these calculations allow us to propose design rules to enhance light harvesting efficiency in conjugated polymers.

ID 226 - Poster

Unintentional doping in n-type microcrystalline silicon carbide thin-films

**M. Pomaska[1], S. Muthmann[1], J. Mock[1], F. Köhler[1], O. Astakhov[1], R. Carius[1], F. Finger[1], K. Ding[1]*
[1]Forschungszentrum Jülich GmbH, Institute of Energy and Climate Research - Photovoltaics (IEK-5), Jülich, Germany

Microcrystalline silicon carbide (µc-SiC:H) is a very promising window layer material for silicon heterojunction and silicon thin-film solar cells. Although not intentionally doped during the hot-wire CVD or plasma-enhanced CVD growth process, the µc-SiC:H layers turn out to be n-type semiconductors that offer high electrical conductivity combined with high optical transparency. In this work, we investigated empirically the structural properties and the deposition conditions that seem to be responsible for the high conductivity in “undoped” µc-SiC:H. The results of our study suggest that the electrical properties are closely related to the crystalline volume fraction and Si-C stoichiometry of the layers, and further seem to be very sensible to the conditions of the vacuum chamber for highly crystalline µc-SiC:H. This is indicated by a systematic abrupt increase of the conductivity after intended chamber openings followed by a stepwise decrease of the conductivity for similar depositions with accumulated deposition time. Secondary ion mass spectroscopy measurements suggest oxygen as the crucial impurity element to increase the electrical conductivity in highly crystalline µc-SiC:H. The samples were deposited with the same deposition parameters but strongly differ in the electrical conductivity and show a notable difference in the oxygen content, while the Si-C stoichiometry and the N/H content were found to comparable. Thermal removal of residual oxygen from the chamber walls that is incorporated into the material during growth is indicated by the strong increase in the dark conductivity whenever the heater temperature was raised for the first time to higher temperatures followed by a decrease by several orders of magnitude when repeating the depositions. This work suggests that intentional n-type doping using oxygen precursors might give rise to reproducible growth conditions for highly conductive µc-SiC:H thin-films.

ID 227 - Poster

Influence of Atmosphere on Damp Heat Degradation of ZnO:Al

*J. Hüpkes[1]
[1]Forschungszentrum Jülich GmbH, IEK5-Photovoltaik, Jülich, Germany

Aluminum-doped zinc oxide (ZnO:Al) is widely used as transparent conductor for opto-electronic devices such as photovoltaic (PV) modules. It is used as front contact or as part of the back contact in thin-film PV technology [1]. Solar modules and in particular the contact material must withstand long-term out-door operation. The estimation of out-door stability comprises the exposure of solar modules to a humid environment at elevated temperature (damp heat). During normal operation, the devices are encapsulated to minimize detrimental effects of the environment. Nevertheless, the stability of the non-encapsulated device is considered an important life-time limiting parameter. ZnO:Al conductivity usually degrades under damp heat exposure. However, the degradation mechanism is still not understood in detail and the actual effect was suggested to be related to the combination of humidity and other atmospheric species such as CO_2 [2,3].

This contribution reports on the electrical properties of ZnO:Al thin films on glass after damp heat treatments under various atmospheric conditions. The ZnO:Al films were prepared by in-line magnetron sputtering. One set of ZnO:Al films was annealed under a protective silicon layer, because those ZnO:Al films have been reported to be stable in damp heat treatments after the cap had been removed [4]. The damp heat treatments took place in humid air, or mixtures of hydrogen, nitrogen, argon, and carbon dioxide (CO_2). 500 ml glass vessels were filled with a few milliliters of water and flushed with the respective gas mixture. The amount of water in the glass vessels was chosen to exceed the requirements for water vapor pressure at the given temperature or to represent about 300 mbar of water vapor pressure. The glass vessels were placed in an oven at about 90°C. Electrical properties of ZnO:Al films before and after the treatments were investigated by Hall effect measurements.

Figure 1 shows the electron mobility of ZnO:Al films after damp heat treatment in various atmospheres. Dry heat did not deteriorate the electronic properties irrespective of whether CO_2, air, nitrogen, or fully inert argon were present during the treatment. Humidity, however, led to a significant degradation of resistivity by a factor of 1.5 to 10 depending on ZnO:Al preparation conditions and the atmospheric composition. Higher levels of humidity induced stronger degradation, while the type of gas in the humid atmosphere did not play a major role. In particular, air, forming gas (5% H_2 in N_2), 20% CO_2 in Argon, and pure Argon led to the same charge carrier mobility of 26 cm^2/Vs after 1000 h damp heat treatment. Contrary, in humid CO_2 (no Argon dilution) severe corrosion of ZnO:Al films caused a milky appearance and a resistance increase by orders of magnitude after 1000 hours. The only exception from degradation exhibited the damp heat stable ZnO:Al that was annealed under the protective layer. The protective layer and the top 30 nm of the ZnO:Al had been removed by plasma etching and/or wet-chemical etching, respectively, before damp heat. The electrical properties did not degrade at all and an electron mobility of 70 cm^2/Vs even after 1000 h of damp heat treatment in various conditions was prevailed (see Fig. 2).

In conclusion, damp heat degradation of ZnO:Al is related to incorporation of water vapor and formation of zinc hydroxide only and commonly without major impact of other environmental species like CO_2. If a certain amount of CO_2 in the atmosphere is exceeded, the low pH value of the water caused corrosion of the ZnO:Al via chemical etching. Finally, the ZnO:Al stability of annealed films was excluded to be caused by a surface modification during the annealing but it represents a real bulk effect.

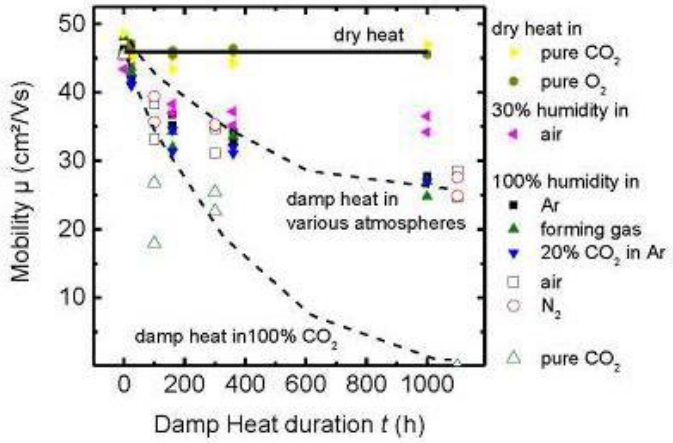

Figure 1: Charge carrier mobility in ZnO:Al films as function of damp heat degradation duration. Several treatments are shown using dry heat as well as damp heat in ambient air or other controlled gas compositions. The lines represent guides to the eye. Dry heat did not harm the electrical properties, damp heat caused degradation of mobility. Humid CO_2 led to chemical corrosion if a certain amount of CO_2 was exceeded.

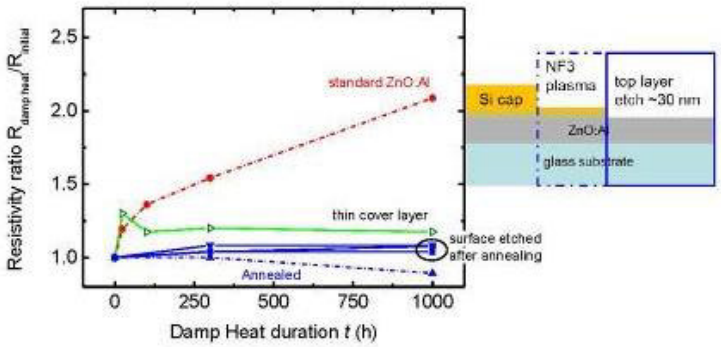

Figure 2: Relative resistivity increase upon damp heat: untreated reference ZnO:Al (red circles), covered by a protection layer (green triangles), annealed under a protective silicon cap layer, and exposed to damp heat after cap removal (blue). The cap was removed by reactive plasma etching (blue dash-dotted line). Additionally the top 30 nm surface layer of the ZnO:Al layer was emliminated by chemical or physical etching (blue solid lines) to assure that there was no remaining surface protection left.

[1] K.L. Chopra, P.D. Paulson, V. Dutta, Progress in Photovoltaics: Research and Applications 12/2-3 (2004) 69.
[2] T. Tohsophon, J. Hüpkes, S. Calnan, W. Reetz, B. Rech, W. Beyer, N. Sirikulrat, Thin Solid Films 511 (2006) 673.
[3] M. Theelen, S. Dasgupta, Z. Vroon, B. Kniknie, N. Barreau, J. van Berkum, M. Zeman, Thin Solid Films 565/0 (2014) 149.
[4] J. Hüpkes, J.I. Owen, M. Wimmer, F. Ruske, D. Greiner, R. Klenk, U. Zastrow, J. Hotovy, Thin Solid Films 555 (2014) 48.

ID 228 - Oral

Light-Driven Vectorial Ion Transport: Using Interdigitated Back-Contact Semiconductors and Organic Photovoltaics for the Photoelectrochemical Generation of Drinking Water from Seawater

*C. Sanborn[1], R. Reiter[1], W. White[1], J. Ma[2], *S. Ardo[1,2]*
[1]University of California Irvine, Chemistry, Irvine, United States
[2]University of California Irvine, Chemical Engineering and Materials Science, Irvine, United States

Many regions of the world are facing massive shortages of clean water for human consumption and agriculture. The earth is an abundant source of water; however, > 95 % of the world's water supply is found in oceans and so is not potable. Thus, an efficient and inexpensive technology to desalinate seawater would be of great benefit to many people. In my presentation I will report on my research group's progress toward the development of two inexpensive, portable, integrated solar-powered desalination devices that will generate water for consumption and agriculture with inputs of only renewable solar energy and salt water.

Semiconductors used in interdigitated back-contact solar cells are uniquely positioned for application in efficient photoelectrochemical devices. The short distance between the positive and negative contacts assures that resistive ionic transport in solution remains small. However, the back contact arrangement also introduces additional design complexity because it requires a complex arrangement of ion-exchange membranes in order to separate photoelectrochemical reaction products. My research group is utilizing this complex arrangement of membranes to design, model, and evaluate photoelectrochemical devices for desalination of salt water. Numerical models and simulations support the validity of the proposed device architectures. Experiments are ongoing to construct a prototype device that demonstrates the desired desalination capabilities using interdigitated back-contact crystalline silicon wafers.

My research group is also focused on fabricating an organic photovoltaic that uses light to drive ion transport - instead of electron transport - to serve as an artificial proton pump. For an initial model system, conical nanopores were selectively track etched in a polyethylene terephthalate plastic sheet, which resulted in pores lined with fixed anionic functional groups. Then, using peptide coupling chemistries, the pores were asymmetrically functionalized with novel photoacids to generate a region containing fixed cationic dyes. The localized distribution of interfacial fixed charge groups mimics a solid-state semiconductor pn-junction with the goal of separating photogenerated charge carriers. Under visible-light illumination and a small reverse bias, excitation of the photoacid molecules resulted in an ionic photocurrent. This initial research and successful demonstration of an artificial light-driven ion pump is being expanded to other polymeric materials with hopes of generating ionic power through sunlight absorption, and incorporating these materials into the device architectures similar to those described above.

ID 229 - Poster

New insight into light-induced degradation of a-Si:H by pulsed EPR on clustered and distributed dangling bonds

*A. Schnegg[1], M. Fehr[2], J. Melskens[3], A. Smets[3], C. Teutloff[1], O. Astakhov[4], F. Finger[4], K. Lips[2,4]
[1]Freie Universität Berlin, Berlin Joint EPR Lab, Fachbereich Physik, Berlin, Germany
[2]Helmholtz Zentrum Berlin für Materialien und Energie, Berlin Joint EPR Lab, Institute for Silicon Photovoltaics, Berlin, Germany
[3]Delft University of Technology, Photovoltaic Materials and Devices, Faculty of Electrical Engineering, Mathematics and Computer Science , Delft, Netherlands
[4]Forschungszentrum Jülich, Institut für Energie- und Klimaforschung - 5 Photovoltaik,, Jülich, Germany

Efficiency-limiting recombination mechanisms in thin film silicon solar cells are to a large extent induced by (meta-)stable paramagnetic dangling bonds. Advanced pulsed electron paramagnetic resonance (EPR) is capable of providing crucial structural and functional information on these paramagnetic states. Herein, pulsed multi-frequency EPR is employed to gain insight into the electronic structure of recombination active defects[1] and the formation of defect clusters during light-induced degradation[2]. Electron-spin echo (ESE) relaxation measurements in the annealed and light-soaked state revealed two types of defects (termed type I and II), which can be discerned by their ESE relaxation. Type I defects exhibit a mono-exponential decay related to indirect flip-flop processes between dipolar coupled electron spins in defect clusters, while the phase relaxation of type II defects is dominated by 1H nuclear spins dynamics and is indicative for isolated spins. The defect concentration for both types is significantly higher in the light-soaked state compared to the annealed state. Our results indicate that in addition to isolated defects, defects on internal surfaces of open volume deficiencies play a role in light-induced degradation of device-quality a-Si:H. This assignment is further corroborated by a comparative study on different a-Si:H materials with varying nanostructures. Finally, Doppler broadening positron annihilation spectroscopy analyses on the same a-Si:H samples suggest that type I defects are likely linked to small open volumes, like divacancies, while type II defects are largely associated with larger open volumes, such as nanosized voids[3].

1. Fehr, M; et al. Metastable defect formation at microvoids identified as the origin of light-induced degradation in a-Si:H, *Phys. Rev. Lett.,* 2014, 112, 066403
2. Fehr, M; et al. Combined multifrequency EPR and DFT study of dangling bonds in a-Si:H.*Phys. Rev B*, 2011, 84, 245203/1-1
3. Melskens, J; et al. unpublished results

ID 230 - Poster

Thin-film mechanics for understanding the phase-change kinetics of amorphous $Ge_2Sb_2Te_5$ doped with Al, C, N and Bi

*J.- Y. Cho[1], Y.- C. Joo[2], M. Wuttig[1]
[1]RWTH Aachen University, I. Physikalisches Institut IA, Aachen, Germany
[2]Seoul National University, Materials Science and Engineering, Seoul, Korea, Republic of

For high switching speed and high reliability of phase-change random access memory (PcRAM), we need to identify materials that enable fast phase-change at elevated temperatures but are stable at and above room temperature. Achieving this goal requires a breakthrough in our understanding of the unique phase-change kinetics of amorphous phase change materials, as a fragile glass described as the non-Arrhenius behavior of atomic mobility [1], [2]. It is a highly rewarding task to unravel the phase-change kinetics, because these properties can be utilized to predict the device characteristics; the switching speed at high temperature and the data retention at low temperature. Thin-film mechanical analysis in this study is an effective approach for the detection of the crystallization kinetics, because energetic and structural changes in amorphous materials result in the significant changes of free volume or mechanical properties. In this study, the phase-change kinetics of the amorphous phase change materials with various doping elements were explored to verify their structural features.

First, we observed crystallization temperature (T_x), glass transition temperature (T_g), super-cooled liquid region (T_x - T_g) and fragility of $Ge_2Sb_2Te_5$ (GST) films doped with various elements through the mechanical stress analysis. Fragile-to-strong transition is observed for C and N doping due to their structural feature as an interstitial dopant, while substitutional Al and Bi doping maintained the fragile behavior of GST (indicated in image 1.). From these data, the temperature dependence of the crystallization growth rate can be derived, which explains the significant degradation of the SET speed in PcRAM for interstitial doping. Doping effects on the thermal stability and atomic mobility show successful matching with the PcRAM characteristics; data retention and SET speed, respectively (indicated in image 2). The correlation between the local atomic structure and the properties relevant to the crystallization kinetics varying with doping provides an explanation of the crystallization kinetics and the prediction of the PcRAM characteristics.

In addition, by measuring the mechanical stress evolution and the thickness changes associated with the crystallization, we also observed that the interstitial doping produces more elastic strain energy than substitutional doping when the GST crystallizes. Thickness changes of film associated with the crystallization was used to calculate the elastic strain energy by assuming elastic deformation according to Hooke's law. From these results, larger elastic strain energy in interstitial doping lowers the difference of G between amorphous and crystalline, thus less driving force for the crystallization in interstitial doping can be expected, which is advantageous for the higher data retention.

The distinct effects of dopants are originated from the changes in free volume and bonding enthalpy by interstitial and substitutional doping. The resulting insight reveals the correlation between the local atomic structure and the properties relevant to the crystallization kinetics varying with doping, providing a thorough relation of the phase-change behaviors and the prediction of the PcRAM characteristics. Consequently, the analysis of materials properties in conjunction with theoretical models helped to build a framework to describe the phase-change kinetics of amorphous materials which can predict and tune the characteristics of functional devices.

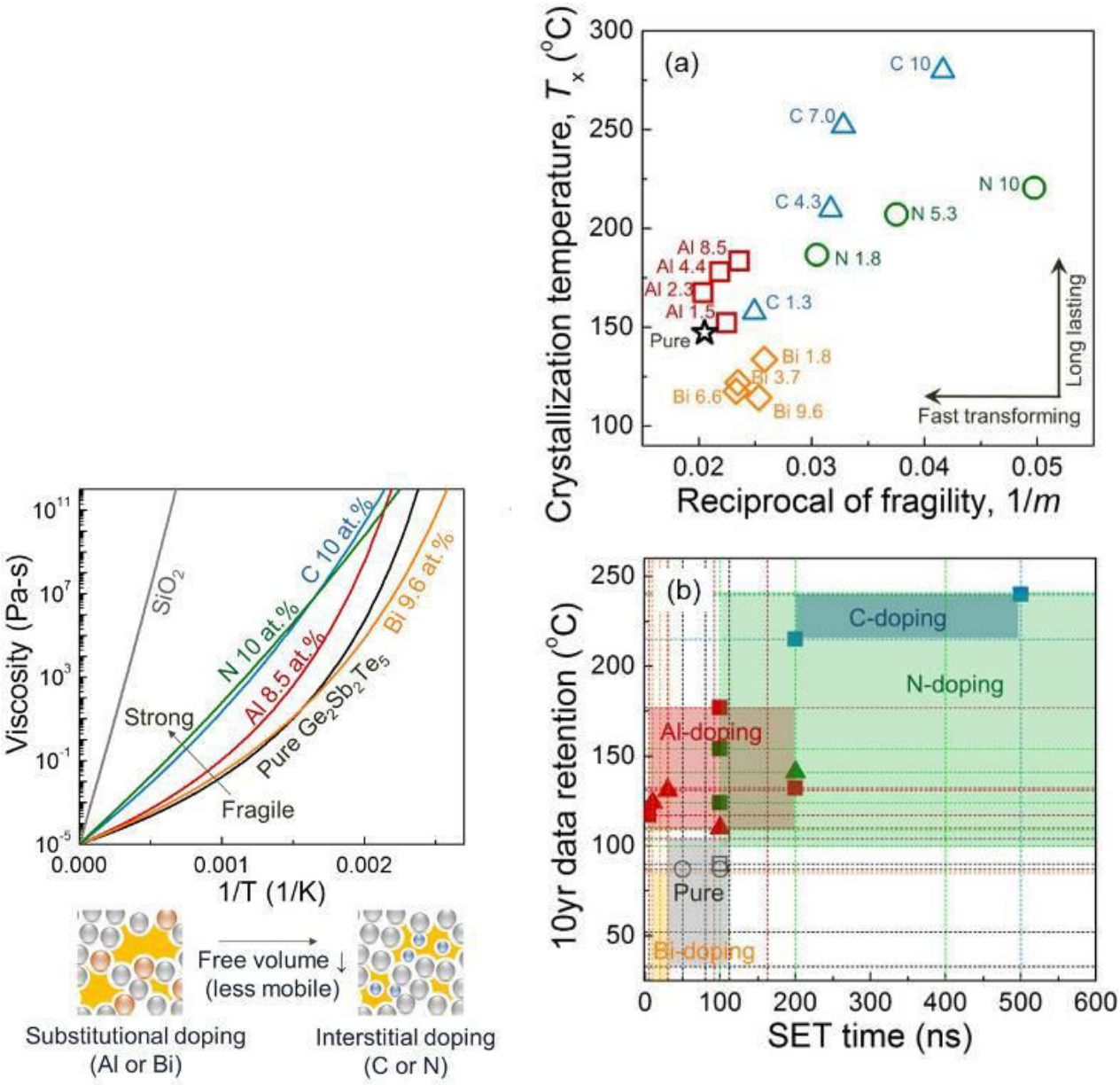

[1] Orava J, Greer AL, Gholipour B, Hewak DW, Smith CE. Characterization of supercooled liquid $Ge_2Sb_2Te_5$ and its crystallization by ultrafast-heating calorimetry. Nature Materials 2012;11:279-83.
[2] Wuttig M, Salinga M. Phase-change materials: Fast transformers. Nature Materials 2012;11:270-.

ID 231 - Poster

Improved Efficiency of Silicon Nanoholes/Gold Nanoparticles /Organic Hybrid Solar Cells Due to Localized Surface Plasmon Resonance

*R. Lu[1], *L. Xu[1], W. Li[1], Z. Ge[1], Z. Liu[1], J. Xu[1], Y. Yu[1], Z. Ma[1], K. chen[1]*
[1]nanjing university, nanjing, China

Silicon is the most widely used material for solar cells due to its abundance, non-toxicity, reliability and mature fabrication process. In this letter, we fabricated silicon nanoholes (SiNHs) / gold nanoparticles （Au NPs）/ organic hybrid solar cells and investigated their spectral and opto-electron conversion properties. SiNHs nanocomposite films were fabricated by metal-assisted electroless etching (EE) method. Then the gold nanoparticles (AuNPs) (including nanospheres/nanorods) of various sizes and shapes were spanned on the SiNHs nanocomposite films. After that, PEDOT:PSS was used to fill on the surface of nanocomposite. The external quantum efficiency (EQE) values of the solar cells with AuNPs are higher than that of the samples without AuNPs in the 400nm-900nm spectral region, which were essential to achieve high performance photovoltaic cells. Compared with the solar cells without AuNPs, the power conversion efficiency of the solar cells incorporate AuNPs have an enhancement of 40%. We thought that the improved efficiency were attributed to localized surface plasmon resonance (LSPR) triggered by gold nanospheres/nanorods on SiNHs nanocomposite films.

ID 232 - Oral

Modulation of Si Nanocrystals Photoluminescence by Local Field Management Using Gold Grating

**D. Zhigunov[1], S. Dyakov[1,2], M. Shcherbakov[1], S. Popov[2], A. Marinins[2], S. Popov[2], M. Qiu[2,3]*
[1]Lomonosov Moscow State University, Physics Department, Moscow, Russian Federation
[2]KTH Royal Institute of Technology, Stockholm, Sweden
[3]Zhejiang University, Department of Optical Engineering, Hangzhou, Sweden

The present work is devoted to the development of effective approach for the control of the optical properties of photonic nanostructures. Recently, certain efforts were addressed to the modification of spontaneous emission of various quantum dots by the resonant coupling with surface plasmons localized in metal nanoparticles [1-3]. However, the efficiency of such coupling is limited by the short interaction distance of localized plasmons, which is usually in the range of several nanometers. In contrast in our study we focus on longer range propagating surface plasmon polaritons and quasi-waveguide modes as promoters for the quantum dots luminescence enhancement [4]. Namely, modulation of luminescence of silicon nanocrystals in a solid matrix was studied since such structures are considered to be promising for optoelectronics [5] and solar cells applications [6].

Ensembles of silicon nanocrystals in SiO_2 matrix were fabricated by the deposition of alternating SiO and SiO_2 layers on quartz substrate followed by 1100 ^oC furnace annealing [7]. Transmission electron microscopy image of resulted multilayered structure showed the array of Si nanocrystals with the mean size of about 2 nm. The presence of crystalline Si phase was confirmed by the Raman spectroscopy. Theoretical calculations using the scattering matrix method predicted the modification of Si nanocrystals photoluminescence spectrum by eigenmodes of the structure. In order to observe such spectrum modification experimentally different gold gratings with the period of 450 nm and variable stripes width were fabricated on the top of the layer with Si nanocrystals by means of e-beam lithography. Angle-resolved transmittance spectroscopy was used to determine the spectral features which represent light-*excited* plasmons. In case of 100 nm stripes width photoluminescence measurements revealed the presence of respective narrow peaks which modulate the broad emission spectrum of Si nanocrystals (Fig. 1). Corresponding calculation of local electric field distribution predicted the excitation of solely localized plasmons (see Fig. 2), while the absence of propagating surface plasmon polaritons can be explained by the large distance between adjacent metal stripes. Thus, the observed in Fig. 1 enhancement of Si nanocrystals photoluminescence arose from the periodic nanostructuring, which led to the excitation of quasi-waveguide mode. The results of theoretical calculations showed good agreement with the obtained experimental transmittance and photoluminescence spectra, which forms the basis of a powerful tool for the design of novel photonic nanostructures.

This work was supported by the Russian Foundation for Basic Research (Grant No. 15-32-21153).

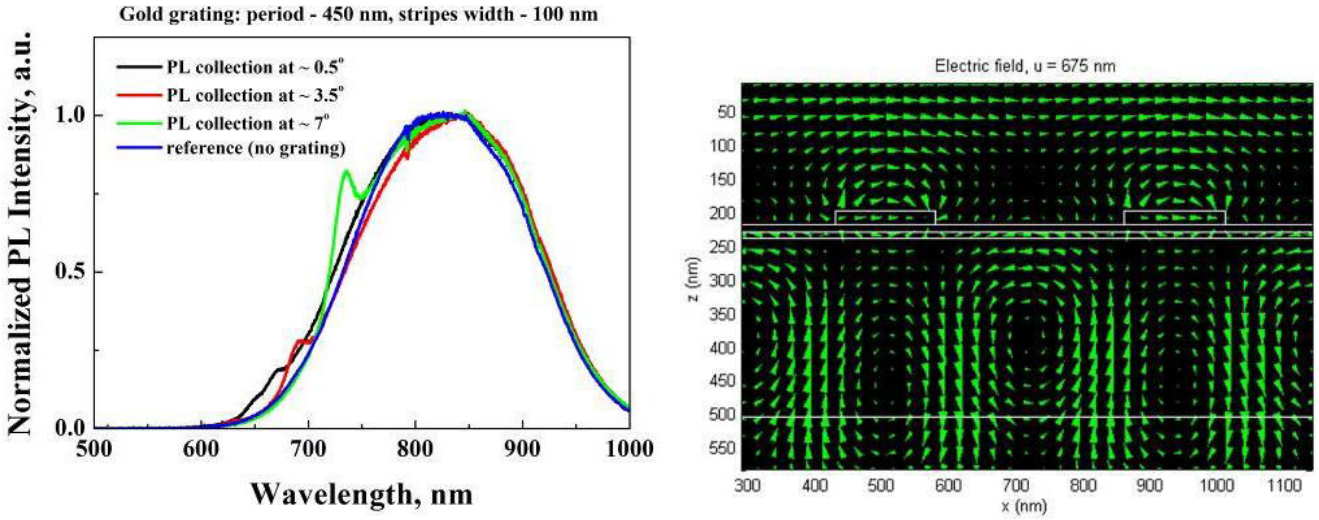

1. T. Nychyporuk, Yu. Zakharko, T. Serdiuk, O. Marty, M. Lemiti, V. Lysenko, “Strong photoluminescence enhancement of silicon quantum dots by their near-resonant coupling with multi-polar plasmonic hot spots”, Nanoscale 3, 2472 (2011).
2. E. Cohen-Hoshen, G.W. Bryant, I. Pinkas, J. Sperling, I. Bar-Joseph, "Exciton-plasmon interactions in quantum dot-gold nanoparticle structures", Nano Lett. 12, 4260-4264 (2012).
3. P.P. Pompa, L. Martiradonna, A. Della Torre, F. Della Sala, L. Manna, M. De Vittorio, F. Calabi, R. Cingolani, R. Rinaldi, “Metal-enhanced fluorescence of colloidal nanocrystals with nanoscale control”, Nature Nanotechnology 1, 126-130 (2006).
4. E. Takeda, T. Nakamura, M. Fujii, S. Miura, S. Hayashi, "Surface plasmon polariton mediated photoluminescence from excitons in silicon nanocrystals", Appl. Phys. Lett. 89, 101907 (2006).
5. N. Daldosso, L. Pavesi, “Nanosilicon photonics”, Laser & Photon. Rev. 3, 508-534 (2009).
6. D. Di, I. Perez-Wurfl, G. Conibeer, M.A. Green, “Formation and photoluminescence of Si quantum dots in SiO_2/Si_3N_4 hybrid matrix for all-Si tandem solar cells”, Sol. Ener. Mat. & Sol. Cells 94, 2238-2243 (2010).
7. M. Zacharias, J. Heitmann, R. Scholz, U. Kahler, M. Schmidt, J. Bläsing, “Size-controlled highly luminescent silicon nanocrystals: A SiO/SiO_2 superlattice approach”, Appl. Phys. Lett. 80, 661 (2002).

ID 233 - Oral

Optimizing the growth of ZnO nanowires by chemical bath deposition for energy applications

*K. Govatsi[1,2], *G. Syrrokostas[1], S. N. Yannopoulos[1]*
[1]FORTH/ICE-HT, Patra, Greece
[2]University, Chemistry, Patra, Greece

Zinc oxide (ZnO) is a wide band gap semiconductor which has received enormous amount of interest over the last decade owing to its flexibility to be grown in a large variety of low-dimensional nanostructures. Nanostructures of ZnO have demonstrated the potential for a wide range of applications in energy, sensing, photonic and optoelectronic devices, etc. This potential arises from a number of advantages such as the low cost of preparation, ease scale up, wide variety of preparation techniques exhibiting different morphologies with high surface area (including nanowires, nanorods, nanotubes, nanorings, nanobelts, etc.) and enhanced light harvesting ability [1,2].Arrays of 1D ZnO nanostructures, such as nanowires (NWs), emerge as the preferred assembly for energy harvesting and conversion.

Among the different preparation techniques chemical bath deposition (CBD) is a facile and low-cost technique used frequently to prepare ZnO NWs with good control over the mean diameter and the aspect ratio [3]. In the CBD method the substrate is usually immersed in an alkaline solution containing a zinc salt and under supersaturation conditions a thin film is deposited on the substrate. A great body of experimental and theoretical investigations has been undertaken over the last decade in order to understand the growth mechanism and how this mechanism is affected by different parameters. Despite this, there are still obstacles to be overcome to achieve large surface area and high aspect ratio of well aligned ZnO NW arrays due to the multi-parametric nature of the growth process. The morphology of the seed layer, the reactants concentrations, the growth time, the bath temperature, the position of the substrate into the reactor, the pH of the solution, the presence of capping agents, mechanical stirring, etc. are among the parameters that affect the morphology of ZnO NWs. In the present study, we systematically explore the role of several of the aforementioned parameters which affect the growth mechanism of NWs and provide some general rules for the controlled growth of ZnO NW arrays with tailored properties.

[1] Z. L. Wang, Mater. Sci. Engineer. R 64, 33 (2009).
[2] K. Govatsi, A. Chrissanthopoulos, S.N. Yannopoulos, in P. Petkov et al. (eds.), *Nanoscience Advances in CBRN Agents Detection, Information and Energy Security, NATO Science for Peace and Security Series A: Chemistry and Biology*, pp. 129-149, (Springer Science, Dordrecht, 2015).
[3] S. Xu and Z. L. Wang, Nano Research 4, 1013-1098 (2011).

ID 234 - Poster

Monolithic Perovskite/µc-Silicon Tandem Solar Cell

*J.- C. Hebig[1], S. Muthmann[1], N. Li[2], C. Quiroz[2], B. Klingebiel[1], R. Carius[1], C. J. Brabec[2,3], U. Rau[1], T. Kirchartz[1,4]
[1]Forschungszentrum Jülich GmbH, IEK-5 Photovoltaik, Jülich, Germany
[2]Friedrich-Alexander-University Erlangen-Nuremberg, Istitute of Materials for Electronics and Energy Technology (i-MEET), Erlangen, Germany
[3]Bavarian Center for Applied Energy Research (ZAE Bayern), Erlangen, Germany
[4]University of Duisburg-Essen, Faculty of Engineering and CENIDE, Duisburg, Germany

Solution processed organometal halide perovskites like methylammonium lead iodide ($CH_3NH_3PbI_3$) are promising candidates for future absorber materials in photovoltaics. Since the report of the first perovskite solar cell in 2009 with a power conversion efficiency of 3.8% [1] the interest in perovskites has increased rapidly. In 2015 perovskite based solar cells reached a conversion efficiency of more than 18 %.[2] Because of its high-performance and the possibility to tune the band gap of the methylammonium lead (mixed) halide between 1.6 eV - 2.3 eV [3] perovskites seem to be a possible tandem partner for mature solar technologies like thin film and even wafer based silicon solar cells.

In this work we present a concept for a monolithic tandem solar cell with a perovskite top cell and a µc-Si:H (pin) bottom cell. The experimental realization of this concept results in tandem cells with a V_{oc} of more than 1.3 V. Starting with an ZnO:Al substrate we deposited a µc-Si pin bottom cell by plasma enhanced chemical vapor deposition (PECVD). On top of this cell we deposited a thin interconnection layer. Using only solution based process steps we build up a hetero junction perovskite top cell by spin-coating PEDOT:PSS, Perovskite, PCBM and ZnO-NP on top of each other. For the front contact we spray-coated a silver nanowire electrode on top of the ZnO-NPs.[4]

One of the challenges for this type of tandem solar cell is the high absorption coefficient of the perovskite in the range of 10^5 cm^{-1} while the light absorption in the µc-Si is relatively low. Currently, the tandem solar cells suffer from insufficient current matching with the perovskite sub cell absorbing more light than the µc-Si sub cell. In order to improve device efficiencies further, we will use structured ZnO:Al substrates for light trapping to increase absorption in the µc-Si bottom cell.

Finally we show that the presented layer stack for the perovskite/µc-Si tandem cell is a very universal concept for building up perovskite/silicon tandem solar cells. This concept can be transferred easily from µc-Si test devices to a wafer based silicon bottom cell. This is highly important because finding a tandem partner as top cell for crystalline silicon is one of the big challenges in today's photovoltaic research.

[1]Kojima A. et al., *J. Am. Chem. Soc.* **2009**, 131, 6050-6051
[2]Jeon N. M., et al., *Nature* **2015**, 517, 476-480
[3]Noh, J. H. et al., *Nano Lett.* **2013**, 13, 1764-1769
[4]Guo F. et al., *Nanoscale* **2015**, 7, 1642-1649

ID 235 - Oral

Hot charges speed up non geminate recombination in polymer-based solar cells but have no effect on device performance

**J. Kurpiers[1], S. Albrecht[1], D. Neher[1]*
[1]University of Potsdam, Institute of Physics and Astronomy, Potsdam-Golm, Germany

In the last years a dramatic increase in the efficiency of solution processed polymer/fullerene solar cells has been reported. However, the fundamental processes involved in the conversion of absorbed photons to free charges are still not fully understood. In this work, we use time delayed collection field (TDCF) [1] experiments with exceptionally high time resolution to investigate the charge carrier dynamics in the highly efficient PCDTBT:$PC_{70}BM$ system. Although this system has a high fill factor of around 70% and an internal quantum efficiency approaching unity under steady state illumination conditions [2], TDCF experiments reveal non-geminate recombination on the 10 ns time-scale, even for charge carrier densities comparable to one sun illumination. This loss becomes significantly accelerated at higher pulse fluence. Interestingly, the short term decay dynamics is not affected by a background steady state carrier density as introduced with a constant background illumination, meaning that the main reason for the nongeminate loss observed at the 10 ns time scale is recombination of hot electrons with hot holes. As recombination occurs mainly between hot carriers, this loss channel seems to be insignificant under steady state illumination. Our results imply that transient experiments which consider exclusively the dynamics of “freshly-generated” charges should be considered with great care when aiming at the understanding of device function under steady-state illumination conditions.

1 S. Albrecht, W. Schindler, J. Kurpiers, J. Kniepert, J. C. Blakesley, et al., Journal of Physical Chemistry Letters 2012 / 3, 640.
2 S. H. Park, A. Roy, S. Beaupre, S. Cho, N. Coates, et al., Nature Photonics 2009 / 3, 297-U5.

ID 236 - Poster

Charge carrier dynamics in PbS quantum dot solar cells

*J. Kurpiers[1], A. Paulke[1], I. Lange[1], S. Albrecht[2], M. A. Loi[3], D. Neher[1]
[1]University of Potsdam, Institute of Physics and Astronomy, Potsdam-Golm, Germany
[2]Helmholtz-Zentrum Berlin für Materialien und Energie GmbH, Institut für Silizium-Photovoltaik, Berlin, Germany
[3]Faculty of Mathematics and Natural Sciences, Photophysics and optoelectronics group, Groningen, Netherlands

Nanocrystal materials are promising materials for optoelectronic applications due to their well-tunable optical and electronic properties. Notably, lead chalconide nanocrystals exhibit a very broad absorption extending into the near infrared region [1]. This makes them particularly attractive for photovoltaic devices. Solar cells comprising PbS nanocrystals show, in fact, high short circuit currents of 20 mA/cm^2, exceeding those of organic solar cells, while open circuit voltages are still rather unsatisfactory. In this work, we use time delayed collection field (TDCF) [2] and Bias assisted charge extraction (BACE) experiments to investigate the charge carrier dynamics in PbS nanocrystal solar cells. We find that free charge carrier creation is slightly field dependent, thus providing an upper limit to the fill factor. BACE measurements reveal a rather high effective mobility of $2x10^{-3}$ cm²/Vs, meaning that charge extraction is efficient. On the other hand, a rather high nongeminate recombination coefficient of $3x10^{-10}$ cm³/s is measured. We, therefore, propose rapid free charge recombination to constitute the main origin for the limited efficiency of PbS nanocrystal cells. This is confirmed by the very good reconstruction of the JV-characteristics with an analytical model, using only experimentally obtained parameters. Interestingly, measurements with TDCF revealed that trap-release assisted recombination predominates upon pulsed illumination. Apparently, these traps are permanently filled under steady state illumination conditions, meaning that they do not contribute to free carrier recombination.

[1] C. Piliego, L. Protesescu, S. Z. Bisri, M. V. Kovalenko, M. A. Loi, Energy & Environmental Science 2013 / 6, 3054-59.
[2] S. Albrecht, W. Schindler, J. Kurpiers, J. Kniepert, J. C. Blakesley, et al., Journal of Physical Chemistry Letters 2012 / 3, 640.

ID 237 - Oral

Ion energy bombardment measurements and simulations from a low temperature VHF PECVD SiH_4-H_2 discharge in the a-Si:H to µ-c-Si transition regime

*K. Landheer[1], W. Goedheer[2], R. E. I. Schropp[3], J. K. Rath[1]
[1]Universiteit Utrecht, Eindhoven, Netherlands
[2]DIFFER, Nieuwegein, Netherlands
[3]Technische Universiteit Eindhoven, Applied Physics, Eindhoven, Netherlands

Ion bombardment plays an important role in the crystalline nucleation in the Si film in the amorphous to crystalline silicon transition regime as well as the defect creation on the substrate in a PECVD process (e.g.[1], [2]). This might have a bearing on the passivation quality of the c-Si/a-Si interface for a silicon heterojunction solar cell when the emitter is deposited at a high hydrogen dilution (H_2/SiH_4) condition. The important question is what happens with the ion bombardment energies in an SiH_4-H_2 VHF PECVD plasma discharge when we increase hydrogen dilution of our standard source gas mixture from 1 to 59 while traversing the transition regime. To that end, we measure and simulate the ion bombardment on the substrate which is at the grounded side of our capacitively coupled VHF PECVD reactor. The ion bombardment intensity is not only determined by the ion energies, but also the ion flux is important and it will be assessed with respect to the deposition rate.

In this work we measured the energies of the positive ions present in the SiH_4-H_2 plasma with an energy resolved mass spectrometer (Hiden EQP 1000 series). Ion flux measurements are not yet performed. Simultaneously, we measured the H_a/Si* ratio with Optical Emission Spectroscopy and monitored the rf voltage, plasma current and the phase difference between the current and the voltage. We compared these measurements with the simulation results of a self-consistent 2D fluid model of the SiH_4-H_2 discharge in our reactor [3]. To refine our simulations, the 2D fluid model was extended with extra H_2 chemistry reactions and DC self bias voltage. We simulate the trajectory of bombarding ions with a Monte Carlo simulation that uses output (a. o. the electric field) from the fluid model. We started the experiment with our standard low temperature VHF PECVD recipe for the deposition of i-a-Si:H with the plasma parameters: power of 57 mW / cm^2 at 60 MHz, pressure of 0.25 mbar, substrate temperature of 130°C, electrode separation of 27 mm and gas flows of 30 sccm SiH_4 and 30 sccm H_2. Subsequently we increased the hydrogen dilution from 1 to 59 to scan the low temperature deposition regime from a-Si:H to µ-c-Si:H deposition.

The ion energy distributions (IED) of H_3^+, SiH_2^+, SiH_3^+ and $S_2H_5^+$ are measured for dilutions from 1 to 59. The SiH_3^+ IED high energy peak position increases from 17 to 20 eV for increasing dilutions from 1 to 5 (see top graph), but stays constant for dilution from 5 to 59. The simulation results of the SiH_3^+ IED show a constant peak position at 19 eV (see bottom graph) for hydrogen dilutions from 2 to 59. Below a hydrogen dilution of 2 the peak position gradually decreases. However, the measured IEDs show also a peak at low energies, usually attributed to a charge exchange reaction. We do not know of any charge exchange reaction for the SiH_3^+ ion with a cross section that could have created the low energy peak. The different intensities of the simulated IED peaks can be explained by the different SiH_3+ production and loss rate in the plasmas and the different chances for an elastic collision with the source gas. Only ions with an incident angle less than 0.26 radians are measured by the ERMS and counted by the simulations. The simulations and measurements show good correspondence for the high energy peak position and both show a nearly constant peak position for hydrogen dilutions above 2.

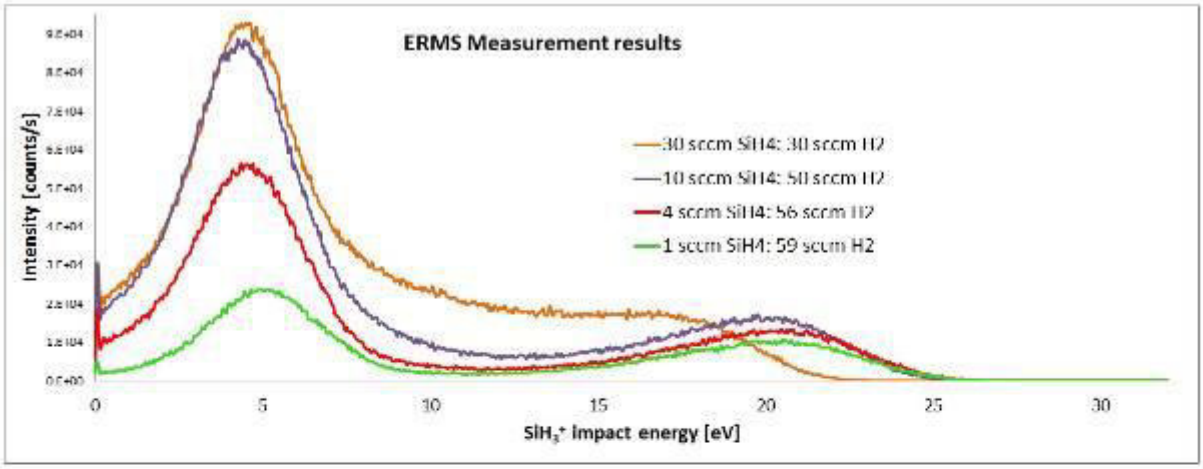

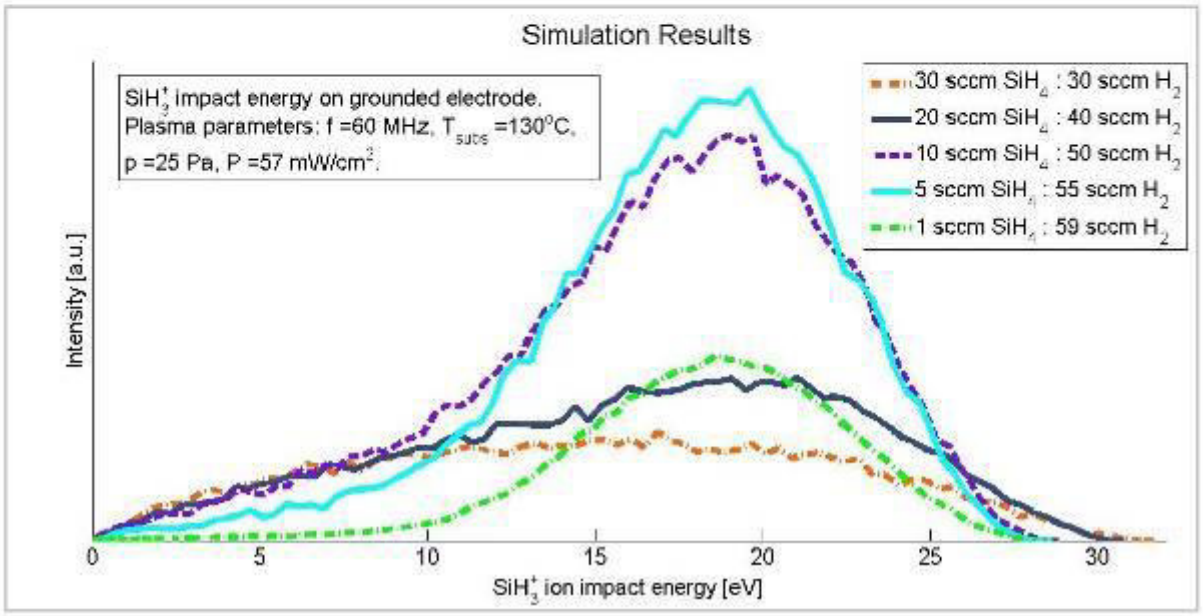

[1] Matsuda, A, “Formation kinetics and control of microcrystallite in μ-c-Si:H from glow discharge plasma”, *Journal of Non-Crystalline Solids*, vol. 59 & 60, 1983.
[2] B. Strahm, A. A. Howling, L. Sansonnens, en C. Hollenstein, “Plasma silane concentration as a determining factor for the transition from amorphous to microcrystalline silicon in SiH_4 /H_2 discharges”, *Plasma Sources Science and Technology*, vol. 16, nr. 1, pp. 80-89, feb. 2007.
[3] G. J. Nienhuis, W. J. Goedheer, E. A. G. Hamers, W. G. J. H. M. van Sark, en J. Bezemer, “A self-consistent fluid model for radio-frequency discharges in SiH_4-H_2 compared to experiments”, *Journal of Applied Physics*, vol. 82, nr. 5, p. 2060, 1997.

ID 238 - Poster

Influence of the ZnO nanowire dimensions on the photoelectrocatalytic properties for water splitting

**K. Govatsi[1,2], A. Seferlis[1], S. Neophytides[1], S. N. Yannopoulos[1]*
[1]FORTH/ICE-HT , Patras, Greece
[2]university, chemistry, Patras, Greece

World demand for energy continues to increase with the passage of time implying a constant depletion of fossil fuels. For this reason, a better exploitation of renewable energy sources is one of the major challenges nowadays in our society. Among the renewable power sources, photocatalytic (PC) water splitting offers a promising way for hydrogen production by solar energy. The development of photoelectrochemical (PEC) cells with high stability and efficiency is mandatory to induce a breakthrough in the daily usage of this technology.

Metal oxide semiconductors such as TiO_2 and ZnO are the best candidates to be used as anodes for PEC cells. TiO_2 nanoparticulate films prepared by various methods have been widely explored as anode materials for PEC cells for more than three decades, while the PEC features of ZnO nanostructured films are still not thoroughly understood. The role of the ZnO nanowire (NW) morphology on hydrogen production is an open issue to be resolved and is the subject of the current work.

ZnO NWs were grown by the chemical bath deposition method on FTO (SnO_2:F) conductive glass substrates. Samples with different diameters ranging from 20 nm to 200 nm (with narrow size distribution) were prepared by properly tuning the NW's growth parameters, and were employed as anodes of a PEC cell. A hydrogen reference electrode (RHE) and a platinum wire (Pt) as cathode were used. The electrolyte was an aqueous solution of NaOH. The ZnO NWs were illuminated with a UV-LED (365 nm). Cyclic voltammetry was used for evaluating the stability and the efficiency of the anode electrode for hydrogen production. The I-V curves of NW arrays exhibit a non-monotonic behavior in relation to the NW diameter, where the photocurrent increased with increasing diameter until an optimum value (for ZnO NW diameter of 120-150 nm). Time resolved cyclic voltammetry experiments of the ZnO NW anodes confirmed their good stability. The high photocurrent, low open circuit potential and good stability suggest that ZnO NW arrays constitute a promising platform for PEC solar hydrogen production.

ID 239 - Poster

Laser processing of SiC: From graphene-coated SiC particles to 3D graphene froths

*A. Antonelou[1], S. N. Yannopoulos[1]
[1]FORTH/ICE-HT, GREECE, Greece

After several years of systematic fundamental research on graphene it is now generally agreed that its exceptional physical properties (optical, electrical, and so on) are well understood. Major experimental challenges are now related to the large-scale production of high-quality graphene and graphene-based structures, which is the prerequisite to evolve fundamental graphene science into viable technological applications. Graphene and graphene-based structures can be prepared in a number of ways using predominantly chemical-vapor-deposition-based approaches and solution chemistry methods. The present work investigates the feasibility of infrared lasers in the controlled graphitization of SiC particles. It is demonstrated that laser-mediated SiC decomposition can result in a manifold of graphene structures depending on the irradiation conditions. In particular, graphene formation, at nearly ambient conditions, can take place in various forms resulting in SiC particles covered by few-layer epitaxially grown films, and particles with a progressively increasing thickness of the graphitized layer, reaching eventually to free-standing 3D graphene froths at higher irradiation doses. Graphene-coated particles and 3D porous graphene scaffolds present implications to a variety of applications, which will be briefly discussed. The present findings testify the potential of lasers towards the tailor-made preparation of high-quality graphene-based structures. The scalability and adaptability of lasers further support their prospect to develop reliable, reproducible, eco-friendly and cost-effective laser-assisted graphene production technologies.

Acknowledgment: The research leading to these results has received funding from the European Union 7th Framework Programme under grant agreement no 607295 - project SMARTPRO.

ID 240 - Oral

**Charge carrier separation at photoactive interfaces:
the role of (de)localized defects**

**M. Rohrmüller[1], M. W. Akhtar[2], A. Schnegg[2], K. Lips[2], W. G. Schmidt[1], U. Gerstman[1]*
[1]Universität Paderborn, Theoretische Physik, Paderborn, Germany
[2]Helmholtz-Zentrum, Berlin, Germany

To develop novel materials for photovoltaic or photocatalytic application a detailed atomistic understanding of charge carrier separation and the corresponding recombination processes is crucial. In this work we show how microscopic modeling of the involved defect states helps to analyze the data obtained from magneto-optical experiments. It will also be demonstrated that theory can give valuable information about the charge carrier separation, which give some hints for further improvement of the materials, even if this kind of information is not directly accessible by experiment.

This is shown using the interface of hydrogenated amorphous silicon and crystalline silicon (a-Si:H/c-Si) in heterojunction solar cells as a prototype example [1]. Combining orientation dependent electrically detected magnetic resonance (EDMR) and density functional theory (DFT) we analyze the spin-dependent recombination in miniature solar cells. By this we find that *(i)* the interface exhibits microscopic roughness, *(ii)* the localized interface defects mimic the famous P_b-centers at the Si/SiO_2 Interface, *(iii)* we identify the microscopic origin of the conduction and valence band tail states, and *(iv)* we discuss how charge carrier separation can be supported by conduction band tail states.

[1] A. B. M. George, J. Behrends, A. Schnegg, T. F. Schulze, M. Fehr, L. Korte, B.Rech, K. Lips, M. Rohrmüller, E. Rauls, W. G. Schmidt, and U. Gerstmann, Phys. Rev. Lett. **110**, 136803 (2013).

ID 241 - Oral

Hydrogen-doped In_2O_3 with high mobility and high transparency prepared by atomic layer deposition for silicon heterojunction solar cells

*Y. Kuang[1], B. Macco[1], Y. Wu[1], C. K. Ande[1], W. M. M. Kessels[1,2], R. E. I. Schropp[1,2]
[1]Eindhoven University of Technology, Department of Applied Physics, Eindhoven, Netherlands
[2]Solliance, Eindhoven, Netherlands

Hydrogen-doped In_2O_3 (In_2O_3:H) with high mobility and high transparency prepared by thermal atomic layer deposition (ALD), is demonstrated as a promising transparent conductive oxide (TCO) electrode for solar cells. The In_2O_3:H was deposited at 100°C and post-annealed in the temperature range of 150-200°C for solid phase crystallization, making the processing temperatures fully compatible with silicon heterojunction solar cell manufacturing. A high mobility of up to 138 cm^2/V s at a relatively low carrier density of 1-2×10^{20} cm^{-3} is obtained, resulting in a significantly reduced parasitic absorption while maintaining a comparable conductivity with respect to the conventional TCO material (Sn-doped In_2O_3 (ITO) by radio frequency magnetron sputtering) [1]. The absorption is reduced in the entire wavelength range of 350-1200 nm, with a more significant reduction in the near infrared region, making the In_2O_3:H particularly interesting for solar cells with low band gap absorbing materials. The damage to the sensitive hydrogenated amorphous silicon (a-Si:H)/crystalline silicon (c-Si) heterojunction interface caused by magnetron sputtering of ITO and atomic layer deposition of In_2O_3:H has been investigated by a direct comparison of minority carrier lifetime degradation after deposition of the two TCOs. ALD offers the important advantage that the TCO can be deposited without ion bombardment damage that is induced by sputtering. Critical issues on the nucleation of the In_2O_3:H on a-Si:H and methods to mitigate these issues will be presented. Optical and electrical properties of a-Si:H/c-Si heterojunction solar cells with In_2O_3:H as the front transparent electrode will be reported.

ID 242 - Oral

From Amorphous Silicon/Organic to Perovskite/Crystalline Silicon Hybrid Multi-Junction Solar Cells

**S. Albtrecht[1], S. Roland[2], S. Neubert[3], F. Lang[1], L. Kegelmann[1], B. Hase[1], M. Seger[4], A. Facchetti[4], B. Stannowski[3], R. Schlatmann[3], L. Korte[1], D. Neher[2], B. Rech[1]*
[1]Helmholtz-Zentrum Berlin, Institut für Silizium Photovoltaik , Berlin, Germany
[2]Universität Potsdam, Physik weicher Materie, Potsdam, Germany
[3]PVcomB/Helmholtz-Zentrum Berlin für Materialien und Energie GmbH, Berlin, Germany
[4]Polyera Corporation, Skokie, United States

Multi-Junction Solar Cells benefit from both reduced thermalization losses and sun light absorption in a broad wavelength range, enabling theoretical efficiencies well above that of single junction solar cells. Absorption spectra that are complementary to silicon (Si), high absorption coefficients, and the ease of fabrication make organic or metal halide perovskite absorbers suitable for the use in multi-junctions in combination with amorphous silicon (a-Si:H) or crystalline silicon (c-Si), respectively. We present efficient monolithic double and triple junction cells incorporating an organic bulk heterojunction sub-cell connected in series with a-Si:H junctions. Optimization of the recombination contacts results in multi-junctions with high fill factors over 70% and very high open-circuit voltage V_{oc} close to the sum of the V_{oc}s of the sub-cells.[1] By applying light trapping using textured transparent front electrodes, a record efficiency for this type of hybrid solar cell of 11.7% is reached for the triple cell.[2] Furthermore, we present tandem solar cells by combining perovskite and a-Si:H/c-Si heterojunction solar cells. By developing a semitransparent perovskite cell with reduced parasitic absorption in the infrared wavelength range, mechanically stacked 4-terminal perovskite/silicon heterojunction solar cells with 13% are realized. A monolithic perovskite/silicon heterojunction integration requires the fabrication of a low temperature electron selective contact for the perovskite cell. However, the typically used TiO_2 needs to be sintered at temperatures that will deteriorate the silicon heterojunction. By replacing TiO_2 with fullerene extraction layers efficient monolithic tandem cells are presented. Using optical simulations of the photocurrent loss in perovskite/silicon heterojunction solar cells together with a parametrization of the I-V curves of the respective reported champion cells, we show that realistic efficiencies of over 25% can be expected for this fascinating tandem cell concept.

(1) Albrecht, S.; Grootoonk, B.; Neubert, S.; Roland, S.; Wördenweber, J.; Meier, M.; Schlatmann, R.; Gordijn, A.; Neher, D. *Solar Energy Materials and Solar Cells* **2014**, *127*, 157. (2) Roland, S.; Neubert, S.; Albrecht, S.; Stannowski, B.; Seger, M.; Facchetti, A.; Schlatmann, R.; Rech, B.; Neher, D. *Advanced Materials* **2015**, *27*, 1262.

ID 243 - Oral

Laser patterning of amorphous silicon thin films deposited on flexible and rigid substrates

*P. Alpuim[1,2], M. D. F. Cerqueira[1], J. Gaspar[2], H. Fonseca[2], V. Iglesias[2], J. Borme[2]
[1]University of Minho, Department of Physics, Braga, Portugal
[2]INL-International Iberian Nanotechnology Laboratory, Nanoelectronics, Braga, Portugal

The possibility of direct writing thin semiconductive channels and structures on insulating substrates in a clean room-free process is attractive for its simplicity, cost effectiveness and the possibility of a wide choice of substrates, including low-temperature plastics. A broad range of applications, such as large-area electronic devices (touch screens, flexible displays), sensors, or optical wave guides could benefit from such process. In the present work we irradiate doped amorphous silicon (a-Si:H) thin films, with thickness in the range from 10 nm to 1 µm, using a Nd-YAG laser operating at 532 nm that is part of a confocal WItec Raman confocal system. The light-matter interactions that occur in the process result in the film crystallization and dopant activation, in the regions exposed to the laser. Since the electrical conductivity of a-Si:H (even of doped a-Si:H) is very low due to disorder and to an inefficient doping mechanism (compensation), the contrast in conductivity between the exposed and unexposed areas is so high that, upon applying a voltage difference between ohmic contacts defined on the sample, essentially all the electrical current flows through the doped, crystallized channels embedded in the amorphous highly resistive matrix.

In this paper, the B- and P-doped a-Si:H writing media were deposited by radio-frequency plasma-enhanced chemical vapor deposition (rf-PECVD), and by hot-wire CVD on three different substrates: polyimide (PI), glass, and oxidized silicon wafers (Si/SiO_2). A systematic study was performed on each type of substrate to find the laser threshold power for crystallization, followed by writing at different laser fluences above the threshold power. The laser threshold power for crystallization of the films increased in the order PI (4 mW), glass (7 mW), and SiO_2 (15 mW) at a writing speed of 62 µm/s. The highest conductivity for each substrate was 75 $\Omega^{-1}cm^{-1}$, for PI, 390 $\Omega^{-1}cm^{-1}$ for glass, and 420 $\Omega^{-1}cm^{-1}$ for Si/SiO_2, obtained at a laser power of 4, 20 and 40 mW, respectively. Both n- and p-doped samples showed similar levels of conductivity after laser crystallization.

We developed a software that generates and fills patterns (with dots, dashes or lines) and converts the resulting files into text files containing a set of instructions that can be read by the control electronics of the X-Y stage onto which the sample is mounted. A shutter installed in front of the laser opens and closes according to the instructions in the file. In this way, any drawing that is contained in the instructions file can be transferred to the substrate using continuous lines, dashes or dots with selected duty cycles. Using this capability we systematically studied the effect of the pattern geometry of the irradiated areas on the crystallization and doping activation of the film. The patterned areas were studied by Raman spectroscopy to measure crystalline fraction and average crystallite size. Scanning Electron Microscopy and Conductive AFM were used to elucidate the crystallization mechanisms and map the conductivity as a function of position. 2D Raman mapping was performed over large areas to confirm and complement the local measurements done by C-AFM.

Piezoresistance will be measured by four-point bending tests where the devices, the contact lines and the pads are encapsulated between polyimide spin coated layers.

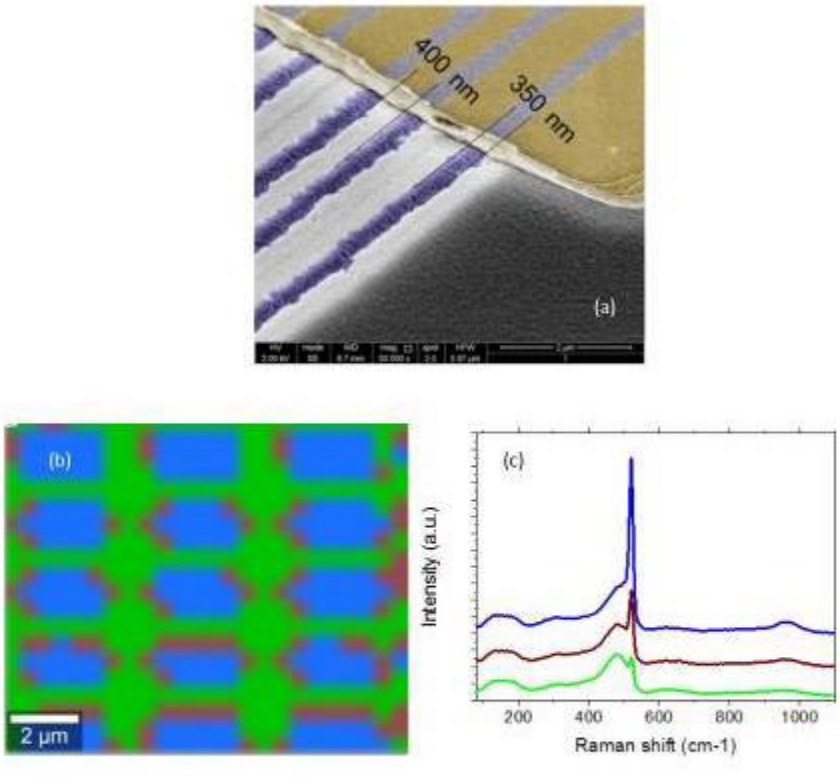

(a) SEM image of lines laser written on a 10 nm thick a-Si:H film deposited on a SiO_2/Si substrate. Four regions are clearly distinguishable: the metal contact on the top area; the laser eroded area (lines); the crystallized areas adjacent to lines; the amorphous region at the bottom right. (b) A 10 µm x 10 µm laser patterned area with parallel dashes depicted by a Raman map (left). The image is obtained by expanding the Raman spectrum stored in each pixel as a linear combination of the three basis spectra shown in the figure on the right. Each pixel color results from adding the colors of the basis spectra in an amount equal to the respective coefficients in the linear

ID 244 - Poster

Graphene field-effect transistors for biosensing applications

*G. Junior[1], N. C. S. Vieira[1,2], M. D. F. Cerqueira[3], N. M. R. Peres[3], J. Borme[1], *P. ALPUIM[3,1]*
[1]INL-International Iberian Nanotechnology Laboratory, Nanoelectronics, Braga, Portugal
[2]IFSC – São Carlos Institute of Physics, University of São Paulo, São Carlos, Brazil
[3]University of Minho, Department of Physics, Braga, Portugal

Soon after the discovery of the possibility of doping graphene through gating, the first graphene-based field-effect transistor (FET) was reported, over a decade ago. Graphene FETs (GFETs) unique electrical characteristics are determined by the astonishing physical properties of graphene itself. Very high carrier mobility makes GFETs attractive for radio-frequency applications; however the output does not saturate, which is a hindrance for speed in these applications. The absence of a bandgap in graphene makes it possible to control the doping level with a voltage. However it reduces the ON/OFF ratio of GFETs to values (~10) that make them unsuitable for logic applications. A graphene film supported on a substrate has a natural 2D electron-gas surface directly exposed to the environment. The channel region in GFETs therefore provides, if uncovered, an extremely sensitive surface to whatever charged objects or electric fields exist in its neighborhood. Graphene is chemically very stable and mechanically rugged. Looking at the above mentioned properties as a whole, one may conclude that GFETs seem to be ideal platforms for the detection of chemical and biological molecules with relevance in many areas, ranging from disease diagnosis, to environmental monitoring, and security. For chemo- and bio-sensing, most of the characteristics that make GFETs not compatible with other technologies are not an issue, or are even desirable.

Graphene science and technology are currently undergoing a critical stage: one in which graphene outstanding properties, demonstrated in many research laboratories across the world, are put to test upon up-scaling to an industrial product, processed for human use. This step has not yet been achieved for most of graphene promised applications. It is obvious that issues related to a high level of device integration, device portability, high fabrication throughput, and reliability, must be addressed and overcome before mass-production of graphene-based products becomes a fact.

In the present work, we report on the wafer-scale fabrication, process yield and uniformity, operation, and modeling of GFETs based on graphene grown by chemical vapor deposition on copper foil catalysts. The fabricated devices are bottom and top gate GFETs with different architectures that are in all cases implemented by use of standard clean-room optical lithographic techniques. One particular device architecture, namely an electrolyte-gated GFET (EGFET) with coplanar source, drain, and gate contacts will be discussed in more detail, since, in our opinion, it shows great promise for chemo- and bio-sensing. This is because, on the one hand aqueous solutions are the natural environment of biomolecules, and, on the other hand the use of a liquid gate allows for a lower operational voltage than the back-gated configuration using a solid-state dielectric. In our EGFET architecture the conventional wire (or silver/silver chloride) gate electrode is replaced with an in-plane receded metallic gate, which provides efficient transistor gating once a droplet of the electrolyte solution (possibly containing an analyte) is placed on the transistor channel. The structure is replicated 264 times in an array that covers the surface of a 200 mm Si oxidized wafer. The transistors can be measured by simply dropping a droplet of solution from a pipette on top of the channel area. Or a microfluidic circuit with a pump to can be used to deliver the solutions. The single-layer graphene transistors resulting from this process consistently perform at the same level as reported for devices based on exfoliated or CVD graphene flakes transferred onto small-area substrates. Transistors with channel length 25 μm, measured in phosphate buffer saline solutions (PBS 1x), showed an average field-effect electron mobility of 1500 $cm^2V^{-1}s^{-1}$ and average hole mobility of 1450 $cm^2V^{-1}s^{-1}$ (these averages were calculated over a population of 90 devices). Raman analysis of the transistor channel shows that it consists essentially of single-layer graphene. The graphene EGFET biosensors will next be used for the detection of a particular cyanotoxin (microcystin), indicative of water contamination, using a detection strategy close to real conditions

(potable water samples). A printed circuit board was designed where the graphene chip, cut from the wafer using a dicing saw, is easily plugged in, thus providing a simple, robust and portable solution in view of a platform for point-of-care or other chemical and biosensing applications.

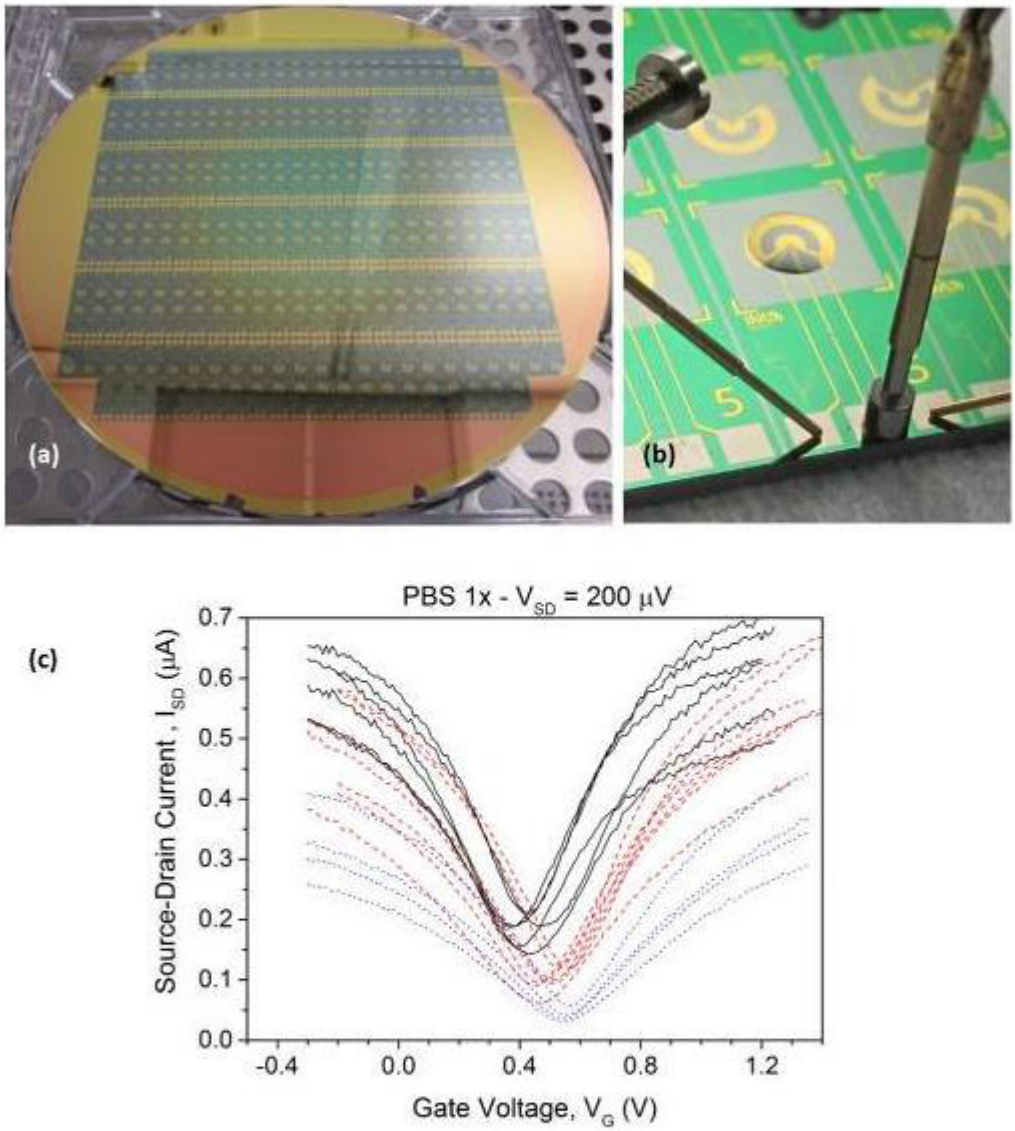

(a) 200 mm wafer containing 264 graphene transistors; (b) Chip with two 5 µm channel transistors being measured before dicing. The gate-electrolyte droplet is clearly visible. The gray, aluminum lines are guides for the wafer dicing process. (c) Transfer curves of 17 graphene EGFETs fabricated on a 200 mm wafer with W/L = 3 (dotted lines), 6 (dashed lines) and 12 (continuous lines). W and L are channel width and length, respectively. Source-drain voltage was V_{SD} = 200 µV. The liquid-gate dielectric was PBS 1×.

ID 245 - Poster

Transport in thin transparent oxides: Nb-doped TiO_2 compared to conventional TCOs

*D. Dorow-Gerspach[1], M. Wuttig[1]
[1]RWTH-Aachen, I.Physikalisches Institut (IA), Aachen, Germany

In many devices such as flat panel displays or solar cells, materials are required, which are both transparent and conducting. A few doped oxides (ZnO, SnO_2 and In_2O_3) combine these properties and are used in the corresponding industries. These conventional TCOs can have resistivities in the range from 100 to 1000 µΩcm depending on dopant concentration and film preparation. All of the metals used to from the oxides (Zn, Sn and In) are located in the same area of the periodic table and the conduction and scattering mechanisms are reasonably well understood. As the conduction band minimum in these materials consist of ***s*-bands**, a large overlap is easily realized enabling high mobilities. This high degree of orbital overlap is also responsible for the low effective mass of about 0.3 m_e, all of these oxides have in common.

In 2005 a new TCO material was discovered, that does not follow this blueprint: Niobium doped TiO_2 [1]. Surprisingly Ti is located far away from the metals used in conventional TCOs. It's also an *n*-type semiconductor, but has a conduction band minimum, which consists of a ***d*-band**. Nevertheless, the effective mass in the direction of the *a*-axis is also around 0.3 m_e only. Most of the TiO_2:Nb films studied so far were prepared with PLD or RF-sputtering on single crystalline substrates. To increase the application potential of such films, we have prepared TiO_2 film by reactive DC magnetron sputtering on glass substrates, both without and with different amounts of Nb doping (1, 2.5, and 5 at % Nb). We have analyzed the dependence of the structural, electrical and optical properties film properties on the oxygen partial pressure and niobium concentration, including the electron mobility and charge carrier density. To analyze the conduction mechanism temperature dependent transport measurements were performed down to 2 K for different samples. These data show significant differences compared to conventional TCOs.

[1] Furubayashi et al., *Appl. Phys. Lett*. 86 (25) 2005

ID 246 - Oral

Copper Sulfide Nanoparticles as Absorber for Photovoltaic Application

**J. Flohre[1], M. Nuys[1], C. Leidinger[1], S. Muthmann[1], F. Köhler[1], J. Mock[1], R. Imlau[2], R. Carius[1,2]*
[1]Forschungszentrum Jülich , Institut für Energie und Klimaforschung 5 - Photovoltaik, Jülich, Germany
[2]Forschungszentrum Jülich , Peter Grünenberg Institut 5, Jülich, Germany

Cost effective solar cells with high efficiency based on abundant, non-toxic material is the long term target of present research and development. Copper Sulfide (Cu_2S) with a suitable band gap of 1.2 eV and high absorption coefficient is an appropriate candidate for an absorber in single or multijunction solar cells.

Copper sulfide nanoparticles (NP) were synthesized in ionic liquid using a microwave reactor. TEM reveals an average diameter of about 70 nm and the NP are partially agglomerated. XRD measurements show that the pristine NP are present in multiple phases which are predominantly djurleite ($Cu_{1.96}S$) as well as high digenite ($Cu_{1.8}S$) and tetragonal chalcocite (Cu_2S). The absorption characteristics deduced from Photothermal Deflection Spectroscopy (PDS) measurements indicate a high free carrier concentration. Taking the free carrier absorption into account the absorption characteristic is in good agreement with the absorption properties of djurleite bulk material. PL spectra of the NP at room temperature exhibit a broad PL peak centered at 1.23 eV with FWHM of 360 meV which is interpreted as a superposition of the emission of different copper sulfide phases.

Pristine NP were embedded in 50 nm amorphous silicon (a-Si:H) via a PECVD process to investigate the suitability of the material with a-Si:H and with the deposition process in terms of compatibility and stability. Embedding reduces the free carrier absorption significantly. Also, the fundamental absorption of the NP changes and exhibits an increase of the absorption between 1.2 eV and 1.3 eV which is in good agreement with the absorption coefficient of chalcocite bulk material. Consequently, the initial multi-phase material is transformed to chalcocite. For energies >1.5 eV the absorption is dominated by a-Si:H. The PL of the embedded NP is significantly increased by about one order of magnitude accompanied by a decrease of the FWHM to 160 meV. The intensive narrower emission is attributed to chalcocite band edge emission indicating a high quality material. However, compared to literature data the peak is little red shifted and broadened. Since the deposition temperature is about 220°C, the improvement of the material quality is likely due to an annealing effect. But the H-plasma and the a-Si:H might also be responsible for a decreased defect concentration, e.g. by surface passivation or saturation of unsaturated bonds of the nanoparticles.

The intensive band edge emission of the embedded copper sulfide NP indicates the suitability of the material as absorber in photovoltaic applications.

ID 247 - Poster

The amorphous / crystalline interface: a computational point of view

*K. Jarolimek[1], E. Hazrati[1], G. de Wijs[1], *R. de Groot[1]*
[1]Radboud University, Institute of Molecules and Materials, Nijmegen, Netherlands

Silicon heterojunction (SHJ) solar cells combine high-efficiency of c-Si wafer technology with high-throughput and low-cost of hydrogenated amorphous silicon (a-Si:H) solar cells. The interface between crystalline and amorphous silicon lies at the heart of the SHJ solar cell. Since a-Si:H has a larger band gap than c-Si, band offsets are formed at the interface.

Experimentally the band offsets can be determined with techniques such as photoelectron spectroscopy and capacitance-voltage measurements. The reported values scatter over a broad range. This can be due to different deposition conditions of the a-Si:H layer or misinterpretation of the experimental results. On average it appears that the offset at the valence band is larger than at the conduction band [1].

In light of the conflicting reports our goal is to calculate the band offsets at the c-Si/a-Si:H interface from first-principles. To this end we construct a simulation cell with dimensions of $1.5 \times 1.3 \times 3.6$ nm^3 and divide it into a crystalline and amorphous part. Periodic boundary conditions are applied in all three dimensions. The crystalline part is terminated with (111) surfaces on both sides. The amorphous structure is generated by simulating an annealing process at 1100 K, with DFT molecular dynamics. Using relatively long annealing times (135 ps) we are able to generate realistic a-Si:H structures.

We use a hybrid functional to calculate the electronic structure of the interface. The position of band edges in the amorphous part is obtained by fitting the calculated density of states to a square root dependence. This is in the spirit of the Tauc band gap often used to interpret optical measurements. Our results show that the valence offset is slightly larger (0.29 eV) than the conduction band offset (0.18 eV).

In total we prepare 28 interface models. All of them contain a small number of defects. We find three types of defects: 3-fold coordinated Si atoms, 5-fold coordinated Si atoms and 2-fold coordinated H atoms. The over-coordinated Si atom is the most common defect. This is in contrast to the prevailing view that considers the 3-fold coordinated Si atom (dangling bond) as the only defect.

[1] G. van Sark, L. Korte and F. Roca (Eds.): Physics and Technology of Amorphous-Crystalline Heterostructure Silicon Solar Cells, (Springer, Berlin, 2012), p. 418.

ID 250 - Oral

Extremely thin and robust interconnecting layer providing 76% Fill Factor in tandem polymer solar cell

*A. Martinez Otero[1], Q. Liu[2], P. Mantilla[2], M. Montes Bajo[2], J. Martorell[2]
[1]FZ Juelich, DUISBURG, Germany
[2]ICFO, Castelldefels, Spain

Bulk-heterojunction (BHJ) polymer solar cells (PSCs) based on mixing polymer donor and fullerene acceptor networks are a proven and promising approach to efficient, cost-effective solar energy conversion. Although PSC performance has improved steadily their metrics are still far away from those of inorganic cells. Multi-junction solar cell configurations, where two or more sub-cells are stacked and connected in series or parallel, offer an exciting approach to overcome the single junction limitations of organic solar cells and further improve their power conversion efficiency (PCE). To improve the efficiency of PSC researchers have focused on maximize current or increase voltage through optimized polymer design[1] or light harvesting.[2] However, raising the fill factor offers an alternative strategy to enhancing PCE.[3] As for the tandem structures the average values of FF reported are around 60%. And in few occasions the FF of the tandem solar cell is higher than any of the FFs of the individual sub-cells.[4]

In this work we report tandem solar cells made of the well-known, low bandgap, high efficiency polymer PTB7 where the FF obtained in the tandem solar cell is not only larger than the FF of the identical sub-cells but it is also, to the best of our knowledge, the highest FF reported for tandem polymer solar cells. PTB7:PC71BM was used in both top and bottom photoactive layers that were connected in series by a novel recombination layer comprising of molybdenum oxide, poly [(9,9-bis(3'-(N,N-dimethylamino)propyl)-2,7-fluorene)-alt-2,7-(9,9-dioctylfluorene) (PFN) and a thin layer of silver in between. The use of this configuration allowed us to obtain a tandem solar cell with FF up to 76% while slightly increasing the current and doubling the voltage yielding a PCE of 8.2% for the tandem cell. The use of this recombination layer with PFN has other important advantages. For instance, there is no need of any thermal annealing that in some cases may be detrimental to the bottom photoactive layer. Moreover, PFN showed to be robust with high transparency and environmental stability and also remarkable solution processability.

Also reported in this work are morphology studies performed by means of atomic force microscopy (AFM) in order to understand the role of the silver layer and PFN thicknesses on the electrical performance of this new interconnection layer. These morphology studies together with optical simulations showed to be interesting tools in order to reach a better understanding of the role the recombination layer has on organic tandem solar cells.

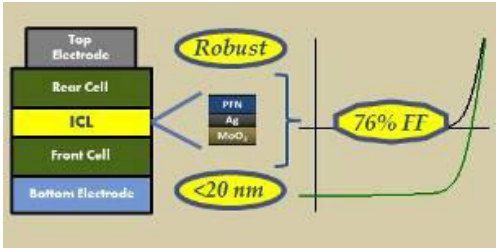

[1] Y. Liang, Z. Xu, J. Xia, S.-T. Tsai, Y. Wu, G. Li, C. Ray, L. Yu. Adv. Mater. 2010, 22, E135.
[2] A. Martínez-Otero, X. Elias, R. Betancur, J. Martorell. Adv. Optical Mater. 2013, 1, 37.
[3] X. Guo, N. Zhou, S. J. Lou, J. Smith, D. B. Tice, J. W. Hennek, R. Ponce Ortiz, J. T. Lopez Navarrete, S. Li, J. Strzalka, L. X. Chen, R. P. H. Chang, A. Facchetti, T. J. Marks. Nat. Photon. 2013, 7, 825.
[4] T. Ameri, N. Li, C. J. Brabec. Energy Environ. Sci. 2013, 6, 2390.

ID 251 - Oral

Comparative Study of the Stability of Amorphous Zinc Tin Oxide Thin Film Transistors with Different Tin Compositions under Positive Bias Stress

*K. M. Niang[1], A. J. Flewitt[1]
[1]Cambridge University, Electrical Engineering, Cambridge, United Kingdom

Amorphous ionic oxide semiconductors have been identified as a promising alternative to hydrogenated amorphous silicon (a-Si:H) for thin film transistors (TFTs) due to their higher carrier mobility and suitability for large-area electronics.[1] Moreover, a large process window exists, as reported for TFTs incorporating amorphous indium gallium zinc oxide (a-IGZO) with various metal cation compositions, where a wide range of compositions achieve high field effect mobility between 27 and 74 $cm^2 V^{-1} s^{-1}$.[2] However, metal oxide TFTs suffer from a threshold voltage (V_{th}) shift when subjected to a gate bias stress and/or light stress.[3-5] Investigation of device stability is an active area of research as it is vitally important for commercial applications.

Most reported bias stress experiments have been performed on devices with an 'optimised' semiconductor oxide, and there are few comparative studies of stability of devices made with different process conditions. Given that there is a large process window in producing high quality TFTs, information on which condition might give the best long term stability is highly desirable. Moreover, stability studies reported in the literature are mainly focussed on a-IGZO TFTs only. Zinc tin oxide (ZTO) is a high-mobility, indium-free alternative amorphous ionic oxide to a-IGZO.[6] Therefore, in this work we performed positive gate bias stress on ZTO TFTs with different tin atomic compositions. The time and temperature dependence of the V_{th} shift was measured and analysed using a thermalization energy concept, which allows two parameters with some physical interpretation to be extracted: a measure of the energy barrier to the threshold voltage shift process and an associated attempt-to-escape frequency. This analysis has previously been used in a-Si:H TFTs and recently in a-IGZO TFTs.[5,7]

The ZTO films are deposited by remote-plasma reactive sputtering using Zn:Sn alloy target with tin atomic compositions of either 10% or 33%, and are annealed at 500 °C for 1 hour in air. Both TFTs are operated in enhancement mode with a V_{th} ~8 V, a switching ratio of ~10^8 and a sub-threshold slope of ~0.6 V dec^{-1}. Field effect mobilities of 15 and 21 $cm^2 V^{-1} s^{-1}$ are obtained for the Sn10% and Sn33% TFTs respectively. The TFTs were subjected to a positive gate bias stress of 20 V for up to 40,000 s at elevated temperatures between 65 and 105 °C. Using the thermalization energy analysis data between Sn10% and Sn33% devices, we quantitatively compare the stability of the two materials which otherwise yield TFTs with very similar transfer and output characteristics.

1) J. K. Jeong *et al.*, *SID Symposium Digest of Technical Papers*, **39**, 1, 1-4 (2008)
2) P. Barquinha *et al.*, Journal of The Electrochemical Society, 156, 3, H161-H168 (2009)
3) M. D. H. Chowdhury, P. Migliorato, and J. Jang, Appl. Phys. Lett. **98**(2011)
4) J.-M. Lee, I.-T. Cho, J.-H. Lee, and H.-I. Kwon, Appl. Phys. Lett. **93** (2008)
5) A. J. Flewitt and M. J. Powell, J. Appl. Phys. **115**, 134501 (2014)
6) H**.** Q. Chiang *et al.,* Appl. Phys. Lett. **86**, 13503 (2005)
7) S. Deane, R. Wehrspohn, and M. Powell, Phys. Rev. B **58**, 12625 (1998)

ID 252 - Poster

Laser annealing of hydrogenated amorphous silicon

**W. Beyer[1,2], J. Bergmann[3], F. Finger[2], S. Haas[2], A. Lambertz[2], N. H. Nickel[1], F. Pennartz[2], T. Schmidt[3], U. Zastrow[2]*
[1]Helmholtzzentrum Berlin für Materialien und Energie, Institut für Silizium-Photovoltaik, Berlin, Germany
[2]Forschungszentrum Jülich GmbH, IEK5-Photovoltaik, Jülich, Germany
[3]Leibniz-Institut für Photonische Technologien e.V. , FA7.3 Photovoltaische Systeme, Jena, Germany

Thermal treatment (annealing) of hydrogenated amorphous silicon (a-Si:H) films is of interest to change/improve the electronic properties for application in electronic devices like thin film silicon or silicon heterojunction solar cells. However, annealing by an oven is often impractical or too expensive. Here we explore the applicability of laser scanning using a green (532 nm) 6W continuous wave laser with a focus diameter of 100 µm. Laser scan speeds of 1- 100 mm/s were applied and the laser line distance was 50 µm. For film characterization, the memory effects of hydrogen out-diffusion and of material microstructure measured by infrared spectroscopy as well as of deuterium-hydrogen interdiffusion detected by secondary mass spectroscopy were used. Plasma grown films (substrate temperature 180 - 240°C) of 0.3 - 1 µm thickness deposited primarily on c-Si substrates were investigated. The results show that the concentration of bonded hydrogen can be reduced considerably. The observed D-H interdiffusion demonstrates that hydrogen diffuses primarily as an atom. By comparison with oven-annealed material, an effective temperature for laser-treatment can be defined and will be discussed. The temperature of laser treatment can be estimated and is found to be largely independent of scan speed. Temperatures as high as 900°C (for laser residence times of 1 - 100 ms) are estimated. The dependence of this latter temperature on parameters like laser power, SiO_2 capping layer thickness etc will be discussed.

ID 253 - Poster

Metal-induced crystallization by homogeneous insertion of metallic species in amorphous silicon and germanium

*A. Zanatta[1], *F. Ferri[2]*
[1]University of São Paulo, Institute of Physics of São Carlos, São Carlos, Brazil
[2]Federal University of São Carlos, Department of Physics, São Carlos, Brazil

The present contribution aims to discuss some aspects related to the metal-induced crystallization of amorphous Si and Ge thin films prepared by cosputtering and probed by Raman scattering spectroscopy. As will be shown, the adopted experimental approach is suitable to investigate the crystallization phenomenon of amorphous thin films containing metallic species (controllably inserted and homogeneously distributed) at various concentration ranges. Additionally, the high sensitivity and spatial resolution provided by Raman spectroscopy is consistent with the detection of minute amounts of either crystalline or amorphous structures in a fast and non-destructive way. The whole process also involves the realization of cumulative thermal annealing treatments that give further insight on the crystallization kinetics of the systems under investigation. In order to illustrate these features, films of amorphous Si and Ge containing manganese will be considered in detail. The main experimental findings involving amorphous Si and Ge films combined with other metals (Ni, Co, Fe, Gd, Er, and Al) will also be briefly discussed.

ID 254 - Oral

Low temperature plasma epitaxy. How does it work ?

*R. I. C. Pere[1], C. W.[1], L. R[1,2], O. J.M[1], H. F[1], C. R[1], D. J-C.[1,2], B. B[1], L. H.L.T[1], N. T[1], V. H[1], S. F.[1], J. E[1]
[1]LPICM, CNRS, Ecole Polytechnique, Palaiseau, France
[2]Total New Energies, Paris La Defense, France*

Plasma Enhanced Chemical Vapor Deposition using a capacitively-coupled RF glow discharge has become the standard technique for the production of amorphous and microcrystalline silicon thin films, which are the basis of a fast expanding large area electronics industry. However, there is still a debate on the growth mechanisms of these films. While standard growth models based on SiH_3 radicals may apply for well controlled and low rate deposition conditions, increasing the deposition rate is synonymous of enhanced gas phase reactions leading to the formation of silicon clusters and nanocrystals in the plasma. Even though “common sense” would suggest that this is something to be avoided, we have been using the plasma synthesized silicon clusters and nanocrystals to improve the electronic properties of polymorphous and microcrystalline silicon while increasing their deposition rate [1].

Interestingly enough the same conditions which result in pm-Si:H on glass substrates lead to epitaxial growth on 100 oriented c-Si substrates [2]. Exploring these plasma conditions over the past ten years has resulted in exciting new results: i) epitaxial growth maintained up to several microns with an improvement of the epi-layer quality ii) fast relaxation of the strain at the interface, iii) successful heteroepitaxy of SiGe on Si as well as on III-V substrates, iv) ultrathin film crystalline silicon cells transferred onto foreign substrates,.. However the detailed epitaxial growth process remains elusive.

In this work we address the various process windows allowing obtaining epitaxial growth at ~200 °C in a plasma environment: the relative roles of silicon radicals, atomic hydrogen, bombardment by silicon ions or by charged clusters will be discussed, based on our large corpus of experimental [2-3] and ab-initio molecular dynamics simulations [4]. The role of charged particles/clusters on the epitaxial growth will be studied with particular emphasis on the role of the impact energy (eV/atom). Recent pulsed discharge studies aiming at selecting the charged nanoparticles (positive or negative) and their impact energy will also be presented.

1) P. Roca i Cabarrocas,Y. Djeridane, Th. Nguyen Tran, E.V. Johnson,A. Abramovand Q. Zhang. Plasma Phys. Control. Fusion 50 (2008) 124037.
2) P. Roca iCabarrocas, R. Cariou and M. Labrune. J. Non Cryst. Solids **358** (2012) pp. 2000.
3) R. Cariou, J. Tang, N. Ramay, R. Ruggeri, and P. Roca i Cabarrocas. Solar Energy Materials and Solar Cells 134 (2015) 15.
4) Ha-Linh Thi Le, Nancy C. Forero-Martinez, and Holger Vach. Chemical Physics Letters **610** (2014) 223.

ID 255 - Poster

Substrate Independent Control of the Thin Film Silicon Crystallinity

**S. Muthmann[1], T. Fink[1], M. Meier[1]*
[1]Forschungszentrum Juelich GmbH, IEK-5 Photovoltaik, Juelich, Germany

The deposition on textured substrates is essential for various types of efficient thin-film solar cells. The textures help to enhance light path by scattering the incoming light and reducing the intensity of the reflectance due to a gradual change of the refractive index. To optimize and to characterize the properties of the deposited layers the influence of the substrate morphology on growing films needs to be taken into account. This is especially important for mixed phase materials like hydrogenated microcrystalline silicon for which optimum device performance is achieved in a narrow process window. In the past we learned that weak intrinsic process drifts tend to change the material properties in growth direction. Here in-situ process control is essential to allow the reproducible fabrication of state of the art layers.

In the present work in-situ Raman spectroscopy was applied to study the evolution of the microcrystalline silicon during layer growth. We deposited thin-film microcrystalline silicon p-i-n junction solar cells on substrates with a wide range of morphologies: Flat glass coated with randomly textured Aluminum doped Zinc Oxide (AZO) which was either prepared by sputtering and consecutive wet chemical etching or low pressure chemical vapor deposition. Also randomly textured glass covered by sputtered AZO and substrates with periodic textures prepared by nano-imprint lithography were studied.

The Raman crystallinity was determined during deposition under constant process parameters. The evolution of the material properties in growth direction is analyzed and compared for the various substrate types. For optimized solar cell performance the well-known increase of the crystalline volume fraction was observed during the initial phase of deposition independent of the substrate type. The source gas flow during the deposition was adjusted to obtain an identical and constant crystalline volume fraction on the various substrate types throughout the layers. It was shown that the fill factor of the devices is particularly improved by the adaption of the growth process. Additionally it was possible to carry out a comparison of the light trapping performance of the different substrate types at well-defined properties of the microcrystalline silicon.

ID 256 - Poster

Nano-structural features of a-Si:H grown by reverse-hydrogen profiling during hot-wire CVD

**C. Arendse[1], B. van Heerden[1], F. Cummings[1], T. Muller[1], P. van Loosdrecht[2], C. Oliphant[3], D. Motaung[4]*
[1]University of the Western Cape, Physics, Bellville, South Africa
[2]University of Cologne, Physikalisches Institut, Cologne, Germany
[3]National Metrology Institute of South Africa, Pretoria, South Africa
[4]Council for Scientific and Industrial Research, Pretoria, South Africa

We report on the evolution of the nano-structural and optical properties of a hydrogenated amorphous silicon thin film series produced by reverse-hydrogen profiling during hot-wire chemical vapour deposition. The hydrogen dilution ratio was increased from 50% to 90% in fixed time intervals. Raman and infrared spectroscopy, corroborated by high resolution transmission electron microscopy, show the preservation of a structurally superior thin film-bulk as the growth progresses with the onset of a porous, nano-crystalline surface in the final deposition step. Infrared spectroscopy and electron energy loss spectroscopy shows low amounts of oxidation confined to the porous crystalline surface. The depth profile of the Si-H and Si-H_2, measured by time-of-flight secondary ion mass spectroscopy, show a homogeneous bulk distribution with a reduction at the surface. The optical properties are determined by the initial growth conditions, which are retained as the growth progresses.

ID 257 - Oral

Glass polymorphism in amorphous germanium probed by first-principle computer simulations

*G. Mancini[1], *M. Celino[2], F. Iesari[2], A. Di Cicco[1]*
[1]University of Camerino, Physics Division, School of Science and Technology, Camerino (Italy), Italy
[2]ENEA, C.R. Casaccia, Rome (Italy), Italy

The low-density (LDA) to high-density (HDA) transformation in amorphous Ge at high pressure is studied by first-principles molecular dynamics (FPMD) simulations in the framework of density functional theory. Previous experiments are accurately reproduced, including the presence of a well-defined LDA-HDA transition above 8 GPa. The LDA-HDA density increase is found to be about 14%. Pair and bond-angle distributions are obtained in the 0-16 GPa pressure range and allowed us a detailed analysis of the transition. The local fourfold coordination is transformed in an average HDA sixfold coordination associated with different local geometries as confirmed by coordination number analysis and shape of the bond-angle distributions.

ID 258 - Oral

Suitability of oxide based (ZnO, CoGaO, and ZnGaO) semiconductor materials for low temperature solid oxide fuel cells as a potential electrolyte

**M. M. Can[1], S. Shawuti[1], M. A. Gülgün[2]*
[1]Istanbul University, Physics Department, Istanbul, Turkey
[2]Sabanci University, Faculty of Engineering and Natural Sciences , Istanbul, Turkey

We analyzed and compared the AC electrical properties of some oxide based (ZnO, $ZnGa_2O_4$ and $CoGa_2O_4$) semiconductors for low temperature solid oxide fuel cells as a potential electrolyte. ZnO, $ZnGa_2O_4$ and $CoGa_2O_4$ powders were synthesized by utilizing solid state reaction method. Each powder was uni-axially pressed to form pellets and annealed at 1200 $^{\circ}$C for 2 hours. Preferentially oriented crystallites in pellets were formed. The AC electrical conductivity responses for the inter and intra granular ionic conduction were analyzed in the temperature range between 25 °C and 700 °C. The capacitance values, which are between ~10^{-12}-10^{-10} F (obtained from Cole-Cole plots), indicate the dominant ionic conductivity was through the grain boundaries. The ionic conductivity values through the grain boundaries were measured as 9.9 x 10^{-8} S cm^{-1} (25 °C), 2.2 x 10^{-8} S cm^{-1} (500 °C), and 1.7 x 10^{-8} S cm^{-1} (500°C) for ZnO, $ZnGa_2O_4$ and $CoGa_2O_4$, respectively. The increase of temperature enhance the ionic conductivity mechanism, which makes the pellets useless at high temperature AC Impedance measurements, 350 °C for ZnO and of 700 °C for $ZnGa_2O_4$ and $CoGa_2O_4$ as found in research. The ionic conductivity of ZnO at 350 °C was up to 1.25 x 10^{-6} S cm^{-1}, and; for $ZnGa_2O_4$ and $CoGa_2O_4$ semiconductors the ionic conductivities at 700 °C were 1.08 x 10^{-6} S cm^{-1} and 2.2 x 10^{-6} S cm^{-1}, respectively. The temperature increase caused an increase in conductivity and thus, leads a corresponding shift in the relaxation time toward the low values. These shifts were correlated with the activation energies (171 meV for ZnO, 1200 meV for $ZnGa_2O_4$ and 1634 meV for $CoGa_2O_4$). Even though the conductivity values (<0.1S/cm) are not enough to commercialize these oxide semiconductors, measured values imply doped oxide semiconductors can be regarded as a potential electrolyte materials for low temperature fuel cell applications.

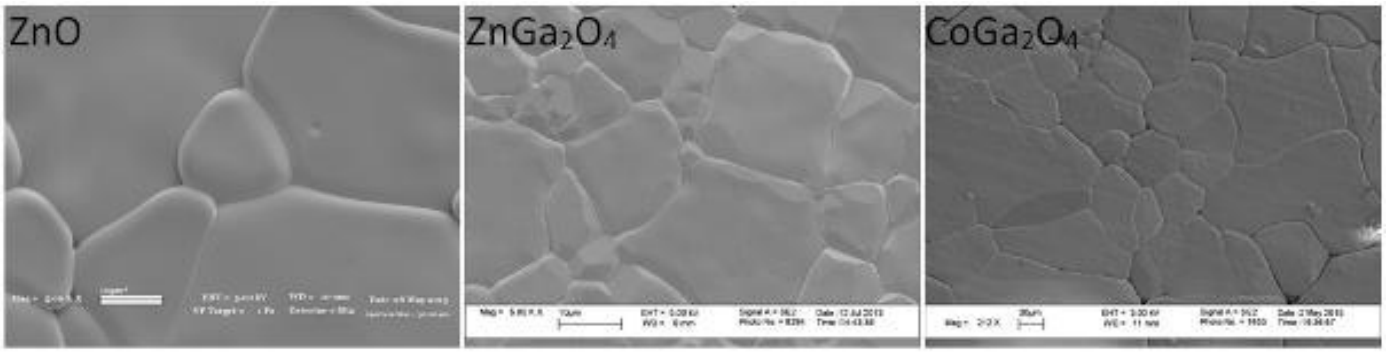

ID 259 - Oral

Crystallization of Phase-Change Materials from First-Principles Simulations

*I. Ronneberger[1], W. Zhang[1], R. Mazzarello[1], P. Zalden[2], M. Xu[1], M. Salinga[1], H. Eshet[3], M. Wuttig[1]
[1]RWTH Aachen, Aachen, Germany
[2]Stanford University, Stanford, Germany
[3]Tel Aviv University, Tel Aviv, Israel

Phase-Change Materials (PCM's) are widely used in optical storage media (CD,DVD, Blu-Ray) because they possess fast and reversible switching capabilities between the amorphous and the crystalline phase and they exhibit strong optical contrast between those phases. In recent years, PCM's have come to the fore as a novel material class suitable for non-volatile memory technology as well. Phase-change memory cells exploit the huge electrical contrast (several orders of magnitude) displayed by the two phases. The switching speed is determined by the crystallization of the amorphous phase.

We study the crystallization of two technologically relevant Phase-Change compounds, namely $Ag_4In_3Sb_{67}Te_{26}$ (AIST) and $Ge_2Sb_2Te_5$ (GST), by means of ab initio molecular dynamics simulationsof large models containing up to 810 atoms. The amorphous phase is obtained byfast quenchingof the melt. We fix 2 crystalline layers during quenching, so as to model the surrounding crystalline matrix. For GST, we also investigate the formation of crystalline nuclei within the amorphous phase using the metadynamics method. From the subsequent production runs,we extract the crystal growth velocities at high temperature (~600K) and obtain ~8 m/s for AIST and ~1 m/s for GST. The observed crystal growth speeds compare well with available experimental data. The differences in growth velocity between AIST and GSTare attributed to both smaller diffusivity and sticking coefficient of GST. Moreover, we demonstrate the formation of the meta-stable cubic phase of GST during crystallization, which was previously reported in experimental studies. The simulation of AIST is extended to low temperatures (between 450 and 550K) and results in growth velocities deviating from the experimental measurements (the latter yielding dramatic slowing down in the crystallization). This discrepancy is attributed to the faster quenching rates of the simulation and the highly fragile energy landscape of AIST, which is not sufficiently sampled within the short simulation times.

Wei Zhang, Ider Ronneberger, Peter Zalden, Ming Xu, Martin Salinga, Matthias Wuttig and Riccardo Mazzarello, "How fragility makes phase-change data storage robust: insights from ab initio simulations", *Sci. Rep.* **4**, 6529 (2014), DOI: 10.1038/srep06529

Ider Ronneberger, Wei Zhang, Hagai Eshet and Riccardo Mazzarello, "Crystallization Properties of the $Ge_2Sb_2Te_5$ Phase-Change Compound from Advanced Simulations", *Adv. Funct. Mater.* (2015), DOI: 10.1002/adfm.201500849

ID 260 - Poster

Charge carrier mobility in Aluminium doped microcrystalline silicon carbide films

**F. Köhler[1], A. Heidt[1], T. Chen[1], J. Mock[1], K. Ding[1], F. Finger[1], J. Ristein[2], R. Carius[1]*
[1]Forschungszentrum Jülich GmbH, IEK-5, Jülich, Germany
[2]Universität Erlangen, Institut für Technische Physik, Erlangen, Germany

Due to its wide band gap in combination with a good electrical conductivity, silicon carbide has proven to be an excellent choice for various applications in thin-film electronics. It can be used e.g. in solar cells, TFTs, Diodes, sensors, micro-electromechanical systems (MEMS) and even shows promising results concerning its biocompatibility for BioMEMS. In order to circumvent high production costs for single crystalline material, it can be produced in a mircrocrystalline phase (µc- SiC:H) e.g. by hot-wire chemical vapor deposition, while still maintaining both acceptable optical transmission and electrical conductivity. When deposited from monomethylsilane, it is unintentionally n-type doped, though for many applications, p-type material is required. P-type conductivity can be obtained by adding an Al precursor (TMAl) during the deposition process.

A series of samples with different Al content up to 6% was prepared by hot-wire chemical vapor deposition and analyzed in terms of chemical, electronic and structural properties. As determined by SIMS measurements, the films were mostly stoichiometric for Al contents of up to 3%, while at higher concentrations an excess of carbon prevails. The data also show an inhomogeneous in-depth distribution of Al, especially for low doping, which is likely related to difficulties in maintaining a constant flow of TMAl. The samples show n-type conductivity without doping. An addition of 0.6% Al leads to a compensation of the material and thus, conductivities as low as 10-10S/cm were obtained. As determined by thermopower measurements, further adding of the dopant yields p-type conductivity up to 0.1 S/cm and charge carrier mobilities in the order of 10-3cm2/Vs, which still is about 5 orders of magnitude below the known values for single crystals. To investigate the origin of this large difference, we measured the density of occupied states in the valence band by total photoelectron yield spectroscopy and found significant contributions of states above the mobility gap in agreement with photothermal deflection spectroscopy. These states are believed to result from impurities that act as scattering centers, and thus limiting the charge carrier mobility. X-ray diffraction was further used to characterize the microstructure of the films in order to find evidence for the origin of the sub-gap states. A relative increase of the diffuse scattering of the {111}-reflection tends decrease to scale with the charge carrier mobility, though, this trend is less pronounced for off-stoichiometric samples. For these samples, it could be assumed that either the excess carbon or an inhomogeneous distribution of Al provides conductivity paths with enhanced mobility.

The diffuse x-ray scattering is linked to the density of stacking faults in the material, which again can give rise to sub-gap states. Furthermore, a continuous lattice dilation up to approximately 1% was found with increasing Al content, while the crystallite size varies independently of the doping concentration. These latter variations are unlikely the dominant cause of the low mobility in the chosen deposition regime, but still might cause variations. We conclude, that defects in the microstructure, especially the high density of stacking faults are the main reason for the comparably low charge carrier mobility.

ID 261 - Poster

Properties of hydrogenated silicon thin films deposited near the nanocrystalline amorphous transition region from argon diluted silane plasma.

*R. Amrani[1,2], P. Abboud[1,2], L. Chahed[1,2], Y. Cuminal[1,2]
[1]IES, Montpellier, France
[2]LPC2ME. Université d'Es-senia, Oran. Algerie, France

Ar diluted silane Si:H thin films were studied by changing the deposition conditions to obtain films from amorphous-like microstructure to highly crystalline. The samples were deposited by 13.56 MHz PECVD (Plasma Enhanced Chemical Vapor Deposition) of silane argon mixture. The argon dilution of silane for all samples studied was 96% by volume. The substrate temperature was fixed at 200 °C. The influence of depositions parameters on optical proprieties of samples was studied by UV-Vis-NIR spectroscopy. The structural evolution was studied by Raman spectroscopy, TEM, AFM, FTIR and X-ray diffraction (XRD). Intrinsic-layer samples depositions were made in this experiment in order to obtain the transition from the amorphous to crystalline phase materials. The deposition pressure varied from 400 mTorr to 1400 mTorr and the rf power from 50 to 250 W. The amorphous-to-nanocrystalline transition in the films is confirmed by micro-Raman spectroscopy and low angle X-ray diffraction analysis. The structural evolution studies show that beyond 160 W, we observed an amorphous-nanocrystalline transition, with an increase in crystalline fraction by increasing rf power and working pressure. Films with different crystalline fractions and crystallite size are achieved by controlling the rf power and process pressure. It was shown that optical and structural properties of nc-Si:H can be tuned by adjusting the deposition conditions. From the present study it has been concluded that the process pressure and rf power are the keys process parameters to induce the crystallinity in the Si:H films prepared by silane diluted in argon PECVD. We have showed that the high dilution of silane in hydrogen is not necessarily essential for promoting crystallinity in Si:H network. Films near the amorphous to nanocrystalline transition region are grown at reasonably high deposition rates (3.5- 8 Å/s), which are highly desirable for the fabrication of cost effective devices. The deposition rate increases with increasing rf power and process pressure. Different crystalline fractions and crystallite size can be achieved by controlling the process pressure and rf power. These structural changes are well correlated to the variation of optical and electrical proprieties of the thin films.

ID 262 - Oral

Analytical model for voltage-dependent photo and dark currents in bulk heterojunction organic solar cells

*M. M. Saleheen[1], S. Arnab[1], *M. Z. Kabir[1]*
[1]Concordia University, Electrical & Computer Engineering, Montreal, Canada

Over the past decade, bulk heterojunction (BHJ) polymer solar cells based on blends of conjugated polymers and fullerene derivatives (e.g., P3HT:PCBM blend) have drawn a huge attention in research due to their high conversion efficiency, solution-based easy fabrication, and abundant availability. Although presently BHJ cells show a reasonable power conversion efficiency (almost 10 %), further efficiency improvements/optimizations seem very likely by better understanding the operating principles through accurate physics-based modeling and optimizations. A high binding energy of the bound electron-hole pairs (EHPs) due to low dielectric constant (ε_r) of organic materials reduces the number of photogenerated free carriers. The free carriers drift across the photoconductor layer (active layer) by the built-in electric field and some of the carriers are lost by recombination. At the optimum operating output voltage, the built-in electric field is decreased which reduces the charge collection efficiency of the photo generated carriers. Moreover, at the same time, the forward diode-like current (commonly known as the dark current) increases considerably. Both the photo and dark currents critically depend on the carrier transport properties of the blend (active layer) and cell structure. Thus the overall cell efficiency is mainly dominated by the photon absorption, dissociation efficiency of bound EHPs, charge collection efficiency and dark current. Therefore, an explicit physics-based model for the voltage-dependent photo and dark currents is highly desirable for enhancing the efficiency and optimizing the design.

In our previous publication [1], we developed an explicit expression for the photocurrent in BHJ cells by incorporating exponential photon absorption, dissociation efficiency of bound EHPs, carrier trapping/recombination, carrier drift and diffusion, and actual solar spectrum. In this paper, the previous model has been modified by considering the contact effects. An explicit expression for the external voltage-dependent forward dark current is also developed by solving the continuity equations for both electrons and holes, and utilizing proper boundary conditions. The external current-voltage characteristics are determined by considering the actual solar spectrum and voltage-dependent photo and dark currents. We examine the effects of the contact properties, blend compositions and cell design on the current-voltage characteristics. The mathematical model is also compared with the published experimental results in order to determine the carrier transport properties (defects, carrier mobility and lifetime) and the effects of initial charge dissociation. We determine the quantitative effects of carrier dissociation and charge collection efficiencies on *J-V* characteristics of various BHJ solar cells. The charge collection efficiency critically depends on the hole transport properties (mobility and carrier lifetime). Low mobility of charge carriers in the blend is one of the main factors limiting the performance of BHJ solar cells. The results of this paper indicate that power conversion efficiency of BHJ solar cells critically depends on charge carrier transport, dissociation of bound EHPs in the blend and contact properties.

[1] S. M. Arnab and M. Z. Kabir, *J. Appl. Phys.* **115**, pp. 034504 (2014)

ID 263 - Poster

Enhancing short-circuit current densities by nanophotonic grating structures at the rear contact of electrically flat silicon heterojunction solar cells

*M. Smeets[1], A. Richter[1], Y. Augarten[1], F. Lentz[1], K. Bittkau[1], K. Ding[1], M. Meier[1], R. Carius[1], U. W. Paetzold[1,2]
[1]Forschungszentrum Jülich GmbH, Institute of Energy and Climate Research - Photovoltaics (IEK-5), Jülich, Belgium
[2]IMEC, Leuven, Belgium

Within the last decade, thin crystalline silicon solar cells with absorber layers down to µm-thicknesses have been realized. With decreasing thickness, the light absorption and, in turn, light trapping in these devices is essential. The currently conventionally applied light-trapping concept for monocrystalline silicon employs etched random pyramids in dimensions up to 10 µm. Facing different crystal orientations inside an absorber, as it is the case in polycrystalline silicon, this concept becomes less effective. Additionally, as soon as the absorber thicknesses reach the height of the random pyramids, these light-trapping structures are no longer feasible. As a result, for both types of absorber layers new light-trapping concepts, which can be applied to versatile types of solar cells and employ alternative implementation processes are needed. The postulated seminal direction: Processing solar cells which are optically rough but electrically flat, leading to optically thick but electrically thin solar cells.

In this contribution, we report on the development and implementation of such a concept at the rear side of silicon heterojunction solar cells, which is also applicable to various solar cell types: In this study, the light-trapping concept is applied to the rear side of flat a-SiO_x:H based prototype silicon heterojunction solar cells after the deposition of the intrinsic passivation layers and doped layers. The nanophotonic grating structures are replicated by nanoimprint lithography. Making use of reactive ion etching a residual layer below the grating structures, unavoidable during the applied nanoimprint lithography process, is removed and working solar cells are realized. The solar cells show light trapping of the incident light due to diffraction at the grating structures. The solar cell parameters of the devices are presented. An increased short-circuit current densitiy compared with flat reference solar cells is demonstrated, while no alteration of the other solar cell parameters are apparent. This promising outcome leads to an increase in the power conversion efficiency of around 0.4 %.

In addition, we have monitored the improvement of the light-trapping effect of different nanophotonic rear contacts also by photoluminescence (PL) imaging. This characterization technique, with measurement times of several milliseconds, provides local information on the improvement of the light trapping via the PL intensity with fairly high spatial resolution. Moreover, the application of PL imaging has thus the potential to, firstly, reduce the time for experimental development as it can be applied for process control early in the processing sequence, and, secondly, for a rough prediction of the relative light-trapping efficiency of the processed grating structures.

All in all, a concept, based on nanoimprint lithoography and reactive ion etching, is presented, which is a first step towards combinations of rear contact structures, independently optimized for light trapping, and front contact structures, independently optimized for incoupling of the incident light.

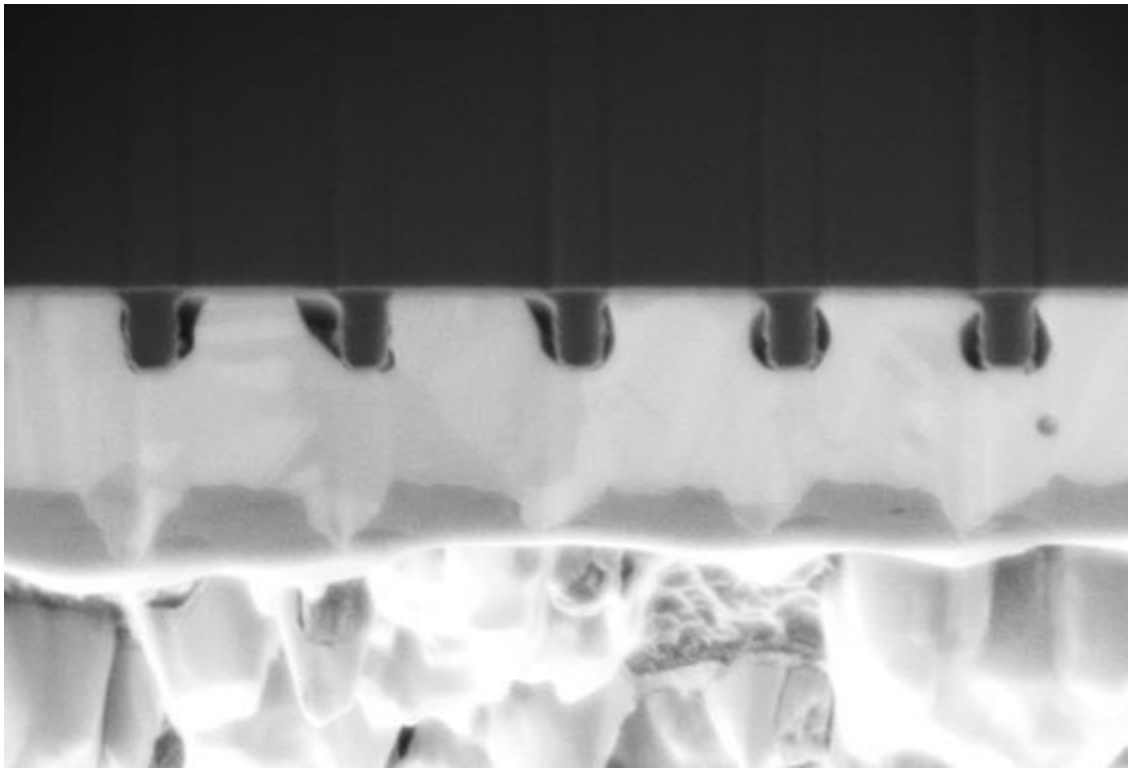

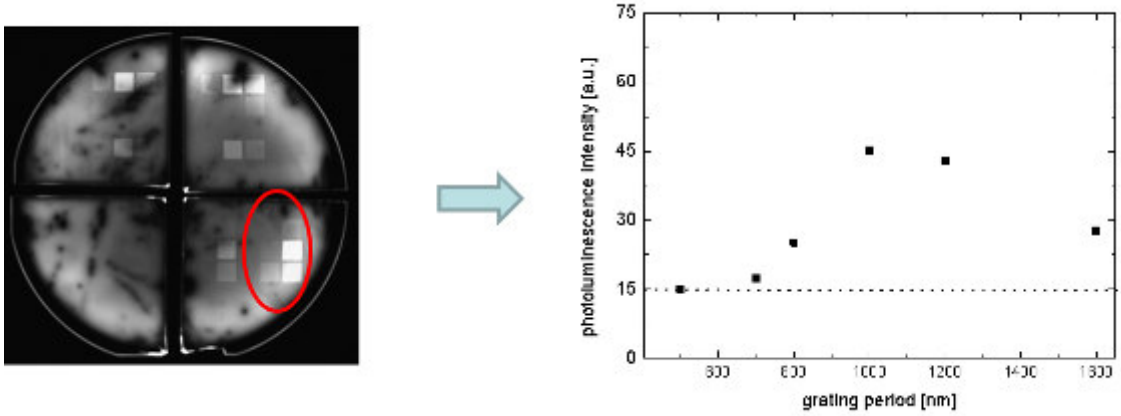
75
60
45
30
15
0
photoluminescence intensity [a.u.]
grating period [nm]

ID 264 - Poster

Assessment of computational methods for the optical characterization of aSi:H

*P. Czaja[1], U. Aeberhard[1], M. Celino[2], R. Grena[2]
[1]Forschungszentrum Jülich GmbH, IEK 5 - Photovoltaik, Jülich, Germany
[2]ENEA, C. R. Casaccia, Rome, Italy

The ab-initio calculation of macroscopic material properties in amorphous materials requires computational approaches that are simple enough to deal with structures of hundreds of atoms but yet do not miss important physical effects.

Our goal is therefore to evaluate and compare different approaches for calculating the absorption spectrum of hydrogenated amorphous Silicon (aSi:H) from ab initio in order to identify the relevant physical effects taking part in the absorption process and to assess to which level of complexity these have to be taken into account.

For that purpose we generate atomic configurations of aSi:H using ab-initio molecular dynamics, and then calculate their electronic structure using density functional theory.

Based on the obtained Kohn-Sham eigenstates, the linear response function is calculated using time-dependent perturbation theory and by solving the Bethe-Salpeter equation respectively, testing different approximations.

In particular we investigate the significance of local field corrections to the dielectric function, quasi-particle corrections to the electronic states, phonon-assisted optical transitions, and excitons.
Special care has to be taken of transitions involving localized defect states, which behave significantly different from extended bulk states.

ID 265 - Oral

Multi-phonon processes in nanocrystal-solids

**D. Bozyigit[1], N. Yazdani[1], M. Yarema[1], K. Vuttivorakulchai[1], O. Yarema[1], W. Lin[1], S. Volk[1], F. Juranyi[1,2], V. Wood[1]*
[1]ETH Zurich, Zurich, Switzerland
[2]PSI, Villingen, Switzerland

Efficiency in any semiconductor device is limited by the electron-phonon interactions, which determine the rate at which electrons can transition between electronic levels by gaining or loosing energy as heat. We perform inelastic neutron scattering and density-functional-theory calculations to study the electron-phonon interactions in nanocrystals. We show that mechanically weakening of the nanocrystal surface induces low energy and frequency surface acoustic phonon modes that couple strongly to electrons. Using thermal admittance spectroscopy to quantify the electronic transition rates in nanocrystal-based diodes and we show direct evidence of the electronic coupling of surface acoustic modes that enable large energy transitions (~1 eV) with very high rates ($10^{25}s^{-1}$) not present in bulk crystals.

ID 266 - Oral

Hybrid photoelectrochemical-photovoltaic devices for water splitting based on silicon wafer hetero-junctions and thin-film silicon multi-junctions

*P. Perez Rodriguez[1], I. A. Digdaya[1], M. Zeman[1], B. Dam[1], L. Han[1], W. Smith[1], *A. Smets[1]*
[1]Delft University of Technology, Delft, Netherlands

Photoelectrochemical water splitting (PEC) has the potential to be a large-scale, sustainable, cost-effective and efficient route to produce hydrogen by harnessing and storing the power of the sun. One single semiconductor material cannot supply the required voltage of 1.5 to 2 V to realize the water splitting reaction between an anode and cathode electrode. Photoelectrochemical-photovoltaic (PEC-PV) multi-junctions are device configurations which can deliver these voltages and therefore can split water under light illumination without any external biasing.

Similar like the photovoltaic (PV) devices, the PEC-PV devices based on III-V semiconductor have the potential to achieve the highest solar-to-hydrogen (STH) conversion efficiencies. However, the PV industry has demonstrated that the technology based on III-V semiconductors cannot compete with the far more cost-effective silicon PV technology. Therefore, the realization of cost effective PEC-PV devices requires a combination of silicon technologies and earth abundant PEC materials.

In this contribution we will discuss three types of silicon based PEC-PV devices and will shows some device demonstrators. The first configuration is based on thin-film silicon (TF Si) PV device power W-gradient doped $BiVO_4$ photoanode. Using this device configuration a 5.2% STH[1,2] conversion efficiency are achieved which is the highest value for PEC-PV device based on metal-oxide photoanode. However, as will be discussed in the contribution the STH conversion efficiency of this technology is limited by 9%.

Two other silicon based PEC-PV structures will be introduced that have the potential to tackle the 10% barrier. The second configuration is based on a-SiC:H photocathode in combination with earth abundant catalyst layers[3,4]. The PV-PEC device structure based on the a-SiC:H phtocathode to reach STH efficiencies above 10% will be presented and challenges will discussed. The third approach is to develop innovative hybrid devices based on TF Si PV junctions and wafer based c-Si/a-Si:H heterojunction solar cells. Results on all three configurations will be presented.

[1]Abdi, Fatwa F, et. al. Nature communications 4, 2195 (2013).
[2]Han, Lihao, et. al. ChemSusChem 7, 2832-2838, (2014).
[3]Han, Lihao; et al. Journal of Materials Chemistry A 3, 4155-4162 (2015).
[4]Digdaya Ibadillah A, et al., Energy Environ. Sci., **DOI:** 10.1039/C5EE00769K (2015).

ID 267 - Poster

Understanding the relation between fill factor and thickness in organic solar cells

*P. Kaienburg[1], T. Kirchartz[2,1]
[1]Forschungszentrum Jülich, IEK-5, Jülich, Germany
[2]University of Duisburg-Essen, Faculty of Engineering and CENIDE, Duisburg, Germany

The efficiency of a solar cell at given illumination is determined by its short circuit current, open circuit voltage and fill factor. While the former two are rather well examined, the understanding of the fill factor especially in thin-film solar cells remains challenging. The fill factor in solar cells made from low mobility semiconductors results from the competition between the extraction and recombination of charge carriers. A high fill-factor in thin-film solar cells is often considered as a qualitative indicator of good electronic quality, i.e. long charge carrier lifetimes and high charge carrier mobilities. The problem with translating the fill factor into a quantitative assay of charge transport and recombination is the complex dependence of the fill factor on a multitude of parameters such as active layer thickness, charge carrier mobilities and lifetimes, illumination and internal electric fields. Here, we explore in how far it is possible to predict a measure of electronic quality from nothing more than thickness, fill factor, open-circuit voltage and short-circuit current. These are parameters that are nearly always measured and available for a large range of materials used in organic photovoltaics.

In order to analyze the thickness-dependent fill factor in a quantitative way, we use numerical simulations to create a huge dataset of possible combinations of thickness, mobilities, lifetimes and interfacial band gaps in a similar way as has been done recently by Bartesaghi et al. [1] We then define a normalized fill factor (FF) to take the effect of the band gap and open-circuit voltage on the fill factor into account [2]. In a second step we define normalized variables that mainly include the effect of recombination, transport and thickness. Both normalizations are chosen carefully to reduce the scatter of the data points. This approach yields three regions as shown in Fig. 1. The two regions with very low and very high normalized FF are difficult to interpret in terms of electronic quality, because huge changes in mobility and lifetime lead to moderate changes in FF if the FF is already nearly ideal or if it is already close to 25%. In the range of intermediate FFs however, changes in mobility and lifetime (or recombination constant) directly translate into changes in FF and information about electronic material quality can under certain assumptions be obtained.

After discussing two different ways of defining normalization schemes based on either Langevin or Shockley-Read-Hall recombination, we compare the predictions based on the simulations with literature data on several generations of organic solar cells and discuss the different assumptions that affect an analysis based mainly on FF and active layer thickness. These assumptions are the properties of the contacts, unintentional doping in the active layer and asymmetry in mobilities.

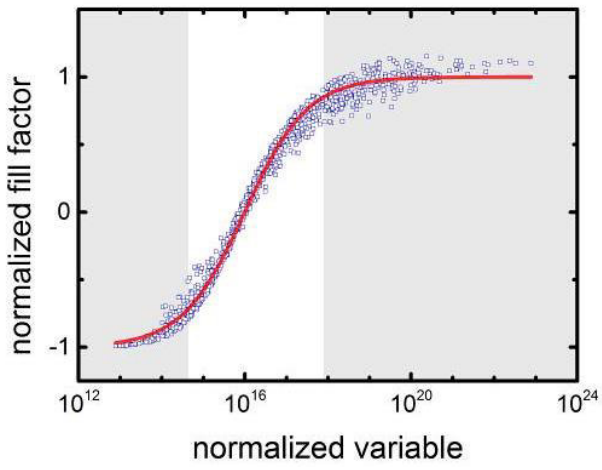

[1] D. Bartesaghi et al., *Nature Communications*, 2015, 6, 7083
[2] M.A. Green, *Solar Cells*, 1982, 7, 337

ID 268 - Poster

Enhanced quantum efficiency of NIP microcrystalline silicon solar cells by hydrogen plasma treatment on the initial intrinsic active layer

*X. Zeng[1], X. Zhang[2], S. Zhang[1], B. Cheng[1]
[1]Laboratory on Integrated Optoelectronics, Institute of Semiconductors, CAS, Beijing, China
[2]Key Laboratory of Semiconductor Materials Science, nstitute of Semiconductors, CAS, Beijing, China

The deposition of hydrogenated microcrystalline silicon (µc-Si:H) solar cells on extremely textured substrates results in improved light trapping in the cell. However, the growth of silicon layers on rough substrates can often cause unwanted current drains, degrading performance of the cells. We show that the use of hydrogen plasma treatment on the initial intrinsic active area of the cell permits in such cases to recover the electrical properties. It is shown that the quantum efficiency in the infrared spectral region from 520 to 800 nm was improved greatly by such treatment. Relative increases of up to 18.3% of short circuit current density J_{SC} (from 14.49 mA/ cm^2 to 17.15 mA/ cm^2) was shown with hydrogen plasma treatment µc-Si:H single-junction cells deposited on rough stainless steel (SS). Finally we applied such regime to solar cells on an optimized Ag/ZnO textured substrate and got short current density as 24.66 mA/cm^2 under xeon lamp illumination (calibrated 100 mW/cm^2). The underlying physics is also discussed in this work by measuring dark J-V curves and capacitance-voltage (C-V) curves of the solar cell.

Light scattering at textured substrates has turned out to be main steps to increase the efficiency of thin-film silicon solar cell [[1],[2],[3],[4],[5]].Owing to the light scattered into different angles a prolonged average optical path-length and hence an enhanced light absorption in the solar cell are obtained[[6]]. For hydrogenated microcrystalline silicon (µc-Si:H) cells light trapping can makeup for the low absorption of the indirect band gap. However, Deposition on textured substrates can cause undesired localized current drain due to low-quality porous film [[7]].In mc-Si:H cells, zones of porous material, called thereafter cracks, appear typically when the device is deposited on substrates with V shape morphology. In particular, substrate topography has been shown to be determinant for growth direction of the microcrystalline material, as it starts perpendicular to the local substrate plane [[8]]. Thus, when growth takes place on steep structures, columnar growth of microcrystalline grains collides over substrate grooves, producing, thus, grain boundaries that extends from the bottom right up to the top of the layers. To mitigate such impact we demonstrated that hydrogen plasma treatment on the initial intrinsic active area of the cell can be used to flatten the as deposited textured intrinsic region. Such treatment can lead to reduce the leaky area thus improved performance of µc--Si:H solar cells deposited on highly textured substrates.

The NIP µc -Si:H solar cells were deposited by plasma-enhanced chemical vapor deposition (PECVD). For the intrinsic µc -Si:H films, the excitation frequencies were 60 MHz Power densities ranged from 100 to 500 mW /cm^2. A 3:100 gas mixture of silane and hydrogen was supplied. The deposition temperature was kept constant at 220°C for intrinsic µc -Si:H films. The pressure p was varied between 1.33 to 2.0 mbar. We made two device differed in the initial growth of µc -Si:H films: One deposited µc -Si:H films without any treatment after n layer growth intrinsic; another fabricated µc -Si:H films by initial deposition µc -Si:H followed 5 min by hydrogen plasma treatment for 2 min. Then intrinsic µc -Si:H and p type amorphous silicon films were fabrication successively to make solar cell.

Hydrogen plasma treatment on the initial intrinsic active area of the solar cells on textured substrates was shown to reduce unwanted current drains and improve the performance of the solar cell.

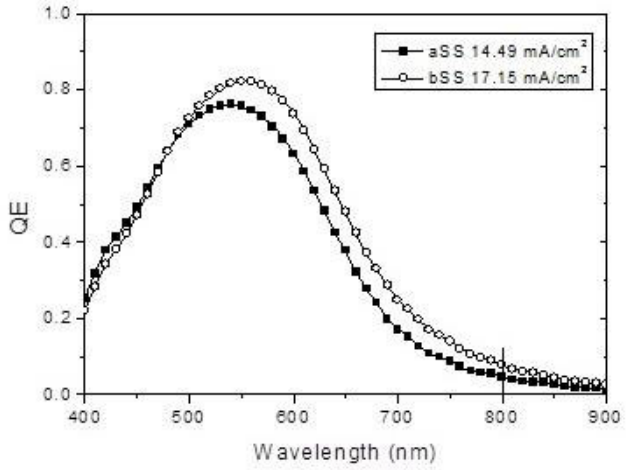

Figure1 Quantum efficiency for μc-Si nip solar cell on rough stainless steel (SS) at 0V without hydrogen treatment (black square) and with hydrogen treatment (open circle)

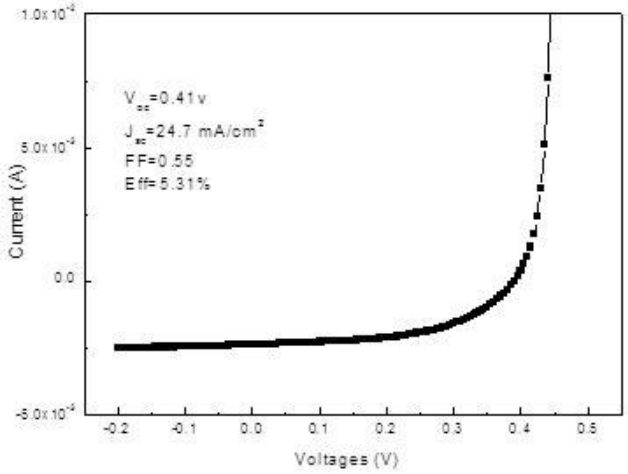

Figure3 Current-voltage (J-V) measurements for μc-Si:H nip solar cell on a Ag/ZnO textured substrate

[1] M. Despeisse,a G. Bugnon, A. Feltrin, M. Stueckelberger, P. Cuony, F. Meillaud, A. Billet,and C. Ballif ,Appl. Phys. Lett. **96**, 073507(2010)
[2] T. Tiedje, B. Abeles, J. M. Cebulka, and J. Pelz, Appl. Phys. Lett. **42**, 712 (1983)
[3] M. Berginski, J. Hupkes, M. Schulte, G. Schope, H. Stiebig, B. Rech, and M. Wuttig, J. Appl. Phys. **101**, 074903 (2007).
[4] J. Springer, B. Recha, W. Reetz, J. M. uller, M. Vanecek, Solar Energy Materials & Solar Cells **85** ,1(2005)
[5] A. Banerjee, J. Yang, K. Hoffman, and S. Guha, Appl. Phys. Lett. **65**, 472 (1994)
[6] J. Krc,, M. Zemanb, O. Kluthc, F. Smolea, M. Topic, Thin Solid Films 426,296 (2003)
[7] Grégory Bugnon , Gaetano Parascandolo , Thomas Söderström , Peter Cuony ,Matthieu Despeisse , Simon Hänni , Jakub Holovský , Fanny Meillaud , and Christophe Ballif, Adv. Funct. Mater. **22**, 3665(2012)
[8] Y. Nasuno, M. Kondo, A. Matsuda, Mater. Res. Soc. Symp. Proc. 664 (2001) A.15.5.1.

ID 269 - Poster

Device simulations of $CH_3NH_3PbI_3$ perovskite / heterojunction crystalline silicon monolithic tandem solar cells using an n-type a-Si:H/p-type µc-$Si_{1-x}O_x$:H tunnel junction.

*A. Nakanishi[1], Y. Takiguchi[1], S. Miyajima[1]
[1]Tokyo Institute of Technology, Physical Electronics, Ookayama, Meguro-ku, Tokyo, Japan

$CH_3NH_3PbI_3$ perovskite has attracted much attention as an absorbing layer for high efficiency and low cost solar cells. This material has a bandgap of about 1.55 eV and it can be increased by adding Cl and prepare $CH_3NH_3PbI_{3-x}Cl_x$. This bandgap is suitable for the absorbing layer of top cell of a tandem solar cell with the crystalline silicon (c-Si) bottom cell [1]. Recently, device simulations of single junction perovskite solar cell [2] and optical simulations of $CH_3NH_3PbI_3$ perovskite / heterojunction c-Si monolithic tandem solar cells [3] have been reported. For further detailed analysis, device simulations of perovskite / heterojunction c-Si monolithic tandem solar cells are required. In this study, we focus on the device simulations of perovskite / heterojunction c-Si monolithic tandem solar cells using silicon based tunnel recombination junction (TRJ) which consists of doped hydrogenated amorphous silicon (a-Si:H) and doped hydrogenated microcrystalline silicon oxide (µc-$Si_{1-x}O_x$:H). The simulations were carried out by using AFOS-HET simulation tool (version 2.4.1). The typical structure used in our simulations is LiF/ITO/spiro-OMeTAD/defective layer/$CH_3NH_3PbI_3$/defective layer/TiO_2/n-type a-Si:H/TRJ/p-type µc-$Si_{1-x}O_x$:H/p-type c-Si/i-type a-Si:H/n-type a-Si:H/Ag. In these simulations, optical constant (n.k) of all the materials are taking into account. It should be noted that LiF, ITO and Ag were only used for optical simulations.

We demonstrates that the TRJ model which is commonly used for a-Si:H/microcrystalline silicon tandem solar cells can be used for simulations of perovskite / heterojunction c-Si monolithic tandem solar cells. We investigated the influence of the doping type of the c-Si wafer. As a result, tandem solar cells with p-type c-Si show higher efficiency than that with n-type c-Si due to the high FF. We also investigated the effect of band offset near the TRJ region. Although our simulations do not take optical confinement in the heterojunction c-Si bottom cell into account, the simulated efficiency reaches to 21.5% (V_{oc} = 1.64 V, J_{sc} =16.0 mA/cm^2 , FF = 0.824) . These results suggest that this simple simulation model is useful to investigate the design of perovskite / heterojunction c-Si monolithic tandem solar cells and further optimizations of the simulation model, especially for taking optical confinement into account, enables more precise simulations.

[1] P. Loper, B. Niesen, Soo-Jin Moon, S. Martin de Nicolas, J. Holovsky, Z. Remes, M. Ledinsky, F.-J. Haug, Jun-Ho Yum, S. De Wolf, and C. Ballif: IEEE Journal of Photovoltaics 4 (2014) 1545.
[2] T. Minemoto and M. Murata: Sol. Energy Mater. Sol. Cell 133 (2015) 8.
[3] M. Filipič, P. Löper, B. Niesen, S. De Wolf, J. Krč, C. Ballif, and M. Topič: Optics Express 23 (2015) A263.

ID 270 - Poster

Influence of synthesis temperature on the morphology of the silicon oxide nanowires synthesized with tin catalyst

**E. Baranov[1], S. Khmel[1], A. Zamchiy[1,2]*
[1]Kutateladze Institute of Thermophysics, Laboratory of rarefied gases, Novosibirsk, Russian Federation
[2]Novosibirsk State University, Department of Physics, Novosibirsk, Russian Federation

Nanowires of various materials are promising candidates for the creation of nanoelectronic devices due to their small size, low power consumption, and unique physical properties. In particular, silica nanowires have good photoluminescence properties and may be used for creation of the optoelectronic devices. Using different both high and low temperature substrates imposes certain limitations on methods for the synthesis of nanostructures, namely on the synthesis temperature. Therefore the study of the morphology of nanostructures depending on the temperature seems an actual task.

Silicon oxide nanowires were synthesized from mixture monosilane-argon with gas diluent hydrogen at different temperatures by gas-jet electron beam plasma CVD method. Oxygen was supplied directly into the vacuum chamber. The synthesis was carried out on c-Si substrate with tin film mass thickness about 120 nm. The process of nanowire synthesis on the substrate with the catalyst consists of three stages: heating up to operating temperature, treatment of hydrogen plasma and the actual growth of nanowires. The synthesis temperature was 280 and 400°C.

SEM observations show that the tin film consists of a submicron size polygonal region. Next annealing leads to strong deformation of the film. At a temperature of 400°C are formed particles of about 10 microns coated with oxide, which are surrounded by particles of nanometer size. At a temperature of 280°C, except the particle size of about 10 microns, are formed micron sized particles, but which are not surrounded by particles of nanometer size. After etching the hydrogen plasma particles acquire a spherical shape, but it should be noted that for temperature 400°C particles are larger. As a result of synthesis the nanostructures morphology varies greatly. At a temperature of 400°C grow up silica "microropes" with the catalyst particles of micron size, and on the surface formed array of silicon oxide nanowires. At a temperature of 280°C, the tin nanoparticles at the surface coated with a silicon thin film, and silicon nanowires grown on the entire surface of the micron-sized catalyst particles. It forms a structure like a sea urchin. We suppose that the low temperature prevents the rapid formation of eutectic tin-silicon solution, which leads to the creation of nanostructures of different morphologies.

ID 271 - Oral

Correlating the density of states with charge transport in conjugated polymers - A study of poly(9,9-dioctylfluorene) using transient photocurrent measurements and drift-diffusion modelling

*X. Shi[1], S. Foster[1], N. Chander[1], A. Perevedentsev[1], X. Wang[1], J.- S. Kim[1], D. Bradley[1], R. MacKenzie[2], J. Nelson[1]
[1]Imperial College London, Dept. of Physics, London, United Kingdom
[2]University of Nottingham, Faculty of Engineering, Nottingham, United Kingdom

Electronic devices based on π-conjugated organic semiconducting materials (OSCs) have attracted much interest as being low-cost, low-embedded energy and mechanically flexible alternatives to their inorganic counterparts. The charge transport process within OSCs is crucial to the performance of devices, and is in turn strongly influenced by variations in the energy and configuration of conjugated segments. Such variations may result from variations in molecular packing, chain conformation, chemical impurities or structural defects, and are characteristic of most OSC layers.

For a given system, the density of states describes the energetic distribution of states that are available to be occupied by charge carriers. For OSCs, the states with the lowest-lying LUMO energies and the highest-lying HOMO energies could act as traps for electrons and holes, respectively. Also, chemical impurities such as species introduced by chemical degradation mechanisms or by unintentional doping may be present, resulting in shallow or deep trap states for the charge carriers. Such defect states are associated with retarded carrier transport and high recombination rates, which in many cases lead to poor device performance.

Here we focus on poly(9,9-dioctylfluorene) (PFO), combining optical (photoluminescence and Raman) spectroscopy with electrical transient techniques to study the influence of processing conditions on hole transport properties. Densities of trap states (DoS) for differently processed films were estimated from temperature-dependent and high-dynamic-range time-of-flight measurements. We find that solvent vapour exposure that is known to induce conformational defects in the polymer film significantly affects the value of the hole mobility as well as the shape of the photocurrent transients. The experimental transport data were rationalised by using a time-domain drift-diffusion model that incorporates energetic disorder via a DoS function. We are able to explain the transport behaviour using a DoS function that is consistent with spectroscopic data for the materials and quantum-chemical calculations of the conformational defect. In addition we address the effect of chemical defects, induced by photodegradation, on the charge transport and DoS in a similar manner. We compare the effects of conformational and chemical defects on the transport properties.

ID 272 - Poster

Impact on the electro-optical properties of very rapid, highly selective laser heating of a solar cell front contact composed of textured ZnO:Al and p-SiOx:H

**F. Maier[1], D. Hauschild[2], S. Haas[1]*
[1]Forschungszentrum Jülich GmbH, IEK-5, Photovoltaik, Jülich, Germany
[2]LIMO Lissotschenko Mikrooptik GmbH, Dortmund, Germany

Improvement of transparent conductive oxides (TCO), especially aluminium doped zinc oxide (ZnO:Al), by post-deposition annealing processes in various atmospheres and with various capping layers is widely studied [1-6]. A promising post-deposition approach is annealing by absorption of intense laser irradiation since it offers layer-selective energy deposition combined with very short processing times.

In this study the influence of continuous wave (cw) laser treatment at λ = 1470 nm on the electrical and optical properties of high quality, texture etched ZnO:Al, capped with a 20 nm thin substoichiometric <p>-SiOx:H layer was investigated. This layer sequence is typically used within thin-film silicon cell structures. The interaction time between laser radiation and TCO material was varied in the ms range for different laser power densities in order to increase conductivity. In contrast, typical furnace annealing times are in the range of some ten hours. At the laser wavelength of 1470nm the absorption coefficient α of ZnO:Al is by orders of magnitude higher than the one of the substrate material or typical photovoltaic absorbers like silicon. Hence the laser energy could be deposited very selectively within the ZnO:Al layer resulting in a very low thermal load to the substrate. On the other hand a total absorption of the radiation of about 40% indicates still a rather uniform heating of the whole ZnO:Al layer in depth.

A twofold improvement of the device grade, texture etched ZnO:Al material, was found although the cap contains oxygen, which is suspected to degenerate ZnO:Al, and is presumed to be rather permeable: (i) the Hall mobility and the carrier density of the capped ZnO:Al increased and simultaneously (ii) its absorption in the short wavelength range could be improved. This tendency corresponds to the findings of Ruske et al. [2] for furnace annealing of ZnO:Al with a dense cap preventing deterioration by oxygen. However, the furnace annealing study revealed a reduction of the specific resistance ρ by -48% within more than 30 hours (ρ=270 down to 140µWcm) compared to laser annealing with a reduction of -22% within milliseconds (ρ=470 down to 365µWcm) for the textured structure of this study.

Furthermore, microscopy data show the formation of cracks starting at a certain threshold laser power. Up to this power level the electrical properties improve while the cracks make the ZnO conductivity fail ($\Delta\rho > 0$). This suggests that the electro-optical material improvement is limited by the simultaneously induced strain. In this context also the changes of Raman spectra are discussed. Further the impact of the TCO annealing on the p-layer transparency and microstructure is presented.

[1] C. Charpentier, P. Prod'homme, and P. Roca i Cabarrocas, Thin Solid Films **531**, 424 (2013).
[2] F. Ruske, M. Roczen, K. Lee, M. Wimmer, S. Gall, J. Hüpkes, D. Hrunski, and B. Rech, J. Appl. Phys. **107**, 013708 (2010).
[3] M. Warzecha, J.I. Owen, M. Wimmer, F. Ruske, J. Hotovy, and J. Hüpkes, IOP Conf. Ser. Mater. Sci. Eng. **34**, 012004 (2012).
[4] V. Schütz, V. Sittinger, S. Götzendörfer, C.C. Kalmbach, R. Fu, P. von Witzendorff, C. Britze, O. Suttmann, and L. Overmeyer, Phys. Procedia **56**, 1073 (2014).
[5] V. Lissotschenko and D. Hauschild, in *Subsecond Annealing Adv. Mater.*, edited by W. Skorupa and H. Schmidt (Springer International Publishing, Cham, 2014), pp. 139-153.
[6] T. Gebel, M. Neubert, R. Endler, J. Weber, M. Vinnichenko, A. Kolitsch, W. Skorupa, and H. Liepack, MRS Proc. **1287**, 75 (2011).

ID 273 - Poster

The nanostructure and light-induced degradation of a-Si:H solar cells produced by expanding thermal plasmas

*T. Nagai[1], J. Melskens[2,3], A. H. M. Smets[2], M. Zeman[2], T. Matsui[1], M. Kondo[4]
[1]National Institute of Advanced Industrial Science and Technology , Research Center for Photovoltaics, Tsukuba, Japan
[2]Delft University of Technology, Photovoltaic Materials and Devices, Delft, Netherlands
[3]Eindhoven University of Technology, Department of Applied Physics, Eindhoven, Netherlands
[4]National Institute of Advanced Industrial Science and Technology (AIST), Fukushima Renewable Energy Institute, Tsukuba, Japan

In this study, we focus on the metastability of *p-i-n* hydrogenated amorphous silicon (a-Si:H) solar cells and the nanostructure of the a-Si:H layer deposited by expanding thermal plasma chemical vapor deposition (ETP-CVD). ETP-CVD yields a different nanostructure for the a-Si:H *i*-layer when compared to the conventional radio frequency plasma-enhanced chemical vapor deposition (RF-PECVD) method. More specifically, the density of the smallest open volume deficiencies in the a-Si:H matrix is significantly smaller for ETP-CVD, while we have indications that the passivation degree of the volume deficiencies appears to be worse in comparison to RF-PECVD. We report on progress in processing of a-Si:H solar cells made by ETP-CVD.

So far, additional DC pulsing and RF biasing on the substrate holder were required to achieve solar cell conversion efficiencies in the order of ~6 % by ETP-CVD. One of the drawbacks of these typical ETP-CVD conditions is the possible negative effect of higher order polysilane molecules, radicals, and ions, which are generated by the reaction of silane with the argon (Ar) ions and excited Ar^* in the reactor chamber. By decreasing both the Ar dilution and the arc current - or in other words increasing the H_2 dilution in the arc head - high-quality a-Si:H solar cells with an initial conversion efficiency of 9.7 % were obtained using purely remote processing conditions without any additional DC pulsing or RF voltage biasing of the substrate.

To investigate the nanostructure of a-Si:H films produced by conventional RF-PECVD and ETP-CVD, we measured the Raman spectra around 2000-2100 cm^{-1}, where the Si-H and Si-H_2 vibrational modes are traditionally assigned, or the Si-H low and high stretching modes, following a more recent interpretation. First, we studied the relation between the nanostructure and the stability of *p-i-n* solar cells. In order to understand the light-induced degradation of the solar cells, the degradation of the external parameters was studied under 1 sun AM1.5 conditions at a controlled temperature of 25 $^{\circ}C$. The short-term (fast defect states) and long-term (slow defect states) degradation are similar for all a-Si:H solar cells and appear to be independent of the ETP-CVD growth conditions. Secondly, the light-soaking evolution of the defect states in the band gap of the *i*-layer in the solar cells is monitored using Fourier Transform Photoconductivity Spectroscopy (FTPS) in combination with external quantum efficiency (EQE) measurements. The FTPS-EQE values in the visible wavelength region drastically decreased during light soaking. Furthermore, at least 3 different distributions that are associated with defect states can be resolved in the sub band gap FTPS-EQE spectra, i.e. in the range of 0.6 to 1.4 eV. The density of these distributions increases non-linearly with light soaking time. Especially, the density of the distribution at 0.6 eV in the FTPS-EQE spectrum is significantly enhanced during light soaking in all cases, while the change in the densities of the other two distributions correlates with the degradation of the external parameters of the solar cells within the first 100 hours of light soaking.

We consider that the light-induced degradation in a-Si:H solar cells produced by the ETP-CVD strongly relates with these sub gap distributions as measured by FTPS and that the generation of defect states during light soaking increases mostly near the *p-i* interface, since blue light is mainly absorbed in the top part of the *i*-layer. The differences and agreements with the stability of a-Si:H *p-i-n* cells deposited by the conventional RF-PECVD will be discussed.

ID 274 - Oral

Progress and challenges in a-Si:H based thin-film solar cells

**T. Matsui[1], A. Bidiville[1], K. Maejima[2], H. Sai[1], T. Koida[1], T. Suezaki[3], M. Matsumoto[4], H. Katayama[4], Y. Takeuchi[5], S. Sugiyama[6], K. Saito[2,7], M. Kondo[1], I. Yoshida[2], K. Matsubara[1]*
[1]National Institute of Advanced Industrial Science and Technology (AIST), Tsukuba, Japan
[2]Photovoltaic Power Generation Technology Research Association (PVTEC), Osaka, Japan
[3]Kaneka Corporation, Osaka, Japan
[4]Panasonic Corporation, Osaka, Japan
[5]Mitsubishi Heavy Industries, Ltd., Tokio, Japan
[6]Sharp Corporation, Tokio, Japan
[7]Fukushima University, Fukushima, Japan

Although high-efficiency (~14-15%) a-Si:H/μc-Si:H tandem solar cells have been demonstrated in the initial state, the stabilized efficiencies of such devices after long-term illumination are limited to ~12% due to the light-induced defect creation in a-Si:H, known as the Staebler-Wronski effect [1]. In our previous studies [2,3], we have demonstrated that high-efficiency and low-degradation a-Si:H solar cells can be obtained when the a-Si:H absorber layer is deposited by a remote plasma process using triode PECVD. By integrating such stable a-Si:H absorber into optimized device designs, we have attained two independently-confirmed record stabilized efficiencies of 10.2% ($\Delta\eta/\eta_{ini}$~10%) for a-Si:H single-junction and 12.7% ($\Delta\eta/\eta_{ini}$~3%) for a-Si:H/μc-Si:H double-junction solar cells [4]. In this paper we show the detailed comparison of the a-Si:H single-junction solar cells fabricated using triode PECVD and conventional diode PECVD with different deposition rates ranging over three orders of magnitude (R_d~10^{-4}-10^{-1} nm/s). Based on this, we discuss the origin of the improved metastability and performance of a-Si:H solar cells developed in this work. In addition, the technologies that led to a marked progress in μc-Si:H solar cells will be introduced including novel light trapping designs, PECVD process and transparent conductive oxide layer [5]. Finally, we discuss the technological challenges and potential for further efficiency improvement in thin-film silicon solar cells.

[1] D. L. Staebler and C. R. Wronski, Appl. Phys. Lett. 31, 292 (1977). [2] S. Shimizu et al., J. Appl. Phys. 97, 033522 (2005). [3] T. Matsui et al., Prog. Photovolt: Res. Appl. 21, 1363 (2013). [4] T. Matsui et al., Appl. Phys. Lett. 106, 053901 (2015). [5] H. Sai et al, Appl. Phys. Lett. 106, 213902 (2015).

ID 275 - Oral

Thin-film silicon MEMS and NEMS

*J. Conde[1]
[1]INESC MN, LISBON, Portugal

Thin-film hydrogenated amorphous silicon (a-Si:H) is a well-established large-area electronics technology, with applications in solar cells, thin-film transistors and photodetector arrays. More recently, thin-film MEMS applications have been demonstrated. Thin-film silicon MEMS processing is CMOS backend compatible, due, in particular, to the low temperature of deposition of the silicon structural layer by PECVD (< 200 ºC). It also allows fabrication on large-area substrates such as glass and (flexible) polymer.

For MEMS applications, the main film properties to consider are the deposition rate, electrical conductivity, and mechanical stress. In the first part of this work, n^+ - doped hydrogenated amorphous/ nanocrystalline silicon thin-films are deposited by rf-PECVD. A wide range of deposition conditions is studied and three different characteristic silicon thin-films, corresponding to three different internal structures, with very distinct mechanical and electrical properties, are identified. These silicon thin-films are used as structural layer of electrostatically actuated thin-film MEMS microresonator bridges and cantilevers, fabricated on glass substrates at temperatures below 200ºC, using surface micromachining and thin-film technology. The effect of the mechanical stress of the structural layer (from tensile to highly compressive) on the device resonance frequency, quality factor and required actuation forces are studied and interpreted with detailed electromechanical models.

In the second part of this work, submicron gap thin-film silicon NEMS are presented and discussed. First, a laterally vibrating square plate fabricated using low temperature (Electrostatic actuation was used to excite the mechanical motion of the thin-film silicon resonators. The total current measured in the network analyzer consists of a motional term, related with the actual motion of the resonator, and a parasitic component, generated by the capacitive coupling between the drive and sense electrodes. In the third part of this work, the mechanical resonant system is be modeled as an equivalent electrical RLC circuit with parallel parasitic capacitance. The model is fit to the experimental results and the motional electrical parameters and quality factor are extracted. The motional resistance, R_m, of a microresonator is a vital parameter when integrating resonators with electronics, in particular with CMOS circuits, since it determines the interface with control electronics, the impedance matching between components and the power consumption. R_m decreases by increasing the electromechanical coupling factor (η) between the excitation signal and the resonator. The dependence of the R_m extracted from fitting the RLC model to the experimental admittance curves with the distance of the transduction gap and the applied dc bias is shown. The results agree with theoretical values until high actuation voltages are considered. The hysteresis associated with high amplitude motion of the resonator is responsible for the asymptotic behavior of R_m.

These results represent an important step towards the development of fully miniaturized and monolithically integrated a-Si:H-based MEMS and NEMS. Using the resonators presented in this work, large-area (on glass and polymer substrates) and CMOS compatible, monolithically integratable thin-film silicon MEMS applications can be envisaged.

ID 276 - Oral

Advances in liquid phase crystallized silicon on glass: growth, electronic properties and solar cell concepts

*D. Amkreutz[1], J. Haschke[1], S. Kühnapfel[1], P. Sonntag[1], C. Becker[2], O. Gabriel[3], B. Rech[1]
[1]Helmholtz-Zentrum Berlin, Silicon Photovoltaics EE-IS, Berlin, Germany
[2]Helmholtz-Zentrum Berlin für Materialien und Energie GmbH, Nanostructured Silcon for Photonic and Photovoltaic Implementations, Berlin, Germany
[3]Helmholtz-Zentrum Berlin für Materialien und Energie GmbH, PVcomB, Berlin, Germany

The direct growth of high quality multicrystalline silicon on glass with a thickness range between 1 and 50 micrometers is a promising approach for future solar cells and has the potential to meet the requirements imposed by the ITR-PV [1] towards thinner wafers. However, the formation of silicon with wafer equivalent electronic quality on glass is challenging due the limited thermal endurance of the substrate. Liquid phase crystallization [2,3] using line shaped energy sources such as CW diode lasers or electron beams has proven to form multicrystalline silicon layers on borosilicate glass which exhibit wafer equivalent grain sizes and electronic quality. Different steps were taken to determine suitable interlayers, dopant density & type as well as post crystallization treatments which finally resulted in open circuit voltages up to 656 mV [3] and efficiencies up to 11.8% [4] using a back-contacted, back- a-Si:H(ip)/mc-Si(n) hetero-junction device with a 10 micrometer silicon absorber. In this contribution, critical process steps with respect to their impact on the absorber properties are discussed and suitable contact systems are compared. In addition, we show latest results obtained using an interdigitated back contact silicon heterojunction scheme. Finally, novel approaches to further improve the film quality in terms of morphology and electronic quality are presented that might open new applications for thin crystalline silicon in the fields of microelectronics or sensors.

[1] ITR-PV roadmap,http://www.itr-pv.net/(2015)
[2] D. Amkreutz et al., Prog. Photovolt. Res. Appl. 19, 937-945 (2011)
[3] J. Dore et al., Prog. Photovolt. Res. Appl. 21, 1377-1383 (2013)
[4] J. Haschke et al., Sol. Energ. Mat. Sol. C. 128, 190-197 (2014)
[5] D. Amkreutz et al., *IEEE J. Photovolt.* 4, 1496-1501 (2014)
[6] O. Gabriel et al., *IEEE J. Photovolt.* 4, 1343-1348 (2014)

ID 277 - Oral

Inverse quantum confinement in luminescent Silicon quantum dots

**T. Niehaus*[1]
[1]*Universität Regensburg, Institut I - Theoretische Physik, Regensburg, Germany*

Research on silicon nanostructures intensified in the past years, due to their potential applications in future technologies, such as nanosensors, molecular electronics and photonic devices. This interest is based on the fact that the electronic structure of these materials depends critically on the size, orientation, passivation and doping level of the nanostructure.

Light absorption and emission of these systems also attracted great attention, because the band gap in bulk crystalline Si is small and indirect, while the band gap in Silicon nanostructures can become large and direct due to the quantum confinement effect. In the past, theoretical descriptions of the optical properties of such nanostructures were mainly restricted to the determination of the absorption spectrum. In order to quantify the luminescence it is often tacitly assumed that the deexcitation occurs resonantly. However, absorption and emission spectra can be quite different due to excited state relaxation and simulations that take this Stokes shift into account are currently rather scarce.

In this talk, an approximate - but parameter-free - method based on time-dependent density functional theory is presented (TD-DFTB) [1-3], which is suitable to investigate the above mentioned topics. We show results on functionalized and reconstructed Silicon nanocrystals [4]. The latter exhibit an unusual inverse quantum confinement effect [5]. If time allows, we also discuss the effect of electron confinement in axial and radial directions of rodlike Silicon nanostructures with large aspect ratio [6]. Formation of self-trapped excitons is observed for short nanostructures; longer wires exhibit fully delocalized excitons with negligible geometrical distortion.

[1] T.A. Niehaus, S. Suhai, F. Della Sala, P. Lugli, M. Elstner, G. Seifert, and Th. Frauenheim Phys. Rev. B
63 085108 (2001)
[2] T.A. Niehaus THEOCHEM 914 38 (2009)
[3] D. Heringer, T.A. Niehaus, M. Wanko, and Th. Frauenheim J. Comp. Chem. 28 2589 (2007)
[4] R.Q. Zhang, A. De Sarkar, T.A. Niehaus, and Th. Frauenheim phys. status solidi b 249 401 (2012)
[5] X. Wang, R.Q. Zhang, S.T. Lee, Th. Frauenheim, and T.A. Niehaus Appl. Phys. Lett. 93 243120 (2008)
[6] Y. Wang, R.Q. Zhang, Th. Frauenheim, and T.A. Niehaus J. Phys. Chem. C 113 12935 (2009)

ID 278 - Oral

What has Bonding Done for Us?

**J. Robertson*[1]
[1]*Cambridge University, Engineering, Cambridge, United Kingdom*

Mott was well known for noting that atoms in amorphous semiconductors obey the 8-N rule of bonding. I use this as a starting point to describe how a knowledge of bonding processes in disordered materials has helped their technological development in many areas. For example, to understand doping in a-Si:H, a general model that includes the 8-N rule. I will continue with VAP defects in chalcogenides, and the different effects of disorder in a-Si:H, a-C, a-InGaZn oxide, and in GeSbTe alloys, relating these to experimental results. It can also help understand some of the unusual properties of the recent perovskite solar cell materials, ABI_3.

ID 279 - Oral

Stability and Aging of Phase Change Materials : An Ab Initio Perspective

**J.- Y. Raty*[1]
[1]*Université de Liège, Physique des Solides, Interfaces et Nanostructures (SPIN), Liège, Belgium*

Data recording with Phase Change Materials is a much studied topic as the writing/erasing characteristics, cyclability and downscaling properties of these materials allow for efficient data storage in future generations of devices. Nevertheless, some aspects of phase change materials are limiting their performances and delaying their wider technological application.

First, aging phenomena are common to all amorphous structures, but of special importance PCMs since it impedes the realization of multi-level memories. Different interpretations have been proposed, but we focus here on the structural relaxation of amorphous GeTe, chosen because it is the simplest system that is representative of the wider class of GST alloys, lying along the GeTe-Sb_2Te_3 composition line of the GeSbTe phase diagram. One difficulty encountered in the simulation of these amorphous systems is that the direct generation of an amorphous structure by quenching a liquid using Density Functional Theory (DFT) based Molecular Dynamics leads to one sample with a small number of atoms, and, hence of small number of atomic environments. Here we sample a large number of local atomic environments, corresponding to different bonding schemes, by chemically substituting different alloys, selected to favor different local atomic structures. This enables spanning a larger fraction of the configuration space relevant to aging. Our results support a model of the amorphous phase and its time evolution that involves an evolution of the local (chemical) order towards that of the crystal. On the other hand its electronic properties drift away from those of the crystal, driven by an increase of the Peierls-like distortion of the local environments in the amorphous, as compared to the crystal [1].

A second problem faced by PCMs is the fact that data recording is limited at high temperature due to the increased propensity to recrystallize. One approach to counter this is to stabilize the PCM using impurity atoms such as C or N. Using DFT and the analysis of the mechanical properties (constraints theory), we demonstrate how these impurity atoms modify the rigidity of the network, which is experimentally correlated with the activation energy for crystallization [2].

Finally, the crystal phase itself has been shown to have variable conductivities depending on the thermal history and annealing conditions. If this could be used profitably for multi-level recording, it also indicates that the crystal is undergoes some temporal evolution. Using DFT, we clarify the stability behavior of GST crystal and show that the metal-insulator transition is driven by the migration of intrinsic vacancies and an Anderson localization transition [3].

[1] J.Y Raty, W. Zhang, J. Luckas, C. Chen, R. Mazzarello, C. Bichara and M. Wuttig, Nat. Comm. (2015)
[2] G. Ghezzi, J.Y. Raty, S. Maitrejean, A. Roule, E. Elkaim and F. Hippert, Applied Physics Letters, 99 (2011) 151906
[3] W. Zhang, A. Thiess, P. Zalden, R. Zeller, P. H. Dederichs, J-Y. Raty, M.Wuttig, S. Blügel et R. Mazzarello, Nature Materials 11 (2012) 952

ID 280 - Oral

Highly efficient single-, double- and triple-junction silicon based thin film solar cells

**X. Zhang[1,2], B. Liu[1], L. Bai[1], J. Fang[1], C. Wei[1], Q. Huang[1], J. Ni[1], X. Chen[1], D. Zhan[1], J. Sun[1], G. Wang[1], G. Hou[1], H. Ren[1], S. Xu[1], B. Li[1], J. Zhang[1], Y. Zhao[1,2]*
[1]Nankai University, Institute of Photo electronics thin Film Devices and Technology, Tianjin, China
[2]Collaborative Innovation Center of Chemical Science and Engineering, Tianjin, China

Great research interest in silicon thin film solar cells (STFSCs), no matter single-, double-, or triple-junction types, has been aroused on account of their unique properties—light weight, sensitivity to low-intensity or non-direct sunlight, and low cost—to meet the imperatives of the increasing global energy demand and environmental sustainability nowadays. Here we present our latest progress in the studies on high-performence single-, double-, and triple- junction STFSCs consisting of pin-type a-Si:H, a-SiGe:H, or μc-Si:H components. By adopting p-type nanocrystalline silicon carbon (p-nc-SiC: H) buffer layers, which show nano-sized silicon crystallites of 4-6 nm embedded in amorphous tissues, at the interfaces between aluminum-doped zinc oxide (AZO) transparent conductive oxide (TCO) front contacts and p-type window layers to reduce the contact potential loss, a high open circuit voltage (V_{oc}) of 0.982 V and a *FF* of 70.00% were successfully acquired for pin-type a-Si:H single-junction TFSCs. Meanwhile, we have also effectively suppressed the high leakage current in pin-type narrow-gap (E_g<1.5 eV) a-SiGe:H single-junction TFSCs by integrating an n-type μc-SiO_x:H layer with a controlled oxygen content, an effective approach giving rise to a highest *FF* of 70.62% and an initial efficiency of 11.45% for pin-type a-SiGe:H single-junction TFSCs (E_g=1.48 eV). Pin-type μc-Si:H single-junction TFSCs were simultaneously improved by sandwiching intrinsic silicon oxide (i-SiO_x:H) buffer layers into p-type window layers and μc-Si:H absorbers to effectively enhance the light coupling, thereby leading to an initial efficiency as high as 10.54%. In addition, on the basis of metal organic chemical vapor deposition (MOCVD) boron-doped zinc oxide (BZO) TCOs, by effectively compensating the band gap discontinuity between wide-gap p-type SiO_x:H window layers and a-Si:H absorbers with i-a-SiO_x:H buffer layers, a high V_{oc} of 0.927 V, *FF* of 72.60%, and initial efficiency of 11.30% can also be realized for pin-type a-Si:H single-junction TFSCs and an initial efficiency of 13.65% for pin-type a-Si:H/μc-Si:H double-junction TFSCs by further tuning the current matching between component cells. Consequently, the successful realization of pin-type a-Si:H/a-SiGe:H/μc-Si:H triple-junction TFSCs on photo-electrically optimized AZO substrates by effectively integrating respective component cells with our electrically lossless tunnel recombination junctions (TRJs) has eventually provided a high initial efficiency of 16.07% (V_{oc}=2.195 V, J_{sc}=9.929 mA/cm^2, and *FF*=73.76%), highlighting the great potential to achieve higher-performance STFSCs and hybrid tandems with other PV cells, such as perovskite, polycrystalline chalcopyrite Cu(In,Ga)Se_2 (CIGS), and organic cells *et al.*.

ID 281 - Oral

Molecular factors influencing charge carrier recombination at donor-acceptor interfaces for organic photovoltaics

*K. Vandewal[1]
[1]Technische Universität Dresden, Institut für Angewandte Photophysik , Dresden, Germany

Electronic processes at the organic hetero-interface between electron donating and electron accepting molecules determine the photocurrent, photovoltage and ultimately, the power conversion efficiency of organic solar cells. While devices with incident-photon-to-extracted-charge conversion yields of over 85%, and absorbed photon-to-extracted-charge conversion yields of 90-100% have been achieved, the difference between the optical gap of main absorber and open-circuit voltage (V_{oc}) is much larger than for inorganic solar cells. The main improvements in the V_{oc} of organic solar cells have so far been made by tailoring donor-acceptor interfacial energetics, taking advantage of well-known principles of molecular design. Nevertheless, for most material systems we consistently find a large (>0.55 eV) difference between eV_{oc} and the energy of the intermolecular charge transfer (CT) state. We present experimental evidence that this difference can be reduced by reducing the physical interfacial area available for free carrier recombination. We quantify this by analyzing the strength of the interfacial CT state absorption and emission signal at photon energies below the optical gap of the neat materials. We further discuss the influence of the measured electronic coupling, molecular reorganization and non-radiative recombination pathways on free carrier recombination and V_{oc}. This work opens up unexplored possibilities for increasing the V_{oc} of organic solar cells, bringing it closer to the optical gap of the main absorber.

ID 282 - Oral

Silicon nanocrystals for future electronics and photonics

**S. Oda*[1]
[1]*Tokyo Institute of Technology, Quantum Nanoelectronics Res. Ctr., Tokyo, Japan*

Quantum dot structures, where electrons are confined three-dimensionally in the sub 10 nm scale, show characteristics quite different from conventional bulk structures. Recent progress in the fabrication technology of silicon nanostructures has made possible observations of novel electrical and optical properties of silicon quantum dots, such as single electron tunneling, ballistic transport, visible photoluminescence and electron emission. Fabrication and characterization of nanocrystalline Si films by plasma processes are discussed.

ID 283 - Oral

Hydrogen incorporation, stability and release effects in thin film silicon

**W. Beyer*[1,2]
[1]*Helmholtzzentrum Berlin für Materialien und Energie, Institut für Silizium-Photovoltaik, Berlin, Germany*
[2]*Forschungszentrum Jülich GmbH, IEK-5 Photovoltaik, Jülich, Germany*

The presence of hydrogen in alloy-type concentrations in plasma-grown silicon films was discovered about 45 years ago. Since then, by scientific interest and due to the high potential for industrial application a multitude of studies have been performed aiming to clarify the role of hydrogen in these materials which, as became clear, have a microstructure highly dependent on deposition conditions. With focus on the experimental techniques of infrared absorption, gas effusion and deuterium-hydrogen interdiffusion measured by SIMS, a number of characteristic and partially surprising hydrogen effects are pointed out which affect hydrogen incorporation, hydrogen stability and hydrogen out-diffusion. These hydrogen effects include severe changes of film microstructure in a certain hydrogen concentration range causing a change of the predominant hydrogen diffusing species from atomic hydrogen in dense material of lower H content to molecular hydrogen in material of higher H concentration. In dense material, H solubility limits deuterium-hydrogen interdiffusion. H stability and diffusion are found to depend (besides of material microstructure) on doping, H concentration, the H diffusion source, treatment time and others. A Meyer-Neldel Rule applies for hydrogen diffusion prefactors and energies. Furthermore, H out-diffusion is found to cause material contraction and formation of microvoids. Similarities and significant differences to single crystalline silicon occur.

0284 - Oral

Novel Approaches to Improve Optical Absorption and Carrier Extraction of Organic Photovoltaic Cells

**W. C. H. Choy*[1]
[1]*The University of Hong Kong, Department of Eletrical and Electronic Engineering, Hongkong*

Several approaches to enhance the light absorption and carrier extraction of organic optoelectronic devices will be investigated. For the light management, a theoretical and experimental study organic solar cells with multiple metallic nanostructures is presented in this talk. From theoretical study, the physics of the performance enhancement of the organic solar cell is explained by multiphysics model of plasmonic organic solar cells. Meanwhile, we have also experimental investigated the plasmonic-optical and plasmonic-electrical effects with various metallic nanostructures such as metallic nanoparticles and metallic nanogratings into different regions of the solar cells. For the plasmonic-optical effects, we demonstrated the enhancement of light absorption in active layer and thus the improvement of photogenerated current. Regarding the electrical effects due to the incorporation of metal nanostructures, we realize the hot carrier effects and charge storage effects separately and achieve high performance organic optoelectronic devices. [1-4]

Besides enhancing light absorption for carrier generation, carrier extraction is also play critical role in the performance of organic optoelectronic devices. Bearing the compatibility with large-area, low-cost, high-throughput production and all-solution technology, we develop various methods to synthesize low-temperature solution-processed transition metal oxides (TMOs) for hole transport layer [5-7] and electron transport layer [8-10] of organic optoelectronic devices. With low temperature treatment or even at room temperature, the TMO films with small amount oxygen vacancies exhibit high film quality and desirable electrical properties for efficient carrier transport layer. The incorporation of metal nanomaterials can further enhance carrier extraction properties of the carrier transport layers. [11]

Recently, we experimentally and theoretically break the intrinsic space-charge limit (SCL) of organic semiconductors by a novel plasmonic-electrical concept [12]. Our results show that the power conversion efficiency of organic solar cells can be enhanced by over 30% and the value of power conversion efficiency can reach about 9.6% depending on the metallic nanostructures, device structures, and the polymer materials. Details of the improvement will be discussed [1-3].

1) W. C. H. Choy, W. K. Chan, Y. Yuan, Adv. Mat., 26, 5368, 2014.
2) W.C.H. Choy, W.E.I. Sha, X. Li, D.Zhang, Progress In Electromagnetics Research, invited, 146, 25, 2014.
3) W.C.H. Choy, Chem. Comm., invited, 50, 11984, 2014.
4) W.E.I. Sha, H.L. Zhu, L. Chen, W.C. Chew, W.C.H. Choy, Scientific Reports, DOI: 10.1038/srep08525
5) F. Jiang, W.C.H. Choy, X.C. Li, D. Zhang, J. Cheng, "Post-Treatment-Free Solution Processed Non-Stoichiometric NiOx Nanoparticles for Efficient Hole Transport Layers of Organic Optoelectronic Devices", Adv. Mat., in press.
6) X.C. Li, F.X. Xie, S.Q. Zhang, J.H. Hou, W.C.H. Choy, (Nature Publishing Group) Light: Science & Applications, doi: 10.1038/lsa.2015.46; X.C.Li, F.X.Xie, S.Q.Zhang, J.H.Hou, W.C.H. Choy, Adv. Function. Mat., DOI: 10.1002/adfm.201401969.
7) F. Xie, W.C.H. Choy, C. Wang, X. Li, S. Zhang, J. Hou, Adv. Mat., 25, 2051, 2013.
8) H.L. Zhu, W.C.H. Choy, W.E.I. Sha, X. Ren, Adv. Opt. Mat., 2, 1082, 2014.
9) F.X. Xie, S.J. Cherng, S. Lu, Y.H. Chang, W.E.I. Sha, S.P. Feng, C.M. Chen, W.C.H. Choy, ACS Appl. Mat. & Interfaces, 6, 5367, 2014.
10) D. Zhang, W.C.H. Choy, F.X. Xie, X. Li, Org. Electron, 13, 2042, 2012.
11) X.C. Li, W.C.H. Choy, F. Xie, S. Zhang, J. Hou, J. Mater. Chem. A, 1, 6614, 2013.
12) W.E.I. Sha, X. Li, W.C.H. Choy, Scientific Reports, 4, 6236, 2014.

ID 285 - Oral

Technological Progress in HIT® - on the long way towards the limit -

*M. Shima[1]
[1]Eco Solutions Company, Panasonic Corp. , Energy System Business Div., Solar BU, Kaizuka

We have been developing a heterojunction solar cell since 1990, that is composed of intrinsic a-Si:H layers and doped a-Si:H layers on an n-type c-Si. As results of R&D, we have already reported a conversion efficiency of 25.6% with a high Voc of 0.740V with our solar cell (designated area: 143.7 cm^2, n-type CZ-Si, confirmed by AIST). This is the highest conversion efficiency achieved in the world as of August 2015 for silicon based solar cells without a concentrating function. We were able to attain this high efficiency by adopting an interdigitated back contact structure to our original a-Si:H/c-Si heterojunction technology in order to reduce optical losses by the grid electrode as compared with a cell having an efficiency 24.7%, which was reported in 2013.

Not only R&D, we have succeeded in the world's first mass production of photovoltaic modules that use heterojunction cells as HIT® in 1997. With its high performance, the HIT® has been strongly supported by our customers since its launch. We have achieved significant improvements in the output power of our photovoltaic module by improving of both solar cell performance and module technologies. As for the solar cell performance improvement, an enhancement of the performance of the passivation characteristics, a reduction of the resistivity of the grid electrodes and a decrease of reflectance on the incident surface are so important. Our past reports demonstrated the high potential of our solar cells. For example, a conversion efficiency of 20.1% with a practical size of more than 100cm2 was reported in 2000, and an excellent Voc and efficiency of 0.750V and 24.7% respectively in a 98 µm-thick cell were reported in 2013 as a result of R&D. On the other hand, as for the module, also many new technologies are developed such as a high performance anti-reflection coating cover glass with long term stability, light confinement structure and so on. We have been fully continuing our efforts to apply our newly developed technologies into mass-production and in order to provide photovoltaic modules HIT® which have the world's highest level conversion efficiency to our customers. We have just announced that HIT® slim type 250W with 25 years warranty of output power will be launched into Japanese market. These modules can be effectively installed in a variety of residential roofs.

In the future, we will continue globally competitive R&D for cell conversion efficiency of over 26%. At the same time, we also promote the development of HIT® by adopting our latest technologies. Hopefully, the latest R&D module efficiency will be announced in this session.

ID 286 - Oral

Singlet Fission – Using Organic Semiconductors and Nanocrystals to Break Efficiency Limits in Photovoltaics

**N. Greenham*[1]
[1]*University of Cambridge, Cavendish Laboratory, Cambridge*

The efficiency of single-junction solar cells, whether silicon, organic or perovskite, is fundamentally limited by inefficient conversion of the high-energy portion of the solar spectrum. I will describe recent progress to overcome this limit using the process of singlet fission, where a photogenerated singlet exciton in an organic semiconductor such as pentacene or tetracene rapidly splits into two lower-energy triplet excitons, each of which may separately contribute to the photocurrent in a solar cell. Very recently, we have shown that these triplet excitons can be efficiently transferred to PbSe nanoparticles, which can then emit photons. This “photon multiplier” structure, combining organic and inorganic semiconductors, could be applied to the front surface of any solar cell. We calculate than in the ideal case, the efficiency of a silicon solar cell could be boosted from 20% to 24%. Current challenges to reaching this limit include improving the luminescence efficiency of the nanoparticles, and tuning the triplet exciton and nanoparticle energies to match the solar cell bandgap. I will describe our recent work to implement singlet fission in devices, and will relate this to some of the physics of the ultrafast fission process, the separation and recombination of pairs of triplet states, and the transfer of excitations from organic to inorganic semiconductors.

ID 287 - Oral

Recent Progress of Nanocrystalline Semiconductor-Based Inorganic/Organic Hybrid Solar Cells

N. Sang Il Seok[1,2]

[1] *School of Energy and Chemical Engineering, Ulsan National Institute of Science and Technology (UNIST), Banyeon 100, Ulsan 689-798, South Korea*
[2] *Division of Advanced Materials, Korea Research Institute of Chemical Technology (KRICT)141 Gajeong-ro, Yuseong-Gu, Daejeon 305-600, Republic of Korea*

Until now, innovative solar energy transforming devices such as dye-sensitized solar cells, organic solar cells, and inorganic-organic hybrid hetero-junction solar cells using inorganic nanocrystalline semiconductors and quantum dots showed a very slow progress in the performance. However, significant improvements to the efficiency of *solar cells* could be possible in the near-future by advent of new technologies or materials. In this presentation, I will talk about recent progress of efficient inorganic-organic hybrid solar cells employing Sb_2S_3 (Sb_2Se_3) and chemically managed perovskite materials. As examples, the surface sulfurization and combination of Sb_2S_3 and Sb_2Se_3 as sensitizer onto mesoporous TiO_2 electrode showed the power conversion efficiency (PCE) of 7.9 % and 8.1 %, respectively, with a metal mask. In inorganic-organic hybrid perovskite materials, a solvent and compositional engineering technology enabled the fabrication of efficient cells exceeding 20% by depositing an extremely uniform, and dense perovskite layers. These results will lead to more efficient and cost-effective inorganic-organic hybrid solar cells in the future. The PCE is the highest value ever reported for each system. These results will lead to more efficient and cost-effective inorganic-organic hybrid heterojunction solar cells in the future.

1. W. S. Yang, J. H. Noh, N. J. Jeon, Y. C. Kim, S. Ryu, J. Seo, **S. I. Seok***, “High-performance photovoltaic perovskite layers fabricated through intramolecular exchange”, ***Science***, 348, 1234 (2015).
2. S. S. Shin, W. S. Yang, J. H. Noh, J. H. Suk, N. J. Jeon, J. H. Park, J. S. Kim, W. M. Seong, **S. I. Seok***, “High-performance flexible perovskite solar cells exploiting Zn_2SnO_4 prepared in solution below 100°C”, ***Nature Comm***. 6, 7410 (2015).
3. N. J, Jeon, J. H. Noh, Y. C. Kim, W. S. Yang, S. Ryu, J. Seo, **S. I. Seok*, “**Compositional engineering of perovskite materials for high performance solar cells”, ***Nature***, 517, 476 (2015).
4. N. J, Jeon, J. H. Noh, Y. C. Kim, W. S. Yang, S. Ryu, **S. I. Seok***, **“**Solvent-engineering for high performance inorganic-organic hybrid perovskite solar cells”, ***Nature Materials*** 13, 897 (2014).
5. Y. C. Choi, T. N. Mandal, W. S. Yang, Y. H. Lee, S. H. Im, J. H. Noh, and **S. I. Seok***, “Sb_2Se_3-Sensitized Inorganic-Organic Heterojunction Solar Cells Fabricated using a Single-Source Precursor”, ***Angew. Chem. Int. Ed.*** 53, 1329-1333 (2014).
6. J. H. Heo, S. H. Im, J. H. Noh, T. N. Mandal, C.-S. Lim, J. A. Chang, Y. H. Lee, H.-j. Kim, A. Sarkar, M.. K. Nazeeruddin, M. Grätzel, **S. I. Seok***, “Efficient inorganic-organic hybrid heterojunction solar cells containing perovskite compound and polymeric hole conductors”, ***Nature Photonics***, 7, 486 (2013).
7. J. A. Chang, S. H. Im, Y. H. Lee, H.-j. Kim, C.-S. Lim, J. H. Heo, **S. I. Seok***, “Panchromatic Photon-Harvesting by Hole-Conducting Materials in Inorganic−Organic Heterojunction Sensitized-Solar Cell through the Formation of Nanostructured Electron Channels”, ***Nano Lett.***, 12, 1863 (2012).

ID 288 - Oral

Relating material properties to charge recombination in organic heterojunction solar cells

Jenny Nelson[1], Jizhong Yao[1], Michelle Vezie[1], Florent Deledalle[1], Thomas Kirchartz[2]

[1]Centre for Plastic Electronics and Department of Physics, Imperial College London, London SW7 2AZ, UK
[2]IEK-5 Photovoltaics, Forschungzentrum Juelich, Germany

The power conversion efficiencies of polymer:fullerene solar cells have increased dramatically over the last decade from 2.5 % in 2001 to over 10% for in recent years. The development has been mainly driven by a better understanding of morphology , improved donor polymers and new device geometries. Nevertheless the best devices still underperform on account of losses to incomplete charge separation and to non-geminate charge recombination. Here, we apply drift-diffusion modelling combined with different experimental techniques to understand the factors that control non-geminate recombination and the impact of recombination on device performance. We study the effects of several factors: trap states in the density of states; purity of the organic semiconductor; recombination at the semiconductor-electrode interface; and unintentional doping. We consider the limits to performance imposed by recombination in different types of solution processed solar cells, and potential approaches to minimise such losses.

Author Index

G ID

H ID

I ID

J ID

K ID

L ID

M ID

T ID

U ID

V ID

W ID

X

Y

Z

Partners and Sponsors:

Walter Schottky Institut
Technische Universität München

Please pay also attention to the previous pages.